universität wien

DISSERTATION

Titel der Dissertation

Geochemistry and provenance of the Upper Cretaceous to Eocene Gosau Group around and beneath the Vienna Basin (Austria and Slovakia)

Verfasser

Gerald Hofer Bakk.rer.nat. MSc

angestrebter akademischer Grad

Doktor der Naturwissenschaften (Dr.rer.nat.)

Wien, 2013

Studienkennzahl lt. Studienblatt:	A 791 426
Dissertationsgebiet lt. Studienblatt:	Erdwissenschaften
Betreuerin / Betreuer:	Ao. Univ. Prof. Dr. Michael Wagreich

…Ton, Steine, Scherben…

Index

1. Summary 7
2. Introduction and targets 11
3. Author´s comment 15
4. Methods 17
4.1 Calcium carbonate, total sulfur and total organic carbon 17
4.2 Bulk rock geochemistry 17
4.3 Stable isotopes 19
4.4 X-ray diffraction and cathodoluminiscence 19
4.5 Heavy minerals 20
5. Publications and manuscript 23
5.1 Publications 23
5.1.1 Stratigraphy and geochemical characterisation of Upper Cretaceous non-marine – marine cycles (Grünbach Formation, Gosau Group, Austria) 24
5.1.2 Carbon, oxygen and strontium isotopes as a tool to decipher marine and non-marine environments: Implications from a case study of cyclic Upper Cretaceous sediments 49
5.1.3 Geochemistry of fine-grained sediments of the Upper Cretaceous to Paleogene Gosau Group (Austria, Slovakia): Implications for paleoenvironmental and provenance studies 75
5.2 Manuscript 99
5.2.1 Provenance of the Upper Cretaceous to Eocene Gosau Group around and beneath the Vienna Basin (Austria and Slovakia) 99
6. Additional results 139
6.1 Bulk rock geochemistry of cuttings 139
6.1.1 Major elements 139
6.1.2 Trace elements 143
7. Discussion 145
7.1 Comparison of core/outcrop and cutting samples 145
7.1.1 Influence of lithology 145
7.1.2 Contamination of drilling mud 146
7.1.3 Contamination of drill bit 146
7.2 Bulk rock and stable isotope geochemistry 147

7.2.1 Geochemical differences between Gosau basins 147
7.2.2 Discrimination between marine and non-marine samples 153
7.3 Provenance analysis 154
7.3.1 Coniacian to Campanian 154
7.3.2 Maastrichtian to Eocene 156
8. Conclusions 157
Acknowledgements 159
References 161
Appendix 183
Geochemistry 184
Heavy mineral assemblages 208
Mineral chemistry 217
Curriculum vitae 233

1. Summary

Bulk rock geochemistry and heavy mineral analysis of outcrop, core and cutting samples of the Upper Cretaceous (Coniacian/Santonian) to Paleogene (up to Eocene) Gosau Group were performed to evaluate differences and similarities, to reconstruct facies, depositional environment and provenance of successions beneath and at the eastern and western margin of the Vienna basin. This PhD thesis concentrates on deposits of the Gießhübl, Glinzendorf and Grünbach basin (Eastern Alps and Alpine subcrop underneath the Vienna basin) as well as the Slovakian Gosau equivalents of the Brezová and Studienka basin (Western Carpathians), today basically arranged in NE-SW-striking synclines.

Bulk rock and stable isotope geochemistry of 247 fine-clastic sediments demonstrate differences between hemipelagic to pelagic samples from the Gießhübl and Studienka basin compared to marginal-marine to non-marine samples from the Grünbach and Glinzendorf basin. B/Al*, $\delta^{13}C$ and $\delta^{18}O$ are reliable geochemical proxies for paleosalinity and can be used to differentiate between marine and limnic intervals. Marine-non-marine cycles are reconstructed in this way (in combination with evaluations of nannofossils) for the proximal Grünbach Formation and the Glinzendorf basin. Enriched Cr and Ni concentrations and Cr/V relative to Y/Ni ratios document ophiolitic detrital influence in mainly non-marine parts of the Glinzendorf Syncline. Statistical factor analysis indicates terrigenous derived elements (e.g. Al_2O_3, SiO_2, K_2O, Th, Rb or Zr), elements representing marine facies (e.g. CaO, Sr, TOT/C, LOI or B/Al*) and ophiolitic detritus (Cr and Ni) to describe the highest variance in a detailed and complex data set. Samples of the Gießhübl and Studienka as well as samples from marine intervals of the Glinzendorf and Grünbach basin can be distinguished from non-marine samples of the Glinzendorf and Grünbach Syncline and non-marine samples of the Glinzendorf succession with dominant ophiolitic input.

Evaluation of heavy mineral assemblages and chemical analysis of single heavy mineral grains provide a provenance concept of that area. Coniacian to Campanian heavy mineral assemblages are generally dominant in chrome spinel, while at least from the Paleocene onwards, garnet is the dominant mineral phase. Tourmaline contents are more abundant in the Studienka Gosau. Chemistry of the dominant heavy minerals garnet, chrome spinel and tourmaline were analyzed by electron microprobe. Detrital garnets with higher proportions of pyrope (and grossular) may report erosion from relics of a metamorphic sole, and chrome spinels of a mixed harzburgite and lherzolite provenance in the Coniacian to Campanian Gosau Group suggests dominant sediment transport from the Tethys suture situated south of the NCA. At this time, a mélange of high metamorphic and ophiolitic nappes from the hanging wall of the

northwards moving thrust complex onto the Austroalpine realm acts as source area for the Gosau basins. Harzburgite dominant chrome spinels in the paleogeographically northern basins indicate only minor influence of the northern Penninic accretionary wedge as a second provenance. From the Maastrichtian on only almandine-rich garnets, which are interpreted as southern, metapelitic provenance, can be observed. Moderate chrome spinel contents represent ultimate erosion of ophiolitic structures in the south. In the Paleogene, almandine-garnets are the only dominant mineral phase that shows similar chemical compositions like garnets from the Austroalpine Crystalline Complexes of the Eastern Alps (Wölz, Rappold, Radenthein, Plankogel, Koralpe and Saualpe Complex).

Gesamtgesteinsgeochemie und Schwermineralanalysen von Aufschluß-, Bohrkern- und Cuttingproben der oberkretazischen (Coniacium/Santonium) bis paläogenen (bis eozänen) Gosau-Gruppe wurden durchgeführt, um Unterschiede und Gemeinsamkeiten herauszuarbeiten, Faziesbereiche, Ablagerungsbedingungen sowie sedimentäre Liefergebiete von den unterschiedlichen Abfolgen am östlichen und westlichen Rand und im Untergrund des Wiener Beckens zu rekonstruieren. Im Rahmen der Dissertation werden Ablagerungen der Gießhübl, Glinzendorf und Grünbach Synklinale (Ostalpen und subalpine Einheiten im Untergrund des Neogenen Wiener Beckens) sowie der Slowakischen Gosau-Äquivalente im Raum Brezová und Studienka (Westkarpaten), welche heute in NE-SW-streichenden Synklinalien vorliegen, untersucht.
Mittels Gesamtgesteinsanalysen und Geochemie stabiler Isotope der 247 feinkörnigen Sedimentproben lassen sich Unterschiede in den hemipelagisch bis pelagischen Proben des Gießhübl- und Studienka-Beckens verglichen mit den randlich-marinen bis nicht-marinen Proben des Grünbach- und Glinzendorf-Beckens erkennen. Dabei erweisen sich B/Al*, $\delta^{13}C$ und $\delta^{18}O$ als brauchbare geochemische Indikatoren (Proxy), um zwischen marinen und nicht-marinen Intervallen zu differenzieren. So konnten (in Kombination mit Nannofossilanalysen) marin – nicht-marine Zyklen in der Beckenrand-nahen Grünbach-Formation und in den Abfolgen der Glinzendorfer Mulde rekonstruiert werden. Erhöhte Cr- und Ni-Konzentrationen sowie eine Anreicherung des Cr/V- im Vergleich zum Y/Ni-Verhältnisses dokumentieren detritären ophiolitischen Einfluss vor allem in nicht-marinen Abschnitten der Glinzendorf Synklinale. Mittels statistischer Faktorenanalyse werden vor allem terrigen-interpretative Elemente (z.B. Al_2O_3, SiO_2, K_2O, Th, Rb or Zr), Elemente, die für marines Milieu charakteristisch sind (z.B. CaO, Sr, TOT/C, LOI or B/Al*) und Ophiolitdetritus (ausgedrückt durch die Elemente Cr und Ni) als entscheidende Faktoren für die Unterscheidung der detailierten und komplexen Daten erkannt. Proben der Gießhübl- und Studienka- sowie Proben mariner Intervalle der

Glinzendorf- und Grünbach-Gosau können so einerseits von nicht-marinen Proben der Glinzendorf und Grünbach Synklinale und andererseits von nicht-marinen Proben mit dominantem ophiolitischen Detritus unterschieden werden.

Evaluierung von Schwermineralspektren und vor allem chemische Analysen einzelner Schwermineralkörner ermöglichen ein detailliertes und erweitertes Konzept der Liefergebiete des Arbeitsgebietes. Schwermineralverteilungen des Coniaciums bis Campaniums sind weitgehend dominant an Chromspinell, während dies spätestens ab dem Paleozän von dominanten Granatspektren abgelöst wird. Turmalinanteile sind hingegen in der Studienka-Gosau merklich erhöht. Chemische Analysen der dominierenden Schwermineralgruppen Granat, Chromspinell und Turmalin wurden mittels Elektronenmikrosonde ermittelt. Dabei zeigen detritäre Granate mit erhöhten Pyrop- und Grossularanteilen Erosion von Resten einer metamorphen Ophiolith-Sohle an, und damit einhergehend lassen Chromspinelle eines gemischten Harzburgit-Lherzolit Liefergebietes in Gosaueinheiten des Coniaciums bis Campaniums auf einen dominanten Sedimenttransport von der südlich der Nördlichen Kalkalpen gelegenen Tethys Sutur schließen. Zu dieser Zeit fungiert eine Mélange aus hochmetamorphen und ophiolitischen Decken einer tektonisch hangenden Einheit der nordwärts gerichteten Überschiebung auf Austroalpine Einheiten als Liefergebiet für die Gosaubecken. In den paläogeographisch nördlich gelegenen Becken sind Chromspinelle vor allem auf eine Harzburgit-Quelle zurückzuführen, was einen geringen Einfluss des nördlichen Penninischen Akkretionskeils als zweites mögliches Lifergebiet vermuten lässt. Ab dem Maastrichtium sind nur mehr Almandin-reiche Granate, die einer südlichen, hauptsächlich metapelitischen Herkunft zuzurechnen sind, in den Schwermineralspektren zu beobachten. Moderate Chromspinellgehalte repräsentieren letzte Erosionen südlicher ophiolitischer Strukturen zu dieser Zeit. Im Paläogen sind Almandin-Granate, welche dieselbe chemische Zusammensetzung wie Granate Austroalpiner Kristallinkomplexe der Ostalpen (Wölz-, Rappold-, Radenthein-, Plankogel-, Koralpe- und Saualpekomplex) zeigen, die einzige dominante Mineralphase.

2. Introduction and targets

The Gosau Group of the Northern Calcareous Alps (NCA) consists of Upper Cretaceous to Paleogene strata unconformably overlying folded and faulted Permian to Lower Cretaceous units, deposited after the climax of Cretaceous Alpine orogeny. Late Cretaceous, diachronous transgression within the NCA started in the Late Turonian, becoming younger towards the southeast of the NCA. Generally the Gosau Group can be divided into a Lower Gosau Subgroup consisting of fluvial, limnic to shallow marine sediments (Turonian to Santonian/Campanian or locally to Maastrichtian) and a deep marine Upper Gosau Subgroup that can last until the Eocene (e.g. Wagreich & Faupl, 1994).

This PhD thesis concentrates on Gosau deposits of the eastern part of the Eastern Alps, the subcrops underneath the Neogene Vienna Basin and the western part of the Western Carpathians. The Gosau Group at the eastern margin of the NCA, today arranged in NE-SW-striking synclines situated on various Alpine nappes, is continued further to the east and can be traced over several industrial boreholes of the subalpine basement of the Vienna Basin. From north to south the Gießhübl Syncline, the Prottes Gosau Group, the Glinzendorf and Grünbach Syncline, and the Slovakian Gosau equivalents of Brezová and Studienka can be distinguished (e.g. Wessely, 1992; 1993; Wagreich & Marschalko, 1995) (Fig. 2.1).

First detailed geological investigations of the Gosau Group of the Grünbach Syncline (Grünbach-Neue Welt) were performed by Plöchinger (1961). Since the 1970s Wessely (1974, 1984, 1990, 1992, 1993, 2000 and 2006) reconstructed the Alpine-Carpathian nappes in the pre-Neogene basement of the Vienna Basin and discussed the position of the various Gosau synclines. Due to distinct heterogeneity of Gosau deposits (e.g. Wagreich, 1986; 2001; Wagreich & Faupl, 1994; Summesberger et al., 2002), especially correlations of different Gosau units and basins in the underground of the Vienna Basin are complex. The tectonic development of the NCA is well understood within the outcrop regions at the western margin of the Vienna Basin (e.g. Wessely, 2006) and also within the Vienna Basin basement. However, because of poor fossil contents and absence of outcrops, the affiliation of the Glinzendorf Syncline is still under debate. Due to coal-bearing sediments at the base and a generally limnic-marine character, the Glinzendorf Syncline is seen as an eastern equivalent of the Grünbach Syncline, analog to the Grünbach Formation (Hamilton et al., 1990; Wessely, 1992; 1993; 2006; Mišík, 1994), but a continuous continuation is unlikely. Additionally, continuations of tectonic units of the NCA into the Slovak part of the Vienna Basin, to outcrops in the Male Karpaty Mountains and the Western Carpathians are poorly known and strongly debated (e.g. Hamilton et al., 1990).

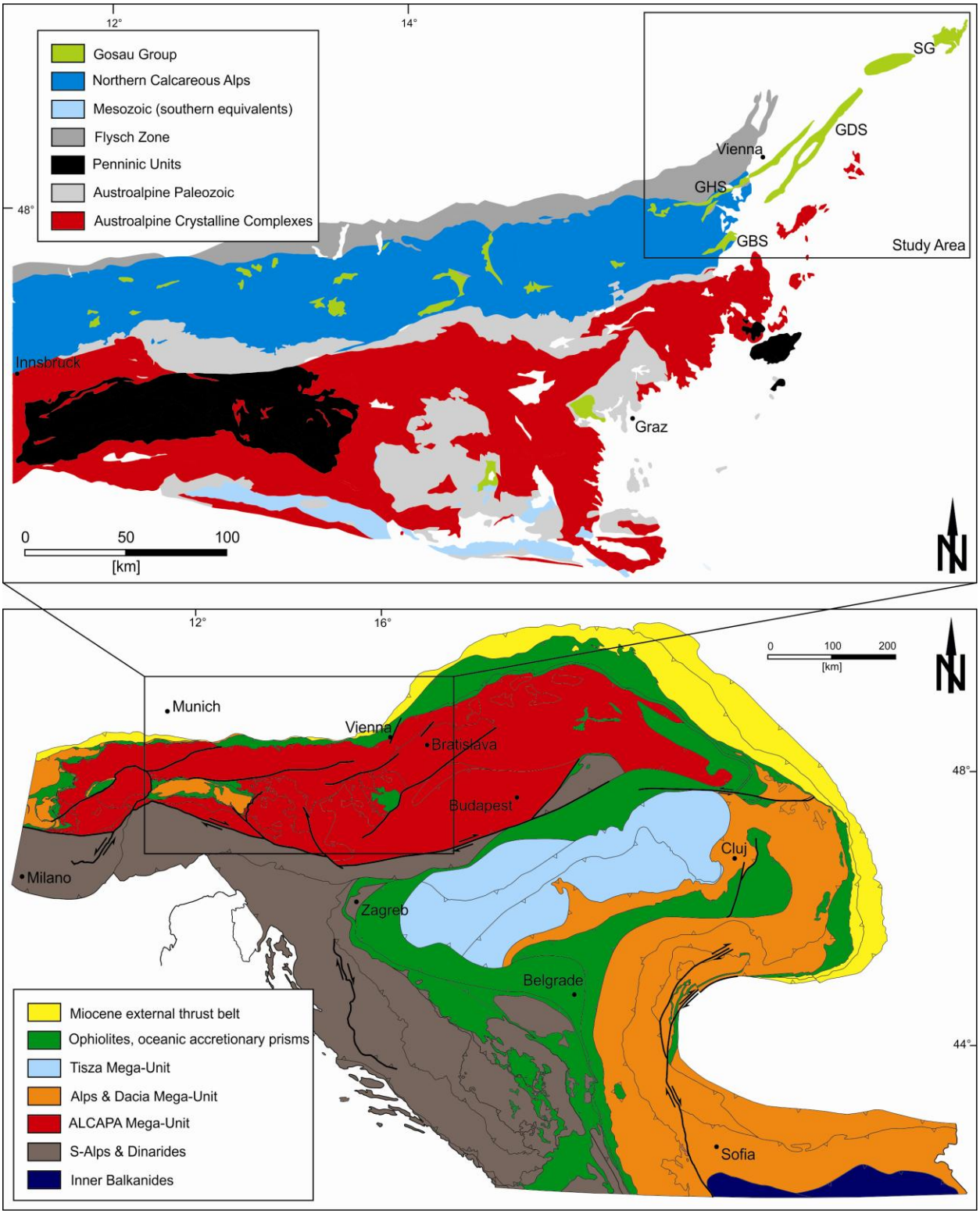


Fig.2.1: Simplified geological map of the Eastern Alps (east of Innsbruck) after Egger et al. (1999) with highlighted study area (upper map) and their location within the Alpine-Carpathian-Dinaridic orogenic system with highlighted major tectonic units of the Alps, Carpathians and Dinarides (lower map) after Schmid et al. (2008). Abbreviations for Gosau basins: GHS: Gießhübl Syncline, GDS: Glinzendorf Syncline, GBS: Grünbach Syncline, SG: Studienka Gosau.

To tackle the main questions on basin correlation and evolution detailed analysis of bulk rock and stable isotope geochemistry, assessment of heavy minerals and chemistry of single heavy minerals from outcrops, drill cores and cuttings of the various Gosau synclines are performed in this PhD thesis. Bulk rock and stable isotope geochemistry of 247 sediment samples are investigated with the aim to evaluate geochemical differences and similarities of the diverse Gosau basins and to reconstruct facies, depositional environment and provenance. Due to the poor outcrop situation of the Grünbach Formation, which is compared to the limnic-marine interval of the Glinzendorf Syncline, an artificial trench was constructed to acquire good reference material. In addition to that, outcrop samples and comprehensive core and cutting material from different boreholes provided a detailed data set. Geochemical indices that are used in literature as indicators and proxies for facies or provenance interpretation are applied and tested. Additionally, the comparability of core and cutting samples (cuttings are prone to various contamination effects) are evaluated and tested.

Evaluation of heavy mineral assemblages and chemical analysis of heavy mineral grains provide a refined provenance concept of that area. Heavy mineral data from literature (Sauer, 1980; Gruber, 1987; Wagreich & Marschalko, 1995) as well as new data (e.g. OMV in-house data) are used to create a detailed review of the heavy mineral development of the various basins. Single grain chemistry (analyzed by electron microprobe) of the dominant heavy minerals garnet, chrome spinel and tourmaline allow precise conclusions of sedimentary provenance. Source areas and sediment transport directions of the different basins are reconstructed and summerized in a general provenance concept.

Bulk rock geochemistry and single grain chemistry of heavy minerals are presented for the first time for the study area.

3. Author´s Comment

Geochemistry data of 16 samples from well Markgrafneusiedl T1 were adopted from the author´s master thesis “Geochemische Untersuchungen an lakustrin-marinen Sedimenten der Bohrung Markgrafneusiedl T1 (Oberkreide, Gosau-Gruppe)” for the sake of data completeness. This data is involved in new analysis, evaluation and interpretation and does not represent duplication or redundant conclusion of parts of the master thesis. Therefore it is not against any ethics in science.

4. Methods

4.1 Calcium carbonate, total sulfur and total organic carbon

Calcium carbonate contents were analyzed using a “Carbonate Bomb” after Müller & Gastner (1971). Total S (TOT/S) and total organic carbon (TOC) were detected by LECO-analysis (detailed description in chapter 5.1.1 and 5.1.3).

4.2 Bulk rock geochemistry

A total of 247 fine-grained sediment samples from 64 outcrop (Maiersdorf, Lilienfeld and Groisbach), 112 drill core (Aderklaa 81, 84, 92, Gänserndorf T3, Glinzendorf T1, Markgrafneusiedl T1, Studienka 83, Závod 57 and 68) and 67 cutting samples (Aderklaa 81, 84, 92, Strasshof T9, Gänserndorf T3, Glinzendorf T1 and Markgrafneusiedl T1) were geochemically analyzed (Fig.4.1). Bulk rock geochemistry of major and trace elements were analyzed by ICP (inductively coupled plasma)- emission/mass spectroscopy (detailed description of sample preparation and methods are given in chapter 5.1.1 and 5.1.3). For the analysis of rare earth elements, ICP-MS was used after leaching a 0.5 g sample in hot (95°C) Aqua Regia. Total S (TOT/S) and total organic carbon (TOC) were detected by LECO-analysis (detailed description in chapter 5.1.1 and 5.1.3). Loss on ignition (LOI) was calculated by weight difference after ignition at 1000°C.

Bulk rock geochemistry of cutting assemblages from the OMV-core sample inventory was performed analogue to core/outcrop samples (see chapter 5.1.1 and 5.1.3). Intervals with relatively high contents of fine-grained sediments (dark grey shales or marls) were selected from washed cuttings. The larger part of visually identified non-shaly components like sandstone or calcite/carbonate fragments were tried to sort out manually. Dependent on particle size and the amount of coarse grains, the samples remained contaminated by sandstone or calcite fragments to some degree (around 1 to 5 %; Fig.4.2). Sorting under the microscope has not been performed. Additionally, four completely unsorted samples (MT1-3649-U, MT1-3870-U, MT1-3975-U and MT1-4055-U) were analysed geochemically to study the influence of perturbing components on geochemistry. A potential contamination product is metallic swarf derived from drill bit. These metallic fragments, which are present in different amounts from sample to sample, were tried to sort out using a magnet. However, residual metallic material is

likely to some degree, which is suggested to affect contents of various metals (Fe, Mn, Cr, etc.) in the geochemical analysis (Fig.4.1). To evaluate the difference of core and cutting samples, only samples from the Gießhübl and Glinzendorf Syncline were compared.

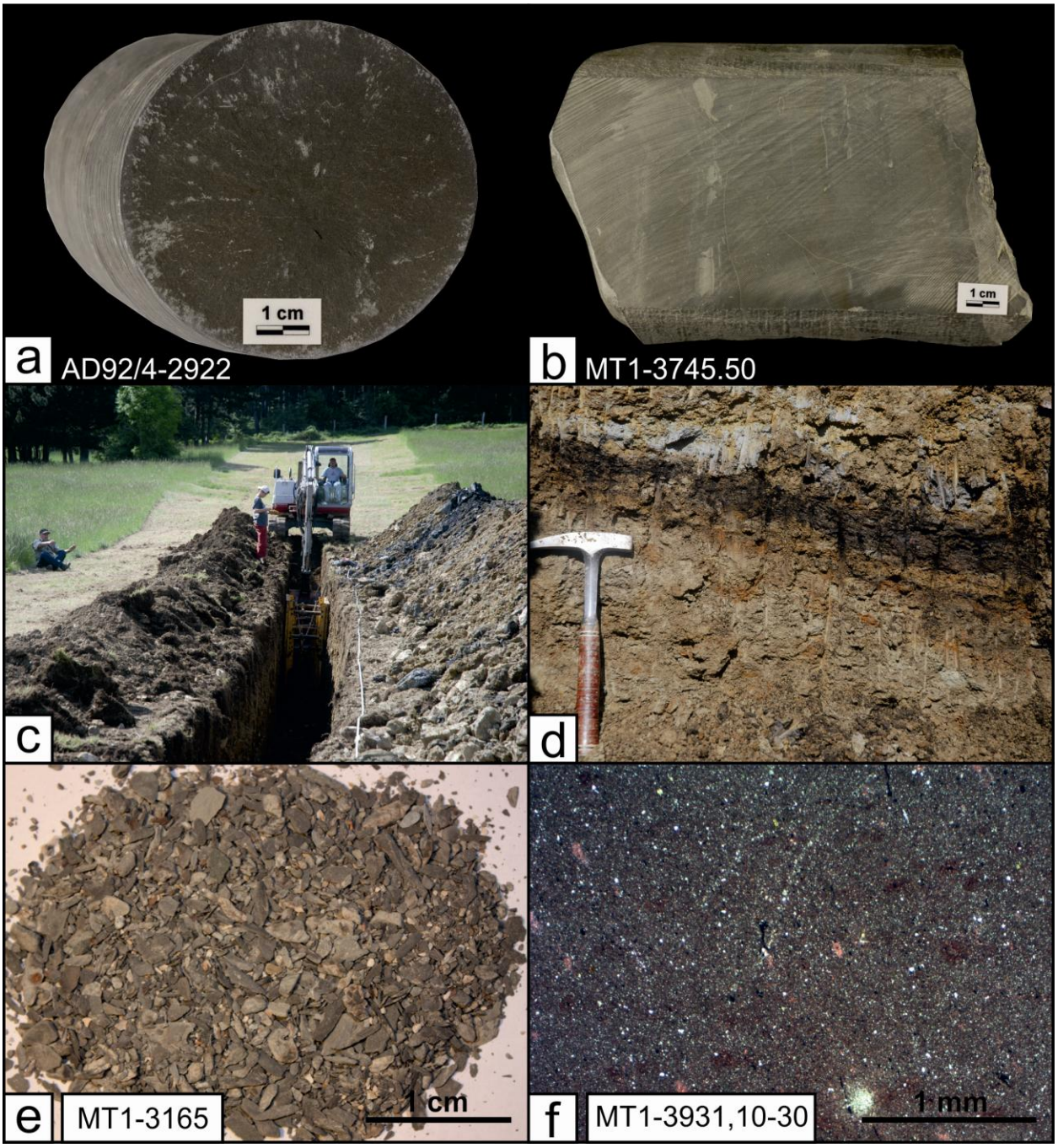


Fig.4.1: a: Example of a fine-clastic drill core sample from the well Aderklaa 92. b: Example of a fine-clastic drill core sample from the well Markgrafneusiedl T1. c: Foto of the artificial trench in Maiersdorf (Grünbach Formation). d: Coal layer from the artificial trench profile in Maiersdorf. e: Example of a cutting sample from the well Markgrafneusiedl T1 before sorting out only fine-clastic chips. f: Example of a thin section from a typically fine-clasic marly drill core sample of the well Markgrafneusiedl T1.

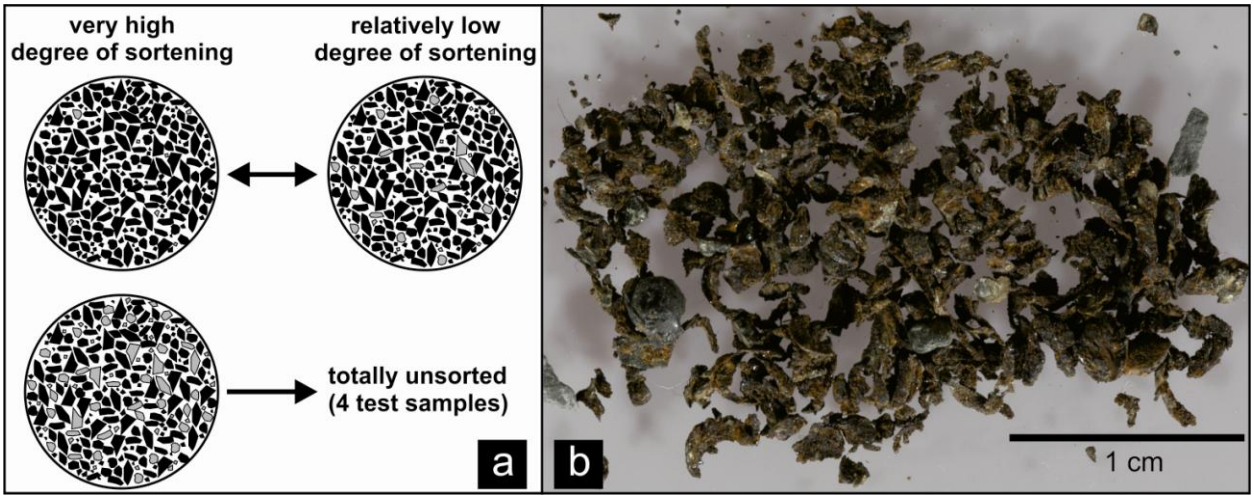


Fig.4.2: a: Schematic figures of cutting samples with maximum and minimum degree of sortening after manual selection and an example for a totally unsorted sample (black chips indicate fine-grained sediment peaces, gray chips indicate coarse-grained sandstone peaces or calcite fragments). b: Metallic swarf (drill dit fragments) sorted out by magnet from a cutting sample of well Markgrafneusiedl T1).

4.3 Stable isotopes

116 fine-grained pelitic outcrop and drill core sediment samples from all Gosau basins were investigated for their stable isotope composition of carbon and oxygen (untreated bulk carbonate) by ThermoFinnigan isotope ratio mass spectrometer at Innsbruck University. The calibration was performed against VPDB calibrated against international reference standards (detailed description of sample preparation and methods are given in chapter 5.1.2).

4.4 X-ray diffraction and cathodoluminiscence

In order to investigate the issue of detrital admixture, 18 samples from different localities were analyzed using powder X-ray diffraction (XRD) to quantify the abundance of dolomite. In addition, several selected thin sections from well Markgrafneusiedl T1 were investigated for cathodoluminiscence (CL) using a cold cathode system (see chapter 5.1.2).

4.5 Heavy minerals

Heavy minerals from the sieve fraction 0.063 to 0.4 mm were separated from 30 silt to sand-sized outcrop (Lilienfeld, Tasshof, Mitterwäldchen, Grünbach, Maiersdorf and Brezová) and drill core (Aderklaa 84, 92, Markgrafneusiedl T1 and Závod 68) sediment samples (detailed description of sample preparation and methods are given in chapter 5.2.1). Element analyses of single heavy mineral grains were carried out using electron microprobe. 1064 measurements on 774 single grains of garnet (263 grains), chrome spinel (269 grains) and tourmaline (242 grains) have been analyzed (detailed description of sample preparation and methods are given in chapter 5.2.1). Heavy mineral data evaluated at the OMV (R. Sauer and W. Hujer) in combination with published data were additionally used for interpretation.

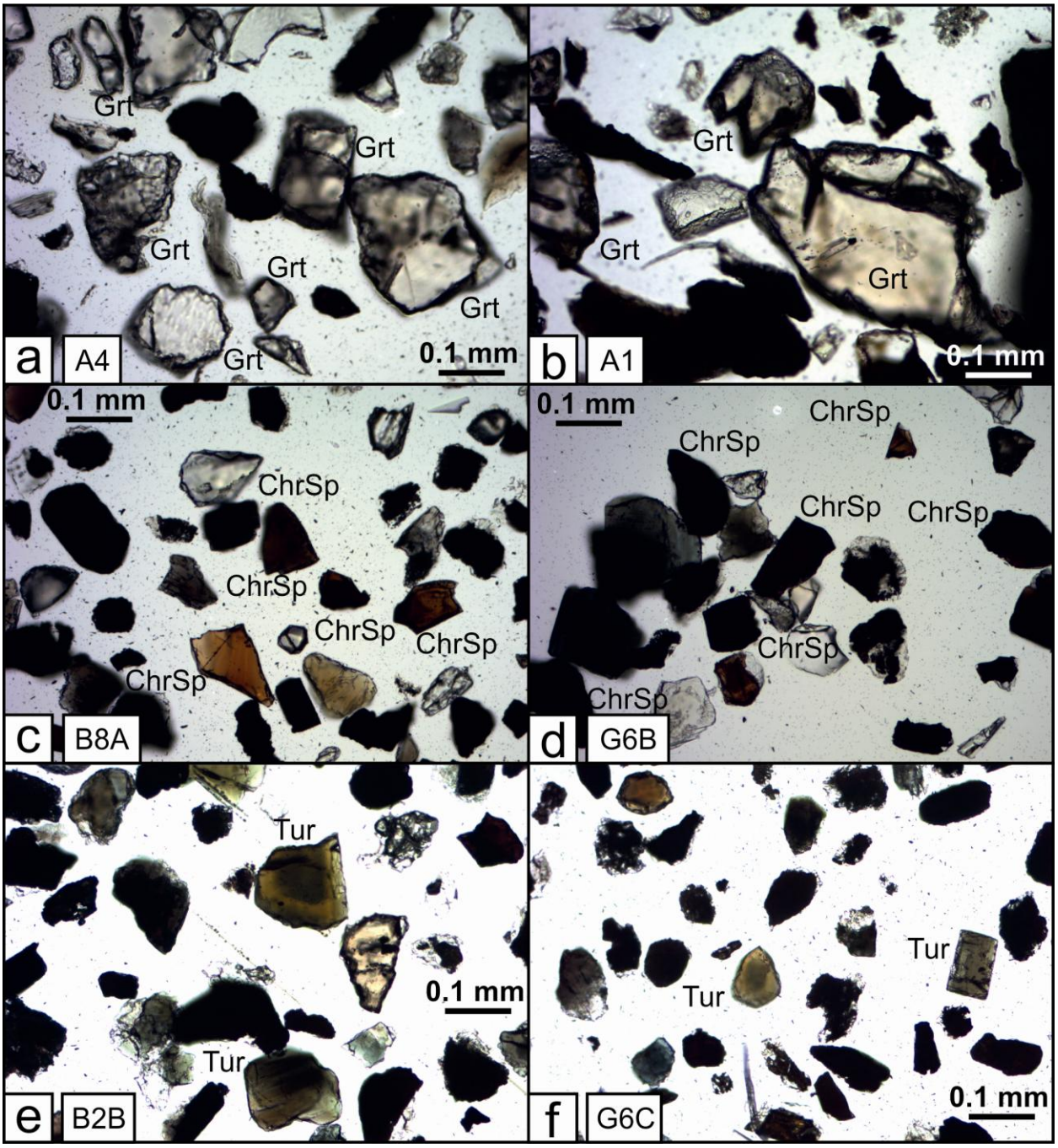


Fig.4.3: a, b: Examples of garnet-rich heavy mineral assemblages of the Gießhübl basin. c, d: Examples of chrome spinel-rich heavy mineral assemblages of the Slovakian Gosau (c) and Grünbach basin (d). e, f: Examples of tourmalines in heavy mineral assemblages of the Slovakian Gosau (e) and Grünbach basin (f).

5. Publications and manuscript

This PhD thesis is a cumulative dissertation and consists of three accepted research papers and one manuscript currently under review. The articles are structured chronologically in order of the date of submission.

5.1 Publications

(1) Hofer, G., Draganits, E., Wagreich, M., Hofmann, C. C., Reischenbacher, D., Grundtner, M. L. & Bottig, M., 2011. Stratigraphy and geochemical characterisation of Upper Cretaceous non-marine – marine cycles (Grünbach Formation, Gosau Group, Austria). Austrian Journal of Earth Sciences 104/2, 90-107.

This paper describes sedimentological and stratigraphical characteristics of the early Campanian Grünbach Formation of the Grünbach Syncline (Gosau Group, Lower Austria). Within an artificial trench profile, five non-marine – marine cycles with an estimated duration of a few 100 kyrs, could be reconstructed by using bulk rock geochemistry, sedimentpetrography and fossil contents.

(2) Hofer, G., Wagreich, M. & Spötl, C., 2013. Carbon, oxygen and strontium isotopes as a tool to decipher marine and non-marine environments: Implications from a case study of cyclic Upper Cretaceous sediments. Geological Society of London, Special Publications: Isotopic Studies in Cretaceous Research 382/1.

This paper investigates stable carbon and oxygen, as well as strontium isotopes of the Gosau Group at the western and eastern border and underneath the Neogene Vienna basin and their applicability as tool to distinguish between marine and non-marine intervals. Marine samples are characterized by significantly higher mean carbon and oxygen isotope values compared to non-marine samples and seem to be reliable tools for the interpretation of paleosalinity.

(3) Hofer, G., Wagreich, M. & Neuhuber, S., 2013. Geochemistry of fine-grained sediments of the Upper Cretaceous to Paleogene Gosau Group (Austria, Slovakia): Implications for paleoenvironmental and provenance studies. Geoscience Frontiers.

This paper discusses comprehensive bulk rock geochemistry data of the study area in terms of paleoenvironmental and provenance reconstruction and evaluation. Main results are constructive applications of paleosalinity proxies (like B/Al*), statistical data assessment by using factor and distriminant analysis, and geochemical provenance analysis.

5.1.1 Stratigraphy and geochemical characterisation of Upper Cretaceous non-marine – marine cycles (Grünbach Formation, Gosau Group, Austria)

Hofer, G., Draganits, E., Wagreich, M., Hofmann, C. C., Reischenbacher, D., Grundtner, M. L. & Bottig, M., 2011. Austrian Journal of Earth Sciences 104/2, 90-107.

Comment of the author concerning the degree of participation
Chapters 3.2, 3.3, 3.4, 4.3, 4.4, 4.5, 5.2, 5.4 and 6 were written by Gerald Hofer. Abstract and chapters 5.3 and 5.5 were written together with other co-authors. Figures 7, 8, 9, 10 and 11 as well as table 1 and appendix B were designed by the author. Gerald Hofer attended sampling and recording of the artificial trench profile, prepared and coordinated sample analysis and interpreted geochemical analysis and general conclusions.
Calcareous nannofossil and palynology data was analyzed and edited by M. Wagreich and C. C. Hofmann.
Maceral analysis of coal particles was analyzed and interpreted by D. Reischenbacher.
Isotope analysis was performed by C. Spötl.

Article structure, numbering and type of quotations are maintained as requested in the journal.

Austrian Journal of Earth Sciences | Volume 104/2 | 90 - 107 | Vienna | 2011

Stratigraphy and geochemical characterisation of Upper Cretaceous non-marine – marine cycles (Grünbach Formation, Gosau Group, Austria)

Gerald HOFER[1*], Erich DRAGANITS[1,2], Michael WAGREICH[1], Christa-Charlotte HOFMANN[3], Doris REISCHENBACHER[4], Marie-Louise GRUNDTNER[1] & Magda BOTTIG[5]

[1] Department of Geodynamics and Sedimentology, University of Vienna, Althanstrasse 14, A-1090 Vienna, Austria;
[2] Department of Prehistoric and Medieval Archaeology, University of Vienna, Franz-Klein-Gasse 1, A-1190 Vienna, Austria;
[3] Department of Palaeontology, University of Vienna, Althanstrasse 14, A-1090 Vienna, Austria;
[4] Department of Applied Geological Sciences and Geophysics, Montanuniversität Leoben, Franz-Joseph-Strasse 18, A-8700 Leoben, Austria;
[5] Geological Survey of Austria, Neulinggasse 38, A-1030 Vienna, Austria;
[*] Corresponding author, gerald.hofer@univie.ac.at

KEYWORDS

Early Campanian
Stable Isotopes
Geochemistry
Gosau Group
Coal cycles
Palynology
Boron

Abstract

Early Campanian non-marine – marine cycles of the Grünbach Formation (Gosau Group, Northern Calcareous Alps, Austria) within the Grünbach Syncline have been investigated using sedimentology, micropaleontology and geochemistry. The succession of the Grünbach Formation comprises clay, marl, siltstone, sandstone as well as rare conglomerate and coal beds deposited in a marginal marine to terrestrial, brackish-limnic environment. Sampling was done from a 45 m section of an artificial trench at Maiersdorf, Lower Austria. Palynological data indicate quite warm and humid depositional conditions. The observation of Nypa pollen represents the northernmost occurrence known so far from the Campanian. Based on geochemical proxies (whole rock geochemistry and bulk carbon and oxygen isotopy) as well as microfossil data, five marine (MC1-5) to non-marine cycles (NC1-5) are reconstructed. Marine intervals were identified basically by the presence of nannofossils and by higher mean $\delta^{13}C$ ratios (-4.51 VPDB), boron contents (mean 165.8 ppm) and B/Al* ratios (mean 167.2) compared to sections interpreted as non-marine (mean $\delta^{13}C$: -6.34 VPDB, B: 139.0 ppm, B/Al*: 149.4). A statistically significant differentiation between marine and non-marine samples is possible using the aluminium-normalized boron ratio and, to a lower degree, the absolute boron values. A duration of a few 100 kyrs is estimated for single non-marine – marine cycles. Low subsidence rates and uniform provenance data argue against a purely tectonic origin of the cycles and are in favor for a mainly climatic control of these transgressive-regressive cycles in the Early Campanian.

Nichtmarin-marine Zyklen im Frühen Campanium der Grünbach-Formation (Gosau-Gruppe, Nördliche Kalkalpen, Österreich) innerhalb der Grünbach-Synklinale wurden mit Hilfe sedimentologischer, mikropaläontologischer und geochemischer Methoden untersucht. Die Abfolge setzt sich aus Tonen, Mergeln, Siltsteinen, Sandsteinen sowie seltener aus Konglomeraten und Kohlelagen zusammen und wurde in einem randmarinen bis terrestrischen Milieu abgelagert. Die Beprobung wurde an einem 45 m mächtigen Profil in einem Schurfgraben bei Maiersdorf (Niederösterreich) durchgeführt. Auf der Grundlage von geochemischen Parametern (Gesamtgesteinschemie und stabile Isotopen des Gesamtgesteins) sowie mikropaläontologischen Daten wurden 5 marine (MC1-5) und nicht-marine (NC1-5) Zyklen rekonstruiert. Marine Intervalle wurden vor allem durch das Auftreten von Nannofossilien identifiziert und sind charakterisiert durch höhere mittlere $\delta^{13}C$ Verhältnisse (-4.51 VPDB), Borgehalte (Mittelwert 165.8 ppm) und B/Al* Verhältnisse (Mittelwert 167.2) im Vergleich zu nicht-marinen Abschnitten (Mittelwert $\delta^{13}C$: -6.34 VPDB, B: 139.0 ppm, B/Al*: 149.4). Eine statistisch signifikante Unterscheidung zwischen marinen und nicht-marinen Proben ist mit Hilfe der Aluminium-normalisierten Borgehalte möglich und, in einem geringeren Maß, mit den absoluten Borgehalten. Die Zeitdauer einzelner marin – nicht-mariner Zyklen wird auf mehrere hunderttausend Jahre geschätzt. Geringe Absenkungsraten und einheitliche Materialherkunft sprechen gegen eine ausschließlich tektonische Kontrolle der Zyklen und weisen eher auf eine klimatische Beeinflussung dieser trangressiv-regressiven Zyklen im Frühen Campanium hin.

1. Introduction

The Cretaceous, especially the mid-Cretaceous, constitutes the last long greenhouse phase of the Earth, characterized by high temperatures and a relatively equable climate. Late Cretaceous times were characterized by the long-term change from the mid-Cretaceous super-greenhouse mode to the Cenozoic icehouse mode of the Earth climate system (e.g., Norris et al., 2002; Forster et al., 2007). Short-term climatic and environmental cycles and events become increasingly recognized during this previously inferred equable warm period of the Cretaceous (e.g., Jenkyns, 2003; Miller et al., 2005a,b, 2008; Wagreich et al., 2011).

Cyclic sea-level changes in the third- to fourth-order time frame are one expression of rapid climate changes, especially during glacial episodes in Earth history (e.g. Ordovician, Carboniferous and Pleistocene) controlled by waning and waxing ice sheets. Recently, also during the Cretaceous such rapid fluctuations of sea-level have been recognized (e.g. Miller et al., 2005a,b; Bornemann et al., 2008).

Gerald HOFER, Erich DRAGANITS, Michael WAGREICH, Christa-Charlotte HOFMANN, Doris REISCHENBACHER, Marie-Louise GRUNDTNER & Magda BÖTTIG

A critical depositional record for the recognition of sea-level cycles constitutes marginal marine and marine to non-marine cyclic archives including coal cycles (McCabe and Parrish, 1992). We describe a cyclic non-marine – marine record from the Upper Cretaceous Gosau Group of the Northern Calcareous Alps of Austria. The principal aim of the paper is the recognition and definition of the cyclic record by using sedimentological features, geochemical proxies and the microfossil record. Cycles are then discussed in terms of eustatic versus regional tectonic control.

2. Geological setting

The Upper Cretaceous-Eocene Gosau Group was deposited unconformably onto folded and faulted Permo-Triassic sediments of the Northern Calcareous Alps (NCA) (Wagreich and Decker, 2001). Widespread erosion and the formation of karst bauxites evidence subaerial exposure before the deposition of the Gosau sediments (Wagreich and Faupl, 1994). Basin analysis indicates a division into a Lower Gosau Subgroup (Upper Turonian to Campanian) with diachronous deposition of continental to shallow marine sediments in only partly connected, fault bounded basins, and an Upper Gosau Subgroup (Santonian/Campanian to Eocene) comprising deep-water sediments (Wagreich, 1993; Wagreich and Faupl, 1994).

This study investigates Early Campanian terrestrial-marine cycles in one of the easternmost Gosau Group occurrences in the NCA (Fig. 1). The Gosau Group of the Grünbach Syncline (Upper Cretaceous to Paleogene) crops out in a ca. 15 km long, mainly SW-NE oriented syncline at the transition from the NCA to the southern part of the Vienna Basin, tectonically positioned on southern (higher) tectonic units of the NCA (Plöchinger, 1961). Lithologically the syncline comprises terrestrial conglomerates, sandstones and shallow marine limestones at the base, followed by a siliciclastic succession with up to eight major coal horizons, succeeded by deeper water sandstones, shales, and marls (Plöchinger, 1961; Sachsenhofer, 1987; Summesberger et al., 2007). The total thickness is around 1200 m (Plöchinger, 1961) with a stratigraphic range from the Late Santonian to Paleocene (Summesberger et al., 2007) (Fig. 2).

The general structure of the Grünbach Gosau is a non-cylindrical, tight, inclined, parallel fold, which can be divided into two parts, based on its structures. In the western part the strike of the syncline is more or less W-E with axial surfaces dipping around 60° towards North, while in the eastern part the syncline strikes SW-NE with axial surfaces dipping towards southeast around 60° (Plöchinger, 1961).

2.1 Age of the Grünbach Formation

The lithostratigraphy and biostratigraphy of the Gosau Group of the Grünbach Syncline has recently been summarized by Summesberger (1997) and Summesberger et al. (2000, 2002, 2007) indicating deposition of the whole group between the Late Santonian and Paleocene. A latest Santonian to earliest Campanian older age limit of the Grünbach Formation, which is studied here, is constrained by the ammonite *Placenticeras polyposis* (Dujardin) and the inoceramid bivalve *Cordicera-*

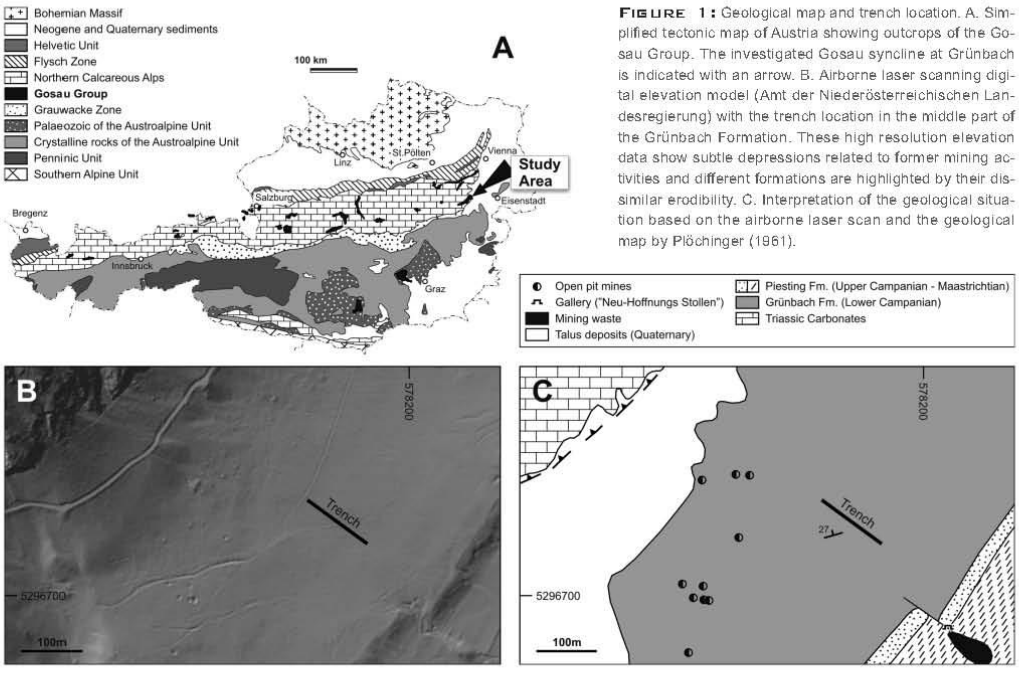


Figure 1: Geological map and trench location. A. Simplified tectonic map of Austria showing outcrops of the Gosau Group. The investigated Gosau syncline at Grünbach is indicated with an arrow. B. Airborne laser scanning digital elevation model (Amt der Niederösterreichischen Landesregierung) with the trench location in the middle part of the Grünbach Formation. These high resolution elevation data show subtle depressions related to former mining activities and different formations are highlighted by their dissimilar erodibility. C. Interpretation of the geological situation based on the airborne laser scan and the geological map by Plöchinger (1961).

mus muelleri Petrascheck from the upper part of the underlying fully marine Maiersdorf Formation (Summesberger et al., 2000). This age is further supported by nannofossils including *Marthasterites furcatus* and *Calculites* cf. *obscurus* (nannofossil standard zone CC16-17; see Summesberger et al., 2002) and a $^{87}Sr/^{86}Sr$ value of 0.707480, indicating an age of 83.3 ± 0.5 Ma, i.e. around the Santonian/Campanian boundary (Scharbert in Summesberger et al., 2002). The Late Campanian younger age limit is constrained by the bivalves *Trochoceramus* cf. *morgani* (Sornay) and *Trochoceramus* cf. *dobrovi* Pavlova (Summesberger et al., 2002) and nannofossil data (CC18-22) in lower parts of the overlying Piesting Formation (Summesberger et al., 2002) and by orbitoids from the base of the Piesting Formation (Plöchinger, 1961, 1967).

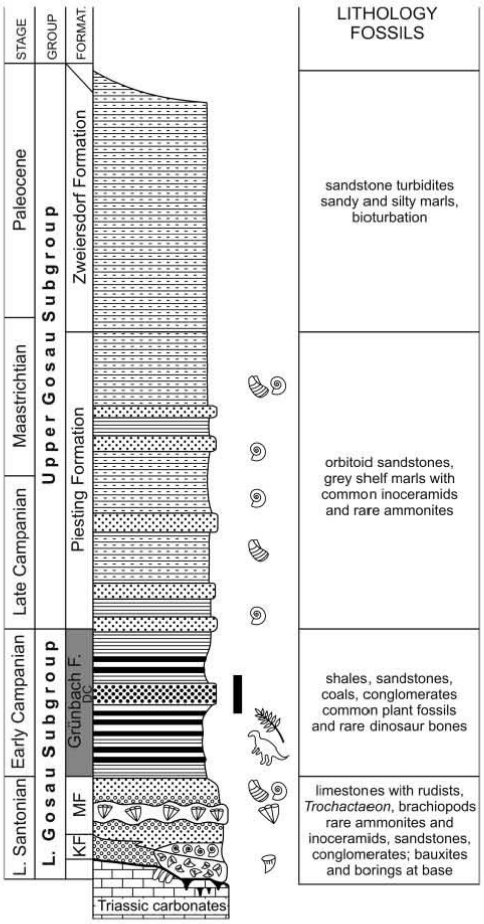


Figure 2: Composite stratigraphy of the Gosau Group of the Grünbach Syncline from Piesting to Grünbach (modified after Summesberger et al., 2002, 2007). Thick vertical line to the right of the section indicates the approximate stratigraphic position of the investigated sediments of the trench at Maiersdorf. Abbreviations: KF - Kreuzgraben Formation, MF - Maiersdorf Formation, DC - Dreistetten conglomerate.

3. Materials and methods

Between 1823 and 1965 the Grünbach Syncline has been well-exposed by huge underground and open pit coal mining (Kreiner, 1994) with mining activity down to 1200 m below surface. At present, the outcrop condition worsened dramatically due to the easily weathering lithologies, high precipitation and recultivation. Due to the virtual lack of outcrops and well data in the area of the Grünbach Gosau an artificial trench was dug to expose the coal-bearing cycles. The trench location has been selected based on a compilation of existing literature, geological maps, mining plans and sections in the archives of the Austrian Geological Survey and their integration into a GIS project (Fig. 1).

Excavation and documentation of the up to 4 m deep trench has been carried out between 25 and 28 May 2010 in the cadastre municipality of Grünbach, on a meadow owned by the Agrargemeinschaft Maiersdorf (cadastral register number 845/1) (Fig. 1). The excavation of the trench is oriented perpendicular to the strike of the syncline and started in the Southeast within the overturned limb of the syncline, progressing up-hill towards older strata of the Lower Campanian Grünbach Formation (Fig. 1). Due to the high instability of the trench faces, the trench had to be back-filled immediately after documentation. In total a 141 m long trench has been excavated, exposing almost 45 m of the Lower Campanian Grünbach Formation (Fig. 3).

3.1 Sedimentology

The sedimentology of the trench section was investigated during trench exposure using standard field logging methods, including grain size estimates, bedding and structure identification complemented by thin section analysis from sandstone and conglomerate beds. In total 92 rock samples have been collected for further analyses; they are housed in the sample archive of the Department of Geodynamics and Sedimentology, University of Vienna (for analyzed samples see Online Appendix B). Samples of the trench have been taken between 4 m to 1.5 m below grassroots.

3.2 Calcium carbonate and total organic carbon content

The calcium carbonate content from 55 samples was analyzed using the "Carbonate Bomb" (after Müller and Gastner, 1971) at the University of Vienna. An absolute error of 1% $CaCO_3$ is given for this method.

Fifty samples were measured for total organic carbon (TOC) with carbon analyzers LECO C200 and LECO RC-412 after dissolving the carbonate with diluted hydrochloric acid (for LECO C200) or measuring at 550°C (LECO RC-412) at the University of Vienna. The accuracy of the measurements is around 0.1%.

3.3 Whole-rock geochemistry

Thirty-seven fine-grained sediments such as shales, marls and some siltstones were used for the geochemical bulk rock analysis. The chemical analysis was done by the AcmeLabs (Acme Analytical Laboratories Ltd., www.acmelab.com) in Van-

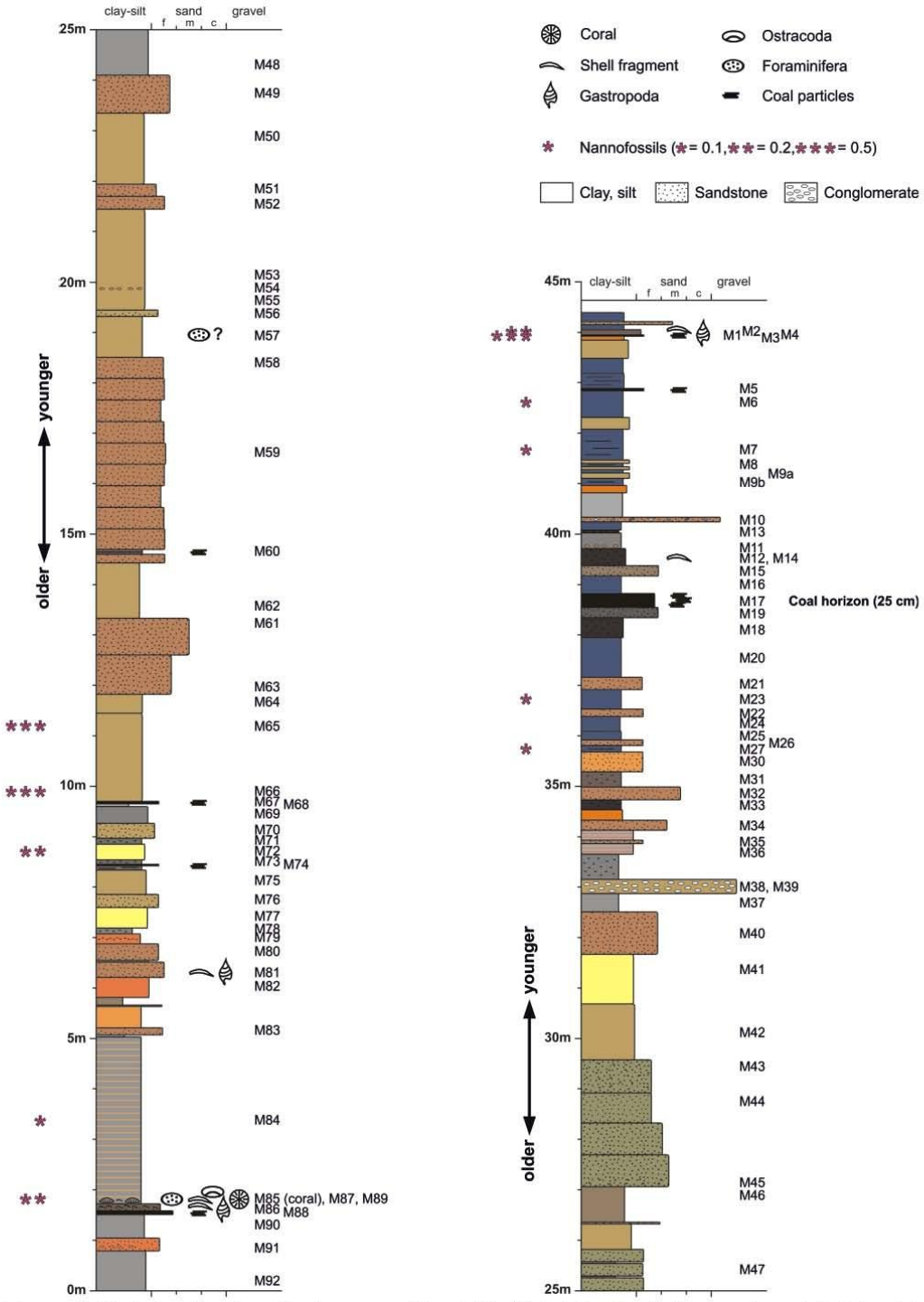


Figure 3: Lithostratigraphic section and fossil occurrences of the part of the Grünbach Formation which has been documented in the trench at Maiersdorf (see Figure 1 for location). Bed colours broadly correspond to the rock colours in the field; M1 to M92 are sample numbers.

couver (Canada).

Oxides (SiO_2, Al_2O_3, Fe_2O_3, MgO, CaO, Na_2O, K_2O, TiO_2, P_2O_5, MnO and Cr_2O_3) and some minor elements (Ba, Be, Co, Cs, Ga, Hf, Nb, Ni, Rb, Sn, Sr, Ta, Th, U, V, W and Zr) as well as the loss on ignition (LOI) were detected by ICP-emission spectroscopy. For the analysis of trace elements (REE: Sc, Y, La, Ce, Pr, Nd, Sm, Eu, Gd, Tb, Dy, Ho, Er, Tm, Yb and Lu; noble and base metals: Mo, Cu, Pb, Zn, Ni, As, Cd, Sb, Bi, Ag, Au, Hg, Tl and Se) ICP-mass spectroscopy was used. For accuracy, precision and detection limits of these analyses see www.acmelab.com.

Major and trace elements are prevalently used as proxies for the interpretation of paleoenvironments. Boron accumulating in (marine) water is attached in clay minerals (mostly in illites) as well as organic substances and remains relatively immobile. Marine sediments are commonly characterised by higher boron concentrations compared to non-marine sediments. Consequently, boron content is commonly used as a paleosalinity indicator (Ernst, 1966; Heling, 1967; Selter et al., 1989, Rügner, 2000). Unfortunately, grain size and source area of the clays can have additional effects on the boron concentration (Dominik and Stanley, 1993). To reduce these of different grain size and mineralogy, boron contents are normalized to aluminium (multiplied with a factor of 100.000 to get natural numbers). This ratio (B/Al*100.000) is used as B/Al* in the following text.

Discriminant function analysis using major elements to determine provenance signatures is applied to the data set (Roser and Korsch, 1988). Other geochemical indices used include U/Th and TOC/S ratios as well as the chemical index of alteration (CIA) and the chemical proxy of alteration (CPA). The TOC is often used in combination with sulphur (TOC/S-ratio) to infer palaeosalinity of sediments, especially when they are organic rich (Sageman and Lyons, 2004). Generally non-marine sediments are characterised by higher TOC/S-ratios than marine samples with similar TOC contents (Berner and Raiswell, 1984). The chemical index of alteration (CIA) expressed as the molar volumes of $[Al_2O_3 / (Al_2O_3 + CaO^* + Na_2O + K_2O)] \times 100$, where CaO* represents the CaO only from the silicate fraction (Nesbitt and Young, 1982, 1989) can be used as a tool for paleoweathering reconstructions (Fedo et al., 1997; Yan et al., 2010). As the samples contain some carbonate, as an approximation, the CaO* is assumed to be equivalent to Na_2O (McLennan, 1993). To avoid errors derived from the unknown CaO content of the silicate fraction, the CPA (chemical proxy of alteration) after Buggle et al., 2011 (or CIW´- chemical index of weathering after Cullers, 2000) is additionally used: $CPA = 100 \times Al_2O_3 / (Al_2O_3 + Na_2O)$.

Cr/Ni- and (Cr/V)/(Y/Ni)-ratios (Garver et al., 1996, and McLennan et al., 1993) are used to indicate ultramafic detritus (ophiolitic input) in provenance studies.

3.4 Bulk carbon and oxygen isotope contents

Stable isotope ratios of carbon and oxygen from 33 samples were analyzed from carbonate bulk (0.1 to 0.3 mg of untreated sample) with a mass spectrometer (on-line preparation using a Gasbench II interfaced to a ThermoFinnigan CF-IRMS) at the University of Innsbruck using the classical phosphoric reaction. The calibration was performed against VPDB with an in-house marble standard standardized against the international reference standard NBS 19. An analytical error (1 s.d.) of 0.06 respectively 0.08 permil for $\delta^{13}C$ and $\delta^{18}O$ based on the long-term performance of quality assurance material is denoted. The results are given in the usual delta notation (for details see Spötl and Vennemann, 2003).

The carbon and oxygen isotopy in carbonates basically depends on the isotopic composition of the water (respectively salinity) from which the carbonate precipitates and to some degree on temperature (Hudson, 1977). Non-marine carbonates are characterised by distinct lower $\delta^{13}C$ and $\delta^{18}O$-values than marine carbonates – that means that they are enriched in the lighter isotopes. Therefore, carbon isotopes are widely used in combination with oxygen isotopy to interpret the genesis and facies (paleoenvironment, paleosalinity, thermometry, etc.) of sediments (Clayton and Degens, 1959; Hudson, 1977; Veizer, 1983; Talbot, 1990, Reinhardt et al., 2003). The statistic evaluation and analysis of the geochemical and isotopic data were done using the software package IBM SPSS Statistics 19.

3.6 Maceral analysis of coal particles

One coal and four clay samples containing coaly particles (M1a, M5, M8A, M14, M17; see Fig. 3 for stratigraphic position) were investigated for maceral composition. Maceral analysis was performed by a single-scan method (Taylor et al., 1998) with a Leica MPV microscope using reflected white and fluorescent light. A maximum of 300 points was counted and the results are given in Online Appendix A. Vitrinite and inertinite macerals were classified according to the nomenclature proposed by ICCP (1998) and ICCP (2001). Vitrinite reflectance of samples was determined following established procedures (Taylor et al., 1998).

3.7 Palynology

Sample preparation for (terrestrial) palynomorphs followed standard procedures: The samples were crushed with a mortar and pestle, and the resultant rock powder treated with standard wet chemical processes using HCl and HF. In order to retain palynomorphs smaller than 10µ the organic extract was not sieved. Instead it was acetolyzed and mixed with glycerine and stored in small glass bottles. For examination under the LM, a drop of well-mixed extract was evenly distributed on a glass slide. For each sample 12 slides were carefully screened to yield both common and accessorial taxa, which occur in small numbers or only as single specimen. For LM photography (Nikon Coolpix) the investigated pollen grains were transferred via glycerine onto a glass slide. For further examination under the SEM (Jeol 6400 and FEI Inspect 500), the pollen grains were moved to a SEM stub, carefully washed with 100% alcohol to remove the glycerine and sputter coated

with gold. Stubs are stored in the Department of Palaeontology, University of Vienna.

3.8 Calcareous nannofossils

Fourty-seven samples of fine-grained sediments were studied using calcareous nannofossil content, applying standard smear slide techniques (e.g., Burnett, 1998). Samples were examined under the light microscope (1000x magnification) for judging the presence and estimating relative abundance of nannofossils (nannofossil specimen per field of view (pfv), using an arbitrary numerical scale by dividing the number of specimens by the number of field(s) of view, i.e. 1 specimen per 5 fields of views gives 1/5 = 0.2 pfv). Additional 22 nannofossil samples were taken from the successions below and above the trench for biostratigraphic evaluation.

4. Results

4.1 Lithostratigraphy

The sediments in the trench are overturned due to folding with an average orientation of 346/24 of the bedding surfaces (Figs. 4A, 5). Only few brittle faults have been observed in the trench (Fig. 4B). They show only small displacements and probably accommodate rheological differences of the diverse bed lithologies. Additionally competent beds within less competent sediments in several examples develop pronounced boudinage structures, which certainly influence the reconstruction of bed thicknesses.

The excavated section exposes only a part of the Lower Campanian Grünbach Formation. Neither the contacts to the Maiersdorf Formation below, nor to the Piesting Formation above have been unearthed (Fig. 2). Figure 1 shows the trench location in the middle part of the Grünbach Formation. The horizontal distance from the respective endpoints to the underlying Maiersdorf Formation and the overlying Piesting Formation is in both directions approximately equal to the trench length (141 m). In the trench almost 45 m lithostratigraphy has been recorded and thus similar thicknesses might be expected for the unexposed sediments of the Grünbach Formation in the hanging wall and foot wall of the trench.

4.2 Sedimentology

The exposed Gosau sediments comprise clay, marl, siltstone, sandstone with rare conglomerate and coal (Figs. 3, 5, 6; see Summesberger et al., 2002). Seven thin, black, organic rich beds have been documented. According to the maceral analyses, however, only one real coal horizon (M17) does exist whereas the others comprise mainly allochthonous accumulation of coal (see Fig. 3).

The exposed section starts with clay (M92, M90), intercalated with a sandstone bed (Fig. 3). Above follows a thin horizon with allochthonous accumulation of coal (M88), directly overlain by a conspicuous brownish limestone which is extremely rich in the green algae *Munieria* sp., indicating fresh-water to brackish environments (Schlagintweit and Wagreich, 1992; Rákosi and

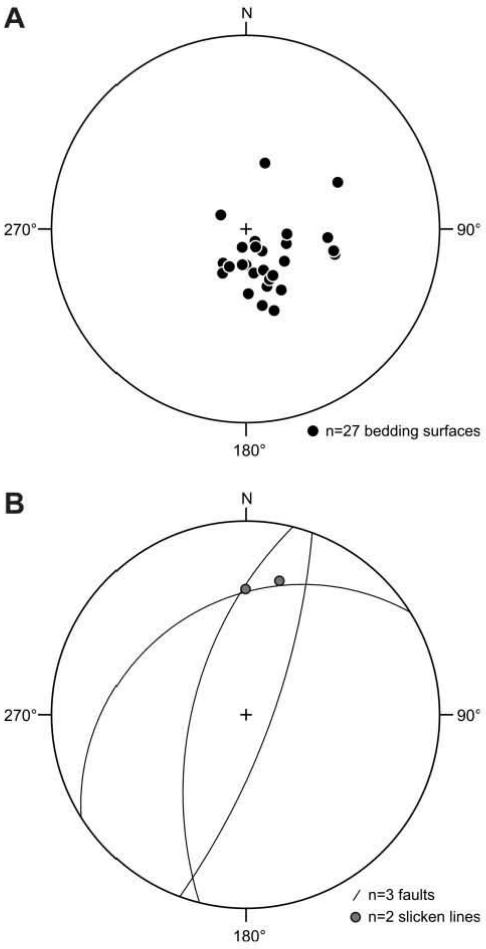


Figure 4: A. Orientation of bedding surfaces exposed in the investigated trench. The bedding surfaces are overturned due to folding with an average orientation of 346/24. B. Fault surfaces and slicken lines exposed in the investigated trench. Faults have been documented at trench running meters 61m, 70.5m and 128.2m. The displacements are generally small and probably result from competence contrasts of different beds during folding. Both plots equal angle projection, lower hemisphere.

Barbacka, 1999/2000) thin-section in Figure 6A). This noticeable limestone additionally contains shell fragments and is succeeded by a thick argillaceous marl layer with marine ostracods, foraminifera and several solitary corals (*Cyclolites* sp., Hannes Loeser, pers. comm. 2010) (Fig. 5B) in life position at its base, confirming the overturned orientation of the beds in the trench.

Above, about 5 m thick alternations of relatively thin marl and sandstone beds with some nannofossils documented in the upper part are present. One of these beds (M81) contains shell fragments and two thin horizons with allochthonous accumulations of coal (M74, M67). In general, the fine grained

beds within the first 10 m show higher carbonate contents compared to similar sediments higher up in the section.

The next 20 m (M65-M43) are dominated by relatively thick sandstone beds interrupted by beds of relatively thick clay and calcareous clays. Brownish colours dominate in both, fine-grained and sand-sized sediments, changing to greenish colours between 25-30 m of the section. Nannofossils in this interval are restricted to the lowermost beds and only one very thin horizon with allochthonous accumulation of coal has been observed. The marl bed M57 contains two fragments of abraded miliolid foraminifera.

Then 2 m of clay (M42-M41) are followed by a some 5 meters thick alternation of relatively thin beds of clay, calcareous clay and sandstone, including two polymict conglomerate layers (M38, M39) (Fig. 3). The fine-grained beds in this part change from brownish to yellowish colours to gradually darker gray.

The final 8 m of the section are dominated by medium to dark gray carbonaceous clay and calcareous clay and three beds with allochthonous accumulations of coal. One of these has a thickness of 25 cm and counts as real coal as indicated by organic petrology (M17, see Online Appendix A). This interval contains several layers with nannofossils and two horizons with shell fragments divided by non-marine clays (Fig. 3).

4.3 Calcium carbonate and total organic carbon content

The calcium carbonate contents of the samples from the trench range from 0 (coaly samples) to 78% with a mean of 22% (Fig. 7, Online Appendix B).

High amounts of TOC correlate with coal and layers with allochthonous accumulations of coal (between 21 and 34% for the samples M1, M5, M67, M74 and M88) up to 52.8% (M17). Moderate TOC contents up to 12% can be seen for many samples (Fig. 7). Shales and marls without visible plant fragments or coal seams have typically TOC contents between 0.05 and 12.05. High sulphur contents of coals and layers with allochthonous accumulation of coal from the trench (e.g. M17, M1, M5, M7) may indicate brackish-marine influence. According to Sachsenhofer (1987 and personal communication 2010) the coals of the eastern part (Piesting, Maiersdorf) of the syncline generally show higher sulphur contents than those of the western part (Grünbach) and are therefore regarded as reworked into the marine intervals (Sachsenhofer, personal communication 2010).

4.4 Whole-rock geochemistry

Results are summarized in Figure 7 and listed in Online Ap-

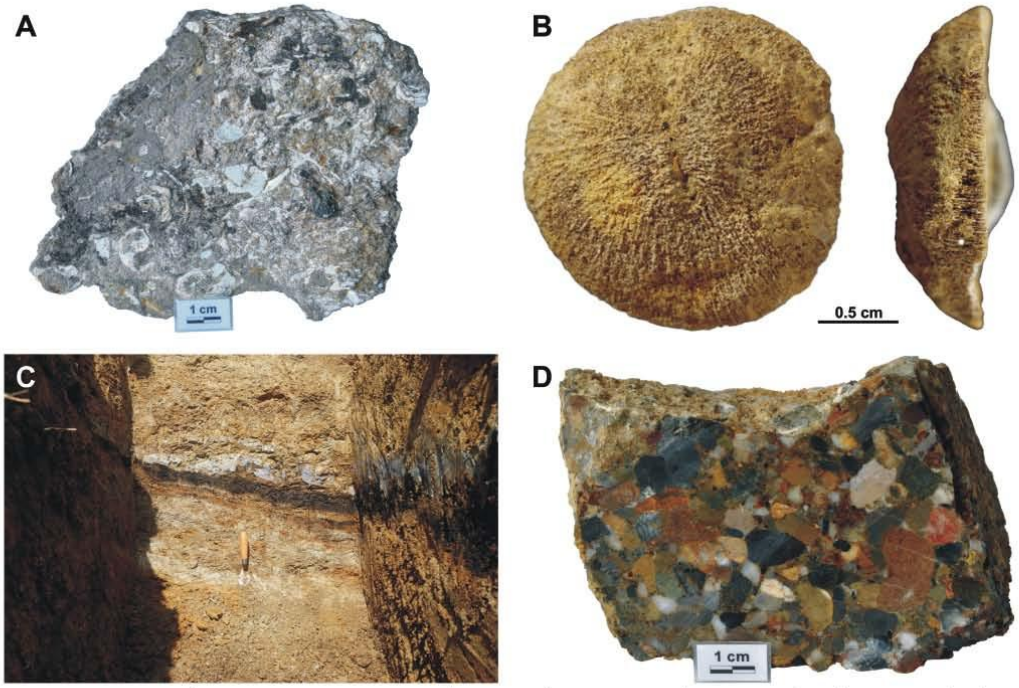


Figure 5: Examples of lithologies documented in the trench (see Figure 3 for samples location). A. Bedding surface of the limestone (M86) with shell fragments. B. Very well preserved solitary coral *Cyclolites* sp. (M85) from directly above the coal layer of M88. C. Typical trench exposure showing the interval at the coal bearing bed M67 and the fine grained beds immediately above and below dipping in overturned orientation at c. 25 degrees towards the NNW. D. Polymict conglomerate (M38) dominated by carbonate clasts from the Northern Calcareous Alps, interpreted to correlate with Dreistetten conglomerate further to the east of the syncline.

pendix B. Samples are generally characterised by relatively high boron concentrations (up to 272 ppm) with a mean of 149 ppm (st.dev.= 41.7) and show a trend from lower to higher values from bottom to top. Only 4 samples have typical non-marine values (between 62 and 89 ppm) which correspond exactly to the coaly horizons (M60, M67, M74 and M88) in the lower part of the profile. Samples from coaly layers in the upper part show shifts to lower boron contents but typical non-marine values (at least under 100ppm) are missing. In the lowermost 10 meters the boron values fluctuate strongly from layer to layer (between 62 and 190 ppm). The middle section between 10 and 35 meters is relatively uniform with boron contents at around 140 ppm. The uppermost 10 meters of the profile are characterised by higher mean values of around 180 ppm and a higher degree of variation including the maximum value of 272 ppm for sample M9B (Fig. 7).

The B/Al* curve shows strong similarities to the boron curve with a mean ratio of 206 (st.dev.= 210.9). While in the lower part of the profile shifts to lower ratios within coaly beds are characteristic, the coaly samples at the top show an extremely high ratio (up to more than 1365), highlighting geochemical differences of the coals respectively coaly sediments in the lower and upper part (Fig. 7).

Th/U ratios alternate between 0.35 and 5.00 (mean=3.19) at which uranium is relative to thorium enriched in mud and organic matter resulting in low Th/U ratios for coaly samples. The lowest ratio of 0.35 (and the highest TOC of 52.8%) is represented by the "real" coal sample M-17 (Fig. 7).

The CIA values are all quite uniform and range between 73.4 and 83.0 with a mean of 76.3 (Figs. 7, 8). The CPA values also have a relatively small range between 92.7 and 98.1 and show similar trends compared to the CIA, which results in a strong positive correlation (r=0.866) (Fig. 7).

Chromium and nickel contents are rather low: chromium concentrations are not higher than 155 ppm (mean=100.8), nickel values range between 5 and 97 ppm with a mean of 53.0 (Fig. 9A).

Cr/V and Y/Ni ratios are uniform and low, between 0.21 and 0.97 (mean=0.68) respectively between 0.29 and 4.73 (mean= 0.65) (Fig. 9B).

The discriminant function plots (after Roser and Korsch, 1988) do not indicate clear results (Fig. 10). The samples cluster around the intersection of the source end members "mafic" (coaly samples are related to this section), "intermediate", "felsic" and "quartzose".

4.5 Bulk carbon and oxygen isotope contents

$\delta^{13}C$ ratios fluctuate between -9.3 and 0.3 ‰ VPDB and with a mean of -5.2 ‰ they are comparatively low. Similar to the boron concentrations a lowermost part with highly variable ratios (most of the extreme low values at around -8 ‰ as well as the maximum value is within these lower 11 meters) and a relatively constant middle interval between 11 and 35 meters (mean around -6.7 ‰) can be observed. At around 33 m the

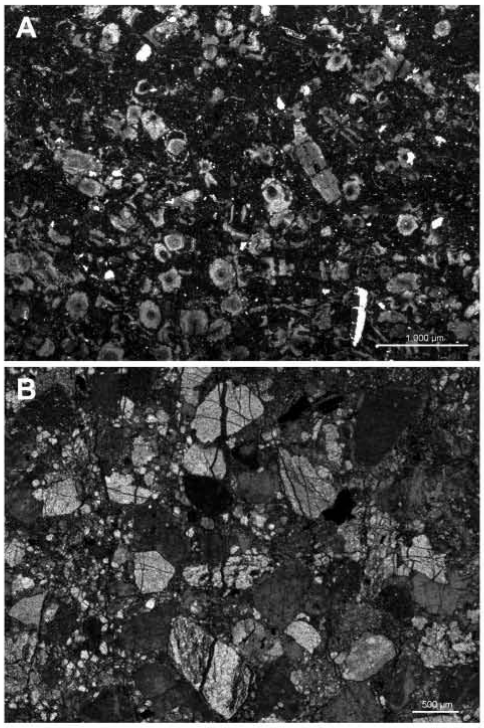


Figure 6: Thin-sections. A. Limestone (M86) with abundant alga *Muneria* sp. B. Medium to coarse grained sandstone (M15) dominated by subangular quartz and rounded carbonate clasts.

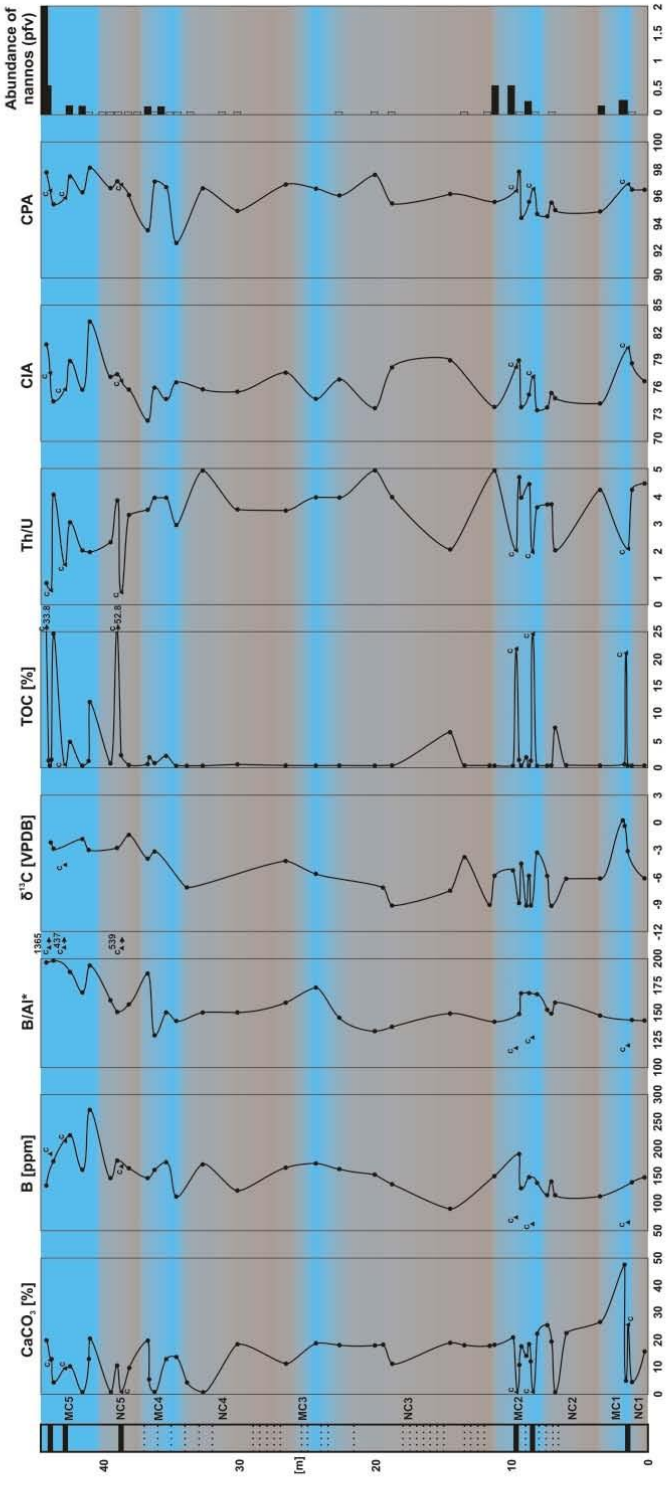
$\delta^{13}C$ isotopy increases to mean values of about -3 ‰ with the highest value up to -1.42 ‰ of this top section between 35 and 44.5 meters (Fig. 7).

$\delta^{18}O$ ratios are also relatively low and fluctuate between -10.0 and -5.2 ‰ VPDB. Generally $\delta^{18}O$ values correlate well with $\delta^{13}C$ ratios with relatively low values typically between -7 and -9 ‰ VPDB in the lower and middle part of the section and higher values between -6 and -5 ‰ VPDB at the top (from around 35 to 44.5 meters).

4.6 Maceral analysis of coal particles

Most of the investigated samples comprise allochthonous accumulation of coals (e.g. Glasspool, 2003), i.e. pieces of vitrinite, gelified wood fragments, and cutinite in clay (e.g. M1A, M5, M8A, M14). Wood structures are faintly indicated by fluorescence. Samples are interpreted as remnants of driftwood or roots in clay. Sample M8A additionally shows liptinite (resinite or flourinite) that appears in otherwise structureless humous masses. The only real coal sample (M17: vitrinite 86 vol.%, liptinite: 11 vol.%, inertinite: 3 %) also contains mainly detrital gelified coal, remnants of leaves (cutinite and phyllohuminite ca. 10 vol.%); additionally spores, inertinite and semiinertinite, and a high pyrite content (Online Appendix A).

The values of vitrinite reflexion 0.50 und 0.52%Rr are slightly



lower than values from Grünbach coal samples measured by Sachsenhofer (1987). The lower values may result from weathering (Ivanova and Zaitseva, 2006) of the near surface samples of the trench compared to fresh samples from underground mining used by Sachsenhofer (1987).

4.7 Palynology

First pollen data of the Grünbach Formation have been provided by Draxler (1997). In all our analyzed samples the palynofloras are very poor and partly badly preserved. All the members of the morphogenera of the pollen are characteristic for the time span between late Santonian to Maastrichtian. The characters of the "Normapolles" (extremely thick walls, very protruding aperture areas) are typical for this period (Scarby, 1986).

The organic facies is generally composed of semi-opaque matter (such as darkened, gelified wood fragments) few fungal spores and hyphen, and very few cuticular, membraneous material. The cavities of many pollen grains are filled with autigenic pyrite crystals.

In the pollen and spores assemblages the most thick-walled and resistant taxa have been preserved. Spores are represented by *Laevigtisporites* and *Concavisporites* types (unknown botanical affiliation), *Cicatricosisporites* and *Cingulatisporites* types (Schizaeales, *Anemia* and *Lygodium*, respectively) and livermoss spores. Angiosperm pollen are generally presented by the "*Norma-*

Figure 7: Simplified profile of the Maiersdorf-trench (black layers represent coal or allochthonous coal layers) with selected geochemical parameters $CaCO_3$, B, B/Al*, $\delta^{13}C$, TOC, Th/U, CIA and CPA. Black dots symbolize pelitic samples, black triangle and "c" stand for coals or allochthonous coal. The trendline of the parameters B, B/Al* and $\delta^{13}C$ does not include coal and allochthonous coal. Semi-quantitative values for the abundance of calcareous Cretaceous nannofossils (pfv, see text) are added: blank bars symbolize blank nannofossil samples, black bars are samples including nannofossils. Five non-marine (NC1 to NC5) to marine cycles (MC1 to MC5) interpreted from geochemical and supported by fossils are highlighted in brown and blue.

polles" group: extremely variable/diverse *Slowakipollis*, *Krutzschipollis*, cf. *Longanulipollis*, cf. *Hungaropollis*, *Trudopollis*, *Oculipollis* and *Nudopolles* species (many of them with strong Juglandalean affinities seen in the exine pattern), *Complexiopollis* spp., (Myricaceae affinities), *Vacuopollis*, etc. All the different existing species (to some extant genera, have been formerly defined under the lightmicroscopy investigation alone) should be handled with care, because of the extreme variability of these ancient genera (compare Scarby, 1986).

Student´s t-test						
Variable	**Interpreted salinity**	**N**	**Mean**	**St. Dev.**	**T**	**Significance**
B [ppm]	non-marine marine	15 16	139.0 165.8	25.26 39.45	-2.232	0.034
B/Al*	non-marine marine	15 16	149.4 167.2	8.57 20.48	-3.189	0.005
$\delta^{13}C$ [VPDB]	non-marine marine	12 20	-6.34 -4.51	2.532 2.644	-1.924	0.064
$\delta^{18}O$ [VPDB]	non-marine marine	12 20	-7.52 -6.90	1.209 1.244	-1.383	0.177

Table 1: Results of the Student´s t-test calculation for the variables B, B/Al*, $\delta^{13}C$ and $\delta^{18}O$ with number of samples (N), mean, standard deviation, T-value (T) and significance for the test (α).

Other angiosperm pollen types are even rarer: Monosulcates (not yet identified taxa), *Minorpollis* (Juglandalean), *Myrtaceadites* (true Myrtaceae), *Clavatipollenites* spp. (*Chloranthaceae*), Platanaceae, tricolpate hamamelidaceous type, tricolpate not affiliated types and *Spinizonocolpites* (Nypa palm).

The occurrences of the megathermal Schizaeles ferns, *Normapolles*, Myrtaceae, Chloranthaceae and *Nypa* (tropical mangrove palm, *Spinizonocolpites*) evidence very warm and humid depositional conditions, somewhere close the coastline. The observation of *Nypa* pollen in trench samples represents the northernmost occurrence so far. The previously northernmost finding of *Nypa* pollen has been from Campanian/Maastrichtian drill cores of northwestern Egypt (Schrank and Ibrahim, 1995).

4.8 Nannofossils

Nannofossils recorded in the trench section do not include marker species that would allow a biostratigraphic zonation. Only a few long-ranging taxa like *Watznaueria barnesae*, *Zeughrabdotus* ssp., *Rhagosdiscus* ssp., *Prediscosphaera* ssp. were found in a few samples. This corroborates the overall marginal marine to non-marine character of sedimentation. However, nannofossil abundance data, though always rare to very rare if not absent at all, can be used to infer possible marine or nonmarine depositional environments and to compare this data with geochemical proxies (Figs. 3, 7).

5. Discussion

5.1. Trench lithostratigraphic position within the Grünbach Formation

Due to the fact that the trench is located entirely within the Grünbach Formation the exact position in meters above the base of the formation and the correlation with published sections (Plöchinger, 1961) remains ambiguous. A small depression with a tree just south from the eastern end of the trench probably represents the location of the former ventilation shaft indicated in the mining plan of the Neuhoffnungs Stollen (gallery). Based on the location of the gallery mouth and the ventilation shaft in the ALS digital elevation data (Fig. 1) and the orientation as well as scale of the mining plan, the sediments of the trench can approximately be correlated to the geological documentation of the gallery. Based on this correlation the sandstone dominated interval with some conglomerate beds between 12 to 33 m of the trench section (Fig. 3) might be correlated with the Dreistetten Conglomerate of Plöchinger (1961) (Fig. 2).

5.2 Paleoenvironment reconstruction based on geochemistry

Considering all geochemical parameters (especially B contents, B/Al* and stable carbon and oxygen isotopic ratios) in combination with calcareous nannofossil abundances and lithofacies characteristics, five large-scale non-marine (NC) to marine facies cycles (MC) can be interpreted. The geochemical characteristics of coals differ significantly from pelitic sediments, and therefore some geochemical features like the TOC or B/Al* ratio can vary drastically in sediments associated with coals. We therefore did not include coaly layers in our general

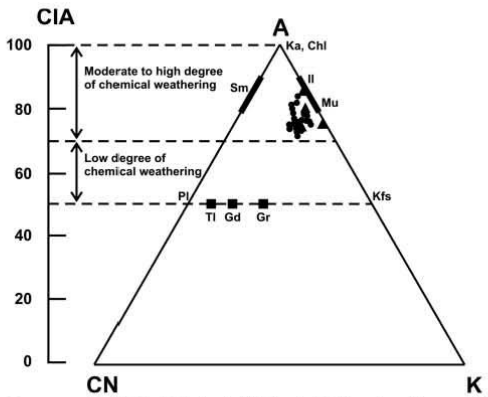


Figure 8: A-CN-K (Al_2O_3-CaO*+Na_2O-K_2O) terniary diagram of samples from Maiersdorf-trench (dots symbolize pelitic samples, triangles coals and coaly samples) and associated chemical index of alteration (CIA) after Nesbitt and Young, 1982. Squares and bars symbolize the average composition of tonalite (Tl), granodiorite (Gd) and granite (Gr) as well as kaolinite (Ka), chlorite (Chl), smectite (Sm), illite (Il), muscovite (Mu), plagioclase (Pl) and K-feldspar (Kfs).

geochemical paleoenvironment interpretations, although values are included into the tables (Online Appendix B) and figures (marked with c).

The stratigraphically lowermost cycle NC1 (0-1.4 m) is characterised by moderate B and B/Al* concentrations as well as low $\delta^{13}C$ and $\delta^{18}O$ ratios. Within this section, no nannofossils could be found which corroborate a non-marine environment. Geochemical and nannofossil data suggest therefore a clearly non-marine interval (Fig. 7, Online Appendix B).

Above a characteristic coaly layer, high $\delta^{13}C$ (up to -0.57 ‰ VPDP) and $\delta^{18}O$ ratios in combination with the rare presence of nannofossils and marine macrofossils (corals, gastropods and bivalves) give evidence for a period of predominantly marine sedimentation (MC1; 1.4-2.8 m of the section). Boron and boron normalized with aluminum, however, show shifts to lower values which do not correspond to the overall interpreted facies trend (Online Appendix B, Fig. 7).

NC2 (2.8-8.0m) shows relatively low B and B/Al* values and a distinct shift to low $\delta^{13}C$ and $\delta^{18}O$ ratios. Additionally, within this interval no nannofossils could be found (Online Appendix B, Fig. 7).

The interval between 8.0-11.5 m is characterized by moderate to high B values and B/Al* ratios as well as relatively low mean $\delta^{13}C$ and $\delta^{18}O$ ratios below -6.50 ‰ VPDB. The two horizons with coaly sediments are geochemically distinct within this interval characterized by low B values below 74 ppm. Nevertheless, high nannofossil abundances suggest a marine depositional environment (MC2) throughout this interval although the chemical evidence for marine sedimentation is ambiguous (Online Appendix B, Fig. 7).

After that, a long period with a lack of nannofossils from 11.5 to 23.9 m is present (NC3). The boron and aluminium normalized values are relatively low and uniform, stable isotope ratios are characteristically low and regarded typical for non-marine environments (Fig. 7, Online Appendix B).

Small positive shifts of boron and carbon isotope ratios as well as a lithological change from yellow to brown mud and sandstones to grey and greenish mud and sandstones may indicate a brackish to marine interval (MC3, 23.9-27.0 m). For this interval, however, no supportive nannofossil or macrofossil data are available to corroborate the brackish-marine interpretation (Online Appendix B, Fig. 7).

NC4 (27.0-34.7m) is very similar to NC3 in lithology (sandstones are dominant) and geochemistry with low B/Al* and carbon isotope ratios as well as low to moderate boron values (Online Appendix B, Fig. 7).

Rare nannofossils have been found in MC4 (34.7-37.1 m); additionally positive shifts especially in the stable carbon isotope and B/Al* ratios can be observed within this section and give evidence for a marine environment.

A lack of nannofossils, dark marls, and a 25 cm coal layer (M-17) characterize NC5 (37.1-40.5 m). Although there is a negative shift of boron concentrations and ratios (except the extremely high value for the coal sample), mean values of B, B/Al* and $\delta^{13}C$ stay overall high and do not fully support the non-marine facies interpretation (Fig. 7) but, compared to the overlying MC5 (40.5-44.7m), values are more "non-marine", i.e. lower in boron and carbon isotopy as a positive shift of boron values and carbon isotopy (mean=-3.0 ‰) is characteristic for the top section MC5. This interval is additionally characterized by a higher amount of nannofossils (pfv up to 2) and a marine macrofossil fauna of bivalves and gastropods. The coaly mud sample M1B has an extremely high B/Al* ratio of 1365 (Online Appendix B, Fig. 7).

Pearson correlation indices of the variables B, B/Al*, $\delta^{13}C$ and $\delta^{18}O$ (Fig. 11) all show positive relations of different significances and illustrate the geochemical coherence of these variables. A positive correlation of r=0.394 between B and B/Al* (excluding coaly samples) as well as distinct discrimination of samples interpreted as marine and non-marine, i.e. higher B and B/Al* values for marine samples, are significant. Further, a significant positive correlation for $\delta^{13}C$ and $\delta^{18}O$ can be ob-

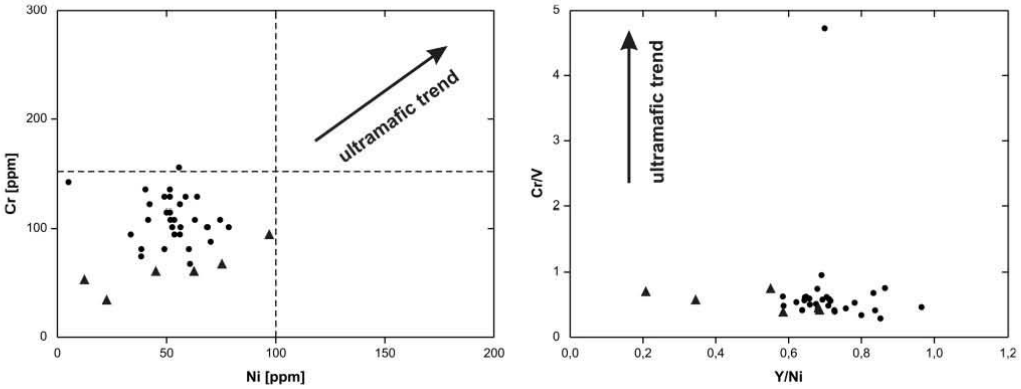


FIGURE 9: Geochemical discrimination plots based on ultramafic/ophiolitic detrital trends. A. Discrimination using Ni and Cr (after Garver et al., 1996) The dashed lines mark the limits enriched Ni (100ppm) and Cr (150ppm). B. Discrimination using Y/Ni and Cr/V (after McLennan et al., 1993). Dots symbolize pelitic samples, triangles coal and allochthonous coal.

served (Fig. 11) but the discrimination effect between marine and non-marine samples is not so distinct. Although this correlation indicates significant diagenetic overprint of the primary isotope signal the isotope data still can be used for the differentiation between marine and non-marine environments as indicated by the statistical significance tests (see Table 1). In contrast, relatively weak positive correlations are characteristic for B and B/Al* in combination with $\delta^{13}C$ (Fig. 11e,f).

Student´s t-test analysis of B, B/Al*, $\delta^{13}C$ and $\delta^{18}O$ were calculated excluding all coaly samples. This comparative method of means and standard deviations demonstrates that boron concentrations are significantly lower in non-marine interpreted intervals (Table 1).

The mean value of the B/Al* ratio is also lower for samples interpreted as non-marine compared to the mean of the marine interpreted sample group. Due to the fact that the variances of the two groups are different for the B/Al*, which was proven by the Levene test, the Student´s t-test for heterogeneous variances was used. With a high significance of α=0.005 marine and non-marine B/Al* ratios are distinctively different (Table 1).

Stable isotope ratios of $\delta^{13}C$ and $\delta^{18}O$ have more negative values within non-marine interpreted intervals relative to marine intervals. While for the $\delta^{13}C$ values the significance is just below the limit, the $\delta^{18}O$ ratios do not differ statistically significantly from marine and non-marine samples (Table 1).

The chemical index of alteration (CIA) values show in general high values between 73 and 85, indicating a significant trend of increasing chemical weathering during the time of deposition of the Grünbach Formation. This is in accordance with the moderate greenhouse climate suggested for the Campanian (e.g. Jenkyns, 2003) and supported by palynology data indicating warm and humid conditions. In detail, there are slight fluctuations recorded from more moderate to higher chemical weathering, which correlate with most of the marine intervals identified by nannofossil and boron content. This may be interpreted as a result of a more pronounced chemical weathering during transgressive to sea level highstand periods.

The TOC/S ratios are fluctuating quite drastic and do not show any systematic variation in regard to identified marine or non-marine intervals and, therefore, doesn't qualify as a reliable means to identify depositional environments in our data.

5.3 Sedimentary Environments and Coal Formation

In general, a non-marine to shallow marine environment of deposition is supposed for the Grünbach Formation (Plöchinger, 1961; Summesberger et al., 2002). High sulphur contents of some of the coals indicate a brackish-marine influence also on coal deposition (Sachsenhofer, 1987, personal communication 2010; see also Schulz and Fuchs, 1991) and, in general, a flood plain to marginal marine environment was inferred for this formation (Summesberger et al., 2002). Our results indicate the presence of large-scale non-marine to brackish-marine cycles and marine environments for at least parts of the Grünbach Formation in contrast to previous, solely non-marine-brackish interpretations (Plöchinger, 1961; Summesberger et al., 2002).

An alluvial fan to fan-delta environment is suggested as the most proximal non-marine facies, and is present as conglomerate layers and conglomerate-sandstone bodies such as the prominent Dreistetten conglomerate, which has a higher thickness to the east of the trench site. Sandstone and shale successions with coals and/or coaly shale layers are interpreted as fluvial-lacustrine to coastal plain sediments in a humid climate with the presence of swamps and mires. Rapid transgressions, as evidenced by fast transitions from coaly layers to fully marine, coral-bearing marls such as at the boundary of cycle NC1-MC1 (Figs 3, 7), raised the groundwater level and fostered coal formation. Marginal marine environments, representing the maximum flooding of transgressive cycles, comprise either sandy fan delta sediments or, as evidenced from the trench section, typically fine-grained marly inner shelf bioturbated pelites with some macrofauna like corals and molluscs, to fine-grained lagoonal deposits with marls and rare

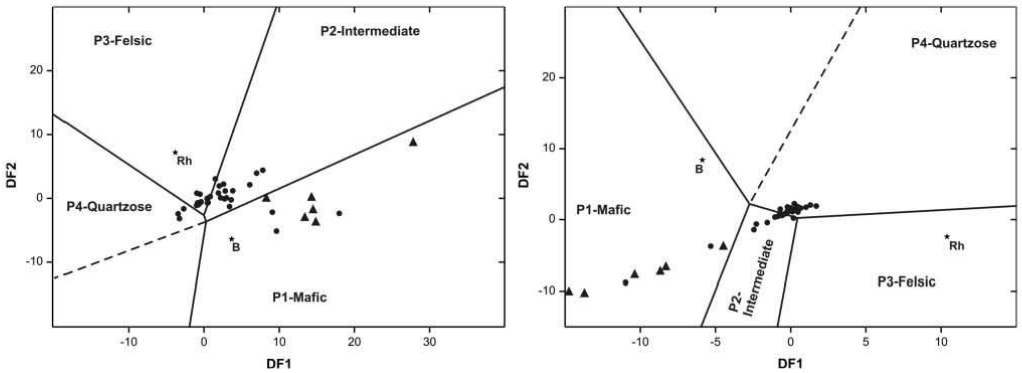


Figure 10: Discrimination plot of discriminant function1 (DF1) and 2 (DF2) showing 4 main provenance groups: P1-mafic, P2-intermediate, P3-felsic and P4-quartzose (after Roser and Korsch, 1988). Dots symbolize pelitic samples, triangles coals and coaly samples. An average basaltic (B) and rhyolithic (Rh) composition is additionally plotted.

miliolid foraminifera and marine ostracods. In-situ positions of corals, the lack of any coarser grained clasts or other fossil fragments argue against significant storm transportation.

5.4 Provenance

Based on sandstone petrology and heavy mineral studies the provenance of Gosau Group sediments of the NCA shows a complex evolution including local, ultramafic ophiolitic and metamorphic sources (e.g. Wagreich and Faupl, 1994). In general, the provenance evolution based on heavy minerals starts with local sources (mainly stable minerals like zircon and tourmaline together with apatite) with variable admixture of ophiolitic detritus (chrome spinel), followed by low- to high-grade metamorphic detritus (garnet, staurolite, chloritoid among other metamorphic minerals).

From the geochemical point of view an ultramafic/ophiolitic

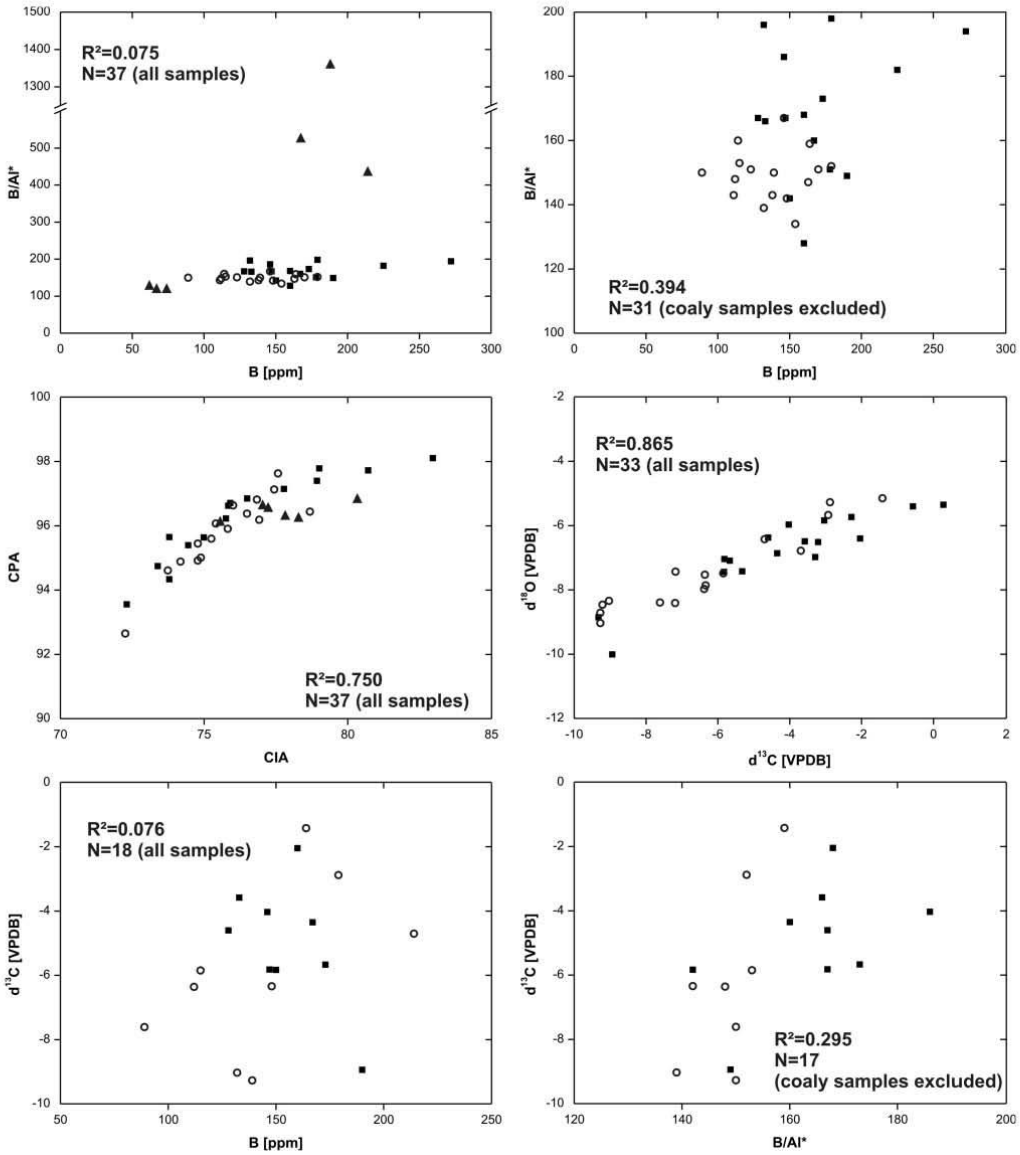


Figure 11: Geochemical discrimination plots of B and B/Al* (for all samples and without coaly samples M1b, M5, M17, M67, M74 and M88), CIA and CPA, $\delta^{13}C$ and $\delta^{18}O$ as well as B and $\delta^{13}C$ (for all samples and without coaly samples M5). Number of samples (N) and squared Pearson correlation index (R^2) is shown in the graphs. Black squares: marine; white circles: non-marine; black triangles: coals.

source cannot be proven. The chromium and nickel limits of 150 ppm respectively 100 ppm indicative of ultramafic sources according to Garver et al. (1996) are not exceeded. Furthermore, no enrichment of the Cr/V ratio relative to the Y/Ni ratio was observed in our data which would be characteristic for ophiolitic detritus (McLennan et al., 1993).

The discriminant function analysis using major elements (Roser and Korsch, 1988) achieves no clear results. The samples plot in all end members of sources and cluster around the intersections. A mixed provenance is most likely for this complex tectonic regime of the Gosau basin in the Early Campanian.

5.5 Marine – non-marine cyclicity

The interpretation of marine - non-marine cycles in the investigated section is mainly based on the occurrence of nannofossils as well as geochemical and isotopic proxies. Due to the rarity of fossils the recognition of cycles is challenging (compare with Herm, 1977; Sanders, 1998). Based on our data 5 large-scale marine – non-marine cycles are reconstructed, some of them associated with coal formation (Figs 3, 7). Generally, the marine cycles are dominated by argillaceous sediments, the terrestrial cycles by sandstone and in rare cases by conglomerate. Brackish-marine influence is also indicated by the high sulphur contents of several coal samples (see maceral analysis; compare Schulz and Fuchs, 1991).

The geochemical proxies for the lowermost 4 beds (NC1) indicate conclusively non-marine environments (Fig. 7), supported by the presence of the limnic/brackish calcareous algae Munieria sp. (Schlagintweit and Wagreich, 1992), overlain by marl with solitary corals in life position, evidencing an abrupt change to marine conditions of MC1 (Fig. 3).

NC2 is dominated by arenaceous beds whereas MC2 is dominated by calcareous mud and marl. Two thin beds with coal particles might indicate short term sea level fluctuations to terrestrial conditions, but the overall marine character is convincingly shown by abundant nannofossils (Fig. 3).

The 12 m thick terrestrial cycle NC3 is the thickest in the section and dominated by sandstone beds. Rare fragments of abraded foraminifera in marl of M57 are interpreted as reworked (question mark in Fig. 3) and could have resulted from coastal wind transport (e.g. Teller et al., 2000). The environmental interpretation of MC3 above is solely based on geochemical data (Fig. 7 and Online Appendix B).

Cycle NC4 is very similar to NC3 and contains one thin conglomerate bed (M38) overlain by MC4, dominated by bluishgrey clay with thin sandstone beds. The terrestrial cycle NC5 is quite rich in organic matter (Online Appendix B) and contains the only unambigous coal seam (M17, Online Appendix A) in the excavated trench. The dominance of allochthonous coal is similar to the (slightly older) coal beds of the Brandenberg Gosau in Tyrol (Schulz and Fuchs, 1991). NC5 ends with a thin conglomerate bed (M10) (Fig. 3) and is followed by MC5, which is dominated by bluish-grey clay and thin beds with coal particles. Nannofossils documented in several samples and geochemical data indicate predominantly marine depositional environments.

The whole Grünbach Formation has an estimated thickness of about 135m at the trench site, with some 45m exposed by the trench, positioned in the middle part of the Grünbach Formation. Given a maximum time span of c. 7.5 Myr for the sedimentation of the Grünbach Formation (Early Campanian, 83.5 Ma for the top of the underlying Maiersdorf Formation, 76 Ma for the base of the overlying Piesting Formation based on Summesberger et al., 2002, using the timescale of Ogg et al., 2004) gives a mean cycle duration of several hundred kyrs. Eustatic cycles recognized by Miller et al. (2005b) at the New Jersey Atlantic margin are one magnitude longer (1-5 Myr), although some shorter cycles are also recognized there (e.g. Mizintseva et al., 2009). Recently, 405 kyr climate cycles resulting in eustatic sea-level changes are increasingly recognized in the Late Cretaceous record (e.g. Gale et al., 2002; Locklair and Sageman, 2008; Voigt and Schönfeld, 2010), and thus may explain the terrestrial-marine cyclic record of the Grünbach Formation.

However, the position of the Grünbach Gosau basin at an active tectonic margin (e.g. Wagreich, 1993) may alternatively suggest tectonically induced relative sea-level changes as cause for "cyclic" rapid marine transgressions and subsequent fill of the generated accommodation space, maybe superposed on eustatic cycles.

The type of cycle control cannot be separated yet with confidence between tectonic and (eustatic) sea-level changes governed by climate. The uniform provenance evolution as suggested by the geochemical and heavy mineral data of our study may point to minor tectonic movements during the deposition of the Grünbach Formation. Also the total thickness of sediment which accumulated during this time span (c. 135 m) is rather low as compared to clearly tectonically driven sedimentation elsewhere in the NCA during this time interval, e.g. 1000 m of Upper Turonian to Santonian sediments in the Gosau pull-apart basin (Wagreich and Decker, 2001). The mean sediment accumulation rate of 1.8 cm/kyr in the investigated Grünbach Formation is rather low compared with > 10 cm/kyr in the Gosau pull-apart basin (Wagreich and Decker, 2001). We therefore see evidence that marine – non-marine cycles in the Grünbach Formation may have had primarily a climatic control.

6. Conclusions

Geochemical parameters can be used to differentiate between marine and non-marine parts of Upper Cretaceous cycles. Marine and non-marine cycle parts can be recognized using boron concentrations and B/Al* ratios in combination with stable carbon isotope ratios. A significant differentiation is present for the ratio B/Al* and absolute boron concentrations after exclusion of coal layers, which have strongly different geochemical characteristics. The aluminium normalized boron ratio is more robust to lithological changes. $\delta^{13}C$ ratios of marine intervals are higher than those of non-marine intervals. Generally, the combination of different geochemical parameters is useful for the interpretation of the paleosalinity.

Five non-marine – marine cycles, with an estimated cycle mean duration of several 100 kyrs are recognized in the trench section. Low subsidence rates and uniform provenance data are in favor of a climatic origin of third-order terrestrial-marine (transgressive-regressive) cycles in the Early Campanian.

Acknowledgements

This work was sponsored by a cooperation project of OMV F&E and the University of Vienna (FA536004). We thank OMV E&P and Philipp Strauss for continuous support. G. Hofer acknowledges a DOC-fellowship of the Austrian Academy of Sciences. Maria Heinrich and Albert Schedl (Geological Survey of Austria) are acknowledged for the possibility to use the old mining documentations in surveys archive. We thank Agrargemeinschaft Maiersdorf and especially its chairman Gerald Wöhrer for the permission to dig the trench and logistic support. Excavation and backfill has been carried out by Ing. Hermann Halbweis GmbH in Maiersdorf. Field work was supported by UNESCO-IGCP 555 "Rapid Environmental/Climate Change in the Cretaceous Greenhouse World: Ocean-Land Interactions" and the Austrian Academy of Sciences. We acknowledge Philipp Strauss, Gerhard Arzmüller, Godfrid Wessely, Herbert Summesberger and Leopold Krystyn for discussion and Ulli Exner for support with differential GPS. Interpretation and drawing of structural data has been carried out by Geocalculator 4.9 (written by Rod Holcombe) and Stereo32 1.0.3 (written by Klaus Röller, Bochum). This manuscript benefited from two anonymous reviews of an earlier version and reviews and editorial remarks by Herbert Summesberger and Martin Zuschin.

References

Berner, R.A. and Raiswell, R., 1984. C/S method for distinguishing freshwater from marine sedimentary rocks. Geology, 12, 365-368.

Bornemann, A., Norris, R.D., Friedrich, O., Beckmann, B., Schouten, S., Sinninghe Damsté, J.S., Vogel, J., Hofmann, T. and Wagner, T., 2008. Isotopic evidence for glaciation during the Cretaceous Supergreenhouse. Science, 319, 189-192.

Buggle, B., Glaser, B., Hambach, U., Gerasimenko, N. and Marković, S., 2011. An evaluation of geochemical weather indices in loess-paleosol studies. Quaternary International, 240, 12-21.

Burnett, J.A., with contributions from Gallagher, L.T., Hampton, M.J., 1998. Upper Cretaceous. In: P.R. Bown (ed.), Calcareous Nannofossil Biostratigraphy. British Micropalaeontological Society Publications Series, Chapman and Hall, London, pp. 132-199.

Clayton, R.N. and Degens, E.T., 1959. Use of carbon isotope analyses of carbonates for differenting freshwater and marine sediments. American Association of Petroleum Geologists Bulletin, 43, 890-897.

Cullers, R.L., 2000. The geochemistry of shales, siltstones and sandstones of Pennsylvanian-Permian age, Colorado, USA: implications for provenance and metamorphic studies. Lithos, 51, 181-203.

Dominik, J. and Stanley, D.J., 1993. Boron, beryllium and sulfur in Holocene sediments and peats of the Nile delta, Egypt: their use as indicators of salinity and climate. Chemical Geology, 104, 203-216.

Draxler, I., 1997. Postconference Excursion: 2.2.2.1. Palynological contribution on the coal-bearing Series of Grünbach. Excursion Guides, Climates: Past, Present and Future, Second European Palaeontological Congress, Vienna 10-12 July 1997, 80-89.

Ernst, W., 1966. Stratigraphisch-fazielle Identifizierung von Sedimenten auf chemisch-geologischem Wege. International Journal of Earth Sciences, 55, 21-29.

Fedo, C.M., Young, G.M. and Nesbitt, G.M., 1997. Paleoclimatic control on the composition of the Paleoproterozoic Serpent Formation, Huronian Supergroup, Canada: A greenhouse to icehouse transition. Precambrian Research, 86, 201-223.

Forster, A., Schouten, S., Baas, M. and Sinninghe Damsté, J.S., 2007. Mid-Cretaceous (Albian-Santonian) sea surface temperature record of the tropical Atlantic Ocean. Geology, 35, 919-922.

Gale, A.S., Hardenbol, J., Hathaway, B., Kennedy, W.J., Young, J.R. and Phansalkar, V., 2002. Global correlation of Cenomanian (Upper Cretaceous) sequences: evidence for Milankovitch control on sea level. Geology, 30, 291-294.

Garver, J.I., Royce, P.R. and Smick, T.A., 1996. Chromium and nickel in shale of the Taconic foreland: a case study for the provenance of fine-grained sediments with an ultramafic source. Journal of Sedimentary Research, 66, 100-106.

Glasspool, I.J., 2003. Hypautochthonous-allochthonous coal deposition in the Permian, South African, Witbank Basin No. 2 seam; a combined approach using sedimentology, coal petrology and palaeontology. International Journal of Coal Geology, 53, 81-135.

Heling, D., 1967. Die Salinitätsfazies von Keupersedimenten aufgrund von Borgehaltsbestimmungen. Sedimentology, 8, 63-72.

Herm, D., 1977. Zyklische Regressions-Sedimentation und Fossil-Vergesellschaftungen in der Gosau (Santonium) von Brandenberg/Tirol. Mitteilungen der Bayerischen Staatssammlung für Paläontologie und Historische Geologie, 17, 257-277.

Hudson, J.D., 1977. Stable isotopes and limestone lithification. Journal of the Geological Society of London, 133, 637-660.

ICCP, 1998. The New Vitrinite Classification (ICCP System 1994). Fuel, 77, 349-358.

ICCP, 2001. The New Inertinite Classification (ICCP System 1994). Fuel, 80, 459-471.

Ivanova, A.V. and Zaitseva, L.B., 2006. Influence of oxidability of carboniferous coals from the Dobrudja foredeep on vitrinite reflectance. Lithology and Mineral Ressources, 41/5, 435-439.

Jenkyns, H.C., 2003. Evidence for rapid climate change in the Mesozoic-Palaeogene greenhouse world. Philosophical Transactions of the Royal Society, Series A 361, 1885-1916.

Kreiner, H., 1994. Der Grünbacher Steinkohlenbergbau und seine Zeit 1823-1965. 2. Auflage, Marktgemeinde Grünbach, Grünbach, 376 pp.

Locklair, R.E. and Sageman, B.B., 2008. Cyclostratigraphy of the Upper Cretaceous Niobrara Formation, Western Interior, U.S.A.: A Coniacian-Santonian orbital timescale. Earth and Planetary Science Letters, 269, 540-553.

McCabe, P.J. and Parrish, J.T., 1992. Tectonic and climatic controls on the distribution and quality of Cretaceous coals. In: P.J. McCabe and J.T. Parrish (eds.), Controls on the distribution and quality of Cretaceous coals. Geological Society of America Special Paper, 267, pp. 1-15.

McLennan, S.M., 1993. Weathering and global denudation. Journal of Geology, 101, 295-303.

McLennan, S.M., Hemming, S., McDaniel, D.K. and Hanson, G.M., 1993. Geochemical approaches to sedimentation, provenance, and tectonics. In: M.J. Johnsson and A. Basu (eds.), Processes Controlling the Composition of Clastic Sediments. Geological Society of America Special Papers 284, pp. 21-40.

Miller, K.G., Kominz, M.A., Browning, J.V., Wright, J.D., Mountain, G.S., Katz, M.E., Sugarman, P.J., Cramer, B.S., Christie-Blick, N. and Pekar, S.F., 2005a. The Phanerozoic record of global sea-level change. Science, 310, 1293-1298.

Miller, K.G., Wright, J.D. and Browning, J.V., 2005b. Visions of ice sheets in a greenhouse world. Marine Geology, 217, 215-231.

Miller, K.G., Wright, J.D., Katz, M.E., Browning, J.V., Cramer, B.S., Wade, B.S. and Mizintseva, S.F., 2008. A view of Antarctic ice-sheet evolution from sea-level and deep-sea isotope changes during the Late Cretaceous-Cenozoic. In: A.K. Cooper, P.J. Barrett, H. Stagg, B. Storey, E. Stump, W. Wise and the 10th ISAES editorial team (eds.), Antarctica: A keystone in a changing world: Proceedings of the 10th International Symposium on Antarctic Earth Sciences. The National Academies Press, Washington DC, pp. 55-70.

Mizintseva, S.F., Browning, J.V., Miller, K.G., Olsson, R.K. and Wright, J.D., 2009. Integrated Late Santonian-Early Campanian sequence stratigraphy, New Jersey Coastal Plain: Implications for global sea-level studies. Stratigraphy, 6, 45-60.

Müller, G. and Gastner, M., 1971. The „Karbonat-Bombe", a simple device for the determination of the carbonate content in sediments, soils, and other materials. Neues Jahrbuch für Mineralogie Monatshefte, 10, 466-469.

Nesbitt, H.W. and Young, G.M., 1982. Early Proterozoic climates and plate motions inferred from major element chemistry of lutites. Nature, 299, 715-717.

Nesbitt, H.W. and Young, G.M., 1989. Formation and diagenesis of weathering profiles. Journal of Geology, 97, 129-147.

Norris, R.D., Bice, K.L., Magno, E.A. and Wilson, P.A., 2002. Jiggling the tropical thermostat in the Cretaceous hothouse. Geology, 30, 299-302.

Ogg, J.G., Agterberg, F.P. and Gradstein, F.M., 2004. The Cretaceous Period. In: F.M. Gradstein, F.P. Agterberg and A.G. Smith (eds.). A Geologic Time Scale 2004, Cambridge University Press, Cambridge, pp. 344-383.

Plöchinger, B., 1961. Die Gosaumulde von Grünbach und der Neuen Welt. Jahrbuch der Geologischen Bundesanstalt, 104, 359-441.

Plöchinger, B., 1967. Erläuterungen zur Geologischen Karte des Hohe Wand-Gebietes (Niederösterreich). Geologische Bundesanstalt, Wien, 142 pp.

Rákosi, L. and Barbacka, M., 1999/2000. Upper Cretaceous flora from Ajka (W Hungary). I. Thallophyta. Studia Botanica Hungarica, 30/31, 27-55.

Reinhardt, E.G., Fitton, R.J. and Schwarcz, H.P., 2003. Isotopic (Sr, O, C) indicators of salinity and taphonomy in marginal marine systems. Journal of Foraminiferal Research, 33, 262-272.

Roser, B.P. and Korsch, R.J., 1988. Provenance signatures of sandstone-mudstone suites determined using discriminant function analysis of major-element data. Chemical Geology, 67, 119-139.

Rügner, O., 2000. Tonmineral-Neubildung und Paläosalinität im Unteren Muschelkalk des südlichen Germanischen Beckens. Unpublished PhD thesis, University of Heidelberg, Heidelberg, 189 pp.

Sachsenhofer, R., 1987. Fazies und Inkohlung mesozoischer Kohlen der Alpen Ostösterreichs. Mitteilungen der Österreichischen Geologischen Gesellschaft, 80, 1-45.

Sageman, B.B. and Lyons, T.W., 2004. Geochemistry of Fine-grained Sediments and Sedimentary Rocks. In: F. MacKenzie (ed.), Sediments, Diagenesis, and Sedimentary Rocks, Treatise on Geochemistry, 7, pp. 115-158.

Sanders, D., 1998. Tectonically controlled Late Cretaceous terrestrial to neritic deposition (Northern Calcareous Alps, Tyrol, Austria). Facies, 39, 139-178.

Scarby, A., 1986. Normapolles anthers from the Upper Cretaceous of southern Sweden. Review of Palaeobotany and Palynology, 46, 235-256.

Schlagintweit, F. and Wagreich, M., 1992. Über ein Vorkommen von *Munieria grambasti sarda* CHERCHI et al. in der obersantonen-untercampanen Gosau Gruppe des Miesenbachtales (Niederösterreich). Mitteilungen der Gesellschaft der Geologie- und Bergbaustudenten in Österreich, 38, 21-29.

Schrank, E. and Ibrahim, M.I.A., 1995. Cretaceous (Aptian-Maastrichtian) palynology of foraminifera dated wells (KRM-1, AG-18) in northwestern Egypt. Berliner Geowissenschaftliche Abhandlungen, Reihe A, 177, 1-44.

Schulz, O. and Fuchs, H.W., 1991. Kohle in Tirol: Eine historische, kohlenpetrologische und lagerstättenkundliche Betrachtung. Archiv für Lagerstättenforschung der Geologischen Bundesanstalt, 13, 123-213.

Selter, V., David, F. and Kraft, T., 1989. Zusammenhänge zwischen Fazies und Borgehalten im nordwestdeutschen Oberkarbon-Becken. Geologisch-Paläontologische Mitteilungen Innsbruck, 16, 108-111.

Spötl, C. and Vennemann, T., 2003. Continuous-flow IRMS analysis of carbonate minerals. Rapid Communications in Mass Spectrometry, 17, 1004-1006.

Summesberger, H., 1997. The Cretaceous of the Grünbach - Neue Welt Basin. In: W.E. Piller, H. Summesberger, I. Draxler, M. Harzhauser and O. Mandic (eds.), Meso- to Cenozoic tropical/subtropical climates – Selected examples from the Northern Calcareous Alps and the Vienna Basin. Excursion Guides Second European Palaeontological Congress Climates: Past, Present and Future, Vienna 1997, Postconference Excursion, 2, pp. 77-89.

Summesberger, H., Wagreich, M., Tröger, K.A. and Scholger, R., 2000. Piesting-Formation, Grünbach-Formation und Maiersdorf-Formation – drei neue lithostratigraphische Termini in der Gosau Gruppe (Oberkreide) von Grünbach und der Neuen Welt (Niederösterreich). In: W.E. Piller (ed.), Austrostrat 2000. 24-26 November 2000 Gossendorf. Vortragskurzfassungen und Exkursionsführer, Berichte des Institutes für Geologie und Paläontologie der Karl-Franzens-Universität Graz/Austria, 2, pp. 23.

Summesberger, H., Wagreich, M., Tröger, K.A. and Scholger, R., 2002. The Upper Cretaceous of Piesting (Austria): Integrated stratigraphy of the Piesting Formation (Gosau Group). In: M. Wagreich (ed.), Aspects of Cretaceous Stratigraphy and Palaeobiogeography. Schriftenreihe der Erdwissenschaftlichen Kommission, 15, pp. 373-399.

Summesberger, H., Machalski, M. and Wagreich, M., 2007. First record of the late Campanian heteromorph ammonite *Nostoceras hyatti* from the Alpine Cretaceous (Grünbach, Go-sau Group, Lower Austria). Acta Geologica Polonica, 57, 443-451.

Talbot, M.R., 1990. A review of the palaeohydrological interpretation of carbon and oxygen isotopic ratios in primary lacustrine carbonates. Chemical Geology (Isotope Geoscience Section), 80, 261-279.

Taylor, G.H., Teichmüller, M., Davis, A., Diessel, C.F.K., Littke, R. and Robert, P., 1998. Organic Petrology. Gebrüder Bornträger, Berlin, 198 pp.

Teller, J.T., Glennie, K.W., Lancaster, N. and Singhvi, A.K., 2000. Calcareous dunes of the United Arab Emirates and Noah's Flood: the postglacial reflooding of the Persian (Arabian) Gulf. Quaternary International, 68-71, 297-308.

Veizer, J., 1983. Trace Elements and Isotopes in Sedimentary Carbonates. In: R.J. Reeder (ed.), Carbonates, mineralogy and chemistry. Reviews in Mineralogy and Geochemistry, 11, pp. 265-299.

Voigt, S. and Schönfeld, J., 2010. Cyclostratigraphy of the reference section for the Cretaceous white chalk of northern Germany, Lägerdorf-Kronsmoor: A late Campanian–early Maastrichtian orbital time scale. Palaeogeography, Palaeoclimatology, Palaeoecology, 287, 67-80.

Wagreich, M., 1993. Subcrustal tectonic erosion in orogenic belts - A model for the Late Cretaceous subsidence of the Northern Calcareous Alps (Austria). Geology, 21, 941-944.

Wagreich, M. and Faupl, P., 1994. Palaeogeography and geodynamic evolution of the Gosau Group of the Northern Calcareous Alps (Late Cretaceous, Eastern Alps, Austria). Palaeogeography, Palaeoclimatology, Palaeoecology, 110, 235-254.

Wagreich, M. and Decker, K., 2001. Sedimentary tectonics and subsidence modelling of the type Upper Cretaceous Gosau basin (Northern Calcareous Alps, Austria). International Journal of Earth Sciences, 90, 714-726.

Wagreich, M., Hu, X. and Sageman, B., 2011. Causes of oxic-anoxic changes in Cretaceous marine environments and their implications for Earth systems. Sedimentary Geology, 235, 1-4.

Wagreich, M. and Krenmayr, H.G., 2005. Upper Cretaceous oceanic red beds (CORB) in the Northern Calcareous Alps (Nierental Formation, Austria): slope topography and clastic input as primary controlling factors. Cretaceous Research, 26, 57-64.

Yan, D., Chen, D., Wang, Q. and Wang, J., 2010. Large-scale climatic fluctuations in the latest Ordovician on the Yangtze block, south China. Geology, 38, 599-602.

For online Appendix and supplementary material to this publication see: www.univie.ac.at/ajes/archive/volume_104_2/

Received: 11 November 2011
Accepted: 13 December 2011

Gerald HOFER[1)*], Erich DRAGANITS[1)2)], Michael WAGREICH[1)], Christa-Charlotte HOFMANN[3)], Doris REISCHENBACHER[4)], Marie-Louise GRUNDTNER[1)] & Magda BOTTIG[5)]

[1)] Department of Geodynamics and Sedimentology, University of Vienna, Althanstrasse 14, A-1090 Vienna, Austria;

[2)] Department of Prehistoric and Medieval Archaeology, University of Vienna, Franz-Klein-Gasse 1, 1190 Vienna, Austria;

[3)] Department of Palaeontology, University of Vienna, Althanstrasse 14, A-1090 Vienna, Austria;

[4)] Department of Applied Geological Sciences and Geophysics, Montanuniversität Leoben, Franz-Joseph-Strasse 18, A-8700 Leoben, Austria;

[5)] Geological Survey of Austria, Neulinggasse 38, A-1030 Vienna, Austria;

[*)] Corresponding author, gerald.hofer@univie.ac.at

APPENDIX

APPENDIX A

Table of maceral analysis (classification of huminites, liptinites, inertinites and matrix) of coal particles for the samples M5, M8A, M14 and M17.

		particles M-5	particles M-8A	coal M-14	coal M-17
Huminite/Vitrinite					
	Telinite				
	Collotelinite	277	141	291	54
	Corpogelinite				
	Detrovitrinite				10
	Collodetrinite				161
	Phyllovitrinite				14
Sum Huminite		277	141	291	239
Liptinite					
	Sporinite				2
	Cutinite				12
	Resinite	12			
	Liptodetrinite				8
	Alginite				5
	Fluorinite				3
Sum Liptinite		12	0	0	30
Inertinite					
	Pyrofusinite				4
	Degradofusinite				2
	Funginite				
	Inertodetrinite				2
Sum Inertinite		0	0	0	8
Matrix					
	Pyrite		8	9	13
	Shale	11	11		10
Sum Matrix		11	19	9	23
	Σ	300	160	300	300
	%	100	100	100	100
	Rr [%]	0.52	0.50	0.52	0.50
	s	0.01	0.01	0.01	0.01
	n	25	16	25	18

Maceral abundance M-5
mineral matter free

95.8 % Telovitrinite
0.0 % Detrovitrinite
0.0 % Gelovitrinite
95.8 % Vitrinite
4.2 % Liptinite
0.0 % Inertinite

Maceral abundance M-8a
mineral matter free

100.0 % Telovitrinite
0.0 % Detrovitrinite
0.0 % Gelovitrinite
100.0 % Vitrinite
0.0 % Liptinite
0.0 % Inertinite

Maceral abundance M-17
mineral matter free

19.5 % Telovitrinite
66.8 % Detrovitrinite
0.0 % Gelovitrinite
86.3 % Vitrinite
10.8 % Liptinite
2.9 % Inertinite

Maceral abundance M-14
mineral matter free

100.0 % Telovitrinite
0.0 % Detrovitrinite
0.0 % Gelovitrinite
100.0 % Vitrinite
0.0 % Liptinite
0.0 % Inertinite

TABLE 1

APPENDIX B

Geochemistry data. List of the sample set (M1-M92) from the Maiersdorf-trench. Analyzed geochemistry (major element oxides: SiO_2, Al_2O_3, Fe_2O_3, MgO, CaO, Na_2O, K_2O, TiO_2, P_2O_5, MnO and Cr_2O_3, minor elements: Ba, Be, Co, Cs, Ga, Hf, Nb, Ni, Rb, Sn, Sr, Ta, Th, U, V, W and Zr, noble and base metals: Mo, Cu, Pb, Zn, Ni, As, Cd, Sb, Bi, Ag, Au, Hg, Tl and Se, rare earth elements: Sc, Y, La, Ce, Pr, Nd, Sm, Eu, Gd, Tb, Dy, Ho, Er, Tm, Yb and Lu, loss on ignition: LOI, total C and S, total organic carbon: TOC, carbonate: $CaCO_3$, some elemental ratios: B/Al*, Th/U, Cr/Ni, Cr/V, Y/Ni, TOC/S, indices of alteration: CIA and CPA and stable carbon and oxygen isotope ratios: $\delta^{13}C$ and $\delta^{18}O$. The interpreted facies determinations (marine or non-marine) used for statistic calculations are added.

Gerald HOFER, Erich DRAGANITS, Michael WAGREICH, Christa-Charlotte HOFMANN, Doris REISCHENBACHER, Marie-Louise GRUNDTNER & Magda BOTTIG

Samples of the Maiersdorf-trench

Sample-Nr.	SiO_2 [%]	Al_2O_3 [%]	Fe_2O_3 [%]	MgO [%]	CaO [%]	Na_2O [%]	K_2O [%]	TiO_2 [%]	P_2O_5 [%]	MnO [%]	Cr_2O_3 [%]	LOI [%]	Sum [%]	Sc [ppm]	Ba [ppm]	Be [ppm]
M-1	24.81	12.75	7.18	0.88	1.28	0.18	2.24	0.51	0.06	0.05	0.012	49.8	99.77	16	1473	4
M-1B	5.94	2.59	3.75	0.42	9.52	0.06	0.49	0.12	0.04	0.17	0.008	73.0	96.09	5	86	0
M-2																
M-3	65.44	17.06	5.12	1.48	0.31	0.50	3.81	0.97	0.20	0.03	0.014	4.9	99.83	16	622	3
M-4																
M-5	27.00	9.26	12.98	1.13	5.56	0.24	1.96	0.47	0.08	0.10	0.009	41.1	99.89	13	290	2
M-6	52.87	23.42	5.92	2.12	0.94	0.38	4.56	1.07	0.08	0.13	0.020	8.3	99.83	24	628	3
M-7	46.62	18.05	7.23	2.13	4.62	0.43	3.96	0.85	0.11	0.09	0.017	15.7	99.84	20	524	2
M-8B																
M-9A																
M-9B	49.69	26.47	3.61	1.82	1.29	0.31	4.03	1.17	0.08	0.03	0.023	11.3	99.83	27	598	4
M-12	42.38	16.56	7.55	1.40	1.59	0.35	3.44	0.77	0.09	0.06	0.015	25.7	99.87	18	441	3
M-13																
M-16	52.92	22.29	6.03	2.40	1.35	0.40	4.72	1.04	0.11	0.17	0.020	8.4	99.82	23	637	2
M-17	11.72	6.01	5.68	0.48	1.95	0.12	1.29	0.23	0.06	0.06	0.005	72.3	99.94	7	183	1
M-18	51.43	19.54	6.68	2.44	3.00	0.48	4.31	0.89	0.12	0.11	0.017	10.8	99.83	20	533	3
M-20																
M-23	52.93	14.82	5.31	2.24	8.56	0.62	3.26	0.83	0.14	0.10	0.011	11.0	99.85	14	480	0
M-24	53.20	23.58	5.91	2.26	0.43	0.42	4.88	1.07	0.09	0.14	0.019	7.8	99.82	24	661	4
M-25																
M-27																
M-31	52.73	22.21	4.93	2.42	2.63	0.46	5.04	1.02	0.11	0.03	0.019	8.2	99.83	22	612	4
M-33	66.30	14.72	4.02	1.65	0.75	0.71	2.95	0.85	0.31	0.02	0.016	7.6	99.87	15	430	2
M-36																
M-37	54.91	21.26	6.33	2.34	1.32	0.45	4.76	1.00	0.12	0.11	0.018	7.2	99.83	21	668	2
M-41																
M-42	66.58	15.37	5.40	1.90	0.49	0.50	3.19	0.97	0.15	0.07	0.014	5.2	99.84	15	491	2
M-46	45.05	19.72	7.66	2.96	6.50	0.39	4.35	0.91	0.13	0.16	0.016	12.0	99.83	21	551	4
M-48	53.49	18.86	6.09	2.23	4.23	0.40	4.27	0.94	0.13	0.09	0.015	9.1	99.84	19	534	2
M-50	54.17	20.93	4.96	2.14	2.89	0.52	4.64	1.01	0.10	0.05	0.016	8.4	99.83	20	624	4
M-53	54.77	21.65	6.34	2.33	0.74	0.32	4.76	1.00	0.06	0.07	0.019	7.8	99.84	22	593	3
M-55																
M-57	54.84	17.95	5.69	1.94	4.72	0.52	3.93	0.94	0.11	0.16	0.014	9.0	99.85	18	526	1
M-60	34.06	11.20	17.19	1.11	10.04	0.27	2.24	0.54	0.08	0.09	0.010	23.1	99.90	14	292	3
M-62																
M-64																
M-65	48.60	19.90	4.40	2.21	6.88	0.55	4.77	0.80	0.09	0.04	0.019	11.6	99.85	19	562	4
M-66																
M-67	31.01	11.89	6.05	0.63	3.87	0.28	2.15	0.47	0.06	0.08	0.010	43.4	99.92	13	315	5
M-68	50.54	24.07	4.71	1.23	1.91	0.33	4.85	1.06	0.05	0.00	0.021	11.1	99.86	25	641	2
M-69	54.83	14.52	7.36	1.65	7.27	0.53	3.07	0.80	0.14	0.17	0.013	9.5	99.86	16	434	2
M-71																
M-72	49.87	16.59	6.49	1.91	7.99	0.46	3.64	0.81	0.13	0.13	0.016	11.8	99.86	18	490	3
M-73																
M-74	21.87	9.17	8.19	0.76	5.56	0.20	1.86	0.37	0.06	0.02	0.009	51.8	99.93	13	263	3
M-75	47.03	15.14	7.24	1.72	10.27	0.51	3.44	0.76	0.13	0.12	0.015	13.5	99.86	16	450	2
M-77	46.04	14.16	5.39	1.52	13.31	0.49	3.09	0.77	0.15	0.14	0.012	14.8	99.87	15	449	3
M-78	50.48	17.53	4.39	1.85	7.95	0.49	3.76	0.85	0.12	0.11	0.015	12.3	99.86	17	539	2
M-79	43.42	13.48	15.62	1.14	1.60	0.43	2.80	0.70	0.09	0.03	0.015	20.5	99.88	16	416	5
M-82																
M-84	44.13	14.35	5.34	1.64	14.33	0.47	3.11	0.72	0.14	0.10	0.012	15.5	99.87	14	441	1
M-85																
M-87																
M-88	28.35	10.62	10.05	0.80	4.48	0.21	1.73	0.46	0.09	0.10	0.014	43.0	99.92	14	263	6
M-89																
M-90	60.27	18.26	3.66	1.72	2.99	0.41	3.26	0.95	0.08	0.02	0.018	8.2	99.86	18	456	2
M-92	49.67	19.69	5.94	2.08	6.07	0.45	4.15	0.90	0.11	0.12	0.016	10.7	99.85	19	575	2

TABLE 2

Samples of the Maiersdorf-trench

Sample-Nr.	Co [ppm]	Cs [ppm]	Ga [ppm]	Hf [ppm]	Nb [ppm]	Rb [ppm]	Sn [ppm]	Sr [ppm]	Ta [ppm]	Th [ppm]	U [ppm]	V [ppm]	W [ppm]	Zr [ppm]	Y [ppm]	La [ppm]
M-1	16.7	14.6	16.4	2.1	8.5	96.3	1	127.1	0.4	7.6	9.1	117	2.0	88.2	22.3	19.2
M-1B	7.2	1.6	12.3	0.9	9.4	20.4	0	255.4	0.1	2.3	4.0	260	3.6	35.0	8.3	5.7
M-2																
M-3	10.5	7.3	21.4	6.5	16.9	139.5	4	89.1	1.3	12.4	3.0	137	2.9	252.6	32.1	43.0
M-4																
M-5	17.3	4.9	14.0	2.6	8.4	73.0	2	191.1	0.5	6.3	4.4	76	2.5	104.0	21.2	19.8
M-6	22.2	14.3	29.0	4.8	17.9	188.8	5	101.2	1.4	14.2	4.6	199	2.9	164.5	30.0	37.5
M-7	19.1	11.2	23.9	4.0	15.5	154.6	4	179.4	1.1	11.9	5.9	163	2.2	145.8	30.8	30.9
M-8B																
M-9A																
M-9B	28.3	19.2	32.6	5.4	21.0	181.5	6	121.5	1.6	16.7	8.7	236	3.1	183.1	28.0	39.6
M-12	16.6	9.0	21.0	3.9	13.5	133.6	3	112.9	1.0	10.1	4.4	159	2.2	133.4	23.4	28.6
M-13																
M-16	24.5	12.3	27.9	4.6	18.1	182.5	5	124.6	1.2	13.6	3.6	189	2.7	154.9	28.7	36.6
M-17	7.2	3.9	9.0	0.9	4.5	52.6	1	149.2	0.2	2.9	8.2	98	1.0	38.1	13.0	10.2
M-18	20.2	12.2	24.5	4.3	16.3	159.6	4	135.9	1.2	13.8	4.2	147	2.7	149.8	27.3	33.4
M-20																
M-23	14.9	7.3	19.0	5.4	14.7	122.0	3	139.3	0.9	11.1	3.2	135	2.6	189.0	28.8	32.6
M-24	27.0	12.8	31.4	5.1	19.1	199.3	5	105.0	1.2	16.3	4.2	219	3.4	177.2	30.9	43.0
M-25																
M-27																
M-31	18.7	12.5	29.6	4.6	17.8	199.3	5	124.6	1.2	13.6	3.5	199	2.9	177.8	30.1	37.3
M-33	15.2	7.5	19.0	4.9	15.2	129.6	3	86.7	1.1	10.6	3.6	125	2.6	194.9	31.4	40.4
M-36																
M-37	17.6	11.4	27.1	5.0	16.9	190.5	6	101.7	1.1	16.0	3.2	189	2.7	178.9	31.8	39.2
M-41																
M-42	21.2	7.5	19.9	7.0	17.1	126.6	4	69.4	1.2	12.5	3.6	146	2.7	271.5	33.4	37.9
M-46	23.0	10.1	25.8	3.9	16.0	168.4	4	136.5	0.8	13.1	3.9	174	2.2	138.4	28.8	35.4
M-48	22.7	10.6	24.1	4.9	16.3	168.1	5	112.5	1.1	13.3	3.4	157	2.7	178.8	32.2	37.3
M-50	23.6	13.0	27.5	5.5	18.1	202.5	5	94.5	1.1	15.3	3.9	185	2.8	185.9	32.4	42.0
M-53	27.2	13.7	28.6	5.2	18.2	196.3	5	92.1	1.3	15.7	3.2	181	2.7	170.5	28.5	39.8
M-55																
M-57	22.4	10.3	22.9	5.9	16.4	156.9	4	85.3	1.1	13.1	3.4	144	2.6	210.3	33.4	39.0
M-60	12.5	7.0	16.1	3.1	10.2	92.7	3	129.5	0.7	9.3	4.5	106	2.3	116.3	25.4	24.8
M-62																
M-64																
M-65	19.4	15.5	25.4	4.2	15.9	198.8	5	94.8	1.1	14.7	3.0	133	3.6	152.8	23.9	34.9
M-66																
M-67	27.2	7.5	15.3	2.6	7.5	89.5	3	67.6	0.5	6.8	3.4	93	2.0	103.1	29.6	21.3
M-68	3.2	21.8	32.6	4.9	18.9	216.6	5	92.2	1.3	17.4	3.7	203	3.2	166.3	24.1	41.6
M-69	18.3	7.4	18.0	4.8	14.1	115.2	3	119.9	0.9	10.4	2.7	116	2.4	182.4	31.2	32.9
M-71																
M-72	24.3	10.2	20.2	4.4	14.3	143.3	4	122.8	1.0	12.4	2.8	149	2.1	153.2	31.0	35.4
M-73																
M-74	7.0	6.8	17.1	2.0	7.1	77.7	2	72.4	0.4	6.9	3.7	90	2.9	71.9	23.0	17.1
M-75	19.9	10.6	19.4	4.9	14.2	137.5	3	145.4	0.8	11.3	3.1	121	2.2	165.3	28.2	34.5
M-77	17.2	8.0	18.4	5.3	14.1	121.8	3	137.3	0.8	11.9	3.2	114	2.7	163.5	28.8	32.5
M-78	18.6	10.9	21.9	4.7	15.0	154.9	4	91.0	1.0	13.3	3.6	148	2.6	157.3	27.6	35.1
M-79	17.8	8.4	18.8	4.4	12.8	112.5	3	61.1	0.9	10.7	5.4	172	2.1	165.7	28.6	30.7
M-82																
M-84	17.6	10.1	17.7	4.1	13.2	126.3	3	140.8	0.7	10.8	2.6	119	2.4	143.6	25.6	30.0
M-85																
M-87																
M-88	16.2	23.5	15.7	2.6	8.1	86.0	2	66.1	0.6	7.2	3.4	111	2.1	100.9	27.9	22.0
M-89																
M-90	23.4	15.0	22.3	5.2	15.8	149.4	4	73.7	1.0	12.5	3.0	146	2.8	186.5	28.6	36.5
M-92	23.6	11.3	24.4	4.0	15.1	163.7	4	100.3	1.0	14.0	3.2	159	3.2	145.9	27.3	35.6

TABLE 2 CONTINUED

Samples of the Maiersdorf-trench

Sample-Nr.	Ce [ppm]	Pr [ppm]	Nd [ppm]	Sm [ppm]	Eu [ppm]	Gd [ppm]	Tb [ppm]	Dy [ppm]	Ho [ppm]	Er [ppm]	Tm [ppm]	Yb [ppm]	Lu [ppm]	TOT/C [%]	TOT/S [%]	Mo [ppm]
M-1	43.4	4.80	20.2	4.02	0.93	3.81	0.64	3.45	0.74	2.10	0.33	2.10	0.30	32.04	3.64	3.3
M-1B	13.3	1.54	5.7	1.36	0.34	1.40	0.27	1.41	0.30	0.84	0.15	0.84	0.14	49.65	0.13	1.0
M-2																
M-3	94.7	10.31	38.1	6.92	1.40	5.89	0.94	5.29	1.07	3.15	0.46	3.14	0.45	0.19	0.00	0.3
M-4																
M-5	45.0	5.11	22.2	4.23	0.97	4.09	0.68	3.72	0.70	2.07	0.33	1.94	0.28	24.72	4.83	5.9
M-6	79.0	8.94	35.3	6.48	1.39	5.56	0.93	5.38	1.09	3.18	0.51	3.22	0.46	0.63	0.11	0.2
M-7	66.9	7.54	31.5	6.04	1.35	5.53	0.91	5.27	1.01	2.94	0.45	3.00	0.44	6.38	3.00	2.3
M-8B																
M-9A																
M-9B	83.8	9.60	38.7	7.02	1.51	5.62	0.91	5.01	1.03	3.14	0.47	3.22	0.50	1.28	0.13	1.5
M-12	58.8	6.71	28.0	5.07	1.13	4.45	0.74	4.27	0.85	2.51	0.37	2.46	0.37	10.73	0.51	2.9
M-13																
M-16	75.7	8.51	33.7	6.37	1.37	5.31	0.92	5.19	1.05	3.05	0.46	3.21	0.44	0.88	0.07	0.6
M-17	23.4	2.67	10.5	2.23	0.52	2.46	0.38	2.03	0.39	1.09	0.16	0.91	0.16	48.96	0.25	5.6
M-18	72.3	7.91	30.8	6.30	1.37	5.36	0.88	4.76	0.94	2.85	0.44	2.83	0.42	2.64	0.98	1.1
M-20																
M-23	71.4	7.91	31.3	5.65	1.21	5.30	0.86	4.77	0.95	2.87	0.44	2.66	0.44	2.10	0.38	1.1
M-24	91.4	10.12	41.6	7.27	1.49	6.44	0.99	5.66	1.16	3.36	0.53	3.31	0.51	0.48	0.25	1.3
M-25																
M-27																
M-31	79.9	8.95	33.8	6.17	1.24	5.28	0.86	5.12	1.00	2.99	0.45	3.04	0.46	0.97	0.02	0.3
M-33	88.6	9.84	39.1	7.09	1.50	6.38	1.03	5.62	1.05	3.13	0.46	2.86	0.46	1.97	0.04	0.3
M-36																
M-37	86.8	9.72	36.8	6.93	1.38	6.05	0.96	5.68	1.08	3.29	0.51	3.26	0.50	0.34	0.00	1.0
M-41																
M-42	80.7	8.91	35.1	6.38	1.40	6.12	1.00	5.79	1.14	3.43	0.52	3.41	0.51	0.07	0.00	0.2
M-46	78.0	8.54	35.5	6.16	1.31	5.51	0.86	4.95	0.96	2.91	0.44	2.79	0.44	1.68	0.00	1.5
M-48	81.9	9.21	35.8	6.54	1.36	5.95	0.98	5.26	1.09	3.36	0.49	3.27	0.48	0.84	0.00	0.1
M-50	88.7	10.22	40.8	7.32	1.51	6.32	1.00	5.58	1.10	3.30	0.51	3.38	0.53	0.69	0.00	1.5
M-53	87.0	9.87	38.0	6.84	1.32	5.53	0.89	5.22	1.03	3.35	0.49	3.26	0.49	0.11	0.00	0.0
M-55																
M-57	83.3	9.61	36.8	6.87	1.44	6.27	1.01	5.99	1.15	3.45	0.51	3.25	0.51	0.99	0.00	0.2
M-60	54.2	6.36	25.6	4.92	1.14	5.03	0.79	4.36	0.89	2.60	0.38	2.44	0.38	7.53	0.13	10.6
M-62																
M-64																
M-65	73.8	8.52	32.8	5.77	1.11	4.89	0.75	4.49	0.89	2.56	0.40	2.54	0.40	1.53	0.00	0.6
M-66																
M-67	48.7	5.76	23.5	5.21	1.18	5.59	0.94	5.41	1.06	3.14	0.47	2.89	0.45	20.88	0.82	17.3
M-68	86.3	9.48	34.8	6.03	1.21	4.73	0.72	4.10	0.85	2.73	0.40	2.75	0.43	1.41	0.00	1.3
M-69	71.7	8.12	31.9	6.22	1.33	5.80	0.92	5.23	1.06	3.10	0.46	3.02	0.46	1.44	0.00	0.8
M-71																
M-72	77.8	8.65	32.8	6.60	1.35	6.26	0.98	5.49	1.07	3.07	0.45	2.96	0.45	1.79	0.00	1.2
M-73																
M-74	36.8	4.27	16.2	3.59	0.83	3.76	0.67	3.70	0.78	2.32	0.36	2.28	0.37	25.61	0.02	5.5
M-75	73.4	8.38	33.3	6.03	1.28	5.44	0.90	4.80	0.98	2.96	0.42	2.78	0.41	2.26	0.00	1.3
M-77	68.8	7.99	31.3	5.87	1.26	5.57	0.91	4.96	1.04	3.04	0.43	2.76	0.43	2.86	0.00	0.4
M-78	74.7	8.53	32.3	6.08	1.23	5.29	0.87	4.65	1.00	2.96	0.44	2.88	0.43	1.80	0.00	0.6
M-79	64.9	7.64	30.8	5.56	1.20	5.10	0.86	4.98	1.00	3.02	0.46	3.01	0.45	7.62	0.25	19.4
M-82																
M-84	65.3	7.24	29.3	5.37	1.07	4.79	0.78	4.38	0.88	2.61	0.40	2.62	0.38	3.07	0.00	0.7
M-85																
M-87																
M-88	45.7	5.44	22.4	4.54	1.03	4.78	0.77	4.47	0.87	2.55	0.38	2.48	0.38	21.43	0.66	5.6
M-89																
M-90	78.2	8.76	34.6	6.32	1.30	5.57	0.90	4.93	1.02	3.03	0.44	2.92	0.44	0.83	0.00	0.0
M-92	74.9	8.68	33.5	6.25	1.33	5.51	0.87	4.74	1.00	2.88	0.42	2.88	0.45	1.33	0.00	0.5

TABLE 2 CONTINUED

Samples of the Maiersdorf-trench

Sample-Nr.	Cu [ppm]	Pb [ppm]	Zn [ppm]	Ni [ppm]	As [ppm]	Cd [ppm]	Sb [ppm]	Bi [ppm]	Ag [ppm]	Au [ppb]	Hg [ppm]	Tl [ppm]	Se [ppm]	B [ppm]	B/Al*	^{13}C [VPDB]
M-1	37.9	9.6	70	38.5	34.4	0.2	1.3	0.3	0.0	1.1	1.54	0.0	2.1	132	196	
M-1B	7.6	4.5	13	12.4	40.5	0.0	4.8	0.0	0.0	0.0	1.25	0.0	0.6	187	1365	
M-2																-2.28
M-3	36.8	9.6	49	33.6	13.3	0.0	1.0	0.5	0.1	2.7	2.55	0.0	0.0	179	198	
M-4																-2.93
M-5	27.6	20.7	42	62.6	300.4	0.2	6.5	0.2	0.1	0.0	4.12	0.3	0.8	214	437	-4.70
M-6	65.3	15.6	55	40.3	3.4	0.0	0.3	0.5	0.1	2.8	0.27	0.0	0.5	225	182	
M-7	41.1	12.7	180	50.0	70.2	0.3	0.9	0.4	0.1	1.5	1.41	0.1	0.9	160	168	-2.04
M-8B																
M-9A																-3.04
M-9B	78.3	21.7	66	55.7	13.4	0.2	1.2	0.6	0.2	1.6	0.96	0.0	1.0	272	194	
M-12	37.6	15.9	55	56.4	59.3	0.1	4.4	0.4	0.0	1.1	2.38	0.1	2.0	146	167	
M-13																
M-16	64.4	12.5	53	51.5	5.9	0.0	0.4	0.5	0.0	2.8	0.34	0.0	0.0	179	152	-2.88
M-17	16.6	5.0	43	22.6	18.9	0.3	0.4	0.1	0.0	0.0	0.78	0.0	1.5	168	528	
M-18	51.6	10.6	50	51.6	24.2	0.1	0.6	0.5	0.1	0.9	0.71	0.0	0.0	164	159	-1.42
M-20																
M-23	40.6	7.5	43	38.4	17.3	0.0	0.7	0.3	0.0	1.0	0.71	0.0	0.5	146	186	-4.03
M-24	67.8	14.6	65	64.0	11.5	0.2	0.3	0.5	0.1	1.4	0.64	0.0	0.0	160	128	
M-25																
M-27																-3.21
M-31	55.3	16.3	49	49.0	9.6	0.0	0.7	0.5	0.0	1.1	0.66	0.0	0.0	178	151	
M-33	45.6	6.0	63	41.6	21.2	0.0	0.8	0.3	0.0	0.6	0.46	0.0	0.6	111	143	
M-36																-7.19
M-37	49.1	10.1	47	56.1	10.6	0.0	0.5	0.4	0.0	2.1	0.66	0.0	0.0	170	151	
M-41																
M-42	50.1	7.9	44	53.6	5.6	0.0	0.4	0.3	0.0	2.3	0.50	0.0	0.0	123	151	
M-46	54.7	12.4	62	53.5	11.7	0.2	0.6	0.4	0.0	2.1	0.51	0.0	0.0	167	160	-4.35
M-48	50.0	13.9	56	52.6	3.1	0.1	0.2	0.4	0.0	2.6	0.74	0.0	0.0	173	173	-5.67
M-50	58.3	17.7	62	51.8	32.5	0.0	0.9	0.4	0.0	1.2	1.66	0.0	0.0	163	147	
M-53	53.9	15.6	54	58.7	0.7	0.0	0.1	0.4	0.0	1.8	1.23	0.0	0.0	154	134	
M-55																-7.18
M-57	51.3	11.4	47	56.1	5.6	0.0	0.2	0.4	0.0	2.3	0.60	0.0	0.0	132	139	-9.03
M-60	26.0	9.9	39	60.7	128.4	0.3	2.6	0.2	0.1	0.0	2.22	0.2	0.8	89	150	-7.61
M-62																-3.69
M-64																-9.21
M-65	38.6	16.2	52	51.5	10.7	0.1	0.1	0.4	0.0	2.1	0.30	0.0	0.0	150	142	-5.83
M-66																-5.32
M-67	28.7	5.8	79	75.4	110.5	0.1	1.6	0.2	0.1	0.9	4.99	0.1	1.9	74	118	
M-68	28.8	25.2	6	5.1	33.9	0.0	0.5	0.5	0.2	3.5	1.85	0.1	0.0	190	149	-8.94
M-69	43.1	12.2	41	70.2	21.0	0.1	0.9	0.3	0.0	1.4	0.81	0.0	0.0	128	167	-4.60
M-71																-9.32
M-72	44.6	13.5	52	74.5	20.6	0.1	0.4	0.4	0.0	1.3	0.63	0.0	0.0	147	167	-5.82
M-73																-9.27
M-74	33.2	10.2	45	45.1	27.5	0.2	2.2	0.2	0.0	0.0	4.95	0.2	1.1	62	128	
M-75	37.1	15.9	63	68.5	41.0	0.2	1.0	0.4	0.0	2.1	1.26	0.0	0.0	133	166	-3.58
M-77	40.1	10.1	39	49.0	11.0	0.0	0.2	0.3	0.0	1.6	0.24	0.0	0.0	115	153	-5.85
M-78	42.1	8.8	41	68.8	26.9	0.2	0.1	0.4	0.0	1.4	0.48	0.0	0.0	139	150	-9.27
M-79	50.7	16.6	46	78.5	80.8	0.4	7.6	0.4	0.2	1.1	4.46	0.4	1.2	114	160	
M-82																-6.38
M-84	34.6	10.1	42	60.2	22.8	0.1	0.4	0.3	0.0	1.3	0.65	0.0	0.0	112	148	-6.36
M-85																0.28
M-87																-0.57
M-88	54.0	13.0	90	97.0	51.4	0.3	3.4	0.2	0.2	0.7	1.83	0.1	1.6	67	119	
M-89																-3.29
M-90	49.1	11.9	39	42.2	21.5	0.0	0.3	0.4	0.0	2.2	0.46	0.0	0.0	138	143	
M-92	49.3	11.6	52	83.0	14.9	0.0	0.3	0.4	0.0	1.9	0.53	0.0	0.0	148	142	-6.34

TABLE 2 CONTINUED

Samples of the Maiersdorf-trench

Sample-Nr.	^{18}O [VPDB]	TOC	$CaCO_3$ [%]	Th/U	Cr/Ni	Cr/V	Y/Ni	TOC/S	CIA	CPA	Interpreted facies
M-1		33.75	0	0.84	2.11	0.69	0.58	9.3	80.71	97.73	marine
M-1B				0.58	4.36	0.21	0.67		77.82	96.33	
M-2	-5.73	1.68	20								marine
M-3		0.15	0	4.13	2.82	0.69	0.96		74.45	95.40	marine
M-4	-5.67	1.80	16								marine
M-5	-6.42	26.30	17	1.43	0.97	0.80	0.34	5.4	75.82	95.91	
M-6		0.56	0	3.09	3.35	0.68	0.74	5.1	78.93	97.40	marine
M-7	-6.40	4.85	12	2.02	2.30	0.70	0.62	1.6	75.76	96.23	marine
M-8B			9								
M-9A	-5.84	0.09	13								marine
M-9B		1.06	4	1.92	2.79	0.66	0.50	8.2	82.96	98.11	marine
M-12		12.05	9	2.30	1.80	0.64	0.41	23.6	77.04	96.64	non-marine
M-13			0								
M-16	-5.27	0.62	10	3.78	2.62	0.72	0.56	8.8	77.44	97.13	non-marine
M-17		52.80	0	0.35	1.49	0.34	0.58	211.2	76.84	96.82	
M-18	-5.15	2.16	13	3.29	2.23	0.78	0.53	2.2	75.54	96.12	non-marine
M-20			0								
M-23	-5.97	0.35	20	3.47	1.94	0.55	0.75	0.9	72.31	93.56	marine
M-24		0.46	0	3.88	2.01	0.59	0.48	1.8	77.78	97.15	marine
M-25			4								
M-27	-6.51	1.72	11								marine
M-31		0.58	0	3.89	2.62	0.65	0.61	29.2	75.91	96.71	marine
M-33		2.09	9	2.94	2.60	0.86	0.75	52.3	72.26	92.65	non-marine
M-36	-8.41	0.12	20								non-marine
M-37		0.18	6	5.00	2.17	0.64	0.57		76.01	96.64	non-marine
M-41			0								
M-42		0.04	0	3.47	1.76	0.65	0.62		74.78	94.92	non-marine
M-46	-6.86	0.33	13	3.36	2.02	0.62	0.54		76.50	96.85	marine
M-48	-7.09	0.09	14	3.91	1.93	0.65	0.61		75.84	96.63	marine
M-50		0.19	4	3.92	2.09	0.58	0.63		75.41	96.07	non-marine
M-53		0.05	0	4.91	2.19	0.71	0.49		77.57	97.63	non-marine
M-55	-7.43	0.11	18								non-marine
M-57	-8.34	0.11	11	3.85	1.69	0.66	0.60		74.78	95.45	non-marine
M-60	-8.39	6.41	19	2.07	1.11	0.64	0.42	49.3	76.92	96.19	non-marine
M-62	-6.78	0.12	18								non-marine
M-64	-8.46	0.14	18								non-marine
M-65	-7.44	0.17	18	4.90	2.49	0.97	0.46		73.79	95.65	marine
M-66	-7.42	0.24	21								marine
M-67		21.45	0	2.00	0.90	0.73	0.39	26.2	78.29	96.27	
M-68	-10.01	1.36	11	4.70	27.82	0.70	4.73		79.01	97.79	marine
M-69	-6.37	0.08	17	3.85	1.25	0.76	0.44		73.79	94.34	marine
M-71	-8.85	1.89	14								marine
M-72	-7.04	0.24	18	4.43	1.45	0.73	0.42		74.99	95.64	marine
M-73	-9.03	0.98	12								marine
M-74		26.90	0	1.86	1.35	0.68	0.51	1345.0	77.21	96.54	
M-75	-6.49	0.17	22	3.65	1.48	0.84	0.41		73.39	94.75	marine
M-77	-7.48	0.13	25	3.72	1.65	0.71	0.59		73.74	94.61	non-marine
M-78	-8.71	0.25	19	3.69	1.47	0.68	0.40		75.25	95.60	non-marine
M-79		7.36	0	1.98	1.29	0.59	0.36	29.4	74.89	95.01	non-marine
M-82	-7.97	0.19	22								non-marine
M-84	-7.53	0.20	27	4.15	1.35	0.68	0.43		74.18	94.89	marine
M-85	-5.35										marine
M-87	-5.40	0.70	47								marine
M-88		21.45	5	2.12	0.98	0.85	0.29	32.5	80.33	96.85	
M-89	-6.98	0.48	26								marine
M-90		0.41	4	4.17	2.88	0.83	0.68		78.68	96.44	non-marine
M-92	-7.86	0.19	16	4.38	1.72	0.68	0.43		76.49	96.38	non-marine

TABLE 2 CONTINUED

5.1.2 Carbon, oxygen and strontium isotopes as a tool to decipher marine and non-marine environments: Implications from a case study of cyclic Upper Cretaceous sediments

Hofer, G., Wagreich, M. & Spötl, C., 2013. Geological Society of London, Special Publications: Isotopic Studies in Cretaceous Research 382/1.

Date of submission: 20.02.2012
Date of acceptance: 08.10.2012

Comment of the author concerning the degree of participation
The entire manuscript was written by Gerald Hofer (supported by co-authors). Sample collection, preparation for isotope analysis and interpretation were performed by the author.
Isotope analysis was performed by C. Spötl.
Calcareous nannofossil data was analyzed and edited by M. Wagreich.

Article structure, numbering and type of quotations are maintained as requested in the journal.

Abstract

The interplay of Late Cretaceous basin subsidence and sea-level oscillations produced a mixed freshwater-marine succession within the Upper Cretaceous Gosau Group of the Northern Calcareous Alps. Cored sections from wells of the Glinzendorf and Gießhübl Syncline, as well as sediments from the outcrop area of Grünbach-Neue Welt and Slovakian equivalents have been investigated for their stable isotopic composition. Bulk carbonate $\delta^{13}C$ and $\delta^{18}O$ values of 116 fine-grained samples (shales, siltstones, marls) and $^{87}Sr/^{86}Sr$ values of 10 samples from the borehole Markgrafneusiedl T1 were analyzed in order to distinguish between non-marine and marine deposits and to compare and correlate isotope characteristics of the different Gosau synclines and basins.

Non-marine samples have significantly lower mean $\delta^{13}C$ values compared to the mean of marine samples. The discrimination between a marine and non-marine group using $\delta^{18}O$ is also statistically highly significant even though the difference between the average non-marine and marine values is small. Strontium isotope values of marine intervals are near the range of values of normal Upper Cretaceous seawater but show a trend towards higher ratios in marginal marine and non-marine deposits. Although diagenesis and detrital carbonate admixture partly influence the isotopic composition, the original environmental signal can still be reliably identified.

Stable carbon and oxygen isotope data are widely used in sedimentology as an indicator for depositional conditions and facies (palaeoenvironment, palaeosalinity, palaeotemperature, etc.) because they reflect primarily the composition of the water from which the carbonate precipitated (Hudson 1977; Anderson & McArthur 1983; Talbot 1990; Reinhardt *et al.* 2003). The primary goals of our study are twofold: (a) to test the applicability of stable isotopes to distinguish between freshwater-brackish and marine deposits, and (b) to evaluate how and to what extent this tool can be used in a complex basinal setting affected by diagenesis and the presence of detrital carbonate.

The data used for this study stem from an applied petroleum geology project aimed at comparing the isotope (C, O, Sr) characteristics of different Upper Cretaceous to Paleocene basins in eastern Austria and western Slovakia, including industrial well data from below the Neogene Vienna Basin. In addition to isotope data other geochemical as well as micropalaeontological data (Hofer *et al*. 2011) are available from these samples. These data are used to unravel palaeogeographic relationships and stratal correlations in this area where the

differentiation of marine and non-marine intervals is challenging. An area of special interest is the Upper Cretaceous Glinzendorf Syncline, where classical facies analysis using thin-sections and micropalaeontologic methods yielded ambiguous results, partly because the fossil content is extremely low (Wessely 2006). These sediments have previously been considered as mainly limnic due to the lack of fossils, and correlated to outcrops of the Campanian Grünbach Formation of the Grünbach Syncline (Wessely 1992, 2006). Recent petrographical and geochemical analyses (Hofer 2009, Hofer *et al*. 2011, and in press), however, indicate a strong marine influence in the Glinzendorf Syncline. Correlations of these Upper Cretaceous to Paleogene strata are of great significance for hydrocarbon exploration in the Vienna Basin, because these successions act as seals for gas (e.g. Zimmer & Wessely 1996).

Carbon and oxygen isotope compositions of carbonate depend in principle on the isotopic composition of the water (related to salinity; Veizer 2003) from which the carbonate precipitates (Anderson & McArthur 1983), as well as on temperature, pH (Hudson 1977; Veizer 2003) and the carbonate speciation. Freshwater is characterised by distinctly lower $\delta^{13}C$ and $\delta^{18}O$ values than seawater (Hoefs 2009). However, carbon and oxygen isotope variations in seawater can be significant especially in coastal regions near river mouths (Schmidt 1999; Schmidt *et al*. 1999; Bigg & Rohling 2000). Diagenesis can influence the isotopic composition in different ways, e.g. by precipitation of new carbonate phases (Hudson 1977). Carbon isotopes are widely used in combination with oxygen isotopes to interpret the origin and facies (palaeoenvironment, palaeosalinity, water temperature, etc.) of carbonate sediments (Clayton & Degens 1959; Hudson 1977; Veizer 1983; Talbot 1990; Reinhardt *et al.* 2003). In general, marine carbonates have $\delta^{13}C$ values between -3 and 5 ‰, while limnic carbonates show values between -2 and -9 ‰ (Hudson 1977). Veizer (1983) characterized typically shallow-marine carbonates by $\delta^{13}C$ values between 2 and 4.5 ‰ and $\delta^{18}O$ values between -0.5 and 1.5 ‰, but the range can locally also be larger and typically biased towards lower $\delta^{13}C$ and $\delta^{18}O$ values (Hamon & Merzeraud 2007; Marquillas *et al*. 2007; Colombié *et al*. 2011). In contrast, deep-sea carbonates show $\delta^{13}C$ and $\delta^{18}O$ values of 0 to 2 ‰ and 1 to 3 ‰, respectively. Freshwater carbonates are characterized with distinctively lower $\delta^{13}C$ values between -2 and -17 ‰ and $\delta^{18}O$ values between 4 (in arid settings) and -10 ‰. Keith & Weber (1964) introduced an empirical Z-value ($Z = 2.048 (\delta^{13}C + 50) + 0.498 (\delta^{18}O + 50)$) in order to discriminate between marine and non-marine carbonates using $\delta^{13}C$ and $\delta^{18}O$ values, which has also been successfully applied in more recent studies (e.g. Cuna *et al*. 2001; Narayanan *et al*. 2007).

Strontium isotopes are incorporated into carbonate minerals without significant fractionation because of the small mass difference. The oceanic $^{87}Sr/^{86}Sr$ ratio is controlled by the riverine input of Sr (tectonic background and erosion rate of the continental crust) and the exchange of

seawater with the young and hot oceanic crust at mid-ocean ridges. The isotopic composition of the seawater has also been influenced by ^{87}Sr production from ^{87}Rb decay over geological times (Veizer 2003). Detailed studies concerning the Sr-isotope composition of the ocean are given by Veizer *et al.* (1999) and Jones & Jenkyns (2001) and used for strontium isotope stratigraphy by, e.g., McArthur *et al.* (2001). $^{87}Sr/^{86}Sr$ isotope ratios are widely used in the literature as an indicator of palaeosalinity mainly in combination with other isotope systems like carbon, oxygen and sulphur (Reinhardt *et al.* 1998, 2003; Schmitz *et al.* 1997; Ingram *et al.* 1998; Holmden & Hudson 2003; Peros *et al.* 2007).

Geological Setting

In the entire Northern Calcareous Alps (NCA), which form part of the Eastern Alps, sediments of the Upper Cretaceous to Paleogene Gosau Group were deposited after the Early Cretaceous Eoalpine orogeny, unconformably overlying folded and faulted Permian to Lower Cretaceous rocks. Generally, the Gosau Group can be divided into the Lower Gosau Subgroup comprising fluvial, lacustrine to shallow-marine sediments of Turonian to Santonian-Campanian (in some areas even Maastrichtian) age, and the Upper Gosau Subgroup characterised by deep-water successions up to Eocene in age (Wagreich & Faupl 1994; Faupl & Wagreich 1996; Hofer *et al.* 2011). Different Gosau Group strata are exposed in the eastern part of the NCA and along the south-western margin of the Vienna Basin (Austria) within all three major thrust systems (i.e. from north to south, the Bajuvaric, Tirolic and Juvavic nappes - e.g. Mandl 2000). These strata continue as NE-SW-striking synclines underneath the Neogene fill of the Vienna Basin (Fig. 1) and can be traced across several oil company wells, and are exposed again at the north-eastern margin of the basin, in the western part of the Western Carpathians (Slovakia). These synclines comprise from north to south the Gießhübl Syncline, the Prottes Gosau Group, the synclines of Brezová and Studienka (Upper Cretaceous to Paleogene Brezová and Myjava Group), the Grünbach Syncline and the Glinzendorf Syncline (Wessely 1974, 1984, 1992, 1993, 2000, 2006; Plöchinger 1961; Zimmer & Wessely 1996; Wagreich & Marschalko 1995; Fig. 1).

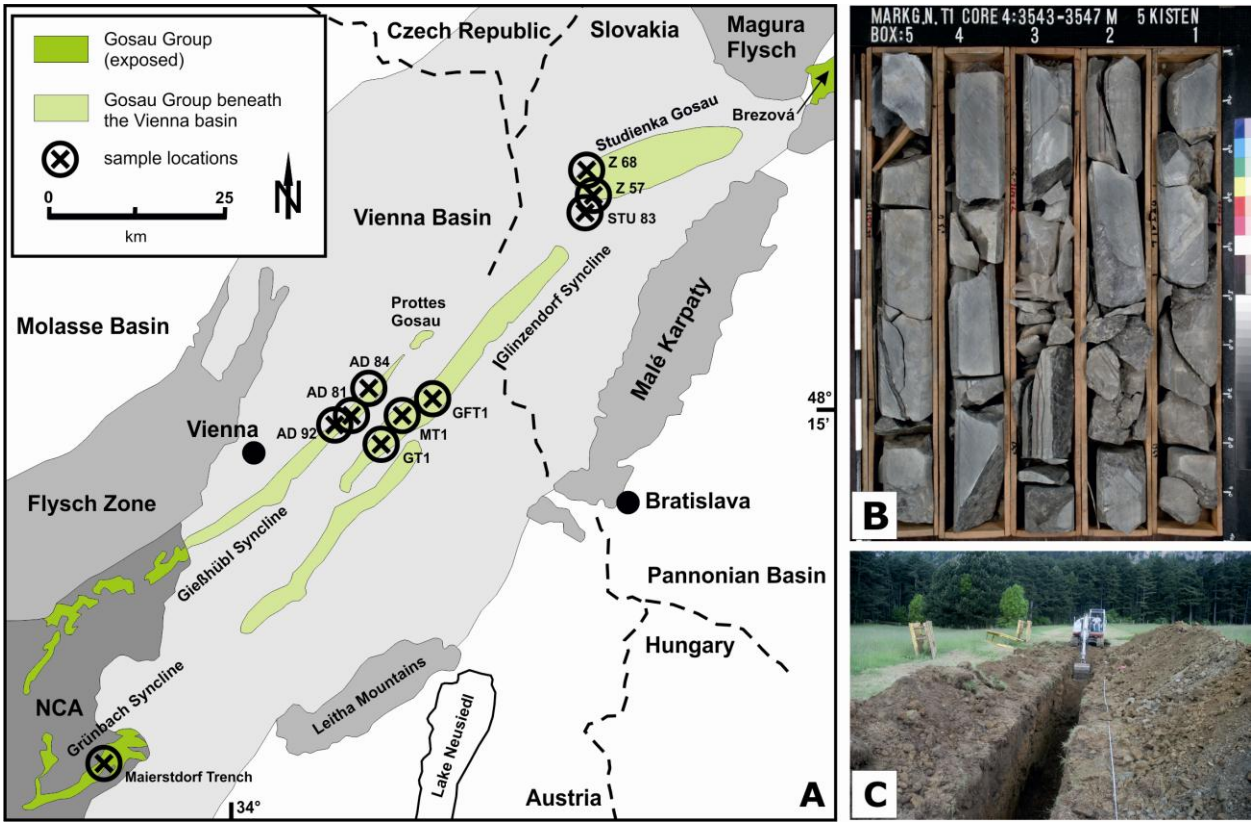


Fig. 1. (a) Simplified geological map of the eastern part of the Eastern Alps (Austria), the pre-Neogene Vienna Basin and the western part of the Western Carpathians (Slovakia) after Wagreich & Marschalko (1995). The Gosau Group in outcrops and underneath the Neogene Vienna Basin is highlighted in green. (b) Cores from Markgrafneusiedl T1 well. (c) Picture of the 141 m-long (45 m stratigraphic profile) trench in Maiersdorf (Lower Austria).

The Coniacian to Paleocene Gosau Group fill of the Gießhübl Syncline, tectonically related to the Bajuvaric thrust system (Faupl & Wagreich 1996), starts with shallow-marine clastics (sandstones and breccias) followed by the Upper Santonian to Lower Maastrichtian Nierental Formation (Wessely 2006), i.e. pelagic to hemipelagic slope strata (see palaeogeographic reconstruction in Fig. 2) which mainly comprise calcareous marls (Krenmayr 1999; Wagreich & Krenmayr 2005; Wagreich *et al.* 2011). The overlying deep-marine Gießhübl Formation, with its flysch turbidites deposited below the calcite compensation depth (CCD), ranges up to the Thanetian (Wessely 1992; Wagreich 2001).

The Prottes Gosau Group is located on top of northern Tirolic units underneath the Neogene of the Vienna Basin. It is mainly composed of coarse-grained clastics such as conglomerates and breccias, as well as marly limestone successions from the Coniacian to the Paleocene (Wessely 2006).

The Tirolic Glinzendorf Syncline, which can be traced over several OMV- and NAFTA wells including Gänserndorf ÜT3, T3, Markgrafneusiedl 1, N1, T1, Glinzendorf 1 and T1 (e.g.

Wessely 2006), Gajary 125 (Ralbovsky & Ostrolucký 1996; Mišík 1994) and Záhorska Ves, is supposed to be an easterly equivalent of the Grünbach Syncline (e.g. Wessely 2006). Limnic to marginal-marine facies dominate the several hundred meter-thick sequence of the Glinzendorf Syncline starting in the Santonian-Campanian with dark marls and mudstones including also some conglomerates and coal layers (Wessely 1992, 2006; Sachsenhofer & Tomschey 1992). Terrigenous mudstones, marls and sandstones top the marine interval (Wessely 2006). Similar to that, a lower and upper conglomeratic non-marine red interval and an intercalation of a marine grey sediment has been described from the Slovakian part (well Gajary 125) of the Glinzendorf Syncline (Mišík 1994). The succession ends probably in the Maastrichtian (Wessely 1992; Pavlishina *et al.* 2004), but a Paleocene age of the topmost sediments cannot be excluded due to ambiguous and spurious microfossil data (Ralbovsky & Ostrolucký 1996).

Gosau Group sediments of the Grünbach Syncline (Santonian to Paleocene) are exposed at the south-western margin of the Vienna Basin near Grünbach – Neue Welt within mainly Juvavic thrust units (Plöchinger 1961) and continue NE-SW-striking underneath the Neogene of the basin. Above Upper Santonian basal conglomerates and breccias follows the shallow-marine Maiersdorf Formation with its sandy limestones (including corals, brachiopods and gastropods) and reef-forming rudist limestones (*Hippurites*) reflecting a major transgressive trend (Summesberger *et al.* 2002; Steuber 2004). The Lower Campanian limnic to brackish/shallow-marine Grünbach Formation is characterized by shales, marls and fine-grained sandstones with coal seams as well as some conglomeratic horizons similar to units at the base of the Glinzendorf Syncline (Summesberger *et al.* 2002; Wessely 2006). Several marine to non-marine cycles were recognized within this formation (Hofer *et al.* 2011). The Piesting Formation (Late Campanian to Maastrichtian) represents deeper marine conditions with marls and sandstones with orbitoids (Hradecká *et al.* 1999), followed by turbiditic sandstones and marls of the Paleocene Zweiersdorf Formation (Summesberger *et al.* 2002).

The correlation of the Slovakian Upper Cretaceous Brezová Group (Coniacian to Maastrichtian) and the Paleogene Myjava Group (Paleocene to Eocene) of the Brezová outcrop area (Wagreich & Marschalko 1995) and the Studienka Gosau Group striking ENE underneath the Slovakian part of the Vienna Basin (Fig. 1) is still being debated. A connection to the Gießhübl Syncline is likely (Wagreich & Marschalko 1995), but a correlation with the Prottes Gosau Group seems also possible (Wessely 1992). Following continentally-influenced transgressive clastics a neritic shelf marl facies was deposited (Wagreich & Marschalko 1995). Calcareous bathyal marls are similar to the Nierental Formation in the NCA. Further deepening of the basin caused the sedimentation of turbiditic sandstones and marls (Upper Campanian to Maastrichtian) and

continues into the Myjava Group. Deposition underneath the CCD is suggested for these formations analogous to the Gießhübl Formation (Wagreich & Marschalko 1995).

A schematic palaeogeographic map of investigated Gosau basins and principal facies distributions of Santonian/Campanian age is given in Fig. 2.

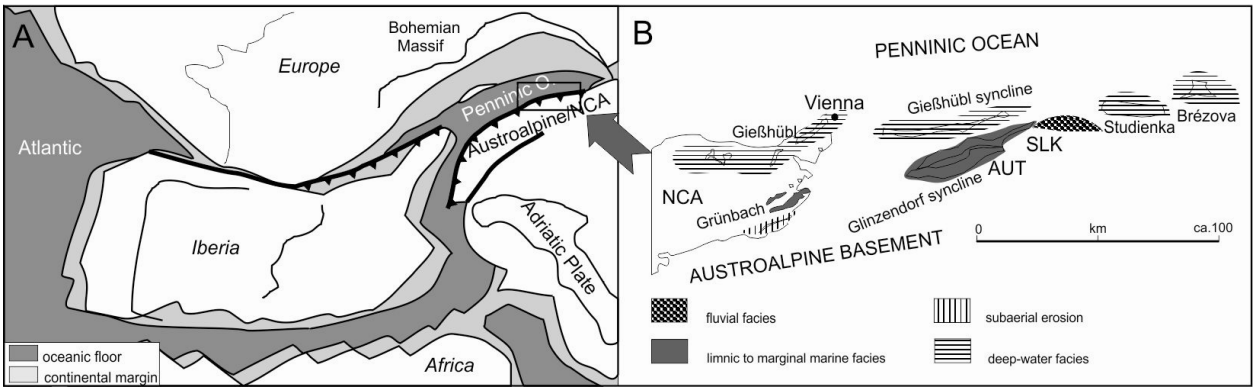


Fig. 2. (a) Schematic palaeogeographic map for the Campanian-Maastrichtian of the western Tethys, simplified from Wagreich *et al.* (2009). NCA – Northern Calcareous Alps. Inset rectangle shows area of detailed map. (b) Palaeogeographic arrangement of Gosau basins and principal facies distribution around Santonian/Campanian boundary; AUT = Austria, SLK = Slovakia.

Methods

Cores of fine-grained pelitic sediments (shales, siltstones or marly sediments) from the OMV core repository (wells Aderklaa 81, 84 and 92, Gänserndorf T3, Glinzendorf T1, Markgrafneusiedl T1, Studienka 83 and Závod 57 and 68) and samples from an artificial trench in Grünbach (Maiersdorf, Lower Austria; Hofer *et al.* 2011) were investigated for their stable isotope composition of carbon and oxygen (Figs. 1 and 3). The $\delta^{13}C$ and $\delta^{18}O$ isotope values of 116 shaly sediment samples from all locations (carbonate content generally around 30 wt.%) as well as the $^{87}Sr/^{86}Sr$ ratios of 10 samples from the Markgrafneusiedl T1 well were analyzed. Only homogeneous samples lacking calcitic veins or visually detectable detrital particles were used. Thin sections of several samples did not show any indication of significant diagenetic effects such as recrystallisation.

Labels of the core samples consist of the well code (Aderklaa = AD, Gänserndorf T3 = GFT3, Glinzendorf T1 = GT1, Markgrafneusiedl MT1 = MT1, Studienka = STU, Závod = Z) and a number representing the depth (or depth range) in metres. Outcrop samples are numbered as collected in the field (Maiersdorf trench = M-No.).

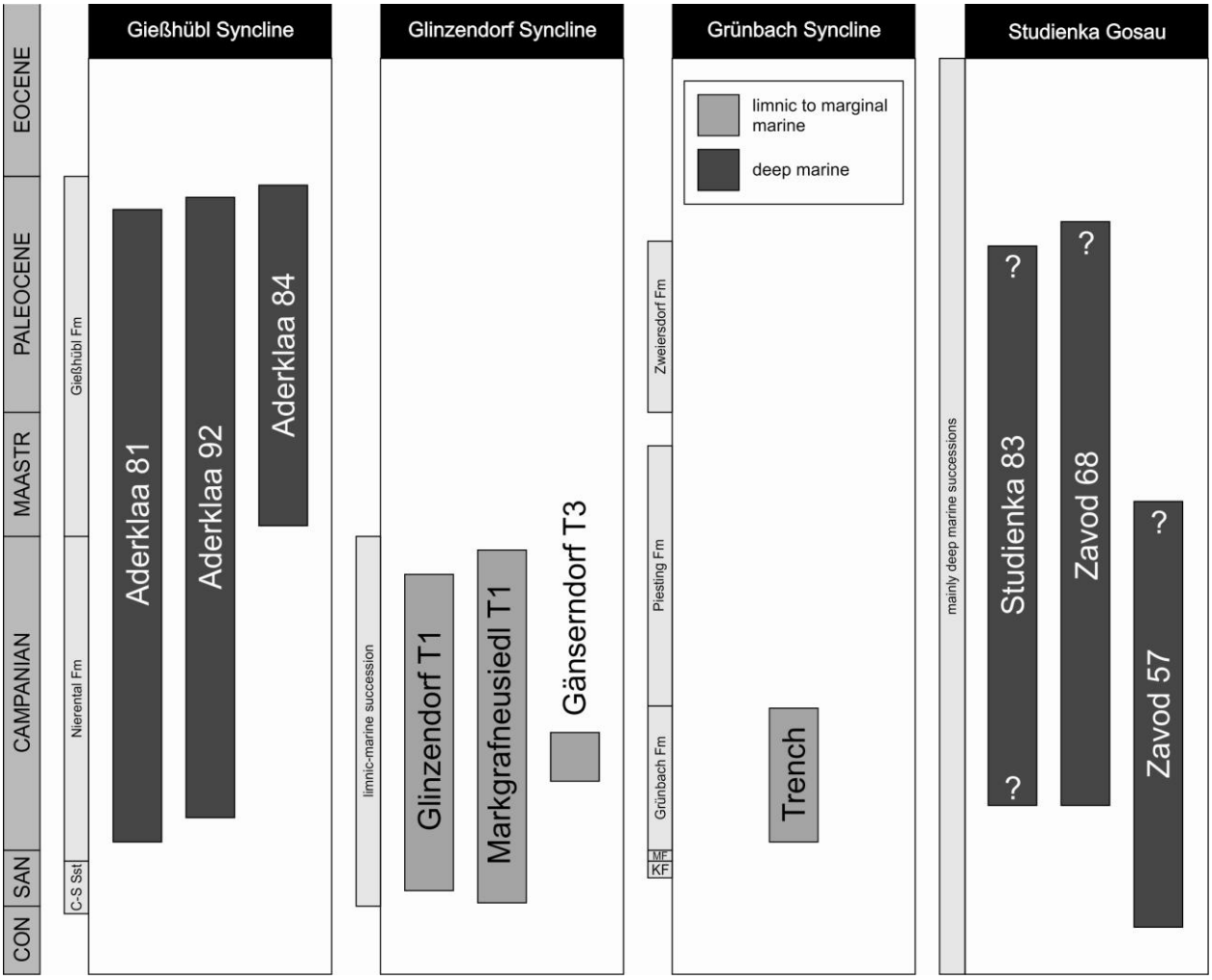


Fig. 3. Schematic stratigraphic distribution of Gosau successions of the boreholes Aderklaa 81, 84 and 92, Glinzendorf T1, Markgrafneusiedl T1, Gänserndorf T3, Studienka 83, Zavod 57 and 68 as well as the artificial trench section in Maiersdorf. The profiles are roughly separated into limnic to marginal marine and deep marine intervals. The stratigraphic classification of the Slovakian wells is very inaccurately (marked with "?") and a correlation to formations of that area not known. C-S Sst: Coniacian-Santonian sandstones; KF: Kreuzgraben Formation; MF: Maiersdorf Formation.

The carbon and oxygen isotope compositions of 0.1 to 0.3 mg of untreated bulk carbonate samples were determined using an on-line preparation device (Gasbench II) interfaced to a ThermoFinnigan isotope ratio mass spectrometer at the University of Innsbruck. The calibration was performed against VPDB using an in-house marble standard previously calibrated against international reference standards. The long-term analytical uncertainty for $\delta^{13}C$ and $\delta^{18}O$ is 0.06 and 0.08 ‰, respectively (for details see Spötl & Vennemann 2003).

In order to investigate the issue of detrital admixture, 18 samples from different localities (Aderklaa 81, 84, 92, Závod 68, Studienka 83 and Maiersdorf trench) were analyzed using powder X-ray diffraction (XRD) and the abundance of dolomite was quantified following Schultz

(1964). The presence of a significant dolomite content is regarded as indicative of reworked Triassic carbonate (mainly Hauptdolomit) even though the dolomite analyzed by XRD cannot be definitely related to a particular Triassic dolomite unit. In addition, several selected thin sections from well Markgrafneusiedl T1 were investigated for cathodoluminescence (CL) using a cold cathode system (CITL 8200 MK3, attached to a Leitz light microscope).

Ten bulk rock carbonate samples were washed and dissolved in 5 N acetic acid and Sr was separated by ion-exchange chromatography. The $^{87}Sr/^{86}Sr$ ratios were analyzed using a Triton thermal ionization mass spectrometer at the Geochronological Laboratory of the Department of Lithospheric Research, Centre for Earth Sciences, University of Vienna). Analytical errors were in the range of ±0.000005. Calibration was performed against standard NBS 987.

Additional samples from non-marine to marginal marine sections (e.g. from the Glinzendorf Syncline and the Grünbach Formation of the Grünbach Syncline) were analyzed for their content of calcareous nannofossils in order to identify marine intervals by an independent method. Standard smear slide techniques (e.g. Wagreich *et al.* 2012) and a light microscope were used for studying nannofossils.

The statistic evaluation of the data (Student´s t-test and the discriminatory analysis) was done using *IBM SPSS Statistics 19.0*. The Student´s t-test investigates the significance of the difference of the mean values between two groups (if equality of variances between the groups was not given, Welch´s t-test was used). The discriminatory analysis is a multivariate statistical technique that studies differences between two or more groups of objects with respect to several variables simultaneously (Bühl 2008; see also Backhaus *et al.* 2006).

Results

Nannofossils

Nannofossil presence data are used to infer marine intervals. Data are available for the Markgrafneusiedl T1 borehole where nannofossils are missing from the lower part and start at a depth of 3933 m with a continuous record in the middle part of the borehole up to 3406 m (nannofossil standard zones CC16/17 of the zonation of Perch-Nielsen 1985, indicating a Santonian age). Above that, samples are again barren of nannofossils, thus indicating an upper non-marine (brackish to freshwater) interval (Fig. 4). Samples from Glinzendorf T1 lack nannofossils except one sample at 3717 m which contains a questionable mixed Cretaceous-Cenozoic nannofossil assemblage which may be attributed to drilling contamination. Above 3249 m, nannofossils are continuously present (Fig. 5; again nannofossil zones CC16/17).

Gänserndorf T3 shows again a lower part without nannofossils and, beginning at 3083 m depth, a poor but continuous presence of nannofossils indicating a marine upper part (Fig. 5).

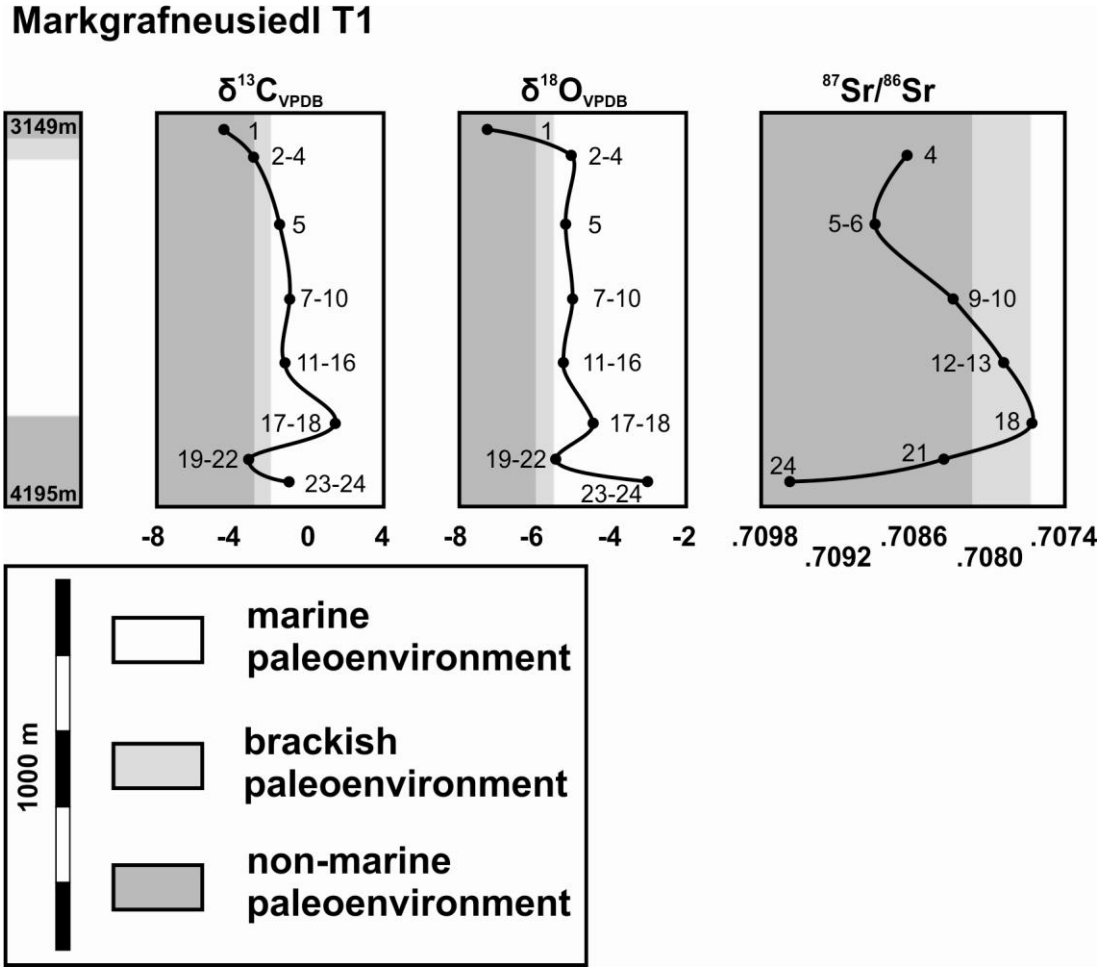


Fig. 4. Carbon, oxygen (in ‰ relative to VPDB) and Sr isotope data and palaeoenvironmental interpretation of sediments in well section Markgrafneusiedl T1. Values from several close-by samples were combined to a single value. Sample numbers in the figure are explained in Table 1.

Nannofossil (and foraminiferal) data from the Gießhübl Syncline boreholes Aderklaa 81, 84 and 92 and the Slovakian boreholes Studienka 83, Závod 57 and 68 indicate a fully marine, deep-water environment (Fig. 5) due to the abundance of nannofossils (and planktonic foraminifera) based on unpublished internal OMV-reports and a few test samples obtained from the Slovakian boreholes. Nannofossil data from the Grünbach Formation of the Grünbach Syncline (Hofer *et al*. 2011) indicate the presence of at least five marine intervals separated by non-marine (nannofossil-barren) intervals (Fig. 6). Nannofossil data from the base of the Grünbach Formation indicate a late Santonian to early Campanian age (CC17).

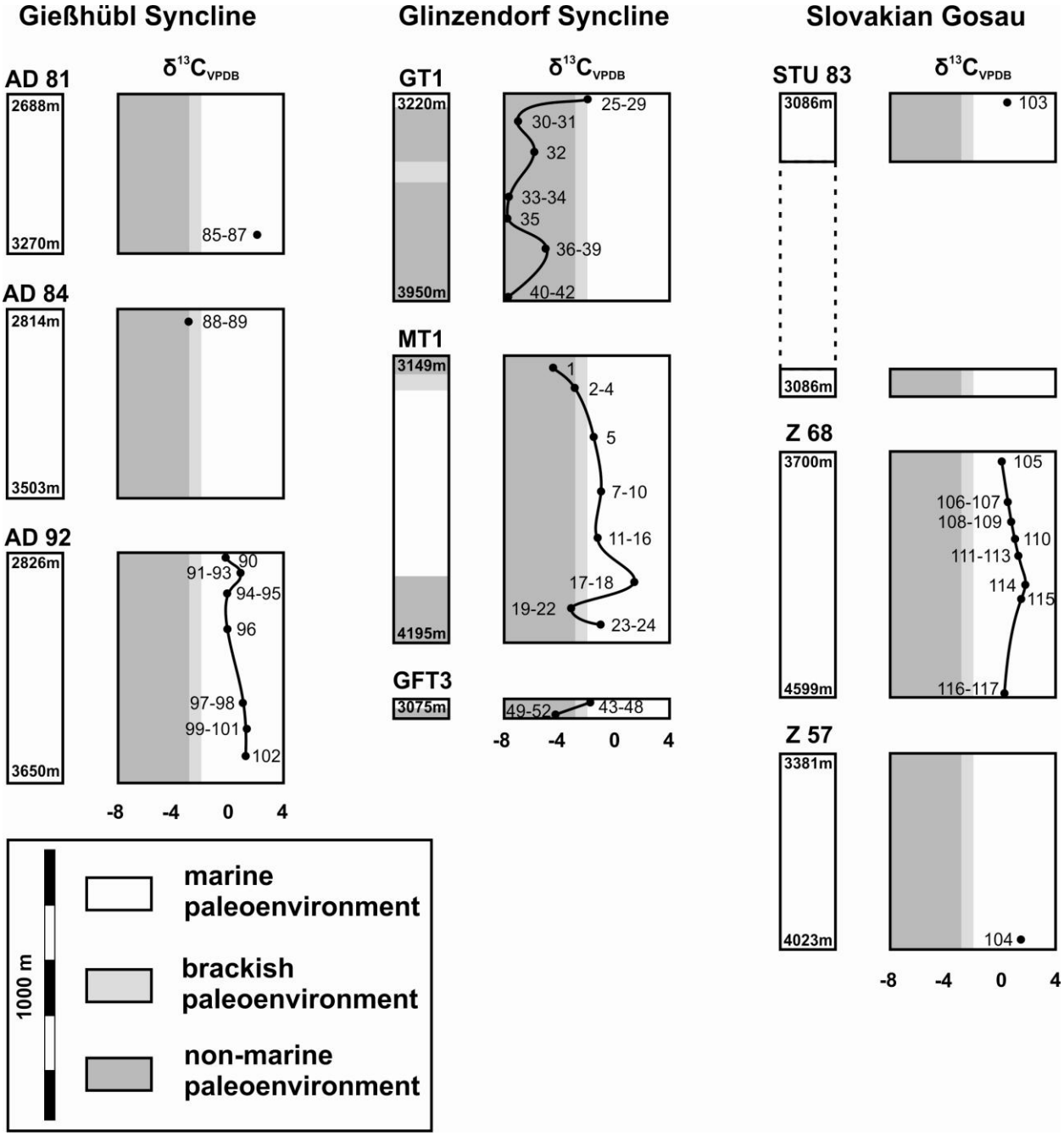


Fig. 5. Carbon isotope data (in ‰ relative to VPDB) and palaeoenvironmental interpretation of sediments in the the wells Aderklaa 81 (AD 81), 84 (AD 84), 92 (AD 92), Glinzendorf T1 (GT1), Markgrafneusiedl T1 (MT1), Gänserndorf T3 (GFT3), Studienka 83 (STU 83), Závod 57 (Z 57) and 68 (Z 68). Values from close-by samples were combined to a single value. Sample numbers in the figure are explained in Table 1.

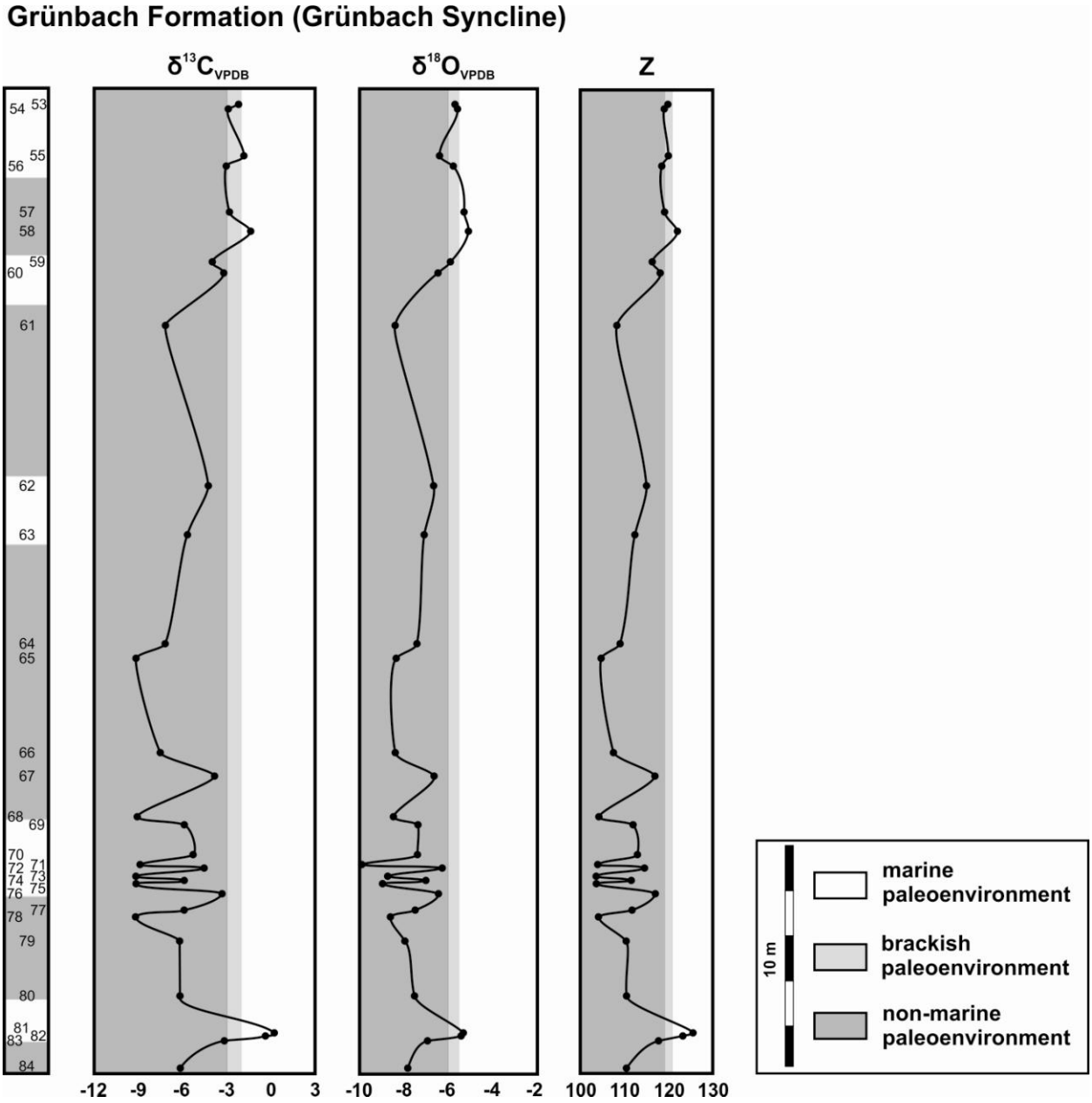


Fig. 6. Schematic profile of the trench in Maiersdorf (Grünbach Fprmation, Grünbach Syncline). Carbon and oxygen isotope values (in ‰ relative to VPDB) and Z-values after Keith & Weber (1964) are plotted. Sample numbers in the figure are explained in Table 1.

Isotopes

$\delta^{13}C$ and $\delta^{18}O$ data scatter between -9.3 and 2.2 ‰ and -10.0 and -1.5 ‰, respectively (Table 1) and show a highly significant positive correlation with a Pearson correlation index of 0.75 (Fig. 7).

Table 1: *Results from isotope analysis.*

Results of the carbon, oxygen and strontium isotope analyses of samples from the well sections Glinzendorf T1 (GT1), Markgrafneusiedl T1 (MT1) and Gänserndorf T3 (GFT3) from the Glinzendorf yncline, Aderklaa 81 (AD 81), 84 (AD 84) and 92 (AD 92) from the Gießhübl Syncline, Studienka 83 (STU 83), Závod 57 (Z 57) and 68 (Z 68) from the Slovakian equivalents and from the artificial trench at Maiersdorf (Grünbach Syncline).

Glinzendorf Syncline:						
Samples	**Sample no. in graphs**	**$d^{13}C$ [VPDB]**	**$d^{18}O$ [VPDB]**	**Z**	**$^{87}Sr/^{86}Sr$**	**interpret. facies**
MT1-3207.80	1	-4.2	-7.4	114.9	na	non-marine
MT1-3272.10	2	-3.2	-4.9	118.3	na	non-marine
MT1-3272.50-60	3	-2.5	-5.3	119.5	na	non-marine
MT1-3275.30-43	4	-3.1	-5.2	118.4	0.7087	non-marine
MT1-3406.20-30	5	-1.6	-5.2	121.4	0.7079	marine
MT1-3409.70-82	6	na	na	na	0.7098	marine
MT1-3544.45-65	7	-1.4	-5.0	122.0	na	marine
MT1-3545.90-3546	8	-1.0	-5.1	122.8	na	marine
MT1-3546.25-55	9	-1.1	-5.1	122.6	0.7083	marine
MT1-3547.50-65	10	-0.8	-5.1	123.1	0.7082	marine
MT1-3743.55-60	11	-1.2	-5.0	122.4	na	marine
MT1-3743.90-3744	12	-1.1	-5.3	122.5	0.7080	marine
MT1-3744.10-20	13	-1.5	-5.3	121.6	0.7079	marine
MT1-3745.50	14	-1.4	-5.4	121.7	na	marine
MT1-3746.50-3747	15	-1.3	-5.1	122.2	na	marine
MT1-3747.20	16	-1.5	-5.4	121.5	na	marine
MT1-3931.10-30	17	2.0	-4.4	129.2	na	marine
MT1-3933.20-50	18	0.8	-4.6	126.7	0.7076	marine
MT1-4023.50 B	19	-3.4	-5.0	118.0	na	non-marine
MT1-4023.50 C	20	-3.7	-5.3	117.1	na	non-marine
MT1-4023.70	21	-2.9	-6.0	118.5	0.7084	non-marine
MT1-4026.20	22	-3.3	-5.4	117.9	na	non-marine
MT1-4106.50	23	1.3	-2.1	128.8	0.7096	non-marine
MT1-4107.10-30	24	-3.2	-4.0	118.8	na	non-marine
GT1-3245	25	-0.7	-5.0	123.4	na	marine
GT1-3246.5	26	-2.3	-6.0	119.5	na	marine
GT1-3247.5	27	-2.9	-6.5	118.2	na	marine
GT1-3249	28	-1.4	-5.2	121.7	na	marine
GT1-3249.5	29	-3.7	-6.7	116.5	na	marine
GT1-3308	30	-5.5	-5.8	113.1	na	non-marine
GT1-3308.8	31	-8.7	-7.3	105.9	na	non-marine
GT1-3361.5	32	-5.5	-6.8	112.7	na	non-marine
GT1-3552	33	-9.0	-3.1	107.4	na	marine
GT1-3554.5	34	-6.3	-6.0	111.4	na	marine
GT1-3615.2	35	-9.1	-7.9	104.7	na	non-marine
GT1-3713.5	36	-6.6	-5.1	111.3	na	non-marine

GT1-3714.5	37	-5.3	-5.9	113.5	na	non-marine
GT1-3716.5	38	-5.2	-5.2	114.1	na	non-marine
GT1-3717	39	-3.3	-5.1	117.9	na	non-marine
GT1-3947.5 R	40	-7.5	-5.6	109.2	na	non-marine
GT1-3948.5	41	-7.6	-5.8	108.8	na	non-marine
GT1-3949.5	42	-7.6	-6.2	108.6	na	non-marine
GFT3-3079	43	0.2	-5.4	124.9	na	marine
GFT3-3079.5	44	-1.6	-6.1	120.9	na	marine
GFT3-3080.5	45	-1.7	-6.5	120.5	na	marine
GFT3-3081	46	-3.5	-7.4	116.5	na	marine
GFT3-3083	47	-0.7	-5.6	123.0	na	marine
GFT3-3083.5	48	-2.2	-5.5	120.1	na	marine
GFT3-3146	49	-4.3	-4.7	116.1	na	non-marine
GFT3-3147 R	50	-4.7	-4.9	115.2	na	non-marine
GFT3-3147 G	51	-4.6	-4.6	115.6	na	non-marine
GFT3-3148	52	-4.8	-4.5	115.1	na	non-marine
Grünbach Syncline:						
Samples	**Sample no. in graphs**	**$d^{13}C$ [VPDB]**	**$d^{18}O$ [VPDB]**	**Z**	**$^{87}Sr/^{86}Sr$**	**interpret. facies**
M-2	53	-2.3	-5.7	119.8	na	marine
M-4	54	-2.9	-5.7	118.5	na	marine
M-7	55	-2.0	-6.4	119.9	na	marine
M-9A	56	-3.0	-5.8	118.2	na	marine
M-16	57	-2.9	-5.3	118.8	na	non-marine
M-18	58	-1.4	-5.2	121.8	na	non-marine
M-23	59	-4.0	-6.0	116.1	na	marine
M-27	60	-3.2	-6.5	117.5	na	marine
M-36	61	-7.2	-8.4	108.4	na	non-marine
M-46	62	-4.4	-6.9	115.0	na	marine
M-48	63	-5.7	-7.1	112.2	na	marine
M-55	64	-7.2	-7.4	108.9	na	non-marine
M-57	65	-9.0	-8.3	104.7	na	non-marine
M-60	66	-7.6	-8.4	107.5	na	non-marine
M-62	67	-3.7	-6.8	116.4	na	non-marine
M-64	68	-9.2	-8.5	104.2	na	non-marine
M-65	69	-5.8	-7.4	111.7	na	marine
M-66	70	-5.3	-7.4	112.7	na	marine
M-68	71	-8.9	-10.0	104.0	na	marine
M-69	72	-4.6	-6.4	114.7	na	marine
M-71	73	-9.3	-8.9	103.8	na	marine
M-72	74	-5.8	-7.0	111.9	na	marine
M-73	75	-9.3	-9.0	103.8	na	marine
M-75	76	-3.6	-6.5	116.7	na	marine
M-77	77	-5.9	-7.5	111.6	na	non-marine
M-78	78	-9.3	-8.7	104.0	na	non-marine

M-82	79	-6.4	-8.0	110.3	na	non-marine
M-84	80	-6.4	-7.5	110.5	na	marine
M-85	81	0.3	-5.4	125.2	na	marine
M-87	82	-0.6	-5.4	123.4	na	marine
M-89	83	-3.3	-7.0	117.1	na	marine
M-92	84	-6.3	-7.9	110.4	na	non-marine
Gießhübl Syncline:						
Samples	**Sample no. in graphs**	**$d^{13}C$ [VPDB]**	**$d^{18}O$ [VPDB]**	**Z**	**$^{87}Sr/^{86}Sr$**	**interpret. facies**
AD81/8-3192.5	85	2.0	-4.9	128.9	na	marine
AD81/8-3193.4	86	2.2	-2.8	130.3	na	marine
AD81/8-3193.5	87	2.2	-3.4	130.1	na	marine
AD84/2-2833.5	88	-2.6	-4.4	119.7	na	marine
AD84/2-2832.5	89	-3.5	-4.9	117.6	na	marine
AD92/3-2840.5	90	-0.2	-3.7	125.0	na	marine
AD92/4-2921.5	91	1.0	-3.2	127.8	na	marine
AD92/4-2922	92	1.0	-3.4	127.7	na	marine
AD92/4-2922.55	93	1.1	-3.3	127.8	na	marine
AD92/5-3009.3	94	-0.1	-3.9	125.1	na	marine
AD92/5-3009.7	95	0.0	-4.0	125.3	na	marine
AD92/6-3111.5	96	-0.2	-3.8	125.0	na	marine
AD92/7-3327.5	97	0.9	-6.3	126.0	na	marine
AD92/7-3329	98	1.4	-4.1	128.1	na	marine
AD92/8-3431.85	99	1.3	-3.3	128.3	na	marine
AD92/8-3432	100	1.4	-3.4	128.5	na	marine
AD92/8-3433	101	1.3	-4.2	127.8	na	marine
AD92/9-3504.4	102	1.1	-5.3	126.9	na	marine
Slovakian Gosau:						
Samples	**Sample no. in graphs**	**$d^{13}C$ [VPDB]**	**$d^{18}O$ [VPDB]**	**Z**	**$^{87}Sr/^{86}Sr$**	**interpret. facies**
STU83-3102-06_3	103	0.2	-1.9	126.8	na	marine
Z57-4020-23	104	1.4	-2.3	129.1	na	marine
Z68-3721-22	105	0.4	-5.4	125.3	na	marine
Z68-3872.5-83.6	106	0.4	-5.0	125.7	na	marine
Z68-3883.6-89	107	0.6	-5.1	126.0	na	marine
Z68-3948-63	108	0.9	-5.0	126.7	na	marine
Z68-3948.5-63	109	0.8	-5.1	126.4	na	marine
Z68-4018-36	110	1.0	-5.0	126.8	na	marine
Z68-4063-81_1	111	1.4	-3.5	128.5	na	marine
Z68-4063-81_2	112	0.7	-5.5	126.0	na	marine
Z68-4063-81_3	113	1.7	-3.0	129.3	na	marine
Z68-4137-42	114	1.8	-2.1	129.9	na	marine
Z68-4183-86.2	115	1.5	-1.5	129.6	na	marine
Z68-4590-99_1	116	0.2	-2.4	126.5	na	marine
Z68-4590-99_2	117	0.2	-2.8	126.3	na	marine

$\delta^{13}C$ values of the Glinzendorf Syncline range between -9.1 and 2.0 ‰. Top and bottom sections of the Markgrafneusiedl T1 borehole are lower (down to -4.3 ‰) - except for one sample with 1.3 ‰ - compared to a relatively higher middle interval with values between -1.5 and 2.0 ‰ (Fig. 4 and 5, Table 1). $\delta^{13}C$ values of the Glinzendorf T1 borehole are generally low and fluctuate between -9.1 and -3.4 ‰, except for higher values from -3.7 to -0.7 ‰ at the top in contrast to intermediate values (-4.8 to -0.8 ‰) of the Gänserndorf T3 borehole (Fig. 5, Table 1). $\delta^{18}O$ values are generally low within the Glinzendorf Syncline (-7.9 to -2.1 ‰) with values typically around -5 ‰ at Markgrafneusiedl T1 (Fig. 4, Table 1). At Glinzendorf T1, $\delta^{18}O$ values range from -7.9 to 3.1 ‰ without specific trends. $\delta^{18}O$ values at Gänserndorf T3 are lower at the bottom compared to the top (Table 1).

$^{87}Sr/^{86}Sr$ ratios of samples from the Markgrafneusiedl T1 borehole well range from 0.70576 to 0.70981 (Fig. 4, Table 1).

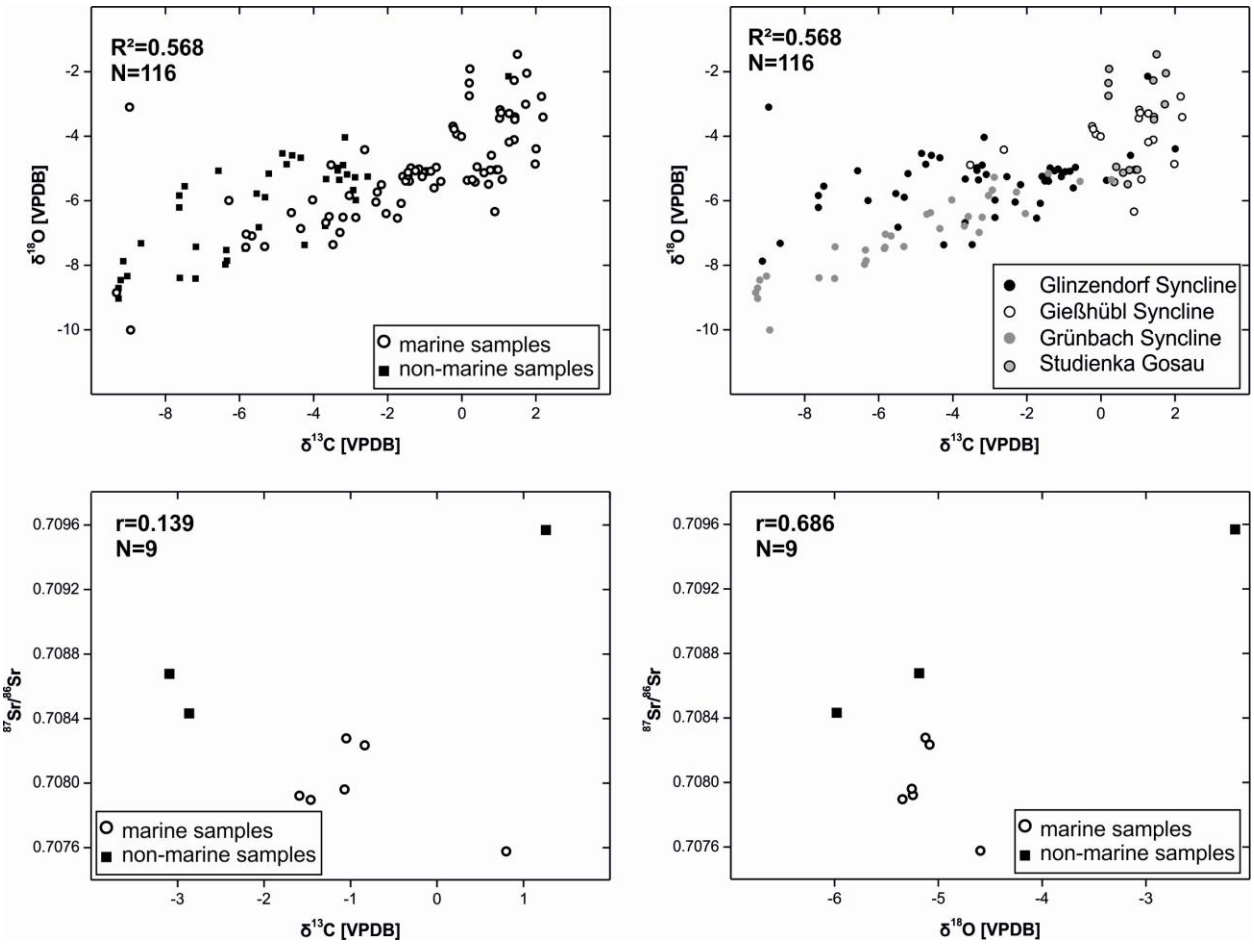


Fig. 7. Discrimination plots of $\delta^{13}C$ versus $\delta^{18}O$ in ‰ relative to VPDB (samples grouped according to depositional origin), $\delta^{13}C$ versus $\delta^{18}O$ (samples grouped according to geographic/tectonic setting), $\delta^{13}C$ versus $^{87}Sr/^{86}Sr$ (samples grouped according to depositional origin) and $\delta^{18}O$ versus $^{87}Sr/^{86}Sr$ (samples also grouped according to depositional origin). Number of samples (N) and Pearson correlation index (r) or squared Pearson correlation index (R^2) are given.

$\delta^{13}C$ and $\delta^{18}O$ values at the Grünbach Syncline are generally low but fluctuate within a few metres (from -9.3 to 0.3 and -10.0 to 5.2 ‰, respectively; Hofer *et al.* 2011; Fig. 6, Table 1).
Profiles of the wells Aderklaa 81, 84 and 92 of the Gießhübl Syncline are characterised by high and uniform $\delta^{13}C$ values ranging from -3.5 to 2.2 ‰ with a mean of 0.6 ±1.5 ‰. Only samples at Aderklaa 84 (Upper Gießhübl Formation) show relatively low values (Fig. 4, Table 1). $\delta^{18}O$ values are moderate within the whole Gießhübl Syncline with a mean of -4.0 ±0.9 ‰ (values between -6.3 and -2.8 ‰; Table 1).
$\delta^{13}C$ values of the Slovakian Gosau deposits of the wells Studienka 83, Závod 57 and 68 are uniformly high and positive and vary from 0.2 to 1.8 ‰ with a mean of 0.9 ±0.6 ‰ (Fig. 5, Table 1). $\delta^{18}O$ values are also relatively high (-5.5 to -1.5 ‰), but not as uniform (mean -3.7 ±1.5 ‰; Table 1).

Results and interpretation of individual sections

Based on the presence or absence of nannofossils and geochemical data (Hofer *et al.* in press) we differentiated between marine (nannofossil-bearing) and non-marine samples (lacking nannofossils). The following interpretation of isotope results is primarily based on this grouping (Table 1) and is discussed in the following section for individual Gosau Group basins.

Glinzendorf Syncline

The non-marine bottom and top sections of Markgrafneusiedl T1 with relatively lower $\delta^{13}C$ mean values of -2.5 ±1.9 and -3.3 ±0.7 ‰, respectively, are accompanied by a marine middle interval with significantly higher mean values of -0.8 ±1.1 ‰ (Fig. 4 and 5). The difference in $\delta^{13}C$ between marine and non-marine samples within this interval is highly significant (Table 2), thus we conclude that $\delta^{13}C$ values reflect the palaeosalinity in the Markgrafneusiedl T1 borehole.
$\delta^{18}O$ values of samples from Markgrafneusiedl T1 are not significantly lower in the non-marine sample group (Table 2). Relatively high mean values of -4.6 ±1.4 and -5.7 ±1.1 ‰ are present at the limnic bottom and top. Relatively constant and typically marine mean values are characteristic for the middle marine section (Fig. 4).
The Z-values of the Markgrafneusiedl T1 well section are significantly lower in non-marine samples (mean 119.0 ±3.7) relative to the mean of marine samples (123.1 ±2.3). Only one sample interpreted as non-marine (MT1-4106.50) exceeds the suggested limit for non-marine Z-values of 120 (Z=128.8; Fig. 8, Tables 1 and 2).

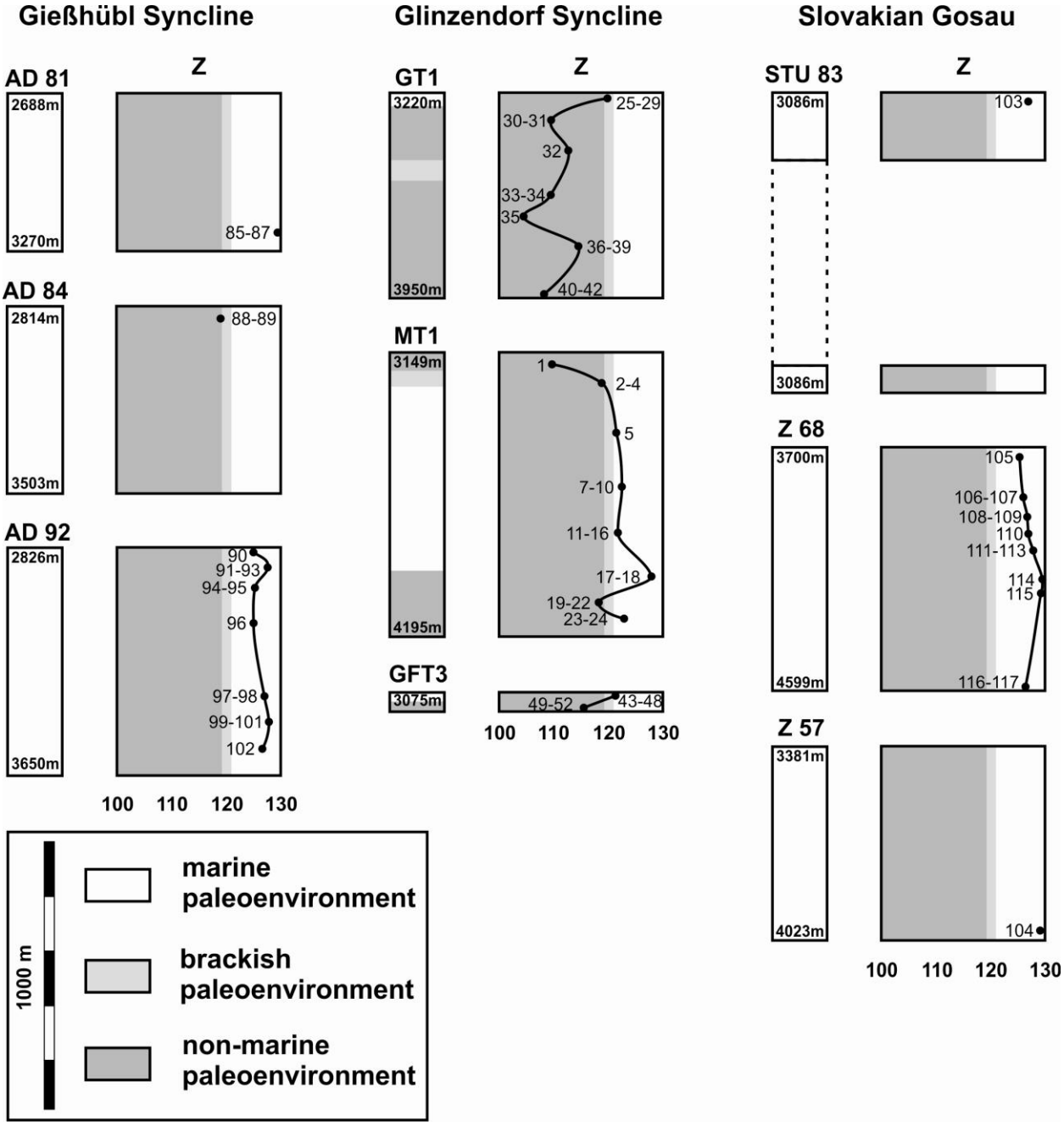


Fig. 8. Z-values after Keith & Weber (1964) of sediments in the well sections Aderklaa 81 (AD 81), 84 (AD 84), 92 (AD 92), Glinzendorf T1 (GT1), Markgrafneusiedl T1 (MT1), Gänserndorf T3 (GFT3), Studienka 83 (STU 83), Závod 57 (Z 57) and 68 (Z 68). Values from close-by samples were combined to mean values. Sample numbers in the figure are explained in Table 1.

The Sr isotope values are not significantly different in marine and non-marine samples of the borehole Markgrafneusiedl T1 (Table 2). Only one marine sample lies on the marine standard curve for the Santonian to Campanian which straddles between 0.7074 and 0.7076 (Howarth & McArthur 1997; McArthur *et al.* 2001). The mean ratio of marine samples is only slightly lower

(and closer to the marine curve) with 0.7082 ±0.0007 compared to the non-marine mean isotope signal of 0.7089 ±0.0006. However, a general trend to ratios closer to the Sr-isotope curve for the marine interval is present (Fig. 4, Table 2).

Table 2: *Student´s t-test.*

Means and standard deviations of $\delta^{13}C$, $\delta^{18}O$ and $^{87}Sr/^{86}Sr$ values are calculated for the marine and non-marine samples, respectively for the different localities (Markgrafneusiedl T1, Glinzendorf T1, Gänserndorf T3, Aderklaa 81, 84, 92, Studienka 83, Závod 57, 68 and Maiersdorf trench), for the different Gosau basins (Glinzendorf Syncline, Gießhübl Syncline, Studienka/Slovakian Gosau and Grünbach Syncline) as well as for the whole sample set. For localities that contain both marine and non-marine samples, the Student´s t-test proves the significance (limit of significance <0.05; significant values are given in bolt) of the difference of the mean values (expressed by T-values).

samples		**facies**	**N**	**mean**	**stand. dev.**	**T**	**significance (t-test)**
Markgrafneusiedl T1	$\delta^{13}C$	non-marine	10	-2.8	1.5	-3.726	**0.001**
		marine	13	-0.8	1.0		
	$\delta^{18}O$	non-marine	10	-5.1	1.3	0.058	0.955
		marine	13	-5.1	0.3		
	Z	non-marine	10	119.0	3.7	-3.259	**0.004**
		marine	13	123.1	2.3		
	$^{87}Sr/^{86}Sr$	non-marine	3	0.7089	0.0006	1.354	0.213
		marine	7	0.7082	0.0007		
Glinzendorf T1	$\delta^{13}C$	non-marine	11	-6.6	1.7	-2.565	**0.021**
		marine	7	-3.8	2.9		
	$\delta^{18}O$	non-marine	11	-6.1	0.9	-1.080	0.296
		marine	7	-5.5	1.2		
	Z	non-marine	11	110.9	3.9	-2.670	**0.017**
		marine	7	116.9	5.7		
Gänserndorf T3	$\delta^{13}C$	non-marine	4	-4.6	0.2	-4.738	**0.001**
		marine	6	-1.6	1.2		
	$\delta^{18}O$	non-marine	4	-4.7	0.1	3.575	0.007
		marine	6	-6.1	0.8		
	Z	non-marine	4	115.5	0.4	-3.744	**0.006**
		marine	6	121.0	2.9		
Glinzendorf Syncline	$\delta^{13}C$	non-marine	25	-4.8	2.3	-4.813	**0.000**
		marine	26	-1.8	2.1		
	$\delta^{18}O$	non-marine	25	-5.4	1.2	-0.030	0.976
		marine	26	-5.4	0.8		
	Z	non-marine	25	114.9	5.1	-4.571	**0.000**
		marine	26	120.9	4.3		
Aderklaa 81	$\delta^{13}C$	marine	3	2.1	0.1		
	$\delta^{18}O$	marine	3	-3.7	1.1		
	Z	marine	3	129.8	0.7		
Aderklaa 84	$\delta^{13}C$	marine	2	-3.1	0.6		
	$\delta^{18}O$	marine	2	-4.7	0.3		
	Z	marine	2	118.7	1.5		
Aderklaa 92	$\delta^{13}C$	marine	13	0.8	0.7		
	$\delta^{18}O$	marine	13	-4.0	0.9		
	Z	marine	13	126.9	1.4		
Gießhübl Syncline	$\delta^{13}C$	marine	18	0.6	1.5		
	$\delta^{18}O$	marine	18	-4.0	0.9		
	Z	marine	18	126.4	3.3		
Studienka 83	$\delta^{13}C$	marine	1	0.2			
	$\delta^{18}O$	marine	1	-1.9			

	Z	marine	1	126.8			
Zavod 57	$\delta^{13}C$	marine	1	1.4			
	$\delta^{18}O$	marine	1	-2.3			
	Z	marine	1	129.1			
Zavod 68	$\delta^{13}C$	marine	13	0.9	0.6		
	$\delta^{18}O$	marine	13	-3.9	1.5		
	Z	marine	13	127.2	1.6		
Slovakian Gosau	$\delta^{13}C$	marine	15	0.9	0.6		
	$\delta^{18}O$	marine	15	-3.7	1.5		
	Z	marine	15	127.3	1.6		
Maiersdorf Trench (Grünbach Syncline)	$\delta^{13}C$	non-marine	12	-6.3	2.5	-1.924	0.064
		marine	20	-4.5	2.6		
	$\delta^{18}O$	non-marine	12	-7.5	1.2	-1.383	0.177
		marine	20	-6.9	1.2		
	Z	non-marine	12	110.6	5.8	-1.880	0.070
		marine	20	114.6	6.0		
all samples	$\delta^{13}C$	non-marine	37	-5.3	2.4	-7.044	**0.000**
		marine	79	-1.4	2.8		
	$\delta^{18}O$	non-marine	37	-6.1	1.5	-3.004	**0.003**
		marine	79	-5.2	1.6		
	Z	non-marine	37	113.5	5.6	-6.723	**0.000**
		marine	79	121.8	6.5		

Negative $\delta^{13}C$ mean values of -6.6 ±1.7 ‰ characterise intervals of the Glinzendorf T1 borehole that are interpreted as non-marine. The section at the top, interpreted as marine based on nannofossil presence, shows a mean $\delta^{13}C$ value of -2.2 ±1.2 ‰. The possibly marine interval (indicated by higher boron concentrations, Hofer *et al*. in press) at around 3550 m is not verified using stable isotope data. The differentiation between marine and non-marine samples within the interval of Glinzendorf T1 is significant (Fig. 5, Table 2).

Samples interpreted as marine based on the presence of nannofossils show slightly higher mean $\delta^{18}O$ values of -5.5 ±1.2 ‰ compared to the non-marine mean value of -6.1 ±0.9 ‰ but this separation is not statistically significant (Table 2).

Z-values of the Glinzendorf T1 borehole differ significantly in marine and non-marine samples (Table 2). Marine mean Z-values are higher (116.9 ±5.7) compared to non-marine mean values (110.9 ±3.9) but only two marine interpreted samples (GT1-3245, GT1-3249) show values higher than 120 (Fig. 8, Table 1 and 2).

The Gänserndorf T3 profile is also represented by characteristically negative (i.e. limnic) $\delta^{13}C$ mean values in the lower part and a less negative (i.e. marine) mean value at the top of the section (Fig. 5) as evidenced by a highly significant discrimination of the means of the two sample groups (Table 2).

Against the general trend, marine mean $\delta^{18}O$ values of -6.1 ±0.8 ‰ at Gänserndorf T3 are even lower than non-marine mean values of -4.7 ±0.1 ‰ (Table 2). This may be due to a stronger diagenetic overprint and/or a higher detrital input at Gänserndorf.

Marine mean Z-values are significantly higher (121.0 ±2.9) in contrast to non-marine mean values (115.5 ±0.4) at Gänserndorf T3 (Fig. 8, Table 2).
The carbon isotopic composition of the carbonate fraction of the whole Glinzendorf Syncline is highly distinctive and successfully separates marine from non-marine samples (Table 2). Even though oxygen isotope ratios are not significantly discriminative, Z-values are significant with non-marine mean values of 114.9 ±5.1 and marine mean values of 120.9 ±4.3 (Table 2).

Grünbach Syncline – Maiersdorf trench

Supported by geochemical parameters, nannofossil content and stable carbon isotopic composition reported here, five marine to non-marine cycles have been recognized in the trench profile of the Grünbach Formation at Maiersdorf (Hofer *et al.* 2011). Samples of the non-marine intervals have lower $\delta^{13}C$ mean values of -6.3 ±2.5 ‰ compared to the marine sample set with a mean of -4.5 ±2.6 ‰. Statistically, the significance is just below the level of significance of α=5 % or 0.05 (Fig. 6, Table 2). However, strong fluctuations exist in the marine intervals (Fig. 6) probably reflecting the presence of some reworked carbonate or stronger diagenetic influence.
Marine samples of the trench profile have higher $\delta^{18}O$ mean values of -6.9 ±1.2 ‰ in contrast to lower mean values of -7.5 ±1.2 ‰ for non-marine samples but the difference is not significant (Fig. 6, Table 2).
Generally, Z-values are relatively low within the Grünbach Formation with marine mean values of only 114.6 ±6.0 compared to a non-marine mean of 110.6 ±5.8. The significance is below the level of significance (Fig. 6, Table 2).

Gießhübl Syncline

$\delta^{13}C$ values of the fully marine samples from the Gießhübl Syncline are uniformly high with a mean of -0.6 ±1.5 ‰. $\delta^{18}O$ values with a mean of -4.0 ±0.9 ‰ also corroborate the marine origin of these sediments (Wessely 2006). Except the two samples of Aderklaa 84, all samples show Z-values above 120 (up to 130.3) representing clearly marine conditions (Fig. 5 and 6, Table 1 and 2) which is in accordance with the micropalaeontologic data.
$\delta^{13}C$ mean values of 2.1 ±0.1 ‰ can be observed in the interval of the bathyal Nierental Formation between 3192.5 and 3193.5 m in the Aderklaa 81 borehole (Fig. 5). The $\delta^{18}O$ mean value of the Aderklaa 81 interval is -3.7 ±1.1 ‰ (Table 2).
Only at Aderklaa 84 the Upper Gießhübl Formation is represented by relatively low $\delta^{13}C$ mean values of -3.1 ±0.5 ‰ but typically marine $\delta^{18}O$ mean values of -4.7 ±0.3 (Fig. 5, Table 2).

The Gießhübl Formation at well Aderklaa 92, representing a deep-marine turbiditic facies (e.g. Wessely 2006) is characterized by marine $\delta^{13}C$ mean values of 0.8 ±0.7 ‰ and $\delta^{18}O$ mean values of 4.0 ±0.9 ‰ (Fig. 5, Table 2).

Slovakian (Studienka) Gosau

$\delta^{13}C$ values of the marine Gosau formations of the Slovakian boreholes Studienka 83, Závod 57 and 68 are all uniform and high (0.2 to 1.5 ‰) with a mean of 0.9 ±0.6 ‰ (Fig. 5, Table 1 and 2). Oxygen isotope values are also suggestive of marine conditions (Table 1 and 2). Z-values are above 120 with a mean of 127.3 ±1.6 (Fig. 8, Tables 1 and 2).

Discussion

Significance of stable isotopes for marine versus non-marine discrimination

The discrimination plot of $\delta^{13}C$ versus $\delta^{18}O$ separates in principle marine samples of the Gießhübl Syncline and Slovakian wells from non- to marginal-marine samples of the Grünbach and Glinzendorf Syncline, and thus allows a distinction of major Gosau Group basin fills. A strongly positive Pearson correlation index of r=0.75 illustrates the correlation between stable carbon and oxygen isotopic composition, thus indicating a similar facies control on both isotope systems. The Student´s t-test suggests a significant discrimination of mean carbon and oxygen isotope ratios and Z-values of marine and non-marine samples for the whole data set (N=116). The mean non-marine carbon isotope value (-5.3 ±2.4 ‰) is significantly lower than the mean marine value of -1.4 ±2.8 ‰. A significance of α=0.000 (T=-7.04) indicates an effective distinction between marine and non-marine samples (Table 2.).

A statistically significant differentiation (α=0.003; T=-3.00) is also present in the oxygen isotope values of marine versus non-marine samples, even though the difference between the mean marine (-5.2 ±1.6 ‰) and the mean non-marine value (-6.1 ±1.5 ‰) is relatively small (Table 2).

Marine samples have higher mean Z-values (121.8 ±6.5) relative to mean values of non-marine samples (113.5 ±5.6) with a significance of α=0.000 (T=-6.72). 94.6 % (N=35 out of 37) of all non-marine samples have Z-values below 120, while only 67.1 % (N=53 out of 79) of all marine samples exceed the limit of 120 which is mainly due to the relatively low values at the Grünbach Syncline (Table 1 and 2).

A discrimination based on $\delta^{13}C$ and $\delta^{18}O$ values of marine and non-marine samples (of the whole data set) is also highly significant (α=0.000; Wilks-lambda=0.649). The histogram of the discriminatory function clearly separates marine from non-marine samples (Fig. 9).

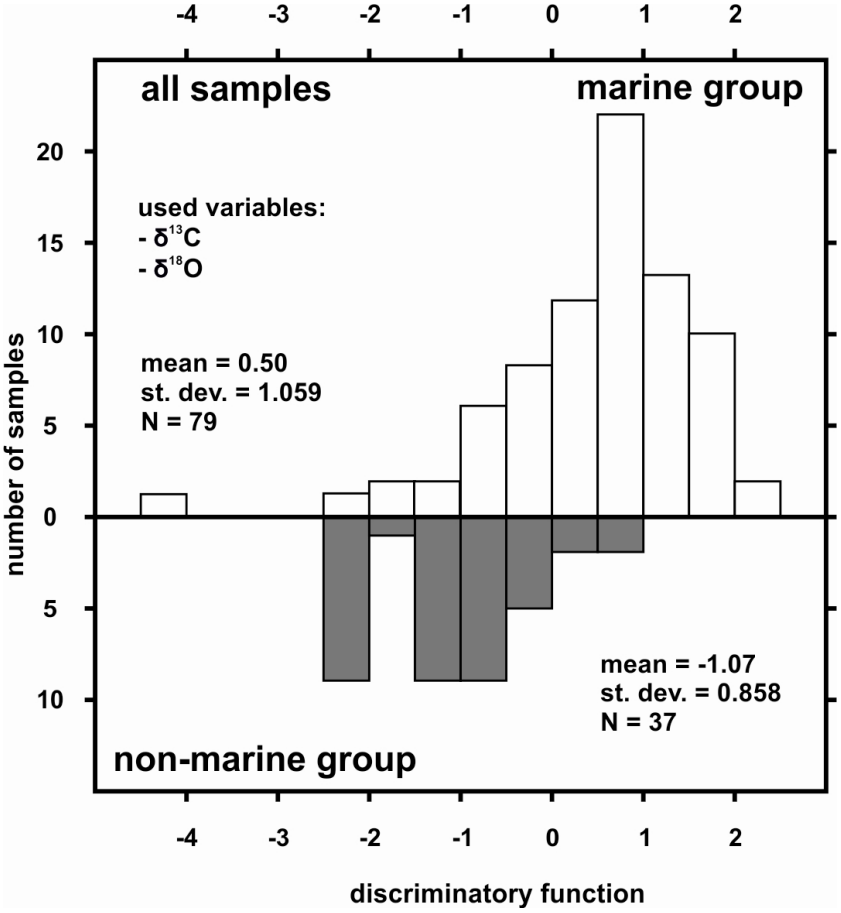


Fig. 9. Histogram of the discriminatory function split for the marine and non-marine group. For details see text.

Influence of diagenesis

The influence of diagenesis on the stable isotope compositions is difficult to assess using bulk-rock samples and considering the fine-grained shaly to marly material used in this study. Most of the samples have low carbonate contents of around 30 wt. %. Only 20 % of the samples had more than 50 wt. % $CaCO_3$. Selected samples of these pelitic rocks from well Markgrafneusiedl T1 where studied by CL. The bulk of the fine-grained carbonate was nonluminescent; only a small fraction of the carbonate in siltstones showed CL. This suggests that the diagenetic overprint of the carbonate is low, which is consistent with the pelitic nature of the sampled material which greatly limits water-rock interaction.

Correlation indices of $\delta^{13}C$ versus $\delta^{18}O$ calculated separately for the different Gosau basins are low for the Gießhübl (r=0.28), Glinzendorf Syncline (r=0.36) and Studienka Gosau (r=0.31) and high only for the Grünbach Syncline (r=0.93; Hofer *et al.* 2011). Therefore, a notable diagenetic imprint is (except for the Grünbach Syncline) unlikely (e.g. Shen & Schidlowski 2000; Hamon & Merzeraud 2007).

Influence of carbonate reworking

An issue especially for bulk-carbonate analysis of clastic sediments is the possible presence of reworked older carbonate material, whose quantification is difficult. Thin-section petrography and CL studies indicate the presence of detrital carbonate grains, mainly limestones, with amounts below 10 %. To further assess the influence of this detrital carbonate material 18 samples (M-6, M-16, M-17, M-31, M-42, M-50, M-65, M-72, M-79, M-85, M-92, AD81/8-3193.4, AD84/2-2833.5, AD92/4-2922, AD92/8-3433, Z68-3883.6, Z68-3433, STU83-3430-35) were quantitatively analyzed for the presence of (detrital) dolomite. Only six samples contained some dolomite and only three of them contained more than 5 % (AD81/8-3193.4: 6.1 %, AD92/8-3433: 8.3 % and Z68-3883.6: 29.9 %). A significant influence of detrital carbonate on the bulk stable isotope composition is therefore regarded as unlikely.

Based on the composition of intercalated coarser grained clastic sediments like conglomerates and sandstones (e.g. Wagreich *et al.* 2011) reworking of older (Mesozoic) carbonates is largely limited to Triassic to Jurassic marine carbonates of the NCA which have $\delta^{13}C$ values generally between -2 and 4 ‰ (e.g. Gawlick & Böhm 2000; Korte *et al.* 2005; Reinhold & Kaufmann 2010). An inferred low influence of detrital carbonates on the stable isotope composition thus cannot explain unusually negative isotope values of marine sections such as in the Grünbach Formation.

Strontium isotopes

Strontium isotope values were measured only from core samples of well Markgrafneusiedl T1. Due to the small number of samples, the correlation indices between $\delta^{13}C$ and $^{87}Sr/^{86}Sr$ as well as $\delta^{18}O$ and $^{87}Sr/^{86}Sr$ are not significant (Fig. 7). The vertical trend of strontium isotopes, however, is clear, from relatively low values in the marine samples to higher values in the transitional to non-marine parts of the section. This trend can be interpreted either as reflecting admixtures of clay minerals and metamorphic minerals (e.g. mica) from the Austroalpine basement and/or detrital Triassic carbonates (Sr isotope values around 0.7076 - 0.7082 according to Korte *et al.* 2003), but does not allow to distinguish marine from non-marine environments. As some values are higher than Triassic (and Jurassic) marine values detritus cannot be the ultimate reason for this shift as already observed in the marine samples, but we attribute this deviation to the high input of clay minerals from eroded basement units.

Unusually negative isotope values of marine sediments in the Grünbach section

Although a statistically significant separation of non-marine and marine environments using carbon isotopes is possible for most of the studied samples, some of the marine samples of the

Grünbach section are isotopically rather negative (up to -9 ‰ $\delta^{13}C$). The very high correlation of carbon and oxygen isotopes (Fig. 7) in this short section suggests a strong influence of diagenesis (probably with precipitation of new carbonate phases). This is consistent with the fact that the Grünbach Syncline experienced the highest thermal overprint of the study area (vitrinite reflectance values above 0.5 % Rr, Hofer *et al.* 2011).

Conclusions

Using stable carbon and oxygen isotope data of bulk carbonate, marine and non-marine fine-clastic shaly sediments from boreholes of the Glinzendorf and Gießhübl Synclines and equivalents from Slovakia as well as sediments of the Grünbach Syncline can be distinguished. Mean carbon and oxygen isotope values of samples containing marine nannofossils and other evidences for marine deposition are distinctively higher (-1.4 and -5.2 ‰, respectively) compared to samples lacking marine indications (-5.3 and -6.1 ‰, respectively). Mean Z-values are higher in marine samples (mean >120) and lower in non-marine samples. This differentiation of marine and non-marine mean values is confirmed statistically by the Student´s t-test and discriminatory analysis. Looking at individual sections and locations, however, the discrimination between marine and non-marine depositional environments is not always statistically significant. $^{87}Sr/^{86}Sr$ ratios of marine samples of the Markgrafneusiedl T1 borehole are closer to the marine isotope curve for the Santonian and Campanian compared to limnic samples, but - possibly because of the limited number of samples – marine and non-marine samples could not be distinguished by this method.

Acknowledgements

This study was funded by the OMV E & P AG within a research project conducted at the University of Vienna under the scientific responsibility of Michael Wagreich and monitored by Philipp Strauss on behalf of OMV. Special thanks to the Austrian Academy of Sciences for the support of a DOC-fellowship to G.H.

References

See reference list of dissertation.

5.1.3 Geochemistry of fine-grained sediments of the Upper Cretaceous to Paleogene Gosau Group (Austria, Slovakia): Implications for paleoenvironmental and provenance studies

Hofer, G., Wagreich, M. & Neuhuber, S. Geochemistry of fine-grained sediments of the Upper Cretaceous to Paleogene Gosau Group (Austria, Slovakia): Implications for paleoenvironmental and provenance studies. Geoscience Frontiers (2013), http://dx.doi.org/10.1016/j.gsf.2012.11.009.

Date of submission: 24.05.2012
Date of acceptance: 10.12.2012

Comment of the author concerning the degree of participation
The entire manuscript was written by Gerald Hofer (supported by co-authors). Sample collection, preparation for geochemical analysis, several analytical methods and interpretations were performed by the author.

Article structure, numbering and type of quotations are maintained as requested in the journal.

ARTICLE IN PRESS

Geoscience Frontiers xxx (2013) 1–20

Contents lists available at SciVerse ScienceDirect

China University of Geosciences (Beijing)

Geoscience Frontiers

journal homepage: www.elsevier.com/locate/gsf

Research paper

Geochemistry of fine-grained sediments of the upper Cretaceous to Paleogene Gosau Group (Austria, Slovakia): Implications for paleoenvironmental and provenance studies

Gerald Hofer*, Michael Wagreich, Stephanie Neuhuber

Department of Geodynamics and Sedimentology, University of Vienna, Althanstrasse 14, A-1090 Vienna, Austria

ARTICLE INFO

Article history:
Received 24 May 2012
Received in revised form
30 October 2012
Accepted 30 November 2012
Available online xxx

Keywords:
Gosau Group
Geochemistry
Pre-Neogene Vienna Basin
Boron
Factor analysis
Provenance

ABSTRACT

Bulk rock geochemistry of 169 fine-grained sediment samples of the upper Cretaceous to Paleogene Gosau Group (Northern Calcareous Alps, Austria and Slovakia) from borehole and outcrop localities was performed to separate non-marine and marine deposits. Geochemical characteristics of different Gosau depositional systems, basins and sediment provenance using major-, trace-, and rare earth elements were also investigated. Geochemical proxies such as boron concentrations were tested for seeking the possibilities of paleosalinity indicators. Due to the fact that several pelagic sections are represented by extremely low boron contents, B/Al* ratios are recognized as more robust and differentiate reliably between marine (mean: 160 ± 34) and non-marine (mean: 133 ± 33) samples. Using statistical factor analysis, hemipelagic to pelagic samples from the Gießhübl Syncline and Slovakian equivalents can be differentiated from marginal-marine to non-marine samples from the Grünbach and Glinzendorf Syncline related to terrigenous- (SiO_2, Al_2O_3, K_2O, Th, Rb, Zr and others) and pelagic indicative elements (CaO, Sr, TOT/C and B/Al*). A clear indication for ophiolitic provenance is traced by high amounts of chromium and nickel. Only non-marine successions of the Glinzendorf Syncline show higher Cr and Ni concentrations (up to 250 and 400 ppm, respectively) and enriched Cr/V and Y/Ni ratios trending to an ultramafic source.

© 2012, China University of Geosciences (Beijing) and Peking University. Production and hosting by Elsevier B.V. All rights reserved.

1. Introduction

Fine-clastic, shaly to marly sediments may be preferentially used to identify overall changes in sediment source areas and depositional conditions such as limnic versus marine, because they normally cover a longer and more continuous time period compared to coarser-grained sediments such as sands and conglomerates (e.g. McLennan et al., 1993; Hofmann et al., 2001; Pearce et al., 2005; Rahman and Suzuki, 2007; Lee, 2009).

This study uses various geochemical proxies and statistical methods that are commonly applied in sedimentology for paleoenvironmental and provenance analyses (e.g. McLennan et al., 1993; Hofmann et al., 2001; Pearce et al., 2005; Rahman and Suzuki, 2007; Lee, 2009; Madhavaraju et al., 2010; Hofer et al., 2011). Several geochemical and statistical tools are tested to infer paleoenvironments, alteration, weathering, and provenance.

We analyzed the bulk rock geochemistry of fine-grained sediments of the upper Cretaceous to Paleogene Gosau Group (e.g. Wagreich and Faupl, 1994) that were deposited after the Eoalpine high pressure orogenic event at ca. 95 Ma (Thöni, 2006). They were deformed and dismembered by Paleogene to Neogene orogeny. The purpose of this study is to compare geochemical characteristics of the different Gosau deposits for separating out freshwater from marine sediments. We determine and differentiate provenance using major-, trace-, and rare earth elements.

* Corresponding author. Tel.: +43 1 4277 53467.
E-mail addresses: gerald.hofer@univie.ac.at (G. Hofer), michael.wagreich@univie.ac.at (M. Wagreich), stephanie.neuhuber@univie.ac.at (S. Neuhuber).

Peer-review under responsibility of China University of Geosciences (Beijing).

Production and hosting by Elsevier

1674-9871/$ – see front matter © 2012, China University of Geosciences (Beijing) and Peking University. Production and hosting by Elsevier B.V. All rights reserved.
http://dx.doi.org/10.1016/j.gsf.2012.11.009

Please cite this article in press as: Hofer, G., et al., Geochemistry of fine-grained sediments of the upper Cretaceous to Paleogene Gosau Group (Austria, Slovakia): Implications for paleoenvironmental and provenance studies, Geoscience Frontiers (2013), http://dx.doi.org/10.1016/j.gsf.2012.11.009

2. Geological setting

The upper Cretaceous to Paleogene sediments of the Gosau Group of the Northern Calcareous Alps (NCA) are unconformably and diachronously overlying Permian to lower Cretaceous units that experienced folding and faulting (Wagreich and Faupl, 1994). The sediments can be divided into a fluvial, lacustrine to shallow-marine lower Gosau Subgroup (Turonian to Santonian/Campanian, in some areas up to Maastrichtian) and into a deep-water dominated up to Eocene upper Gosau Subgroup (Faupl et al., 1987; Wagreich and Faupl, 1994; Faupl and Wagreich, 1996). Originally the Gosau Group sediments were situated at the northern, tectonically active continental margin of the Austroalpine microplate along the northern margin of the Adriatic plate (Faupl and Wagreich, 2000). The Gosau basins represent strike-slip dominated slope basins within an early accretionary structure due to southward subduction of the Penninic Ocean (viz. Alpine Tethys of Stampfli et al., 2002). Today, the original palaeogeographic situation is largely obliterated due to polyphase tectonic deformation and large-scale thrusting within the Eastern Alps (e.g. Faupl and Wagreich, 2000).

Various Gosau Group deposits are exposed in the eastern part of the Eastern Alps (Austria) at the area of Gießhübl and Grünbach – Neue Welt (south-western margin of the Vienna Basin). They are also exposed in the western part of the Western Carpathians at the area of Brezová and Myjava, Slovakia (Fig. 1) (Wagreich and Marschalko, 1995). In between, NE–SW-striking Gosau sediments were drilled in several wells below the Neogene fill of the Vienna Basin (Wessely, 1993). The Gosau Group deposits were deformed during the Alpine orogeny and today forming synclines. From north to south several synclines on different tectonic nappes of the NCA and on Carpathian units are present. There are the northernmost Gießhübl Syncline, the Prottes Gosau Group, its Slovakian equivalents of Studienka, the Glinzendorf Syncline and the southernmost Grünbach Syncline (Plöchinger, 1961; Wessely, 1974, 1984, 1992, 1993, 2000, 2006; Wagreich and Marschalko, 1995; Zimmer and Wessely, 1996) (Fig. 1).

2.1. Tectonic position and sedimentary setting

The Gießhübl Syncline (Coniacian to Paleocene) is part of the Lunz Nappe of the Bajuvaric Nappe system (Faupl and Wagreich, 1996) of the NCA. It is dominated by deep-marine facies from the Campanian onward. In the Coniacian–Santonian shallow-marine sandstones and breccias are deposited, and are overlain by the Nierental Formation (upper Gosau Subgroup) of the upper Santonian-Campanian to lower Maastrichtian (Wessely, 2006). The group mainly consists of calcareous marls of pelagic to hemipelagic slope facies (Krenmayr, 1999; Wagreich and Krenmayr, 2005; Wagreich et al., 2011). The youngest unit is the Gießhübl Formation

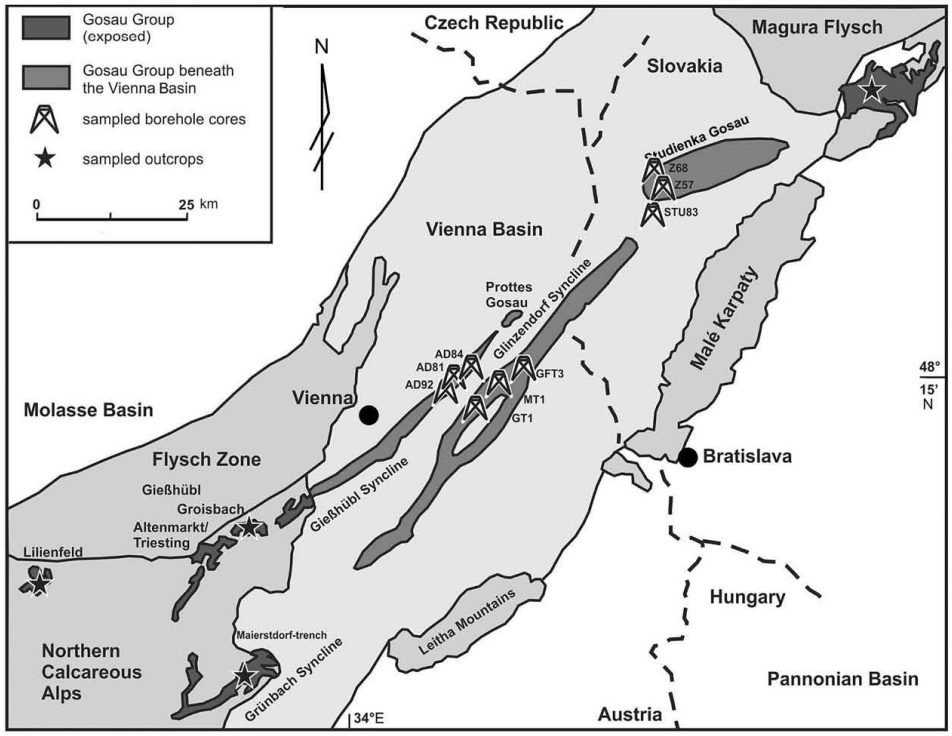


Figure 1. Simplified geological map of the eastern part of the Eastern Alps, the Vienna Basin and the western part of the Western Carpathians with highlighted Gosau Group situated at the border and underneath the Neogene Vienna Basin (modified after Wagreich and Marschalko, 1995; Zimmer and Wessely, 1996). The sampled locations of the wells and outcrops are marked.

Please cite this article in press as: Hofer, G., et al., Geochemistry of fine-grained sediments of the upper Cretaceous to Paleogene Gosau Group (Austria, Slovakia): Implications for paleoenvironmental and provenance studies, Geoscience Frontiers (2013), http://dx.doi.org/10.1016/j.gsf.2012.11.009

(subdivided into a lower, middle and upper Gießhübl Member). It is a massive deep-water turbidite to mass-flow-complex deposited below the calcite compensation depth (Faupl and Sauer, 1978; Wagreich, 2001), with a temporal extent up to the Thanetian (Wessely, 1992). Gosau Group sediments of the Gießhübl Syncline crop out at the area of Gießhübl, Alland and Altenmarkt/Triesting. About 10 km to the west of Altenmarkt/Triesting, equivalents of the Gießhübl Syncline are exposed around Lilienfeld, where the Gosau Group is consisted of Coniacian-Santonian lower Gosau Subgroup units followed by the hemipelagic-pelagic Nierental, Spitzenbach and Gießhübl formations of Campanian to Maastrichtian age (Wagreich, 1986; Wagreich et al., 2011).

The Prottes Gosau Group (Coniacian to Paleocene) is a small, isolated, mainly conglomeratic complex lying on Tirolic nappes underneath the Neogene of the Vienna Basin between Prottes and Altenmarkt/Triesting (Wessely, 2006).

The Tirolic Glinzendorf Syncline (Santonian to Campanian or Maastrichtian) is sometimes interpreted as an eastern equivalent of the Grünbach Syncline (Wessely, 2006) because of its similar limnic character with interbedded coal horizons. However, a continuous connection from the Grünbach Syncline underneath the Vienna Basin to the Glinzendorf Syncline is due to borehole informations doubtful. The sediments of the Glinzendorf Syncline are detected exclusively in the subsurface and can be found in several industrial wells of the oil and gas companies OMV and NAFTA, like Gänserndorf ÜT3, T3, Markgrafneusiedl 1, N1, T1, Glinzendorf 1 and T1 (Wessely, 2006), Gajary 125 (Misík, 1994; Ralbovsky and Ostrolucký, 1996) or Záhorska Ves. Basically, limnic to marginal-marine facies is dominant in the several hundred metre thick succession starting in the Santonian with dark marls and mudstones and some minor coal layers (Sachsenhofer and Tomschey, 1992; Wessely, 1992, 2006). Marls, mudstones and minor conglomerates are continued up to the Campanian. Above a middle-part, consisting of marine mudstones, marls and sandstones, clastics are present at the top (Wessely, 2006). Generally, this succession is also reported from the Slovakian part of the syncline (Gajary 125 well) with lower and upper conglomeratic non-marine red intervals, and intercalation of a marine grey interval (Mišík, 1994). Here, a Maastrichtian (Wessely, 1992; Pavlishina et al., 2004) or even Paleocene top cannot be excluded (Ralbovsky and Ostrolucký, 1996).

The Grünbach Syncline (Santonian to Paleocene) is exposed at the south-western margin of the Vienna Basin in the area of Grünbach – Neue Welt (Plöchinger, 1961) (Fig. 1). The connection to upper Cretaceous rocks beneath the Neogene fill of the Vienna Basin is controversial (e.g. Hofer et al., 2011). The Gosau Group of Grünbach starts at the base with a characteristic red conglomerate and breccia horizon of an alluvial fan in the upper Santonian (Kreuzgraben Formation; see also Erkan, 1972 for description of Gosau conglomerates). A transgressive trend is documented by the overlying shallow-marine Maiersdorf Formation that contains calcareous breccias, minor sandy limestones (including corals, brachiopods and gastropods) and reef-forming rudist limestones (Summesberger et al., 2002). This might correspond to the global transgression at the end of the Santonian.

Similar facies compared to units at the base of the Glinzendorf Syncline occurs in the limnic to marginal-marine Grünbach Formation of the lower Campanian that contains coal layers within marls and fine-clastic sandstones as well as a conglomeratic horizon (Summesberger et al., 2002; Wessely, 2006). From the late Campanian onward the facies is deep-marine with *Inoceramus* marls and *Orbitoides* bearing sandstones of the Piesting Formation, which lasted until the Maastrichtian (Hradecká et al., 1999). The maximum depth of the basin is estimated with the turbiditic Zweiersdorf Formation of Paleocene age (Summesberger et al., 2002).

The correlation of the Cretaceous Brezová Group (Coniacian to Maastrichtian) and the Paleogene Myjava Group (Paleocene to Eocene) of the so-called Brezová Depression striking ENE underneath the Slovakian part of the Neogene Vienna Basin with exposures at the north-eastern margin at the area of Brezová with the Gosau Group is still being debated because of unlike continuous distribution (Fig. 1). An affiliation to the Gießhübl Syncline is likely (Wagreich and Marschalko, 1995) due to its bathyal character but a correlation with the Prottes Gosau Group is also possible (Wessely, 1992).

The stratigraphic succession starts, above local conglomerates, with the marl-dominated Santonian Hurbanova Dolina Formation representing a neritic shelf facies followed by calcareous marls of the Campanian Košariská Formation (similar to the Nierental Formation in Austria) that documents a fast deepening of the basin. This deepening continues further and produced massive turbidite units of the Podbradlo, Podlipovec (upper Campanian to Maastrichtian), Priepastné and Jablonka (Paleogene of the Myjava Group) Formations. A deposition below the calcite compensation depth (3600 m for the Cretaceous) (Tyrell and Zeebe, 2004) is assumed for the Jablonka Formation analogous to the Gießhübl Formation (Wagreich and Marschalko, 1995).

3. Methods

169 samples of fine-grained sediments such as shales, marls and siltstones are collected from cores of the OMV-core sample repository (wells Aderklaa 81, 84 and 92, Gänserndorf T3, Glinzendorf T1, Markgrafneusiedl T1, Studienka 83 and Zavod 57 and 68), from outcrops in Lilienfeld and Groisbach (Gießhübl Syncline) and from an artificial trench in Maiersdorf (Grünbach Syncline, Hofer et al., 2011) for bulk rock geochemistry. Core samples are numbered with the well code (Aderklaa = AD, Gänserndorf T3 = GFT3, Glinzendorf T1 = GT1, Markgrafneusiedl T1 = MT1, Studienka = STU, Závod = Z) and the depth (or depth range) in metres. Facies, formations and Gosau units of the samples are shown in Appendix I. First, the samples were classified as marine or non-marine by the presence or absence of marine fossils, especially calcareous nannofossils, or by identification of geological formations based on literature data, mainly on fossil content (e.g. planktonic foraminifera, etc.; see Wagreich and Marschalko, 1995; Summesberger et al., 2002). Clearly, continuous fully marine deep-water conditions are known for the profiles of the Gießhübl Syncline and Slovakian equivalents (Wessely, 1992, 2006; Wagreich and Marschalko, 1995) and OMV in-house data. The non-marine to marginal-marine sections of the Glinzendorf Syncline and the Grünbach Formation (Hofer et al., 2011) were additionally analyzed during this study for presence of calcareous nannofossils in order to have an independent facies control. Blank nannofossil sections, in combination with corresponding geochemical features, are classified as non-marine.

Chemical bulk rock analyses were done by *AcmeLabs* (Acme Analytical Laboratories Ltd., www.acmelab.com) in Vancouver (Canada). Oxides (SiO_2, Al_2O_3, Fe_2O_3, MgO, CaO, Na_2O, K_2O, TiO_2, P_2O_5, MnO and Cr_2O_3) and some minor elements (Ba, Be, Co, Cs, Ga, Hf, Nb, Ni, Rb, Sn, Sr, Ta, Th, U, V, W and Zr) were detected by ICP (inductively coupled plasma)-emission spectroscopy. A Lithium metaborate/tetraborate fusion and nitric acid digestion of a 0.2 g sample was used. Loss on ignition (LOI) was calculated by weight difference after ignition at 1000 °C. For the analysis of trace elements, ICP-mass spectroscopy was used after leaching a 0.5 g sample in hot (95 °C) Aqua Regia. B was also detected by ICP-MS after Na_2O_2 fusion (www.acmelab.com). Total S (TOT/S) was detected by LECO analysis. Detection limits (DL) for the elements are given in Appendix I.

Please cite this article in press as: Hofer, G., et al., Geochemistry of fine-grained sediments of the upper Cretaceous to Paleogene Gosau Group (Austria, Slovakia): Implications for paleoenvironmental and provenance studies, Geoscience Frontiers (2013), http://dx.doi.org/10.1016/j.gsf.2012.11.009

159 samples were analyzed for total organic carbon (TOC) with a LECO C200 and a LECO RC-412 after dissolving the carbonate with diluted hydrochloric acid (for LECO C200) or measuring at 550 °C (LECO RC-412) at the University of Vienna (analytical error is around 0.1%).

Major and trace elements are commonly used as proxies for the interpretation of paleoenvironments. Discrimination plots and index numbers have been introduced in recent years (e.g. Nesbitt and Young, 1982; Roser and Korsch, 1988; Hofmann et al., 2001). The chemical index of alteration (CIA) expressed as the molar volumes of $[Al_2O_3/(Al_2O_3 + CaO^* + Na_2O + K_2O)] \times 100$, where CaO^* represents the CaO only from silicate fraction (Nesbitt and Young, 1982, 1989), can be used as a tool for paleoclimate reconstructions (Yan et al., 2010). As our samples contain a large portion of marine carbonate, we assume that CaO^* is equivalent to Na_2O (McLennan et al., 1993) as an approximation. To avoid errors derived from the unknown CaO content of the silicate fraction, the chemical proxy of alteration (CPA after Buggle et al., 2011) or chemical index of weathering (CIW after Cullers, 2000) is also used ($CPA = 100 \times Al_2O_3/[Al_2O_3 + Na_2O]$). The aluminium ratios Si/Al (proxy for quartz content in clays), K/Al (proxy for illite content) and Na/Al (proxy for smectite content) are used to identify mineralogical variations within the samples (Hofmann et al., 2001). Discriminant function analysis of major elements is performed for the determination of provenance signals (Roser and Korsch, 1988).

Boron concentrations in sediments are depending on the paleosalinity of the depositional environment (Ernst, 1966; Heling, 1967; Selter et al., 1989; Rügner, 2000). They are commonly used as tracers for marine facies. Because of its high solubility, boron accumulates at higher salinities in the sea (around 4440 μg/l of B in seawater in contrast to 18 μg/l in freshwater; Martin and Whitfield, 1983). Boron is mainly adsorbed to clay minerals (illites offer the highest adsorption capacity) or organic matter and behaves immobile after the integration into the phyllosilicate structure (Rügner, 2000). Unfortunately, grain size can also affect boron concentration (positive correlation with decreasing grain size) as well as variations in the primary composition (source area) of the clays (Dominik and Stanley, 1993). To reduce effects of variable grain size and mineralogy, and to optimize the comparability of sediments with different sedimentation and clay accumulation rates, we normalize the boron contents with respect to aluminium (multiplied with a factor of 100,000 to get small numbers). This ratio (B/Al × 100,000) is used as B/Al* in the following text (Hofer et al., 2011). A B/Al* ratio of 150 correlates with a boron content of 100 ppm in fine-grained sediments of mostly marine origin. In comparison, Goodarzi and Swaine (1994) used boron concentrations of 50 and 110 ppm to separate fresh/brackish and brackish/marine boundaries in coals. But B concentrations can vary quite drastic in TOC-rich sediments (Hofer et al., 2011).

Geochemical proxies for the interpretation of sediment provenance and paleoenvironment rely mainly on trace element concentrations/ratios such as Cr, V, Ni, Th, U, and others. Cr/Ni and (Cr/V)/(Y/Ni) (McLennan et al., 1993; Garver et al., 1996) are used in this study to infer ultramafic provenance. Jones and Manning (1994) used several geochemical index numbers like U/Th, TOC/S (=C/S), Ni/Co or V/Cr for the interpretation of paleoredox conditions. Chromium is mainly derived from detrital, clastic components, while vanadium is commonly linked to organic matter (deposited under reducing environments). V/Cr ratios above 2 are seen as sedimentation under anoxic paleoconditions. The TOC/S ratio is frequently used to assess the paleosalinity of the environment of (commonly organic rich) sediments (Berner and Raiswell, 1984; Morse and Berner, 1995; Sageman and Lyons, 2004). Typically, less pyrite is formed in organic rich sediments derived from freshwater compared to analogous marine equivalents. Hence, non-marine sediments commonly have higher TOC/S ratios (Berner and Raiswell, 1984).

Th/Sc and Zr/Sc ratios are used to identify sediment recycling and sorting processes (McLennan et al., 1993). Th/Sc monitors the compositional variation of the source, while higher Zr/Sc ratios are associated with zircon enrichments due to sedimentary recycling.

Immobile trace elements like Th, Sc, La, Zr and Ti/Zr as well as La/Sc ratios are used to discriminate between various (palaeo) tectonic settings (Bhatia and Crook, 1986). Light REE (La), incompatible element (Th), compatible element (Sc) and heavy mineral fraction are compared. Th-Sc-Zr/10, La-Th-Sc and La/Sc-Ti/Zr plots were originally tested for graywackes (Bhatia and Crook, 1986) but also adopted for shales and sandstones (Mader and Neubauer, 2004; Kutterolf et al., 2008; Lee, 2009; Descourvieres et al., 2011).

To manage, group, and interpret our geochemical data we use factor analysis, *t*-tests and discriminant analysis.

Factor analysis, which belongs to the dimension-reducing statistical methods, generally analyzes correlations of variables or objects within a large data set. A low number of hypothetical variables – so-called factors – are mathematically defined and summarize the essential information in the data set. Thereby the complexity of the data is reduced based on data-intern dependent relationships. As a result only a low number of factors represent the roughly identical information of a much more voluminous underlying data set. In other words, the method describes the variability among observed variables in terms of a potentially lower number of unobserved variables (factors) and it is used to classify variables by detecting structures in the relationships between variables (Reyment and Jöreskog, 1996). Positive and negative correlations of variables are summarized into factors and the user has to interpret why element associations exist and what they may indicate. One critical aspect is that number of factors and variables are selected by the user, so that the result is influenced by input parameters (Swan and Sandilands, 1995). On the other hand it allows users to optimize the results based on the expert knowledge. Factor analysis is used in geosciences especially for large geochemical data sets (Ohta, 2004; Filzmoser et al., 2009).

To investigate the significance of the difference in mean values between two groups we use the Student's *t*-test if equality of the variances between the two (tested by Levene test) is given, otherwise Welch's *t*-test is used.

Discriminant analysis is a multivariate statistical technique that simultaneously studies differences between groups of objects with respect to several variables. Thus, it determines which variables discriminate between two or more naturally occurring groups (Bühl, 2008). It investigates predetermined groups and does not generate groups (like the cluster analysis for example does) (Backhaus et al., 2006). A separation into groups is more distinct if variation between groups is large, while that within groups is small.

Statistic operations (Student's *t*-test, factor and discriminant analysis) were performed with the statistical software package *IBM SPSS Statistics 19.0*. For the statistical analyses coal-bearing samples (M-1B, M-5, M-17, M-67, M-74 and M-88) were excluded because the geochemistry of coals is extremely different from pelitic sediments and therefore they would influence the statistics to a large degree. The following variables (elements) were used for calculations of the factor analysis: SiO_2, Al_2O_3, Fe_2O_3, MgO, CaO, Na_2O, K_2O, TiO_2, P_2O_5, MnO, Cr_2O_3, Ba, Co, Nb, Ni, Rb, Sn, Sr, Th, U, V, Zr, Mo, Cu, Pb, Zn, Cd, Sb, Tl, Se, B, TOT/C, TOT/S, LOI and B/Al*. These elements and ratios were selected because they play an important role for the interpretation of paleoenvironments (Dominik and Stanley, 1993; McLennan et al., 1993; Garver et al., 1996; Hofmann et al., 2001; Sageman and Lyons, 2004; Lee, 2009). For example, REEs are excluded because they show due to related provenance similar trends in the different sample sets. Other elements like Ag are also

Please cite this article in press as: Hofer, G., et al., Geochemistry of fine-grained sediments of the upper Cretaceous to Paleogene Gosau Group (Austria, Slovakia): Implications for paleoenvironmental and provenance studies, Geoscience Frontiers (2013), http://dx.doi.org/10.1016/j.gsf.2012.11.009

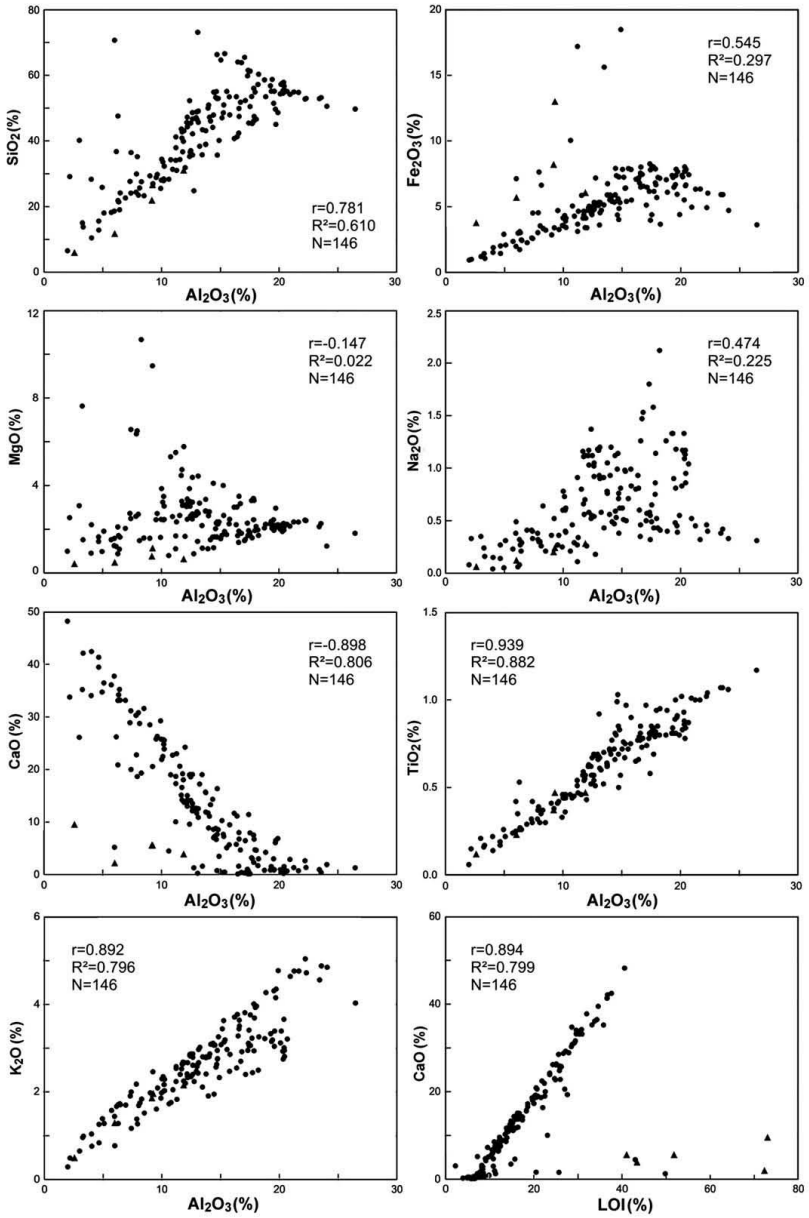


Figure 2. Discrimination plots of major element oxides SiO_2, Al_2O_3, Fe_2O_3, Na_2O, CaO, TiO_2, K_2O and loss on ignition (LOI). SiO_2, Fe_2O_3, Na_2O, TiO_2 and K_2O show a positive correlation with Al_2O_3; CaO is strongly negative correlated. LOI and CaO are strongly positive correlated. Pearson correlation coefficients (r), squared Pearson correlation coefficients (R^2) and number of samples (N) are given in the graphs. Coals and coaly samples (M-1B, M-5, M-17, M-67, M-74 and M-88; plotted as triangles) are excluded for the calculation of the correlation indices.

Please cite this article in press as: Hofer, G., et al., Geochemistry of fine-grained sediments of the upper Cretaceous to Paleogene Gosau Group (Austria, Slovakia): Implications for paleoenvironmental and provenance studies, Geoscience Frontiers (2013), http://dx.doi.org/10.1016/j.gsf.2012.11.009

excluded because it is below detection limit. The analysis was performed using the principle components extraction method and varimax rotation, which is the most common orthogonal rotation criterion (Davis, 2002).

Student's *t*-tests were calculated for the variables B, B/Al*, SiO_2, Al_2O_3, TiO_2, CaO, LOI, Sr, Zr and factor 1 (calculated by factor analysis) as well as $\delta^{13}C$ and $\delta^{18}O$ (Hofer et al., 2011, in press). The limit of significance is determined as <0.05.

For the calculation of the discriminant analysis parameters (variables) such as B, B/Al*, SiO_2, Al_2O_3, TiO_2, CaO, LOI, Sr and Zr as well as $\delta^{13}C$ and $\delta^{18}O$ are used in four different scenarios and compared within two defined groups: a "marine" group and a "non-marine" group (variables B, B/Al*, $\delta^{13}C$ and $\delta^{18}O$ for scenario a; B, B/Al* and $\delta^{13}C$ for scenario b; B/Al* and $\delta^{13}C$ for scenario c and B, B/Al*, $\delta^{13}C$, $\delta^{18}O$, SiO_2, Al_2O_3, TiO_2, CaO, LOI, Sr and Zr for scenario d). B, B/Al*, $\delta^{13}C$ and $\delta^{18}O$ are seen as proxies for paleosalinity (Clayton and Degens, 1959; Hudson, 1977; Anderson and Arthur, 1983; Veizer, 1983; Talbot, 1990). SiO_2, Al_2O_3, TiO_2 and Zr are the end members representing the terrigenous trends. CaO, LOI (here the LOI represents carbonate minerals, largely calcite). Sr served as end members for pelagic trends. Samples from non-marine to marginal-marine sections (from the Glinzendorf Syncline and the Grünbach Formation at the trench in Maiersdorf) were analyzed for their content of calcareous nannofossils to identify marine intersections.

4. Results

4.1. Major elements

Major element chemistry can vary due to lithology and grain size differences quite drastically – coaly samples from the Grünbach Syncline are very heterogeneous (Hofer et al., 2011). SiO_2, Al_2O_3, Fe_2O_3, Na_2O, K_2O and TiO_2 are all associated with strong positive correlations, while CaO and LOI show negative Pearson correlation indices with these elements (Fig. 2 and Table 1). CIA and CPA values range from 57 to 83 and 80 to 98, respectively (Appendix I). CIA and CPA have a high Pearson correlation index of $r = 0.891$, which means that both indices are matchable. Si/Al ratios are generally low (mean: 2.98 ± 1.39). K/Al and Na/Al are relatively constant with a mean of 0.32 ± 0.06 and 0.07 ± 0.03, respectively (Appendix I).

4.2. Trace elements

Boron contents are ranging between 14 and 272 ppm and show strong positive correlations to trace elements such as Ga, V, Th, U or Rb (Fig. 3, Table 1 and Appendix I). B and B/Al* values are varying within the Gießhübl Syncline from 45 to 132 ppm and 121 to 191, respectively (Appendix I). While absolute B concentrations are low (mean: 62.3 ± 16.2 ppm) at Aderklaa 81 well, B/Al* values are relatively high with a mean of 178 ± 11. Aderklaa 84 shows relatively high B values with a mean of 107.5 ± 5.0 ppm and moderate B/Al* ratios (mean: 134 ± 14). B concentrations of the Aderklaa 92 borehole are higher (around 120 ppm) at the bottom interval (3505–3110 m) and lower (down to 74 ppm) at the top. In contrast to that, B/Al* ratios are relatively uniform (moderate to low with a mean of 139 ± 11). The lower Gießhübl Formation of Aderklaa 92 is characterized by mean boron values of 116.0 ± 19.6 ppm with one outlier (74 ppm) at 3329 m. The middle Gießhübl Formation has mean boron values of 96.5 ± 0.5 ppm at around 3009 m and lower mean values of 77.3 ± 4.2 ppm at a section around 2922 m. One sample from the upper Gießhübl Formation gives 112 ppm (analogue to Aderklaa 84 with 108 ppm) (Table 2 and Appendix I). At Aderklaa 84 and 92, B/Al* ratios are low at the lower and upper Gießhübl Formation. They show higher values (around 140 are characteristic) in the middle Gießhübl Formation (Table 2 and Appendix I). Outcrop samples from Groisbach also have low boron contents (mean: 48.0 ± 2.5 ppm) but higher B/Al* ratios (mean: 156 ± 22) (Appendix I). Outcrop samples from Lilienfeld are characterized by relatively low B values ranging from 45 to 114 ppm. But they also have high B/Al* ratios up to 282. Boron values at Glinzendorf vary from 14 to 145 ppm. Accordingly, B/Al* ranges between 92 and 193. B concentrations of Markgrafneusiedl T1 well are lower in the lower part of the section with an average of 88.2 ± 14.9 ppm and significantly higher in the middle and upper intervals where they reach up to 133 ppm. A notably uniform signal of enriched boron concentration can be observed in the interval between 3747.2 m and 3406.2 m with an average of 115.0 ± 8.8 ppm. B/Al* ratios show similar trends ranging from 95 to 192 (Table 3 and Appendix I). B values are generally moderate in the profile of Glinzendorf T1 with only one short interval of higher values (up to 145 ppm) between 3555 and 3480 m. They show a larger variation and fluctuation compared to results from Markgrafneusiedl T1. In some sections there is a range of 40 ppm and

Table 1
Pearson correlation indices.

$N = 146$	SiO_2 (%)	Al_2O_3 (%)	Fe_2O_3 (%)	MgO (%)	CaO (%)	Na_2O (%)	K_2O (%)	TiO_2 (%)	LOI (%)
SiO_2 (%)	1	0.781	0.507	−0.159	−0.927	0.554	0.649	0.868	−0.954
Al_2O_3 (%)	0.781	1	0.545	−0.147	−0.898	0.474	0.892	0.939	−0.834
Fe_2O_3 (%)	0.507	0.545	1	−0.108	−0.677	0.378	0.409	0.512	−0.520
MgO (%)	−0.159	−0.147	−0.108	1	0.100	0.169	−0.068	−0.171	0.096
CaO (%)	−0.927	−0.898	−0.677	0.100	1	−0.550	−0.761	−0.919	0.894
Na_2O (%)	0.554	0.474	0.378	0.169	−0.550	1	0.296	0.457	−0.581
K_2O (%)	0.649	0.892	0.409	−0.068	−0.761	0.296	1	0.854	−0.714
TiO_2 (%)	0.868	0.939	0.512	−0.171	−0.919	0.457	0.854	1	−0.878
LOI (%)	−0.954	−0.834	−0.520	0.096	0.894	−0.581	−0.714	−0.878	1
$N = 146$	B (ppm)	B/Al*	Ga (ppm)	V (ppm)	Th (ppm)	U (ppm)	Rb (ppm)	Cr (ppm)	
B (ppm)	1	−0.032	0.878	0.836	0.742	0.324	0.829	−0.043	
B/Al*	−0.032	1	−0.440	−0.435	−0.538	−0.145	−0.366	−0.016	
Ga (ppm)	0.878	−0.440	1	0.946	0.909	0.333	0.928	−0.054	
V (ppm)	0.836	−0.435	0.946	1	0.881	0.338	0.856	−0.043	
Th (ppm)	0.742	−0.538	0.909	0.881	1	0.271	0.815	0.063	
U (ppm)	0.324	−0.145	0.333	0.338	0.271	1	0.208	0.062	
Rb (ppm)	0.829	−0.366	0.928	0.856	0.815	0.208	1	−0.045	
Cr (ppm)	−0.043	−0.016	−0.054	−0.043	0.063	0.062	−0.045	1	

Please cite this article in press as: Hofer, G., et al., Geochemistry of fine-grained sediments of the upper Cretaceous to Paleogene Gosau Group (Austria, Slovakia): Implications for paleoenvironmental and provenance studies, Geoscience Frontiers (2013), http://dx.doi.org/10.1016/j.gsf.2012.11.009

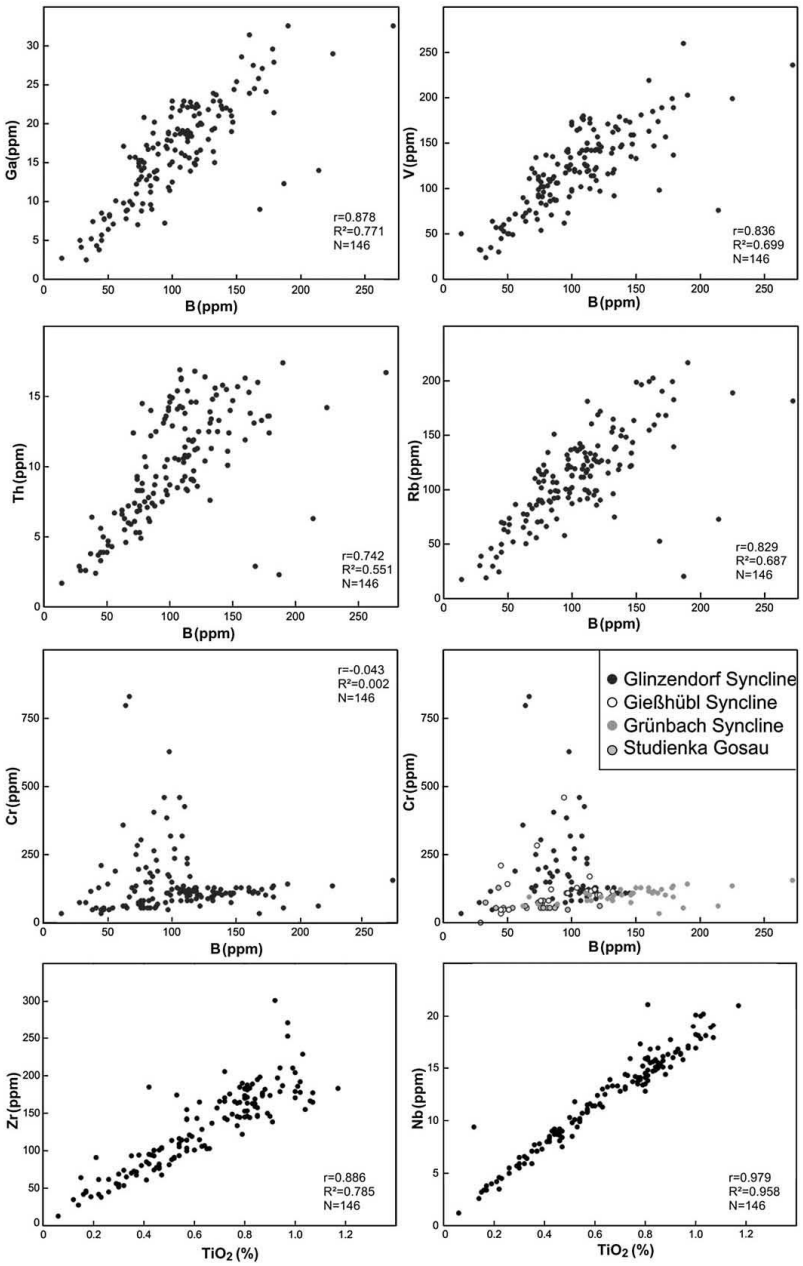


Figure 3. Discrimination plots of trace elements B, Ga, V, Th, Rb, Cr and TiO_2. Ga, V, Th and Rb show a positive correlation with B. A general positive trend can also be observed for Cr vs. B, but most of the samples from the Glinzendorf Syncline (samples from different Gosau synclines are separated supplementary) follow a rather negative trend. Zr and Nb correlate strongly positive with TiO_2. Pearson correlation coefficients (r), squared Pearson correlation coefficients (R^2) and number of samples (N) are given in the graphs.

Please cite this article in press as: Hofer, G., et al., Geochemistry of fine-grained sediments of the upper Cretaceous to Paleogene Gosau Group (Austria, Slovakia): Implications for paleoenvironmental and provenance studies, Geoscience Frontiers (2013), http://dx.doi.org/10.1016/j.gsf.2012.11.009

Table 2
Means of B and B/Al* of the Gießhübl Syncline.

Gießhübl Syncline			B (ppm)	B/Al*
Aderklaa 81	Marine	Mean	62.3	178
		Stand. dev.	16.2	11
		N	3	3
Aderklaa 84	Marine	Mean	107.5	134
		Stand. dev.	4.9	14
		N	2	2
Aderklaa 92	Marine	Mean	103.8	139
		Stand. dev.	21.7	11
		N	13	13
Lilienfeld	Non-marine	Mean	70.7	239
		Stand. dev.	24.6	37
		N	3	3
	Marine	Mean	81.3	197
		Stand. dev.	26.0	35
		N	4	4
Groisbach	Marine	Mean	48.0	156
		Stand. dev.	2.4	22
		N	5	5
Nierental Formation		Mean	55.4	169
		Stand. dev.	12.5	28
		N	10	10
Lower Gießhübl Formation		Mean	116.0	137
		Stand. dev.	19.6	13
		N	7	7
Middle Gießhübl Formation		Mean	85.0	140
		Stand. dev.	10.9	8
		N	5	5
Upper Gießhübl Formation		Mean	109.0	137
		Stand. dev.	4.4	12
		N	3	3
Gießhübl Syncline (marine samples)		Mean	86.6	147
		Stand. dev.	30.3	19
		N	23	23

more within only a few metres while other parts are quite uniform. The lowermost 350 m of strata are characterized by mean values of around 90 ppm, but with some high standard deviations. After a short maximum, concentrations decrease to average values of 132.5 to 86.6 ppm at depths between 3550 and 3245 m, whereas the top section between 3245 and 3249.5 m has a low mean value

Table 3
Means of B and B/Al* of the Glinzendorf Syncline.

Glinzendorf Syncline			B (ppm)	B/Al*
Markgrafneusiedl T1	Non-marine	Mean	94.2	140
		Stand. dev.	20.4	10
		N	5	5
	Marine	Mean	103.2	167
		Stand. dev.	29.3	19
		N	11	11
Glinzendorf T1	Non-marine	Mean	100.9	115
		Stand. dev.	19.7	17
		N	33	33
	Marine	Mean	111.8	158
		Stand. dev.	24.8	31
		N	8	8
Gänserndorf T3	Non-marine	Mean	69.8	156
		Stand. dev.	11.0	7
		N	4	4
	Marine	Mean	61.5	132
		Stand. dev.	34.1	14
		N	6	6
Glinzendorf Syncline (all samples)	Non-marine	Mean	97.6	120
		Stand. dev.	20.5	20
		N	42	42
	Marine	Mean	94.9	156
		Stand. dev.	34.1	26
		N	26	26

Table 4
Means of B and B/Al* of the Studienka (Slovakian) Gosau.

Slovakian Gosau			B (ppm)	B/Al*
Studienka 83	Marine	Mean	76.3	140
		Stand. dev.	46.5	48
		N	3	3
Zavod 57	Marine	Mean	41.0	238
		Stand. dev.		
		N	1	1
Zavod 68	Marine	Mean	72.0	169
		Stand. dev.	18.6	57
		N	13	13
Slovakian Gosau (all samples)	Marine	Mean	70.9	168
		Stand. dev.	24.3	56
		N	17	17

of 86.6 ± 11.4 ppm. In contrast to that B/Al* ratios are generally low and fluctuate around 110 with one interval of higher ratios up to 193 at the very top (Table 3 and Appendix I). B concentrations and B/Al* ratios from the Gänserndorf T3 borehole are low to moderate ranging from 14 to 112 ppm and 116 to 163, respectively (Table 4 and Appendix I).

B values of the Slovakian Gosau Group deposits from the Studienka 83, Závod 57 and 68 wells are generally low and are varying from 29 to 122 ppm with a mean of 70.9 ± 24.3. The only enriched boron signal (122 ppm) is present in the lowermost interval of Studienka 83. In the top section boron values decrease to 29 ppm (Table 4 and Appendix I). At Závod 68 mean boron values are generally low (72.0 ± 17.9 ppm), starting with extremely low values of around 38 ppm in the lowermost section. Above that, the B signal increases up to almost 100 ppm at depths around 4070 m and decreases again to slightly lower values between 3950 and 3720 m (Table 4 and Appendix I). The Závod 57 borehole is represented by only one sample at around 4022 m with a boron concentration of 41 ppm. On the other hand B/Al* ratios of Slovakian profiles are high (up to 286) with a mean of 168 ± 56 (Table 4 and Appendix I). Geochemical results from the Maiersdorf trench (Grünbach Syncline) are given in Hofer et al. (2011).

Th/Sc ratios are relatively high and ranging from 0.41 to 1.30 (mean: 0.76 ± 0.14). Zr/Sc ratios are relatively low with values between 5.08 and 32.10 (mean: 9.77 ± 4.06). V/Cr ratios are generally low and ranging between 0.21 and 12.46. Th/U ratios are quite variable and fluctuating between 0.14 and 6.22 (mean: 3.80 ± 1.29). La/Sc ratios are low and ranging between 1.14 and 4.70 (mean: 2.09 ± 0.47). Ti/Zr ratios have a broad range from 13.62 to 41.62 (mean: 29.78 ± 5.23) (Appendix I).

4.3. Organic carbon

TOC contents are generally low and below 1% (Appendix I). Some samples from the Glinzendorf Syncline (Markgrafneusiedl T1, Glinzendorf T1 and Gänserndorf T3) are enriched in organic carbon up to 4.3%. Some samples from the trench (coals and coaly shales from the Grünbach Syncline) contain even high amounts of TOC up to 52.8% (Hofer et al., 2011). TOC/S ratios range from 0.1 to 52.3 (and even up to 1345 in coaly sediments) with a mean of 6.6 ± 10.4 (Appendix I).

4.4. Statistics

The calculated factors 1 and 2 of the factor analysis explain 39.9% and 10.5% of the variance. Factor 1 shows significant positive factor loadings (Table 5: bold numbers indicate significant factor loadings > 0.500) with Al_2O_3, TiO_2, Th, Nb, V, SiO_2, Sn, K_2O, Zr, Rb, B, Fe_2O_3, Co, Cu, Zn and Na_2O and negative factor loadings with CaO,

Please cite this article in press as: Hofer, G., et al., Geochemistry of fine-grained sediments of the upper Cretaceous to Paleogene Gosau Group (Austria, Slovakia): Implications for paleoenvironmental and provenance studies, Geoscience Frontiers (2013), http://dx.doi.org/10.1016/j.gsf.2012.11.009

Table 5
Factors 1 and 2 calculated at the factor analysis.

Variables	Factor 1	Factor 2
Al_2O_3	**0.968**	<0.1
TiO_2	**0.965**	<0.1
Th	**0.962**	<0.1
Nb	**0.960**	<0.1
CaO	**−0.957**	<0.1
V	**0.914**	<0.1
LOI	**−0.914**	<0.1
SiO_2	**0.885**	<0.1
Sn	**0.865**	−0.177
K_2O	**0.864**	−0.221
Zr	**0.855**	<0.1
Rb	**0.853**	−0.150
B	**0.804**	−0.140
TOT/C	**−0.716**	0.138
Sr	**−0.705**	−0.156
Fe_2O_3	**0.621**	0.222
Cu	**0.586**	<0.1
Zn	**0.584**	0.247
Na_2O	**0.524**	−0.165
B/Al*	**−0.505**	−0.192
Ba	0.408	−0.233
Pb	0.367	0.303
MnO	0.227	<0.1
Tl	0.224	0.196
P_2O_5	0.189	−0.145
MgO	−0.143	0.117
Ni	<0.1	**0.900**
Cr_2O_3	<0.1	**0.807**
Co	**0.605**	**0.690**
U	0.284	0.333
Cd	−0.312	0.313
Se	<0.1	0.269
TOT/S	<0.1	0.266
Sb	0.195	0.239
Mo	<0.1	0.233

LOI, TOT/C, Sr and B/Al*. Factor 2 groups only Ni, Cr_2O_3 and Co with large positive loading values. The screeplot demonstrates the eigen values for all detected factors of the analysis (Fig. 4).

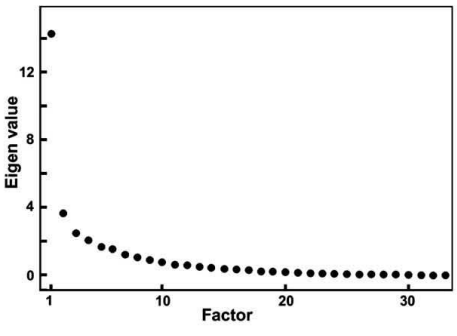


Figure 4. Screeplot showing the eigen values of the factors calculated at the factor analysis. The first two factors have the highest eigen values of around 14 and 4; the other factors have eigen values <2.2.

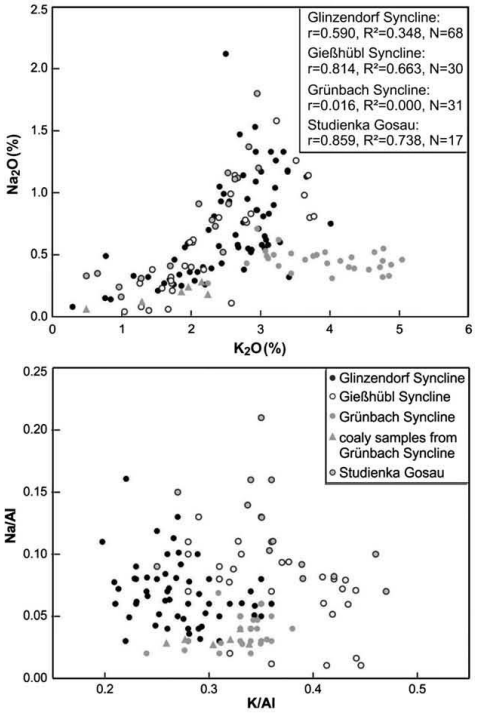


Figure 5. Discrimination plots of K_2O vs. Na_2O and K/Al vs. Na/Al as proxies for smectite and illite contents. Pearson correlation coefficients (r), squared Pearson correlation coefficients (R^2) and number of samples (N) are given separately for the various groups of samples. Different Gosau locations can be distinguished to some degree.

5. Discussion

5.1. Major elements

Major element chemistries are plotted against Al_2O_3 (Fig. 2). Terrigenous derived oxides (e.g. SiO_2 and especially TiO_2) show a strong positive correlation with Al_2O_3, which means that quartz content is not influenced by a special paleoenvironment favouring growth of siliceous tests and skeletons (e.g. radiolarian or siliceous sponges). Strong negative correlation can be only observed between CaO and Al_2O_3. This demonstrates that nearly all Ca is of marine origin and is not influenced significantly by a detrital source (e.g. feldspars). Therefore, the use of Na_2O as a substitute for CaO* is interpreted as valid. A strong positive correlation between CaO and LOI ($r = 0.599$ for all samples and 0.810 excluding coaly samples M-1B, M-5, M-17, M-67 and M-74) supports the assumption that CaO is largely derived from carbonates (Von Eynatten, 2003). Low and relatively constant Si/Al ratios indicate minor influence of detrital quartz for the whole data set. Only a few samples show higher ratios up to 11.8. K/Al and Na/Al ratios are relatively constant and do not suggest drastic fluctuations in illite and smectite contents (Appendix I). But there is an identifiable variance of Na_2O and K_2O contents as well as Na/Al and K/Al, respectively between the different Gosau locations. Especially samples from the Grünbach Syncline show different K_2O/Na_2O ratios ($r = 0.016$) compared to the other groups of samples (r range between 0.590 and 0.859; Fig. 5). K/Al vs. Na/Al plot suggests higher illite and smectite contents for samples from the Gießhübl and Studienka area, medium illite and smectite concentrations from the Glinzendorf Syncline and medium illite and low smectite contents for samples from the Grünbach Syncline (Fig. 5). But generally, variations in lithology or mineralogy are small except coaly samples from

Please cite this article in press as: Hofer, G., et al., Geochemistry of fine-grained sediments of the upper Cretaceous to Paleogene Gosau Group (Austria, Slovakia): Implications for paleoenvironmental and provenance studies, Geoscience Frontiers (2013), http://dx.doi.org/10.1016/j.gsf.2012.11.009

Grünbach Syncline, which makes the geochemical interpretation of the depositional environment robust.

CIA values are ranging between 57 and 83 with a general trend of a lower degree of chemical weathering for the Studienka Gosau and relatively high alteration indices for the Grünbach Syncline. Samples from the Glinzendorf and Gießhübl Synclines indicate a lower moderate to higher degree of weathering (Fig. 6). This indicates a shorter exposure time and faster erosion and transport in the Studienka and Gießhübl realm, and a longer exposure and more vigorous transport of the sediments in Glinzendorf and Grünbach.

5.2. Boron

5.2.1. Gießhübl Syncline

The pelagic section of the Nierental Formation at well Aderklaa 81 is characterized by atypically low boron concentrations (Fig. 7, Table 2 and Appendix I). Using B/Al*, there is a drastic shift to high (tentatively marine-) values. Comparably, this effect can be observed for all samples from the Nierental Formation (e.g. Groisbach and Lilienfeld) (Fig. 7, Table 2 and Appendix I).

At Aderklaa 84 the upper Gießhübl Member is represented by typically marine mean boron values, but relatively low B/Al* ratios (Fig. 7, Table 2 and Appendix I).

The lower Gießhübl Formation of Aderklaa 92 is generally characterized by typically marine boron values (>115 ppm). The middle Gießhübl Formation has boron values slightly lower than 100 ppm. The one sample of the upper Gießhübl Formation is analogous to Aderklaa 84, which has clear marine interpretation (Fig. 7, Table 2 and Appendix I). Low B/Al* ratios are characteristic at lower and upper Gießhübl Formation, and higher in the middle Gießhübl Formation (Fig. 7, Table 2 and Appendix I).

Outcrop samples from the Nierental Formation at Groisbach and Lilienfeld (analogous to Aderklaa 81) show extremely uniform and abnormally low boron values in contrast to high aluminium normalized boron ratios (Table 2 and Appendix I). Samples from Lilienfeld, which represent non-marine strata, have slightly lower B concentrations compared to marine samples from the same area (Fig. 7, Table 2 and Appendix I).

While only the aluminium normalized B values represent the paleodepositional character of the pelagic Nierental Formation, absolute boron concentrations reflect the paleosalinity of the Gießhübl Formation.

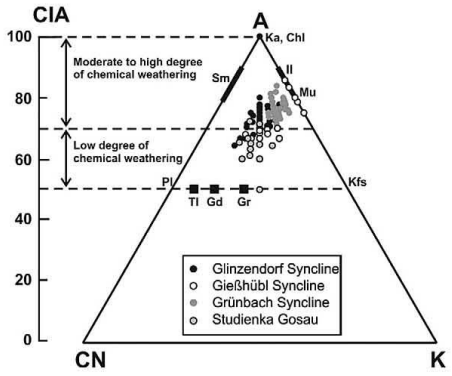


Figure 6. A-CN-K (Al_2O_3-CaO* + Na_2O-K_2O) ternary diagram of the sample set grouped in Glinzendorf-, Gießhübl-, Grünbach Syncline and Studienka Gosau with associated chemical index of alteration (CIA) after Nesbitt and Young (1982). Squares and bars symbolize the average composition of tonalite (Tl), granodiorite (Gd) and granite (Gr) as well as kaolinite (Ka), chlorite (Chl), smectite (Sm), illite (Il), muscovite (Mu), plagioclase (Pl) and K-feldspar (Kfs).

5.2.2. Glinzendorf Syncline

At Markgrafneusiedl T1 well (Figs. 1, 7 and 8 and Table 3) the non-marine basal section is characterized by significantly lower B values than those from the marine middle section. The interpreted limnic top, which is represented by one geochemistry sample (MT1-3275.30-43) and a boron concentration of 119 ppm, does not show a shift to lower values. The reason for that high value is most likely a grain size effect, because this sample comprises relatively high amount of silt compared to other samples (Figs. 7 and 8, Table 3 and Appendix I). The general boron trend of this well is also traced by the B/Al* ratio, beginning with lower values in the lowermost non-marine part, higher values in the middle marine section and shift back to lower values at the non-marine top. This shift at the top section can only be observed by aluminium normalized boron values (Figs. 7 and 8, Table 3 and Appendix I).

While absolute B concentrations are relatively high at the Glinzendorf T1 well, B/Al* ratios mainly represent non-marine character of this section with low values. A possible short marine interval at around 3550 m is expressed by high boron (up to 145 ppm) and slightly enriched B/Al* values. The marine top can only be represented by high normalized values – absolute B concentrations do not show a shift to higher values. Although a direct correlation with the Markgrafneusiedl T1 profile is not possible, a general similarity may be characteristic. Both profiles have the highest boron concentrations in the middle section and lower values at bottom and top (Figs. 7 and 8, Table 3 and Appendix I).

The Gänserndorf T3 well is generally characterized by low boron contents with high variations in absolute concentrations (mean: 64.8 ± 25.2 ppm). The lower non-marine interval from 3146 to 3148 m has low boron contents similar like the marine top from 3079 to 3083.5 m that varies drastically between 14 and 112 ppm. The same trend can be observed using B/Al*.

5.2.3. Grünbach Syncline – Maiersdorf trench

Five marine to non-marine cycles have been reconstructed from the 45 m trench section using B, B/Al*, $\delta^{13}C$ and calcareous nannofossil contents (Hofer et al., 2011). Absolute and normalized B concentrations differ in that interval, but B/Al* are more robust to lithological variations (Table 6).

5.2.4. Slovakian (Studienka) Gosau

In general, boron values from the marine Gosau Formations of the Slovakian wells (Studienka 83, Závod 57 and 68) are abnormally low. At Závod 68 boron values of <100 ppm do not represent the marine sedimentary environment. In contrast to that, mean values with marine interpretation of 168 ± 54 can be observed for the Slovakian Gosau wells by using B/Al* ratios. Except for the upper part of the Závod 68 borehole, all samples are clearly over 150 up to 286 (Fig. 7, Table 4 and Appendix I).

Generally, boron normalized values are more robust to lithological variation and reflect the paleosalinity of the sediments in large parts. 71.7% of non-marine samples from all Gosau locations have B/Al* ratios lower than 150, and 57.0% of marine samples are greater than the postulated transition value of 150.

5.3. Boron and trace elements

Dominant positive correlations can be observed in plots of B vs. Ga, V, Rb and Th. The B vs. Cr plot corroborates the connection of high detrital chrome spinel contents within limnic intervals, which are the sections associated with low boron contents from the

Please cite this article in press as: Hofer, G., et al., Geochemistry of fine-grained sediments of the upper Cretaceous to Paleogene Gosau Group (Austria, Slovakia): Implications for paleoenvironmental and provenance studies, Geoscience Frontiers (2013), http://dx.doi.org/10.1016/j.gsf.2012.11.009

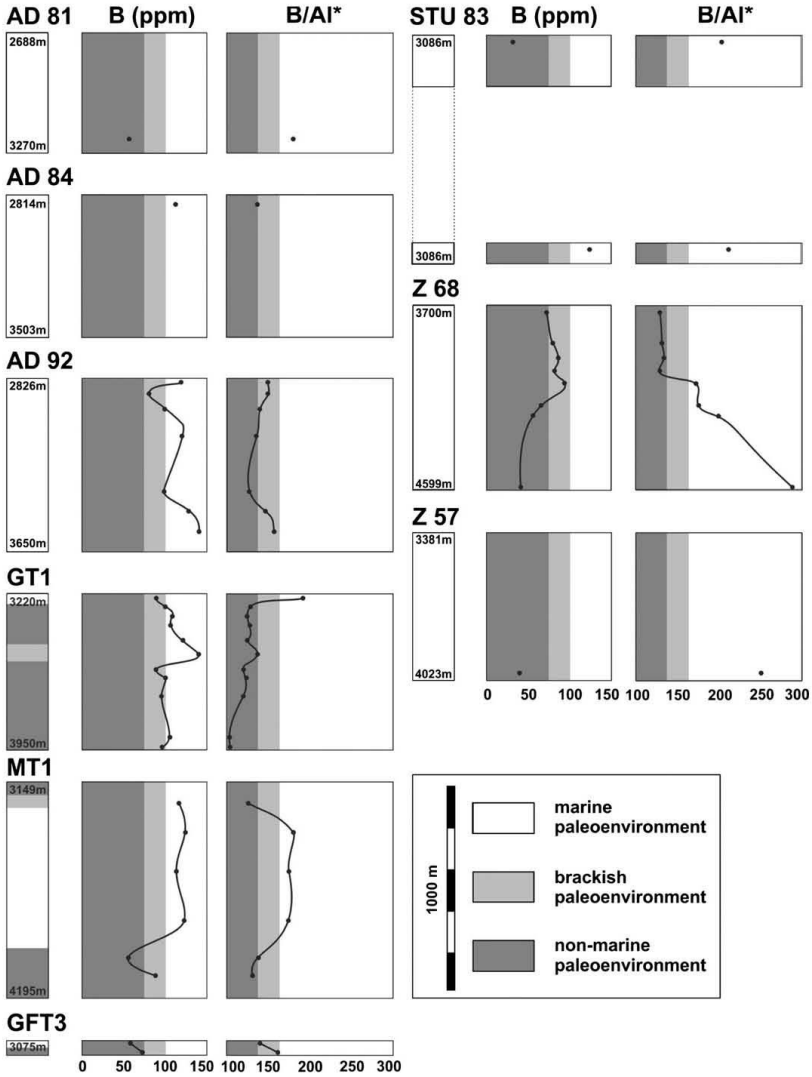


Figure 7. B and B/Al* are plotted for all wells (AD81 = Aderklaa 81, AD84 = Aderklaa 84, AD92 = Aderklaa 92, GT1 = Glinzendorf T1, MT1 = Markgrafneusiedl T1, GFT3 = Gänserndorf T3, STU83 = Studienka 83, Z68 = Závod 68 and Z57 = Závod 57). Known or suggested paleosalinities are drawn in white (marine), light grey (brackish) and dark grey (non-marine).

Glinzendorf Syncline (unpublished OMV in-house data from Markgrafneusiedl T1 and Glinzendorf T1). While there is a strong positive correlation between boron and chromium in the rest of the data set, lots of samples from the Glinzendorf Syncline show significantly different trends. Especially non-marine samples do not follow the general trend (Fig. 3).

Another important factor when using B as paleosalinity indicator is the possible influence of the boron-silicate tourmaline. Heavy mineral analyses show that tourmaline contents are very low in general, and are relatively constant within all investigated locations. Therefore, influence from detrital tourmaline on boron fluctuations within the sections can be excluded.

V/Cr ratios do not suggest periods of anoxic conditions. Except 2 coal samples (M-1B and M-17) from the Grünbach Syncline, all samples have V/Cr less than 2 (Appendix I).

TOC/S ratios are generally higher in non-marine (with a mean of 10.2 ± 13.9) compared to a mean of 4.3 ± 6.4 in marine samples. The high standard deviations are due to high TOC values from the trench.

Relatively high Th/Sc (mean: 0.76 ± 0.14) and low Zr/Sc ratios (maximum value of 32.1) suggest no (or at least minor) sediment

Please cite this article in press as: Hofer, G., et al., Geochemistry of fine-grained sediments of the upper Cretaceous to Paleogene Gosau Group (Austria, Slovakia): Implications for paleoenvironmental and provenance studies, Geoscience Frontiers (2013), http://dx.doi.org/10.1016/j.gsf.2012.11.009

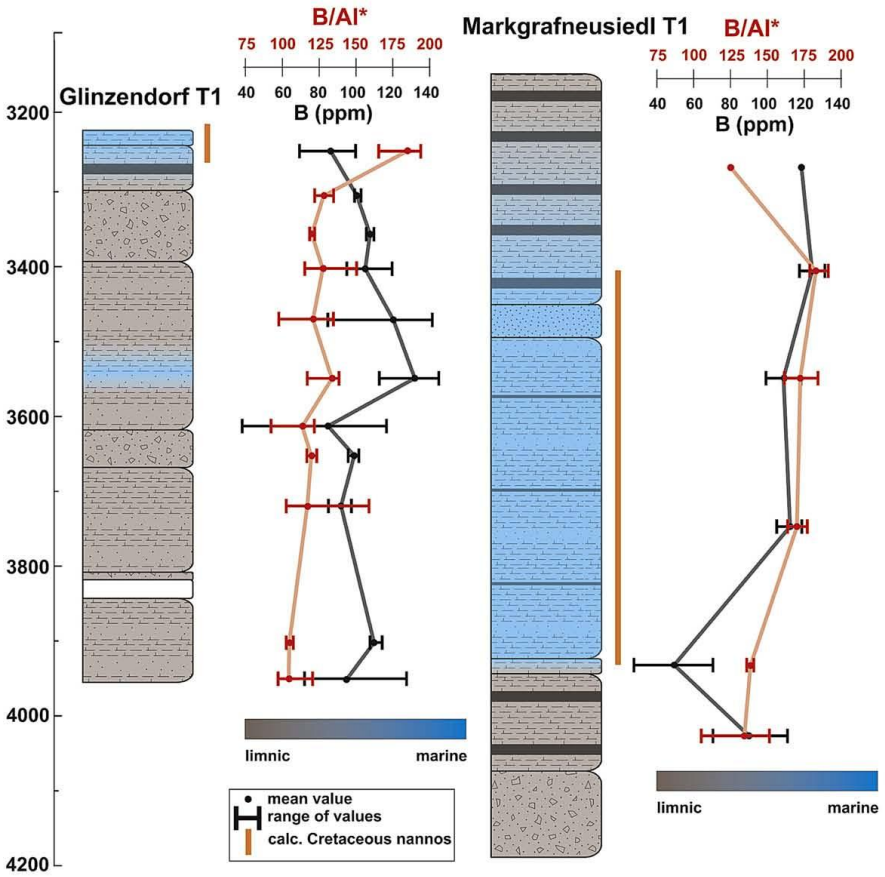


Figure 8. Profiles of the wells Glinzendorf T1 and Markgrafneusiedl T1 from the Glinzendorf Syncline. Interpreted marine and non-marine facies are coloured in blue and brown. Values of B (ppm) and B/Al* are plotted in black and red. Orange lines symbolize (marine) segments where Cretaceous calcareous nannofossils were found. A schematic interpretation-bar for the paleosalinity is given (the transition from non-marine to marine condition is marked at 100 ppm for boron and 150 for B/Al*).

recycling and sorting expressed by zircon enrichments (McLennan et al., 1993) (Fig. 9). This is in accordance with a generally immature "syntectonic" character of the Gosau Group deposition (e.g. Wagreich and Decker, 2001).

The predominant part of the samples has characteristic Th/U ratios of around 3–5 but some samples vary extremely from that. Looking at the results from the trench-profile in detail clear relationship between the Th/U ratio and the coal or rather TOC content in the sediments is recognized. Sediments with high TOC have significantly lower Th/U ratios compared to sediments with low

Table 6
Means of B and B/Al* of the Grünbach Syncline (Maiersdorf trench).

Grünbach syncline			B (ppm)	B/Al*
Maiersdorf trench	Non-marine	Mean	147.4	213
		Stand. dev.	43.5	230
		N	31	31
	Marine	Mean	156.7	166
		Stand. dev.	37.2	18
		N	6	6

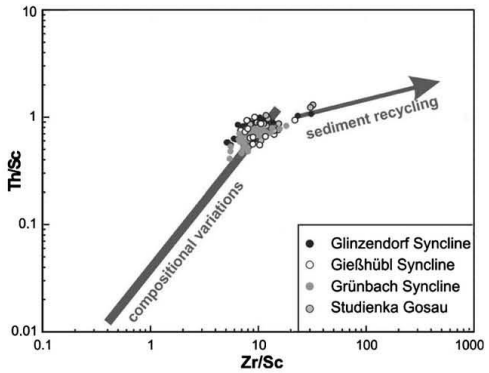


Figure 9. Discrimination plot of Zr/Sc vs. Th/Sc (McLennan et al., 1993) monitoring sediment recycling processes.

Please cite this article in press as: Hofer, G., et al., Geochemistry of fine-grained sediments of the upper Cretaceous to Paleogene Gosau Group (Austria, Slovakia): Implications for paleoenvironmental and provenance studies, Geoscience Frontiers (2013), http://dx.doi.org/10.1016/j.gsf.2012.11.009

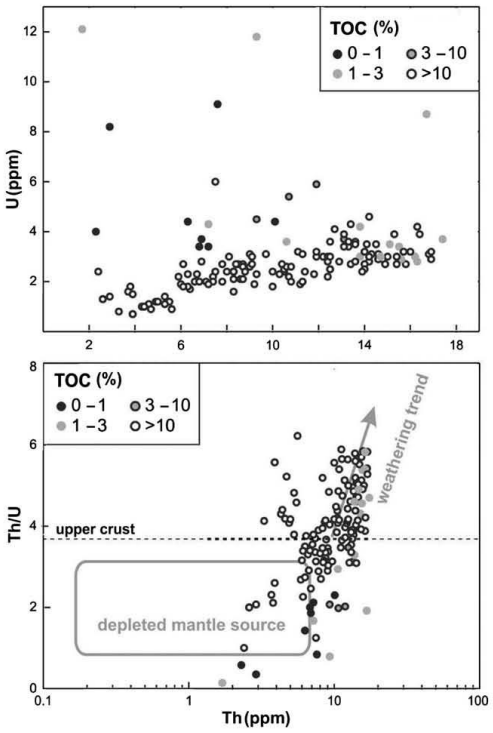


Figure 10. Discrimination plots of Th vs. U and Th vs. Th/U (McLennan et al., 1993). TOC content influences the Th/U ratio (U is enriched in samples with higher TOC).

TOC. Four samples (MT1-4023.50B, MT1-4023.50C, MT1-4023.70 and MT1-4025.40-50) from the Markgrafneusiedl T1 borehole, which plot close to coaly sediments from the trench, are also related to a coal horizon at parts of this depth level (Fig. 10). The Th vs. Th/U graph (McLennan et al., 1993) indicates that during weathering the Th/U ratio increases (and exceeds the upper crustal igneous values of 3.5–4.0) distinctively for most of the samples from Glinzendorf T1, Aderklaa 81, 84, 92, Studienka 83 and Závod 68. Samples from Markgrafneusiedl T1 and Gänserndorf T3 plot below this limit. Such relatively low Th/U ratios are commonly reported from active margin sediments (McLennan et al., 1993). Coal-bearing samples from the trench have distinct lower Th/U ratios. The high U content in organic matter results in lower Th/U ratios. Thus it cannot be used to differentiate different provenances (Fig. 10).

The influence of (detrital) heavy minerals on geochemistry is tested using binary diagrams with TiO_2, which can occur in clay minerals (illite) and heavy minerals (rutile, anatase) (Ratcliffe et al., 2004; Pearce et al., 2005). A strong positive correlation ($r = 0.943$) between TiO_2 and Al_2O_3 (proxy for clay minerals) suggests illite as the primary source of titanium. TiO_2 and Zr also have high positive correlation coefficient ($r = 0.892$) indicating heavy minerals as potential sources. Nb and TiO_2, which are both associated with clay as well as heavy minerals, show clear positive linear trend ($r = 0.973$) (Fig. 3).

5.4. Factor analysis

Components in the rotated space (component 1 vs. component 2) illustrate the information of coherences in element contents (Fig. 11). Variables that plot close to each other have a strong correlation index (Table 5). Component 1 contains terrigenous elements such as Al_2O_3, K_2O, Th, Rb, Zr that plot on the positive x-axis. Elements indicating for marine environments (e.g. CaO, Sr, TOT/C, LOI, B/Al* as well as Cd to some degree) plot on the negative part of the x-axis. The vertical spread, created by component 2, additionally separates elements associated with ultramafic rocks (Cr_2O_3 and Ni) at the positive end of the y-axis (Fig. 11).

Factor 1 plotted against factor 2 (Fig. 11) separates the samples affected by continental influence (proximal samples) and pelagic samples along the x-axis. Most of the samples from Glinzendorf T1 and the trench at Grünbach as well as some samples from the three Aderklaa wells, Markgrafneusiedl T1, Gänserndorf T3 and Studienka 83 are plotted in the so-called "terrigenous" sector. Interestingly most of the samples from the Glinzendorf and Grünbach Syncline plot also within this sector, and are classified as non-marine. Deep-marine (or pelagic) sediments like most of the samples from the Gießhübl Syncline, the Slovakian wells, Markgrafneusiedl T1 and Gänserndorf T3 are set in the "pelagic" sector influenced by the marine variables CaO, Sr, TOT/C, LOI and B/Al* (but not including absolute B, which is located at the positive part of the axis). Strongly marine influenced samples therefore shift to the negative part of the x-axis. Marine samples from the Glinzendorf Syncline and the Slovakian Gosau as well as some samples from the Glinzendorf Syncline are prominent in this sector. The ophiolitic signal could be detected for some samples from the Glinzendorf Syncline producing a shift to positive values of factor 2. In particular samples from Gänserndorf T3, which shows ophiolitic input from geochemistry and heavy minerals, are affected by that shift (Fig. 11).

It must be kept in mind that variations in grain sizes influence the geochemistry and the factor analysis to a low degree (Ohta, 2004). We tried to avoid this effect by using only fine-grained sediment samples.

5.5. Student's t-test

This test compares mean values and standard deviations and uses postulated indicators of paleosalinity (B/Al*, $\delta^{13}C$ and $\delta^{18}O$) to discriminate between two end members. Results from Student's t-test show highly significant separation into marine and non-marine values of the whole data set (Appendix II). Means of B/Al*, $\delta^{13}C$ and $\delta^{18}O$ (Hofer et al., 2011, in press) are significantly lower in non-marine samples compared to marine samples. Because of the heterogeneity of the variance, Welch's t-test was used for comparison of mean boron values of marine and non-marine samples. Mean values of SiO_2, Al_2O_3, TiO_2, CaO, LOI, Sr and Zr (except for Al_2O_3 homogeneity of variance is not given) differ also significantly in marine and non-marine samples illustrating the terrigenous and pelagic affiliation of these elements. Factor 1 values, separating pelagic and terrigenous samples in the factor analysis (Fig. 11), are also significantly different (Appendix II). Due to this effect, some pelagic samples have extremely low B concentrations. Mean boron values are slightly higher in non-marine samples in contrast to marine samples. Therefore, the use of B concentrations to separate marine and non-marine samples is not significant for our data set and cannot be recommended without using additional evidence.

T-test was also used to detect differences of major element concentrations and ratios (normalized with respect to Al_2O_3) between the different Gosau locations (Appendix III). Generally, absolute element concentrations are discernible between most of the different locations. Samples from the Gießhübl and Studienka area only have similar major element contents. Al_2O_3 normalized major elements like SiO_2, Fe_2O_3 or TiO_2 do not show any differences in most of the cases. The Na_2O/Al_2O_3 ratio (smectite content) is for

Please cite this article in press as: Hofer, G., et al., Geochemistry of fine-grained sediments of the upper Cretaceous to Paleogene Gosau Group (Austria, Slovakia): Implications for paleoenvironmental and provenance studies, Geoscience Frontiers (2013), http://dx.doi.org/10.1016/j.gsf.2012.11.009

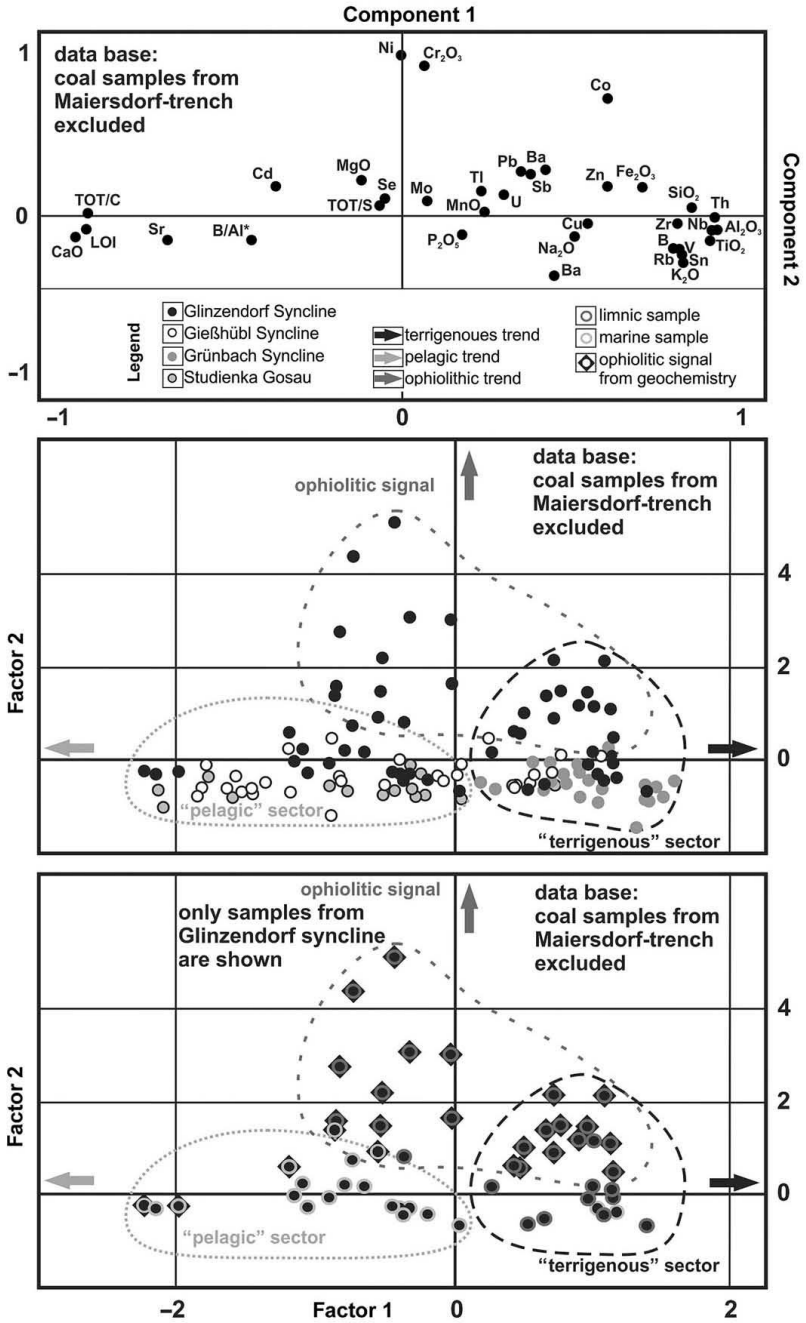


Figure 11. Factor analysis including data of all samples except coaly samples from the Maiersdorf trench (Grünbach Syncline). Statistic was calculated with varimax rotation using the variables SiO_2, Al_2O_3, Fe_2O_3, MgO, CaO, Na_2O, K_2O, TiO_2, P_2O_5, MnO, Cr_2O_3, Ba, Co, Nb, Ni, Rb, Sn, Sr, Th, U, V, Zr, Mo, Cu, Pb, Zn, Cd, Sb, Tl, Se, B, TOT/C, TOT/S, LOI and B/Al*. Component plot (component 1 vs. component 2, topmost graph) shows the distribution of the variables (elements/oxides) in relation to components 1 and 2. The factor plots (factor 1 vs. factor 2) give the distribution of the samples grouped in different Gosau synclines (middle graph) and in detail for the Glinzendorf Syncline showing marine and non-marine samples and samples with assumed ophiolitic detritus determinate by geochemistry and heavy minerals (lowermost graph).

Please cite this article in press as: Hofer, G., et al., Geochemistry of fine-grained sediments of the upper Cretaceous to Paleogene Gosau Group (Austria, Slovakia): Implications for paleoenvironmental and provenance studies, Geoscience Frontiers (2013), http://dx.doi.org/10.1016/j.gsf.2012.11.009

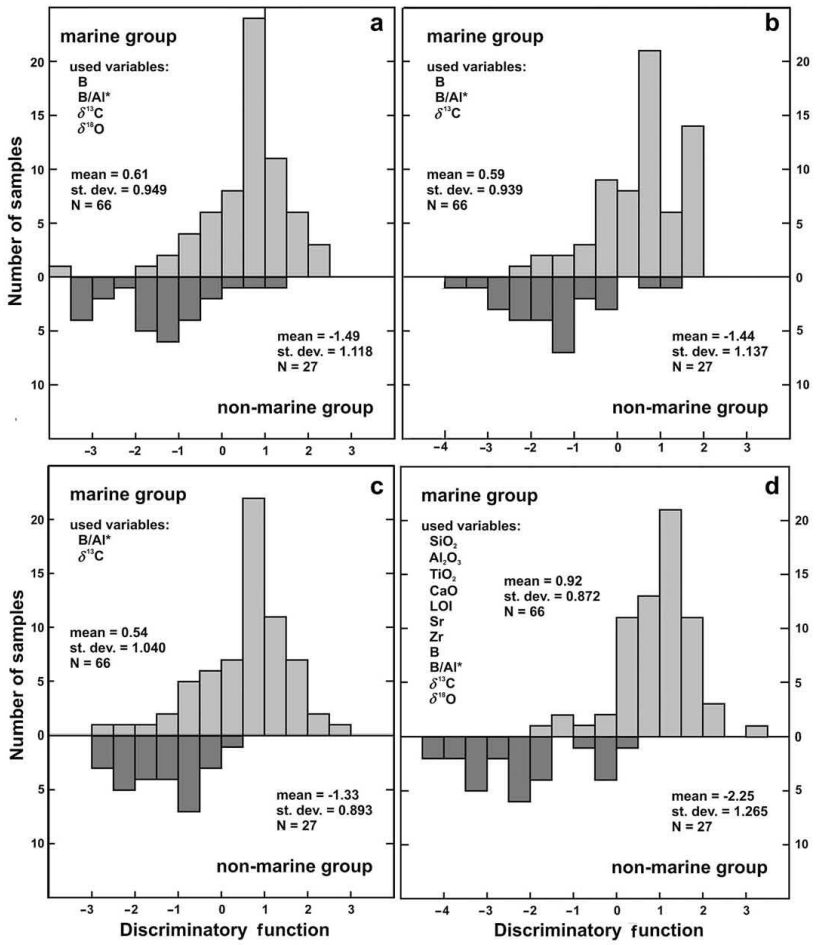


Figure 12. Histogram of the canonical discriminatory function of the two predetermined groups (marine and non-marine) for four calculated scenarios. Used variables for scenario a: B, B/Al*, $\delta^{13}C$ and $\delta^{18}O$ (Isotope data see Hofer et al., 2011); scenario b: B, B/Al* and $\delta^{13}C$; scenario c: B/Al* and $\delta^{13}C$; scenario d: B, B/Al*, $\delta^{13}C$, $\delta^{18}O$, SiO_2, Al_2O_3, TiO_2, CaO, LOI, Sr and Zr. The separation of the two groups using these variables is highly significant ($\alpha = 0.000$).

all sampled locations statistically significantly discriminable. Samples from the Glinzendorf Syncline, which is supposed to be an equivalent of the Grünbach Syncline by Wessely (1992, 2006), are statistically different compared to samples from the Grünbach Syncline considering major elements (e.g. MgO, CaO, Na_2O, K_2O and TiO_2) (Appendix III).

Welch's *t*-test suggests also a significant discrimination (significance = 0.023) between marine and non-marine samples using TOC/S.

5.6. Discriminant analysis

Mean values of the variables from marine and non-marine groups are slightly different to the means calculated by the Student's *t*-test because only samples that contain all variables could be used for this analysis. We have excluded 78 samples from the calculation because at least one discriminatory variable is missing (Appendix IV). Wilks-lambda describes the dimension of the quality of the discrimination into the groups. Lower Wilks-lambda values indicate distinct separation between the groups. Discriminatory functions of all four scenarios are with $\alpha = 0.000$ highly significant, demonstrating the relevance of the variables for the discrimination of marine and non-marine samples (Fig. 12 and Appendix IV). Most of these variables are additionally dominant parameters for factor analysis (resulting in high factor loadings; Fig. 11 and Table 5).

5.7. Provenance

Discriminant function analysis using major elements (Roser and Korsch, 1988) indicates generally a mixed provenance. Different sample groups plot in all end-member sources ("mafic", "intermediate", "felsic" and "quartzose"), and cluster mainly around the intersections. Coal-bearing samples plot within the "mafic" domain, which is simply due to the geochemistry of coals and not

Please cite this article in press as: Hofer, G., et al., Geochemistry of fine-grained sediments of the upper Cretaceous to Paleogene Gosau Group (Austria, Slovakia): Implications for paleoenvironmental and provenance studies, Geoscience Frontiers (2013), http://dx.doi.org/10.1016/j.gsf.2012.11.009

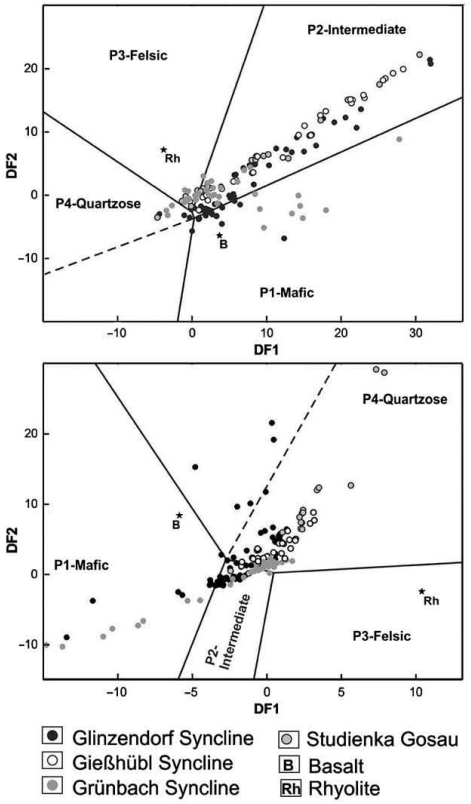


Figure 13. Discrimination plot of discriminant function 1 (DF1) and 2 (DF2) showing 4 main provenance groups: P1-mafic, P2-intermediate, P3-felsic and P4-quartzose (Roser and Korsch, 1988). An average basaltic (B) and rhyolitic (Rh) composition is additionally plotted.

a provenance effect. Generally, no distinct differences were observed between the various Gosau synclines and basins, reflecting the complex tectonic regime (Fig. 13).

In discrimination plots of Cr vs. Ni (Garver et al., 1996) and Cr/V vs. Y/Ni (McLennan et al., 1993), only some samples from the Glinzendorf Syncline (Markgrafneusiedl T1, Glinzendorf T1 and Gänserndorf T3) trend to ultramafic (ophiolitic) source. This is probably detritus from the obducted ophiolitic Tethys suture to the south (e.g. Pober and Faupl, 1988). However, samples from other Gosau regions do not show this trend (Fig. 14). Although the limits of 150 ppm for Cr and 100 ppm for Ni (Garver et al., 1996) are exceeded by lower non-marine samples (4023.5–4025.5 m) from Markgrafneusiedl T1 and several samples from Glinzendorf T1 and Gänserndorf T3, the suggested Cr/Ni ratios of 1.3–1.5 for clear evidence of ultramafic source are not reached in most of the cases. Only 2 samples (GT1-3249 and GT1-3361.5) have additionally this suggested ratio. In the Cr/V vs. Y/Ni plot, samples from the lower non-marine part between 4023.5 and 4025.5 m (and one sample at 3931.2 m) as well as several samples from Glinzendorf T1 and most of the samples from Gänserndorf T3 (mainly from the lower limnic part) trend again to ultramafic (ophiolitic) detritus. Similar to Markgrafneusiedl T1, samples from the middle section of Glinzendorf T1 (between around 3400 and 3650 m) do not show any indication for an ultramafic source (Fig. 14). These Cr enrichments within limnic intervals of the Glinzendorf Syncline correlate with chrome spinels as the dominant mineral of the heavy mineral assemblages (unpublished OMV in-house data). According to Woletz (1963), Stattegger (1987), Pober and Faupl (1988) and Wagreich and Marschalko (1995), the typical evolution of heavy minerals of the Gosau Group begins with chrome spinel (and zircon) dominant assemblages up to the lower Campanian, followed by a decrease of chrome spinel and an increase of garnet. Garnet is getting the dominant heavy mineral up to the Paleogene. This anomaly of the Glinzendorf Syncline with respect to chromium (chrome spinel) can also be observed in the discrimination plot of B vs. Cr, where lots of samples from the Glinzendorf Syncline do not follow the general trend line of the data set (positive correlation). Some of them rather follow a negative trend (Fig. 3).

A mean Th/Sc ratio of 0.76 ± 0.14, which is a sensitive parameter of average provenance compositions (Taylor and McLennan, 1985; Lee, 2009), indicates a generally intermediate to higher silicic provenance (Fig. 9).

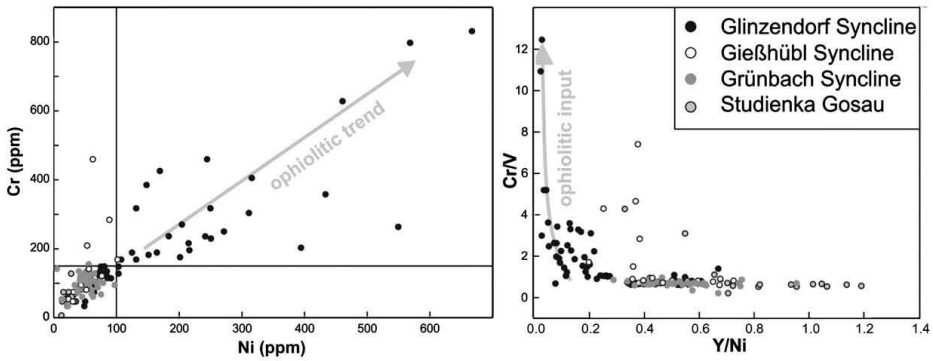


Figure 14. Discrimination plots between Ni and Cr after Garver et al. (1996) (left graph) as well as Y/Ni and Cr/V after McLennan et al. (1993) (right graph). Samples that exceed the limits of 100 ppm Ni and 150 ppm Cr and that are enriched in the Cr/V ratio suggesting ophiolitic input. Only samples from the Glinzendorf Syncline have characteristic geochemical signals for ophiolitic input.

Please cite this article in press as: Hofer, G., et al., Geochemistry of fine-grained sediments of the upper Cretaceous to Paleogene Gosau Group (Austria, Slovakia): Implications for paleoenvironmental and provenance studies, Geoscience Frontiers (2013), http://dx.doi.org/10.1016/j.gsf.2012.11.009

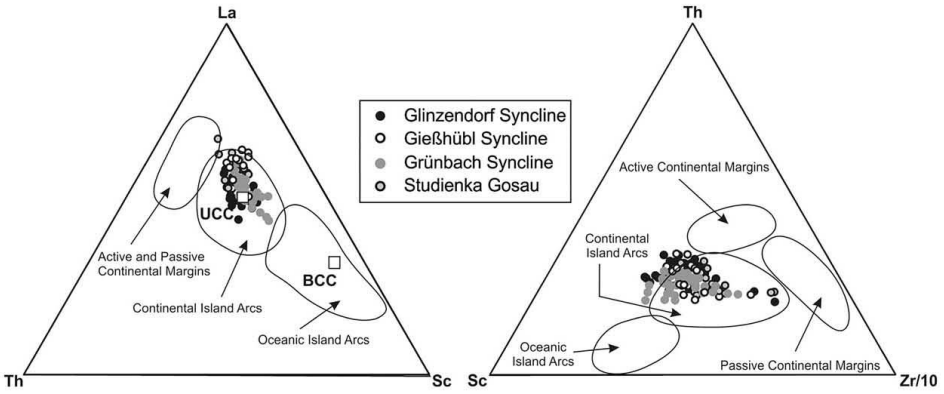


Figure 15. Discrimination plots La-Th-Sc and Th-Sc-Zr/10 for tectonic settings (Bhatia and Crook, 1986). The tectonic regimes active and passive continental margins and continental and oceanic island arcs are distinct. Average upper continental crust (UCC) and bulk continental crust (BCC) are additionally plotted.

The discrimination plots La-Th-Sc and Th-Sc-Zr/10 (Bhatia and Crook, 1986) draw a similar picture: The samples plot close to the average composition of the upper continental crust (UCC) and more or less within the sector of continental island arcs (Fig. 15). However, the tectonic regime of the NCA after the Eoalpine orogenic event is clearly an active continental margin (Wagreich and Faupl, 1994; Wagreich et al., 2011). A reason for this incorrect tectonic classification could be the influence of ophiolitic detritus within the samples. This admixture of an ultramafic/mafic source could lead to higher Sc concentrations (Taylor and McLennan, 1985; Lee, 2009). Bock et al. (2000) and Kutterolf et al. (2008) also reported using bulk rock geochemistry is problematic for discrimination between active continental margins and island arc provenances. Similar to that, most of the samples cluster around the sector of continental island arcs at the La/Sc vs. Ti/Zr plot after Bhatia and Crook (1986). However, some samples plot in or around the regime of active continental margins (Fig. 16).

5.8. Summary for geochemical indices and discrimination diagrams

Based on the large data set and the complex and mixed nature of the Gosau Group sediments in an "orogenic", active margin setting we can evaluate some commonly used geochemical indices for paleoenvironmental and provenance interpretations. The usability of some tested proxies is summarized in Table 7.

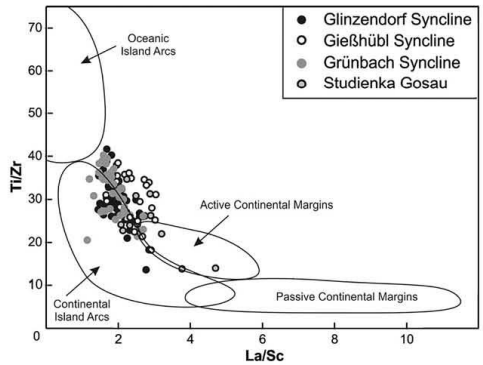


Figure 16. Discrimination plot La/Sc vs. Ti/Zr for tectonic settings (Bhatia and Crook, 1986). The tectonic regimes active and passive continental margins and continental and oceanic island arcs are distinct.

The use of B as a paleosalinity indicator is only sensible if normalized with Al. This B/Al* index is a useful proxy to determine paleosalinity of sediments and seems to work in different environmental settings and basins. Only a comparison between sediments with drastically diverse amount of organic matter is problematic (Hofer et al., 2011). Stable carbon and oxygen isotopes show excellent coherence with B/Al*, and provide a robust and statistically significant discrimination between marine and non-marine samples (Hofer et al., 2011, in press) even under conditions of possible older carbonate reworking as evident for the Gosau basins within the Northern Calcareous Alps (e.g. Wagreich and Decker, 2001). The discrimination plot between $\delta^{13}C$ and $\delta^{18}O$ generally separates marine (pelagic) samples of the Gießhübl Syncline and Slovakian wells (plotting in the "marine" sector) from non- to marginal-marine samples of the Grünbach and Glinzendorf Syncline (plotting in the "limnic" sector) (Fig. 17). Carbon isotope and B/Al* ratios are in good accordance with the interpreted facies, even though the correlation index between B/Al* and $\delta^{13}C$ is low (Fig. 17). Total boron concentrations seem to deviate stronger, especially within pelagic intervals. This is also expressed by the discrimination plot of B vs. B/Al* indicating no correlation ($r = -0.036$) (Fig. 17).

According to our data, we do not recommend the TOC/S ratio as a reliable paleosalinity proxy, although statistically proven, because of low difference of means in marine and non-marine samples. But the higher average non-marine values are mainly derived from a few samples that are rich in organic matter. In general, low TOC

Table 7
Usability of tested geochemical proxies.

Proxy	Useful	Not useful	Purpose
B		×	Paleosalinity
B/Al*	×		Paleosalinity
TOC/S		×	Paleosalinity
Cr/Ni	×		Ultramafic detritus
(Cr/V)/(Y/Ni)	×		Ultramafic detritus
(Th/Sc)/(Zr/Sc)	×		Sediment recycling
Th-Sc-Zr/10		×	Tectonic setting
La-Th-Sc		×	Tectonic setting
(La/Sc)/(Ti/Zr)		×	Tectonic setting

Please cite this article in press as: Hofer, G., et al., Geochemistry of fine-grained sediments of the upper Cretaceous to Paleogene Gosau Group (Austria, Slovakia): Implications for paleoenvironmental and provenance studies, Geoscience Frontiers (2013), http://dx.doi.org/10.1016/j.gsf.2012.11.009

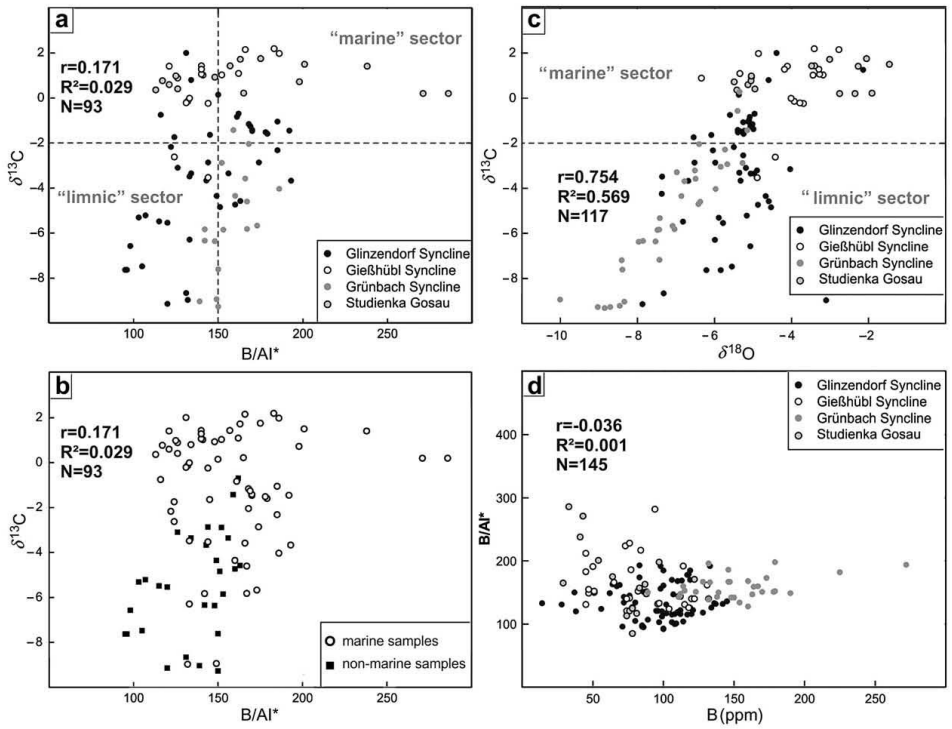


Figure 17. (a) Discrimination plots of B/Al* vs. $\delta^{13}C$ (Isotope data see Hofer et al., 2011, in press) grouped in different Gosau synclines/basins. For approximate orientation a "marine" sector (B/Al* > 150 and $\delta^{13}C > -2$) and a "limnic" sector (B/Al* < 150 and $\delta^{13}C < -2$) are given. (b) Discrimination plots of B/Al* vs. $\delta^{13}C$ grouped in marine and non-marine samples. (c) Discrimination plots of $\delta^{18}O$ vs. $\delta^{13}C$ (Isotope data see Hofer et al., 2011, in press) grouped in different Gosau synclines/basins. For approximate orientation a "marine" sector ($\delta^{13}C > -2$) and a "limnic" sector ($\delta^{13}C < -2$) are given. (d) Discrimination plots of B vs. B/Al* grouped in different Gosau synclines/basins. Pearson correlation coefficients (r), squared Pearson correlation coefficients (R^2) and number of samples (N) are given in the graphs.

contents of our sediments seem to blur results obtained by this method.

CIA and CPA indices can only give an overall picture of alteration, weathering or climate conditions. Significant fluctuations or climate-controlled cyclicity within single profiles or successions of formations are not given, although significant climate changes from upper Cretaceous to Paleogene formations are suspect. CIA and CPA indices seem to be robust and persistent throughout the sections and from one basin to the other.

The detection of ophiolitic detritus using Cr and Ni ratios (McLennan et al., 1993; Garver et al., 1996) is sensitive, and is also screened by factor analysis. This signal clearly applies to the Gosau basins and can be used to correlate or discriminate sections. In contrast, general provenance discrimination plots using major and trace elements achieved inaccurate and complex results and can be hardly interpreted. Trace element discrimination plots (Bhatia and Crook, 1986) classified mainly false (paleo)tectonic settings, probably due to the mixed provenance within an evolving orogen that shares sources of continental crust, accretionary wedges and terranes, and some ophiolites (e.g. Stattegger, 1987; Pober and Faupl, 1988).

The statistical factor analysis turned out to be an excellent tool to deal with large multivariate data sets and to get a good overview of the characteristics of data, especially in respect to correlations of basins. With that, paleoenvironmental as well as provenance questions were accurately determined.

6. Conclusions

This study shows by detailed geochemical analysis and statistical data treatment that fine-grained sediments may be separated into proximal and distal depositional areas within the Gosau Group in the Eastern Alps and its succession into the Carpathians. Geochemical investigation indicates that Gosau sediments of Grünbach, Glinzendorf and Gießhübl have a more proximal signal during the early stages (Coniacian and Santonian) of sediment deposition and tend to get more pelagic from the Campanian onward. In contrast, Carpathian sediments of the Studienka development plot in the pelagic marine sector. In summary, a combination of geochemical parameters can be used to distinguish limnic, marginal-marine, and pelagic fine-clastic sediment intervals within upper Cretaceous to Paleogene samples from outcrops and drill cores. Aluminium normalized boron and stable carbon and oxygen ratios are significantly different in marine and non-marine samples. In this data set absolute boron concentrations are not robust because they rather reflect lithological variations. In this way B/Al* may be used as indicator for paleosalinity. The combination of B/Al*, $\delta^{13}C$ and $\delta^{18}O$ are reliable geochemical proxies to determine the paleosalinity and paleodepositional conditions in sediments with low or nonexistent fossil abundances and uncertain paleoenvironment. However, only an overall assessment of major, minor, and trace element geochemistry provides reliable results.

Please cite this article in press as: Hofer, G., et al., Geochemistry of fine-grained sediments of the upper Cretaceous to Paleogene Gosau Group (Austria, Slovakia): Implications for paleoenvironmental and provenance studies, Geoscience Frontiers (2013), http://dx.doi.org/10.1016/j.gsf.2012.11.009

Using factor analysis, pelagic influenced samples (i.e. deposits from the distal continental margin such as the Gießhübl Syncline and Slovakian equivalents) can be separated from marginal-marine to non-marine samples (Grünbach and Glinzendorf Syncline) owing to the content of terrigenous-indicative elements. On the other hand, a discrimination of samples with a supposed ophiolitic detritus related to elements associated with ultramafic genesis (Cr, Ni) can be observed only for several samples of the Glinzendorf Syncline. In this way huge and complex multivariate data sets with multidimensional variables can be reduced and displayed easily. We suggest a preliminary application of data reduction in an initial stage of a research and an advanced selection of input variable in a final stage, when there is more knowledge on the data set. In this way some redundant variables can be excluded.

Geochemical provenance analysis indicates generally a mixed provenance of Gosau Group sediments within a continental island arc with an exceptional position of parts of the Glinzendorf Syncline that identify an ultramafic/ophiolitic source.

Acknowledgements

This study was funded by the OMV AG within a scientific research project at the University of Vienna (University of Vienna Commission No. FA 536004). This research article is part of G.Hs PhD thesis which is partly funded by the DOC program of Austrian Academy of Sciences.

Appendix I–IV. Supplementary data

Supplementary data related to this article can be found at http://dx.doi.org/10.1016/j.gsf.2012.11.009.

References

Anderson, T.F., Arthur, M.A., 1983. Stable isotopes of oxygen and carbon and their application to sedimentologic and palaeoenvironmental problems. In: Arthur, M.A., Anderson, T.F., Kaplan, I.R., Veizer, J., Land, L.S. (Eds.), Stable Isotopes in Sedimentary Geology. SEPM. Short Course, vol. 10. Geological Society of London, London, pp. 1–151.

Backhaus, K., Erichson, B., Plinke, W., Weiber, R., 2006. Multivariate Analysemethoden. Eine anwendungsorientierte Einführung. Springer, Berlin.

Berner, R.A., Raiswell, R., 1984. C/S method for distinguishing freshwater from marine sedimentary rocks. Geology 12, 365–368.

Bhatia, M.R., Crook, K.A.W., 1986. Trace element characteristics of graywackes and tectonic setting discrimination of sedimentary basins. Contributions to Mineralogy and Petrology 92, 181–193.

Bock, B., Bahlburg, H., Wörner, G., Zimmermann, U., 2000. Ordovician arcs and terranes in NW-Argentina and N-Chile? Geochemical and isotope evidence. Journal of Geology 108, 513–535.

Buggle, B., Glaser, B., Hambach, U., Gerasimenko, N., Marković, S., 2011. An evaluation of geochemical weather indices in loess-paleosol studies. Quaternary International 240, 12–21.

Bühl, A., 2008. SPSS 16. Einführung in die moderne Datenanalyse. Pearson Studium, München.

Clayton, R.N., Degens, E.T., 1959. Use of carbon isotope analyses of carbonates for differentiating freshwater and marine sediments. American Association of Petroleum Geologists Bulletin 43, 890–897.

Cullers, R.L., 2000. The geochemistry of shales, siltstones and sandstones of Pennsylvanian-Permian age, Colorado, USA: implications for provenance and metamorphic studies. Lithos 51, 181–203.

Davis, J.C., 2002. Statistics and Data Analysis in Geology. John Wiley & Sons, New York.

Descourvieres, C., Douglas, G., Leyland, L., Hartog, N., Prommer, H., 2011. Geochemical reconstruction of the provenance, weathering and deposition of detrital-dominated sediments in the Perth Basin: the Cretaceous Leederville Formation, south-west Australia. Sedimentary Geology 236, 62–76.

Dominik, J., Stanley, D.J., 1993. Boron, beryllium and sulfur in Holocene sediments and peats of the Nile delta, Egypt: their use as indicators of salinity and climate. Chemical Geology 104, 203–216.

Erkan, E., 1972. Die exotischen Gerölle in der Gosaukreide der nordöstlichen Kalkalpen (Stratigraphische Gliederung, Bestand, Schüttungsrichtungen). Mitteilungen der Geologischen Gesellschaft in Wien 65, pp. 33–108.

Ernst, W., 1966. Stratigraphisch-fazielle Identifizierung von Sedimenten auf chemisch-geologischem Wege. International Journal of Earth Sciences 55 (1), 21–29.

Faupl, P., Pober, E., Wagreich, M., 1987. Facies development of the Gosau Group of the eastern parts of the Northern Calcareous Alps during the Cretaceous and Paleogene. In: Flügel, H.W., Faupl, P. (Eds.), Geodynamics of the Eastern Alps. Deuticke, Vienna, pp. 142–155.

Faupl, P., Sauer, R., 1978. Zur Genese roter Pelite in Turbiditen der Flyschgosau in den Ostalpen (Oberkreide-Alttertiär). Neues Jahrbuch für Geologie und Paläontologie, Monatshefte, 65–86.

Faupl, P., Wagreich, M., 1996. Basin analysis of the Gosau Group of the Northern Calcareous Alps (Turonian-Eocene, Eastern Alps). In: Wessely, G., Liebl, W. (Eds.), Oil and Gas in Alpidic Thrustbelts and Basins of Central and Eastern Europe. EAGE Special Publication No. 5, pp. 127–135.

Faupl, P., Wagreich, M., 2000. Late Jurassic to Eocene paleogeography and geodynamic evolution of the Eastern Alps. Mitteilungen der Österreichischen Geologischen Gesellschaft 92, 79–94.

Filzmoser, P., Hron, K., Reimann, C., Garrett, R., 2009. Robust factor analysis for compositional data. Computers & Geosciences 35, 1854–1861.

Garver, J.I., Royce, P.R., Smick, T.A., 1996. Chromium and nickel in shale of the Taconic foreland: a case study for the provenance of fine-gained sediments with an ultramafic source. Journal of Sedimentary Research 66, 100–106.

Goodarzi, F., Swaine, D.J., 1994. Paleoenvironmental and Environmental Implications of the Boron Content of Coals. Geological Survey of Canada Bulletin, Ottawa, vol. 471.

Heling, D., 1967. Die Salinitätsfazies von Keupersedimenten aufgrund von Borgehaltsbestimmungen. Sedimentology 8 (1), 63–72.

Hofer, G., Draganits, E., Wagreich, M., Hofmann, C.C., Reischenbacher, D., Neuhuber, S., Grundtner, M.L., Bottig, M., 2011. Stratigraphy and geochemical characterisation of Upper Cretaceous non-marine – marine cycles (Grünbach Formation, Gosau Group, Austria). Austrian Journal of Earth Sciences 104 (2), 90–107.

Hofer, G., Wagreich, M., Spötl, C. Carbon, Oxygen and Strontium Isotopes as a Tool to Decipher Marine and Non-marine Environments: Implications from a Case Study of Cyclic Upper Cretaceous Sediments, The Geological Society of London, Special Publications, in press.

Hofmann, P., Ricken, W., Schwark, L., Leythaeuser, D., 2001. Geochemical signature and related climatic-oceanographic processes for early Albian black shales: site 417D, North Atlantic Ocean. Cretaceous Research 22, 243–257.

Hradecká, L., Lobitzer, H., Ottner, F., Švábenická, L., Svobodová, M., 1999. Biostratigraphy and facies of selected exposures in the Grünbach-Neue Welt Gosau-Group (Coal-bearing series, Inoceramus-Marl and Zweiersdorf-Formation, Late Cretaceous and Paleocene, Lower Austria). Abhandlungen der Geologischen Bundesanstalt 56 (2), 519–551.

Hudson, J.D., 1977. Stable isotopes and limestone lithification. Journal of the Geological Society of London 133, 637–660.

Jones, B., Manning, D.A.C., 1994. Comparison of geochemical indices used for the interpretation of paleoredox conditions in ancient mudstones. Chemical Geology 111, 111–129.

Krenmayr, H.G., 1999. Die Nierental-Formation der Oberen Gosau Gruppe (Oberkreide-Paleozän, Nördliche Kalkalpen) in Berchtesgaden: Definition, Fazies und Environment. Jahrbuch der Geologischen Bundesanstalt 141 (4), 409–447.

Kutterolf, S., Diener, R., Schacht, U., Krawinkel, H., 2008. Provenance of the Carboniferous Hochwipfel Formation (Karawanken Mountains, Austria/Slovenia) – geochemistry versus petrography. Sedimentary Geology 203, 246–266.

Lee, Y.I., 2009. Geochemistry of shales of the Upper Cretaceous Hayang Group, SE Korea: implications for provenance and source weathering at an active continental margin. Sedimentary Geology 215, 1–12.

Mader, D., Neubauer, F., 2004. Provenance of Palaeozoic sandstones from the Carnic Alps (Austria): petrographic and geochemical indicators. International Journal of Earth Sciences 93, 262–281.

Madhavaraju, J., González-León, C.M., Lee, Y.I., Armstrong-Altrin, J.S., Reyes-Campero, L.M., 2010. Geochemistry of the Mural Formation (Aptian-Albian) of the Bisbee Group, Northern Sonora, Mexico. Cretaceous Research 31, 400–414.

Martin, J.M., Whitfield, M., 1983. The significance of the river input of chemical elements to the ocean. In: Wong, C.S., Boyle, E.A., Bruland, K.W., Burton, J.D., Goldberg, E.D. (Eds.), Trace Metals in Sea Water. Plenum Publ. Corp., New York, pp. 265–296.

McLennan, S.M., Hemming, S., McDaniel, D.K., Hanson, G.M., 1993. Geochemical approaches to sedimentation, provenance, and tectonics. In: Johnsson, M.J., Basu, A. (Eds.), Processes Controlling the Composition of Clastic Sediments. Geological Society of America, Special Papers, vol. 284, pp. 21–40.

Mišík, M., 1994. Senonian continental sediments with marine intercalation (Gosau complex) in the basement of the Slovakian part of Vienna basin (borehole Gajary Ga-125). Mineralia Slovaca 26, 297–310.

Morse, J.W., Berner, R.A., 1995. What determines sedimentary C/S ratios? Geochimica et Cosmochimica Acta 59, 1073–1077.

Nesbitt, H.W., Young, G.M., 1982. Early Proterozoic climates and plate motions inferred from major element chemistry of lutites. Nature 299, 715–717.

Nesbitt, H.W., Young, G.M., 1989. Formation and diagenesis of weathering profiles. Journal of Geology 97, 129–147.

Ohta, T., 2004. Geochemistry of Jurassic to earliest Cretaceous deposits in the Nagato Basin, SW Japan: implication of factor analysis to sorting effects and provenance signatures. Sedimentary Geology 171, 159–180.

Please cite this article in press as: Hofer, G., et al., Geochemistry of fine-grained sediments of the upper Cretaceous to Paleogene Gosau Group (Austria, Slovakia): Implications for paleoenvironmental and provenance studies, Geoscience Frontiers (2013), http://dx.doi.org/10.1016/j.gsf.2012.11.009

ARTICLE IN PRESS

Pavlishina, P., Verreussel, R., Leereveld, H., Summesberger, H., Wagreich, M., 2004. Palynological study of Gosau group deposits (Upper Cretaceous) of the Northern Calcareous Alps (Austria). Annalen des Naturhistorischen Museums in Wien 106A, 67–90.

Pearce, T.J., Wray, D., Ratcliffe, K., Wright, D.K., Moscariello, A., 2005. Chemostratigraphy of the Upper Carboniferous Schooner Formation, southern North Sea. In: Collinson, J.D., Evans, D.J., Holliday, D.W., Jones, N.S. (Eds.), Carboniferous Hydrocarbon Geology: The Southern North Sea and Surrounding Onshore Areas. Yorkshire Geological Society 7, pp. 147–164.

Plöchinger, B., 1961. Die Gosaumulde von Grünbach und der Neuen Welt. Jahrbuch der Geologischen Bundesanstalt 104, 359–441.

Pober, E., Faupl, P., 1988. The chemistry of detrital chromium spinels and its implications for the geodynamic evolution of the Eastern Alps. Geologische Rundschau 77, 641–670.

Ralbovsky, E., Ostrolucký, P., 1996. The Glinzendorf Syncline below the Vienna Basin in Slovakia. In: Wessely, G., Liebl, W. (Eds.), Oil and Gas in Alpidic Thrustbelts and Basins of Central and Eastern Europe. EAGE Special Publication No. 5, pp. 145–146.

Rahman, M.J.J., Suzuki, S., 2007. Composition of Neogene shales from the Surma Group, Bengal Basin, Bangladesh: implications for provenance and tectonic setting. Austrian Journal of Earth Sciences 100, 54–64.

Ratcliffe, K.T., Wright, A.M., Hallsworth, C., Morton, A., Zaitlin, B.A., Potocki, D., Wray, D.S., 2004. An example of alternative correlation techniques in a low-accommodation setting, nonmarine hydrocarbon system: the (Lower Cretaceous) Mannville Basal Quartz succession of southern Alberta. AAPG Bulletin 88 (10), 1419–1432.

Reyment, R.A., Jöreskog, K.G., 1996. Applied Factor Analysis in the Natural Sciences. Cambridge University Press, Cambridge.

Roser, B.P., Korsch, R.J., 1988. Provenance signatures of sandstone-mudstone suites determined using discriminant function analysis of major-element data. Chemical Geology 67, 119–139.

Rügner, O., 2000. Tonmineral-Neubildung und Paläosalinität im Unteren Muschelkalk des südlichen Germanischen Beckens. Ph.D. Thesis, University of Heidelberg, Germany, 189 pp.

Sachsenhofer, R.F., Tomschey, O., 1992. Gosau-type coals of Austria and Hungary – a preliminary geochemical comparison. Acta Geologica Hungarica 35 (1), 49–57.

Sageman, B.B., Lyons, T.W., 2004. Geochemistry of fine-grained sediments and sedimentary rocks. In: MacKenzie, F. (Ed.), Sediments, Diagenesis, and Sedimentary Rocks. Treatise on Geochemistry, vol. 7. Elsevier Publ., New York, pp. 115–158.

Selter, V., David, F., Kraft, T., 1989. Zusammenhänge zwischen Fazies und Borgehalten im nordwestdeutschen Oberkarbon-Becken. Geologisch-Paläontologische Mitteilungen Innsbruck 16, 108–111.

Stampfli, G.M., Borel, G., Marchant, R., Mosar, J., 2002. Western Alps geological constraints on western Tethyan reconstructions. Journal Virtual Explorer 8, 77–106.

Stattegger, K., 1987. Heavy minerals and provenance of sands: modelling of lithological end members from river sands of northern Austria and from sandstones of the Austroalpine Gosau Formation (Late Cretaceous). Journal of Sedimentary Petrology 57, 301–310.

Summesberger, H., Wagreich, M., Tröger, K.A., Scholger, R., 2002. The Upper Cretaceous of Piesting (Austria): integrated stratigraphy of the Piesting Formation (Gosau Group). In: Wagreich, M. (Ed.), Aspects of Cretaceous Stratigraphy and Palaeobiogeography. Schriftenr. d. Erdwiss. Komm. 15, pp. 373–399.

Swan, A.R.H., Sandilands, M., 1995. Introduction to Geological Data Analysis. Blackwell Science Ltd, London.

Talbot, M.R., 1990. A review of the palaeohydrological interpretation of carbon and oxygen isotopic ratios in primary lacustrine carbonates. Chemical Geology (Isotope Geoscience Section) 80, 261–279.

Taylor, S.R., McLennan, S.M., 1985. The Continental Crust: Its Composition and Evolution. Blackwell, Oxford.

Thöni, M., 2006. Dating eclogite-facies metamorphism in the Eastern Alps – approaches, results, interpretations: a review. Mineralogy and Petrology 88, 123–148.

Tyrell, T., Zeebe, R.E., 2004. History of carbonate ion concentration over the last 100 million years. Geochimica et Cosmochimica Acta 68, 3521–3530.

Veizer, J., 1983. Trace elements and isotopes in sedimentary carbonates. In: Reeder, R.J. (Ed.), Carbonates, Mineralogy and Chemistry 11, pp. 265–299.

Von Eynatten, H., 2003. Petrography and chemistry of sandstones from the Swiss Molasse Basin: an archive of the Oligocene to Miocene evolution of the Central Alps. Sedimentology 50, 703–724.

Wagreich, M., 1986. Schichtfolge und Fazies der Gosau von Lilienfeld (Oberkreide; niederösterreichische Kalkvoralpen). Mitteilungen der Gesellschaft der Geologie- und Bergbaustudenten Österreichs 32, 19–38.

Wagreich, M., 2001. Paleocene-Eocene paleogeography of the Northern Calcareous Alps (Gosau Group, Austria). In: Piller, W.E., Rasser, M.W. (Eds.), Paleogene of the Eastern Alps. Schriftenreihe der Erdwissenschaftlichen Kommission 14, pp. 57–75.

Wagreich, M., Decker, K., 2001. Sedimentary tectonics and subsidence modelling of the type Upper Cretaceous Gosau basin (Northern Calcareous Alps, Austria). International Journal of Earth Sciences 90, 714–726.

Wagreich, M., Faupl, P., 1994. Palaeogeography and geodynamic evolution of the Gosau Group of the Northern Calcareous Alps (Late Cretaceous, Eastern Alps, Austria). Palaeogeography, Palaeoclimatology, Palaeoecology 110, 235–254.

Wagreich, M., Ilickovic, T., Popovic, A., Porpaczy, C., Steinbrener, J., Wessely, G., 2011. Biostratigraphy and sedimentology of Campanian deep-water sections (Nierental Formation, Gosau Group) in Lower Austria. Austrian Journal of Earth Sciences 104 (2), 108–121.

Wagreich, M., Krenmayr, H.G., 2005. Upper Cretaceous oceanic red beds (CORB) in the Northern Calcareous Alps (Nierental Formation, Austria): slope topography and clastic input as primary controlling factors. Cretaceous Research 26, 57–64.

Wagreich, M., Marschalko, R., 1995. Late Cretaceous to Early Tertiary palaeogeography of the Western Carpathians (Slovakia) and the Eastern Alps (Austria): implications from heavy mineral data. Geologische Rundschau 84, 187–199.

Wessely, G., 1974. Rand und Untergrund des Wiener Beckens – Verbindungen und Vergleiche. Mitteilungen der Geologischen Gesellschaft in Wien 66–67, 265–287.

Wessely, G., 1984. Der Aufschluß auf kalkalpine und subalpine Tiefenstrukturen im Untergrund des Wiener Beckens. The exploration to limestone-alpine deep structures in the basement of the Vienna basin. Erdoel-Erdgas 100, 285–292.

Wessely, G., 1992. The Calcareous Alps below the Vienna Basin in Austria and their structural and facial development in the Alpine-Carpathian border zone. Geologica Carpathica 43 (6), 347–353.

Wessely, G., 1993. Der Untergrund des Wiener Beckens. In: Brix, F., Schultz, O. (Eds.), Erdöl und Erdgas in Österreich. Naturhistorisches Museum Wien, Wien, pp. 249–280.

Wessely, G., 2000. Sedimente des Wiener Beckens und seiner alpinen und subalpinen Unterlagerung. The Vienna Basin and its alpine and subalpine basement. Mitteilungen der Gesellschaft der Geologie- und Bergbaustudenten in Österreich 44, 191–214.

Wessely, G., 2006. Niederösterreich. Geologie der österreichischen Bundesländer. Geologische Bundesanstalt, Wien.

Woletz, G., 1963. Charakteristische Abfolgen der Schwermineralgehalte in Kreide- und Alttertiär-Schichten der nördlichen Ostalpen. Jahrbuch der Geologischen Bundesanstalt 106, 89–119.

Yan, D., Chen, D., Wang, Q., Wang, J., 2010. Large-scale climatic fluctuations in the latest Ordovician on the Yangtze block, south China. Geology 38, 599–602.

Zimmer, W., Wessely, G., 1996. Exploration results in thrust and subthrust complexes in the Alps and below the Vienna Basin in Austria. In: Wessely, G., Liebl, W. (Eds.), Oil and Gas in Alpidic Thrustbelts and Basins of Central and Eastern Europe. EAGE Special Publication No. 5, pp. 81–107.

Please cite this article in press as: Hofer, G., et al., Geochemistry of fine-grained sediments of the upper Cretaceous to Paleogene Gosau Group (Austria, Slovakia): Implications for paleoenvironmental and provenance studies, Geoscience Frontiers (2013), http://dx.doi.org/10.1016/j.gsf.2012.11.009

Appendix

Appendix I: see appendix A (of dissertation)

Appendix II:

Student´s t-test		**N**	**mean**	**stand. dev.**	**T**	**α**
Non-marine group:	B	60	106.6	29.2	0.996	0.321
	B/Al*	60	133	33	-4.726	0.000
	$\delta^{13}C$	37	-5.3	2.4	-7.044	0.000
	$\delta^{18}O$	37	-6.1	1.5	-3.004	0.003
	SiO_2	60	50.5	10.5	6.451	0.000
	Al_2O_3	60	15.8	4.5	4.092	0.000
	TiO_2	60	0.7	0.2	4.152	0.000
	CaO	60	7.1	8.5	-6.468	0.000
	LOI	60	12.5	7.0	-5.846	0.000
	Sr	60	159.4	84.7	-9.551	0.000
	Zr	60	151.3	42.8	4.518	0.000
	factor 1	70	0.41	0.85	4.372	0.000
Marine group:	B	86	100.5	45.2	0.996	0.321
	B/Al*	86	160	34	-4.726	0.000
	$\delta^{13}C$	79	-1.4	2.9	-7.044	0.000
	$\delta^{18}O$	79	-5.2	1.6	-3.004	0.003
	SiO_2	86	37.5	13.9	6.451	0.000
	Al_2O_3	86	12.3	5.5	4.092	0.000
	TiO_2	86	0.6	0.3	4.152	0.000
	CaO	86	18.5	12.7	-6.468	0.000
	LOI	86	20.5	9.6	-5.846	0.000
	Sr	86	439.8	252.6	-9.551	0.000
	Zr	86	114.3	56.0	4.518	0.000
	factor 1	100	-0.24	1.10	4.372	0.000

Appendix III:

Student´s t-test for major elements and ratios (significant values in bolt)

SiO_2	GDS	GBS	SG
GHS	**0.004**	**0.000**	0.999
GDS		**0.016**	**0.011**
GBS			**0.000**

SiO_2/Al_2O_3	GDS	GBS	SG
GHS	0.641	0.092	0.070
GDS		0.074	0.094
GBS			**0.035**

Fe_2O_3	GDS	GBS	SG
GHS	**0.032**	**0.019**	**0.021**
GDS		0.393	**0.000**
GBS			**0.000**

Fe_2O_3/Al_2O_3	GDS	GBS	SG
GHS	0.598	0.633	**0.016**
GDS		0.298	**0.008**
GBS			0.769

MgO	GDS	GBS	SG
GHS	0.986	**0.002**	**0.009**
GDS		**0.001**	**0.009**
GBS			**0.001**

MgO/Al_2O_3	GDS	GBS	SG
GHS	0.473	**0.000**	**0.013**
GDS		**0.000**	**0.010**
GBS			**0.002**

CaO	GDS	GBS	SG
GHS	**0.004**	**0.000**	0.741
GDS		**0.000**	**0.003**
GBS			**0.000**

CaO/Al_2O_3	GDS	GBS	SG
GHS	0.141	**0.000**	0.207
GDS		**0.002**	**0.034**
GBS			**0.003**

Na_2O	GDS	GBS	SG
GHS	0.965	**0.005**	0.483
GDS		**0.000**	0.419
GBS			**0.008**

Na_2O/Al_2O_3	GDS	GBS	SG
GHS	**0.019**	**0.000**	**0.000**
GDS		**0.000**	**0.000**
GBS			**0.000**

K_2O	GDS	GBS	SG
GHS	0.919	**0.000**	0.097
GDS		**0.000**	**0.046**
GBS			**0.000**

K_2O/Al_2O_3	GDS	GBS	SG
GHS	**0.000**	0.081	0.645
GDS		**0.000**	**0.000**
GBS			**0.039**

TiO_2	GDS	GBS	SG
GHS	0.140	**0.000**	0.111
GDS		**0.000**	**0.001**
GBS			**0.000**

TiO_2/Al_2O_3	GDS	GBS	SG
GHS	0.165	0.207	0.519
GDS		**0.001**	**0.035**
GBS			0.768

Al_2O_3	GDS	GBS	SG
GHS	**0.016**	**0.000**	0.119
GDS		**0.000**	**0.000**
GBS			**0.000**

GHS: Gießhübl Syncline
GDS: Glinzendorf Syncline
GBS: Grünbach Syncline
SG: Studienka Gosau

Appendix IV:

Dikriminant Analysis					
Variable	**Group**	**Mean**	**St. Dev.**	**Wilks-Lambda**	**Significance**
B	non-marine	98.8	32.2	0.999	0.737
	marine	96.1	37.1		
B/Al*	non-marine	131.7	22.9	0.862	0.000
	marine	158.2	33.0		
$\delta^{13}C$	non-marine	-5.5	2.2	0.611	0.000
	marine	-1.1	2.7		
$\delta^{18}O$	non-marine	-6.0	1.3	0.896	0.002
	marine	-4.9	1.6		
SiO_2	non-marine	46.8	10.6	0.873	0.000
	marine	39.7	12.7		
Al_2O_3	non-marine	14.4	4.2	0.945	0.024
	marine	11.9	4.8		
TiO_2	non-marine	0.7	0.2	0.946	0.026
	marine	0.6	0.3		
CaO	non-marine	10.3	7.5	0.869	0.000
	marine	19.2	11.5		
LOI	non-marine	14.4	6.8	0.886	0.001
	marine	20.6	8.3		
Sr	non-marine	191.3	95.8	0.726	0.000
	marine	485.7	253.1		
Zr	non-marine	135.8	42.3	0.942	0.020
	marine	110.6	48.3		

Test of Discr. Funktion:			
Scenario	**Wilks-Lambda**	**Chi-Quadrat**	**Significance**
a.	0.518	58.529	0.000
b.	0.537	55.614	0.000
c.	0.575	49.845	0.000
d.	0.320	97.302	0.000

5.2 Manuscript

The manuscript titled *Provenance of the Upper Cretaceous to Eocene Gosau Group around and beneath the Vienna Basin (Austria and Slovakia)* by Hofer G. and Wagreich M. was submitted at the *Swiss Journal of Geosciences*. The main purpose of this article is to reconstruct the provenance of the Gosau Group at the border zone between the eastern Alps and western Carpathians. Garnet and chrome spinel chemistry suggest dominant sediment transport from the Tethys suture to the south. Detrital garnets related to a metamorphic sole are present from the Coniacian to the Campanian.

5.2.1 Provenance of the Upper Cretaceous to Eocene Gosau Group around and beneath the Vienna Basin (Austria and Slovakia)

Hofer, G. & Wagreich, M.

Submitted at: Swiss Journal of Geosciences
Date of submission: 18.12.2012
Status: Under review

Comment of the author concerning the degree of participation
The entire manuscript was written by Gerald Hofer (supported by co-author). Sample collection, preparation, sieving, heavy mineral separation, embedding and polishing of mounts, analysis by electron microprobe as well as calculations and interpretation of the data were performed by the author.
Counting of heavy minerals was partly performed by OMV (R. Sauer and W. Hujer).

Article structure, numbering and type of quotations are maintained as requested in the journal.

Abstract

Chemistry of detrital garnets, chrome spinels and tourmalines in combination with the general heavy mineral distribution from the Upper Cretaceous to Eocene Gosau Group of the eastern part of the Eastern Alps and the western West Carpathians approve a precise picture of sedimentary provenance and paleogeographic evolution of that area. Coniacian to Campanian garnets are partly derived from high metamorphic rocks, probably from a metamorphic sole remnant of the southern Tethys ophiolitic suture zone. From there, tectonically high ophiolitic nappes, later on completely eroded, support mainly the paleogeographically southern Grünbach and Glinzendorf basin with ultramafic detritus represented by chrome spinels of a mixed harzburgite/lherzolite composition. A second possible ophiolitic source, the Penninic accretionary wedge to the north of the Gosau basins, only plays (if at all) a minor role. In contrast to that, only almandine-rich garnets could be observed from the Maastrichtian to the Eocene. Garnet chemistry suggests low-grade metamorphic metapelites from southern provenance. Ophiolite detritus is reduced in the Maastrichtian and disappears in the Paleocene (or Eocene in the Slovakian Gosau basin).

1 Introduction

The well documented sedimentation history of the Upper Cretaceous to Paleogene Gosau Group reflects ongoing tectonic processes at the active margin of the Austroalpine microplate (e.g. Faupl and Wagreich 1996). Several studies of heavy mineral assemblages contributed significantly to the understanding of detrital sources and moreover the paleogeographic evolution of that area during the Late Cretaceous to Paleogene (Woletz 1967; Faupl 1983; Gruber 1987; Winkler 1988; Wagreich and Marschalko 1995). But reconstructions of provenance are still puzzling and paleogeographic positions or correlations of various Gosau basins at the transition zone between the Eastern Alps and the Western Carpathians are still under debate (e.g. Wagreich and Marschalko 1995; Hofer et al. in press). Single grain chemistry of heavy minerals is an important tool in provenance analysis techniques (e.g. Henry and Guidotti 1985; Pober and Faupl 1988; Morton 1991; Von Eynatten and Gaupp 1999; Weltje and Von Eynatten 2004; Mange and Morton 2007; Meinhold et al. 2009; Aubrecht et al. 2009) but so far was only applied selectively to the Gosau Group (Pober and Faupl 1988). This study gives an overview of Gosau Group heavy mineral assemblages (old and new data) of the eastern part

of the Eastern Alps and the western part of the West Carpathians, plus new insights from single grain chemistry with the goal to improve provenance conceptions and to reconstruct the paleotectonic evolution of that area during the Late Cretaceous to Paleogene.

2 Geological setting

The Gosau Group of the Northern Calcareous Alps (NCA) comprises Upper Cretaceous to Paleogene sediments overlying folded and faulted Permian to Lower Cretaceous units (Wagreich and Faupl 1994). A subdivision into a fluvial, lacustrine to shallow-marine Lower Gosau Subgroup (Turonian to Santonian/Campanian, in some areas up to Maastrichtian) and into a deepwater dominated Upper Gosau Subgroup up to Eocene is defined (Faupl et al. 1987; Wagreich and Faupl 1994; Faupl and Wagreich 1996).

Various Gosau Group deposits are exposed at the eastern part of the Eastern Alps (Austria) at the area of Gießhübl and Grünbach – Neue Welt at the south-western margin of the Vienna Basin and in the western part of the West Carpathians at the area of Brezová and Myjava (Slovakia) (Wagreich and Marschalko 1995) (Fig. 1). Beneath Neogene sediments of the Vienna Basin, NE-SW-striking Gosau units can be traced over several wells down to depths of more than 4000 m (Wessely 1993; Zimmer and Wessely 1996). During the Alpine orogeny, sediments of the Gosau Group were folded and are today arranged in synclines on different tectonic nappes of the NCA and on Carpathian units (Fig. 1). From north to south the Gießhübl Syncline, the Prottes Gosau Group, its Slovakian equivalents of Studienka and Brezová (here labeled as Slovakian Gosau), the Glinzendorf Syncline and the Grünbach Syncline are defined (Plöchinger 1961; Wessely 1974; 1984; 1992; 1993; 2000; 2006; Wagreich and Marschalko 1995; Zimmer and Wessely 1996). These various Gosau depressions are interpreted as different basins.

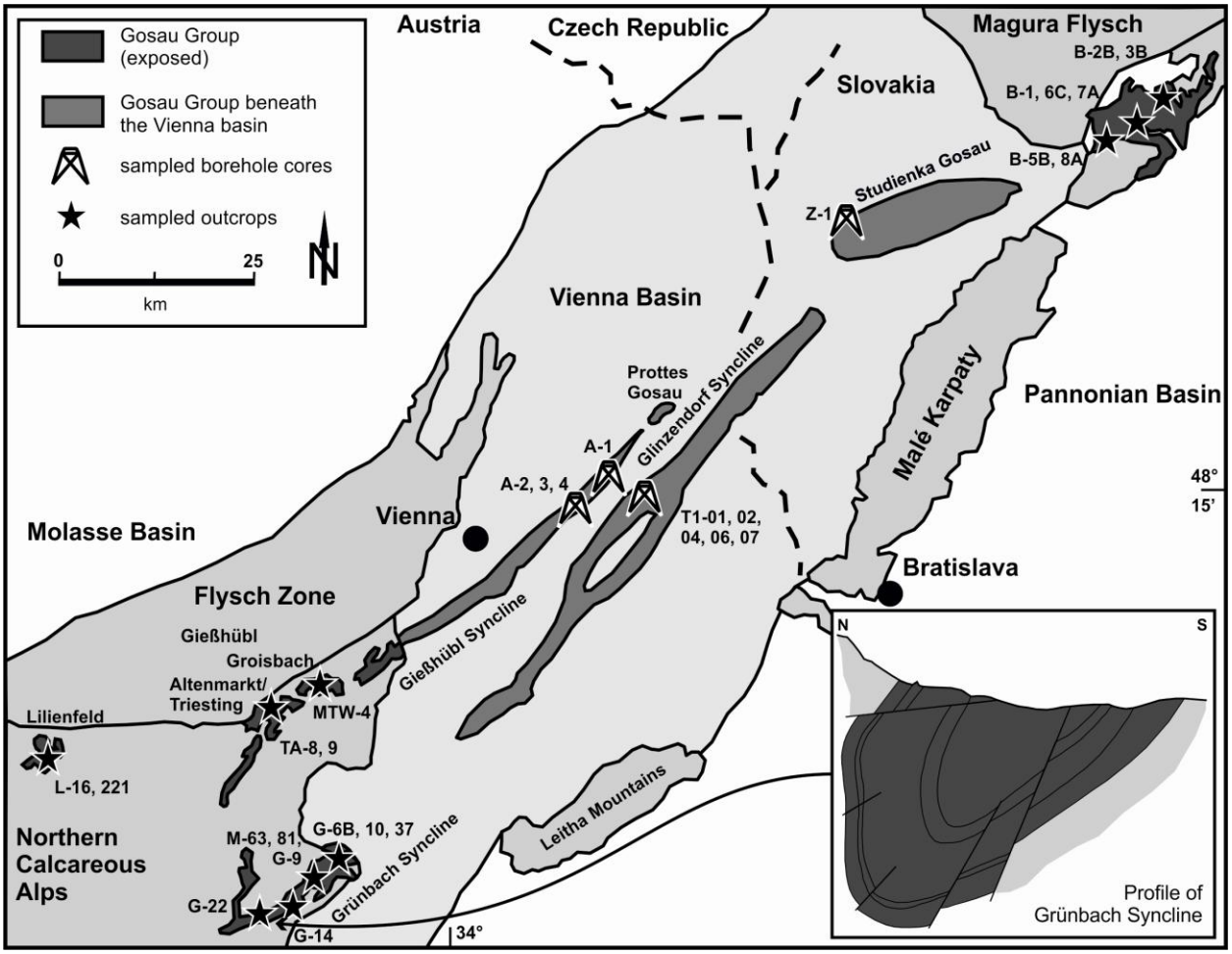


Fig. 1: Simplified geological map of the eastern part of the Eastern Alps, the Vienna Basin and the western part of the West Carpathians with highlighted Gosau Group situated at the border and underneath the Neogene Vienna Basin (modified after Wagreich and Marschalko 1995; Zimmer and Wessely 1996). Sampled locations of wells and outcrops are marked. A N-S profile of the Grünbach area (after Plöchinger 1961) illustrates the recent arrangement of the Gosau Group in synclines.

3 Stratigraphy

Strata of the Gießhübl basin (Coniacian to Paleocene), which is part of the Lunz Nappe of the Bajuvaric Nappe system (Faupl and Wagreich 1996) of the NCA, starts with shallow-marine sandstones and breccias of the Coniacian/Santonian. The overlaying Nierental Formation of the Upper Santonian/Campanian to Lower Maastrichtian (Wessely 2006) is already attributed to the Upper Gosau Subgroup and comprises mainly calcareous marls of a pelagic to hemipelagic slope facies (Krenmayr 1999; Wagreich and Krenmayr 2005; Wagreich et al. 2011). The main part of the strata is represented by the Gießhübl Formation (subdivided into a Lower, Middle

and Upper Gießhübl Member), a massive deep-water turbidite to mass-flow-complex deposited below the calcite compensation depth (Faupl and Sauer 1978; Wagreich 2001a), with a temporal extent up to the Thanetian (Wessely 1992). Gosau Group sediments of the Gießhübl basin crop out at the area of Gießhübl, Alland and Altenmarkt/Triesting (Fig. 1). Equivalents of the Gießhübl Syncline are exposed around Lilienfeld, where the Gosau Group comprises Coniacian-Santonian Lower Gosau Subgroup units followed by the hemipelagic-pelagic Nierental, Spitzenbach and Gießhübl Formations of the Campanian to Maastrichtian (Wagreich 1986; Wagreich et al. 2011).

The Prottes Gosau Group (Coniacian to Paleocene) is a small, isolated, mainly conglomeratic subcrop complex lying on Tirolic nappes underneath the Neogene of the Vienna Basin between Prottes and Altenmarkt / Triesting (Wessely 2006).

Because of the limnic to shallow-marine character with interbedded coal horizons of the Tirolic Glinzendorf basin (Santonian to Campanian or maybe Maastrichtian), it is sometimes interpreted as an easterly equivalent of the Grünbach basin (Wessely 2006). However, a continuous connection from the Grünbach Syncline underneath the Vienna Basin to the Glinzendorf Syncline is doubtful. Sediments of the Glinzendorf basin appear exclusively in the subsurface, detected by several oil-industry (OMV and NAFTA) wells like Gänserndorf ÜT3, T3, Markgrafneusiedl 1, N1, T1, Glinzendorf 1 and T1 (Wessely 2006), Gajary 125 (Mišík 1994; Ralbovsky and Ostrolucký 1996) or Záhorska Ves (Fig. 1). Basically, limnic to marginal-marine facies is dominant in the several hundred meter thick succession starting in the Santonian with dark marls and mudstones with some minor coal layers intercalated (Sachsenhofer and Tomschey 1992; Wessely 1992; 2006). Marls, mudstones and minor conglomerates continue up to the Campanian with a marine middle-part and non-marine clastics at the top (Wessely 2006). Generally, this succession is also reported from the Slovakian part of the syncline (Gajary 125) with a lower and upper conglomeratic non-marine red interval and an intercalation of a marine grey interval (Mišík 1994). Here, a Maastrichtian (Wessely 1992; Pavlishina et al. 2004) or even Paleocene top cannot be excluded (Ralbovsky and Ostrolucký 1996).

The Grünbach basin (Santonian to Paleocene) is exposed at the south-western margin of the Vienna Basin in the area of Grünbach – Neue Welt (Plöchinger 1961) (Fig. 1). The connection to Upper Cretaceous rocks beneath the Neogene fill of the Vienna Basin is controversial (e.g. Hofer et al. 2011). The base of the Grünbach Gosau starts in the Upper Santonian with a characteristic red conglomerate and breccia horizon of an alluvial fan (Kreuzgraben Formation; e.g. Erkan 1972). A transgressive trend is documented by the overlying shallow-marine Maiersdorf Formation that contains calcareous breccias, minor sandy limestones (including corals, brachiopods and gastropods) and reef-forming rudist limestones (Summesberger et al.

2002). The limnic to marginal-marine Grünbach Formation of the Lower Campanian contains coal layers within marls and fine-clastic sandstones as well as a conglomeratic horizon (Summesberger et al. 2002; Wessely 2006) and is comparable to units at the base of the Glinzendorf Syncline. With the Upper Campanian to Maastrichtian Piesting Formation the facies changed to deep-marine *Inoceramus* marls and *Orbitoides* bearing sandstones (Hradecká et al. 1999). The maximum depth of the basin is reached with the turbiditic Zweiersdorf Formation of up to Paleocene age (Summesberger et al. 2002).

Slovakian Gosau outcrop equivalents are subdivided into the Upper Cretaceous Brezová Group (Coniacian to Maastrichtian) and the Paleogene Myjava Group (Paleocene to Eocene) (Wagreich and Marschalko 1995). A correlation of the so-called Brezová Depression striking ENE underneath the Slovakian part of the Neogene Vienna Basin with exposures at the north-eastern margin at the area of Brezová with the Gosau Group is still being debated (a continuous distribution is unlikely). An affiliation to the Gießhübl Syncline is likely (Wagreich and Marschalko 1995) due to its bathyal character but also a correlation with the Prottes Gosau Group is debated (Wessely 1992). Strata start with the Upper Coniacian coarse-clasic to marly Ostriež Formation. Above the marl-dominated Santonian Hurbanova Dolina Formation of a neritic shelf facies, calcareous marls of the Campanian Košariská Formation (similar to the Nierental Formation) document a fast deepening of the basin. Further deepening results in massive turbidite units of the Podbradlo and Podlipovec Formation (Upper Campanian to Maastrichtian) with the intermediary Bradlo Formation. Again deep-marine turbiditic facies is recorded in the Paleocene to Eocene Priepastné and Jablonka Formation of the Myjava Group. A deposition underneath the calcite compensation depth is supposed for the Jablonka Formation analogue to the Gießhübl Formation (Wagreich and Marschalko 1995).

4 Paleogeography

Originally, Gosau Group sediments, as part of the NCA, were situated at the northern, tectonically active continental margin of the Austroalpine microplate, along the northern margin of the Adriatic plate (Faupl and Wagreich 1996; 2000). To the north, oblique subduction of the Penninic Ocean (Alpine Tethys of Stampfli et al. 2002) underneath the Austroalpine plate controlled the tectonic evolution of the continental margin (Wagreich, 1993a). The Gosau basins represent strike-slip dominated slope basins within an early accretionary structure due to southward subduction of the Penninic Ocean. This accretionary wedge existed from the Turonian to the Campanian and was composed of Austroalpine units, obduced ophiolites and

exhumed metamorphic units (Winkler 1988; Faupl and Wagreich 1996). Elevation above sea level is supposed for parts of this transpressional feature, and detritus supply (including ophiolitic detritus) is reported from the north into the Gosau basin (Dietrich and Franz 1976; Stattegger 1986; 1987; Pober and Faupl 1988; Faupl and Pober 1991). Paleotransport direction data from sediments of the Upper Aptian to Lower Cenomanian Tannheim-Losenstein basin (Wagreich 2001b) and the Lower Gosau Group suggest sediment transport mainly from northern provenance (Faupl 1983; Wagreich 1988). A second ophiolitic source area at this time is the Tethys suture zone (also Vardar/Meliata suture) to the south that supplied material for the Transdanubian Range and Dinarides as well (Pober and Faupl 1988; Von Eynatten and Gaupp 1999; Árgyelán and Horváth 2002; Lužar-Oberiter et al. 2009). From the Santonian/Campanian to Eocene, subcrustal tectonic erosion of the accretionary wedge caused a collisional regime in the NCA and led to northwards deepening of the Gosau basin (Wagreich 1993a; 1995). The northern (Penninic) source area became more and more deactivated from that time on (Faupl and Wagreich 1996; Von Eynatten and Gaupp 1999). Only northwards-directed paleocurrents are documented in Upper Gosau sediments (Faupl 1983; Wagreich 1986; 1988). Today, the original palaeogeographic situation of the Gosau basins is largely obliterated due to polyphase tectonic deformation and large-scale thrusting within the Eastern Alps (e.g., Faupl and Wagreich 2000).

5 Heavy mineral assemblages

The stable heavy minerals zircon, tourmaline and rutile are combined to the ZTR-index (Hubert 1962), reflecting the mineralogical maturity of sediments (e.g. Pettijohn et al. 1973; Kutterolf 2001; Garzanti and Andò 2007). During weathering and transport, these minerals accumulate and ZTR-index rises (ZTR-index increases with higher amounts of quartz and chert).
Metamorphic heavy minerals are grouped as META = garnet + chloritoid + glaucophan + epidote group + titanite + staurolite + hornblende + disthene (Von Eynatten 1996; Von Eynatten and Gaupp 1999).

6 Mineral chemistry

Geochemistry of single heavy mineral grains analyzed by microprobe techniques for questions of provenance has become widespread in sedimentology in the last decades (e.g. Henry and Guidotti 1985; Pober and Faupl 1988; Morton 1991; Von Eynatten 1996; Von Eynatten and Gaupp 1999; Weltje and Von Eynatten 2004; Mange and Morton 2007; Mikes et al. 2008; Aubrecht et al. 2009; Meinhold et al. 2009). Especially garnet, chrome spinel and tourmaline are reliable minerals because of their frequency and chemical variability.

6.1 Garnet

Garnet geochemistry is the most widely used single grain determination and discrimination tool for sedimentary provenance. This is because garnet is a frequent component in heavy mineral assemblages, it is relatively stable during weathering and diagenesis, and it shows a wide range in major element compositions, which is useful for provenance analysis (Morton 1985; 1991; Von Eynatten and Gaupp 1999; Mange and Morton 2007; Morton and Hallsworth 2007). The general formula of garnet is $(Mg,Fe^{2+},Mn,Ca)_3(Al,Cr,Ti,Fe^{3+})_2(SiO_4)_3$ with some other possible substitutions (Deer et al. 1962). Most garnets belong to the solid solution series between the most common end members almandine ($Fe^{2+}{}_3Al_2[SiO_4]_3$), pyrope ($Mg_3Al_2[SiO_4]_3$), spessartine ($Mn_3Al_2[SiO_4]_3$) and grossular ($Ca_3Al_2[SiO_4]_3$). Garnets are common in various metamorphic rocks of different P-T-facies but also in plutonic igneous rocks, pegmatites or even in ultramafic varieties and some acid volcanics. Generally, garnet-rich heavy mineral assemblages are associated with metamorphic provenance (Morton 1991; Von Eynatten 1996). Dominant pyrope contents are related to higher-pressure events of the host rock (Wright 1938; Preston et al. 2002; Méres et al. 2012). Provenance discrimination is mainly based on triangle plots between various end members (Barth 1962; Von Eynatten 1996; Von Eynatten and Gaupp 1999; Preston et al. 2002; Morton et al. 2003; Méres 2008; Aubrecht et al. 2009). Almandine garnets from magmatic rocks can be classified by using binary diagram of MnO and CaO (Harangi et al. 2001).

6.2 Chrome spinel

Detrital chrome spinel (also chromian or brown spinel, $[Mg,Fe^{2+}][Cr,Al,Fe^{3+}]_2O_4$) is seen as an indicator of mafic and ultramafic provenance (such as peridotites and serpentinites) and commonly associated with ophiolites (Zimmerle 1984; Pober and Faupl 1988; Árgyelán and Horváth 2002; Mange and Morton 2007; Aubrecht et al. 2009; Meinhold et al. 2009). An increase of chrome spinel, which is chemically and mechanically relatively stable, in sediments during orogenic periods can be observed in the geological record (Mange and Maurer 1992). Due to the different behavior of the elements Cr, Mg and Al during fractional crystallization and partial melting processes and the temperature-dependent relation of Fe^{2+} and Mg between the mineral and silicate melt, chrome spinel geochemistry is a capable petrogenetic tool (Dick and Bullen 1984; Arai 1992). Different chemical ratios and concentrations of spinels are used to identify the tectonic setting of source rocks (Dick and Bullen 1984; Pober and Faupl 1988; Cookenboo et al. 1997; Lužar-Oberiter et al. 2009; Meinhold et al. 2009), although discrimination diagrams for provenance studies have also been criticized, e.g. by Power et al. (2000). Al_2O_3/TiO_2 discrimination diagram after Kamenetsky et al. (2001) separates tectonic provenance regimes MORB (mid-ocean ridge basalt), OIB (ocean-island basalt), LIP (large igneous province), ARC (island-arc magmas) and SSZ (supra-subduction zone). Several plots use Cr# (= Cr/[Cr+Al]) and Mg# (= Mg/[Mg+Fe^{2+}]) to discriminate spinel chemistry concerning questions of provenance (Dick and Bullen 1984; Pober and Faupl 1988; Arai 1992; Sciunnach and Garzanti 1997; Barnes and Roeder 2001; Hisada et al. 2004). Barnes and Roeder (2001) use the triangle plot Cr-Al-Fe^{3+} to display geotectonic settings.

6.3 Tourmaline

Tourmaline geochemistry is highly complex with a huge range of compositional variations (general formula: $Na[Mg,Fe,Mn,Li,Al]_3Al_6[Si_6O_{18}][BO_3]_3[OH,F]$) comprising of three end members: dravite (Mg-tourmaline), schorl (Fe-tourmaline) and elbaite (Li-tourmaline). Dravite and schorl as well as schorl and elbaite form a continuous solid solution series (Deer et al. 1962). Detrital tourmaline originates mainly from granites, granite pegmatites, contact and regionally metamorphosed rocks or as recrystallized grains, or formed by metasomatic processes from schists, gneisses or phyllites (Mange and Maurer 1992). Because of its stability during weathering and diagenesis, tourmaline is a common detrital heavy mineral in siliciclastic sediments. The wide range of chemical composition provides the potential for geochemical

discrimination of provenance (Henry and Guidotti 1985; Henry and Dutrow 1992; Aubrecht and Krištín 1995; Mange and Morton 2007; Tsikouras et al. 2011). Provenance discrimination is mainly based on triangle plots of Fe-Mg-Al and Fe-Mg-Ca after Henry and Guidotti (1985). Discrimination (MgO vs. FeO) between the different tourmaline varieties is given in Morton (1991).

7 Methods

7.1 Sample preparation for electron microprobe

30 silt to sand-sized Gosau sediment samples were taken and analyzed from outcrops and drill cores (wells Aderklaa 84, 92, Markgrafneusiedl T1 and Závod 68) of the OMV-core sample repository (Fig. 1 and Table 1). The samples were crushed to small pieces and decalcified in acetic acid (at the University of Vienna) or hydrochloric acid (at OMV), which partly solve apatite. Heavy minerals were separated from the sieve fraction 0.063 to 0.4 mm by gravity settling in tetrabromethane with a specific gravity of 2.96 g/cm^3 (Mange and Maurer 1992). This grain size fraction was selected because data from different studies and OMV in-house data, which all used this range of fraction, was used and compared to our data. The grain concentrates containing the whole heavy mineral fraction were embedded in epoxy resin (araldite mount) and polished (up to 1 µm on grinding disc).

7.2 Electron microprobe

Element analyses of single heavy mineral grains were carried out using a *Cameca SX 100* electron microprobe at the University of Vienna (Department of Lithospheric Research) at operating conditions of 15 kV and 20 nA. The analyses were made and calibrated against mineral standards followed by a PAP correction (after Pouchou and Pichoir 1984) applied to the data. 1064 measurements on 774 single grains of garnet (263 grains), chrome spinel (269 grains) and tourmaline (242 grains) have been analyzed. B_2O_3 concentrations in tourmalines were defined between 9.660 and 9.982 as usual contents in common tourmalines. Oxygen and H_2O were stoichiometrically calculated. The analytical error for the elements is controlled by

several factors, but generally below 5% (e.g. Bjerg et al. 2009). Subjective influence (of a special group of grains) was tried to minimize by randomly selecting grains one after another. Formula parameters and end members for the different minerals analyzed by electron microprobe were calculated using the software *MINSORT* (Petrakakis and Dietrich 1985) based on 12 oxygens for garnets and 32 oxygens for spinels.

Gosau	Formation	Sample	Age	Sample	Location	Mineral Chemistry
Gießhübl	U-Gießhübl Fm	A-1	Paleocene	drill core	Aderklaa 84, 2834.5 m	Grt
Gießhübl	M-Gießhübl Fm	A-2	Paleocene	drill core	Aderklaa 92, 3011.5 m	Grt
Gießhübl	L-Gießhübl Fm	A-4	Maastr-Paleoc	drill core	Aderklaa 92, 3112 m	Grt, Tur
Gießhübl	L-Gießhübl Fm	A-3	Maastr-Paleoc	drill core	Aderklaa 92, 3505 m	Grt, Chr, Tur
Gießhübl	Nierental Fm	TA-9	Campanian	outcrop	Tasshof	Chr
Gießhübl	Nierental Fm	TA-8	Campanian	outcrop	Tasshof	Grt, Chr, Tur
Gießhübl	Con-San Sst	L-221	Con-San	outcrop	Lilienfeld	Grt, Chr, Tur
Gießhübl	Con-San Sst	L-16	Con-San	outcrop	Lilienfeld	Grt, Chr, Tur
Gießhübl	Con-San Sst	MTW-4	Con-San	outcrop	Mitterwäldchen	Chr, Tur
Glinzendorf	limnic-marine succession	T1-01	San-Camp	drill core	Markgrn. T1, 3207.8 m	Chr, Tur
Glinzendorf	limnic-marine succession	T1-04	San-Camp	drill core	Markgrn. T1, 3272.56-60 m	Grt
Glinzendorf	limnic-marine succession	T1-02	San-Camp	drill core	Markgrn. T1, 3409.70-82 m	Grt, Chr, Tur
Glinzendorf	limnic-marine succession	T1-07	San-Camp	drill core	Markgrn. T1, 3546.25-55 m	Grt
Glinzendorf	limnic-marine succession	T1-06	San-Camp	drill core	Markgrn. T1, 3744.10-20 m	Grt, Tur
Grünbach	Zweiersdorf Fm	G-14	Paleocene	outcrop	Zweiersdorf-Oberhöflein	Grt, Rut
Grünbach	Piesting Fm	G-37	Camp-Maastr	outcrop	Malleiten-Fischau	Tur
Grünbach	Piesting Fm	G-10	Camp-Maastr	outcrop	Dreistätten-Muthmannsdorf	Grt, Tur
Grünbach	Grünbach Fm	G-22	Campanian	outcrop		Grt, Chr, Tur
Grünbach	Grünbach Fm	M-63	Campanian	outcrop	Maiersdorf trench	Chr, Tur
Grünbach	Grünbach Fm	M-81	Campanian	outcrop	Maiersdorf trench	Grt, Chr
Grünbach	Maiersdorf Fm	G-9	Santonian	outcrop		Grt, Chr
Grünbach	Kreuzgraben Fm	G-6B	Santonian	outcrop		Grt, Chr
Slovakian	Jablonka Fm	B-3B	Eocene	outcrop		Grt, Tur
Slovakian	Dekov Vrch Fm	Z-1	Paleocene	drill core	Závod 68, 3872.5-3883.6 m	Grt, Tur
Slovakian	Paleogene (without precision)	B-1	Paleogene	outcrop	Solosnica	Grt, Tur
Slovakian	Priepastné Fm	B-2B	Paleocene	outcrop	Jablonka	Grt, Chr, Tur
Slovakian	Podbradlo Fm	B-7A	Campanian	outcrop	Bradlo (monument)	Chr, Tur
Slovakian	Košariská Fm	B-6C	Campanian	outcrop	Košariská	Grt, Chr, Tur
Slovakian	Štvernik Fm	B-8A	Con-San	outcrop	Štvernik	Chr
Slovakian	Coniacian-Santonian (w. p.)	B-5B	Con-San	outcrop	Brezová-Košariská	Tur

Table 1: Sample locations and affiliation to Gosau formations of all samples with analyzed heavy minerals by electron microprobe.

7.3 Evaluation/counting of heavy minerals

523 samples have been used to evaluate and assess the assemblage of heavy minerals of the Gosau Group in the study area. 139 heavy mineral analyses (all of them have the same grain size fraction of 0.063 to 0.4 mm) have been taken from literature (Sauer 1980; Gruber 1987; Wagreich and Marschalko 1995); 384 samples were analyzed at the OMV laboratory (editor: R. Sauer) or taken from OMV in-house data (unpublished data; edited by W. Hujer, R. Sauer or unknown editors). Heavy mineral data from a different grain size spectrum (e.g. Woletz 1967: 0.063 to 0.1 mm; or Mišík 1994: unknown grain size spectrum and preparation procedure) were ignored because heavy mineral assemblages are dependent on grain size (e.g. Garzanti et al. 2009). Apatite percentages were omitted because this mineral was at least partly solved by OMV preparation methods with HCl. The heavy mineral spectra were grouped in formations, members, age- or depth intervals (in case of well data) and averaged (Appendix I). Only samples with more than 50 counted grains (in most of the cases the number of counted grains is higher than 100) are used for statistics and the generalized heavy mineral profiles.

8 Results

8.1 Heavy mineral assemblages

Data from the following generalized heavy mineral profiles (Fig. 2) have been adopted from literature (Sauer 1980; Gruber 1987; Wagreich and Marschalko 1995) and OMV in-house data (unpublished data; edited by W. Hujer, R. Sauer or unknown editors).

The Gießhübl basin is generally characterized by a drastic rise of garnet concentrations and hand in hand with that, a drop in chrome spinel and zircon from the Coniacian/Santonian up to the Paleocene (Figs. 2, 3 and 4). Rutile (mean: 8.2 ± standard deviation: 7.9%) and tourmaline (5.3 ±4.9%) percentages are moderate/low and constant, some chloritoide is only found in the Nierental Formation (up to 8%) and in the base of the Lower Gießhübl Formation (up to 7%). Basal sandstones of the Coniacian/Santonian age (data from OMV wells Aderklaa 82, Schönkirchen T11 and T90, Strasshof T1, T9, T9a and T9b; N=27; Appendix I) are dominant in chrome spinel (49.1 ±32.1%) and zircon (28.7 ±21.5%) with low garnet concentrations (7.9 ±16.3%). Garnet populations rise to 32.8 ±22.2%, while chrome spinel (21.7 ±13.6%) and zircon (17.8 ±9.3%) is depleted in samples of the Nierental Formation (data from OMV wells of

Aderklaa 92; N=14; Appendix I). The base of the Lower Gießhübl Formation (N=6) is quite different to the rest of the formation and characterized by a dominant amount of chrome spinel (37.8 ±29.3%) with a garnet content of 22.0 ±18.5% (Sauer 1980). Generally, assemblages of the Gießhübl Formation are dominated by garnet (Lower G-Fm: 78.2 ±17.9%, N=139; Middle G-Fm: 66.6 ±29.6%, N=52; Upper G-Fm: 82.0 ±6.9%, N=52) while chrome spinel is almost inexistent (Sauer 1980).

Heavy mineral assemblages of the limnic-marine successions of the Glinzendorf basin are generally garnet-rich (45.4 ±27.5%) with moderate and fluctuating chrome spinel (24.4 ±30.0%) as well as moderate zircon (14.4 ±12.8%) and rutile contents (9.4 ±6.0%) and low tourmaline concentrations (3.1 ±2.5%) (Figs. 2, 3, 4 and 5). Chrome spinel dominant parts (up to 91.7%) correlate with non-marine strata within the wells Markgrafneusiedl T1 and Glinzendorf T1 (Hofer et al. in press). The Santonian/Campanian (maybe Maastrichtian; Wessely 2006) section is subdivided into five depth-sections of the wells Markgrafneusiedl T1 and Glinzendorf T1 that show similar heavy mineral assemblages. It has to be kept in mind, that the correlation between the two wells by depth level is certainly not accurate, because tectonic deformation is relatively complex within the subcrop of the Glinzendorf Syncline (Wessely 1992; 2006; Mišík 1994; Ralbovsky and Ostrolucký 1996). Generally, garnet contents rise and chrome spinel concentrations drop in marine and top sections and vice versa (Figs. 2, 3 and 4). The bottom interval between 4200 and 3900 m is characterized by relatively high amounts of chrome spinel (32.5 ±25.1%; up to 77%) and moderate amounts of garnet (37.4 ±25.0%). Garnet contents slowly increase between 3900 and 3700m (47.7 ± 33.9%) and 3700 and 3500m (54.5 ±22.8%), while chrome spinel is reduced (12.3 ±22.7%) between 3700 and 3500m. High chrome spinel (31.7 ±30.2%) and zircon (21.8 ±20.8%) contents characterize the interval between 3500 and 3300m. At the top between 3300 and 3100m garnet accumulation dominates with 71.1 ±9.7%, while chrome spinel is more or less inexistent (2.3 ±2.5%). Similar heavy mineral assemblages (dominance of ZTR and chrome spinel) are observed for the borehole Gajary 125 (Mišík 1994), but, due to unknown grain size spectrum and preparation procedure, this data was ignored for further evaluation during the present study.

Late Cretaceous (Santonian to Maastrichtian) heavy mineral assemblages of the Grünbach basin are generally rich in chrome spinel, tourmaline, garnet, zircon, rutile and chloritoide, while in the Paleocene Zweiersdorf Formation garnet is the only dominant heavy mineral phase (Sauer 1980; Gruber 1987) (Figs. 2, 3, 4 and 5). Late Santonian Kreuzgraben and Maiersdorf formations are dominated by garnet (46.7 ±24.7% and 34.0 ±17.5%) with moderate, but fluctuating concentrations of chrome spinel (14.8 ±14.7% and 18.4 ±10.7%) and tourmaline (9.9 ±9.6% and 19.9 ±14.2%). Tourmaline (22.8 ±12.8%), chloritoide (17.1 ±14.7%), zircon (16.4

±11.4%) and rutile (16.1 ±12.6%) are present in high amounts in the Campanian Grünbach Formation (N=67). Chrome spinel and garnet contents are highly variable (between 0 and 61% and 0 and 86%, respectively), but relatively low in average (8.9 ±12.8% and 9.1 ±16.0%). With 26.5 ±23.4% in average, chrome spinel is the dominant heavy mineral phase in the Piesting Formation but also tourmaline (20.1 ±9.9%), zircon (15.8 ±10.4%) and chloritoide (10.2 ±11.2%) concentrations are moderate to high. Garnet (13.3 ±20.1%) already predominates in the youngest intervals (Maastrichtian?) of the Piesting Formation with maximum values of 86% (Gruber 1987). Within the overlying Paleocene Zweiersdorf Formation this trend continues, and garnet is the dominant heavy mineral with a mean concentration of 86.3 ±4.6%.

Tourmaline is the dominant heavy mineral of the Slovakian Gosau equivalents with 31.1 ±14.2% in average (Figs. 2 and 5). High to medium chrome spinel concentrations are characteristic for the Coniacian to Maastrichtian, medium to high amounts of garnet can be observed from the Late Campanian onwards (Wagreich and Marschalko 1995) (Figs. 2, 3 and 4). The ZTR index is higher compared to the Austrian Gosau equivalents due to the high tourmaline and constantly medium to high zircon percentages. Coniacian to Santonian strata is (except one zircon-rich sample at the base) characterized by chrome spinel (51.6 ±14.7%). Tourmaline contents are enriched as well (23.4 ±14.0%), while garnet is rare or even absent (4.0 ±4.7%) in these sediments. From the Campanian on chrome spinel concentrations are reduced (they typically scatter between 10 and 20%) and do not occur in the Eocene any more. While garnet is still depleted in the Campanian (6.0 ±5.1%) it rises up to 24.4 ±4.2% in the Bradlo Formation. Tourmaline is the dominant heavy mineral in the Campanian and Maastrichtian (35.2 ±10.4%), zircon is relatively high and constant as well in these sediments (22.0 ±8.0%). In the Paleocene, tourmaline concentrations are even slightly higher with a mean of 43.8 ±18.1% and a maximum content of 68% (Priepastné Formation). Garnet percentages are higher (17.1 ±8.7%), chrome spinel concentrations lower (9.7 ±5.1%) in the Paleocene as compared to the Late Cretaceous. Zircon (13.3 ±3.3%) and even chloritoide contents (8.0 ±5.7%) are relatively high as well. In the Eocene, garnet is the dominant heavy mineral phase with an average amount of 45.2 ±4.6%. Tourmaline concentrations are still high (28.1 ±7.9%) as it is characteristic for the whole Brezová and Myjava Group. Zircon contents are similar to the Paleocene, while chrome spinel is inexistent.

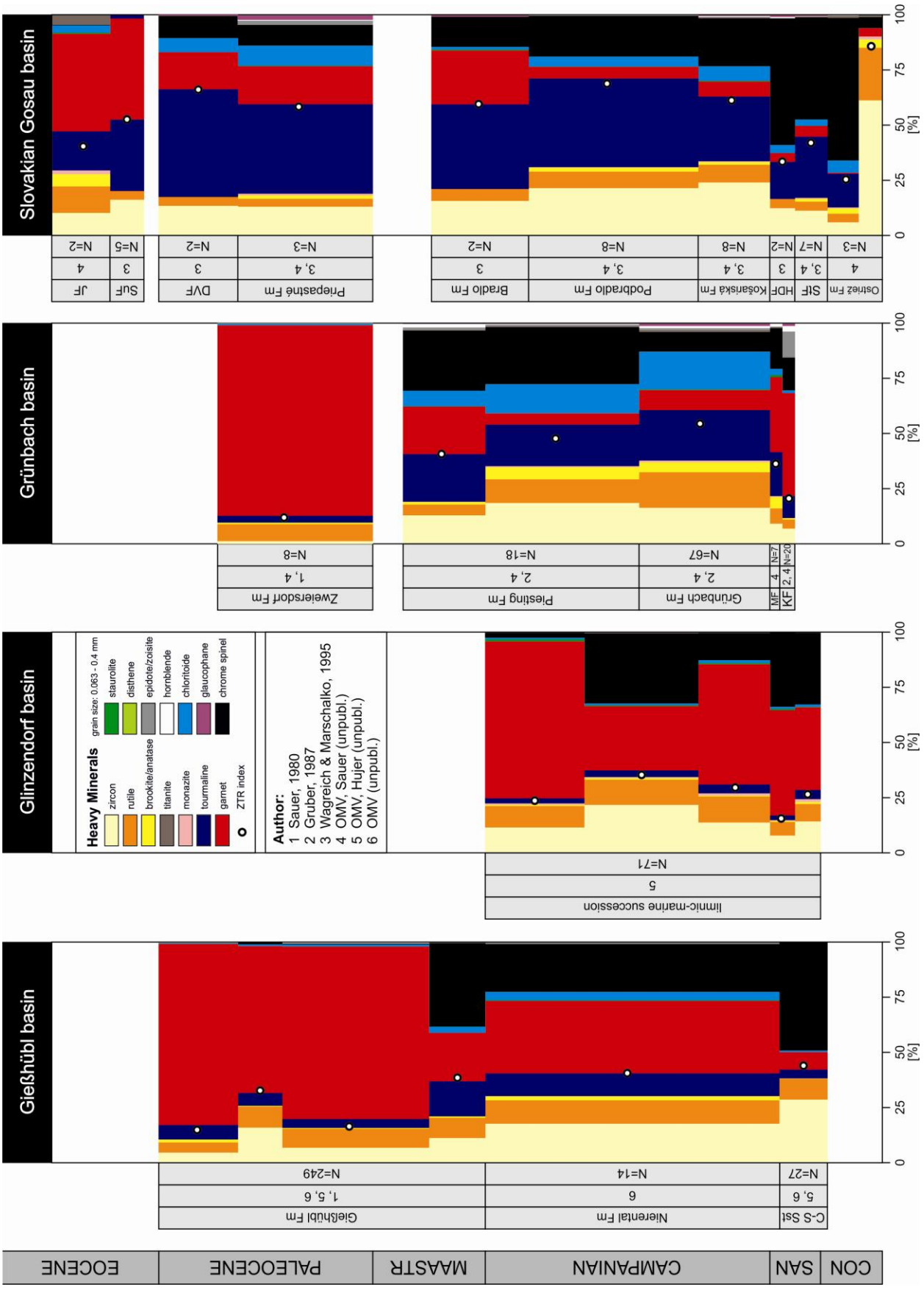

CON
SAN
CAMPANIAN
MAASTR
PALEOCENE
EOCENE
Gießhübl basin
Glinzendorf basin
Grünbach basin
Slovakian Gosau basin
C-S Sst
Nierental Fm
Gießhübl Fm
limnic-marine succession
Grünbach Fm
Piesting Fm
Zwelersdorf Fm
Osnież Fm
HDF
StF
Košariská Fm
Podbradlo Fm
Bradlo Fm
Priepastné Fm
DVF
SuF
JF
N=27
N=14
N=249
N=71
N=67
N=18
N=8
N=3
N=7
N=2
N=8
N=2
N=2
N=5
5, 6
6
1, 5, 6
5
2, 4
1, 4
3, 4
4
MF
KF
N=7
N=20
0
25
50
75
100
[%]
Heavy Minerals
grain size: 0.063 - 0.4 mm
zircon
rutile
brookite/anatase
titanite
monazite
tourmaline
garnet
ZTR index
staurolite
disthene
epidote/zoisite
hornblende
chloritoide
glaucophane
chrome spinel
Author:
1 Sauer, 1980
2 Gruber, 1987
3 Wagreich & Marschalko, 1995
4 OMV, Sauer (unpubl.)
5 OMV, Hujer (unpubl.)
6 OMV (unpubl.)

Fig. 2: Synthetic, composite heavy mineral profiles of the area of the Gießhübl, Glinzendorf, Grünbach and Slovakian Gosau basin. Number of samples (N) and authors (1-6) are given. Data has been taken from literature (1: Sauer 1980; 2: Gruber 1987 and 3: Wagreich and Marschalko 1995), OMV in-house data (unpublished data; edited by 5: W. Hujer, 4: R. Sauer or 6: unknown editors) or have been edited by 4: R. Sauer at the OMV lab. Apatite percentages were omitted because it was partly solved. The heavy mineral spectra were grouped in formations (C-S Sst = Coniacian-Santonian sandstones; KF = Kreuzgraben Formation; MF = Maiersdorf Formation; StF = Štvernik Formation; HDF = Hurbanova Dolina Formation; DVF = Dedkov Vrch Formation; SuF = Surovin; JF = Jablonka Formation), members, age- or depth intervals (in case of well data) and averaged.

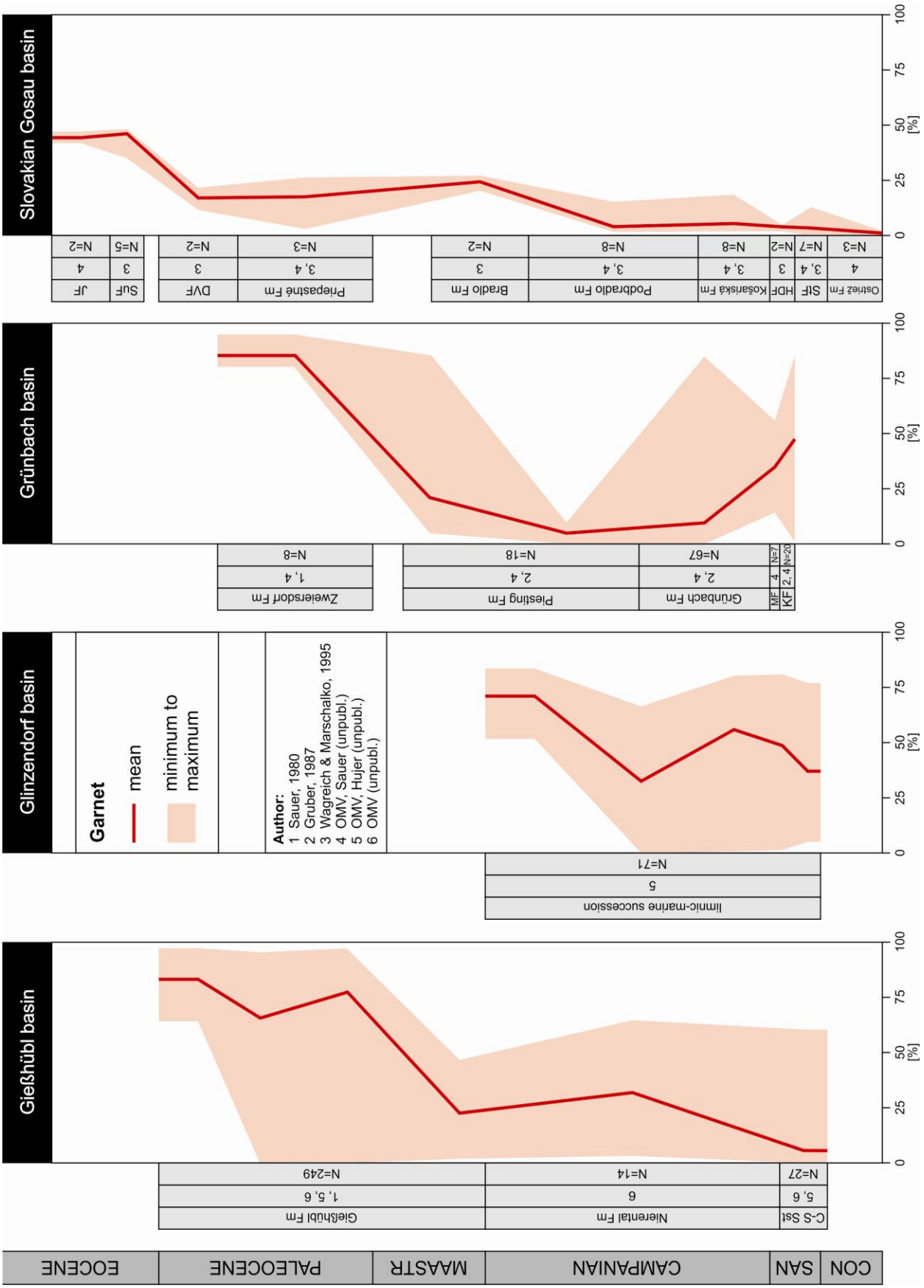

Slovakian Gosau basin
Grünbach basin
Glinzendorf basin
Gießhübl basin
Garnet
mean
minimum to maximum
Author:
1 Sauer, 1980
2 Gruber, 1987
3 Wagreich & Marschalko, 1995
4 OMV, Sauer (unpubl.)
5 OMV, Hujer (unpubl.)
6 OMV (unpubl.)
limnic-marine succession
5
N=71
Zweiersdorf Fm
1, 4
N=8
Piesting Fm
2, 4
N=18
Grünbach Fm
2, 4
N=67
MF 4 N=7
KF 2, 4 N=20
Ostrež Fm
4
N=3
StF
3, 4
N=7
HDF
3
N=2
Košariská Fm
3, 4
N=8
Podbradlo Fm
3, 4
N=8
Bradlo Fm
3
N=2
Priepastné Fm
3, 4
N=3
DVF
3
N=2
SuF
3
N=5
JF
4
N=2
C-S Sst
5, 6
N=27
Nierental Fm
6
N=14
Gießhübl Fm
1, 5, 6
N=249
CON
SAN
CAMPANIAN
MAASTR
PALEOCENE
EOCENE
0
25
50 [%]
75
100

Fig. 3: Synthetic, composite profiles of garnet contents (mean, minimum and maximum values) of the area of the Gießhübl, Glinzendorf, Grünbach and Slovakian Gosau basin. Number of samples (N) and authors (1-6) are given. Data has been taken from literature (1: Sauer 1980; 2: Gruber 1987 and 3: Wagreich and Marschalko 1995), OMV in-house data (unpublished data; edited by 5: W. Hujer, 4: R. Sauer or 6: unknown editors) or have been edited by 4: R. Sauer at the OMV lab. Apatite percentages were omitted because it was partly solved. The heavy mineral spectra were grouped in formations (C-S Sst = Coniacian-Santonian sandstones; KF = Kreuzgraben Formation; MF = Maiersdorf Formation; StF = Štvernik Formation; HDF = Hurbanova Dolina Formation; DVF = Dedkov Vrch Formation; SuF = Surovin; JF = Jablonka Formation), members, age- or depth intervals (in case of well data) and averaged.

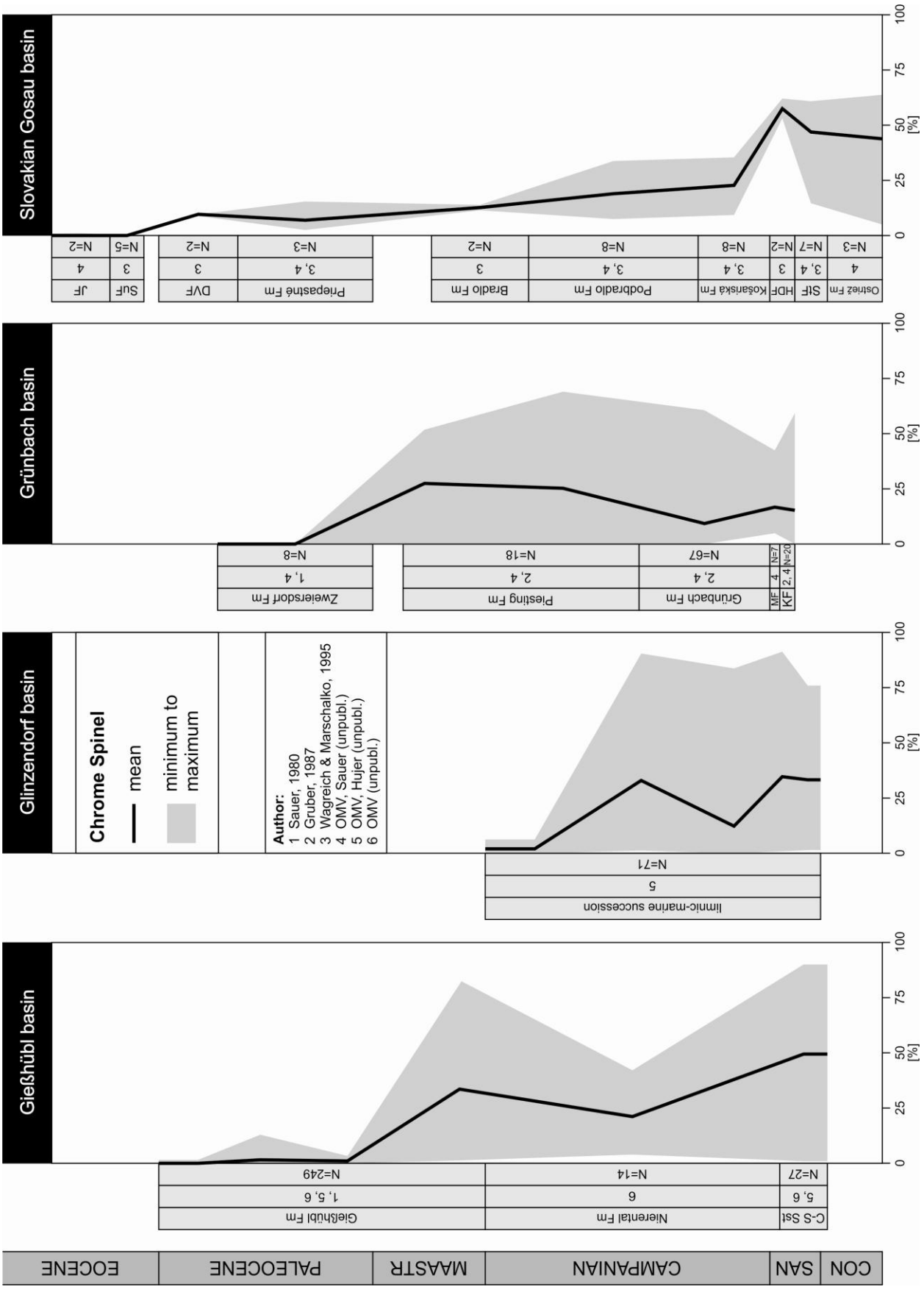

Slovakian Gosau basin
Grünbach basin
Glinzendorf basin
Gießhübl basin
Chrome Spinel
mean
minimum to maximum
Author:
1 Sauer, 1980
2 Gruber, 1987
3 Wagreich & Marschalko, 1995
4 OMV, Sauer (unpubl.)
5 OMV, Hujer (unpubl.)
6 OMV (unpubl.)
limnic-marine succession
N=71
Zweiersdorf Fm
Piesting Fm
Grünbach Fm
Ostrež Fm
Stř
HDF
Košariská Fm
Podbradlo Fm
Bradlo Fm
Priepastné Fm
DVF
SuF
JF
C-S Sst
Nierental Fm
Gießhübl Fm
CON
SAN
CAMPANIAN
MAASTR
PALEOCENE
EOCENE
[%]

Fig. 4: Synthetic, composite profiles of chrome spinel contents (mean, minimum and maximum values) of the area of the Gießhübl, Glinzendorf, Grünbach and Slovakian Gosau basin. Number of samples (N) and authors (1-6) are given. Data has been taken from literature (1: Sauer 1980; 2: Gruber 1987 and 3: Wagreich and Marschalko 1995), OMV in-house data (unpublished data; edited by 5: W. Hujer, 4: R. Sauer or 6: unknown editors) or have been edited by 4: R. Sauer at the OMV lab. Apatite percentages were omitted because it was partly solved. The heavy mineral spectra were grouped in formations (C-S Sst = Coniacian-Santonian sandstones; KF = Kreuzgraben Formation; MF = Maiersdorf Formation; StF = Štvernik Formation; HDF = Hurbanova Dolina Formation; DVF = Dedkov Vrch Formation; SuF = Surovin; JF = Jablonka Formation), members, age- or depth intervals (in case of well data) and averaged.

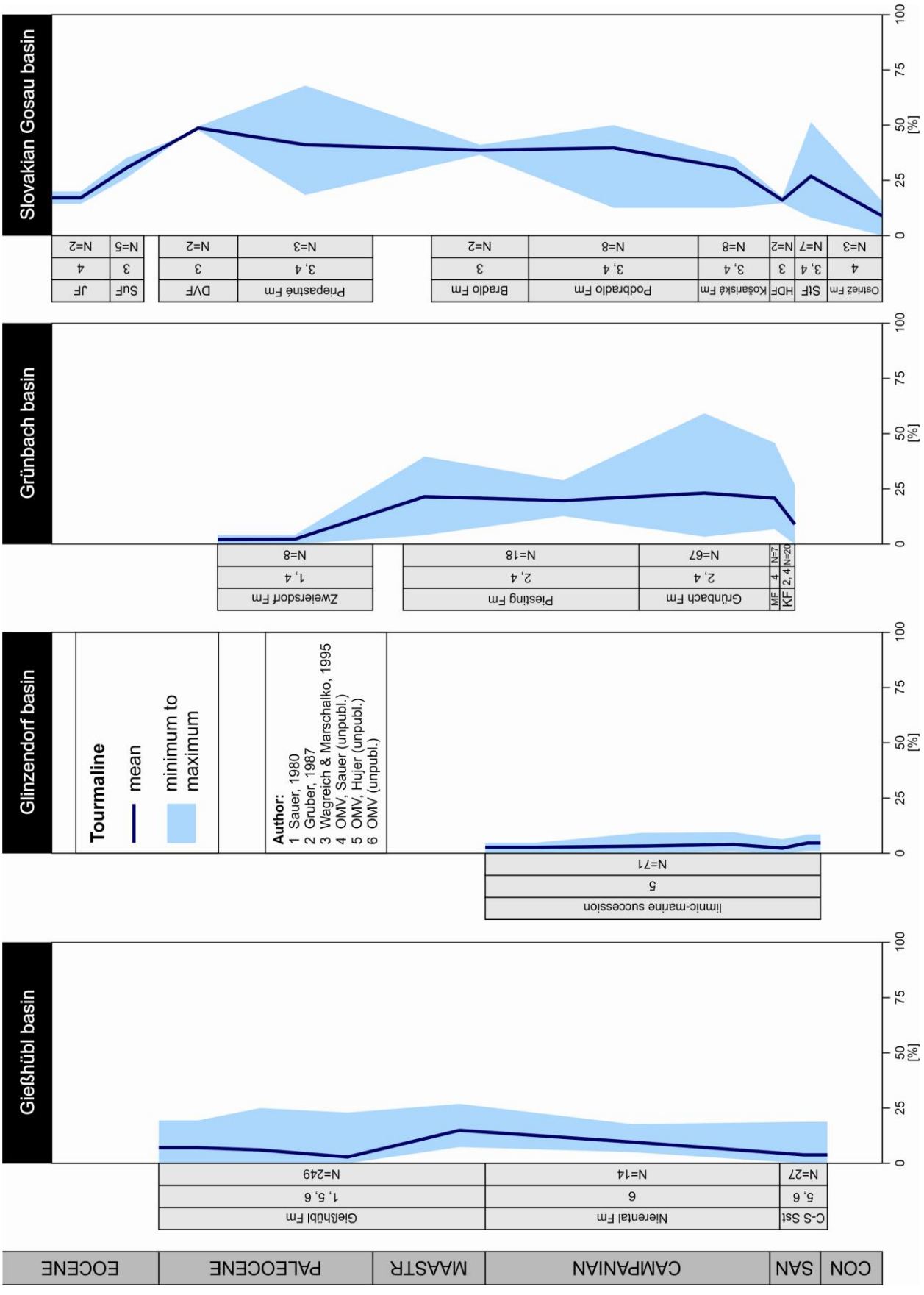

Slovakian Gosau basin
Grünbach basin
Glinzendorf basin
Gießhübl basin
Tourmaline
mean
minimum to maximum
Author:
1 Sauer, 1980
2 Gruber, 1987
3 Wagreich & Marschalko, 1995
4 OMV, Sauer (unpubl.)
5 OMV, Hujer (unpubl.)
6 OMV (unpubl.)
limnic-marine succession
5
N=71
Zweiersdorf Fm
1, 4
N=8
Piesting Fm
2, 4
N=18
Grünbach Fm
2, 4
N=67
MF 4 N=7
KF 2, 4 N=20
Ostrez Fm
4
N=3
StF
3, 4
N=7
HDF
3
N=2
Košariská Fm
3, 4
N=8
Podbradlo Fm
3, 4
N=8
Bradlo Fm
3
N=2
Priepastné Fm
3, 4
N=3
DVF
3
N=2
SuF
3
N=5
JF
4
N=2
C-S Sst
5, 6
N=27
Nierental Fm
6
N=14
Gießhübl Fm
1, 5, 6
N=249
0
25
50
75
100
[%]
CON
SAN
CAMPANIAN
MAASTR
PALEOCENE
EOCENE

Fig. 5: Synthetic, composite profiles of tourmaline contents (mean, minimum and maximum values) of the area of the Gießhübl, Glinzendorf, Grünbach and Slovakian Gosau basin. Number of samples (N) and authors (1-6) are given. Data has been taken from literature (1: Sauer 1980; 2: Gruber 1987 and 3: Wagreich and Marschalko 1995), OMV in-house data (unpublished data; edited by 5: W. Hujer, 4: R. Sauer or 6: unknown editors) or have been edited by 4: R. Sauer at the OMV lab. Apatite percentages were omitted because it was partly solved. The heavy mineral spectra were grouped in formations (C-S Sst = Coniacian-Santonian sandstones; KF = Kreuzgraben Formation; MF = Maiersdorf Formation; StF = Štvernik Formation; HDF = Hurbanova Dolina Formation; DVF = Dedkov Vrch Formation; SuF = Surovin; JF = Jablonka Formation), members, age- or depth intervals (in case of well data) and averaged.

Triangle plots of metamorphic minerals (META), stable minerals (ZTR) and ophiolite detritus (chrome spinel) (Pober and Faupl 1988) illustrate the general decrease of ophiolitic detrital influence from the Coniacian to the Eocene with a mixed source from the Coniacian to the Maastrichtian and an ophiolitic-free provenance in the Paleogene (Fig. 6).

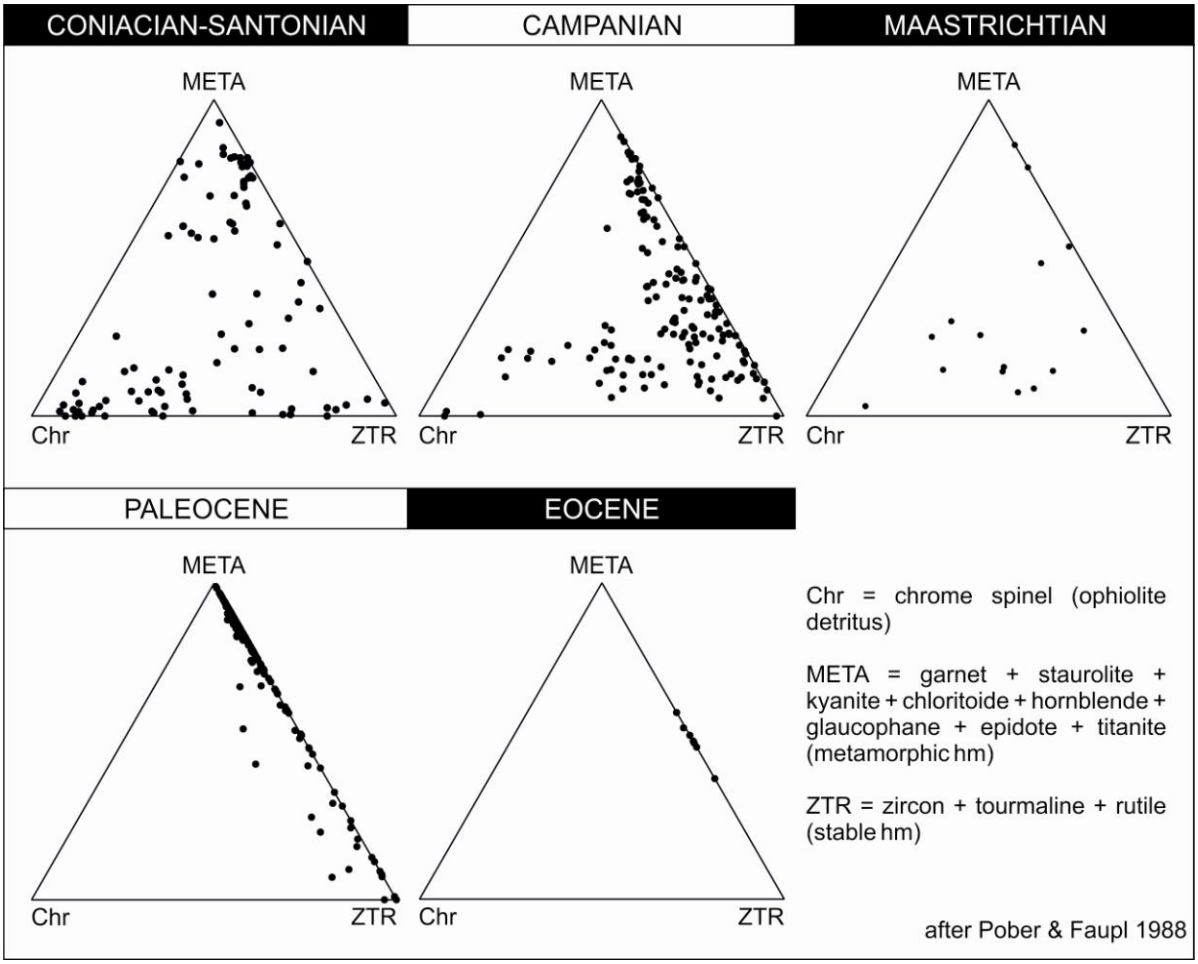


Fig. 6: Triangular plot of chrome spinel (ophiolite detritus), metamorphic (META = garnet + staurolite + kyanite + chloritoide + hornblende + glaucophane + epidote + titanite) and stable heavy minerals (ZTR = zircon + tourmaline + rutile) after Pober and Faupl (1988). Data set is grouped in age intervals.

8.2 Correlations and logratios of heavy minerals

Pearson correlation indices of heavy minerals are shown in Appendix II. Ultrastable minerals zircon and rutile are (except for the Glinzendorf basin) positively correlated (r is up to 0.747). A significant positive correlation with tourmaline is not present (only for rutile and tourmaline at the Glinzendorf basin; r=0.476). Negative correlations between zircon/rutile and garnet can be observed for the Gießhübl and Grünbach basin and between rutile and chrome spinel for the Glinzendorf and Grünbach basin. The highest negative correlation indices are given between garnet and chrome spinel (Gießhübl basin: r=-0.704; Glinzendorf basin: r=-0.844; Grünbach basin: r=-0.144; Slovakian Gosau basin: r=-0.627).

Logratio discrimination plots (Fig. 7) use the four dominant heavy mineral phases (garnet and chrome spinel) and indices (ZTR and META) (e.g. Von Eynatten 1996; Wagreich 1998). That creates four quadrants with specific heavy mineral associations: Quadrant I (Q I), with samples that are dominant in garnet and chrome spinel. Quadrant II (Q II) is characteristic for assemblages that are rich in garnet and other metamorphic associated heavy minerals. Quadrant III (Q III) contains samples with dominant concentrations of the stable heavy minerals zircon, tourmaline and rutile as well as metamorphic minerals. At quadrant IV (Q IV), samples with dominant amounts of chrome spinels and stable heavy minerals plot.

Due to strong negative correlations between garnet and chrome spinel (Appendix II), only two percent of the data set plot in Q I implying that a dominance of garnet hand in hand with high amounts of chrome spinel is extremely rare (Fig. 7). Samples from the Coniacian-Santonian age are either dominated by chrome spinel and stable minerals or garnet and metamorphic minerals (46 and 41% plot in Q IV and II, respectively). Especially samples from the Gießhübl basin and Slovakian Gosau basin plot in Q IV, while samples from the Grünbach basin are dominated by garnet and metamorphic minerals. Generally, marine samples from the Glinzendorf basin plot in Q II, non-marine samples in Q IV (Fig. 7). Campanian heavy mineral assemblages of the Gießhübl basin show balanced amounts of garnet, chrome spinel, metamorphic and stable minerals and plot in the central part of Q II, III and IV. Samples from the Glinzendorf basin are mainly dominated by garnet; the Slovakian Gosau basin is rich in chrome spinel and stable minerals and plot in Q IV. Only samples from the Grünbach basin are neither dominant in garnet nor in chrome spinel and plot in Q III (Fig. 7). 69% of Maastrichtian samples group in Q IV, symbolizing dominance of chrome spinel and stable minerals (Fig. 7). Absence of chrome spinel and dominance of garnet in the Paleocene and Eocene result in dominant samples in Q II (80%) and Q III (18%) (Fig. 7).

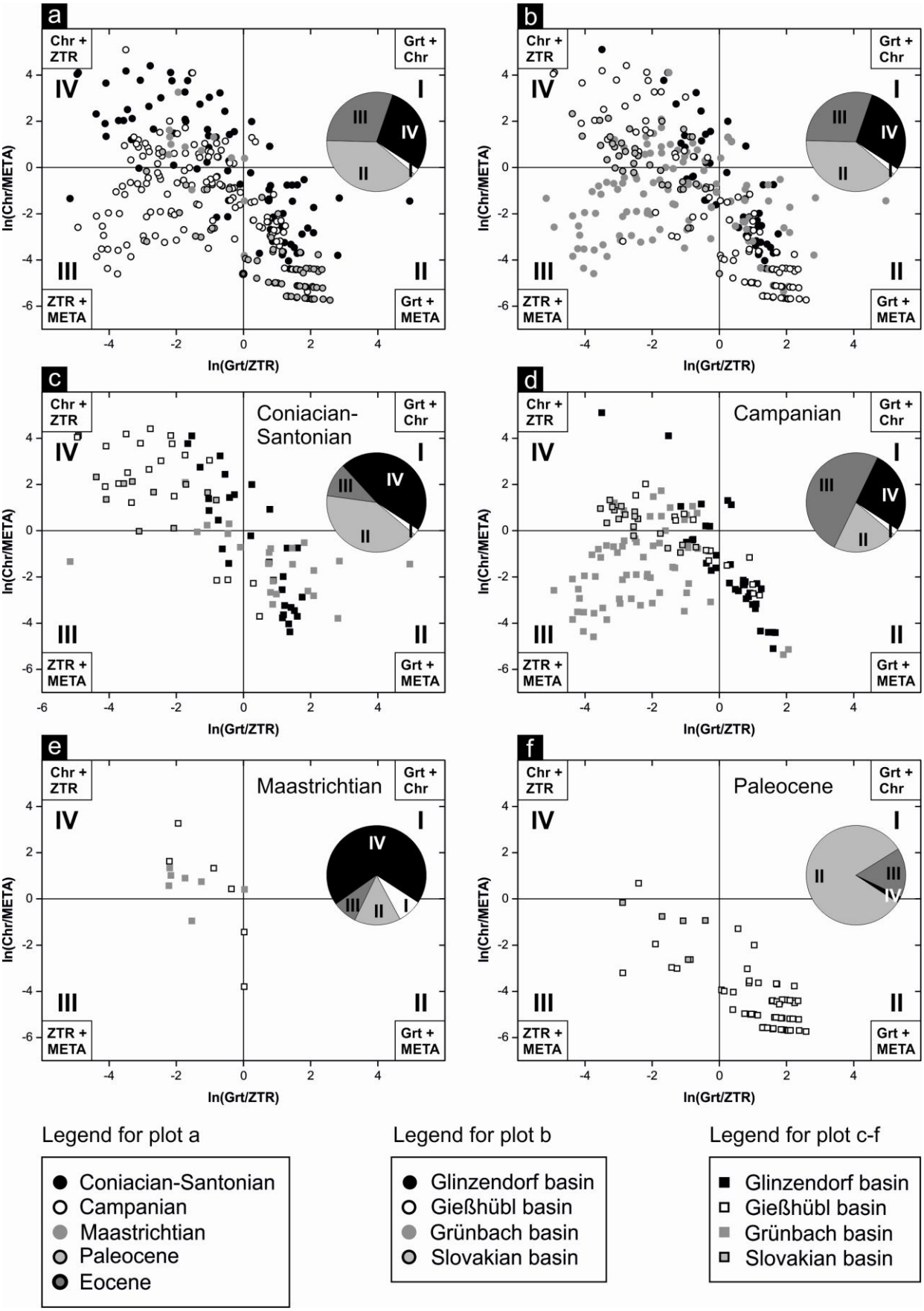

a
b
c
d
e
f
Chr + ZTR
Grt + Chr
ZTR + META
Grt + META
I
II
III
IV
ln(Chr/META)
ln(Grt/ZTR)
Coniacian-Santonian
Campanian
Maastrichtian
Paleocene
Legend for plot a
Coniacian-Santonian
Campanian
Maastrichtian
Paleocene
Eocene
Legend for plot b
Glinzendorf basin
Gießhübl basin
Grünbach basin
Slovakian basin
Legend for plot c-f
Glinzendorf basin
Gießhübl basin
Grünbach basin
Slovakian basin

Fig. 7: Logratio-diagrams of ln(Grt/ZTR) vs. ln(Chr/META) grouped in age intervals (a), Gosau basins (b) and Gosau basins for individual age intervals (c-f). Grt = garnet; Chr = chrome spinel; META = garnet + staurolite + kyanite + chloritoide + hornblende + glaucophane + epidote + titanite; ZTR = zircon + tourmaline + rutile. Pie charts illustrate the percentage of samples plotting in quadrant I to IV.

8.3 Mineral Chemistry

8.3.1 Garnet

Analyzed detrital garnets (mean values of multiple analyzes from single grains are used for further calculations) are usually almandine-rich with 63 ±9% in average and a maximum of 85%. Only 12% of 263 analyzed garnet grains have compositions lower than 50% almandine. Grossular proportions are generally moderate to low with a mean of 18 ±9%. Only two grains show a dominant grossular component with 56 (B-3B) and 93% (G-22). Pyrope contents vary between 0 and 46% with a low average of 12 ±7% (half of the samples have concentrations lower than 10%) (Fig. 8). Mean pyrope contents are summarized in table 2. While low spessartine proportions are characteristic (6 ±6% in average), andratite and uvarovite is almost inexistent (Appendix III).

Mean pyrope contents of detrital garnets [wt.%]

Con-San	**Mean**	**Stand. Dev.**	**N**
GHB	0.36	0.14	2
GDB			0
GBB	0.20	0.05	30
SGB			0
Campanian	**Mean**	**Stand. Dev.**	**N**
GHB	0.16		1
GDB	0.14	0.09	18
GBB	0.17	0.07	19
SGB	0.03	0.01	3
Maastrichtian	**Mean**	**Stand. Dev.**	**N**
GHB	0.10	0.06	31
GDB			0
GBB			0
SGB			0
Paleocene	**Mean**	**Stand. Dev.**	**N**
GHB	0.09	0.04	62
GDB			0
GBB	0.11	0.06	39
SGB	0.09	0.06	52
Eocene	**Mean**	**Stand. Dev.**	**N**
GHB			0
GDB			0
GBB			0
SGB	0.09	0.09	6

Table 2: Mean pyrope contents of detrital garnets of various time and Gosau basin (GHB: Gießhübl basin, GDB: Glinzendorf basin, GBB: Grünbach basin, SGB: Slovakian Gosau basin).

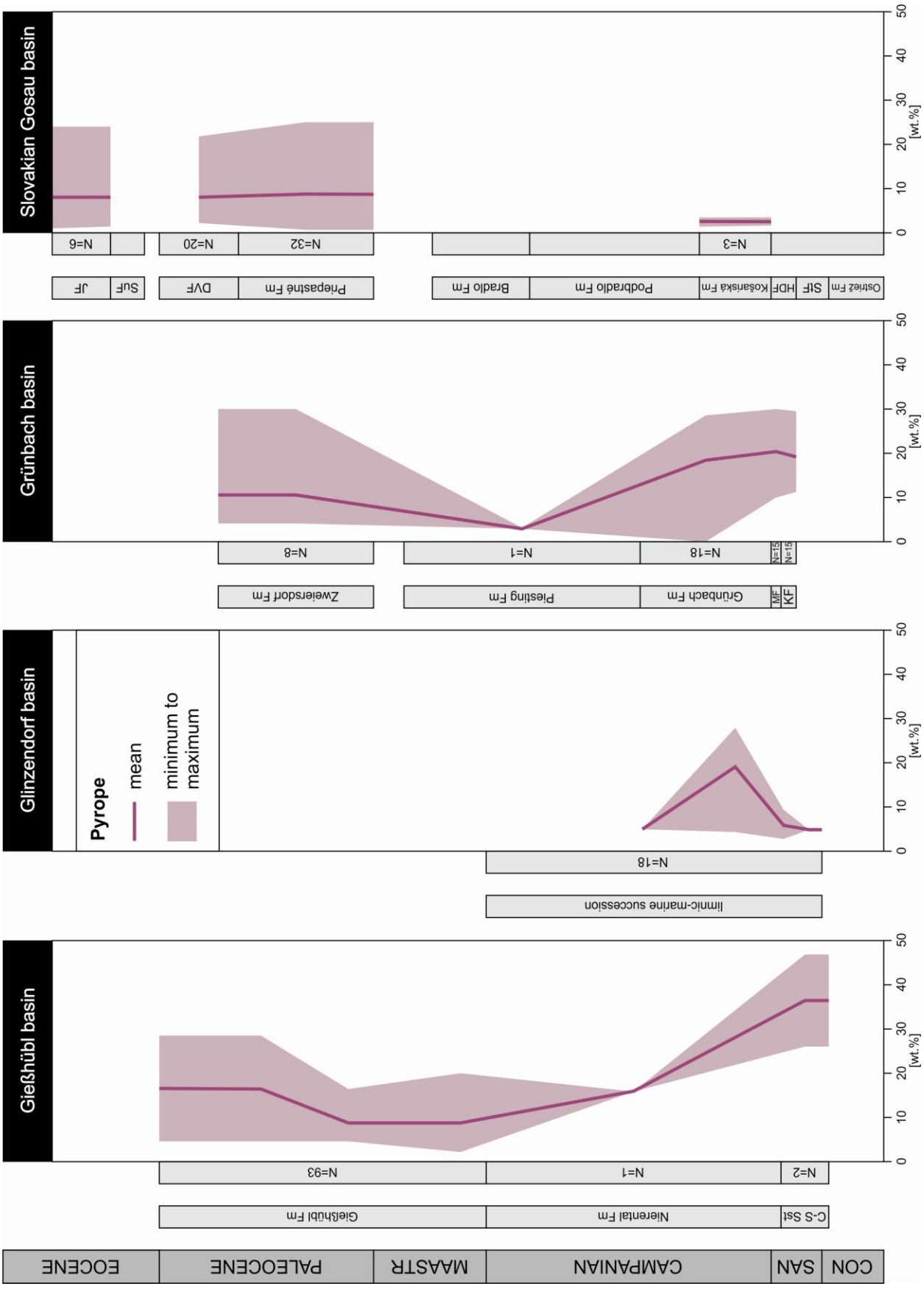

CON
SAN
CAMPANIAN
MAASTR
PALEOCENE
EOCENE
Gießhübl basin
C-S Sst
Nierental Fm
Gießhübl Fm
N=2
N=1
N=93
0
10
20
30
40
50
[wt.%]
limnic-marine succession
N=18
Glinzendorf basin
Pyrope
mean
minimum to maximum
Grünbach basin
Grünbach Fm
Piesting Fm
Zwelersdorf Fm
MF
KF
N=15
N=15
N=18
N=1
N=8
Slovakian Gosau basin
Ostrež Fm
StF
HDF
Košariská Fm
Podbradlo Fm
Bradlo Fm
Priepastné Fm
DVF
SuF
JF
N=3
N=32
N=20
N=6

Fig. 8: Synthetic, composite profiles of pyrope contents (mean, minimum and maximum values) in wt.% of garnets of the area of the Gießhübl, Glinzendorf, Grünbach and Slovakian Gosau basin. Number of samples (N) for different formations (C-S Sst = Coniacian-Santonian sandstones; KF = Kreuzgraben Formation; MF = Maiersdorf Formation; StF = Štvernik Formation; HDF = Hurbanova Dolina Formation; DVF = Dedkov Vrch Formation; SuF = Surovin; JF = Jablonka Formation), members, age- or depth intervals (in case of well data) is given.

Various triangle plots show similar systematic trends of garnet populations in time and space (different Gosau basins) (Fig. 9). Generally, garnets of such compositions cannot be explicitly assigned to a specific lithology, because garnet chemistry is dependent on paragenesis and coexisting mineral phases. Higher amounts (around 20 and 30%) of pyrope and grossular are commonly associated with amphibolites, blueschist-associated eclogite or granulite source rocks. Pyrope contents of <50% exclude garnet peridotites and associated eclogites as possible source (Von Eynatten and Gaupp 1999). Components of high-grade metamorphic garnets supposed of being derived from amphibolites and granulites (mainly expressed by high contents of pyrope and grossular) are prominent from the Coniacian to the Campanian and disappear in the Maastrichtian to the Eocene, where dominant almandine-rich garnets suggest biotite schist and granite source. Mean pyrope values are high in the Coniacian-Santonian (20.6 ±7.0%) and Campanian (14.5 ±8.7%) and significantly lower in the Maastrichtian (9.7 ±5.8%), Paleocene (9.8 ±5.4%) and Eocene (8.8 ±9.1%). Discrimination diagram (almandine+spessartine – pyrope – grossular; Fig. 9) of Preston et al. (2002) indicates 49% of amphibolites and 29% of eclogite provenance in Coniacian-Santonian age. This “high-metamorphic” source is dominant compared to lower metamorphic-grade derived garnets from biotite schists (10%) and granites/pegmatites (10%). This influence of a high metamorphic character of garnets is still present (but reduced) in the Campanian (35% indicate amphibolites, 15% eclogites, 23% biotite schists and 17% granities as possible provenance). From the Maastrichtian to the Eocene there are no indications for high-grade metamorphic garnets any more. Biotite schists (around 70% plot in this field) are the supposed dominant source. The same trend can be demonstrated using the boundary conditions after Morton et al. (2003) with dominant garnets derived from amphibolites/granulite facies from the Coniacian to the Campanian in contrast to prevailing low-grade metamorphosed almandine-rich garnets from the Maastrichtian onwards (Fig. 9). The general retrograde metamorphic character in time can also be observed in the almandine – pyrope – grossular plot (Fig. 9) after Méres (2008): The bigger part of Coniacian to Campanian garnets suggest compositions from granulite, eclogite and high amphibolites to granulite facies, and high-pressure eclogites, high-pressure mafic granulites and amphibolites as interpreted source rocks. Maastrichtian to Eocene detrital garnets plot more or less in the field of amphibolite facies and suggest a lower degree of metamorphism (e.g. Aubrecht et al. 2009).

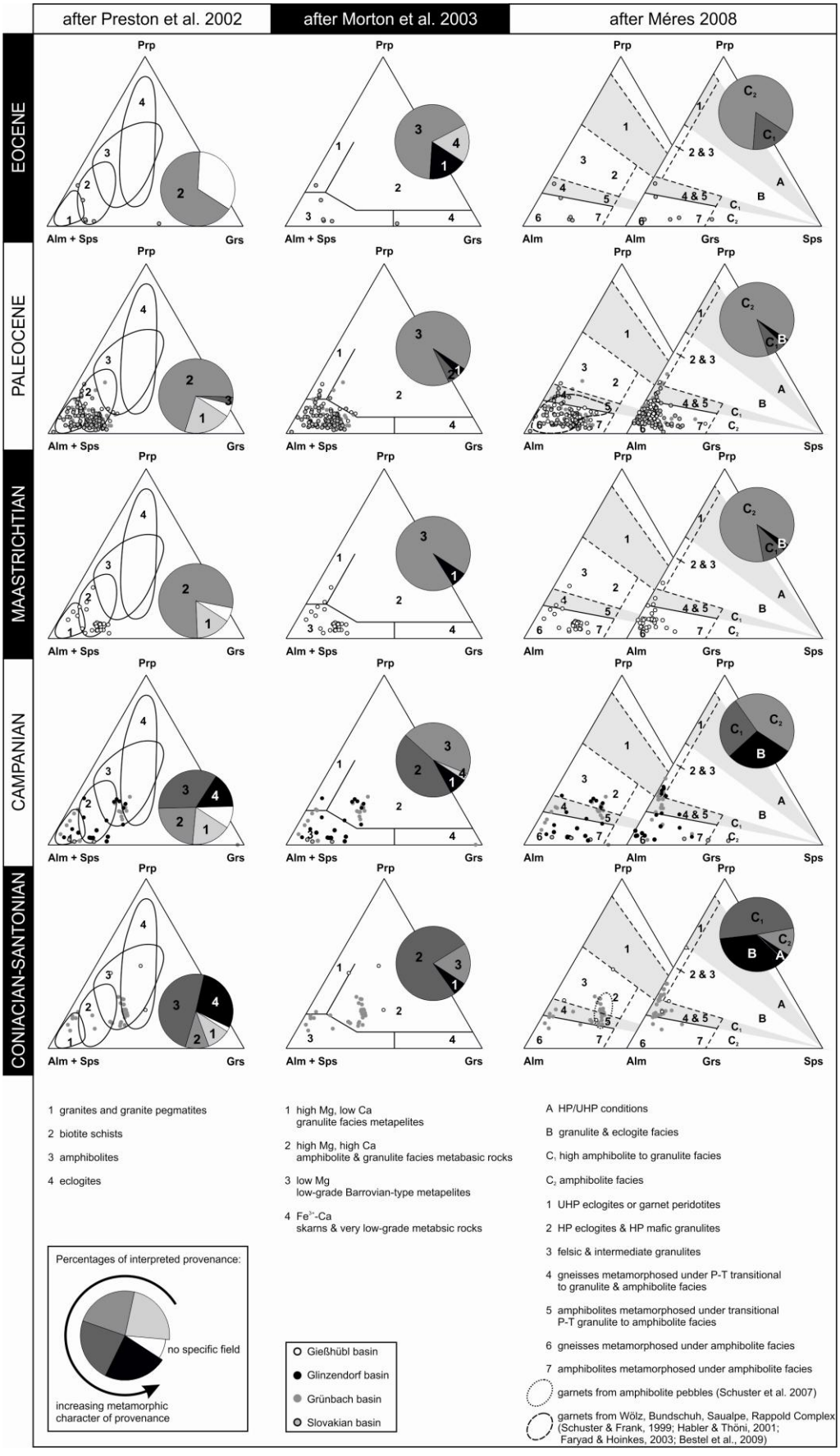

after Preston et al. 2002
after Morton et al. 2003
after Méres 2008
EOCENE
PALEOCENE
MAASTRICHTIAN
CAMPANIAN
CONIACIAN-SANTONIAN
Prp
Alm + Sps
Grs
Alm
Grs
Sps
1 granites and granite pegmatites
2 biotite schists
3 amphibolites
4 eclogites
1 high Mg, low Ca
granulite facies metapelites
2 high Mg, high Ca
amphibolite & granulite facies metabasic rocks
3 low Mg
low-grade Barrovian-type metapelites
4 Fe3+-Ca
skarns & very low-grade metabsic rocks
A HP/UHP conditions
B granulite & eclogite facies
C1 high amphibolite to granulite facies
C2 amphibolite facies
1 UHP eclogites or garnet peridotites
2 HP eclogites & HP mafic granulites
3 felsic & intermediate granulites
4 gneisses metamorphosed under P-T transitional to granulite & amphibolite facies
5 amphibolites metamorphosed under transitional P-T granulite to amphibolite facies
6 gneisses metamorphosed under amphibolite facies
7 amphibolites metamorphosed under amphibolite facies
garnets from amphibolite pebbles (Schuster et al. 2007)
garnets from Wölz, Bundschuh, Saualpe, Rappold Complex (Schuster & Frank, 1999; Habler & Thöni, 2001; Faryad & Hoinkes, 2003; Bestel et al., 2009)
Percentages of interpreted provenance:
no specific field
increasing metamorphic character of provenance
Gießhübl basin
Glinzendorf basin
Grünbach basin
Slovakian basin

Fig. 9: Almandine (Alm) + spessartine (Sps) – pyrope (Prp) – grossular (Grs)-triangle plot after Preston et al., 2002 (left column) and Morton et al. (2003; middle column), and almandine (Alm) – pyrope (Prp) – spessartine (Sps)-triangle plot after Méres (2008; right column) of detrital garnets. Plots are shown for individual age intervals with samples grouped in different Gosau basins (Gießhübl, Glinzendorf, Grünbach and Slovakian Gosau basin). Fields for interpreted provenance (lithologies or metamorphic facies) from where the garnets are supposed to be derived are given below the plots according to the authors. Pie charts illustrate the percentage of samples plotting in the different fields of provenance (gray scale indicates the metamorphic character of the provenance).

There can be also a difference in the spatial distribution of detrital garnets observed. The Grünbach and Glinzendorf basins, which were paleogeographically located in the south of the Gosau depositional area, are generally characterized by a higher amount of garnets derived from a higher-metamorphic source compared to the northern Gießhübl and Slovakian basins. A statistical evaluation of this observation is not possible, because the different time periods are not always represented by samples from all Gosau basins. In the Slovakian basin, garnets do not suggest input of high-grade metamorphic (e.g. upper-amphibolitic, eclogitic) source rocks (Fig. 9).

A clear interpretation of the almandine discrimination diagram (MnO vs. CaO) after Harangi et al. (2001) is not possible, because most of the sample points do not plot within the classification fields. Generally high-pressure garnets from M/I-type magmas and garnets from S-type magmas and metapelites are common (Fig. 10).

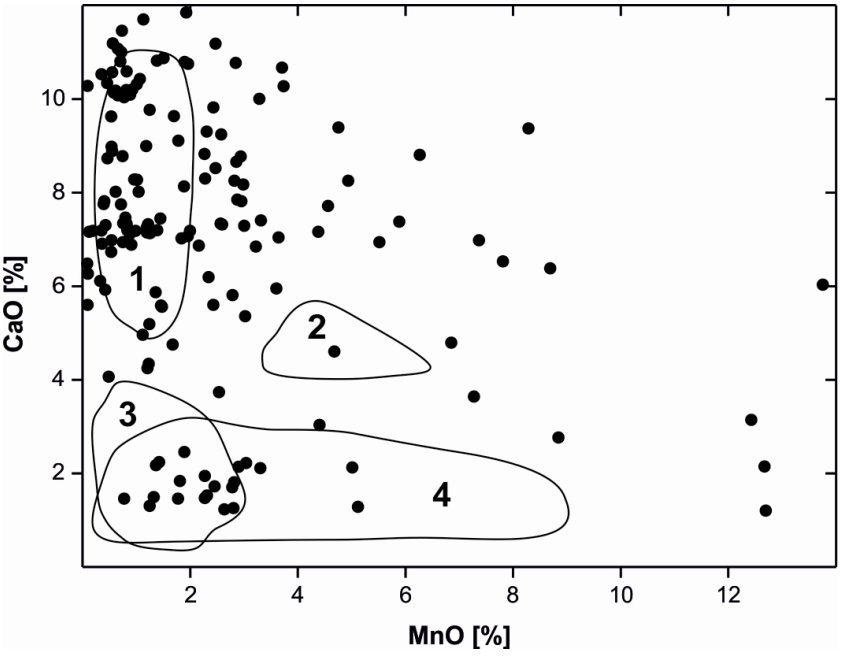


Fig. 10: Binary discrimination diagram (MnO vs. CaO) for almandine garnets from magmatic rocks after Harangi et al. (2001). 1: high-pressure garnets from M/I-type magmas; 2: low-pressure garnets from M/I-type magmas; 3: garnets from S-type magmas; 4: garnets from metapelites.

8.3.2 Chrome spinel

MgO contents of the analyzed detrital chrome spinels (mean values of multiple analyses from single grains are used for further calculations) range from 6.8 to 19.7% with 13.3 ±2.4% in average. Mean Cr_2O_3 concentrations of 40.5 ±9.9% fluctuate between 10.7 and 58.5%. Mg# and Cr# show a broad range between 0.29 and 1.0 as well as 0.2 and 0.88, respectively, with means of 0.62 ±0.14 and 0.65 ±0.14. Trace element concentrations are constantly low with TiO_2<0.43, NiO<0.38, MnO<0.33 and ZnO<0.31 (Appendix IV). Generally, zoned spinels could not be observed thus representing unaltered chemical composition (Pober and Faupl 1988).
According to the Al_2O_3/TiO_2 diagram of Kamenetsky et al. (2001), most of the detrital chrome spinels were derived from MOR-type peridotites and supra-subduction zone (SSZ) peridotites. Only a few samples trend to volcanic rock sources from island-arc basalts or MORB-type rocks (Fig. 11).

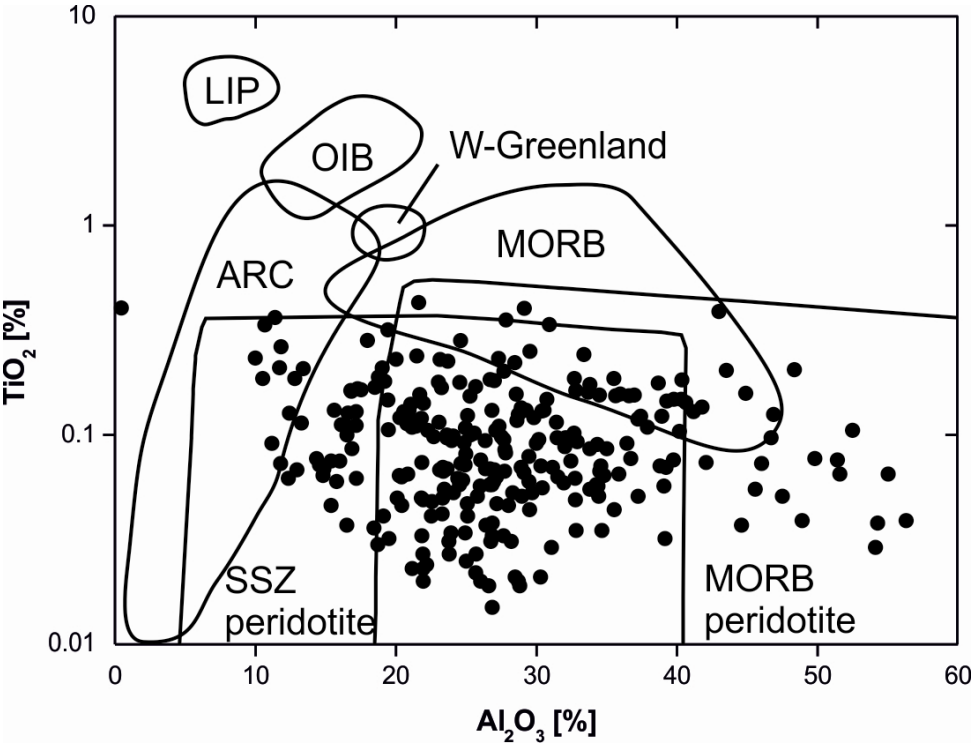


Fig. 11: Discrimination diagram (Al_2O_3 vs. TiO_2) of chrome spinels derived from various types of mafic and ultramafic rocks after Kamenetsky et al. (2001). LIP: large igneous province; OIB: ocean-island basalt; MORB: mid-ocean ridge basalt; ARC: island-arc basalt; SSZ: supra-subduction zone.

Generally, chrome spinels fit well to the field of ophiolites (peridotites of alpine type) using the Mg# vs. Cr#-diagram of Pober and Faupl (1988) (Fig. 12). The influence of metamorphic spinel is negligible. Most of the samples plot in the field of type II ophiolite (peridotite) provenance, which is a transitional classification comprising type I and III (Pober and Faupl 1988). Samples derived from type I (Cr#<0.6; lherzolite composition) and III (Cr#>0.6; harzburgite composition)

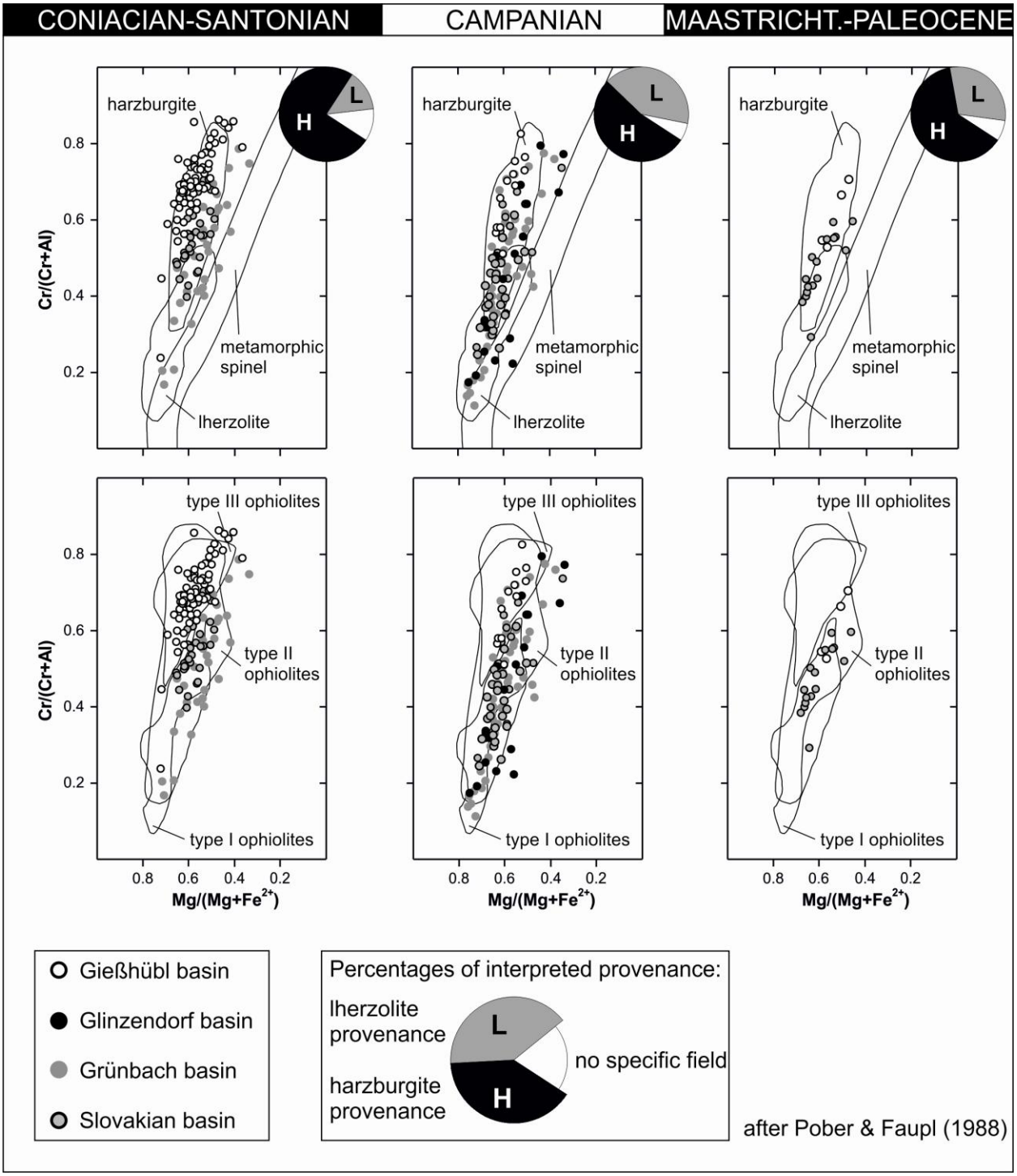


Fig. 12: Mg/(Mg+Fe^{2+}) vs. Cr/(Cr+Al) of detrital chrome spinels after Pober and Faupl (1988). Plots are shown for individual age intervals with samples grouped in different Gosau basins (Gießhübl, Glinzendorf, Grünbach and Slovakian Gosau basin). Pie charts illustrate the percentage of samples plotting in harzburgite (H) or lherzolite (H) provenance field.

ophiolites are similarly distributed for the whole dataset. About two-thirds of the analyzed grains are related to harzburgite composition compared to lherzolite provenance. Looking in detail,

there is a significant difference in time and space (various Gosau basins). In the Coniacian-Santonian, harzburgite composition is with around 75% dominant compared to 14% of lherzolite related source. This dominance of harzburgite peridotites is reduced in the Campanian (53% harzburgite compared to 41% lherzolite composition). The mean of Cr# of the Coniacian-Santonian is with 0.68 ±0.11 significantly different from the Campanian with 0.61 ±0.16. A significance of 0.000 (T=3.773) is proved by Welch´s t-test, which was used because equality of variance is not given. 63 and 30% of Maastrichtian to Paleocene spinels are related to harzburgite respectively lherzolite source. Paleogeographically northern basins have a significant higher influence of harzburgite character (74% in the Gießhübl basin; 65% in the Slovakian basin) compared to southern basins (44% in the Glinzendorf basin; 47% in the Grünbach basin).

8.3.3 Tourmaline

Generally, tourmaline chemistry of the analyzed formations (mean values of multiple analyzes from single grains are used for further calculations) range to a great degree in major element concentrations: Al_2O_3: 22.4 - 39.3 (mean: 32.1 ±2.2), FeO: 0.3 – 23.4 (mean: 8.1 ±2.8), MgO: 0.0 – 14.8 (mean: 6.6 ±1.6), CaO: 0.0 – 17.4 (mean: 0.5 ±1.1) (Appendix V). Mixtures of dravite and schorl are most common with no specific differences in time or space (Fig. 13). Minor and trace element concentrations fluctuate between 0.0 and 3.1 (Na_2O), 1.9 (TiO_2), 1.4 (F), 1.0 (K_2O) and 0.4 (MnO). Chemistry of cores and rims vary differently strong between almost zero and a few weight percentages (Appendix V).

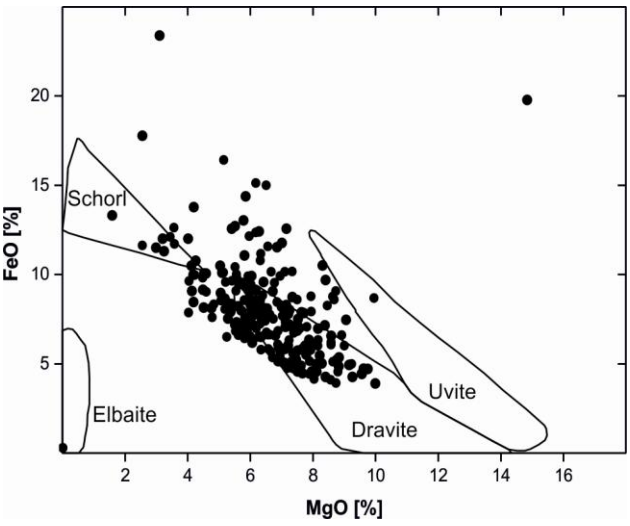


Fig. 13: Discrimination diagram (MgO vs. FeO) of tourmalines after Morton (1991) indicating the various tourmaline varieties (schorl, dravite, uvite and elbaite).

Provenance-discrimination plots (Fe-Mg-Al and Fe-Mg-Ca after Henry and Guidotti 1985) indicate a generally mixed source of various metapelites, Fe^{3+}-rich quartz-tourmaline rocks and granitoids (Fig. 14). Neither in time, nor in space (paleogeographic adjustment of the Gosau basins), no clear change in the source is identifiable. According to these plots, there is no clear evidence for the occurrence of tourmalines derived from metaultramafic rocks and Cr, V-rich metasediments, which would be indicative for an ophiolitic provenance.

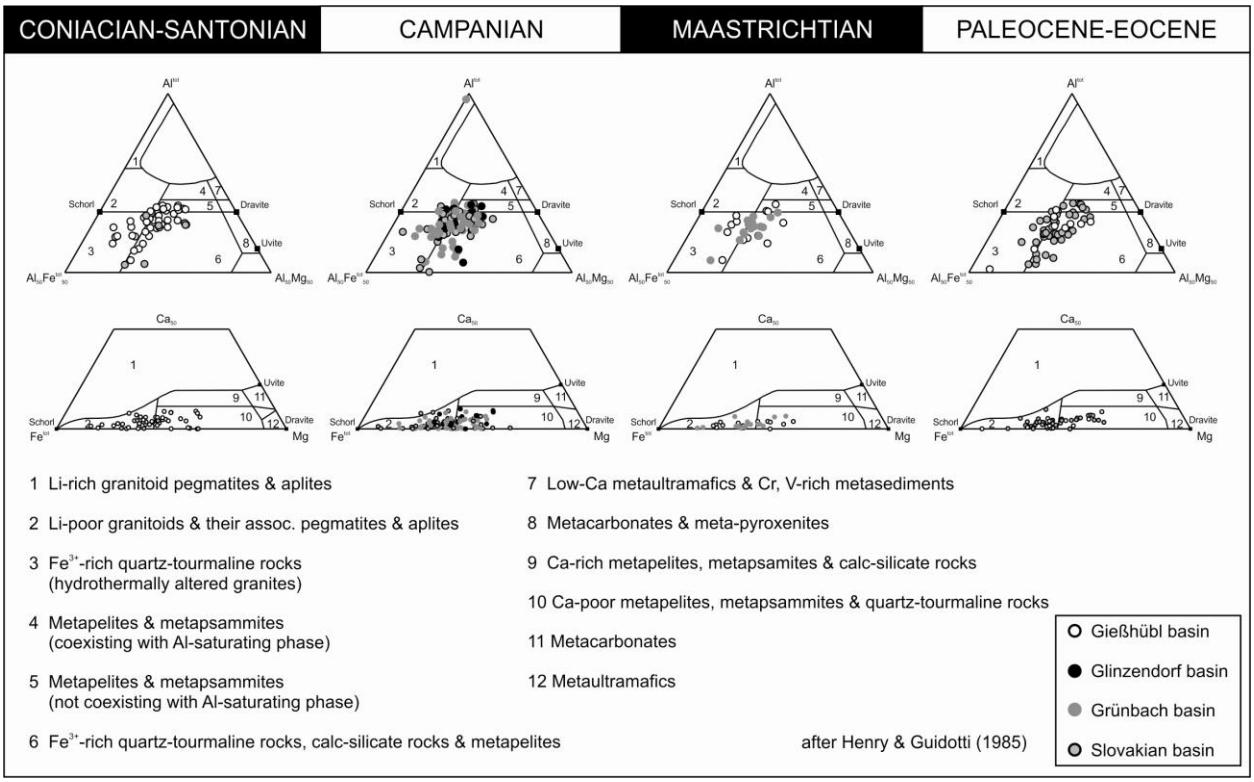


Fig. 14: Fe^{tot} – Al^{tot} – Mg and Fe^{tot} – Ca – Mg-triangle plot of detrital tourmalines after Henry and Guidotti (1985). Plots are shown for individual age intervals with samples grouped in different Gosau basins (Gießhübl, Glinzendorf, Grünbach and Slovakian Gosau basin). Fields for interpreted provenance from where the tourmalines are supposed to be derived are given below the plots according to the authors.

9 Discussion

Heavy mineral assemblages of Coniacian-Campanian sediments are characterized by prevailing chrome spinel, followed by zircon, tourmaline and garnet in all Gosau basins (Fig. 2). This indicates erosion of an ophiolitic source. Primarily, this detritus was interpreted only to be derived from northern Penninic provenance (Dietrich and Franz 1976; Stattegger 1986). Chemical analysis of detrital chrome spinels (Pober and Faupl 1988) and sedimentological

evaluation of serpentinitic sandstones (Wagreich 1993b) introduced the ophiolitic Tethys suture zone to the south as a significant second source area (Fig. 15). This southern ophiolite complex supplied clastic material at least since the Early Cretaceous (Decker et al. 1987; Von Eynatten and Gaupp 1999) up to the Maastrichtian and is now fully eroded. Today, the only evidence for this ophiolitic thrust unit(s) gives basic volcanic components of conglomerates (Gruber et al. 1992), serpentine fragments in sandstones (Wagreich 1993b) and (extremely) chrome spinel-rich heavy mineral assemblages. These ophiolite massifs of the Vardar/Meliata suture support chrome spinel-rich detritus in larger regional scale (Pober and Faupl 1988; Árgyelán 1996; Von Eynatten and Gaupp 1999; Lenaz et al. 2009; Lužar-Oberiter et al. 2009; 2012). In addition, high amounts of Cr and Ni in non-marine fine-grained clastic sediments of the Glinzendorf basin suggest a dominant ophiolitic detrital supply in proximal, paleogeographically southern basins (Hofer et al. in press). Generally, serpentinites that provided those massive amounts of detrital chrome spinels are much more common in Tethyan ophiolites and relatively scarce in Penninic units. Chrome spinels from northern Gosau basins have characteristically higher Cr# (mean: 0.67 ±0.10) compared to spinels from southern basins (0.60 ±0.18) and indicate harzburgite source (Fig. 12). Spinels from Penninic ophiolites from the Tauern, Unterengadin (Pober and Faupl 1988) and Rechnitz window (Mikuš and Spišiak 2007), which are probably comparable to a possible northern ophiolitic provenance, commonly have lower Cr# indicating lherzolitic composition. Generally, chemistry of chrome spinels is hardly distinguishable between Meliata and Penninic ultramafics (Pober and Faupl 1988; Mikuš and Spišiak 2007). Hence, chrome spinel data do not confirm dominant detrital input of Penninic ophiolite source, but however minor influence is likely. Detrital supply from the accretionary wedge is supposed at least for the Tannheim-Losenstein basin in the Early Cretaceous (Wagreich 2001b).

Chrome spinel chemistry of southern Gosau basins point to a provenance from a mixed harzburgite and lherzolite source of the Tethys suture sensu Pober and Faupl (1988) and Faupl and Wagreich (2000). Analogue detrital chrome spinels from Dinaric Cretaceous basins (Lužar-Oberiter et al. 2009) and chrome spinels from Dinaric ophiolites (Maksimovic and Majer, 1981), probably comparable to the fully eroded southern provenance, show equal chemistry. Supplementary to dominant spinel portions, metamorphic derived minerals are important in Coniacian to Campanian heavy mineral assemblages (Fig. 2). Garnet chemistry indicates a mixed source of high- to low-grade metamorphosed provenance (Fig. 9). High amounts of garnets derived from HP/UHP conditions of granulite, eclogite and amphibolite facies can be observed in the Gießhübl, Glinzendorf and Grünbach basin. Garnets from the Slovakian basin do not suggest higher metamorphic character, which can also be an effect of low number of samples. Garnet chemistry and spatial distribution of these high-grade metamorphosed grains

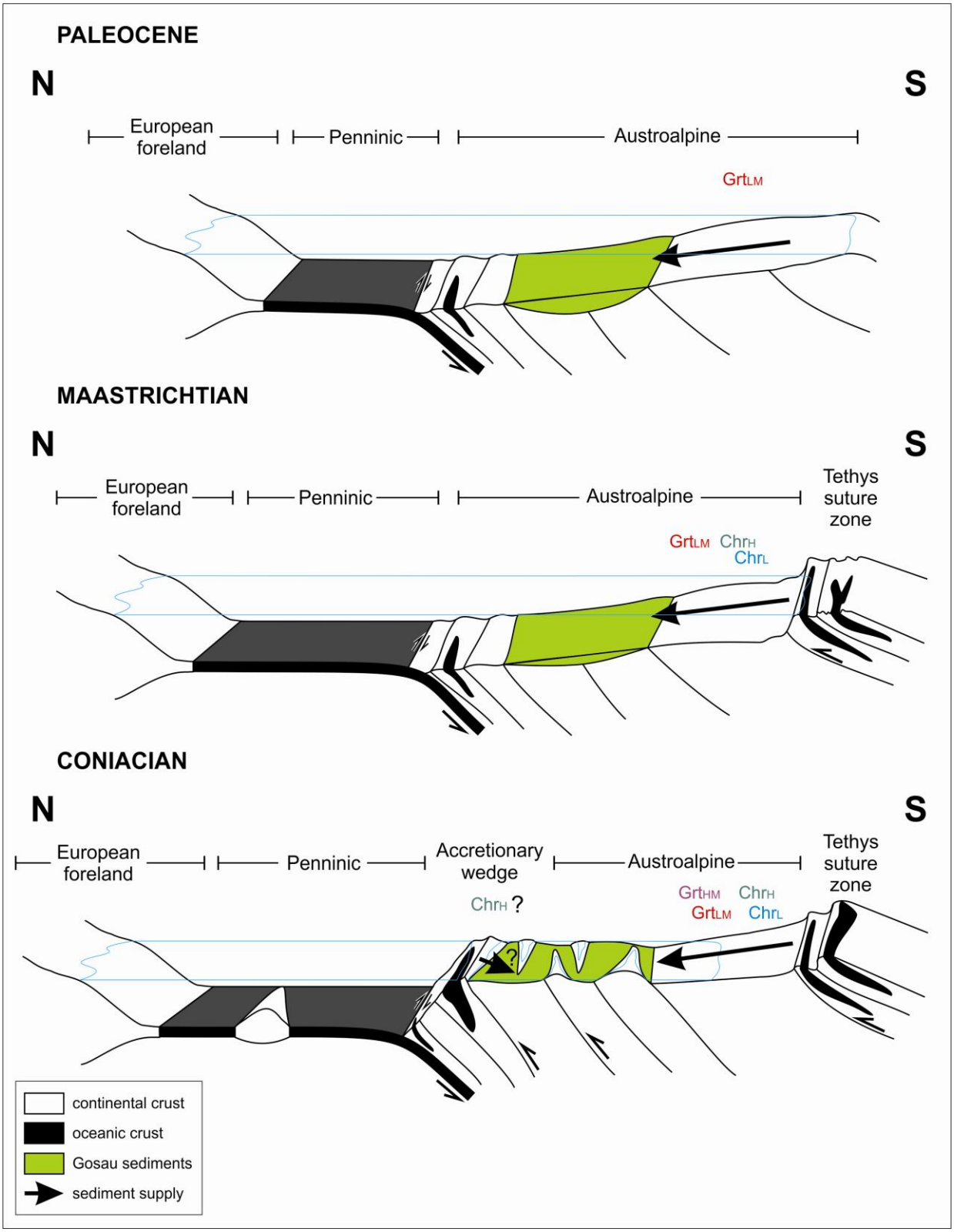


Fig. 15: Plate tectonic model for the Eastern Alps and Western Carpathians during the deposition of the Gosau Group with associated souce areas of detritus. Types of detrital garnets and chrome spinels are marked from various provenances: Grt_{LM}: low-grade metamorphosed garnets, Grt_{HM}: high-grade metamorphosed garnets, Chr_{H}: chrome spinels from mainly harzburgite-provenance, Chr_{L}: chrome spinels from mainly lherzolite-provenance.

point to high metamorphic units of the Tethys suture to the south as the most likely source area. Investigations on amphibolite pebbles (upper amphibolites facies) from the Grünbach Syncline suggest remnants of the metamorphic sole of Tethys ophiolite sheets as ultimate provenance (Schuster et al. 2007). Similarities (e.g. symplectitic textures and cooling ages) to amphibolites from the metamorphic sole at the base of the Dinaric ophiolites are conspicuous, and are not known from Austroalpine metamorphic units. These (upper) amphibolite-facies metamorphic soles generally indicate basaltic and sedimentary protoliths (Carosi et al. 1996; Dimo-Lahitte et al. 2001; Elitok and Drüppel 2008; Mikes et al. 2008). Garnet chemistry from Schuster et al. (2007; data from amphibolite pebbles of the Lower Gosau Group) and Balen et al. (2003; data from the Dinaric Krivaja-Konjuh ultramafic massif, Bosnia) are identical to our results (Fig. 9). Similar compositions of detrital garnets are also observed in the Dinaride Ophiolite Zone mélange in Bosnia, which are attributed to the sub-ophiolitic metamorphic sole (Mikes et al. 2008).

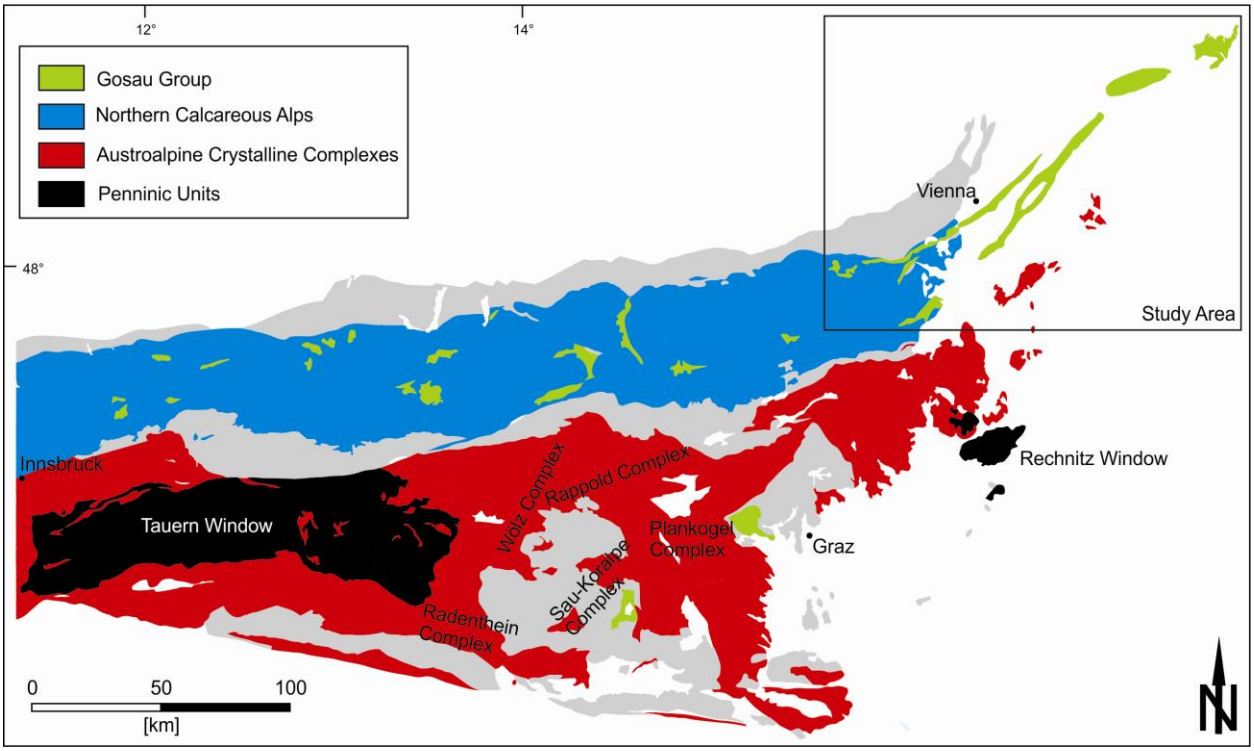


Fig. 16: Simplified geological map of the Eastern Alps (east of Innsbruck) after Egger et al. (1999). Highlighted Austroalpine crystalline complexes are supposed to be the source area for Paleogene almandine-rich garnets of the Gosau Group in the study area.

The influence of ophiolitic detritus is present until the Maastrichtian with chrome spinels of harzburgite dominant source (Figs. 2, 6, 12 and 15). At this time, detrital input only comes from

the south (Wagreich and Faupl 1994). Nappes of high metamorphic facies in the south are already eroded at this time and garnet chemistry generally indicates low metamorphic metapelites as provenance (Fig. 9).

Paleogene heavy mineral assemblages are only dominated by garnet (around 80%), and tourmaline in the Slovakian basin (Fig. 2). Chrome spinel is inexistent, except minor amounts in the Slovakian Gosau, probably due to reworking of older Gosau sediments. Garnet chemistry is analogue to the Maastrichtian from low metamorphic, probably metapelitic source (Fig. 9). Garnet chemistry is uniform and almandine-rich, equal to garnets from the Austroalpine Crystalline Complexes of the Eastern Alps like the Wölz, Rappold, Radenthein, Plankogel, Koralpe and Saualpe Complex (Schuster and Frank 1999; Habler and Thöni 2001; Faryad and Hoinkes 2003; Bestel et al. 2009) (Fig. 16). Abundant amounts of garnet mica schist lithoclasts e.g. in the Gießhübl Formation corroborate these units as the most likely sources (Sauer 1980). High metamorphic and ophiolitic nappes from the Tethys suture zone are already eroded (Fig. 15). Local ophiolitic remnants only provide clastic material for the easternmost Slovakian Gosau basin. Equivalent crystalline complexes like in the Eastern Alps do not exist in the Carpathians. Significantly higher ZTR-indices and slightly higher degrees of roundness of garnets from Paleogene heavy mineral assemblages in the Slovakian part compared to the Gießhübl and Grünbach basin imply a more distal paleogeographical position of that sedimentation area.

10 Conclusions

Occurrence of detrital garnets from high metamorphic source and chrome spinels of a mixed harzburgite and lherzolite provenance in the Coniacian to Campanian Gosau Group suggests dominant sediment transport from the Tethys suture situated south of the NCA. At this time, a mélange of high metamorphic and ophiolitic nappes from the hanging wall of the northwards thrust onto the Austroalpine realm acts as source area for the Gosau basins. Detrital garnets with high proportions of pyrope (and grossular) may report erosion from relics of a metamorphic sole. Harzburgite dominant chrome spinels especially in the paleogeographically northern basins indicate only minor influence of the northern Penninic accretionary wedge as a second provenance. From the Maastrichtian on, only low- to medium-grade metamorphic garnets mainly from metapelites of southern provenance can be observed. Moderate chrome spinel contents represent ultimate erosion of ophiolitic structures in the south. In the Paleogene nearly no ultramafic detritus is supported by the hinterland and garnets from low grade metamorphic source dominate the heavy mineral assemblages. These almandine-rich garnets show equal

chemical composition like garnets from the Austroalpine Crystalline Complexes of the Eastern Alps (Wölz, Rappold, Radenthein, Plankogel, Koralpe and Saualpe Complex). Tourmaline chemistry generally indicates a mixed source of metapelites and granitoids, but no significant variation in time can be observed.

Acknowledgements

Thanks to the OMV for providing in-house data and support of heavy mineral preparation and counting. Special thanks to Roman Sauer and Wolfgang Hujer for counting thousands of grains. Finally, thanks to the Austrian Academy of Sciences for the support of a DOC-fellowship to Gerald Hofer.

References

See reference list of dissertation.

Appendix

Appendix I: see appendix B (of dissertation)

Appendix II:

Gosau		zrn	rut	bkt/ana	mon	tur	grt	sta	cld	chr	tit	epi	hbl	gln	N
Gießhübl	rut	**.467**													290
	bkt/ana	-.131	**-.207**												
	mon	.126	.015	.132											
	tur	.112	-.031	.211	.033										
	grt	**-.759**	**-.462**	.077	-.098	**-.273**									
	sta	.005	-.043	.175	-.038	.076	-.002								
	cld	.054	.086	.104	.135	**.347**	-.143	.024							
	chr	.182	-.052	-.047	.020	.038	**-.704**	-.031	-.036						
	tit	-.059	.027	-.067	-.051	.149	-.044	-.016	.049	.007					
	epi	.038	.030	.149	-.045	.166	-.094	**.322**	.113	.006	.000				
	hbl	-.052	.038	-.048	-.036	.131	-.031	-.038	.024	-.051	**.634**	.141			

Glinzendorf	rut	.105												71
	bkt/ana	-.056	-.045											
	mon	.179	.375	.127										
	tur	.148	**.476**	.221	**.454**									
	grt	-.324	.249	.065	-.006	-.042								
	sta	-.208	.149	.142	-.149	-.018	.343							
	cld	-.205	.301	.062	-.010	.170	**.421**	.183						
	chr	-.160	**-.542**	-.085	-.225	-.235	**-.844**	-.280	**-.411**					
	tit	.312	.295	.101	.165	.256	-.098	-.021	-.010	-.144				
	epi	.139	-.048	-.081	-.083	.238	-.138	-.092	-.113	.068	-.068			
	hbl	-.051	-.018	-.081	-.032	.041	.123	.089	.119	-.094	-.068	-.014		
	gln	-.090	-.027	-.116	-.045	-.048	.189	.372	.070	-.133	.016	-.020	-.020	
Grünbach	rut	**.353**												120
	bkt/ana	**.409**	**.462**											
	mon	**.590**	**.348**	**.493**										
	tur	.077	-.037	-.049	-.111									
	grt	**-.531**	**-.457**	**-.364**	-.277	**-.454**								
	sta	-.042	-.176	-.106	-.101	.218	.017							
	cld	.126	**.323**	**.321**	.146	-.017	**-.507**	-.065						
	chr	-.224	**-.347**	**-.329**	-.262	.073	-.144	-.092	-.271					
	tit	.112	**.417**	**.316**	.302	-.016	-.294	-.126	.184	-.008				
	epi	-.103	-.216	-.200	-.142	-.141	.018	.024	-.189	-.089	-.171			
	hbl	-.160	-.289	-.208	-.185	.003	.050	.208	.045	-.009	-.202	.030		
	gln	-.015	-.181	-.224	-.151	.010	-.109	.230	.027	-.072	-.116	.344	.284	
	dis	.065	-.063	.126	.038	-.049	.006	.087	.044	-.041	.158	-.038	.025	-.045
Slovakia	rut	**.747**												42
	bkt/ana	.105	**.515**											
	mon	.105	.451	**.832**										
	tur	-.280	-.381	-.338	-.343									
	grt	-.138	-.092	-.137	-.052	-.012								
	sta	.021	.002	-.119	-.096	.008	.095							
	cld	-.095	-.081	.121	.238	.202	-.265	-.076						
	chr	-.341	-.310	.010	-.053	-.408	**-.627**	-.116	-.061					
	tit	-.041	.447	**.592**	**.683**	-.399	.234	.138	-.026	-.102				
	epi	-.025	-.094	-.074	-.056	-.118	.062	.284	.023	-.009	-.067			
	hbl	-.037	-.130	-.314	-.285	.002	-.133	.438	.072	.137	-.214	.350		
	gln	-.153	-.261	-.281	-.219	-.186	-.023	.301	.188	.209	-.200	**.755**	.363	
	dis	-.042	-.099	.008	.270	.036	.067	-.083	**.665**	-.153	-.061	-.037	-.091	.196

Appendix III: see appendix C1 (of dissertation)

Appendix IV: see appendix C2 (of dissertation)

Appendix V: see appendix C3 (of dissertation)

6. Additional results

In this result section, only results that were not presented in any of the publications or manuscripts are reported. 67 cutting samples of wells from the Gießhübl (Aderklaa 81, 84, 92 and Strasshof T9) and Glinzendorf Syncline (Gänserndorf T3, Glinzendorf T1 and Markgrafneusiedl T1) were geochemically analyzed analogue to core and outcrop samples (appendix A).

6.1 Bulk rock geochemistry of cuttings

Before using geochemistry of cutting samples equivalent together with core and outcrop samples, possible contamination effects like drilling mud or drill bit fragments, that could influence the geochemical signal respectively paleodepositional, facies or provenance interpretations, are evaluated and compared to core/outcrop samples. Interactions with drilling mud and (permeable) sediments are reported in various studies (Kleven et al., 1997; Lepland et al., 2000; Bottig, 2008). Artificial abrasion remnants from drill heads are also common accessories in cutting samples. On the other hand, core and cutting samples are equivalently used together in recent geochemical or chemostratigraphic studies (e.g. Pearce et al., 2005).

6.1.1 Major elements

Major element oxides can vary due to lithological and grain size differences quite drastic (appendix A). Element oxides SiO_2, Fe_2O_3, CaO, MgO, Na_2O, TiO_2, Cr_2O_3 and K_2O are normalized to Al_2O_3 to reduce these effects. Pearson correlation indices are calculated separately for Glinzendorf and Gießhübl sample group as well as for core/outcrop and cutting samples. Generally, SiO_2, Fe_2O_3, Na_2O, TiO_2, and K_2O show strong positive correlations with Al_2O_3 while CaO is negative correlated. MgO and Cr_2O_3 do not show any significant correlation trends with Al_2O_3 (Figs. 6.1, 6.2).

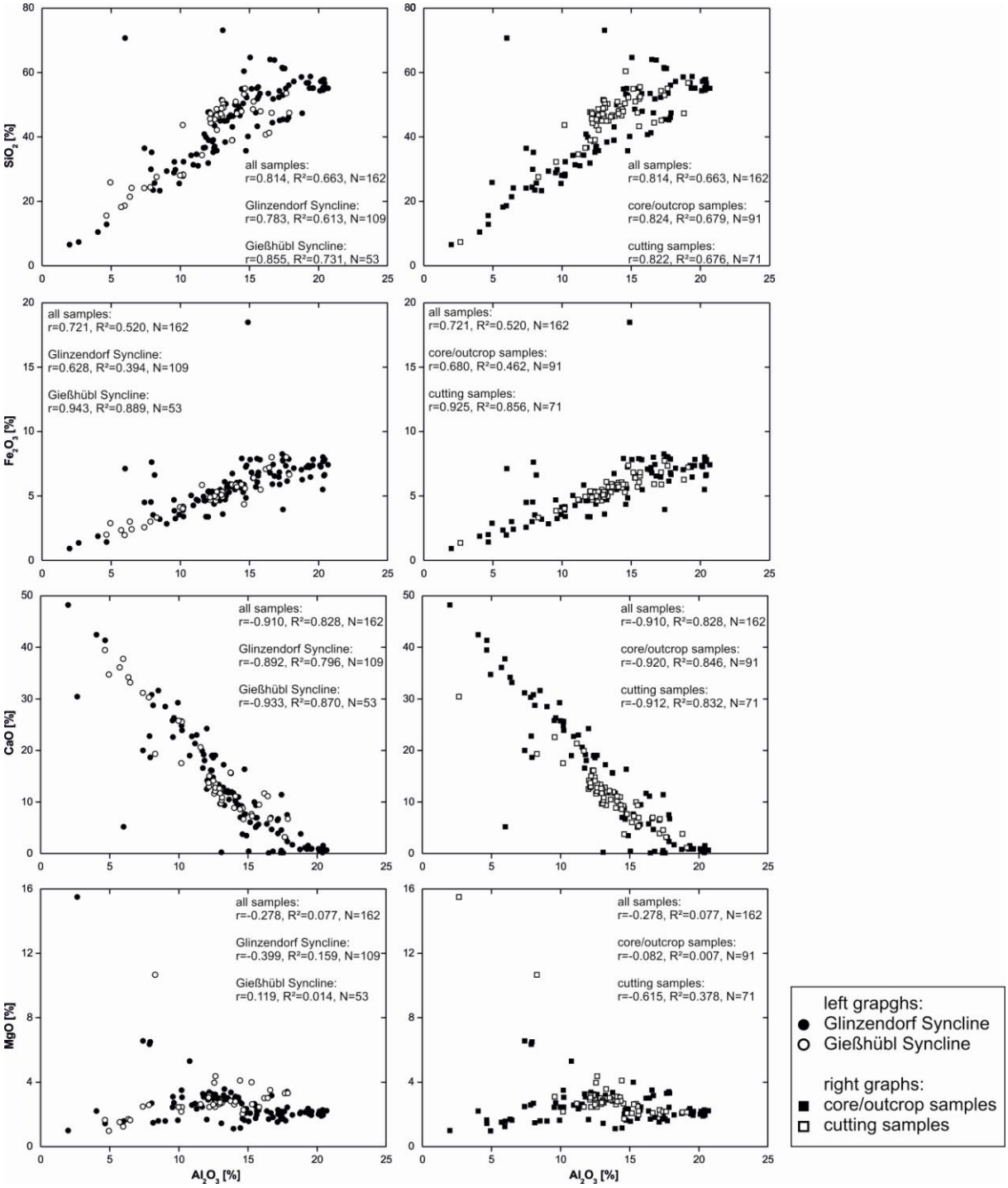


Fig. 6.1: Discrimination plots of the major element oxides SiO_2, Fe_2O_3, CaO and MgO against Al_2O_3. Graphs on the left column are grouped in samples from the Glinzendorf and Gießhübl Syncline; plots on the right side are divided into core/outcrop and cutting samples. Pearson correlation index (r), squared Pearson correlation index (R^2) and number of samples (N) are given.

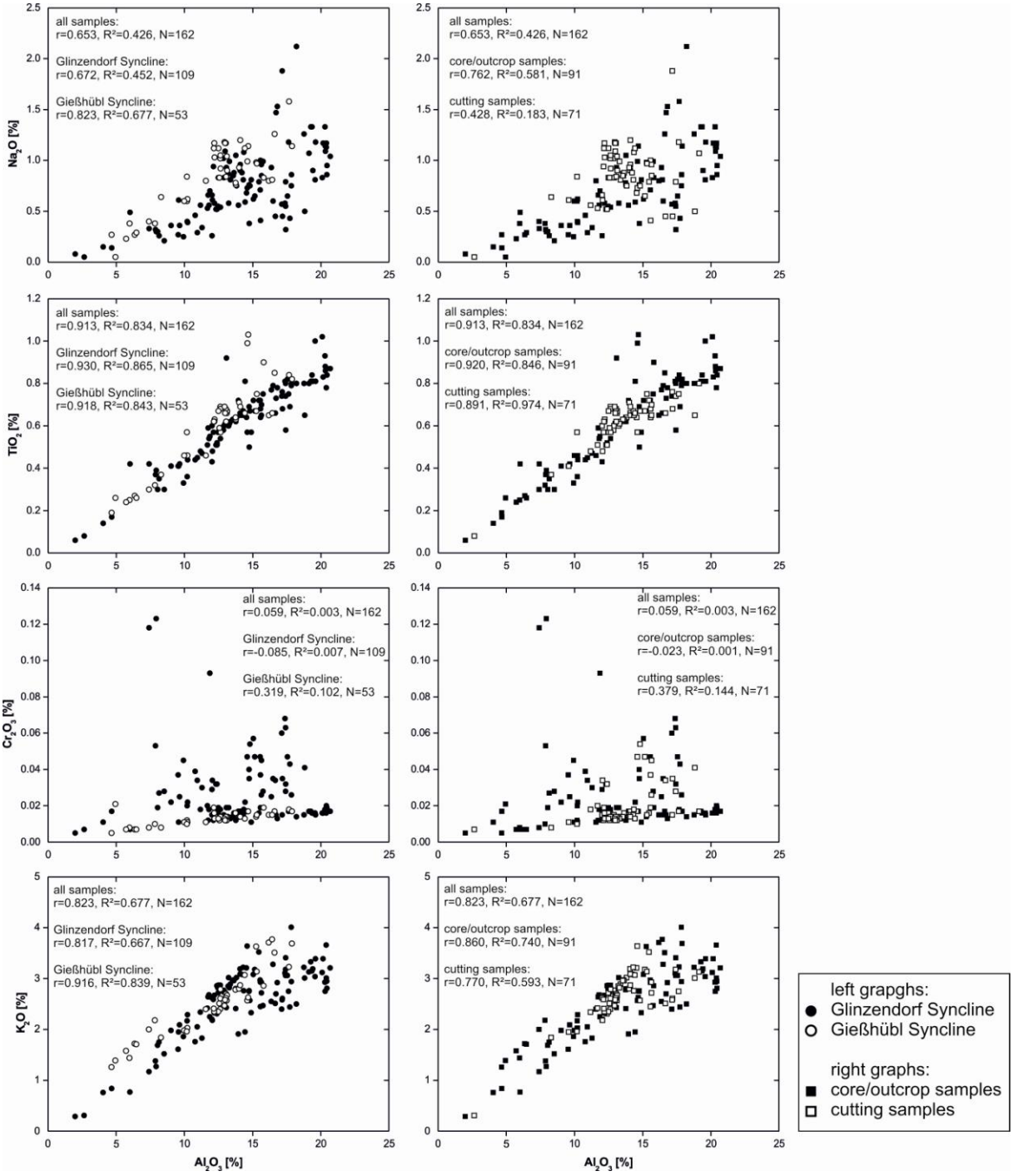


Fig. 6.2: Discrimination plots of the oxides Na_2O, TiO_2, Cr_2O_3 and K_2O against Al_2O_3. Graphs on the left column are grouped in samples from the Glinzendorf and Gießhübl Syncline; plots on the right side are divided into core/outcrop and cutting samples. Pearson correlation index (r), squared Pearson correlation index (R^2) and number of samples (N) are given.

SiO_2 contents are generally higher (mean=45.5 ±12.7) and fluctuate stronger within the Glinzendorf Syncline resulting in a lower correlation index of SiO_2 and Al_2O_3 (r=0.783) compared to the Gießhübl Syncline (mean=39.3 ±11.3; r=0.855). SiO_2 values of cuttings do not differ from core/outcrop samples of the data set (Fig. 6.1). Si/Al ratios, a proxy for quartz content in clays (Hofmann et al., 2001), vary from 2.14 to 10.41 (mean=2.9 ±0.8). Fe_2O_3 concentrations of the Glinzendorf Syncline are slightly higher (mean=5.9 ±2.0) showing several outliers from the general trend compared to Gießhübl samples (mean=4.8 ±1.5). These outliers (GT1-3409.5 shows the highest Fe_2O_3 accumulation of 18.49%) are all associated with core samples (cores/outcrops: r=0.680; cuttings: r=0.925; Fig. 6.1). A strong negative correlation between CaO and Al_2O_3 is given for core and cutting samples (r=-0.910). CaO values are generally lower and constant in cutting samples (mean=12.7 ±6.5) compared to core/outcrop samples (mean=14.3 ±12.7; Fig. 6.1). MgO values fluctuate between 1 and 15.5% with a mean of 2.7 ±1.5. Trends between MgO and Al_2O_3 of Glinzendorf and Gießhübl samples are not significantly different. Only cutting samples show a negative correlation of r=0.615 (Fig. 6.1). Correlations between Na_2O and Al_2O_3 of Glinzendorf (r=0.672) and Gießhübl samples (r=0.823) are slightly different. Cutting samples do not show a distinct correlation (r=0.428), while core/outcrop samples (r=0.762) do (Fig. 6.2). According to that, Na/Al ratios (proxy for smectite content; Hofmann et al., 2001) are generally comparably but slightly higher for Gießhübl and cutting samples (mean=0.09 ±0.03) in relation to Glinzendorf and core/outcrop samples (mean=0.07 ±0.03 and 0.07 ±0.02). TiO_2 and Al_2O_3 is strongly positive correlated within all groups of samples (r=0.913, Fig. 6.2). A rather different trend can be observed for Gießhübl samples at the Cr_2O_3/Al_2O_3 discrimination plot. While there are some Cr enrichments for samples of the Glinzendorf Syncline (r=-0.085), Cr concentrations remain low and constant within Gießhübl samples (r=0.319). These higher Cr concentrations of some Glinzendorf samples are present in core and cutting samples as well (Fig. 6.2). K_2O values achieve up to 4% and are strongly positive correlated with Al_2O_3. Cutting samples have a slightly lower correlation index of r=0.770 compared to core/outcrop samples of r=0.860 (Fig. 6.2). K/Al ratios (proxy for illite content; Hofmann et al, 2001) are with a mean of 0.09 ±0.03 generally low. CaO and LOI are strongly positive correlated for all types of samples (r=0.964). Only some cutting samples do not strictly follow the trend line resulting in a slightly lower correlation index (cuttings: r=0.885; cores/outcrops: r=0.987; Fig. 6.3). In relation to that, a clearly negative correlation can be observed between SiO_2 and LOI (r=0.975; Fig. 6.3).

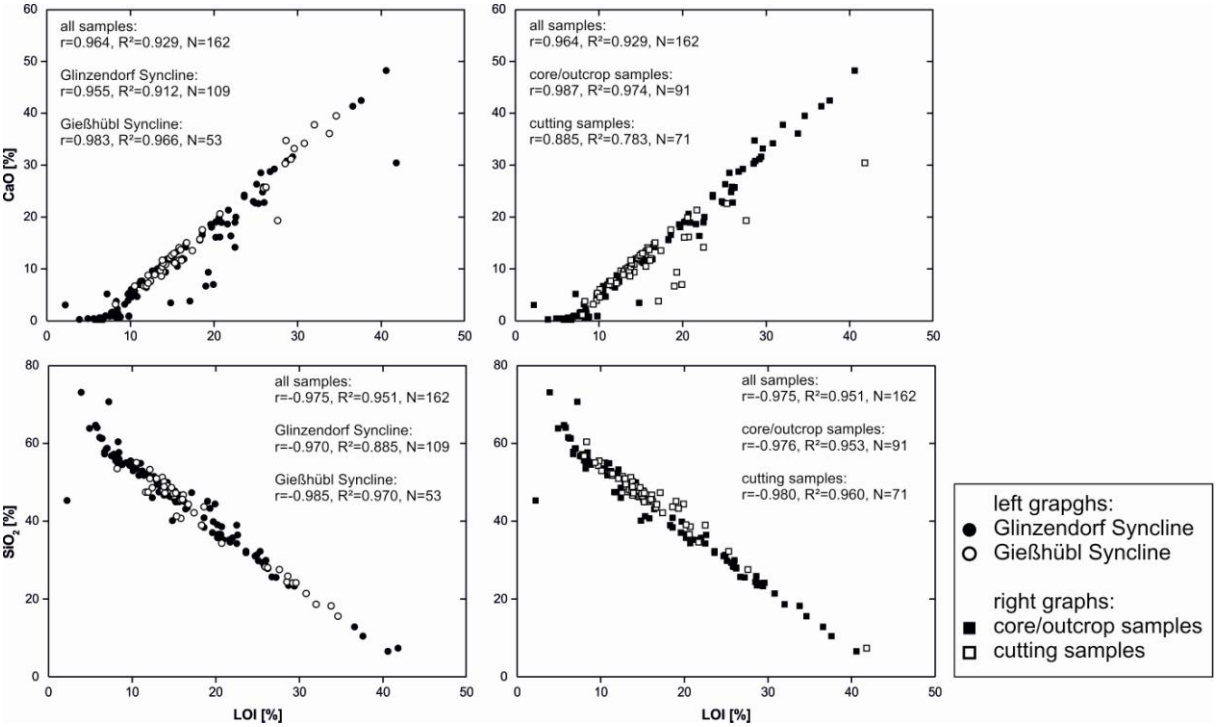


Fig. 6.3: Discrimination plots of CaO, SiO_2 and LOI (loss on ignition). Graphs on the left column are grouped in samples from the Glinzendorf and Gießhübl Syncline; plots on the right side are divided into core/outcrop and cutting samples. Pearson correlation index (r), squared Pearson correlation index (R^2) and number of samples (N) are given.

6.1.2 Trace elements

Ba concentrations range from 88 up to 1670 ppm, the latter is an outlier from core sample AD81/8-3192.5. Ba is significantly enriched with a mean of 358.3 ±119.3 ppm in cuttings compared to core samples with a mean of 269.1 ±183.7 ppm. Average Ba concentrations are also higher in samples from the Gießhübl Syncline (mean=385.8 ±218.0 ppm) compared to samples from the Glinzendorf Syncline (mean=270.5 ±114.0 ppm).

Some extreme high concentrations of the metals Cu, Zn and Pb can be observed for two cutting samples with 10 to 20 times higher values than average (2264 ppm of Cu and 1742 of Zn at MT1-3250 and 2349 ppm of Pb at STRHT9-3610). Mean values of Cu (cores/outcrops: 30.2 ±27.0 ppm; cuttings: 68.7 ±264.7), Zn (cores/outcrops: 57.8 ±22.0 ppm; cuttings: 94.7 ±199.4) and Pb (cores/outcrops: 16.5 ±13.3 ppm; cuttings: 58.9 ±276.8) are due to outliers higher in cuttings but comparable with core/outcrop samples.

7. Discussion

This discussion part connects results, conclusions and speculations from the independent puplications and manuscripts and integrates geochemistry data of cutting samples. Topics that are discussed in detail in one of the publications or manuscrips are only described or summarized in relation with new aspects. Therefore, this discussion does not substitute discussion parts of the publications and manuscripts.

7.1 Comparison of core/outcrop and cutting samples

Before using cutting samples hand in hand with core and outcrop samples, disturbing factors, which are more likely in cuttings, have to be assessed. To evaluate these differences, only samples from the Gießhübl and Glinzendorf Syncline of the same intervals were compared.

7.1.1 Influence of lithology

The problem of sampling only fine-clastic material for geochemical analysis is bigger in cutting samples. Investigated cuttings are suggested to have slightly higher amounts of sandstone-sized pieces, especially in samples with small cutting size and similar looking sand and shale fragments in terms of color. Additionally, downhole contamination of cuttings ranging between almost zero and probably some meters can mix various lithologies.

Strong positive correlations with Al_2O_3 are associated with terrigenous derived oxides (e.g. SiO_2 and TiO_2) explaining quartz content as not influenced by a special paleoenvironment favouring growth of siliceous tests (e.g. radiolarian or siliceous sponges). Low variations of the Si/Al ratio suggest only minor fluctuations in quartz contents for all types of samples. Hence, grain size variations are low and picking of coarse-grained cutting chips could reduce disturbing influences of sandstone intervals in cutting samples (student´s t-test between cutting and core/outcrop samples: T=-1.46; α=0.147). Strong negative correlation between CaO and Al_2O_3 (Fig. 6.1) demonstrates that most of the Ca is of marine origin and not from detrital source (e.g. feldspars). Strong positive correlation between CaO and LOI (Fig. 6.3) supports the assumption that CaO is largely derived from carbonates (Von Eynatten, 2003). Small but recognizable enrichments of smectite and illite contents are likely for samples of the Gießhübl Syncline

resulting in higher Na/Al and K/Al ratios. Na_2O concentrations and Na/Al ratios are additionally different in cutting samples (student´s t-test: Na_2O: T=-2.60; α=0.010; Na/Al: T=-4.93; α=0.000). Another remarkable effect is the discrepancy of Mg content in cutting samples, which is expressed by different absolute mean MgO values (T=-2.99; α=0.003) and MgO/Al_2O_3 ratios (cuttings: r=-0.615; cores/outcrops: r=-0.082; Fig. 6.1). In cutting samples MgO shows a negative correlation with CaO (r=-0.432) which could be related to some influence of dolomite, while there is no correlation in core/outcrop samples (r=0.021). Detrital carbonatic/dolomitic material may not be recognized by the selection procedure of cuttings.
The accuracy of the sorting of cutting samples influences the quality of the geochemical analysis to some degree. Depending on the “contaminated” lithology (sandstones or carbonates) unsorted test-samples (symbolized with “-U”) can have higher quartz or carbonate contents resulting in slightly higher SiO_2 and CaO contents than their sorted equivalents.

7.1.2 Contamination of drilling mud

Impact of drilling mud on geochemistry is more likely in cutting samples because surface area is increased and fluid circulation is limited in compact fine-grained core samples. Main components of drilling mud are bentonite, barite, potassium carbonate, potassium chloride, citric acid, water and many other complex chemicals (Bottig, 2008). Significantly higher Ba concentrations (T=-3.55; α=0.001) in cutting samples suggest influence of drilling mud, which is associated with barium sulfate usually used in drilling mud. Accumulation of Ba (and barite) due to drilling mud is generally known from various investigations (e.g. Lepland et al., 2000; Bottig, 2008). Average Ba concentrations are also significantly higher (T=-4.43; α=0.000) in samples from the Gießhübl Syncline compared to samples from the Glinzendorf Syncline. Maybe this is due to generally higher amounts of coarse-grained cutting pieces (and therefore higher fluid absorptive capacities) at Gießhübl within the cutting samples.

7.1.3 Contamination of drill bit

Fe concentrations do not show differences between cutting and core/outcrop samples. In fact, Fe contents are slightly higher in core/outcrop samples (8.1 ±3.4 %) compared to cuttings (7.6 ±1.6 %). Magnetic extraction of drill bit chips seems to be a reliable tool. Different mean values between cores and cuttings of Cu, Zn and Pb are only triggered by extreme contents of two

outlying cutting samples (MT1-3250 and STRHT9-3610). A general discrimination between cores and cuttings concerning these elements is not given. Student t-tests of Cu, Zn and Pb do not explain significant differences between those two groups (Cu: T=-1.38; α=0.169; Zn: T= -1.75; α=0.082; Pb: T=-1.29; α=0.201). However, mean values of the metallic elements Sn, W, Cd, Au and Tl are significantly higher in cutting samples (student´s t-test: Sn: core: 2.51 ±0.99 ppm, cutting: 3.30 ±1.90 ppm, T=-3.32, α=0.001; W: core: 1.90 ±0.61 ppm, cutting: 6.05 ±12.84 ppm, T=-2.72, α=0.008; Cd: core: 0.08 ±0.11 ppm, cutting: 0.15 ±0.16 ppm, T=-3.01, α=0.003; Au: core: 0.77 ±0.83 ppm, cutting: 1.60 ±2.28 ppm, T=-2.92, α=0.004; Tl: core: 0.03 ±0.07 ppm, cutting: 0.12 ±0.09 ppm, T=-6.74, α=0.000). These element enrichments are probably related to contaminations of drill bit fragments, but are extremely low and do not influence the sediment-geochemical interpretation.

Geochemistry of core/outcrop and cutting samples are generally comparably. Precise magnetic extraction of drill bit fragments is possible and enrichments of metallic elements cannot be observed in cutting samples. Contamination of drilling mud in cutting samples is resulting in significantly higher Ba concentrations. Geochemical distinction between the Gießhübl and Glinzendorf Syncline is identifiable, while it is not between core/outcrop and cutting samples. By using the performed preparation procedure of cutting samples, they can be combined with core/outcrop samples.

7.2 Bulk rock and stable isotope geochemistry

7.2.1 Geochemical differences between Gosau basins

Bulk rock geochemistry shows, that basic relationships concerning major and trace element concentrations and correlations are similar in the various Gosau basins with generally low variations in lithology and mineralogy. Elements (oxides) of terrigenous origin (e.g. SiO_2 or TiO_2) are strongly positive correlated with Al_2O_3 in contrast to a strong negative correlation with CaO, indicating Ca as only derived from marine source. Additionally, strong positive correlation between CaO and LOI supports the assumption that CaO is largely derived from carbonates (Von Eynatten, 2003). However, geochemical evaluation demonstrates distinct differences of depositional environments and detrital influence between various units. Detailed discussion of geochemical data is given in chapter 5.1.3.

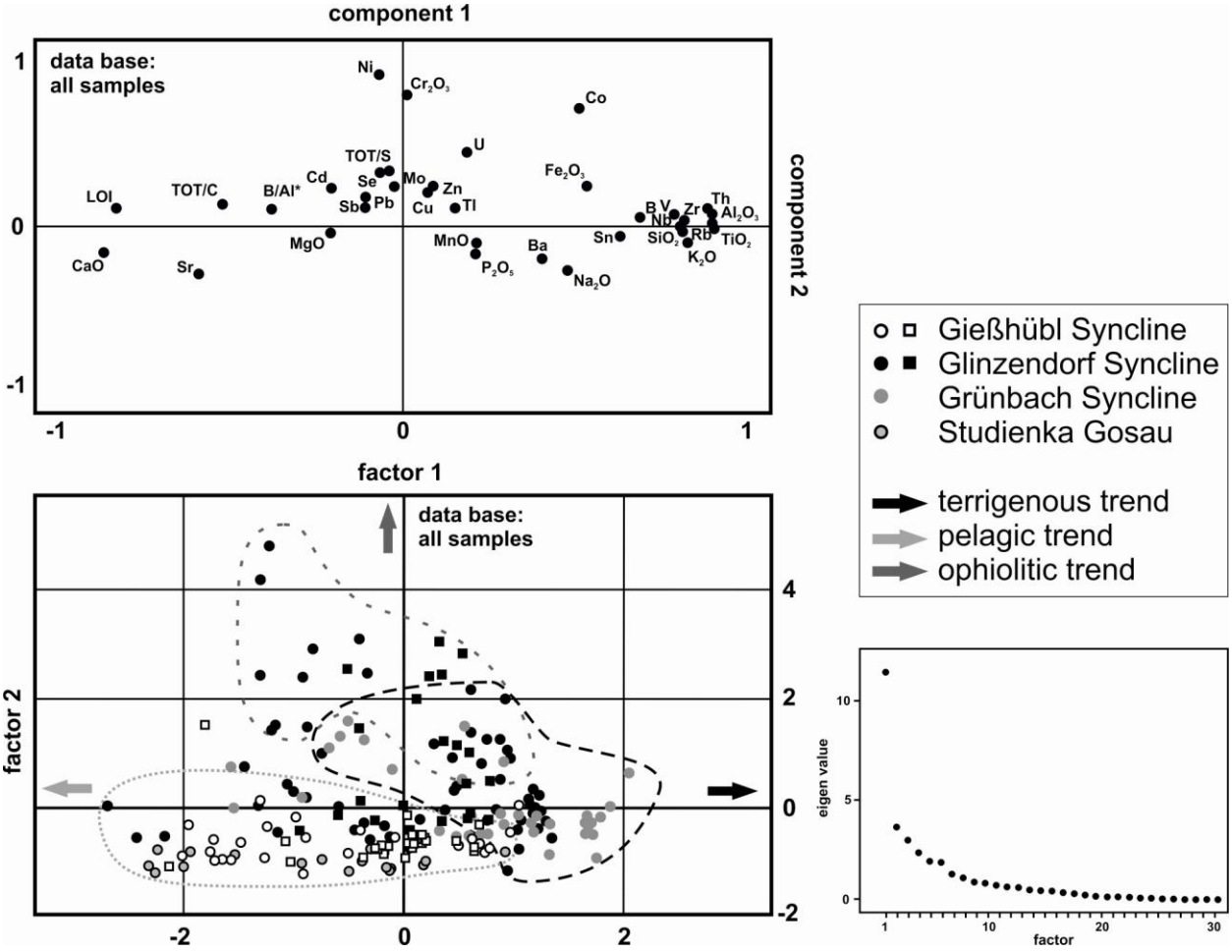


Fig. 7.1: Factor analysis including data of all samples. Statistic was calculated with Varimax rotation using the variables SiO_2, Al_2O_3, Fe_2O_3, MgO, CaO, Na_2O, K_2O, TiO_2, P_2O_5, MnO, Cr_2O_3, Ba, Co, Nb, Ni, Rb, Sn, Sr, Th, U, V, Zr, Mo, Cu, Pb, Zn, Cd, Sb, Tl, Se, B, TOT/C, TOT/S, LOI and B/Al*. Component plot (component 1 vs. component 2) shows distribution of the variables (elements/oxides) in relation to component 1 and 2. Factor plot (factor 1 vs. factor 2) give distribution of samples grouped in different Gosau synclines (circles: outcrop/core samples, squares: cutting samples). Eigen values of all factors indicate factor 1 as the dominant factor.

Differences between the paleogeographically northern, more distal and pelagic Gießhübl and Studienka basin, and the proximal (southern), limnic to marginal-marine Glinzendorf and Grünbach basin can be detected by geochemistry. Terrigenous interpretive elements (e.g. Al_2O_3, SiO_2, K_2O, Th, Rb or Zr) on the one hand and elements representing marine facies (e.g. CaO, Sr, TOT/C, LOI or B/Al*) on the other hand demonstrate the highest variability in the data set. These groups of variables represent the end-members of factor 1 (factor analysis; Fig. 7.1) and separate pelagic samples of the Gießhübl and Studienka basin as well as samples from marine intervals of the Glinzendorf and Grünbach basin, from non-marine samples (Glinzendorf and Grünbach) (see also chapter 5.1.3). Addition of cutting samples for factor analysis (statistical procedure analogue to the publication in chapter 5.1.3) only slightly changes results

presented in chapter 5.1.3. Analogue to the analysis described in the publication in chapter 5.1.3, the dominant factor 1 (eigen value of 11.4, explains 34 % of the variance) basically divides samples with prominent terrigenous input and samples with marine influence (Fig. 7.1). Factor 2 is mainly influenced by the index elements for ophiolitic detritus Cr and Ni. Only (non-marine) samples from the Glinzendorf Syncline are influenced by factor 2 as well and trend to input of ophiolite detritus (Fig. 7.1).

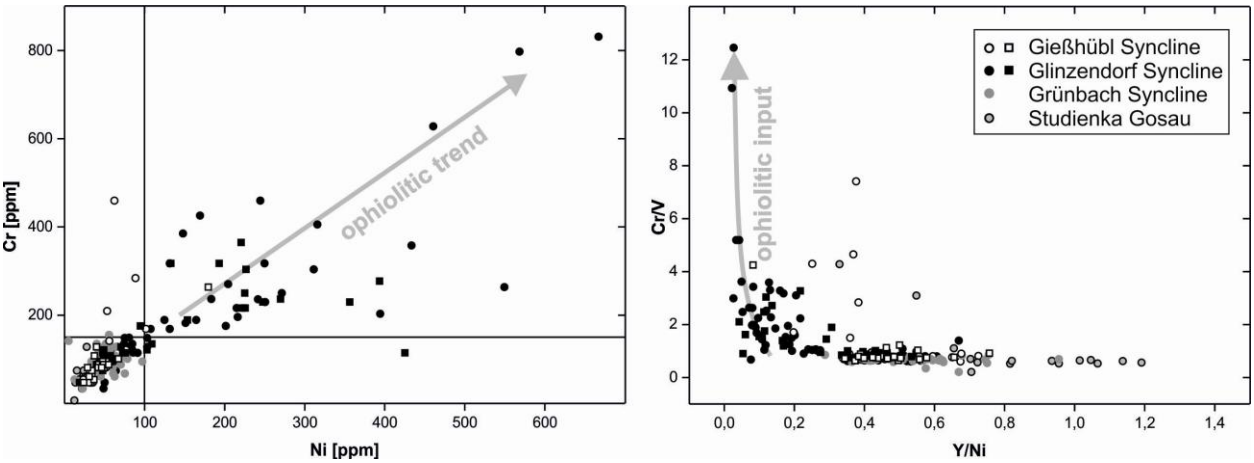


Fig. 7.2: Discrimination plots between Ni and Cr after Garver et al. (1996) as well as Y/Ni and Cr/V after McLennan et al. (1993). Samples that exceed the limits of 100 ppm Ni and 150 ppm Cr and that are enriched in the Cr/V ratio suggest ophiolitic input. Only samples from the Glinzendorf Syncline have characteristic geochemical signals for ophiolitic input (circles: outcrop/core samples, squares: cutting samples).

Geochemical comparison between the limnic-marine Glinzendorf basin and the Grünbach Formation, which also has a paleogeographically marginal depositional position, suggest some differences of the sedimentary facies. Generally, both units show various fluctuations in limnic and fully (marginal-) marine facies. Due to several coal horizons, the Grünbach Formation is usually interpreted as a non-marine succession (Summesberger et al., 2000; 2002; Wessely, 2006). Fluctuation of geochemical proxies (like B/Al*, $\delta^{13}C$ or $\delta^{18}O$) and occurrance of calcareous nannofossils indicate at least five marine to non-marine cycles (for detailed discussion see chapter 5.1.1). Marine intervals are also recognized in all analyzed well profiles (Glinzendorf T1, Markgrafneusiedl T1 and Gänserndorf T3) of the Glinzendorf Syncline using the same indicators (for detailed discussion see chapter 5.1.3). The extension of marine facies segments is unexpected high in both, Grünbach and Glinzendorf successions. Variances between Grünbach and Glinzendorf equivalents can be observed in Na and K contents or ratios suggesting higher smectite and lower illite concentrations in the Glinzendorf successions. Higher illite contents (and stable isotope data) may suggest higher diagenetic influence in the

Grünbach Formation compared to the Glinzendorf unit. Detrital ophiolitic material in fine-clastic samples indicated by Cr/Ni and (Cr/V)/(Y/Ni) ratios (McLennan et al., 1993; Garver et al., 1996) is only detected in mainly non-marine intervals of the Glinzendorf Syncline (Figs. 7.2, 7.3). One sample from Strasshof T9 (STRHT9-3610) shows enriched Cr and Ni contents, which is only an artificial effect due to drill bit contamination (see extreme Pb values of 2346 ppm; appendix A). Cutting samples confirm the trend that prominent ophiolitic detritus is only present in non-marine strata and correlates well with higher chrome spinel concentrations in heavy mineral assemblages (Fig. 7.3). Additionally, samples with enriched Cr and Ni concentrations are close to the characteristic Cr/Ni ratio of 1.3 - 1.5 (Garver et al., 1996). As mentioned before, this distinction is significant and additionally highlighted by the dimension-reducing statistical factor analysis (factor 2) (Fig. 7.1).

Rare earth element (REE) concentrations are in spite of minor fluctuations in absolute values, generally uniform in all sampled Gosau locations (Fig. 7.4). REE geochemistry is normalized to the North American Shale (NASC) after Gromet et al. (1984) and shows similar composition. REE compositions, which are suggested being sensitive to provenance signals (Lee, 2009), do not vary significantly in different Gosau basins, age-intervals or facies. Strong positive correlation between Al_2O_3 and La (r=0.909), plus positive correlation between CaO and La (r= -0.825) indicate, that REEs are enriched in the clay fraction and depleted in samples with higher carbonate content (due to dilution of clay minerals at higher carbonate contents) (Fig. 7.5).

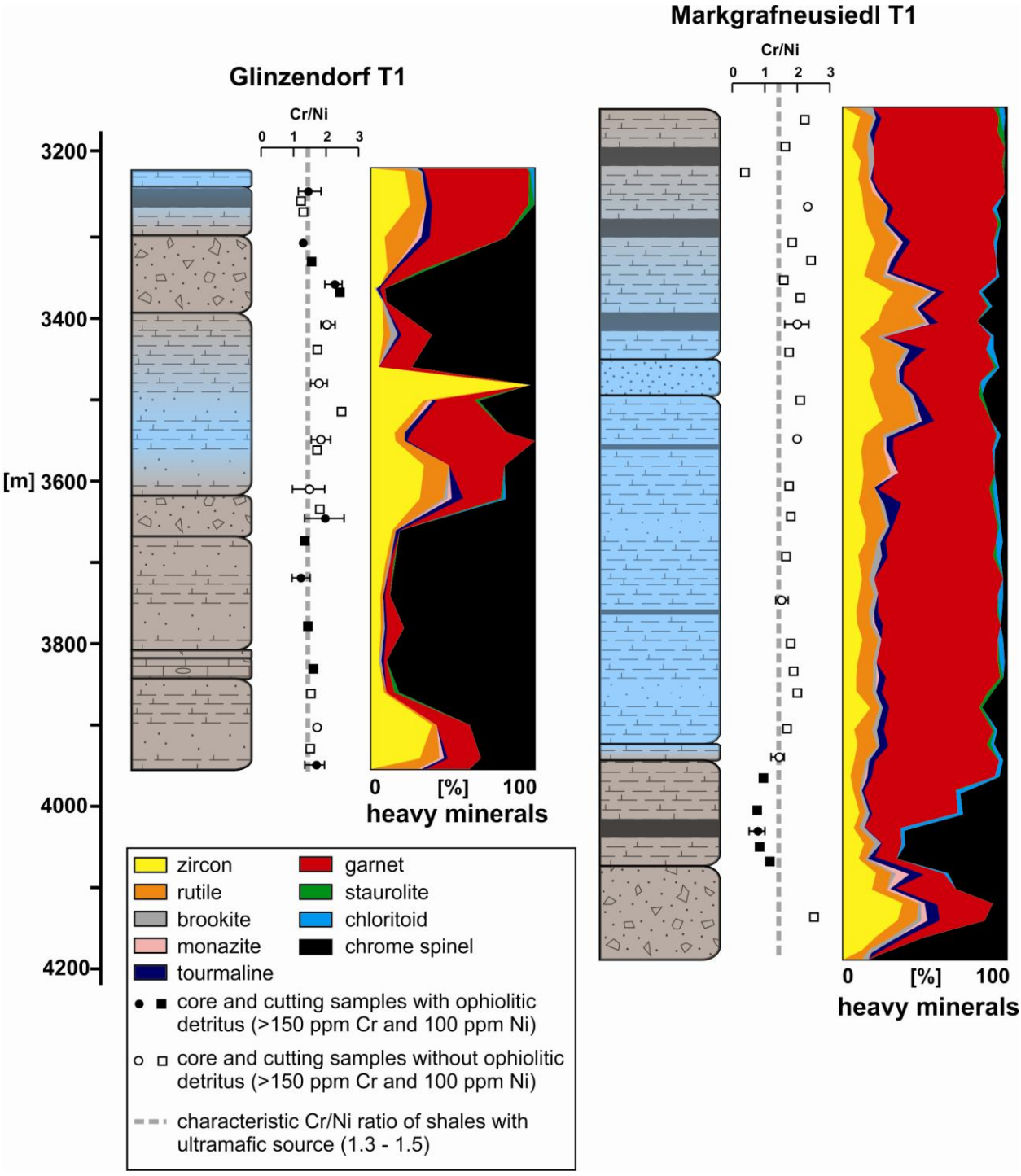


Fig. 7.3: Profiles of the wells Markgrafneusiedl T1 and Glinzendorf T1 (marine intervals: blue; non-marine intervals: brown) from the Glinzendorf Syncline with heavy mineral assemblages. Cr/Ni ratios of core (circle) and cutting samples (squares) are shown (dashed line indicate characteristic Cr/Ni ratio between 1.3 and 1.5 of shales with ultramafic source after Garver et al., 1996). Filled dots indicate samples that exceed the limits of 150 ppm Cr and 100 ppm Ni suggesting ophiolitic detritus after Garver et al. (1996).

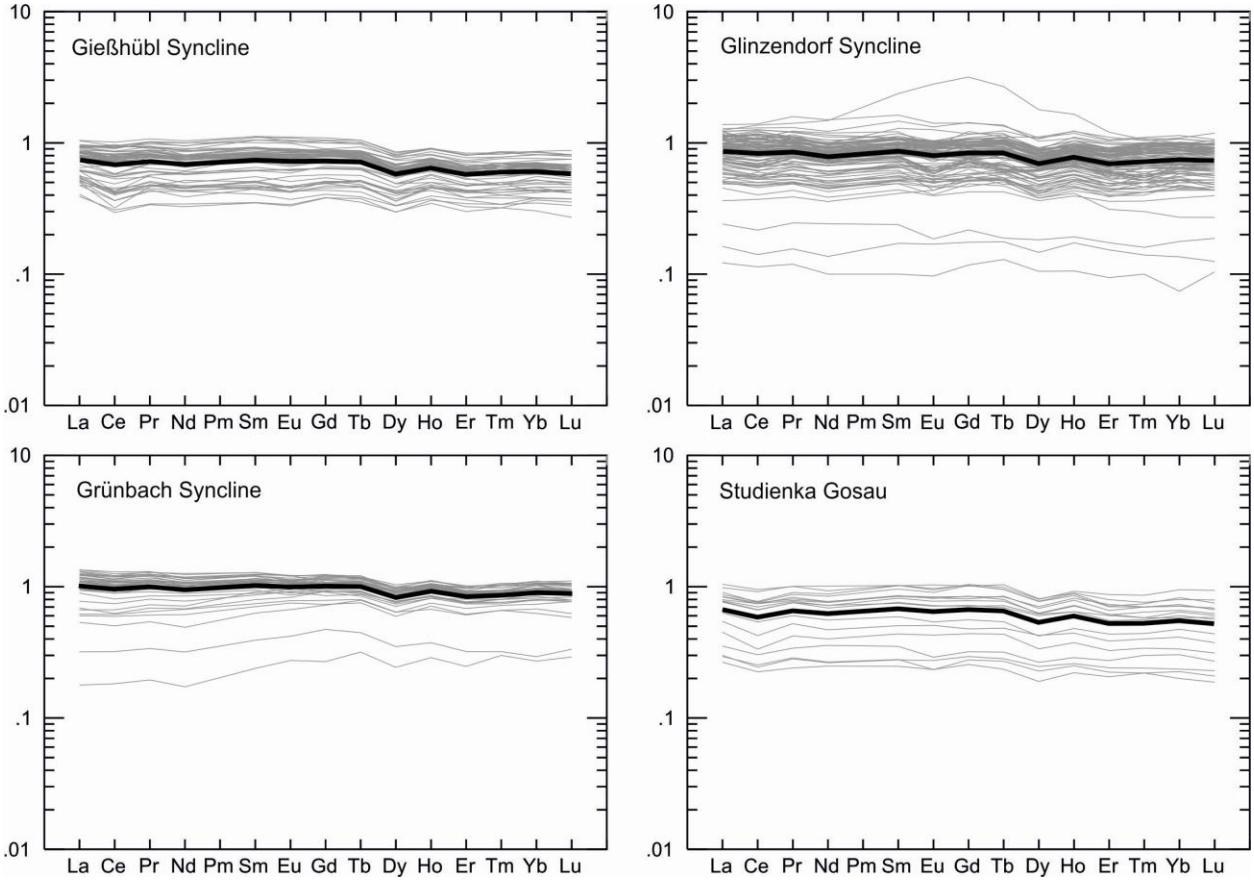


Fig. 7.4: Spider plots of REEs from Gießhübl, Glinzendorf, Grünbach Syncline and Studienka Gosau with average composition in black normalized to NASC after Gromet et al. (1984).

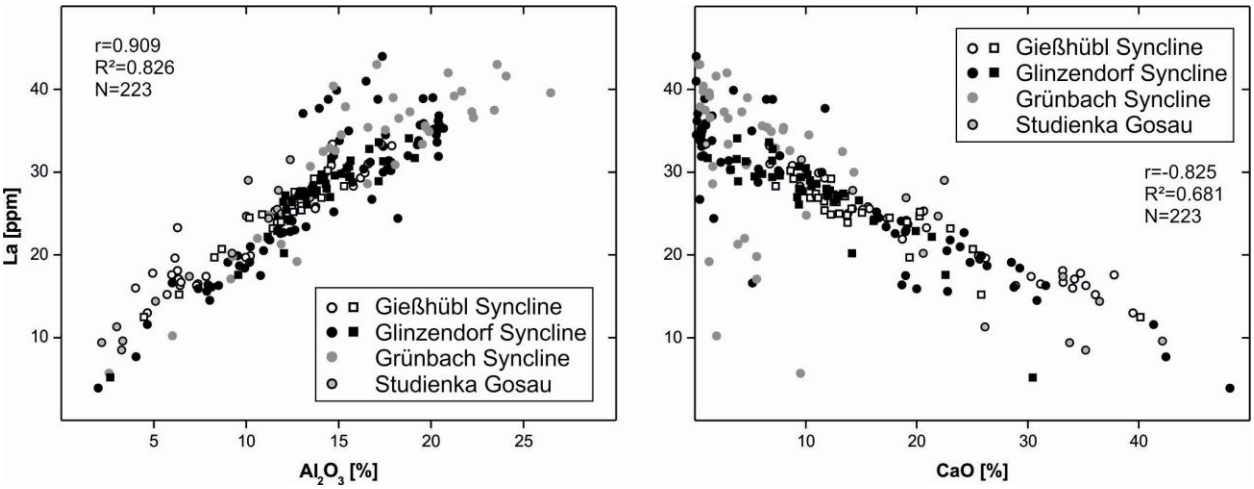


Fig. 7.5: Discrimination plots of Al_2O_3 and CaO versus La for core/outcrop (circles) and cutting samples (squares). Pearson correlation index (r), squared Pearson correlation index (R^2) and number of samples (N) are given.

Reconstructions of (paleo)tectonic settings by using major (Roser & Korsch, 1988) and trace element discrimination plots (La-Th-Sc, Th-Sc-Zr/10 and [La/Sc]/[Ti/Zr]) of bulk rock samples (Bhatia & Crook, 1986) do not allow coherent interpretation (for discussion see chapter 5.1.3).

7.2.2 Discrimination between marine and non-marine samples

Several geochemical proxies were tested for their potential as indicators of paleosalinity. Facies and thus paleosalinity of the limnic-marine successions of the Glinzendorf Syncline and the Grünbach Formation (Grünbach Syncline) are hard to interpret due to poor contents of macro- and microfossils. Salinity-indicative geochemical proxies in combination with analysis of nannofossils are applied to these intervals to have an independent control factor.

B concentrations, which are supposed as being an indicator for paleosalinity (Ernst, 1966; Heling, 1967; Selter et al., 1989; Rügner, 2000), do not show any systhematic variations, and mean values are not different in marine and non-marine samples. Absolute B values are influenced by grain size effects (positive correlation with decreasing grain size) as well as variations in the primary composition (source area) of the clays (Dominik & Stanley, 1993) and therefore do not qualify for a reliable proxy of the salinity facies.

In contrast B/Al* (=B/Al*100,000; see chapter 5.1.1 and 5.1.3) ratios reduce grain size and mineralogical effects and are a reliable tool to discriminate between marine and non-marine sediments. Mean B/Al* ratios are significantly (T=-4.57; α=0.000) lower in non-marine (131.4 ±31.5) compared to marine samples (151.5 ±31.3). A detailed discussion is given in chapter 5.1.1 and 5.1.3.

Stable isotope ratios of carbon and oxygen (for detailed discussion see chapter 5.1.2) are also statistically different in marine and non-marine intervals. Especially, mean $\delta^{13}C$ values are significantly (T=-7.04; α=0.000) lower in non-marine samples (-5.3 ±2.4 ‰) compared to marine ones (-1.4 ±2.8 ‰). The shift between mean $\delta^{18}O$ values of non-marine (-6.1 ±1.5 ‰) and marine samples (-5.1 ±1.6 ‰) is much lower but also statistically proven (T=-3.00; α=0.003). An issue especially for bulk carbonate analysis of clastic sediments is the possible presence of reworked older carbonate material and diagenetic influence. The influence of diagenesis by carbonate cement precipitation is interpreted as low because of the pelitic nature of the sampled material and the extremely low amount of visible cements under the (CL) microscope. Low correlation indices between $\delta^{13}C$ and $\delta^{18}O$ can be observed for the Gießhübl, Glinzendorf Syncline and Studienka Gosau, and is exclusively high in the Grünbach Syncline. Therefore, a notable diagenetic imprint is (except for the Grünbach Syncline) unlikely (e.g. Shen &

Schidlowski, 2000; Hamon & Merzeraud, 2007). Thin-section petrography and CL studies indicate only low presence of detrital carbonate grains, mainly limestones, with amounts below 10 %. Amounts of detrital dolomite are also extremely low, quantified by XRD investigations. A significant influence of detrital carbonate on the bulk stable isotope composition is therefore regarded as unlikely.

Discriminant analysis using the parameters B/Al*, $\delta^{13}C$ and $\delta^{18}O$ is with α=0.000 highly significant, demonstrating the relevance of the variables for the discrimination of marine and non-marine samples (detailed description of method and discussion see chapter 5.1.3).

According to this data set, the TOC/S ratio, frequently used to assess paleosalinity (Berner & Raiswell, 1984; Morse & Berner, 1995; Sageman & Lyons, 2004), cannot be recommended as a reliable paleosalinity proxy, although statistically proven, because of low difference of means in marine and non-marine samples. Higher average of non-marine values is mainly derived from a few samples that are rich in organic matter. In general, low TOC contents of samples seem to blur results obtained by this method (see chapter 5.1.1 and 5.1.3).

The combination of B/Al*, $\delta^{13}C$ and $\delta^{18}O$ are reliable geochemical proxies to distinguish between marine and non-marine sediments with low or nonexistent fossil abundances and uncertain paleoenvironment. However, only an overall assessment of major, minor, and trace element geochemistry provides reliable results.

7.3 Provenance analysis

Provenance analysis is based on interpretations of heavy mineral assemblages (appendix B) and single grain chemistry (appendix C1, C2, C3; see results and discussion in chapter 5.2.1). Bulk rock trace element geochemistry (Cr, Ni, etc.) provides supplementary indications. REEs, which are suggested being sensitive to provenance signals (Lee, 2009), do not show any distinct differences in various Gosau basins or time intervals.

7.3.1 Coniacian to Campanian

Heavy mineral assemblages of the Coniacian to Campanian are generally characterized by prevailing chrome spinel, followed by zircon, tourmaline and garnet in all Gosau basins indicating erosion of an ophiolitic source (see chapter 5.2.1). Chrome spinel chemistry generally suggests a mixed harzburgite/lherzolite provenance, whereas chrome spinels from northern

Gosau basins (Gießhübl and Slovakian Gosau) have higher Cr# compared to spinels from southern basins (Glinzendorf and Grünbach) and indicate a harzburgite dominant source. This chrome spinel chemistry points to the Tethys suture sensu Pober & Faupl (1988) and Faupl & Wagreich (2000) as the dominant source. Analogue detrital chrome spinels from Dinaric Cretaceous basins (Lužar-Oberiter et al., 2009) and chrome spinels from Dinaric ophiolites (Maksimovic & Majer, 1981), probably comparable to the fully eroded southern provenance, show similar chemical trends. This southern ophiolite complex supplied clastic material at least since the Early Cretaceous (Decker et al., 1987; Von Eynatten & Gaupp, 1999) up to the Maastrichtian. Today, the only evidences for this ophiolitic thrust unit(s) are a few tiny tectonic slices and basic volcanic components of conglomerates (Gruber et al., 1992), serpentine fragments in sandstones (Wagreich, 1993b) and chrome spinel-rich heavy mineral assemblages. In contrast to that, spinels from Penninic ophiolites from the Tauern, Unterengadin (Pober & Faupl, 1988) and Rechnitz window (Mikuš & Spišiak, 2007), which are probably comparable to a possible northern ophiolitic provenance, commonly show lherzolitic composition. Additionally, Cr and Ni-rich, ophiolitic detritus of fine-grained sediments can only be observed in the paleogeographically southern Glinzendorf basin (Figs. 7.2, 7.3) suggesting predominant ophiolitic sediment fluxes from south. Hence, these data do not confirm dominant detrital input of a hypothetic Penninic ophiolite source, but, however, minor influence cannot be excluded. Detrital supply from the north (northern accretionary wedge) is supposed at least for the Tannheim-Losenstein basin in the Early Cretaceous based on basin configuration and paleocurrent data (Wagreich, 2001b). Paleocurrent reconstructions of the Lower Gosau Subgroup are heterogenous and indicate partly paleocurrent from the north (Faupl et al., 1987; Faupl & Wagreich, 1996). This is maybe due to a multitude of local source areas in a pronounced and complex subsidence area and may also be explained by redepositions of sediment input generally from the south.

Metamorphic derived minerals are supplementary important in Coniacian to Campanian heavy mineral assemblages. Garnet chemistry indicates a mixed source of supposed high- to low-grade metamorphosed provenance. High amounts of garnets trend to HP/UHP conditions of granulite, eclogite and amphibolite facies of the source area and can be observed in the Gießhübl, Glinzendorf and Grünbach basin. This group of garnet is characterized by abundant portions of pyrope and grossular compared to a second group of exclusively almandine-rich minerals. Garnets from the Slovakian basin do not suggest higher metamorphic character, which is maybe only an effect of low number of samples. Garnet chemistry and spatial distribution of these high-grade metamorphosed grains (they are dominant in paleogeographically southern basins) point to the metamorphic sole of the Tethys ophiolites

from a Tethys suture to the south as the most likely source area. Investigations on amphibolite pebbles (upper amphibolites facies) from the Grünbach Syncline suggest remnants of this metamorphic sole of Tethys ophiolite sheets as ultimate provenance (Schuster et al., 2007). Garnet chemistry data of Schuster et al. (2007) and data from Balen et al. (2003; from the Dinaric Krivaja-Konjuh ultramafic massif, Bosnia) are identical to garnets of this study (see chapter 5.2.1). Similar compositions of detrital garnets are also reported from the Dinaride Ophiolite Zone mélange in Bosnia, which are attributed to the sub-ophiolitic metamorphic sole (Mikes et al., 2008).

7.3.2 Maastrichtian to Eocene

The influence of ophiolitic detritus is present until the Maastrichtian with chrome spinels of harzburgite-dominant source. Due to northwards deepening of the Gosau basin, detrital input is only delivered from south (Wagreich & Faupl, 1994). Crystalline nappes of increasing metamorphic grade are already eroded in the south at this time, and garnet chemistry generally indicates relatively uniform almandine-rich garnets of a supposed low metamorphic, metapelitic provenance (see chapter 5.2.1).

Paleogene heavy mineral assemblages are only dominated by garnet (around 80%), and tourmaline in the Slovakian Gosau basin. Chrome spinel is, except minor amounts in the Slovakian Gosau probably due to reworking of older Gosau sediments, inexistent. High metamorphic and ophiolitic nappes from the Tethys suture zone are already eroded. Garnet chemistry is analogue to the Maastrichtian uniform and almandine-rich. These garnets are equal to garnets from Austroalpine Crystalline Complexes of the Eastern Alps like the Wölz, Rappold, Radenthein, Plankogel, Koralpe and Saualpe Complex (Schuster & Frank, 1999; Habler & Thöni, 2001; Faryad & Hoinkes, 2003; Bestel et al., 2009). Abundant amounts of garnet mica schist lithoclasts e.g. in the Gießhübl Formation corroborate these units as the most likely sources (Sauer, 1980). Significantly higher ZTR-indices and slightly higher degrees of roundness of garnets in the Slovakian part compared to the Gießhübl and Grünbach basin imply a more distal paleogeographical position of that sedimentation area. Equivalent crystalline complexes like in the Eastern Alps do not exist in the Carpathians (see chapter 5.2.1).

8. Conclusions

Detailed geochemical bulk rock analysis of fine-clastic sediments, stable carbon and oxygen isotope data of bulk carbonate and statistical data treatment are used to separate Gosau Group successions into proximal and distal depositional areas in the Eastern Alps and its continuation into the Carpathians. A combination of those geochemical parameters can be used to distinguish limnic, marginal-marine, and pelagic fine-clastic sedimentary intervals within Upper Cretaceous to Eocene samples from outcrops, drill cores and cuttings. Thereby, cutting samples do not show significant geochemical anomalies compared to outcrop and core samples (except for the element Ba) and can be successfully used for geochemical separation.

The combination of B/Al*, $\delta^{13}C$ and $\delta^{18}O$ are reliable geochemical proxies to determine the paleosalinity and paleodepositional conditions in sediments with low or nonexistent fossil abundances and uncertain paleoenvironment. In this dataset absolute boron concentrations are not robust because they rather reflect lithological variations. Using factor analysis, pelagic influenced samples deposited at the distal continental margin (Gießhübl Syncline and Slovakian equivalents) can be separated from marginal-marine to non-marine samples (Grünbach and Glinzendorf Syncline) owing to the content of terrigenous- and marine-indicative elements. On the other hand, a discrimination of samples with ophiolitic detritus related to elements associated with ultramafic genesis (Cr, Ni) can be observed only for several samples of the Glinzendorf Syncline. In this way huge and complex multivariate data sets with multidimensional variables can be reduced and displayed easily.

Geochemical comparison between the limnic-marine Glinzendorf succession and the Grünbach Formation suggest some differences of the sedimentary facies. Generally, both units show various fluctuations in limnic and marine facies, whereas the extent of marine facies intervals is unexpectedly high. Variances between Grünbach and Glinzendorf equivalents can be observed in Na and K contents and ratios. Higher illite contents and a relatively high correlation between stable C abd O isotopes may suggest a significant diagenetic influence in the Grünbach Formation.

Evaluation of heavy mineral assemblages and chemistry of detrital heavy minerals provide a revised provenance concept. Occurrence of garnets from high metamorphic source and generally chrome spinel dominant heavy mineral assemblages of a mixed harzburgite and lherzolite provenance in the Coniacian to Campanian Gosau Group suggest dominant sediment transport from the Tethys suture situated south of the NCA. At this time, a mélange of high metamorphic and ophiolitic nappes from the hanging wall of the northwards moving thrust complex onto the Austroalpine realm acts as the main source area for the Gosau basins.

Detrital garnets with enriched proportions of pyrope and grossular may report erosion from relics of a metamorphic sole. Harzburgite dominant chrome spinels especially in the paleogeographically northern basins indicate only minor influence of the northern Penninic accretionary wedge as a second provenance. From the Maastrichtian onwards, only garnets derived from low- to medium-grade metamorphic source mainly from metapelites of southern provenance can be observed. Moderate chrome spinel contents represent ultimate erosion of ophiolitic structures in the south. In the Paleogene nearly no ultramafic detritus is supported by the hinterland and garnets from low grade metamorphic source dominate the heavy mineral assemblages. These almandine-rich garnets show equal chemical composition like garnets from the Austroalpine Crystalline Complexes of the Eastern Alps (Wölz, Rappold, Radenthein, Plankogel, Koralpe and Saualpe Complex). Tourmaline chemistry generally indicates a mixed source of metapelites and granitoids, but no significant variation in time can be observed.

Acknowledgements

First of all I want to thank my supervisor Michael Wagreich for great professional (and private) support and a smooth cooperation. Thanks also to Stephanie Neuhuber for plenty of geochemical advice. Special thanks to the Austrian Academy of Sciences for the support of a DOC-fellowship and the OMV for founding the *Gosau Inventory Project* in cooperation with the University of Vienna. Last but not least, thanks to Godfried Wessely and all my co-authors. Franz Biedermann, Magda Bottig, Erich Draganits, Susanne Gier, Sabine Hruby-Nichtenberger, Wolfgang Hujer, Franz Kiraly, Norbert Kohlmayer, Konstantin Petrakakis, Hugh Rice, Roman Sauer, Andrea Schicker, Ralf Schuster, Christoph Spötl, Philipp Strauss and Helga Zeitlhofer, to all of you thanks for your support.
Finally, thanks to my lovely wife Iris, my family and friends for mental support.

References

Anderson, T.F. & Arthur, M.A., 1983. Stable isotopes of oxygen and carbon and their application to sedimentologic and palaeoenvironmental problems. In: Arthur, M.A., Anderson, T.F., Kaplan, I.R., Veizer, J. & Land, L.S. (Eds.), Stable isotopes in sedimentary geology, SEPM Short course 10, 1-151.

Arai, S., 1992. Chemistry of chromian spinel in volcanic rocks as a potential guide to magma chemistry. Mineralogical Magazine 56, 173-184.

Árgyelán, G.B., 1996. Geochemical investigations of detrital chrome spinels as a tool to detect an ophiolitic source area (Gerecse Mountains, Hungary). Acta Geologica Hungarica 39, 341-368.

Árgyelán, G.B. & Horváth, P., 2002. Heavy mineral assemblages of Senonian formations in the Transdanubian Range, Hungary. Acta Geologica Hungarica 45, 319-339.

Aubrecht, R. & Krištín, J., 1995. Provenance of detrital tourmaline in the Lower Jurassic of the Malé Karpaty Mts. Mineralia Slovaca 27, 37-44.

Aubrecht, R., Méres, Š., Sýkora, M. & Mikuš, T., 2009. Provenance of the detrital garnets and spinels from the Albian sediments of the Czorsztyn Unit (Pieniny Klippen Belt, Western Carpathians, Slovakia). Geologica Carpathica 60/6, 463-483.

Aubrecht, R., Méres, Š., Sýkora, M. & Mikuš, T., 2012. Provenance of the detrital garnets and spinels from the Albian sediments of the Czorsztyn Unit (Pieniny Klippen Belt, Western Carpathians, Slovakia). Geologica Carpathica 60, 463-483.

Backhaus, K., Erichson, B., Plinke, W. & Weiber, R., 2006. Multivariate Analysemethoden. Eine anwendungsorientierte Einführung. Springer, Berlin, 831pp.

Balen, D., Operta, M. & Pamic, J., 2003. The geothermobarometry of Alpine amphibolites from the metamorphic sole of the Krivaja-Konjuh ultramafic massif (Dinaride Ophiolite Zone, Bosnia). Annales Universitatis Scientiarum Budapestinensis, Sectio Geologica 35, 131-132.

Barnes, S.J. & Roeder, P.L., 2001. The range of spinel compositions in terrestrial mafic and ultramafic rocks. Journal of Petrology 42/12, 2279-2302.

Barth, T.F.W., 1962. Theoretical Petrology. John Whiley & Sons, New York, 416pp.

Berner, R.A. & Raiswell, R., 1984. C/S method for distinguishing freshwater from marine sedimentary rocks. Geology 12, 365-368.

Bestel, M., Gawronski, T., Abart, R. & Rhede, D., 2009. Compositional zoning of garnet porphyroblasts from the polymetamorphic Woelz Complex, Eastern Alps. Mineralogy and Petrology 97, 173-188.

Bhatia, M.R. & Crook, K.A.W., 1986. Trace element characteristics of graywackes and tectonic setting discrimination of sedimentary basins. Contributions to Mineralogy and Petrology 92, 181-193.

Bigg, G.R. & Rohling, E.J., 2000. An oxygen isotope data set for marine water. Journal of Geophysical Research 105, 8527-8535.

Bjerg, E.A., Ntaflos, T., Thöni, M., Aliani, P. & Labudia, C.H., 2009. Heterogeneous lithospheric mantle beneath northern Patagonia: evidence from Prahuaniyeu garnet- and spinel-peridotites. Journal of Petrology 50, 1267-1298.

Bock, B., Bahlburg, H., Wörner, G. & Zimmermann, U., 2000. Ordovician arcs and terranes in NW-Argentina and N-Chile? Geochemical and isotope evidence. Journal of Geology 108, 513-535.

Bornemann, A., Norris, R.D., Friedrich, O., Beckmann, B., Schouten, S., Sinninghe Damsté, J.S., Vogel, J., Hofmann, T. & Wagner, T., 2008. Isotopic evidence for glaciation during the Cretaceous Supergreenhouse. Science 319, 189-192.

Bottig, M., 2008. Diagenetische Umwandlungen in Sandsteinen der gasgesättigten, der sekundär verwässerten, der Wasser-, und der Übergangszone des Erdgas-Speichers Haidach in der Molasse Zone, Österreich. Diploma thesis, University of Vienna, 74pp.

Buggle, B., Glaser, B., Hambach, U., Gerasimenko, N. & Marković, S., 2011. An evaluation of geochemical weather indices in loess-paleosol studies. Quaternary International 240, 12-21.

Bühl, A., 2008. SPSS 16. Einführung in die moderne Datenanalyse. Pearson Studium, München.

Burnett, J.A., with contributions from Gallagher, L.T. & Hampton, M.J., 1998. Upper Cretaceous. In: P.R. Bown (Ed.), Calcareous Nannofossil Biostratigraphy. British Micropalaeontological Society Publications Series, Chapman and Hall, London, 132–199.

Carosi, R., Cortesogno, L., Gaggero, L. & Marroni, M., 1996. Geological and petrological features of the metamorphic sole from the Mirdita Nappe, northern Albania. Ofioliti 21, 21-40.

Clayton, R.N. & Degens, E.T., 1959. Use of carbon isotope analyses of carbonates for differenting freshwater and marine sediments. American Association of Petroleum Geologists Bulletin 43, 890-897.

Colombié, C., Lécuyer, C. & Strasser, A., 2011. Carbon- and oxygen-isotope records of palaeoenvironmental and carbonate production changes in shallow-marine carbonates (Kimmeridgian, Swiss Jura). Geological Magazine 148, 133-153.

Cookenboo, H.O., Bustin, R.M. & Wilks, K.R., 1997. Detrital chromian spinel compositions used to reconstruct the tectonic setting of provenance: implications for orogeny in the Canadian Cordillera. Journal of Sedimentary Research 67, 116-123.

Cullers, R.L., 2000. The geochemistry of shales, siltstones and sandstones of Pennsylvanian-Permian age, Colorado, USA: implications for provenance and metamorphic studies. Lithos 51, 181-203.

Cuna, S., Pop, D. & Hosu, A., 2001. Carbon and oxygen isotope ratios in Rona limestone, Romania. Studia Universitatis Babes-Bolyai, Geologia 46, 139-15.

Davis, J.C., 2002. Statistics and data analysis in Geology. John Wiley & Sons, New York, 656pp.

Decker, K., Faupl, P. & Müller, A., 1987. Synorogenic sedimentation on the Northern Calcareous Alps during the Early Cretaceous. In: Flügel, H.W. & Faupl, P. (Eds.), Geodynamics of the Eastern Alps. Deuticke, Vienna, 126-141.

Deer, W.A., Howie, R.A. & Zussman, J., 1962. The Rock-Forming Minerals. Vol. 1 Ortho- and Ring Silicates, Longman, London, 333pp.

Descourvieres, C., Douglas, G., Leyland, L., Hartog, N. & Prommer, H., 2011. Geochemical reconstruction of the provenance, weathering and deposition of detrital-dominated sediments in the Perth Basin: The Cretaceous Leederville Formation, south-west Australia. Sedimentary Geology 236, 62-76.

Dick, H.J.B. & Bullen, T., 1984. Chromian spinel as a petrogenetic indicator in abyssal and alpine-type peridotites and spatially associated lavas. Contributions to Mineralogy and Petrology 86, 54-76.

Dietrich, V.J. & Franz, U., 1976. Ophiolith-Detritus in den santonen Gosau-Schichten (Nördliche Kalkalpen). Geotektonische Forschungen 50, 85-109.

Dimo-Lahitte, A., Monié, P. & Vergély, P., 2001. Metamorphic soles from the Albanian ophiolites: Petrology $^{40}Ar/^{39}Ar$ geochronology, and geodynamic evolution. Tectonics 20, 78-96.

Dominik, J. & Stanley, D.J., 1993. Boron, beryllium and sulfur in Holocene sediments and peats of the Nile delta, Egypt: their use as indicators of salinity and climate. Chemical Geology 104, 203–216.

Draxler, I., 1997. Postconference Excursion: 2.2.2.1. Palynological contribution on the coal-bearing Series of Grünbach. Excursion Guides, Climates: Past, Present and Future, Second European Palaeontological Congress, Vienna 10-12 July 1997, 80-89.

Egger, H., Krenmayr, H.G., Mandl, G.W., Matura, A., Nowotny, A., Pascher, G., Pestal, G., Pistotnik, J., Rockenschaub, M. & Schnabel, W., 1999. Geologische Übersichtskarte der Republik Österreich 1:15000000 (ohne Quartär). Geologische Bundesanstalt, Wien.

Elitok, Ö. & Drüppel, K., 2008. Geochemistry and tectonic significance of metamorphic sole rocks beneath the Beyşehir-Hoyran ophiolite (SW-Turkey). Lithos 100, 322-353.

Erkan, E., 1972. Die exotischen Gerölle in der Gosaukreide der nordöstlichen Kalkalpen (Stratigraphische Gliederung, Bestand, Schüttungsrichtungen). Mitteilungen der Geologischen Gesellschaft in Wien 65, 33-108.

Ernst, W., 1966. Stratigraphisch-fazielle Identifizierung von Sedimenten auf chemisch-geologischem Wege. International Journal of Earth Sciences 55, 21-29.

Ertl, A., 2000. Druckabschätzungen in Metabsiten und Metapeliten mittels des Pyropanteils in Granaten. Eigenverlag Andreas Ertl, Wien, 21pp.

Faryad, S.W. & Hoinkes, G., 2003. P-T gradient of Eo-Alpine metamorphism within the Austroalpine basement units east of the Tauern Window (Austria). Mineralogy and Petrology 77, 129-159.

Faupl, P., 1983. Die Flyschfazies in der Gosau der Weyerer Bögen (Oberkreide, Nördliche Kalkalpen, Österreich). Jahrbuch der Geologischen Bundesanstalt 126, 219-244.

Faupl, P., Pober, E. & Wagreich, M., 1987. Facies development of the Gosau Group of the eastern parts of the Northern Calcareous Alps during the Cretaceous and Paleogene. In: Flügel, H.W. & Faupl, P. (Eds.), Geodynamics of the Eastern Alps. Deuticke, Vienna, 142-155.

Faupl, P. & Pober, E., 1991. Zur Bedeutung detritischer Chromspinelle in den Ostalpen: Ophiolitischer Detritus aus der Vardarsutur. Jubiläumsschrift 20 Jahre geologische Zusammenarbeit Österreich-Ungarn 1, 133-143.

Faupl, P. & Sauer, R., 1978. Zur Genese roter Pelite in Turbiditen der Flyschgosau in den Ostalpen (Oberkreide-Alttertiär). Neues Jahrbuch für Geologie und Paläontologie, Monatshefte 1978, 65-86.

Faupl, P. & Wagreich, M., 1996. Basin analysis of the Gosau Group of the Northern Calcareous Alps (Turonian-Eocene, Eastern Alps). In: Wessely, G. & Liebl, W. (Eds.), Oil and Gas in Alpidic Thrustbelts and Basins of Central and Eastern Europe. EAGE Special Publication 5, 127-135.

Faupl, P. & Wagreich, M., 2000. Late Jurassic to Eocene paleogeography and geodynamic evolution of the Eastern Alps. Mitteilungen der Österreichischen Geologischen Gesellschaft 92, 79-94.

Fedo, C.M., Young, G.M. & Nesbitt, G.M., 1997. Paleoclimatic control on the composition of the Paleoproterozoic Serpent Formation, Huronian Supergroup, Canada: A greenhouse to icehouse transition. Precambrian Research 86, 201–223.

Filzmoser, P., Hron, K., Reimann, C. & Garrett, R., 2009. Robust factor analysis for compositional data. Computers & Geosciences 35, 1854-1861.

Forster, A., Schouten, S., Baas, M. & Sinninghe Damsté, J.S., 2007. Mid-Cretaceous (Albian–Santonian) sea surface temperature record of the tropical Atlantic Ocean. Geology 35, 919-922.

Gale, A.S., Hardenbol, J., Hathaway, B., Kennedy, W.J., Young, J.R. & Phansalkar, V., 2002. Global correlation of Cenomanian (Upper Cretaceous) sequences: evidence for Milankovitch control on sea level. Geology 30, 291-294.

Garver, J.I., Royce, P.R. & Smick, T.A., 1996. Chromium and nickel in shale of the Taconic foreland: a case study for the provenance of fine-gained sediments with an ultramafic source. Journal of Sedimentary Research 66, 100-106.

Garzanti, E. & Andò, S., 2007. Heavy mineral concentration in modern sands: Implications for provenance interpretation. In: Mange, M.A. & Wright, D.T. (Eds.), Heavy Minerals in Use. Developments in Sedimentology 58, 517-545.

Garzanti, E., Andò, S. & Vezzoli, G., 2009. Grain-size dependence of sediment composition and environmental bias in provenance studies. Earth and Planetary Science Letters 277. 422-432.

Gawlick, H.J. & Böhm, F., 2000. Sequence and isotope stratigraphy of Late Triassic distal periplatform limestones from the Northern Calcareous Alps (Kälberstein Quarry, Berchtesgaden Hallstatt Zone). International Journal of Earth Sciences 89, 108-129.

Glasspool, I.J., 2003. Hypautochthonous-allochthonous coal deposition in the Permian, South African, Witbank Basin No. 2 seam; a combined approach using sedimentology, coal petrology and palaeontology. International Journal of Coal Geology 53, 81-135.

Goodarzi, F. & Swaine, D.J., 1994. Paleoenvironmental and environmental implications of the Boron content of coals. Geological Survey of Canada Bulletin 471, Ottawa, 76pp.

Gromet, L.P., Dymek, R.F., Haskin, L.A. & Korotev, R.L., 1984. The "North American shale composite"; its compilation, major and trace element characteristics. Geochimica et Cosmochimica Acta 48, 2469-2482.

Gruber, P., 1987. Sedimentologische und stratigraphische Untersuchungen der Gosaugruppe zwischen Puchberg/Schneeberg und Waidmannsfeld (Miesenbachtal, Niederösterreich). PhD thesis, University of Vienna, 142pp.

Gruber, P., Faupl, P. & Koller, F., 1992. Zur Kenntnis basischer Vulkanitgerölle aus Gosaukonglomeraten der östlichen Kalkalpen – Ein Vergleich mit Vulkaniten aus dem Haselgebirge. Mitteilungen der Österreichischen Geologischen Gesellschaft 84, 77-100.

Habler, G. & Thöni, M., 2001. Preservation of Permo-Triassic low-pressure assemblages in the Cretaceous high-pressure metamorphic Saualpe crystalline basement (Eastern Alps, Austria). Journal of Metamorphic Geology 19, 679-697.

Hamilton, W., Jiříček, R. & Wessely, G., 1990. The alpine-carpathian floor of the Vienna basin in Austria and ČSSR. In: Minaříková, D. & Lobitzer, H. (Eds.), Thirty years of geological cooperation between Austria and Czechoslovakia, 46-56.

Hamon, Y. & Merzeraud, G., 2007. C and O isotope stratigraphy in shallow-marine carbonate: a tool for sequence stratigraphy (example from the Lodève region, peritethian domain). Swiss Journal of Geosciences 100, 71-84.

Harangi, S., Downes, H., Kósa, L., Szabó, C., Thirlwall, M.F., Mason, P.R.D. & Mattay, D., 2001. Almandine garnet in calc-alkaline volcanic rocks of the Northern Pannonian Basin (eastern-central Europe): Geochemistry, petrogenesis and geodynamic implications. Journal of Petrology 42/10, 1813-1843.

Heling, D., 1967. Die Salinitätsfazies von Keupersedimenten aufgrund von Borgehaltsbestimmungen. Sedimentology 8, 63-72.

Henry, D.J. & Guidotti, C.V., 1985. Tourmaline as a petrogenetic indicator mineral: an example from the staurolite-grade metapelites of NW Maine. American Mineralogist 70, 1-15.

Henry, D.J. & Dutrow, B.L., 1992. Tourmaline in a low grade clastic metasedimentary rock: an example of the petrogenetic potential of tourmaline. Contributions to Mineralogy and Petrology 112, 203-218.

Herm, D., 1977. Zyklische Regressions-Sedimentation und Fossil-Vergesellschaftungen in der Gosau (Santonium) von Brandenberg/Tirol. Mitteilungen der Bayerischen Staatssammlung für Paläontologie und Historische Geologie 17, 257-277.

Hisada, K.I., Sugiyama, M., Ueno, K., Charusiri, P. & Arai, S., 2004. Missing ophiolitic rocks along the Mae Yuam Fault as the Gondwana-Tethys divide in north-west Thailand. The Island Arc 13, 119-127.

Hoefs, J., 2009. Stable isotope geochemistry. 6th edition, Springer, Berlin, 300pp.

Hofer, G., 2009. Geochemische Untersuchungen an lakustrin-marinen Sedimenten der Bohrung Markgrafneusiedl T1 (Oberkreide, Gosau-Gruppe). Master thesis, University of Vienna, 102pp.

Hofmann P., Ricken, W., Schwark, L. & Leythaeuser, D., 2001. Geochemical signature and related climatic-oceanographic processes for early Albian black shales: Site 417D, North Atlantic Ocean. Cretaceous Research 22, 243-257.

Holmden, C. & Hudson, J.D., 2003. $^{87}Sr/^{86}Sr$ and Sr/Ca Investigation of Jurassic mollusks from Scotland: Implications for paleosalinities and the Sr/Ca ratio of seawater. Geological Society of America Bulletin 115, 1249-1264.

Howarth, R.J. & McArthur, J.M., 1997. Statistics for strontium isotope stratigraphy. A robust LOWESS fit to the marine Sr-isotope curve for 0 to 509 Ma and accompanying look-up table for deriving numerical age. Journal of Geology 105, 441-456.

Hradecká, L., Lobitzer, H., Ottner, F., Švábenická, L. & Svobodová, M., 1999. Biostratigraphy and facies of selected exposures in the Grünbach-Neue Welt Gosau-Group (Coal-Bearing Series, Inoceramus-Marl and Zweiersdorf-Formation, Late Cretaceous and Paleocene, Lower Austria). Abhandlungen der Geologischen Bundesanstalt 56, 519-551.

Hubert, J.F., 1962. A zircon-tourmalin-rutile maturity index and the interdependence of the composition of heavy mineral assemblages with the gross composition and texture of sandstones. Journal of Sedimentary Petrology 32, 440-450.

Hudson, J.D., 1977. Stable isotopes and limestone lithification. Journal of the Geological Society of London 133, 637-660.

ICCP, 1998. The New Vitrinite Classification (ICCP System 1994). Fuel 77, 349-358.

ICCP, 2001. The New Inertinite Classification (ICCP System 1994). Fuel 80, 459-471.

Ingram, B.L., De Deckker, P., Chivas, A.R., Conrad, M.E. & Byrne, A.R., 1998. Stable isotopes, Sr/Ca, and Mg/Ca in biogenic carbonates from Petaluma Marsh, northern California, USA. Geochimica et Cosmochimica Acta 62, 3229-3237.

Ivanova, A.V. & Zaitseva, L.B., 2006. Influence of oxidability of carboniferous coals from the Dobrudja foredeep on vitrinite reflectance. Lithology and Mineral Ressources 41/5, 435-439.

Jenkyns, H.C., 2003. Evidence for rapid climate change in the Mesozoic-Palaeogene greenhouse world. Philosophical Transactions of the Royal Society, Series A 361, 1885-1916.

Jones, C.E. & Jenkyns, H.C., 2001. Seawater strontium isotopes, oceanic anoxic events and seafloor hydrothermal activity in the Jurassic and Cretaceous. American Journal of Science 301, 112-149.

Jones, B. & Manning, D.A.C., 1994. Comparison of geochemical indices used for the interpretation of paleoredox conditions in ancient mudstones. Chemical Geology 111, 111-129.

Kamenetsky, V.S., Crawford, A.J. & Meffre, S., 2001. Factors controlling chemistry of magmatic spinel: an empirical study of associated olivine, Cr-spinel and melt inclusions from primitive rocks. Journal of Petrology 42, 655-671.

Keith, M.L. & Weber, J.N., 1964. Carbon and oxygen isotopic composition of selected limestones and fossils. Geochimica et Cosmochimica Acta 28, 1787-1816.

Korte, C., Kozur, H.W., Bruckschen, P. & Veizer, J., 2003. Strontium isotope evolution of Late Permian and Triassic seawater. Geochimica et Cosmochimica Acta 67, 47– 62.

Korte, C., Kozur, H.W. & Veizer, J., 2005. d13C and d18O values of Triassic brachiopods and carbonate rocks as proxies for coeval seawater and palaeotemperature. Palaeogeography, Palaeoclimatology, Palaeoecology 226, 287–306.

Kreiner, H., 1994. Der Grünbacher Steinkohlenbergbau und seine Zeit 1823-1965. Marktgemeinde Grünbach, Grünbach, 356pp.

Krenmayr, H.G., 1999. Die Nierental-Formation der Oberen Gosau Gruppe (Oberkreide-Paleozän, Nördliche Kalkalpen) in Berchtesgaden: Definition, Fazies und Environment. Jahrbuch der Geologischen Bundesanstalt 141, 409-447.

Kutterolf, S., 2001. Die klastischen Sedimente der karbonen Hochwipfel- und Auerning-Formation der Ostkarawanken (Österreich/Slowenien). Sedimentologie, Geochemie und Provenanz. PhD thesis, University of Stuttgart, 182pp.

Kutterolf, S., Diener, R., Schacht, U. & Krawinkel, H., 2008. Provenance of the Carboniferous Hochwipfel Formation (Karawanken Mountains, Austria/Slovenia) – Geochemistry versus petrography. Sedimentary Geology 203, 246-266.

Lee, Y.I., 2009. Geochemistry of shales of the Upper Cretaceous Hayang Group, SE Korea: Implications for provenance and source weathering at an active continental margin. Sedimentary Geology 215, 1-12.

Lenaz, D., Mazzoli, C., Spišiak, J., Princivalle, F. & Maritan, L., 2009. Detrital Cr-spinel in the Šambron-Kamenica Zone (Slovakia): evidence for an ocean-spreading zone in the Northern Vardar suture?. International Journal of Earth Sciences (Geologische Rundschau) 98, 345-355.

Lepland, A., Sæther, O., Thorsnes, T., Accumulation of barium in recent Skagerrak sediments: sources and distribution controls. Marine Geology 163, 13-26.

Locklair, R.E. & Sageman, B.B., 2008. Cyclostratigraphy of the Upper Cretaceous Niobrara Formation, Western Interior, U.S.A.: A Coniacian–Santonian orbital timescale. Earth and Planetary Science Letters 269, 540-553.

Lužar-Oberiter, B., Mikes, T., Von Eynatten, H. & Babić, L., 2009. Ophiolithic detritus in Cretaceous clastic formations of the Dinarides (NW Croatia): evidence from Cr-spinel chemistry. International Journal of Earth Sciences 98, 1097-1108.

Lužar-Oberiter, B., Mikes, T., Dunkl, I., Babić, L. & Von Eynatten, H., 2012. Provenance of Cretaceous synorogenic sediments from the NW Dinarides (Croatia). Swiss Journal of Geosciences, DOI 10.1007/s00015-012-0107-3.

Mader, D. & Neubauer, F., 2004. Provenance of Palaeozoic sandstones from the Carnic Alps (Austria): petrographic and geochemical indicators. International Journal of Earth Sciences 93, 262-281.

Madhavaraju, J., González-León, C.M., Lee, Y.I., Armstrong-Altrin, J.S. & Reyes-Campero, L.M., 2010. Geochemistry of the Mural Formation (Aptian-Albian) of the Bisbee Group, Northern Sonora, Mexico. Cretaceous Research 31, 400-414.

Maksimovic, Z. & Majer, V., 1981. Accessory spinels of two main zones of alpine ultramafic rocks in Yugoslawia. Bull. Sci. Nat. Serb. Acad. Sci. Arts 21, 47-58.

Mandl, G.W., 2000. The Alpine sector of the Tethyan shelf—Examples of Triassic to Jurassic sedimentation and deformation from the Northern Calcareous Alps. Mitteilungen der Österreichischen Geologischen Gesellschaft 92, 61–77.

Mange, M.A. & Maurer, H.F.W., 1992. Heavy minerals in colour. Chapman & Hall, London, 147pp.

Mange, M.A. & Morton, A.C., 2007. Geochemistry of heavy minerals. In: Mange, M.A. & Wright, D.T. (Eds.), Heavy Minerals in Use. Developments in Sedimentology 58, 345-391.

Marquillas, R., Sabino, I., Sial, A.N., Del Papa, C., Ferreira, V. & Matthews, S., 2007. Carbon and oxygen isotopes of Maastrichtian-Denian shallow marine carbonates: Yacoraite Formation, northwestern Argentina. Journal of South American Earth Sciences 23, 304-320.

Martin, J.M. & Whitfield, M., 1983. The significance of the river input of chemical elements to the ocean. In: Wong, C.S., Boyle, E.A, Bruland, K.W, Burton, J.D & Goldberg, E.D. (Eds.), Trace Metals in Sea Water. Plenum Publ. Corp., New York, 265-296.

McArthur, J.M., Howarth, R.J. & Bailey, T.R., 2001. Strontium isotope stratigraphy: LOWESS Version 3. Best-fit line to the marine Sr-isotope curve for 0 to 509 Ma and accompanying look-up table for deriving numerical age. Journal of Geology 109, 155-169.

McCabe, P.J. & Parrish, J.T., 1992. Tectonic and climatic controls on the distribution and quality of Cretaceous coals. In: McCabe, P.J. & Parrish, J.T. (Eds.), Controls on the distribution and quality of Cretaceous coals. Geological Society of America Special Paper 267, 1-15.

McLennan, S.M., 1993. Weathering and global denudation. Journal of Geology 101, 295-303.

McLennan, S.M., Hemming, S., McDaniel, D.K. & Hanson, G.M., 1993. Geochemical approaches to sedimentation, provenance, and tectonics. In: Johnsson, M.J. & Basu, A. (Eds.), Processes Controlling the Composition of Clastic Sediments. Geological Society of America Special Papers 284, 21-40.

Meinhold, G., Kostopoulos, D., Reischmann, T., Frei, D. & BouDaher-Fadel, M.K., 2009. Geochemistry, provenance and stratigraphic age of metasedimentary rocks from the eastern Vardar suture zone, northern Greece. Palaeogeography, Palaeoclimatology, Palaeoecology 277, 199-225.

Méres, Š., 2008. Garnets – important information resource about source area and parental rocks of the siliciclasic sedimentary rocks. In: Jurcovič, L. (Ed.), Conference “Cambelove dni 2008”. Abstract Book, Comenius University, Bratislava, 37-43.

Méres, Š., Aubrecht, R., Gradziński, M. & Sýkora, M., 2012. High (ultrahigh) pressure metamorphic terrane rocks as the source of the detrital garnets from the Middle Jurassic sands and sandstones of the Cracow Region (Cracow-Wieluń Upland, Poland). Acta Geologica Polonica 62, 231-245.

Mikes, T., Christ, D., Petri, R., Dunkl, I., Frei, D., Báldi-Beke, M., Reitner, J., Wemmer, K., Hrvatović, H. & Von Eynatten, H., 2008. Provenance of the Bosnian Flysch. Swiss Journal of Geosciences Supplement Volume 3, 31-54.

Mikuš, T. & Spišiak, J., 2007. Chemical composition and alteration of Cr-spinels from Meliata and Penninic serpentinized peridotites (Western Carpathians and Eastern Alps). Geological Quarterly 51, 257-270.

Miller, K.G., Kominz, M.A., Browning, J.V., Wright, J.D., Mountain, G.S., Katz, M.E., Sugarman, P.J., Cramer, B.S., Christie-Blick, N. & Pekar, S.F., 2005a. The Phanerozoic record of global sea-level change. Science 310, 1293-1298.

Miller, K.G., Wright, J.D. & Browning, J.V., 2005b. Visions of ice sheets in a greenhouse world. Marine Geology 217, 215-231.

Miller, K.G., Wright, J.D., Katz, M.E., Browning, J.V., Cramer, B.S., Wade, B.S. & Mizintseva, S.F., 2008. A view of Antarctic ice-sheet evolution from sea-level and deep-sea isotope changes during the Late Cretaceous-Cenozoic. In: Cooper, A.K., Barrett, P.J., Stagg, H., Storey, B., Stump, E., Wise, W. & the 10th ISAES editorial team (Eds.), Antarctica: A keystone in a changing world: Proceedings of the 10th International Symposium on Antarctic Earth Sciences. The National Academies Press, Washington DC, 55-70.

Mišík, M., 1994. Senonian continental sediments with marine intercalation (Gosau complex) in the basement of the Slovakian part of Vienna basin (borehole Gajary Ga-125). Mineralia Slovaca 26, 297-310.

Mizintseva, S.F., Browning, J.V., Miller, K.G., Olsson, R.K. & Wright, J.D., 2009. Integrated Late Santonian-Early Campanian sequence stratigraphy, New Jersey Coastal Plain: Implications for global sea-level studies. Stratigraphy 6, 45-60.

Morse, J.W. & Berner, R.A., 1995. What determines sedimentary C/S ratios? Geochimica et Cosmochimica Acta 59, 1073-1077.

Morton, A.C., 1985. A new approach to provenance studies: electron microprobe analysis of detrital garnets from Middle Jurassic sandstones of the northern North Sea. Sedimentology 32, 553-566.

Morton, A.C., 1991. Geochemical studies of detrital heavy minerals and their application to provenance research. In: Morton, A.C., Todd, S.P. & Haughton, P.D.W. (Eds.), Developments in Sedimentary Provenance Studies. Geology of London Special Publication 57, 31-45.

Morton, A.C., Allen, M., Simmons, M., Spathopoulos, F., Still, J., Hinds, D., Ismail-Zadeh, A. & Kroonenberg, S., 2003. Provenance patterns in a neotectonic basin: Pliocene and Quaternary sediment supply to the South Caspian. Basin Research 15, 321-337.

Morton, A.C. & Hallsworth, C.R., 2007. Stability of detrital heavy minerals during burial diagenesis. In: Mange, M.A. & Wright, D.T. (Eds.), Heavy Minerals in Use. Developments in Sedimentology 58, 215-245.

Müller, G. & Gastner, M., 1971. The „Karbonat-Bombe“, a simple device for the determination of the carbonate content in sediments, soils, and other materials. Neues Jahrbuch für Mineralogie Monatshefte 10, 466-469.

Narayanan, V., Anirudhan, S. & Grottoli, A.G., 2007. Oxygen and carbon isotope analysis of the Miocene limestone of Kerala and its implications to palaeoclimate and its depositional setting. Current Science 93, 1155-1159.

Nesbitt, H.W. & Young, G.M., 1982. Early Proterozoic climates and plate motions inferred from major element chemistry of lutites. Nature 299, 715-717.

Nesbitt, H.W. & Young, G.M., 1989. Formation and diagenesis of weathering profiles. Journal of Geology 97, 129-147.

Norris, R.D., Bice, K.L., Magno, E.A. & Wilson, P.A., 2002. Jiggling the tropical thermostat in the Cretaceous hothouse. Geology 30, 299-302.

Ogg, J.G., Agterberg, F.P. & Gradstein, F.M., 2004. The Cretaceous Period. In: Gradstein, F.M., Agterberg, F.P. & Smith, A.G. (Eds.), A Geologic Time Scale 2004, Cambridge University Press, Cambridge, 344–383.

Ohta, T., 2004. Geochemistry of Jurassic to earliest Cretaceous deposits in the Nagato Basin, SW Japan: implication of factor analysis to sorting effects and provenance signatures. Sedimentary Geology 171, 159-180.

Pavlishina, P., Verreussel, R., Leereveld, H., Summesberger, H. & Wagreich, M., 2004. Palynological study of Gosau group deposits (Upper Cretaceous) of the Northern Calcareous Alps (Austria). Annalen des Naturhistorischen Museums in Wien 106A, 67-90.

Pearce, T.J., Wray, D., Ratcliffe, K., Wright, D.K. & Moscariello, A., 2005. Chemostratigraphy of the Upper Carboniferous Schooner Formation, southern North Sea. In: Collinson, J.D., Evans, D.J., Holliday, D.W. & Jones, N.S. (Eds.), Carboniferous hydrocarbon geology: the southern North Sea and surrounding onshore areas. Vol. 7, Yorkshire Geological Society, 147-164.

Perch-Nielsen, K., 1985. Mesozoic calcareous nannofossils. In: Bolli, H.M., Saunders, J.B., Perch-Nielsen, K. (Eds.), Plankton Stratigraphy. Cambridge University Press, Cambridge, 329-426.

Peros, M.C., Reinhardt, E.G., Schwarcz, H.P. & Davis, A.M., 2007. High-resolution paleosalinity reconstruction from Laguna de la Leche, north coastal Cuba, using Sr, O, and C isotopes. Palaeogeography, Palaeoclimatology, Palaeoecology 245, 535-550.

Pettijohn, F.J., Potter, P.E. & Siever, R., 1973. Sand and sandstones. Springer, New York, 618pp.

Petrakakis, K. & Dietrich, H., 1985. MINSORT: a program for the processing and archivation of microprobe analyses of silicate and oxide minerals. Neues Jahrbuch für Mineralogie – Monatshefte 8, 379-384.

Plöchinger, B., 1961. Die Gosaumulde von Grünbach und der Neuen Welt. Jahrbuch der Geologischen Bundesanstalt 104, 359-441.

Plöchinger, B., 1967. Erläuterungen zur Geologischen Karte des Hohe Wand-Gebietes (Niederösterreich). Geologische Bundesanstalt, Wien.

Pober, E. & Faupl, P., 1988: The chemistry of detrital chromium spinels and its implications for the geodynamic evolution of the Eastern Alps. Geologische Rundschau 77, 641-670.

Pouchou, L.J. & Pichoir, F. A new model for quantitative X-ray microanalysis. Part 1. Applications to the analysis of homogenous samples. Recherche Aerospatiale 3, 13-38.

Power, M.R., Pirrie, D., Andersen, J.C.O. & Wheeler, P.D., 2000. Testing the validity of chrome spinel chemistry as a provenance and petrogenetic indicator. Geology 28, 1027-1030.

Preston, J., Hartley, A., Mange-Rajetzky, M., Hole, M., May, G., Buck, S. & Vaughan, L., 2002. The provenance of Triassik continental sandstones from the Beryl Field, northern North Sea: mineralogical, geochemical and sedimentological constraints. Journal of Sedimentary Research 72, 18-29.

Rákosi, L. & Barbacka, M., 1999/2000. Upper Cretaceous flora from Ajka (W Hungary). I. Thallophyta. Studia Botanica Hungarica 30/31, 27-55.

Ralbovsky, E. & Ostrolucký, P., 1996. The Glinzendorf Syncline below the Vienna Basin in Slovakia. In: Wessely, G. & Liebl, W. (Eds.), Oil and Gas in Alpidic Thrustbelts and Basins of Central and Eastern Europe. EAGE Special Publication 5, 145-146.

Rahman, M.J.J. & Suzuki, S., 2007. Composition of Neogene shales from the Surma Group, Bengal Basin, Bangladesh: Implications for provenance and tectonic setting. Austrian Journal of Earth Sciences 100, 54-64.

Ratcliffe, K.T., Wright, A.M., Hallsworth, C., Morton, A., Zaitlin, B.A., Potocki, D. & Wray, D.S., 2004. An example of alternative correlation techniques in a low-accommodation setting, nonmarine hydrocarbon system: The (Lower Cretaceous) Mannville Basal Quartz succession of southern Alberta. AAPG Bulletin 88/10, 1419-1432.

Reinhardt, E.G., Stanley, D.J. & Patterson, R.T., 1998. Strontium isotopic-paleontological method as a high-resolution paleosalinity tool for lagoonal environments. Geology 26, 1003-1006.

Reinhardt, E.G., Fitton, R.J. & Schwarcz, H.P., 2003. Isotopic (Sr, O, C) indicators of salinity and taphonomy in marginal marine systems. Journal of Foraminiferal Research 33, 262-272.

Reinhold, C. & Kaufmann, B., 2010. Sea-level changes as controlling factor of early diagenesis: the reefal limestones of Adnet (Late Triassic, Northern Calcareous Alps, Austria). Facies 56, 231-248.

Reyment, R.A. & Jöreskog, K.G., 1996. Applied Factor Analysis in the Natural Sciences. Cambridge Univ. Press, Cambridge, 384pp.

Roser, B.P. & Korsch, R.J., 1988. Provenance signatures of sandstone-mudstone suites determined using discriminant function analysis of major-element data. Chemical Geology 67, 119-139.

Rügner, O., 2000. Tonmineral-Neubildung und Paläosalinität im Unteren Muschelkalk des südlichen Germanischen Beckens. PhD thesis, University of Heidelberg,189pp.

Sachsenhofer, R., 1987. Fazies und Inkohlung mesozoischer Kohlen der Alpen Ostösterreichs. Mitteilungen der Österreichischen Geologischen Gesellschaft 80, 1-45.

Sachsenhofer, R.F. & Tomschey, O., 1992. Gosau-type coals of Austria and Hungary – a preliminary geochemical comparison. Acta Geologica Hungarica 35, 49-57.

Sageman, B.B. & Lyons, T.W., 2004. Geochemistry of Fine-grained Sediments and Sedimentary Rocks. In: MacKenzie, F. (Ed.), Sediments, Diagenesis, and Sedimentary Rocks, Treatise on Geochemistry, 7, pp. 115-158.

Sanders, D., 1998. Tectonically controlled Late Cretaceous terrestrial to neritic deposition (Northern Calcareous Alps, Tyrol, Austria). Facies 39, 139-178.

Sauer, R., 1980. Zur Stratigraphie und Sedimentologie der Gießhübler Schichten im Bereich der Gießhübler Gosaumulde (Nördliche Kalkalpen). PhD thesis, University of Vienna, 181pp.

Scarby, A., 1986. Normapolles anthers from the Upper Cretaceous of southern Sweden. Review of Palaeobotany and Palynology 46, 235-256.

Schlagintweit, F. & Wagreich, M., 1992. Über ein Vorkommen von Munieria grambasti sarda CHERCHI et al. in der obersantonen-untercampanen Gosau Gruppe des Miesenbachtales (Niederösterreich). Mitteilungen der Gesellschaft der Geologie- und Bergbaustudenten in Österreich 38, 21-29.

Schmid, S.M., Bernoulli, D., Fügenschuh, B., Matenco, L., Schefer, S., Schuster, R., Tischler, M. & Ustaszewski, K., 2008. The Alpine-Carpathian-Dinaridic orogenic system: correlation and evolution of tectonic units. Swiss Journal of Geosciences 101, 139-183.

Schmidt, G.A., Bigg, G.R. & Rohling, E.J., 1999. Global Seawater Oxygen-18 Database - v1.21. http://data.giss.nasa.gov/o18data/

Schmitz, B., Ingrain, S.L., Dockery, D.T. & Aberg, G., 1997. Testing $^{87}Sr/^{86}Sr$ as a paleosalinity indicator on mixed marine, brackish-water and terrestrial vertebrate skeletal apatite in late Paleocene-early Eocene near-coastal sediments, Mississippi. Chemical Geology 140, 275-287.

Schrank, E. & Ibrahim, M.I.A., 1995. Cretaceous (Aptian-Maastrichtian) palynology of foraminifera dated wells (KRM-1, AG-18) in northwestern Egypt. Berliner Geowissenschaftliche Abhandlungen, Reihe A 177, 1-44.

Schultz, L.G., 1964. Quantitative interpretation of mineralogical composition from X-ray and chemical data for the Pierre shale. U.S. Geological Survey Professional Paper 391-C, 33.

Schulz, O. & Fuchs, H.W., 1991. Kohle in Tirol: Eine historische, kohlenpetrologische und lagerstättenkundliche Betrachtung. Archiv für Lagerstättenforschung der Geologischen Bundesanstalt 13, 123-213.

Schuster, R. & Frank, W., 1999. Metamorphic evolution of the Austroalpine units east of the Tauern Window: indications for Jurassic strike slip tectonics. Mitteilungen der Gesellschaft der Geologie- und Bergbaustudenten in Österreich 42, 37-58.

Schuster, R., Koller, F. & Frank, W., 2007. Pebbles of upper-amphibolite facies amphibolites in the Gosau Group of the Eastern Alps: relics of a metamorphic sole?. Abstract Volume, 8th Workshop on Alpine Geological Studies, Alpshop 2007, Davos, Switzerland, October 8-10, 2007, 74pp.

Sciunnach, D. & Garzanti, E., 1997. Detrital chromian spinels record tectono-magmatic evolution from Carboniferous rifting to Permian spreading in neotethys (India, Nepal and Tibet). Ofioliti 22/1, 101-110.

Selter, V., David, F. & Kraft, T., 1989. Zusammenhänge zwischen Fazies und Borgehalten im nordwestdeutschen Oberkarbon-Becken. Geologisch-Paläontologische Mitteilungen Innsbruck 16, 108-111.

Shen, Y. & Schidlowski, M., 2000. New C isotope stratigraphy from southwest China: Implications for the placement of the Precambrian-Cambrian boundary on the Yangtze Platform and global correlations. Geology 28, 623-626.

Spötl, C. & Vennemann, T., 2003. Continuous-flow IRMS analysis of carbonate minerals. Rapid Communications in Mass Spectrometry 17, 1004-1006.

Stampfli, G.M., Borel, G., Marchant, R. & Mosar, J., 2002. Western Alps geological constraints on western Tethyan reconstructions. Journal Virtual Explorer 8, 77-106.

Stattegger, K., 1986. Multivariate statistische Auswertung von Schwermineraldaten der alpinen Gosau und Bezüge zur plattentektonischen Entwicklung der Ostalpen während der Oberkreide. Geologische Rundschau 75, 341-352.

Stattegger, K., 1987. Heavy minerals and provenance of sands: modelling of lithological end members from river sands of northern Austria and from sandstones of the Austroalpine Gosau Formation (Late Cretaceous). Journal of Sedimentary Petrology 57, 301-310.

Steuber, T., 2004. Turonian-Campanian Plagioptychidae (Mollusca: Hippuritoidea) of Gosau-type rudist formations of the Alps (Austria). Annalen des Naturhistorischen Museums in Wien 106A, 103-121.

Summesberger, H., 1997. The Cretaceous of the Grünbach - Neue Welt Basin. In: Piller, W.E., Summesberger, H., Draxler, I., Harzhauser, M. & Mandic, O. (Eds.), Meso- to Cenozoic tropical/subtropical climates – Selected examples from the Northern Calcareous Alps and the Vienna Basin. Excursion Guides Second European Palaeontological Congress Climates: Past, Present and Future, Vienna 1997, Postconference Excursion 2, 77-89.

Summesberger, H., Wagreich, M., Tröger, K.A. & Scholger, R., 2000. Piesting-Formation, Grünbach-Formation und Maiersdorf-Formation – drei neue lithostratigraphsche Termini in der Gosau Gruppe (Oberkreide) von Grünbach und der Neuen Welt (Niederösterreich). In: Piller, W.E. (Ed.), Austrostrat 2000. 24-26 November 2000 Gossendorf. Vortragskurzfassungen und Exkursionsführer, Berichte des Institutes für Geologie und Paläontologie der Karl-Franzens-Universität Graz/Austria 2, 23pp.

Summesberger, H., Wagreich, M., Tröger, K.A. & Scholger, R., 2002. The Upper Cretaceous of Piesting (Austria): Integrated stratigraphy of the Piesting Formation (Gosau Group). In: Wagreich, M. (Ed.), Aspects of Cretaceous Stratigraphy and Palaeobiogeography. Schriftenreihe der Erdwissenschaftlichen Kommission 15, 373-399.

Summesberger, H., Machalski, M. & Wagreich, M., 2007. First record of the late Campanian heteromorph ammonite Nostoceras hyatti from the Alpine Cretaceous (Grünbach, Gosau Group, Lower Austria). Acta Geologica Polonica 57, 443-451.

Swan, A.R.H. & Sandilands, M., 1995. Introduction to Geological Data Analysis. Blackwell Science Ltd, London, 464pp.

Talbot, M.R., 1990. A review of the palaeohydrological interpretation of carbon and oxygen isotopic ratios in primary lacustrine carbonates. Chemical Geology (Isotope Geoscience Section) 80, 261-279.

Taylor, S.R. & McLennan, S.M., 1985. The Continental Crust: Its Composition and Evolution. Blackwell, Oxford, 312pp.

Taylor, G.H., Teichmüller, M., Davis, A., Diessel, C.F.K., Littke, R. & Robert, P., 1998. Organic Petrology. Gebruder Borntraeger, Berlin, 704pp.

Teller, J.T., Glennie, K.W., Lancaster, N. & Singhvi, A.K., 2000. Calcareous dunes of the United Arab Emirates and Noah's Flood: the postglacial reflooding of the Persian (Arabian) Gulf. Quaternary International 68-71, 297-308.

Thöni, M., 2006. Dating eclogite-facies metamorphism in the Eastern Alps - approaches, results, interpretations: a review. Mineralogy and Petrology 88, 123-148.

Tsikouras, B., Pe-Piper, G., Piper, D.J.W. & Schaffer, M., 2011. Varietal heavy mineral analysis of sediment provenance, Lower Cretaceous Scotian Basin, eastern Canada. Sedimentary Geology 237, 150-165.

Tyrell, T., Zeebe, R.E., 2004, History of carbonate ion concentration over the last 100 million years. Geochimica et Cosmochimica Acta 68, 3521-3530.

Veizer, J., 1983. Trace Elements and Isotopes in Sedimentary Carbonates. In: R.J. Reeder (Eds.), Carbonates, mineralogy and chemistry. Reviews in Mineralogy and Geochemistry 11, 265-299.

Veizer, J., 2003. Isotopic evolution of seawater on geological time scales: sedimentogical perspective. In: Lentz, D.R. (Ed.) Geochemistry of Sediments and Sedimentary Rocks: Evolutionary Considerations to Mineral Deposit-Forming Environments. Geological Association of Canada, GEOtext 5, 99-114.

Veizer, J., Ala, D., Azmy, K., Bruckschen, P., Buhl, D., Bruhn, F., Carden, G.A.F., Diener, A., Ebneth, S., Godderis, Y., Jasper, T., Korte, C., Pawellek, F., Podlaha, O.G. & Strauss, H., 1999. $^{87}Sr/^{86}Sr$, $\delta^{13}C$ and $\delta^{18}O$ evolution of Phanerozoic seawater. Chemical Geology 161, 59-88.

Voigt, S. & Schönfeld, J., 2010. Cyclostratigraphy of the reference section for the Cretaceous white chalk of northern Germany, Lägerdorf-Kronsmoor: A late Campanian–early Maastrichtian orbital time scale. Palaeogeography, Palaeoclimatology, Palaeoecology 287, 67-80.

Von Eynatten, H., 1996. Provenanzanalyse kretazischer Siliziklastika aus den Nördlichen Kalkalpen. PhD thesis, University of Mainz, 145pp.

Von Eynatten, H., 2003. Petrography and chemistry of sandstones from the Swiss Molasse Basin: an archive of the Oligocene to Miocene evolution of the Central Alps. Sedimentology 50, 703-724.

Von Eynatten, H. & Gaupp, R., 1999. Provenance of Cretaceous synorogenic sandstones in the Eastern Alps: constraints from framework petrography, heavy mineral analysis and mineral chemistry. Sedimentary Geology 124, 81-111.

Wagreich, M., 1986. Schichtfolge und Fazies der Gosau von Lilienfeld (Oberkreide; niederösterreichische Kalkvoralpen). Mitteilungen der Gesellschaft der Geologie- und Bergbaustudenten Österreichs 32, 19-38.

Wagreich, M., 1988. Sedimentologie und Beckenentwicklung des tieferen Abschnittes (Santon-Untercampan) der Gosauschichtgruppe von Gosau und Rußbach (Oberösterreich – Salzburg). Jahrbuch der Geologischen Bundesanstalt 131, 663-685.

Wagreich, M., 1993a. Subcrustal tectonic erosion in orogenic belts - A model for the Late Cretaceous subsidence of the Northern Calcareous Alps (Austria). Geology 21, 941-944.

Wagreich, M., 1993b. Serpentinitreiche Sandsteine als Anzeiger verschwundener Suturzonen am Beispiel der Oberkreide der Nördlichen Kalkalpen (Gosau-Gruppe, Österreich). Zentralblatt für Geologie und Paläontologie, Teil I 1992, 663-673.

Wagreich, M., 1998. Lithostratigraphie, Fazies und Sequenzstratigraphie der Gosau Gruppe von Bad Ischl und Strobl am Wolfgangsee (Oberturon-Maastricht, Nördliche Kalkalpen, Österreich). Jahrbuch der Geologischen Bundesanstalt 141, 209-234.

Wagreich, M., 2001a. Paleocene-Eocene paleogeography of the Northern Calcareous Alps (Gosau Group, Austria). In: Piller, W.E. & Rasser, M.W. (Eds.), Paleogene of the Eastern Alps. Schriftenreihe der Erdwissenschaftlichen Kommission 14, 57-75.

Wagreich, M., 2001b. A 400-km-long piggyback basin (Upper Aptian-Lower Cenomanian) in the Eastern Alps. Terra Nova 13, 401-406.

Wagreich, M. & Decker, K., 2001. Sedimentary tectonics and subsidence modelling of the type Upper Cretaceous Gosau basin (Northern Calcareous Alps, Austria). International Journal of Earth Sciences 90, 714-726.

Wagreich, M. & Faupl, P., 1994. Palaeogeography and geodynamic evolution of the Gosau Group of the Northern Calcareous Alps (Late Cretaceous, Eastern Alps, Austria). Palaeogeography, Palaeoclimatology, Palaeoecology 110, 235-254.

Wagreich, M., Hohenegger, J. & Neuhuber, S., 2012. Nannofossil biostratigraphy, strontium and carbon isotope stratigraphy, cyclostratigraphy and an astronomically calibrated duration of the Late Campanian Radotruncana calcarata Zone. *Cretaceous Research* (2012), doi:10.1016/j.cretres.2012.04.006.

Wagreich, M., Hu, X. & Sageman, B., 2011. Causes of oxic-anoxic changes in Cretaceous marine environments and their implications for Earth systems. Sedimentary Geology 235, 1-4.

Wagreich, M., Ilickovic, T., Popovic, A., Porpaczy, C., Steinbrener, J. & Wessely, G., 2011. Biostratigraphy and sedimentology of Campanian deep-water sections (Nierental Formation, Gosau Group) in Lower Austria. Austrian Journal of Earth Sciences 104/2, 108-121.

Wagreich, M. & Krenmayr, H.G., 2005. Upper Cretaceous oceanic red beds (CORB) in the Northern Calcareous Alps (Nierental Formation, Austria): slope topography and clastic input as primary controlling factors. Cretaceous Research 26, 57-64.

Wagreich, M. & Marschalko, R., 1995. Late Cretaceous to Early Tertiary palaeogeography of the Western Carpathians (Slovakia) and the Eastern Alps (Austria): implications from heavy mineral data. Geologische Rundschau 84, 187-199.

Weltje, G.J. & Von Eynatten, H., 2004. Quantitative provenance analysis of sediments: review and outlook. Sedimentary Geology 171, 1-11.

Wessely, G., 1974. Rand und Untergrund des Wiener Beckens – Verbindungen und Vergleiche. Mitteilungen der Geologischen Gesellschaft in Wien 66-67, 265-287.

Wessely, G., 1984. Der Aufschluß auf kalkalpine und subalpine Tiefenstrukturen im Untergrund des Wiener Beckens. Erdoel-Erdgas 100, 285-292.

Wessely, G., 1992. The Calcareous Alps below the Vienna basin in Austria and their structural and facial development in the alpine-carpathian border zone. Geologica Carpathica 43, 347-353.

Wessely, G., 1993. Der Untergrund des Wiener Beckens. In: Brix, F. & Schultz, O. (Eds.), Erdöl und Erdgas in Österreich. Naturhistorisches Museum Wien, Wien, 249-280.

Wessely, G., 2000. Sedimente des Wiener Beckens und seiner alpinen und subalpinen Unterlagerung. The Vienna Basin and its alpine and subalpine basement. Mitteilungen der Gesellschaft der Geologie- und Bergbaustudenten in Österreich 44, 191-214.

Wessely, G., 2006. Niederösterreich. Geologie der Österreichischen Bundesländer. Geologische Bundesanstalt, Wien, 416pp.

Winkler, W., 1988. Mid- to early Late Cretaceous flysch and melange formations in the western part of the Eastern Alps. Paleotectonic implications. Jahrbuch der Geologischen Bundesanstalt 131, 341-389.

Woletz, G., 1963. Charakteristische Abfolgen der Schwermineralgehalte in Kreide- und Alttertiär-Schichten der nördlichen Ostalpen. Jahrbuch der Geologischen Bundesanstalt 106, 89-119.

Wright, W.I., 1938. The composition and occurrence of garnets. American Mineralogist 23, 436-449.

Yan, D., Chen, D., Wang, Q. & Wang, J., 2010. Large-scale climatic fluctuations in the latest Ordovician on the Yangtze block, south China. Geology 38, 599-602.

Zimmer, W. & Wessely, G., 1996. Exploration results in thrust and subthrust complexes in the Alps and below the Vienna Basin in Austria. In: Wessely, G. & Liebl, W. (Eds.), Oil and Gas in Alpidic Thrustbelts and Basins of Central and Eastern Europe. EAGE Special Publication 5, 81-107.

Zimmerle, W., 1984. The geotectonic significance of detrital brown spinel in sediments. Mitteilungen des Geologisch-Paläontologischen Instituts der Universität Hamburg 56, 337-360.

Appendix

Geochemistry

Appendix A (page 184 to 207): Bulk rock geochemistry of outcrop, core and cutting samples. Parts of this table appear in online appendices of the publications 1, 2 and 3 (chapter 5.1.1, 5.1.2 and 5.1.3).

Heavy mineral assemblages

Appendix B (page 208 to 216): Heavy mineral assemblages of outcrop and core samples (edited by OMV). Abbreviations of heavy minerals: zrn: zircon, tur: tourmaline, rut: rutile, grt: garnet, chr: chrome spinel, cld: chloritoid, sta: staurolite, mon: monazite, tit: titanite, epi: epidote, hbl: hornblende, gln: glaucophane, dis: disthene, sil: sillimanite, bkt/ana: brookite/anatase. This table is also part of the online appendix of the manuscript (chapter 5.2).

Mineral chemistry

Appendix C1 (page 217 to 222): Garnet chemistry of outcrop and core samples. This table is also part of the online appendix of the manuscript (chapter 5.2.1).

Appendix C2 (page 223 to 228): Chrome spinel chemistry of outcrop and core samples. This table is also part of the online appendix of the manuscript (chapter 5.2.1).

Appendix C3 (page 229 to 232): Tourmaline chemistry of outcrop and core samples. This table is also part of the online appendix of the manuscript (chapter 5.2.1).

Gosau	Samples	Location	Type	Unit	SiO_2 [%]	Al_2O_3 [%]	Fe_2O_3 [%]	MgO [%]	CaO [%]	Na_2O [%]	K_2O [%]	TiO_2 [%]	P_2O_5 [%]	MnO [%]	Cr_2O_3 [%]	LOI [%]	Sum [%]	Sc [ppm]	Ba [ppm]	Be [ppm]
				DL	0.01	0.01	0.04	0.01	0.01	0.01	0.01	0.01	0.01	0.01	0.002	-5.1	0.01	1	1	1
Gießhübl S.	AD81-3150	Aderklaa 81	cutting		47.90	14.42	5.90	4.10	8.62	1.12	3.07	0.66	0.12	0.13	0.013	13.7	99.79	14	300	2
Gießhübl S.	AD81-3175	Aderklaa 81	cutting		42.14	12.64	5.27	4.37	13.52	0.92	2.79	0.57	0.10	0.11	0.013	17.4	99.81	13	317	1
Gießhübl S.	AD81/8-3192,5	Aderklaa 81	core		24.38	7.83	3.02	2.59	30.30	0.38	2.18	0.32	0.07	0.09	0.010	28.5	99.67	8	1670	0
Gießhübl S.	AD81/8-3193,4	Aderklaa 81	core		24.11	7.39	2.58	2.49	31.16	0.40	2.00	0.30	0.06	0.10	0.008	29.2	99.81	7	569	0
Gießhübl S.	AD81/8-3193,5	Aderklaa 81	core		15.56	4.65	2.01	1.65	39.49	0.27	1.26	0.19	0.09	0.08	0.005	34.6	99.86	5	229	0
Gießhübl S.	AD81-3225	Aderklaa 81	cutting		27.58	8.28	3.33	10.67	19.34	0.64	1.84	0.37	0.06	0.06	0.008	27.6	99.74	8	173	1
Gießhübl S.	AD84-2800	Aderklaa 84	cutting		51.24	13.05	4.93	2.88	9.73	0.84	2.70	0.62	0.10	0.09	0.012	13.6	99.82	13	313	2
Gießhübl S.	AD84-2817	Aderklaa 84	cutting		46.75	12.56	4.63	3.97	11.65	0.83	2.51	0.59	0.10	0.11	0.012	16.1	99.80	12	310	1
Gießhübl S.	AD84/2-2832,5	Aderklaa 84	core		53.23	14.61	4.37	2.03	8.79	0.99	2.57	0.99	0.09	0.04	0.017	12.1	99.82	15	345	2
Gießhübl S.	AD84/2-2833,5	Aderklaa 84	core		47.96	15.80	5.50	2.46	9.48	0.83	2.86	0.90	0.08	0.04	0.019	13.9	99.80	17	382	2
Gießhübl S.	AD84-2850	Aderklaa 84	cutting		43.70	10.17	4.03	2.17	17.55	0.84	1.96	0.57	0.10	0.10	0.010	18.6	99.81	10	279	2
Gießhübl S.	AD84-2890	Aderklaa 84	cutting		50.10	13.10	5.17	2.76	10.39	1.04	2.57	0.66	0.11	0.10	0.012	13.8	99.81	13	393	2
Gießhübl S.	AD92/3-2840,5	Aderklaa 92	core		55.04	14.67	5.60	2.28	6.69	1.14	2.63	1.03	0.10	0.11	0.017	10.5	99.80	15	415	2
Gießhübl S.	AD92-2870	Aderklaa 92	cutting		50.97	15.30	6.42	2.63	7.28	0.97	3.14	0.75	0.10	0.08	0.015	12.1	99.80	16	476	2
Gießhübl S.	AD92-2890	Aderklaa 92	cutting		50.90	14.00	5.88	2.62	8.88	0.93	2.80	0.71	0.11	0.10	0.014	12.9	99.81	15	396	2
Gießhübl S.	AD92/4-2921,5	Aderklaa 92	core		27.86	10.18	4.17	2.43	25.67	0.60	2.02	0.46	0.09	0.07	0.012	26.2	99.77	11	509	1
Gießhübl S.	AD92/4-2922	Aderklaa 92	core		28.24	10.22	4.13	2.45	25.56	0.62	2.03	0.46	0.10	0.07	0.011	25.9	99.78	11	435	1
Gießhübl S.	AD92/4-2922,55	Aderklaa 92	core		28.07	9.97	4.14	2.45	25.75	0.60	1.98	0.46	0.09	0.07	0.011	26.2	99.78	10	428	2
Gießhübl S.	AD92-2950	Aderklaa 92	cutting		49.07	13.12	5.32	2.73	10.89	0.90	2.67	0.67	0.11	0.09	0.014	14.2	99.79	13	524	2
Gießhübl S.	AD92-2980	Aderklaa 92	cutting		48.62	12.62	4.91	2.47	12.11	1.02	2.40	0.69	0.09	0.09	0.014	14.7	99.80	13	413	2
Gießhübl S.	AD92/5-3009,3	Aderklaa 92	core		38.98	13.76	5.88	2.84	15.60	0.76	2.80	0.63	0.11	0.06	0.016	18.3	99.77	14	304	1
Gießhübl S.	AD92/5-3009,7	Aderklaa 92	core		38.92	13.74	5.89	2.83	15.72	0.78	2.78	0.64	0.10	0.07	0.016	18.3	99.76	14	295	0
Gießhübl S.	AD92-3040	Aderklaa 92	cutting		44.29	12.20	4.90	2.46	15.05	1.03	2.33	0.63	0.10	0.08	0.013	16.7	99.78	12	400	1
Gießhübl S.	AD92-3080	Aderklaa 92	cutting		46.70	12.63	5.33	2.70	12.76	1.05	2.61	0.68	0.10	0.08	0.014	15.1	99.79	14	407	2
Gießhübl S.	AD92/6-3111,5	Aderklaa 92	core		47.46	16.60	8.01	3.51	6.75	1.26	3.51	0.85	0.14	0.04	0.017	11.6	99.76	17	346	2
Gießhübl S.	AD92-3170	Aderklaa 92	cutting		46.48	13.03	5.33	2.80	12.47	1.17	2.62	0.68	0.11	0.08	0.014	15.0	99.76	14	502	2
Gießhübl S.	AD92-3230	Aderklaa 92	cutting		47.08	12.93	5.11	2.64	12.62	1.18	2.47	0.69	0.11	0.09	0.013	14.9	99.78	13	402	2
Gießhübl S.	AD92-3270	Aderklaa 92	cutting		45.41	12.48	5.01	2.61	14.12	1.12	2.35	0.67	0.11	0.10	0.013	15.8	99.78	13	527	1
Gießhübl S.	AD92/7-3327,5	Aderklaa 92	core		53.50	17.66	8.03	3.31	3.19	1.58	3.23	0.84	0.15	0.06	0.018	8.2	99.79	18	491	2
Gießhübl S.	AD92/7-3329	Aderklaa 92	core		34.33	11.56	5.86	2.63	20.62	0.80	2.40	0.46	0.18	0.22	0.011	20.7	99.81	11	282	1
Gießhübl S.	AD92-3360	Aderklaa 92	cutting		47.21	14.08	5.71	2.80	11.11	1.20	2.87	0.69	0.11	0.12	0.014	13.9	99.79	15	406	1
Gießhübl S.	AD92-3400	Aderklaa 92	cutting		48.84	12.98	5.10	2.74	11.69	1.17	2.58	0.66	0.11	0.12	0.012	13.8	99.81	13	331	2
Gießhübl S.	AD92/8-3431,85	Aderklaa 92	core		40.70	16.18	7.09	3.01	11.68	0.80	3.71	0.65	0.08	0.11	0.015	15.8	99.80	15	421	3
Gießhübl S.	AD92/8-3432	Aderklaa 92	core		41.25	16.43	7.20	3.02	11.14	0.81	3.77	0.66	0.09	0.10	0.015	15.3	99.80	15	424	2
Gießhübl S.	AD92/8-3433	Aderklaa 92	core		47.46	17.88	6.67	3.32	6.73	1.14	3.69	0.82	0.08	0.05	0.017	11.9	99.79	17	458	2
Gießhübl S.	AD92-3460	Aderklaa 92	cutting		47.21	12.18	4.70	3.16	13.01	1.17	2.35	0.62	0.10	0.12	0.016	15.2	99.81	12	322	2
Gießhübl S.	AD92/9-3504,4	Aderklaa 92	core		48.58	15.26	6.40	4.00	7.65	0.98	3.63	0.67	0.12	0.08	0.014	12.4	99.81	14	373	2
Gießhübl S.	AD92-3530	Aderklaa 92	cutting		45.62	12.15	4.90	3.04	13.71	1.12	2.41	0.62	0.10	0.11	0.019	16.0	99.77	12	666	1
Gießhübl S.	STRHT9-3610	Strasshof T9	cutting		30.49	6.38	3.22	5.45	25.81	0.42	1.65	0.31	0.07	0.06	0.039	25.6	99.54	7	151	0
Gießhübl S.	STRHT9-3680	Strasshof T9	cutting		14.70	4.47	1.62	1.84	40.15	0.23	1.11	0.18	0.05	0.11	0.007	35.4	99.82	4	146	0
Gießhübl S.	STRHT9-3780	Strasshof T9	cutting		45.15	11.67	4.34	4.09	13.77	0.79	3.09	0.58	0.09	0.07	0.013	16.2	99.81	11	284	2
Gießhübl S.	STRHT9-4110	Strasshof T9	cutting		34.01	12.25	5.21	2.67	20.24	0.52	3.17	0.53	0.10	0.12	0.013	20.9	99.75	12	539	2
Gießhübl S.	STRHT9-4250	Strasshof T9	cutting		34.34	12.55	5.07	2.60	20.28	0.59	2.97	0.54	0.10	0.13	0.013	20.6	99.77	12	373	2
Gießhübl S.	STRHT9-4290	Strasshof T9	cutting		31.54	11.44	4.69	2.39	23.03	0.54	2.69	0.50	0.10	0.14	0.012	22.6	99.72	11	590	2
Gießhübl S.	STRHT9-4360	Strasshof T9	cutting		47.00	13.68	5.50	2.70	12.28	1.34	2.83	0.71	0.11	0.11	0.013	13.5	99.77	14	352	2

Samples	Co [ppm]	Cs [ppm]	Ga [ppm]	Hf [ppm]	Nb [ppm]	Rb [ppm]	Sn [ppm]	Sr [ppm]	Ta [ppm]	Th [ppm]	U [ppm]	V [ppm]	W [ppm]	Zr [ppm]	Y [ppm]	La [ppm]	Ce [ppm]	Pr [ppm]	Nd [ppm]	Sm [ppm]	Eu [ppm]	Gd [ppm]	Tb [ppm]	Dy [ppm]	Ho [ppm]
Unit	[ppm]	[ppm]	[ppm]	[ppm]	[ppm]	[ppm]	[ppm]	[ppm]	[ppm]	[ppm]	[ppm]	[ppm]	[ppm]	[ppm]	[ppm]	[ppm]	[ppm]	[ppm]	[ppm]	[ppm]	[ppm]	[ppm]	[ppm]	[ppm]	[ppm]
DL	0.2	0.1	0.5	0.1	0.1	0.1	1	0.5	0.1	0.2	0.1	8	0.5	0.1	0.1	0.1	0.1	0.02	0.3	0.05	0.02	0.05	0.01	0.05	0.02
AD81-3150	17.7	7.6	17.9	3.9	12.6	124.6	18	224.0	1.0	10.9	2.1	137	23.3	126.0	22.8	30.2	68.6	7.40	26.7	5.22	1.09	4.63	0.74	3.87	0.80
AD81-3175	16.6	6.9	15.2	3.2	10.9	110.9	4	264.0	0.7	9.4	2.1	116	3.0	105.9	20.8	27.1	58.8	6.51	24.9	4.63	0.97	4.12	0.66	3.47	0.71
AD81/8-3192,5	10.2	7.1	9.7	1.5	5.9	88.1	2	629.3	0.4	4.9	1.2	91	1.1	53.7	17.0	17.4	30.7	3.78	14.1	2.64	0.58	2.65	0.43	2.40	0.48
AD81/8-3193,4	9.1	5.2	8.9	1.5	5.9	77.1	2	524.5	0.3	4.6	1.1	85	1.3	51.6	16.2	16.5	30.0	3.55	14.3	2.58	0.57	2.55	0.39	2.30	0.47
AD81/8-3193,5	6.3	3.5	5.7	1.3	4.0	49.9	0	593.8	0.3	3.9	0.7	56	0.7	38.6	14.7	13.0	21.5	2.67	10.8	1.99	0.41	1.98	0.32	1.72	0.38
AD81-3225	10.2	4.4	9.7	2.3	7.1	73.7	2	219.2	0.4	6.2	2.4	85	2.2	74.1	13.7	19.7	38.8	4.36	16.4	3.15	0.63	2.82	0.43	2.38	0.45
AD84-2800	12.9	8.4	15.8	3.7	11.7	121.0	3	357.2	0.9	11.3	2.9	107	3.6	127.8	21.1	27.7	59.4	6.74	25.6	4.57	0.94	4.13	0.64	3.56	0.71
AD84-2817	12.4	7.9	14.8	3.9	11.3	111.3	4	328.5	0.8	10.6	3.0	102	2.7	119.8	20.2	26.5	55.7	6.42	23.6	4.46	0.90	3.95	0.63	3.44	0.68
AD84/2-2832,5	16.5	6.8	18.7	6.0	19.0	115.8	3	457.7	1.4	10.3	2.3	142	2.1	210.1	26.0	30.8	66.8	7.76	31.4	6.02	1.25	5.21	0.83	4.47	0.89
AD84/2-2833,5	17.0	7.7	19.3	4.9	17.7	135.6	3	506.2	1.3	10.6	2.6	164	1.9	173.6	23.4	28.3	58.7	6.97	28.3	5.15	1.08	4.61	0.73	4.28	0.78
AD84-2850	10.3	5.3	12.4	4.3	10.6	83.6	3	494.5	0.8	8.4	2.4	90	93.5	137.8	19.8	24.5	50.8	5.79	21.8	4.18	0.84	3.70	0.60	3.21	0.65
AD84-2890	14.3	7.7	15.6	3.8	12.0	116.8	3	377.2	1.0	10.1	2.3	111	3.1	125.5	21.8	26.9	57.2	6.46	24.5	4.64	0.96	4.14	0.67	3.69	0.76
AD92/3-2840,5	15.3	6.5	18.2	6.8	20.2	118.4	3	396.1	1.4	11.4	2.4	150	2.2	228.7	27.7	33.4	73.8	8.47	34.2	6.36	1.28	5.38	0.85	4.72	0.94
AD92-2870	20.2	9.1	19.8	4.0	14.5	145.4	4	322.4	1.1	11.5	1.8	141	2.8	129.4	23.2	28.3	62.7	6.97	26.7	5.03	1.07	4.49	0.71	3.92	0.80
AD92-2890	16.7	8.2	17.7	3.8	13.6	127.7	4	349.9	1.0	10.7	2.4	129	2.4	133.7	22.9	29.2	62.3	6.89	26.2	5.19	1.07	4.41	0.72	3.93	0.78
AD92/4-2921,5	11.1	5.0	13.3	2.0	9.0	89.9	2	834.5	0.7	7.1	2.0	110	1.2	78.2	16.9	19.5	40.0	4.76	19.0	3.49	0.78	3.30	0.53	2.84	0.60
AD92/4-2922	11.3	5.3	14.0	2.3	8.6	90.1	2	823.3	0.6	7.2	1.9	107	1.3	82.2	17.5	19.9	41.9	4.81	18.9	3.51	0.78	3.33	0.54	2.83	0.52
AD92/4-2922,55	10.6	5.1	12.8	2.3	9.0	90.4	2	844.6	0.6	6.8	2.0	110	1.2	77.8	16.5	19.7	40.6	4.83	19.2	3.71	0.76	3.36	0.54	2.84	0.56
AD92-2950	13.5	8.1	16.0	4.0	12.6	119.5	3	382.9	1.0	10.3	2.5	120	2.4	131.2	21.7	27.4	59.2	6.59	25.0	4.70	1.00	4.21	0.67	3.65	0.72
AD92-2980	13.8	6.9	14.9	3.8	13.0	104.2	3	465.4	1.0	9.3	2.2	119	3.1	132.9	21.4	27.6	56.9	6.36	24.8	4.62	0.99	4.12	0.66	3.51	0.73
AD92/5-3009,3	15.6	8.0	17.9	3.1	13.0	131.8	3	923.2	0.9	10.0	1.8	141	1.5	105.9	21.6	25.8	56.2	6.40	25.7	4.73	1.05	4.34	0.69	3.66	0.74
AD92/5-3009,7	16.9	7.9	18.7	3.4	12.5	128.0	2	906.1	0.9	9.2	1.9	140	1.6	106.9	22.3	25.6	54.7	6.31	25.8	4.67	1.02	4.28	0.69	3.72	0.71
AD92-3040	12.5	6.4	14.1	3.2	12.0	101.9	3	602.6	0.9	9.0	2.2	108	3.3	121.3	20.9	25.1	53.7	6.26	24.7	4.46	0.97	4.11	0.66	3.61	0.71
AD92-3080	13.5	7.2	15.7	3.6	12.5	115.2	3	581.9	1.0	10.1	2.3	118	3.2	130.7	21.5	26.4	57.3	6.55	25.0	4.62	1.02	4.20	0.68	3.65	0.75
AD92/6-3111,5	17.0	9.5	22.2	4.3	16.9	160.3	4	788.7	1.1	10.8	2.0	142	2.2	147.2	26.6	31.0	68.7	7.96	32.9	6.39	1.37	5.68	0.89	4.84	0.95
AD92-3170	14.7	7.2	15.8	4.0	12.4	113.3	3	599.5	1.0	10.2	2.2	118	6.2	134.6	22.1	27.3	59.0	6.77	26.0	4.83	1.06	4.34	0.71	3.81	0.73
AD92-3230	14.4	6.6	16.3	3.8	12.2	106.0	3	616.9	0.9	9.1	2.2	112	5.4	129.6	23.0	26.7	56.0	6.50	25.5	4.76	1.01	4.29	0.71	3.99	0.78
AD92-3270	13.5	5.7	14.6	3.5	11.8	101.1	3	565.7	0.9	9.2	2.0	112	5.0	131.0	21.5	25.6	55.0	6.22	24.7	4.39	1.02	4.17	0.68	3.72	0.73
AD92/7-3327,5	22.8	7.5	22.0	4.9	15.8	131.8	3	371.0	1.1	11.8	2.3	142	2.3	168.9	27.4	30.3	65.9	7.98	31.2	6.28	1.35	5.46	0.89	4.95	0.94
AD92/7-3329	11.6	6.4	14.9	2.3	9.2	106.9	3	666.3	0.7	8.3	1.6	91	1.9	76.5	22.2	25.3	52.1	5.82	23.3	4.48	0.95	4.16	0.65	3.61	0.71
AD92-3360	16.2	7.3	16.8	3.7	12.3	118.6	3	440.5	1.0	9.9	2.0	126	5.1	123.6	22.0	26.9	60.3	6.74	26.3	4.88	1.09	4.46	0.73	3.94	0.77
AD92-3400	13.9	6.4	14.9	3.5	11.3	108.4	3	427.0	0.8	9.0	1.9	111	4.7	120.4	21.2	25.4	56.3	6.39	26.0	4.71	1.04	4.21	0.69	3.75	0.73
AD92/8-3431,85	13.7	11.7	19.8	3.2	13.2	168.7	4	517.8	1.1	11.2	1.9	143	2.2	102.8	20.9	29.3	68.7	7.31	28.6	5.24	1.11	4.46	0.71	3.72	0.77
AD92/8-3432	16.4	12.1	20.1	3.2	13.9	172.0	4	508.7	1.0	11.3	2.0	141	2.3	103.0	21.3	29.9	67.8	7.46	28.8	5.30	1.09	4.37	0.71	4.01	0.78
AD92/8-3433	27.1	11.0	23.9	4.1	16.8	164.8	4	420.6	1.2	13.9	2.4	162	2.2	144.2	24.9	33.2	69.2	8.08	33.1	5.73	1.23	4.68	0.79	4.58	0.85
AD92-3460	13.5	5.8	14.2	3.7	11.4	96.9	3	391.6	0.7	8.5	2.1	105	7.6	130.3	20.6	25.0	53.8	6.18	24.4	4.53	0.99	4.07	0.67	3.64	0.70
AD92/9-3504,4	16.0	9.0	19.2	4.0	13.3	152.9	4	275.0	1.1	12.5	2.5	139	2.2	136.7	24.3	29.9	63.0	7.38	29.9	5.20	1.12	4.53	0.74	4.33	0.84
AD92-3530	12.9	5.8	14.2	3.6	11.1	100.1	3	408.9	0.9	9.0	2.1	105	12.2	124.6	19.9	24.8	52.2	6.09	24.4	4.54	0.96	3.93	0.64	3.50	0.69
STRHT9-3610	13.2	5.0	8.2	2.6	6.3	66.8	1	710.7	0.5	5.2	2.0	62	1.2	81.4	14.7	15.2	33.1	3.75	14.8	2.87	0.56	2.57	0.44	2.42	0.50
STRHT9-3680	6.7	3.0	5.7	0.7	3.5	48.3	1	755.5	0.2	3.0	0.7	42	0.7	34.4	11.1	12.5	22.5	2.71	11.3	2.00	0.42	1.99	0.30	1.73	0.36
STRHT9-3780	12.6	7.9	14.1	3.1	10.6	113.2	2	402.8	0.8	8.4	2.4	99	6.5	121.4	18.9	23.9	54.1	5.72	22.5	4.29	0.91	3.67	0.61	3.33	0.66
STRHT9-4110	16.1	7.9	16.7	2.6	11.0	130.1	3	699.8	0.8	8.1	1.5	110	2.4	90.9	18.9	24.7	54.8	5.65	22.3	4.49	0.94	3.85	0.61	3.45	0.69
STRHT9-4250	16.8	7.5	17.5	2.5	11.1	135.1	3	710.2	0.7	8.7	1.4	115	2.0	95.2	19.4	25.2	58.2	5.81	23.4	4.41	0.93	3.94	0.62	3.18	0.67
STRHT9-4290	15.4	7.3	15.9	2.4	10.7	120.6	2	1022.7	0.8	7.9	1.5	111	1.6	84.9	18.5	23.2	53.2	5.39	23.0	4.08	0.92	3.76	0.60	3.26	0.65
STRHT9-4360	18.7	6.2	17.9	3.7	12.5	115.2	2	665.0	0.8	9.4	2.0	123	3.2	139.8	25.7	29.2	70.7	7.15	29.3	5.99	1.30	5.20	0.86	4.64	0.93

Samples	Unit	Er [ppm]	Tm [ppm]	Yb [ppm]	Lu [ppm]	TOT/C [%]	TOT/S [%]	Mo [ppm]	Cu [ppm]	Pb [ppm]	Zn [ppm]	Ni [ppm]	As [ppm]	Cd [ppm]	Sb [ppm]	Bi [ppm]	Ag [ppm]	Au [ppm]	Hg [ppm]	Tl [ppm]	Se [ppm]	B [ppm]	$\delta^{13}C$ [VPDB]	$\delta^{18}O$ [VPDB]
	DL	0.03	0.01	0.05	0.01	0.02	0.02	0.1	0.1	0.1	1	0.1	0.5	0.1	0.1	0.1	0.1	0.5	0.01	0.1	0.5	3	0.06	0.08
AD81-3150		2.24	0.35	2.04	0.32	2.69	0.03	0.9	44.3	27.9	118	45.9	9.2	0.2	0.4	0.4	0.0	14.0	0.07	0.2	0.0	95		
AD81-3175		2.05	0.30	1.91	0.28	3.82	0.03	0.6	30.8	24.4	70	49.1	8.9	0.0	0.3	0.3	0.0	7.4	0.04	0.1	0.0	93		
AD81/8-3192,5		1.44	0.23	1.51	0.23	6.95	0.77	0.2	30.4	8.1	39	31.8	6.6	0.0	0.2	0.2	0.0	2.2	0.02	0.1	0.0	77	1.98	-4.86
AD81/8-3193,4		1.44	0.21	1.36	0.20	7.16	0.58	0.1	9.8	8.9	36	28.9	5.2	0.1	0.2	0.2	0.0	2.9	0.02	0.1	0.0	65	2.15	-2.77
AD81/8-3193,5		1.17	0.17	1.08	0.16	8.87	0.60	0.0	33.4	6.4	25	21.8	7.9	0.2	0.2	0.2	0.0	1.4	0.00	0.0	0.0	45	2.19	-3.41
AD81-3225		1.30	0.20	1.18	0.18	7.25	0.08	1.7	20.3	19.7	38	36.7	6.4	0.0	0.3	0.2	0.0	2.4	0.03	0.2	0.0	62		
AD84-2800		1.97	0.31	1.98	0.30	3.04	0.16	1.1	36.4	21.4	77	43.6	10.5	0.8	0.2	0.3	0.0	3.9	0.07	0.1	0.6	107		
AD84-2817		1.96	0.31	1.83	0.29	3.54	0.14	0.8	34.1	18.2	100	42.2	8.7	0.2	0.2	0.3	0.0	3.1	0.06	0.1	0.0	96		
AD84/2-2832,5		2.62	0.39	2.52	0.39	2.07	0.00	0.2	17.6	10.0	64	46.7	4.1	0.1	0.0	0.2	0.0	1.1	0.00	0.1	0.0	111	-3.53	-4.89
AD84/2-2833,5		2.43	0.35	2.28	0.36	2.38	0.00	0.1	21.0	12.5	72	57.0	7.2	0.0	0.2	0.3	0.0	1.2	0.00	0.0	0.0	104	-2.62	-4.42
AD84-2850		1.92	0.28	1.78	0.27	4.32	0.08	0.4	33.0	15.0	53	34.3	9.2	0.3	0.3	0.2	0.0	1.9	0.06	0.1	0.6	74		
AD84-2890		2.06	0.33	2.01	0.31	3.02	0.12	0.6	41.3	17.2	66	49.5	8.3	0.2	0.2	0.3	0.0	4.3	0.07	0.2	0.0	90		
AD92/3-2840,5		2.84	0.42	2.67	0.42	1.77	0.09	0.0	47.3	11.5	77	42.6	10.5	0.1	0.1	0.3	0.0	1.9	0.03	0.0	0.0	112	-0.24	-3.69
AD92-2870		2.23	0.35	2.19	0.32	2.49	0.11	0.2	62.6	30.5	71	67.4	11.4	0.1	0.2	0.4	0.0	4.1	0.09	0.4	0.0	115		
AD92-2890		2.25	0.34	2.17	0.33	2.52	0.10	0.4	48.7	20.0	74	51.9	12.4	0.2	0.2	0.4	0.0	4.3	0.08	0.3	0.5	109		
AD92/4-2921,5		1.67	0.24	1.72	0.25	6.21	0.14	0.3	40.6	11.6	58	39.9	9.1	0.4	0.2	0.3	0.0	0.8	0.03	0.0	1.0	82	1.03	-3.18
AD92/4-2922		1.61	0.24	1.54	0.24	6.12	0.13	0.3	37.9	11.2	58	38.2	8.9	0.4	0.2	0.3	0.0	1.4	0.03	0.0	1.0	76	1.02	-3.44
AD92/4-2922,55		1.62	0.25	1.62	0.23	6.25	0.13	13.9	38.2	11.2	56	37.5	8.3	0.4	0.2	0.3	0.0	1.6	0.03	0.0	1.2	74	1.06	-3.27
AD92-2950		2.11	0.32	2.07	0.31	3.08	0.14	0.5	36.9	18.7	66	44.1	11.4	0.2	0.2	0.3	0.0	2.8	0.08	0.2	0.0	104		
AD92-2980		2.17	0.32	2.01	0.31	3.38	0.11	0.5	39.2	20.3	65	45.0	9.4	0.1	0.2	0.3	0.0	2.4	0.07	0.2	0.5	98		
AD92/5-3009,3		2.11	0.32	2.08	0.29	3.95	0.09	0.1	51.3	14.8	70	48.2	4.5	0.2	0.2	0.4	0.0	1.4	0.03	0.0	0.6	96	-0.14	-3.93
AD92/5-3009,7		2.16	0.32	2.09	0.30	3.96	0.10	0.0	50.0	15.4	72	54.2	5.6	0.2	0.2	0.4	0.0	1.0	0.04	0.0	0.6	97	-0.01	-4.01
AD92-3040		1.95	0.31	1.97	0.30	4.20	0.14	0.3	39.9	19.7	59	41.4	9.6	0.2	0.3	0.3	0.0	3.9	0.05	0.2	0.0	92		
AD92-3080		2.20	0.33	2.16	0.31	3.56	0.12	0.3	42.0	21.6	74	47.2	7.9	0.2	0.2	0.3	0.0	2.4	0.06	0.2	0.0	95		
AD92/6-3111,5		2.73	0.42	2.53	0.38	1.65	0.08	0.1	31.5	14.3	84	44.7	6.0	0.0	0.2	0.4	0.0	3.1	0.09	0.2	0.0	115	-0.21	-3.78
AD92-3170		2.13	0.33	2.02	0.33	3.31	0.10	0.4	45.2	20.2	66	47.4	8.3	0.1	0.3	0.3	0.0	1.3	0.06	0.2	0.8	97		
AD92-3230		2.23	0.35	2.09	0.32	3.17	0.09	0.3	43.3	18.0	67	47.5	8.2	0.1	0.3	0.3	0.0	2.5	0.07	0.2	0.6	88		
AD92-3270		2.07	0.33	2.09	0.30	4.43	0.11	0.2	55.4	15.3	71	42.7	7.6	0.2	0.3	0.3	0.0	4.1	0.06	0.2	0.7	71		
AD92/7-3327,5		2.76	0.41	2.65	0.39	0.88	0.04	0.4	28.1	13.3	109	65.5	8.5	0.0	0.3	0.5	0.0	1.1	0.13	0.1	0.0	118	0.89	-6.34
AD92/7-3329		2.10	0.30	1.90	0.29	4.69	0.00	5.7	15.9	10.5	48	30.6	3.9	0.1	0.2	0.2	0.0	1.2	0.01	0.0	0.0	74	1.41	-4.11
AD92-3360		2.17	0.34	2.12	0.32	2.83	0.05	0.2	61.5	14.3	69	47.5	5.8	0.1	0.3	0.4	0.0	2.5	0.05	0.2	0.0	87		
AD92-3400		2.12	0.33	2.05	0.30	3.03	0.06	0.2	44.7	12.6	65	42.1	5.4	0.1	0.2	0.3	0.0	2.4	0.06	0.2	0.0	86		
AD92/8-3431,85		2.13	0.33	2.15	0.31	2.83	0.00	0.3	44.2	15.1	71	44.5	4.3	0.1	0.2	0.4	0.0	1.3	0.07	0.2	0.0	120	1.28	-3.29
AD92/8-3432		2.34	0.33	2.13	0.30	2.63	0.04	0.2	56.3	16.6	70	48.9	5.3	0.0	0.2	0.5	0.0	1.7	0.09	0.2	0.0	122	1.43	-3.40
AD92/8-3433		2.49	0.39	2.52	0.38	1.88	0.30	2.9	53.1	32.1	90	65.5	91.5	0.0	0.2	0.5	0.1	1.0	0.06	0.3	0.9	132	1.28	-4.18
AD92-3460		2.01	0.32	1.92	0.29	3.65	0.07	0.4	35.4	19.2	134	37.3	7.4	0.2	0.3	0.3	0.0	1.6	0.04	0.2	0.0	84		
AD92/9-3504,4		2.42	0.38	2.36	0.36	2.17	0.03	0.4	28.0	11.9	65	43.3	5.0	0.0	0.3	0.4	0.0	2.1	0.06	0.1	0.0	131	1.09	-5.34
AD92-3530		1.93	0.30	1.90	0.29	3.78	0.11	0.5	46.5	18.8	60	39.8	7.8	0.1	0.4	0.3	0.1	1.3	0.06	0.2	0.0	84		
STRHT9-3610		1.46	0.22	1.36	0.21	6.72	0.18	0.2	13.7	2345.8	38	179.5	24.5	0.0	40.3	0.8	0.2	0.0	0.04	0.0	0.0	52		
STRHT9-3680		1.02	0.16	0.94	0.13	9.46	0.00	0.1	10.9	6.3	29	24.0	4.2	0.0	0.2	0.1	0.0	0.0	0.01	0.0	0.0	28		
STRHT9-3780		2.06	0.30	1.93	0.28	3.87	0.39	0.7	27.3	16.1	54	48.6	5.6	0.0	0.3	0.2	0.0	0.0	0.04	0.0	0.0	94		
STRHT9-4110		1.92	0.29	1.82	0.28	4.89	0.00	0.4	46.3	18.6	81	49.3	5.6	0.1	0.3	0.3	0.0	0.0	0.03	0.2	0.0	69		
STRHT9-4250		1.95	0.30	1.92	0.29	4.89	0.00	0.5	52.7	15.8	76	48.6	7.3	0.2	0.3	0.3	0.0	0.0	0.04	0.1	0.0	69		
STRHT9-4290		1.79	0.27	1.82	0.26	5.53	0.00	0.4	51.1	15.6	68	46.4	4.1	0.1	0.3	0.3	0.0	0.0	0.03	0.1	0.0	65		
STRHT9-4360		2.73	0.43	2.62	0.39	3.02	0.12	0.3	41.5	16.1	79	55.2	23.4	0.2	0.3	0.3	0.0	0.0	0.05	0.1	0.0	65		

Samples	$^{87}Sr/^{86}Sr$	$CaCO_3$	TOC	CIA	CPA	Si/Al	K/Al	Na/Al	B/Al*	Th/U	Cr/V	Y/Ni	Cr/Ni	Th/Sc	Zr/Sc	La/Sc	Ti/Zr	TOC/S
Unit		[%]	[%]															
DL	0.000005	1	0.1															
AD81-3150				67.29	88.67	2.93	0.33	0.11	124.51	5.19	0.64	0.50	1.91	0.78	9.00	2.16	31.40	
AD81-3175				67.64	89.31	2.95	0.35	0.10	139.06	4.48	0.76	0.42	1.79	0.72	8.15	2.08	32.27	
AD81/8-3192,5		61	0.09	68.44	92.61	2.75	0.44	0.07	185.86	4.08	0.74	0.53	2.12	0.61	6.71	2.18	35.72	0.12
AD81/8-3193,4		56	0.18	67.98	91.82	2.88	0.42	0.08	166.24	4.18	0.64	0.56	1.87	0.66	7.37	2.36	34.85	0.30
AD81/8-3193,5		73	0.12	67.37	91.28	2.96	0.43	0.08	182.90	5.57	0.60	0.67	1.55	0.78	7.72	2.60	29.51	0.20
AD81-3225				66.90	88.72	2.94	0.35	0.11	141.52	2.58	0.64	0.37	1.47	0.78	9.26	2.46	29.93	
AD84-2800				69.65	90.42	3.47	0.32	0.09	154.97	3.90	0.76	0.48	1.86	0.87	9.83	2.13	29.08	
AD84-2817				69.75	90.19	3.29	0.31	0.09	144.46	3.53	0.79	0.48	1.92	0.88	9.98	2.21	29.52	
AD84/2-2832,5		19	0.30	70.75	89.97	3.22	0.28	0.10	143.59	4.48	0.81	0.56	2.46	0.69	14.01	2.05	28.25	
AD84/2-2833,5		23	0.41	73.06	92.05	2.68	0.28	0.07	124.41	4.08	0.78	0.41	2.25	0.62	10.21	1.66	31.08	
AD84-2850				67.55	88.04	3.80	0.30	0.12	137.52	3.50	0.75	0.58	1.97	0.84	13.78	2.45	24.80	
AD84-2890				67.86	88.45	3.38	0.31	0.11	129.85	4.39	0.73	0.44	1.64	0.78	9.65	2.07	31.53	
AD92/3-2840,5		18	0.31	68.98	88.67	3.31	0.28	0.11	144.29	4.75	0.77	0.65	2.70	0.76	15.25	2.23	27.00	3.47
AD92-2870				69.89	90.56	2.94	0.32	0.09	142.06	6.39	0.72	0.34	1.50	0.72	8.09	1.77	34.75	
AD92-2890				69.68	90.15	3.21	0.31	0.09	147.15	4.46	0.73	0.44	1.82	0.71	8.91	1.95	31.84	
AD92/4-2921,5		54	0.44	70.99	91.16	2.42	0.31	0.08	152.24	3.55	0.74	0.42	2.03	0.65	7.11	1.77	35.26	3.13
AD92/4-2922		51	0.48	70.69	90.93	2.44	0.31	0.09	140.55	3.79	0.69	0.46	1.95	0.65	7.47	1.81	33.55	3.69
AD92/4-2922,55		46	0.44	70.77	90.99	2.49	0.31	0.08	140.28	3.40	0.68	0.44	1.98	0.68	7.78	1.97	35.45	3.38
AD92-2950				69.16	89.86	3.30	0.32	0.10	149.82	4.12	0.79	0.49	2.15	0.79	10.09	2.11	30.61	
AD92-2980				67.95	88.26	3.40	0.30	0.11	146.77	4.23	0.79	0.48	2.10	0.72	10.22	2.12	31.13	
AD92/5-3009,3		31	0.56	71.33	91.67	2.50	0.32	0.08	131.86	5.56	0.77	0.45	2.24	0.71	7.56	1.84	35.66	6.21
AD92/5-3009,7		34	0.55	71.13	91.46	2.50	0.32	0.08	133.43	4.84	0.77	0.41	1.99	0.66	7.64	1.83	35.89	5.50
AD92-3040				67.36	87.80	3.21	0.30	0.12	142.52	4.09	0.81	0.50	2.12	0.75	10.11	2.09	31.14	
AD92-3080				66.79	87.97	3.27	0.32	0.12	142.16	4.39	0.80	0.46	2.00	0.72	9.34	1.89	31.19	
AD92/6-3111,5		17	0.26	67.63	88.90	2.53	0.33	0.11	130.93	5.40	0.81	0.60	2.57	0.64	8.66	1.82	34.62	3.31
AD92-3170				66.09	87.13	3.15	0.32	0.13	140.70	4.64	0.80	0.47	2.00	0.73	9.61	1.95	30.29	
AD92-3230				66.36	86.95	3.22	0.30	0.13	128.63	4.14	0.78	0.48	1.85	0.70	9.97	2.05	31.92	
AD92-3270				66.71	87.14	3.21	0.30	0.13	107.52	4.60	0.78	0.50	2.06	0.71	10.08	1.97	30.66	
AD92/7-3327,5		11	0.13	67.01	87.17	2.68	0.29	0.13	126.29	5.13	0.86	0.42	1.86	0.66	9.38	1.68	29.82	3.29
AD92/7-3329		35	0.14	68.85	89.78	2.62	0.33	0.10	120.99	5.19	0.82	0.73	2.43	0.75	6.95	2.30	36.05	
AD92-3360				66.62	87.70	2.96	0.32	0.12	116.78	4.95	0.75	0.46	1.99	0.66	8.24	1.79	33.47	
AD92-3400				66.15	87.09	3.32	0.31	0.13	125.22	4.74	0.73	0.50	1.93	0.69	9.26	1.95	32.86	
AD92/8-3431,85		22	0.18	70.88	92.48	2.22	0.36	0.07	140.17	5.89	0.71	0.47	2.28	0.75	6.85	1.95	37.91	
AD92/8-3432		24	0.18	70.89	92.50	2.22	0.36	0.07	140.34	5.65	0.72	0.44	2.07	0.75	6.87	1.99	38.41	4.58
AD92/8-3433		17	0.37	69.78	90.51	2.34	0.32	0.09	139.53	5.79	0.71	0.38	1.75	0.82	8.48	1.95	34.09	1.23
AD92-3460				65.58	86.35	3.42	0.30	0.13	130.34	4.05	1.03	0.55	2.90	0.71	10.86	2.08	28.53	
AD92/9-3504,4		19	0.14	68.08	90.44	2.81	0.37	0.09	162.25	5.00	0.68	0.56	2.18	0.89	9.76	2.14	29.38	4.80
AD92-3530				65.88	86.83	3.32	0.31	0.13	130.67	4.29	1.22	0.50	3.23	0.75	10.38	2.07	29.83	
STRHT9-3610				66.82	90.23	4.22	0.41	0.09	154.04	2.60	4.25	0.08	1.47	0.74	11.63	2.17	22.83	
STRHT9-3680				69.54	92.20	2.91	0.39	0.07	118.39	4.29	1.13	0.46	1.97	0.75	8.60	3.13	31.37	
STRHT9-3780				66.25	89.98	3.42	0.42	0.09	152.24	3.50	0.89	0.39	1.81	0.76	11.04	2.17	28.64	
STRHT9-4110				70.43	93.47	2.45	0.41	0.06	106.46	5.40	0.80	0.38	1.78	0.68	7.58	2.06	34.95	
STRHT9-4250				70.88	92.82	2.42	0.37	0.07	103.91	6.21	0.76	0.40	1.81	0.73	7.93	2.10	34.01	
STRHT9-4290				70.93	92.79	2.44	0.37	0.07	107.39	5.27	0.73	0.40	1.75	0.72	7.72	2.11	35.31	
STRHT9-4360				64.67	86.12	3.04	0.32	0.14	89.80	4.70	0.71	0.47	1.59	0.67	9.99	2.09	30.45	

Gosau	Samples	Location	Type	Unit	SiO_2 [%]	Al_2O_3 [%]	Fe_2O_3 [%]	MgO [%]	CaO [%]	Na_2O [%]	K_2O [%]	TiO_2 [%]	P_2O_5 [%]	MnO [%]	Cr_2O_3 [%]	LOI [%]	Sum [%]	Sc [ppm]	Ba [ppm]	Be [ppm]
				DL	0.01	0.01	0.04	0.01	0.01	0.01	0.01	0.01	0.01	0.01	0.002	-5.1	0.01	1	1	1
Gießhübl S.	STRHT9-4420	Strasshof T9	cutting		28.63	8.68	4.42	4.21	25.05	0.51	2.10	0.38	0.16	0.18	0.009	25.5	99.79	9	208	0
Gießhübl S.	STRHT9-4550	Strasshof T9	cutting		34.10	11.88	4.33	4.52	19.11	0.55	3.05	0.50	0.10	0.08	0.011	21.6	99.78	11	330	2
Gießhübl S.	STRHT9-4645	Strasshof T9	cutting		49.23	10.86	3.96	4.04	12.26	1.02	2.48	0.56	0.10	0.06	0.012	15.2	99.81	10	304	2
Gießhübl S.	LI08-11	Lilienfeld	outcrop		41.20	11.22	3.11	1.70	18.70	0.11	2.58	0.54	0.12	0.03	0.025	20.5	99.89	13	177	1
Gießhübl S.	LI08-13	Lilienfeld	outcrop		19.02	6.42	2.47	1.09	35.24	0.21	1.73	0.26	0.07	0.10	0.007	33.2	99.89	6	184	0
Gießhübl S.	LI08-15R	Lilienfeld	outcrop		36.76	6.15	2.99	1.22	26.21	0.06	1.67	0.35	0.05	0.06	0.042	24.3	99.92	8	73	0
Gießhübl S.	LI08-15G	Lilienfeld	outcrop		28.33	4.02	1.51	0.91	34.05	0.04	1.04	0.22	0.06	0.07	0.031	29.6	99.93	6	46	0
Gießhübl S.	LI08-16	Lilienfeld	outcrop		47.58	6.29	1.73	0.88	20.88	0.08	1.28	0.53	0.06	0.03	0.068	20.5	99.91	8	99	0
Gießhübl S.	LI08-20	Lilienfeld	outcrop		21.80	6.29	3.10	2.11	33.15	0.32	1.71	0.26	0.09	0.10	0.012	30.9	99.88	6	154	1
Gießhübl S.	LI08-22	Lilienfeld	outcrop		27.67	7.31	2.62	2.73	28.89	0.41	1.91	0.32	0.07	0.05	0.018	27.9	99.88	7	123	0
Gießhübl S.	P-6	Groisbach	outcrop		18.62	5.97	1.97	1.25	37.78	0.38	1.44	0.25	0.07	0.08	0.008	32.0	99.87	6	202	0
Gießhübl S.	P-30	Groisbach	outcrop		25.85	4.94	2.90	0.98	34.75	0.05	1.39	0.26	0.05	0.07	0.021	28.6	99.87	7	355	0
Gießhübl S.	P-121	Groisbach	outcrop		18.23	5.72	2.36	1.52	36.10	0.23	1.58	0.24	0.06	0.07	0.007	33.8	99.88	5	131	0
Gießhübl S.	P-182R	Groisbach	outcrop		21.43	6.35	3.02	1.71	34.21	0.27	1.72	0.27	0.07	0.06	0.007	30.8	99.88	6	126	0
Gießhübl S.	P-182G	Groisbach	outcrop		24.17	6.47	2.42	1.64	33.19	0.29	1.71	0.26	0.04	0.07	0.007	29.6	99.89	6	123	0
Glinzendorf S.	MT1-3165	Markgrafneusiedl T1	cutting		47.81	12.85	4.65	2.95	11.98	1.02	2.74	0.58	0.12	0.12	0.013	14.9	99.77	13	393	1
Glinzendorf S.	MT1-3195	Markgrafneusiedl T1	cutting		51.48	12.98	5.36	2.96	9.64	1.09	2.73	0.61	0.14	0.12	0.012	12.6	99.75	12	641	1
Glinzendorf S.	MT1-3207,80	Markgrafneusiedl T1	core																	
Glinzendorf S.	MT1-3250	Markgrafneusiedl T1	cutting		47.82	14.07	5.85	3.05	10.38	0.90	3.19	0.66	0.12	0.09	0.017	13.6	99.76	15	397	2
Glinzendorf S.	MT1-3272,10	Markgrafneusiedl T1	core																	
Glinzendorf S.	MT1-3272,50-60	Markgrafneusiedl T1	core																	
Glinzendorf S.	MT1-3275,30-43	Markgrafneusiedl T1	core		46.03	17.83	6.81	3.41	7.53	0.75	4.01	0.79	0.10	0.13	0.017	12.4	99.79	18	481	2
Glinzendorf S.	MT1-3305	Markgrafneusiedl T1	cutting		47.51	15.45	5.71	2.66	9.99	0.79	3.52	0.72	0.11	0.11	0.016	13.2	99.79	17	475	2
Glinzendorf S.	MT1-3335	Markgrafneusiedl T1	cutting		50.38	14.54	5.30	2.68	9.23	0.68	3.21	0.64	0.09	0.09	0.017	12.9	99.81	16	474	2
Glinzendorf S.	MT1-3355	Markgrafneusiedl T1	cutting		49.48	14.21	5.76	2.90	9.55	0.88	3.08	0.65	0.12	0.10	0.014	13.0	99.78	14	597	2
Glinzendorf S.	MT1-3380	Markgrafneusiedl T1	cutting		46.45	13.81	5.72	2.85	11.95	0.75	3.02	0.64	0.11	0.12	0.015	14.4	99.81	14	440	3
Glinzendorf S.	MT1-3406,20-30	Markgrafneusiedl T1	core		37.04	12.48	4.66	3.21	18.59	0.54	2.87	0.57	0.09	0.09	0.019	19.6	99.80	12	238	2
Glinzendorf S.	MT1-3409,24-30	Markgrafneusiedl T1	core		73.09	13.07	3.60	1.45	0.26	0.93	2.43	0.92	0.13	0.00	0.019	3.9	99.84	13	286	1
Glinzendorf S.	MT1-3409,70-82	Markgrafneusiedl T1	core																	
Glinzendorf S.	MT1-3445	Markgrafneusiedl T1	cutting		48.04	14.08	6.04	3.11	10.15	0.96	3.09	0.65	0.12	0.10	0.015	13.4	99.80	14	428	2
Glinzendorf S.	MT1-3500	Markgrafneusiedl T1	cutting		47.67	12.01	5.34	3.13	12.51	0.66	2.62	0.60	0.11	0.10	0.015	15.1	99.82	13	363	1
Glinzendorf S.	MT1-3544,45-65	Markgrafneusiedl T1	core																	
Glinzendorf S.	MT1-3545,90-3546	Markgrafneusiedl T1	core																	
Glinzendorf S.	MT1-3546,25-55	Markgrafneusiedl T1	core		44.31	12.19	5.03	3.38	14.20	0.58	2.67	0.63	0.14	0.07	0.013	16.6	99.83	12	251	2
Glinzendorf S.	MT1-3547,50-65	Markgrafneusiedl T1	core		40.86	11.73	4.65	3.28	16.58	0.66	2.64	0.59	0.12	0.07	0.012	18.6	99.81	11	256	2
Glinzendorf S.	MT1-3605	Markgrafneusiedl T1	cutting		46.66	14.30	6.07	3.05	10.96	0.81	3.22	0.67	0.12	0.11	0.015	13.8	99.81	15	406	3
Glinzendorf S.	MT1-3650	Markgrafneusiedl T1	cutting		46.22	13.57	5.94	2.96	11.85	0.85	2.97	0.63	0.13	0.10	0.014	14.6	99.81	14	384	2
Glinzendorf S.	MT1-3695	Markgrafneusiedl T1	cutting		45.02	13.36	5.70	2.92	12.01	0.81	2.89	0.62	0.12	0.10	0.013	16.2	99.80	14	395	3
Glinzendorf S.	MT1-3695-U	Markgrafneusiedl T1	cutting		46.74	13.62	5.73	2.91	10.50	0.88	2.96	0.63	0.12	0.10	0.016	15.6	99.77	14	719	2
Glinzendorf S.	MT1-3743,55-60	Markgrafneusiedl T1	core		35.23	12.38	4.92	3.28	18.96	0.52	2.86	0.52	0.11	0.09	0.017	20.9	99.78	12	228	2
Glinzendorf S.	MT1-3743,90-3744	Markgrafneusiedl T1	core																	
Glinzendorf S.	MT1-3744,10-20	Markgrafneusiedl T1	core		36.68	11.79	4.64	3.09	19.19	0.56	2.68	0.54	0.11	0.10	0.018	20.4	99.81	11	226	1
Glinzendorf S.	MT1-3745,50	Markgrafneusiedl T1	core		38.37	13.24	4.73	3.19	17.24	0.58	3.02	0.60	0.08	0.09	0.019	18.6	99.81	13	254	2
Glinzendorf S.	MT1-3746,50-3747	Markgrafneusiedl T1	core		35.74	12.63	4.79	3.24	19.04	0.54	2.87	0.54	0.10	0.10	0.018	20.2	99.79	12	235	2
Glinzendorf S.	MT1-3747,20	Markgrafneusiedl T1	core		36.54	12.44	4.39	3.05	19.05	0.55	2.82	0.57	0.10	0.08	0.018	20.2	99.81	12	251	1

Samples	Co	Cs	Ga	Hf	Nb	Rb	Sn	Sr	Ta	Th	U	V	W	Zr	Y	La	Ce	Pr	Nd	Sm	Eu	Gd	Tb	Dy	Ho
Unit	[ppm]	[ppm]	[ppm]	[ppm]	[ppm]	[ppm]	[ppm]	[ppm]	[ppm]	[ppm]	[ppm]	[ppm]	[ppm]	[ppm]	[ppm]	[ppm]	[ppm]	[ppm]	[ppm]	[ppm]	[ppm]	[ppm]	[ppm]	[ppm]	[ppm]
DL	0.2	0.1	0.5	0.1	0.1	0.1	1	0.5	0.1	0.2	0.1	8	0.5	0.1	0.1	0.1	0.1	0.02	0.3	0.05	0.02	0.05	0.01	0.05	0.02
STRHT9-4420	8.8	4.9	11.9	1.7	7.9	90.2	2	633.5	0.5	6.2	1.8	79	1.4	74.9	20.2	20.7	49.6	5.06	20.2	4.42	0.94	4.07	0.66	3.47	0.71
STRHT9-4550	10.4	7.0	15.5	2.6	10.2	120.9	3	559.6	0.7	8.6	2.5	109	1.9	102.2	19.0	24.0	53.2	5.62	21.5	4.23	0.86	3.68	0.62	3.43	0.66
STRHT9-4645	10.4	5.1	14.3	4.3	11.0	97.1	3	330.1	0.8	8.4	2.5	88	2.2	162.7	21.8	24.9	58.0	6.09	24.8	4.86	0.97	4.29	0.70	3.95	0.80
LI08-11	17.3	9.9	13.9	2.9	10.1	112.2	2	207.8	0.6	8.3	2.4	100	1.6	109.2	20.2	21.9	42.2	5.43	22.2	4.02	0.87	3.61	0.59	3.31	0.67
LI08-13	7.7	4.6	8.3	1.4	5.0	68.1	1	445.8	0.3	4.4	1.0	66	1.1	45.1	15.5	16.3	26.6	3.45	12.8	2.54	0.53	2.36	0.39	2.17	0.47
LI08-15R	9.4	7.2	7.0	2.5	5.9	70.3	1	192.8	0.4	5.3	1.1	66	1.1	93.3	22.2	19.6	31.0	4.48	19.8	3.53	0.77	3.34	0.54	3.12	0.66
LI08-15G	4.8	4.2	5.0	1.8	3.5	42.6	0	225.2	0.2	3.3	0.8	45	0.6	61.7	19.6	16.0	23.3	3.68	17.1	2.89	0.69	2.97	0.48	2.66	0.59
LI08-16	9.8	6.7	7.2	4.4	9.4	57.9	1	163.2	0.7	7.5	2.4	62	1.4	174.2	23.4	23.3	42.5	5.55	22.9	4.06	0.82	3.72	0.63	3.70	0.73
LI08-20	6.4	5.0	8.8	1.8	5.5	70.8	2	393.8	0.3	5.3	1.4	54	1.3	61.8	18.6	18.1	30.3	3.79	15.1	2.73	0.53	2.61	0.44	2.47	0.52
LI08-22	8.2	5.9	9.0	1.8	6.6	81.1	2	341.3	0.5	6.1	1.8	71	1.4	74.1	15.1	16.3	32.1	3.94	15.1	2.92	0.57	2.55	0.43	2.51	0.48
P-6	7.1	4.0	7.7	1.5	5.5	63.5	2	633.1	0.4	3.9	1.5	60	1.2	53.5	15.9	17.6	29.7	3.78	15.6	2.52	0.52	2.44	0.40	2.08	0.47
P-30	6.0	4.2	6.4	1.9	4.7	61.3	1	512.4	0.3	3.9	0.7	50	0.8	62.3	21.4	17.8	35.6	4.51	19.1	3.50	0.73	3.46	0.55	3.20	0.63
P-121	7.5	4.1	7.8	1.2	5.3	69.1	1	570.2	0.3	5.0	1.2	53	1.0	46.2	12.6	15.2	26.5	3.37	14.1	2.32	0.46	2.11	0.33	1.92	0.39
P-182R	5.2	4.5	8.1	1.5	5.4	73.6	1	512.4	0.3	4.7	0.9	50	1.2	47.8	14.2	17.1	31.2	4.02	15.5	2.84	0.56	2.64	0.41	2.09	0.49
P-182G	5.2	4.2	8.5	1.3	5.6	70.1	2	479.8	0.4	5.6	0.9	57	1.0	46.9	12.0	16.7	29.2	3.70	15.0	2.65	0.53	2.27	0.36	1.94	0.41
MT1-3165	12.3	8.7	16.4	3.5	11.8	117.3	3	488.0	0.9	10.6	3.1	111	1.8	118.6	21.3	27.1	58.0	6.43	25.0	4.67	0.92	3.88	0.66	3.67	0.73
MT1-3195	13.2	8.1	15.8	3.7	11.6	118.7	3	471.7	0.9	10.9	3.5	109	2.0	138.8	22.5	27.7	59.4	6.73	26.6	4.80	0.99	4.00	0.69	3.85	0.78
MT1-3207,80																									
MT1-3250	22.7	9.6	16.9	3.7	13.9	128.3	4	457.3	6.2	12.0	3.5	127	54.6	120.7	22.7	29.0	62.7	7.03	28.4	5.07	1.05	4.30	0.72	4.06	0.81
MT1-3272,10																									
MT1-3272,50-60																									
MT1-3275,30-43	19.9	9.0	22.5	3.8	13.4	125.8	3	189.5	1.0	11.9	3.0	143	2.1	122.0	24.6	30.2	63.5	7.90	31.1	5.60	1.01	4.71	0.68	4.30	0.88
MT1-3305	19.5	10.2	20.6	3.8	12.7	140.7	4	371.2	1.1	12.9	4.2	131	4.5	132.0	23.5	30.5	64.3	7.20	27.5	5.12	1.04	4.39	0.72	3.98	0.82
MT1-3335	16.1	9.7	18.6	3.4	11.3	126.3	4	245.8	0.9	11.0	4.0	123	11.0	116.5	21.0	27.0	59.2	6.45	25.7	4.51	0.98	3.96	0.65	3.87	0.74
MT1-3355	19.7	9.2	18.5	3.8	12.8	129.0	4	356.7	3.3	11.0	3.5	123	27.0	125.7	22.1	29.4	63.4	6.92	27.3	4.97	1.05	4.29	0.73	4.13	0.82
MT1-3380	16.1	9.1	18.1	3.5	12.4	120.7	4	321.8	0.9	11.0	3.7	116	2.0	124.2	21.9	27.8	58.7	6.55	25.9	4.69	1.00	4.27	0.69	3.91	0.80
MT1-3406,20-30	14.7	9.6	14.7	3.6	11.1	99.1	3	512.3	0.7	9.1	3.0	121	2.0	103.5	20.7	24.1	50.4	6.34	23.4	4.48	0.76	3.75	0.56	3.71	0.78
MT1-3409,24-30	16.6	7.6	15.0	8.9	16.5	75.0	3	111.5	1.3	13.4	4.3	92	3.1	301.1	36.0	37.1	79.1	9.72	39.2	6.93	1.17	6.34	0.94	6.44	1.27
MT1-3409,70-82																									
MT1-3445	17.4	9.4	19.4	3.8	12.8	129.9	3	368.5	1.0	11.8	3.2	122	2.3	138.3	23.4	29.7	65.1	7.18	28.0	5.03	1.09	4.39	0.71	4.00	0.81
MT1-3500	14.6	7.2	16.3	4.2	10.7	107.1	3	253.1	0.8	9.1	3.0	108	2.4	149.5	22.7	26.4	56.7	6.45	25.2	4.68	0.98	4.04	0.69	3.81	0.76
MT1-3544,45-65																									
MT1-3545,90-3546																									
MT1-3546,25-55	12.4	7.1	15.4	3.8	11.3	85.9	2	273.4	0.8	9.7	3.1	109	1.9	128.5	24.6	25.6	53.2	6.69	26.7	5.11	0.89	4.51	0.65	4.43	0.88
MT1-3547,50-65	11.3	7.2	15.1	3.9	11.4	87.3	2	267.1	1.2	8.7	2.7	99	1.8	119.1	21.5	24.5	49.8	6.30	24.5	4.37	0.79	4.01	0.56	3.80	0.77
MT1-3605	15.6	9.0	18.3	3.4	12.1	129.0	4	294.7	0.9	11.4	3.5	125	2.2	125.6	23.0	28.6	62.4	6.95	26.8	4.99	1.06	4.53	0.72	4.15	0.78
MT1-3650	16.8	8.7	17.7	3.4	12.1	124.0	4	347.0	0.8	10.7	3.4	119	2.3	124.7	23.3	28.0	60.8	6.81	27.1	5.08	1.07	4.37	0.73	3.99	0.85
MT1-3695	14.9	8.6	17.6	3.7	11.7	121.3	3	384.9	0.9	10.0	3.3	118	2.2	126.8	23.0	27.5	60.0	6.70	24.7	4.86	1.04	4.33	0.72	4.07	0.82
MT1-3695-U	15.4	8.8	17.2	3.4	11.8	125.5	4	369.1	0.9	10.2	3.2	121	2.2	129.1	22.7	28.3	62.8	6.90	27.3	5.06	1.06	4.36	0.72	3.74	0.78
MT1-3743,55-60	13.2	9.2	15.9	3.6	10.1	99.8	3	569.9	0.6	9.0	2.6	127	1.7	91.1	19.4	22.8	46.9	6.04	24.0	4.24	0.72	3.72	0.51	3.56	0.68
MT1-3743,90-3744																									
MT1-3744,10-20	12.9	8.8	14.4	3.4	9.9	90.7	2	534.9	0.7	8.5	2.7	118	1.8	105.3	20.6	23.7	48.1	6.04	23.6	4.50	0.73	3.88	0.53	3.60	0.69
MT1-3745,50	12.9	9.5	16.3	3.5	11.4	99.1	2	477.6	0.7	9.0	3.1	123	2.0	100.9	19.3	23.4	48.6	6.05	23.0	4.28	0.69	3.52	0.50	3.52	0.71
MT1-3746,50-3747	12.7	9.5	15.6	3.1	10.0	97.0	2	567.8	0.8	8.4	2.7	120	1.9	93.4	20.4	23.0	47.8	6.15	23.1	4.57	0.76	3.87	0.53	3.60	0.70
MT1-3747,20	14.1	9.8	14.9	2.6	10.8	95.1	2	486.9	0.7	9.1	2.7	114	1.8	99.8	20.2	24.2	50.8	6.20	23.5	4.37	0.73	3.70	0.51	3.60	0.69

Samples	Er	Tm	Yb	Lu	TOT/C	TOT/S	Mo	Cu	Pb	Zn	Ni	As	Cd	Sb	Bi	Ag	Au	Hg	Tl	Se	B	$\delta^{13}C$	$\delta^{18}O$
Unit	[ppm]	[ppm]	[ppm]	[ppm]	[%]	[%]	[ppm]	[ppm]	[ppm]	[ppm]	[ppm]	[ppm]	[ppm]	[ppm]	[ppm]	[ppm]	[ppm]	[ppm]	[ppm]	[ppm]	[ppm]	[VPDB]	[VPDB]
DL	0.03	0.01	0.05	0.01	0.02	0.02	0.1	0.1	0.1	1	0.1	0.5	0.1	0.1	0.1	0.1	0.5	0.01	0.1	0.5	3	0.06	0.08
STRHT9-4420	1.90	0.28	1.86	0.27	6.50	0.00	0.4	20.8	11.6	50	30.8	4.4	0.1	0.3	0.2	0.0	0.6	0.05	0.0	0.0	55		
STRHT9-4550	2.01	0.31	1.97	0.28	5.44	0.14	0.6	23.8	14.8	57	34.1	11.1	0.0	0.4	0.3	0.0	0.0	0.06	0.0	0.0	93		
STRHT9-4645	2.27	0.34	2.20	0.32	3.60	0.09	0.3	19.1	9.4	50	28.8	5.0	0.1	0.2	0.2	0.0	8.0	0.07	0.0	0.0	77		
LI08-11	1.96	0.30	1.99	0.30	4.07	0.00	0.0	29.8	8.0	46	101.7	6.6	0.1	0.0	0.3	0.0	1.5	0.01	0.0	0.0	114		
LI08-13	1.41	0.21	1.34	0.20	7.91	0.00	0.2	12.8	6.1	27	33.2	6.2	0.1	0.2	0.2	0.0	0.6	0.03	0.0	0.0	51		
LI08-15R	2.03	0.30	1.85	0.28	5.73	0.00	0.0	7.8	4.5	41	88.5	3.4	0.2	0.0	0.1	0.0	0.0	0.00	0.0	0.0	73		
LI08-15G	1.59	0.25	1.30	0.21	7.51	0.00	0.0	8.1	4.3	23	53.2	5.4	0.2	0.0	0.1	0.0	1.8	0.00	0.0	0.0	45		
LI08-16	2.23	0.34	2.16	0.32	5.07	0.00	0.2	18.4	7.2	33	62.2	3.8	0.2	0.0	0.1	0.0	0.0	0.01	0.0	0.0	94		
LI08-20	1.48	0.22	1.43	0.22	7.61	0.00	0.2	8.7	6.5	27	51.8	5.7	0.1	0.2	0.2	0.0	0.9	0.01	0.0	0.6	76		
LI08-22	1.48	0.20	1.30	0.21	6.77	0.00	0.1	10.6	9.3	40	76.5	7.9	0.1	0.0	0.2	0.0	0.8	0.02	0.0	0.7	84		
P-6	1.46	0.22	1.42	0.20	8.16	0.00	0.1	14.2	5.2	33	23.5	3.8	0.2	0.0	0.1	0.0	0.9	0.01	0.0	0.0	47		
P-30	1.83	0.24	1.61	0.24	7.28	0.00	0.2	5.3	12.0	19	55.9	8.6	0.2	0.3	0.1	0.0	0.0	0.03	0.0	0.0	50		
P-121	1.11	0.16	1.14	0.17	8.08	0.00	0.1	14.0	6.8	30	35.3	3.5	0.2	0.0	0.2	0.0	0.0	0.02	0.0	0.0	47		
P-182R	1.30	0.19	1.17	0.18	7.53	0.00	0.2	13.0	6.8	28	33.1	3.5	0.1	0.2	0.2	0.0	0.0	0.07	0.0	0.0	51		
P-182G	1.25	0.17	1.18	0.18	7.27	0.00	0.0	13.8	3.7	35	30.3	3.1	0.1	0.0	0.1	0.0	0.5	0.01	0.0	0.0	45		
MT1-3165	2.04	0.30	1.95	0.29	3.40	0.25	1.3	29.5	227.1	87	39.8	12.2	0.3	0.5	0.3	0.0	0.5	0.09	0.1	0.8	85		
MT1-3195	2.09	0.32	2.03	0.31	2.77	0.47	1.8	27.5	26.4	68	48.0	21.0	0.3	1.2	0.3	0.0	0.0	0.14	0.2	1.2	86		
MT1-3207,80																						-4.25	-7.37
MT1-3250	2.38	0.34	2.22	0.33	3.14	0.45	1.5	2263.9	20.0	1742	425.1	24.4	1.0	1.1	0.4	2.9	0.0	0.64	0.1	0.6	99		
MT1-3272,10																						-3.21	-4.90
MT1-3272,50-60																						-2.54	-5.26
MT1-3275,30-43	2.49	0.37	2.46	0.44	2.41	0.03	0.0	38.0	14.6	43	48.7	10.9	0.0	0.2	0.4	0.0	1.4	0.46	0.0	0.0	119	-3.10	-5.19
MT1-3305	2.41	0.35	2.22	0.35	2.96	0.33	1.6	36.9	22.0	72	57.3	27.0	0.1	1.5	0.4	0.1	0.5	2.71	0.1	0.0	119		
MT1-3335	2.23	0.33	2.10	0.32	2.96	0.30	1.1	34.5	106.8	61	47.6	26.4	0.0	1.3	0.3	0.0	0.0	1.14	0.0	0.0	135		
MT1-3355	2.31	0.36	2.10	0.33	2.80	0.42	2.0	39.8	21.7	77	58.5	22.2	0.1	1.6	0.3	0.0	0.0	0.63	0.2	0.7	104		
MT1-3380	2.30	0.33	2.11	0.31	3.09	0.25	1.2	30.5	16.0	53	49.0	19.9	0.1	1.3	0.3	0.0	0.0	0.57	0.1	0.0	119		
MT1-3406,20-30	2.16	0.32	2.01	0.37	4.83	0.35	0.4	17.8	13.0	40	79.3	24.1	0.1	0.2	0.3	0.0	0.0	0.29	0.0	0.0	118	-1.59	-5.25
MT1-3409,24-30	3.76	0.52	3.38	0.57	0.12	0.77	2.9	35.5	24.8	58	53.8	32.7	0.0	0.3	0.3	0.0	1.2	0.83	0.1	0.5	133		
MT1-3409,70-82																							
MT1-3445	2.30	0.35	2.29	0.35	2.93	0.37	1.6	28.7	18.1	62	55.6	20.7	0.2	1.1	0.3	0.0	0.0	0.49	0.1	0.0	116		
MT1-3500	2.22	0.33	2.17	0.32	3.70	0.27	1.5	26.0	20.3	66	48.9	20.2	0.0	1.3	0.3	0.0	0.8	0.58	0.1	0.0	92		
MT1-3544,45-65																						-1.38	-4.99
MT1-3545,90-3546																						-0.97	-5.10
MT1-3546,25-55	2.43	0.35	2.33	0.36	3.95	0.13	0.3	21.9	10.7	40	42.9	13.4	0.1	0.3	0.3	0.0	0.0	0.43	0.0	0.0	119	-1.05	-5.13
MT1-3547,50-65	2.26	0.29	2.14	0.33	4.50	0.19	0.4	20.1	11.3	40	41.9	18.1	0.2	0.3	0.3	0.0	0.0	0.45	0.0	0.0	100	-0.84	-5.09
MT1-3605	2.27	0.36	2.38	0.35	3.33	0.29	1.6	33.4	19.3	55	55.7	31.9	0.1	1.6	0.3	0.0	0.0	1.13	0.2	0.6	101		
MT1-3650	2.30	0.36	2.20	0.34	3.52	0.49	1.2	28.9	19.3	54	51.1	27.3	0.2	1.3	0.3	0.0	0.5	0.63	0.1	0.0	96		
MT1-3695	2.45	0.35	2.40	0.36	4.71	0.59	1.5	29.9	17.4	55	50.0	26.4	0.3	1.2	0.3	0.0	0.0	18.68	0.2	0.0	113		
MT1-3695-U	2.28	0.33	2.18	0.33	4.44	0.52	1.2	29.9	17.6	68	48.9	19.9	0.2	0.8	0.3	0.0	0.0	0.52	0.1	0.0	105		
MT1-3743,55-60	2.03	0.27	2.00	0.30	5.10	0.26	0.4	17.5	13.9	46	85.7	28.1	0.0	0.3	0.3	0.0	0.0	0.26	0.0	0.6	110	-1.16	-5.02
MT1-3743,90-3744																						-1.07	-5.26
MT1-3744,10-20	2.06	0.28	1.98	0.30	5.06	0.19	0.3	16.4	12.6	46	75.4	14.6	0.1	0.2	0.3	0.0	0.0	0.22	0.0	0.0	106	-1.46	-5.35
MT1-3745,50	2.01	0.27	2.00	0.31	4.57	0.24	0.3	21.4	13.8	47	76.9	17.6	0.1	0.2	0.3	0.0	0.0	0.26	0.0	0.0	119	-1.42	-5.40
MT1-3746,50-3747	2.00	0.26	1.97	0.30	4.88	0.22	0.3	20.8	14.1	49	77.1	14.2	0.1	0.2	0.3	0.0	0.0	0.25	0.0	0.0	113	-1.26	-5.07
MT1-3747,20	1.98	0.28	1.88	0.30	4.96	0.31	0.4	21.6	14.7	50	84.3	17.9	0.1	0.3	0.3	0.0	0.0	0.31	0.0	0.0	117	-1.52	-5.39

Samples	$^{87}Sr/^{86}Sr$	$CaCO_3$	TOC	CIA	CPA	Si/Al	K/Al	Na/Al	B/Al*	Th/U	Cr/V	Y/Ni	Cr/Ni	Th/Sc	Zr/Sc	La/Sc	Ti/Zr	TOC/S
Unit		[%]	[%]															
DL	0.000005	1	0.1															
STRHT9-4420				68.72	91.19	2.91	0.38	0.08	119.76	3.44	0.77	0.66	1.97	0.69	8.32	2.30	30.42	
STRHT9-4550				69.92	92.92	2.54	0.40	0.06	147.95	3.44	0.68	0.56	2.18	0.78	9.29	2.18	29.33	
STRHT9-4645				64.26	86.62	4.00	0.36	0.13	134.01	3.36	0.92	0.76	2.82	0.84	16.27	2.49	20.63	
LI08-11			0.24	78.05	98.41	3.24	0.36	0.01	192.03	3.46	1.69	0.20	1.66	0.64	8.40	1.68	29.65	
LI08-13			0.09	71.46	94.89	2.62	0.42	0.05	150.14	4.40	0.72	0.47	1.42	0.73	7.52	2.72	34.56	
LI08-15R				75.41	98.42	5.28	0.43	0.01	224.34	4.82	4.30	0.25	3.21	0.66	11.66	2.45	22.49	
LI08-15G				76.17	98.39	6.23	0.41	0.01	211.57	4.13	4.65	0.37	3.94	0.55	10.28	2.67	21.38	
LI08-16			0.60	79.23	97.95	6.68	0.32	0.02	282.45	3.13	7.41	0.38	7.39	0.94	21.78	2.91	18.24	
LI08-20			0.14	68.42	92.28	3.06	0.43	0.07	228.36	3.79	1.50	0.36	1.57	0.88	10.30	3.02	25.22	
LI08-22			0.20	68.15	91.55	3.34	0.41	0.08	217.18	3.39	1.71	0.20	1.59	0.87	10.59	2.33	25.89	
P-6			0.09	68.00	90.52	2.76	0.38	0.09	148.79	2.60	0.90	0.68	2.30	0.65	8.92	2.93	28.01	
P-30			0.05	74.75	98.36	4.62	0.44	0.01	191.30	5.57	2.84	0.38	2.54	0.56	8.90	2.54	25.02	
P-121			0.11	69.87	93.80	2.82	0.43	0.06	155.30	4.17	0.89	0.36	1.34	1.00	9.24	3.04	31.14	
P-182R			0.08	69.78	93.46	2.98	0.43	0.06	151.80	5.22	0.95	0.43	1.43	0.78	7.97	2.85	33.86	
P-182G				69.76	93.13	3.30	0.41	0.06	131.45	6.22	0.83	0.40	1.56	0.93	7.82	2.78	33.23	
MT1-3165				67.03	88.45	3.29	0.33	0.11	125.02	3.42	0.79	0.54	2.21	0.82	9.12	2.08	29.32	
MT1-3195				66.49	87.86	3.50	0.33	0.12	125.22	3.11	0.74	0.47	1.69	0.91	11.57	2.31	26.35	
MT1-3207,80		16																
MT1-3250				68.69	90.48	3.00	0.36	0.09	132.99	3.43	0.90	0.05	0.27	0.80	8.05	1.93	32.78	
MT1-3272,10		21																
MT1-3272,50-60		22																
MT1-3275,30-43	0.7087	17	0.14	72.37	93.53	2.28	0.35	0.06	126.14	3.97	0.80	0.51	2.36	0.66	6.78	1.68	38.82	4.63
MT1-3305				70.68	92.24	2.72	0.36	0.07	145.57	3.07	0.83	0.41	1.89	0.76	7.76	1.79	32.70	
MT1-3335				71.80	92.86	3.06	0.35	0.07	175.48	2.75	0.93	0.44	2.41	0.69	7.28	1.69	32.93	
MT1-3355				69.52	90.75	3.08	0.34	0.09	138.33	3.14	0.77	0.38	1.62	0.79	8.98	2.10	31.00	
MT1-3380				70.65	91.80	2.97	0.34	0.08	162.86	2.97	0.87	0.45	2.07	0.79	8.87	1.99	30.89	
MT1-3406,20-30	0.7079	37	0.56	71.88	93.35	2.62	0.36	0.06	178.70	3.03	1.06	0.26	1.62	0.76	8.63	2.01	33.02	1.60
MT1-3409,24-30		1	0.17	69.67	89.52	4.94	0.29	0.10	192.33	3.12	1.40	0.67	2.39	1.03	23.16	2.85	18.32	0.22
MT1-3409,70-82	0.7098	1																
MT1-3445				68.40	89.91	3.01	0.34	0.10	155.71	3.69	0.83	0.42	1.82	0.84	9.88	2.12	28.18	
MT1-3500				70.57	91.71	3.51	0.34	0.08	144.78	3.03	0.94	0.46	2.07	0.70	11.50	2.03	24.06	
MT1-3544,45-65		31																
MT1-3545,90-3546		30																
MT1-3546,25-55	0.7083	28	0.44	71.75	92.74	3.21	0.34	0.07	184.50	3.13	0.81	0.57	2.05	0.81	10.71	2.13	29.39	3.42
MT1-3547,50-65	0.7082	35	0.40	69.99	91.53	3.08	0.35	0.08	161.13	3.22	0.82	0.51	1.94	0.79	10.83	2.23	29.70	2.11
MT1-3605				69.92	91.48	2.88	0.35	0.08	133.49	3.26	0.81	0.41	1.82	0.76	8.37	1.91	31.98	
MT1-3650				69.30	90.66	3.01	0.34	0.09	133.71	3.15	0.79	0.46	1.85	0.76	8.91	2.00	30.29	
MT1-3695				69.75	90.93	2.98	0.34	0.09	159.86	3.03	0.74	0.46	1.76	0.71	9.06	1.96	29.31	
MT1-3695-U				69.07	90.39	3.03	0.34	0.09	145.70	3.19	0.89	0.46	2.21	0.73	9.22	2.02	29.26	
MT1-3743,55-60		37	0.46	72.03	93.54	2.51	0.36	0.06	167.93	3.46	0.90	0.23	1.34	0.75	7.59	1.90	34.22	1.75
MT1-3743,90-3744	0.7080	35																
MT1-3744,10-20	0.7079	37	0.52	71.31	92.75	2.75	0.36	0.07	169.92	3.15	1.03	0.27	1.61	0.77	9.57	2.15	30.74	2.74
MT1-3745,50		36	0.46	71.89	93.28	2.56	0.36	0.06	169.87	2.90	1.04	0.25	1.67	0.69	7.76	1.80	35.65	1.93
MT1-3746,50-3747		36	0.43	72.12	93.43	2.50	0.36	0.06	169.10	3.11	1.01	0.26	1.58	0.70	7.78	1.92	34.66	1.96
MT1-3747,20		37	0.53	71.90	93.22	2.59	0.36	0.06	177.76	3.37	1.07	0.24	1.44	0.76	8.32	2.02	34.24	1.70

Gosau	Samples	Location	Type	Unit	SiO_2 [%]	Al_2O_3 [%]	Fe_2O_3 [%]	MgO [%]	CaO [%]	Na_2O [%]	K_2O [%]	TiO_2 [%]	P_2O_5 [%]	MnO [%]	Cr_2O_3 [%]	LOI [%]	Sum [%]	Sc [ppm]	Ba [ppm]	Be [ppm]
				DL	0.01	0.01	0.04	0.01	0.01	0.01	0.01	0.01	0.01	0.01	0.002	-5.1	0.01	1	1	1
Glinzendorf S.	MT1-3800	Markgrafneusiedl T1	cutting		46.24	13.53	5.30	3.03	12.17	0.85	2.96	0.63	0.12	0.10	0.014	14.8	99.80	13	420	1
Glinzendorf S.	MT1-3835	Markgrafneusiedl T1	cutting		44.98	12.88	5.50	3.01	13.37	0.83	2.77	0.60	0.11	0.10	0.015	15.6	99.80	13	420	2
Glinzendorf S.	MT1-3870	Markgrafneusiedl T1	cutting		43.49	12.47	5.08	2.99	14.79	0.83	2.72	0.57	0.14	0.10	0.016	16.6	99.80	12	368	2
Glinzendorf S.	MT1-3870-U	Markgrafneusiedl T1	cutting		47.74	12.12	4.73	2.91	12.84	0.94	2.59	0.57	0.14	0.10	0.012	15.1	99.77	12	372	1
Glinzendorf S.	MT1-3905	Markgrafneusiedl T1	cutting		44.95	13.21	6.10	2.98	12.81	0.87	2.85	0.60	0.12	0.10	0.014	15.2	99.80	13	374	3
Glinzendorf S.	MT1-3931,10-30	Markgrafneusiedl T1	core		10.45	4.04	1.89	2.21	42.45	0.15	0.76	0.14	0.07	0.05	0.011	37.6	99.84	4	92	0
Glinzendorf S.	MT1-3933,20-50	Markgrafneusiedl T1	core		28.43	10.19	3.91	3.50	24.81	0.40	2.17	0.36	0.10	0.05	0.020	25.8	99.70	10	144	0
Glinzendorf S.	MT1-3975	Markgrafneusiedl T1	cutting		38.57	12.31	5.37	3.09	16.16	0.52	2.32	0.51	0.09	0.09	0.032	20.7	99.81	13	257	2
Glinzendorf S.	MT1-3975-U	Markgrafneusiedl T1	cutting		39.04	12.38	5.27	3.20	16.10	0.52	2.31	0.51	0.09	0.09	0.032	20.2	99.78	13	281	2
Glinzendorf S.	MT1-4005	Markgrafneusiedl T1	cutting		47.34	18.81	6.27	2.14	3.81	0.50	3.01	0.65	0.08	0.04	0.041	17.1	99.83	18	249	3
Glinzendorf S.	MT1-4023,50 B	Markgrafneusiedl T1	core		31.00	11.28	4.65	2.34	23.01	0.34	1.83	0.47	0.09	0.12	0.030	24.7	99.85	13	153	0
Glinzendorf S.	MT1-4023,50 C	Markgrafneusiedl T1	core		28.88	9.54	4.70	2.44	25.82	0.27	1.61	0.41	0.10	0.11	0.037	25.9	99.85	11	147	1
Glinzendorf S.	MT1-4023,70	Markgrafneusiedl T1	core		35.68	14.74	4.86	2.34	16.37	0.38	2.76	0.50	0.08	0.05	0.035	22.0	99.84	16	193	2
Glinzendorf S.	MT1-4025,40-50	Markgrafneusiedl T1	core		31.35	10.94	4.28	2.58	22.72	0.29	2.05	0.45	0.12	0.08	0.034	24.9	99.84	11	159	1
Glinzendorf S.	MT1-4026,20	Markgrafneusiedl T1	core		45.31	17.72	6.16	1.61	3.05	0.43	2.44	0.69	0.09	0.02	0.043	2.2	99.84	17	204	3
Glinzendorf S.	MT1-4055	Markgrafneusiedl T1	cutting		45.13	17.18	5.90	2.01	6.70	0.45	2.61	0.68	0.09	0.07	0.035	19.0	99.83	17	315	2
Glinzendorf S.	MT1-4055-U	Markgrafneusiedl T1	cutting		44.41	16.66	5.93	2.09	7.00	0.45	2.51	0.66	0.10	0.07	0.034	19.9	99.83	16	310	2
Glinzendorf S.	MT1-4075	Markgrafneusiedl T1	cutting		43.26	15.57	6.08	2.53	9.36	0.41	2.45	0.64	0.09	0.08	0.037	19.3	99.81	16	300	2
Glinzendorf S.	MT1-4106,50	Markgrafneusiedl T1	core																	
Glinzendorf S.	MT1-4107,10-30	Markgrafneusiedl T1	core																	
Glinzendorf S.	MT1-4135	Markgrafneusiedl T1	cutting		7.35	2.65	1.37	15.50	30.45	0.05	0.31	0.08	0.02	0.04	0.007	41.8	99.65	2	276	0
Glinzendorf S.	GT1-3245	Glinzendorf T1	core		23.46	8.03	3.53	2.69	30.82	0.30	1.69	0.30	0.09	0.11	0.019	28.7	99.78	7	118	1
Glinzendorf S.	GT1-3246.5	Glinzendorf T1	core		32.28	10.23	3.41	3.06	23.91	0.39	2.29	0.44	0.07	0.07	0.022	23.6	99.83	10	163	1
Glinzendorf S.	GT1-3247.5	Glinzendorf T1	core		29.37	9.01	2.85	1.59	28.52	0.36	1.98	0.41	0.07	0.06	0.022	25.6	99.87	9	130	0
Glinzendorf S.	GT1-3249	Glinzendorf T1	core		29.81	9.64	3.26	2.72	26.32	0.36	2.09	0.42	0.06	0.06	0.025	25.1	99.84	10	155	2
Glinzendorf S.	GT1-3249.5	Glinzendorf T1	core		25.66	8.13	6.63	1.48	28.75	0.26	1.75	0.35	0.06	0.08	0.027	26.7	99.85	8	132	0
Glinzendorf S.	GT1-3270	Glinzendorf T1	cutting		34.63	11.17	4.72	2.68	21.36	0.56	2.34	0.48	0.10	0.09	0.018	21.7	99.83	11	209	1
Glinzendorf S.	GT1-3280	Glinzendorf T1	cutting		36.57	11.68	4.96	2.47	19.91	0.53	2.42	0.51	0.10	0.08	0.020	20.6	99.83	12	236	1
Glinzendorf S.	GT1-3308	Glinzendorf T1	core		55.09	15.55	7.90	1.76	5.12	0.71	2.97	0.72	0.12	0.06	0.047	9.7	99.83	16	208	2
Glinzendorf S.	GT1-3308.8	Glinzendorf T1	core		52.89	14.73	7.26	1.64	7.65	0.76	2.75	0.69	0.11	0.10	0.040	11.2	99.82	15	204	2
Glinzendorf S.	GT1-3330	Glinzendorf T1	cutting		54.92	15.15	6.84	2.07	6.07	0.65	3.18	0.67	0.11	0.08	0.047	10.1	99.86	15	236	2
Glinzendorf S.	GT1-3361.5	Glinzendorf T1	core		61.50	17.37	8.26	1.71	0.11	0.58	3.11	0.81	0.12	0.04	0.068	6.1	99.82	17	242	2
Glinzendorf S.	GT1-3362.5	Glinzendorf T1	core		61.23	17.54	8.07	1.72	0.13	0.65	3.06	0.82	0.11	0.04	0.047	6.4	99.82	17	252	3
Glinzendorf S.	GT1-3364.5	Glinzendorf T1	core		61.23	17.41	7.80	1.75	0.60	0.55	3.06	0.80	0.15	0.05	0.063	6.3	99.81	17	231	2
Glinzendorf S.	GT1-3370	Glinzendorf T1	cutting		60.40	14.60	5.89	1.73	3.77	0.73	3.64	0.57	0.10	0.09	0.047	8.3	99.87	13	264	2
Glinzendorf S.	GT1-3406.5	Glinzendorf T1	core		55.15	19.60	7.84	2.18	0.95	1.18	3.39	0.81	0.13	0.38	0.015	8.2	99.80	18	349	2
Glinzendorf S.	GT1-3406.8	Glinzendorf T1	core		43.11	13.76	6.74	3.37	11.90	1.05	2.41	0.62	0.13	0.30	0.012	16.4	99.79	13	260	2
Glinzendorf S.	GT1-3407.8	Glinzendorf T1	core		51.75	16.71	7.45	3.17	4.69	1.47	2.70	0.73	0.11	0.20	0.015	10.8	99.80	16	250	2
Glinzendorf S.	GT1-3409.5	Glinzendorf T1	core		40.14	14.89	18.49	2.34	3.47	0.81	2.33	0.57	1.36	0.57	0.011	14.8	99.76	16	564	2
Glinzendorf S.	GT1-3440	Glinzendorf T1	cutting		51.75	15.57	6.61	2.50	6.97	1.00	2.93	0.68	0.13	0.22	0.019	11.4	99.83	15	318	2
Glinzendorf S.	GT1-3477.5	Glinzendorf T1	core		63.83	16.80	6.55	1.82	0.43	1.53	2.92	0.78	0.18	0.05	0.013	4.9	99.85	15	317	2
Glinzendorf S.	GT1-3478.5	Glinzendorf T1	core		58.60	18.76	7.05	2.06	0.80	1.26	3.22	0.80	0.22	0.15	0.015	6.9	99.84	17	270	2
Glinzendorf S.	GT1-3479.5	Glinzendorf T1	core		57.25	20.16	7.27	2.19	0.53	1.17	3.39	0.83	0.15	0.18	0.016	6.7	99.81	19	298	2
Glinzendorf S.	GT1-3480.5	Glinzendorf T1	core		57.84	20.39	6.59	2.27	0.19	1.13	3.66	0.78	0.10	0.14	0.016	6.7	99.80	19	271	3
Glinzendorf S.	GT1-3510	Glinzendorf T1	cutting		48.60	14.35	5.65	2.84	9.38	1.08	2.76	0.65	0.12	0.14	0.018	14.2	99.83	14	277	2

Samples	Co [ppm]	Cs [ppm]	Ga [ppm]	Hf [ppm]	Nb [ppm]	Rb [ppm]	Sn [ppm]	Sr [ppm]	Ta [ppm]	Th [ppm]	U [ppm]	V [ppm]	W [ppm]	Zr [ppm]	Y [ppm]	La [ppm]	Ce [ppm]	Pr [ppm]	Nd [ppm]	Sm [ppm]	Eu [ppm]	Gd [ppm]	Tb [ppm]	Dy [ppm]	Ho [ppm]
Unit	[ppm]	[ppm]	[ppm]	[ppm]	[ppm]	[ppm]	[ppm]	[ppm]	[ppm]	[ppm]	[ppm]	[ppm]	[ppm]	[ppm]	[ppm]	[ppm]	[ppm]	[ppm]	[ppm]	[ppm]	[ppm]	[ppm]	[ppm]	[ppm]	[ppm]
DL	0.2	0.1	0.5	0.1	0.1	0.1	1	0.5	0.1	0.2	0.1	8	0.5	0.1	0.1	0.1	0.1	0.02	0.3	0.05	0.02	0.05	0.01	0.05	0.02
MT1-3800	14.4	8.8	17.1	3.4	12.1	125.5	3	404.4	0.8	10.6	3.0	117	2.0	127.8	22.8	27.8	60.4	6.79	26.0	4.90	1.01	4.29	0.71	3.71	0.80
MT1-3835	14.5	8.3	16.5	4.0	11.4	118.6	3	391.4	0.9	10.3	3.2	115	2.4	131.4	21.3	27.4	60.9	6.67	26.0	4.79	0.97	4.32	0.69	3.67	0.76
MT1-3870	13.0	7.8	16.1	3.5	11.4	116.0	2	461.7	0.9	9.6	3.1	111	2.2	122.1	21.4	26.6	59.5	6.49	24.5	4.71	0.95	4.18	0.68	3.68	0.73
MT1-3870-U	12.6	7.4	16.5	4.2	12.1	115.7	3	696.1	0.9	10.1	3.1	106	2.2	132.7	21.8	27.2	60.6	6.49	25.2	4.89	0.98	4.17	0.69	3.83	0.75
MT1-3905	16.3	8.9	17.8	3.6	11.8	118.0	3	399.0	0.9	10.2	3.2	115	2.5	120.5	21.7	27.1	59.0	6.55	26.5	4.71	1.00	4.22	0.70	3.68	0.76
MT1-3931,10-30	6.8	9.3	5.0	1.1	2.6	30.2	0	749.8	0.2	2.9	1.4	33	0.5	27.6	6.2	7.7	15.8	1.94	8.0	1.36	0.23	1.13	0.16	1.06	0.20
MT1-3933,20-50	10.4	8.0	12.2	2.1	7.7	85.9	1	1280.0	0.6	7.4	2.2	134	1.1	72.8	16.3	19.1	40.0	4.93	19.0	3.53	0.54	2.90	0.41	2.74	0.57
MT1-3975	22.6	10.0	16.5	3.3	10.1	106.0	3	398.7	0.8	8.5	4.1	108	3.0	103.2	19.1	24.3	54.1	5.72	22.4	4.14	0.80	3.67	0.59	3.19	0.67
MT1-3975-U	21.4	9.6	15.6	2.8	10.2	105.8	3	395.1	0.8	8.9	4.2	110	2.6	101.4	18.8	24.1	53.7	5.63	21.4	4.16	0.80	3.62	0.58	3.32	0.69
MT1-4005	29.4	13.9	24.5	4.0	13.5	146.8	4	181.8	1.0	13.1	6.3	171	2.5	130.6	23.6	34.1	76.8	8.04	30.7	5.19	1.00	4.15	0.69	4.15	0.86
MT1-4023,50 B	32.3	10.1	12.8	2.1	9.0	66.2	2	376.4	0.7	7.5	6.0	82	1.4	67.7	20.4	21.8	44.4	5.67	22.1	4.44	0.75	3.96	0.54	3.56	0.71
MT1-4023,50 C	26.4	7.9	11.0	1.9	8.0	56.0	1	398.3	0.5	6.1	2.7	73	1.4	61.1	22.3	19.9	40.2	4.98	18.9	4.01	0.72	3.76	0.52	3.65	0.71
MT1-4023,70	29.4	16.2	18.7	2.4	10.3	99.1	2	297.8	0.8	9.3	11.8	125	1.8	81.3	21.5	25.2	52.9	6.46	25.7	5.34	0.94	4.77	0.63	4.12	0.75
MT1-4025,40-50	26.4	9.1	12.9	2.1	8.7	73.3	2	347.5	0.6	7.2	4.3	87	1.4	77.8	17.8	20.5	41.0	5.16	20.1	3.79	0.64	3.28	0.46	3.11	0.64
MT1-4026,20	33.4	31.9	20.9	4.4	14.4	119.5	3	144.0	0.8	13.6	15.7	154	1.8	141.6	23.4	31.4	69.4	7.56	29.0	4.98	1.01	4.01	0.75	4.36	0.81
MT1-4055	24.5	26.3	20.9	3.5	13.9	124.7	4	191.1	0.9	13.5	10.4	153	2.7	136.5	26.8	33.6	72.7	7.89	30.2	5.51	1.13	4.80	0.80	4.15	0.95
MT1-4055-U	23.7	24.9	20.4	3.9	12.8	122.2	3	202.6	0.9	12.1	11.0	154	2.7	133.3	26.7	32.8	72.4	7.60	29.7	5.52	1.08	4.94	0.80	4.20	0.88
MT1-4075	22.5	21.2	20.7	3.4	12.9	114.1	3	231.0	1.0	11.9	7.4	142	3.0	128.6	25.8	30.7	70.7	7.37	27.8	5.27	1.04	4.56	0.76	4.26	0.90
MT1-4106,50																									
MT1-4107,10-30																									
MT1-4135	2.3	3.9	2.7	0.5	1.6	13.8	2	151.4	0.1	1.5	4.7	25	0.7	23.8	5.7	5.2	10.3	1.23	4.5	0.98	0.21	0.91	0.15	0.85	0.18
GT1-3245	15.5	9.3	9.6	1.5	5.5	82.8	2	779.9	0.5	5.9	2.2	122	0.9	55.1	11.8	14.5	29.3	3.44	12.7	2.50	0.49	2.20	0.36	2.10	0.41
GT1-3246.5	16.9	10.4	12.5	3.1	9.2	102.0	2	363.2	0.7	8.7	2.6	97	1.5	93.3	18.0	21.0	44.8	5.20	20.1	3.87	0.77	3.37	0.57	3.16	0.65
GT1-3247.5	12.4	9.4	11.2	2.3	8.0	88.7	2	351.8	0.6	7.8	2.7	93	1.5	85.2	16.2	19.1	39.1	4.59	16.5	3.34	0.66	2.95	0.51	2.80	0.60
GT1-3249	16.3	11.7	11.4	2.5	8.5	97.1	2	404.7	0.6	8.0	2.4	91	1.4	82.5	15.7	18.7	38.5	4.45	16.1	3.21	0.65	2.79	0.49	2.69	0.55
GT1-3249.5	14.4	10.6	9.6	2.1	7.1	88.8	2	359.8	0.5	6.3	2.3	108	1.3	70.4	13.9	16.1	33.3	3.84	14.0	2.80	0.57	2.42	0.43	2.28	0.47
GT1-3270	14.2	9.4	12.8	2.6	9.2	100.7	3	429.1	0.7	8.8	2.4	102	5.0	89.5	17.4	22.2	45.1	5.18	19.9	3.69	0.76	3.37	0.54	2.98	0.59
GT1-3280	14.6	9.6	14.6	2.6	9.5	104.4	3	406.8	0.7	8.9	2.7	108	2.3	94.1	18.4	22.9	47.5	5.46	22.1	4.08	0.86	3.67	0.59	3.20	0.63
GT1-3308	26.9	9.5	17.8	5.0	14.4	136.6	3	151.4	1.0	14.2	2.8	126	2.2	170.5	29.9	35.0	73.7	8.52	32.9	6.18	1.23	5.50	0.93	5.06	1.02
GT1-3308.8	23.4	8.6	16.6	4.6	13.3	119.1	3	191.2	1.0	12.9	2.8	119	2.1	157.0	27.1	32.0	69.8	7.91	30.8	6.00	1.18	5.51	0.93	5.15	0.97
GT1-3330	23.8	8.7	17.6	4.6	13.3	131.4	4	165.0	0.9	12.8	2.9	117	12.4	159.4	26.3	29.8	63.0	7.19	28.7	5.32	1.04	4.88	0.84	4.56	0.89
GT1-3361.5	30.3	9.5	18.7	5.5	15.8	142.4	3	104.5	1.2	14.1	3.5	139	2.6	187.5	31.9	44.0	101.6	12.53	49.4	9.28	1.75	7.36	1.16	5.97	1.13
GT1-3362.5	27.2	9.9	19.1	5.7	15.5	139.2	3	105.4	1.1	14.3	3.1	142	2.5	183.5	28.5	34.5	77.1	8.30	32.6	5.97	1.29	5.58	0.93	5.33	1.08
GT1-3364.5	26.4	9.2	18.7	5.2	14.5	133.8	3	103.6	1.0	14.2	3.0	134	2.4	183.1	28.6	33.1	72.2	8.05	30.5	5.76	1.17	5.25	0.88	5.06	1.00
GT1-3370	18.0	7.4	16.5	5.2	14.1	140.1	4	146.6	1.1	13.8	3.1	97	4.8	176.3	28.8	31.6	67.6	7.80	30.8	5.70	0.99	5.27	0.90	4.97	1.00
GT1-3406.5	15.8	8.7	22.2	4.6	21.1	140.2	4	120.3	1.0	16.8	3.1	157	2.6	146.2	27.4	35.9	79.0	8.85	34.8	5.97	1.27	4.97	0.83	4.81	0.96
GT1-3406.8	11.2	6.4	16.2	3.4	11.6	111.6	2	333.9	0.9	10.5	2.4	102	1.9	114.7	23.9	27.3	57.5	6.74	25.9	5.09	1.18	4.94	0.80	4.21	0.89
GT1-3407.8	15.5	7.7	20.9	4.0	14.3	120.6	3	160.0	1.0	14.0	2.7	134	2.0	141.5	22.7	31.2	68.4	7.56	28.2	5.12	1.04	4.36	0.73	4.00	0.82
GT1-3409.5	12.2	6.4	17.1	3.2	11.5	100.4	3	137.6	0.8	13.1	3.7	117	1.6	114.2	53.3	39.9	99.6	11.13	48.7	13.51	3.48	16.49	2.28	10.37	1.72
GT1-3440	17.4	8.3	17.9	4.3	13.2	120.7	3	238.0	1.0	12.6	2.9	127	2.9	146.3	24.8	29.4	64.7	7.05	28.0	5.29	1.11	4.71	0.78	4.29	0.85
GT1-3477.5	14.6	6.0	18.8	5.0	14.1	112.3	3	56.0	1.1	12.2	3.0	111	2.6	164.3	25.6	26.7	58.6	6.70	26.1	5.29	1.11	5.36	0.87	4.63	0.92
GT1-3478.5	20.2	9.2	21.3	5.4	13.5	125.2	3	98.9	1.0	14.6	3.1	149	3.0	169.8	27.3	32.0	74.8	7.74	28.8	5.76	1.25	5.54	0.94	5.22	1.00
GT1-3479.5	21.5	9.6	23.7	5.0	15.6	139.2	4	122.8	1.1	14.8	2.9	168	2.9	162.9	27.6	35.2	88.4	8.81	32.2	6.07	1.27	5.20	0.86	5.12	1.01
GT1-3480.5	23.2	10.5	22.0	4.4	17.3	148.4	4	107.6	1.0	15.8	2.7	175	2.8	144.6	24.3	36.2	90.2	8.50	31.9	5.66	1.15	4.66	0.77	4.40	0.92
GT1-3510	15.1	8.1	17.7	3.9	12.5	115.8	4	291.8	0.9	11.2	2.8	120	4.0	131.3	21.1	28.0	59.2	6.66	26.7	4.80	1.03	4.25	0.72	3.83	0.76

Samples	Unit / DL	Er [ppm] 0.03	Tm [ppm] 0.01	Yb [ppm] 0.05	Lu [ppm] 0.01	TOT/C [%] 0.02	TOT/S [%] 0.02	Mo [ppm] 0.1	Cu [ppm] 0.1	Pb [ppm] 0.1	Zn [ppm] 1	Ni [ppm] 0.1	As [ppm] 0.5	Cd [ppm] 0.1	Sb [ppm] 0.1	Bi [ppm] 0.1	Ag [ppm] 0.1	Au [ppm] 0.5	Hg [ppm] 0.01	Tl [ppm] 0.1	Se [ppm] 0.5	B [ppm] 3	$\delta^{13}C$ [VPDB] 0.06	$\delta^{18}O$ [VPDB] 0.08
MT1-3800		2.39	0.37	2.28	0.34	3.30	0.27	1.2	29.4	16.6	59	52.6	14.9	0.2	0.7	0.3	0.0	0.0	0.38	0.1	0.0	101		
MT1-3835		2.23	0.34	2.10	0.33	3.53	0.23	1.1	25.9	16.8	55	52.8	23.0	0.2	0.9	0.3	0.0	0.0	0.35	0.1	0.0	89		
MT1-3870		2.12	0.36	2.12	0.32	3.98	0.30	0.9	73.3	18.7	57	54.1	17.7	0.2	0.9	0.3	0.0	0.0	0.33	0.0	0.7	78		
MT1-3870-U		2.21	0.32	2.09	0.31	3.43	0.20	1.1	26.8	15.7	61	45.8	16.2	0.2	0.7	0.3	0.0	0.0	0.23	0.0	0.6	86		
MT1-3905		2.22	0.35	2.15	0.32	3.54	0.43	1.5	29.8	20.4	64	55.6	23.7	0.2	1.1	0.3	0.0	0.0	0.37	0.1	0.8	98		
MT1-3931,10-30		0.59	0.08	0.55	0.09	10.66	0.82	0.7	10.4	4.9	26	64.1	14.8	0.0	0.0	0.0	0.0	0.0	0.02	0.0	0.0	28	2.01	-4.39
MT1-3933,20-50		1.53	0.22	1.61	0.23	6.78	0.87	0.1	9.7	10.7	41	84.5	16.4	0.0	0.0	0.2	0.0	0.0	0.02	0.0	0.0	72	0.80	-4.60
MT1-3975		1.94	0.32	2.00	0.29	6.40	0.91	1.8	31.2	30.8	132	225.6	19.4	0.2	0.7	0.3	0.0	0.0	0.22	0.1	0.7	96		
MT1-3975-U		1.92	0.31	2.08	0.30	5.86	0.82	1.5	30.6	30.2	140	222.5	18.6	0.0	0.6	0.3	0.0	0.0	0.21	0.1	0.5	89		
MT1-4005		2.52	0.41	2.60	0.39	5.40	1.83	2.0	50.2	28.8	93	393.6	22.0	0.2	0.6	0.4	0.0	0.0	0.14	0.1	0.5	120		
MT1-4023,50 B		1.93	0.26	1.88	0.27	6.40	0.49	1.8	24.0	25.7	49	394.2	17.4	0.2	0.2	0.3	0.0	0.0	0.02	0.0	0.6	80	-3.35	-4.98
MT1-4023,50 C		1.84	0.26	1.72	0.28	6.87	0.49	1.1	22.5	21.6	56	271.4	19.6	0.2	0.2	0.2	0.0	0.0	0.02	0.0	0.0	72	-3.67	-5.33
MT1-4023,70		2.08	0.27	2.11	0.30	6.77	1.64	1.8	32.0	21.1	68	241.7	27.6	0.2	0.2	0.3	0.0	0.0	0.04	0.0	1.4	112	-2.87	-5.98
MT1-4025,40-50		1.76	0.23	1.80	0.26	7.17	1.14	0.8	25.7	22.9	78	250.6	26.6	0.2	0.3	0.3	0.0	0.0	0.04	0.0	0.0	88		
MT1-4026,20		2.31	0.39	2.59	0.38	11.62	2.64	2.6	41.8	24.9	110	261.4	16.1	0.3	0.5	0.4	0.0	0.0	0.05	0.0	2.3	89	-3.31	-5.36
MT1-4055		2.76	0.42	2.68	0.42	7.71	1.33	2.6	40.1	26.4	87	269.7	16.7	0.2	0.5	0.3	0.0	0.0	0.11	0.2	1.7	77		
MT1-4055-U		2.65	0.42	2.72	0.40	8.36	1.33	3.1	42.7	27.4	98	247.6	18.4	0.2	0.5	0.3	0.0	0.0	0.12	0.2	1.6	82		
MT1-4075		2.60	0.39	2.58	0.38	6.80	1.13	2.0	39.0	29.4	81	225.2	16.8	0.2	0.5	0.3	0.0	0.0	0.11	0.2	1.4	91		
MT1-4106,50																							1.26	-2.14
MT1-4107,10-30																							-3.16	-4.04
MT1-4135		0.52	0.07	0.42	0.06	11.07	0.24	5.8	109.6	25.5	122	18.6	8.4	0.1	0.4	0.0	0.0	0.0	0.03	0.0	0.0	11		
GT1-3245		1.22	0.18	1.18	0.19	7.56	0.41	0.7	10.7	21.3	48	103.2	19.3	0.1	0.3	0.2	0.0	0.0	0.04	0.0	0.5	69	-0.69	-4.96
GT1-3246.5		1.89	0.29	1.82	0.28	6.13	0.32	0.2	15.0	12.9	36	103.1	11.4	0.1	0.3	0.2	0.0	0.0	0.07	0.0	0.8	100	-2.32	-6.04
GT1-3247.5		1.66	0.25	1.60	0.25	6.73	0.35	0.2	5.4	14.8	32	80.7	11.4	0.0	0.2	0.3	0.0	0.0	0.07	0.0	2.9	83	-2.86	-6.52
GT1-3249		1.68	0.25	1.54	0.24	6.56	0.39	0.3	6.2	14.4	36	107.6	14.2	0.1	0.3	0.2	0.0	0.0	0.05	0.0	0.6	98	-1.45	-5.22
GT1-3249.5		1.44	0.21	1.35	0.21	6.54	0.03	0.6	17.3	10.6	61	151.2	9.6	0.2	1.2	0.2	0.0	0.0	0.00	0.0	0.0	83	-3.67	-6.68
GT1-3270		1.66	0.26	1.61	0.25	5.62	0.35	0.7	23.7	18.4	59	103.0	17.5	0.1	0.3	0.3	0.0	1.1	0.06	0.0	0.0	63		
GT1-3280		1.82	0.29	1.80	0.27	4.78	0.21	0.5	23.8	18.3	50	109.1	18.9	0.1	0.3	0.3	0.0	1.8	0.05	0.0	1.1	125		
GT1-3308		3.09	0.45	2.81	0.47	1.17	0.00	0.6	38.3	10.0	63	249.9	12.2	0.1	0.6	0.3	0.0	0.8	0.05	0.0	0.0	99	-5.54	-5.78
GT1-3308.8		2.97	0.41	2.73	0.44	1.76	0.00	0.4	38.0	10.3	59	204.2	10.9	0.0	0.5	0.3	0.0	1.5	0.03	0.1	0.0	102	-8.66	-7.32
GT1-3330		2.59	0.42	2.68	0.41	1.76	0.11	1.0	20.7	19.8	69	193.1	25.5	0.0	0.4	0.4	0.0	1.9	0.09	0.2	0.0	121		
GT1-3361.5		3.31	0.48	3.05	0.50	0.06	0.00	1.2	8.9	23.9	79	244.5	17.2	0.0	1.1	0.4	0.0	1.9	0.07	0.2	0.7	106	-5.48	-6.82
GT1-3362.5		3.10	0.47	2.99	0.48	0.05	0.00	1.0	10.3	21.2	81	131.4	16.1	0.0	0.9	0.4	0.0	2.3	0.06	0.2	0.0	108		
GT1-3364.5		3.01	0.46	3.00	0.46	0.06	0.00	1.0	12.0	19.3	78	169.3	12.6	0.0	0.9	0.4	0.0	1.4	0.09	0.2	0.0	110		
GT1-3370		3.01	0.47	2.92	0.45	1.52	0.07	0.7	28.5	17.7	62	132.7	12.3	0.0	0.5	0.3	0.0	1.6	0.05	0.1	0.0	59		
GT1-3406.5		2.98	0.46	2.98	0.47	1.39	0.15	0.8	40.0	20.6	71	50.9	14.4	0.0	0.2	0.5	0.0	1.0	0.04	0.0	0.6	120		
GT1-3406.8		2.50	0.37	2.30	0.35	4.08	0.23	0.2	9.0	16.7	97	39.4	4.6	0.1	0.1	0.3	0.0	0.0	0.04	0.0	0.0	107		
GT1-3407.8		2.50	0.38	2.51	0.39	2.07	0.08	0.1	34.1	19.3	66	55.1	6.1	0.0	0.1	0.3	0.0	0.0	0.03	0.0	0.0	99		
GT1-3409.5		4.10	0.53	3.10	0.43	3.45	0.10	0.5	2.2	10.7	60	32.9	4.6	0.0	0.2	0.2	0.0	0.0	0.03	0.0	0.0	95		
GT1-3440		2.47	0.39	2.45	0.37	2.43	0.33	0.8	39.3	21.6	61	70.5	51.0	0.0	0.4	0.5	0.3	2.8	0.15	0.2	0.5	112		
GT1-3477.5		2.80	0.43	2.78	0.40	0.53	0.23	0.6	3.9	10.0	61	42.2	9.9	0.0	0.4	0.3	0.0	0.0	0.11	0.0	0.0	85		
GT1-3478.5		2.95	0.48	3.02	0.43	0.93	0.28	0.6	13.8	10.5	64	56.6	12.7	0.0	0.3	0.5	0.0	1.2	0.09	0.0	0.0	121		
GT1-3479.5		3.13	0.50	3.12	0.47	0.71	0.15	0.6	13.6	6.4	71	62.8	10.3	0.0	0.2	0.5	0.0	0.0	0.09	0.0	0.0	134		
GT1-3480.5		2.90	0.48	2.88	0.43	0.41	0.05	0.2	120.6	4.8	80	69.1	4.8	0.0	0.1	0.4	0.0	1.0	0.21	0.0	0.0	142		
GT1-3510		2.20	0.36	2.16	0.33	3.33	0.30	1.0	37.5	23.7	67	48.9	12.2	0.4	0.2	0.3	0.0	0.7	0.07	0.1	0.0	124		

Samples	$^{87}Sr/^{86}Sr$	$CaCO_3$	TOC	CIA	CPA	Si/Al	K/Al	Na/Al	B/Al*	Th/U	Cr/V	Y/Ni	Cr/Ni	Th/Sc	Zr/Sc	La/Sc	Ti/Zr	TOC/S
Unit		[%]	[%]															
DL	0.000005	1	0.1															
MT1-3800				69.28	90.63	3.02	0.34	0.09	141.09	3.53	0.81	0.43	1.80	0.82	9.83	2.14	29.55	
MT1-3835				69.21	90.41	3.08	0.34	0.09	130.60	3.22	0.88	0.40	1.92	0.79	10.11	2.11	27.37	
MT1-3870				68.72	90.13	3.08	0.34	0.09	118.22	3.10	0.97	0.40	2.00	0.80	10.18	2.22	27.99	
MT1-3870-U				67.27	88.68	3.48	0.34	0.11	134.11	3.26	0.76	0.48	1.77	0.84	11.06	2.27	25.75	
MT1-3905				68.96	90.22	3.01	0.34	0.09	140.21	3.19	0.82	0.39	1.70	0.78	9.27	2.08	29.85	
MT1-3931,10-30		81	0.96	75.43	94.24	2.28	0.30	0.05	130.99	2.07	2.25	0.10	1.16	0.73	6.90	1.93	30.41	1.17
MT1-3933,20-50	0.7076	48	0.45	73.55	93.93	2.46	0.33	0.06	133.54	3.36	1.01	0.19	1.60	0.74	7.28	1.91	29.65	0.52
MT1-3975				74.46	93.50	2.77	0.30	0.06	147.39	2.07	2.00	0.08	0.96	0.65	7.94	1.87	29.63	
MT1-3975-U				74.62	93.54	2.79	0.29	0.06	135.87	2.12	1.97	0.08	0.97	0.68	7.80	1.85	30.15	
MT1-4005				79.32	95.81	2.22	0.25	0.04	120.57	2.08	1.62	0.06	0.70	0.73	7.26	1.89	29.84	
MT1-4023,50 B		44	0.82	78.44	95.28	2.43	0.25	0.04	134.04	1.25	2.47	0.05	0.51	0.58	5.21	1.68	41.62	1.68
MT1-4023,50 C		52	0.59	78.38	95.55	2.67	0.26	0.04	142.64	2.26	3.42	0.08	0.92	0.55	5.55	1.81	40.23	1.20
MT1-4023,70	0.7084	32	2.36	77.67	95.93	2.14	0.29	0.04	143.61	0.79	1.89	0.09	0.98	0.58	5.08	1.58	36.87	1.44
MT1-4025,40-50		44	1.69	77.52	95.82	2.53	0.29	0.04	152.03	1.67	2.64	0.07	0.92	0.65	7.07	1.86	34.68	1.49
MT1-4026,20		49		81.37	96.16	2.26	0.22	0.03	94.93	0.87	1.89	0.09	1.11	0.80	8.33	1.85	29.21	
MT1-4055				79.96	95.87	2.32	0.24	0.04	84.71	1.30	1.55	0.10	0.88	0.79	8.03	1.98	29.87	
MT1-4055-U				79.88	95.75	2.35	0.24	0.04	93.03	1.10	1.49	0.11	0.93	0.76	8.33	2.05	29.68	
MT1-4075				79.56	95.85	2.45	0.25	0.04	110.46	1.61	1.76	0.11	1.11	0.74	8.04	1.92	29.84	
MT1-4106,50	0.7096	42																
MT1-4107,10-30		98																
MT1-4135				84.13	96.99	2.45	0.18	0.03	78.45	0.32	1.89	0.31	2.54	0.75	11.90	2.60	20.15	
GT1-3245		55	0.50	74.03	94.21	2.58	0.33	0.05	162.40	2.68	1.05	0.11	1.24	0.84	7.87	2.07	32.64	1.21
GT1-3246.5		44	0.49	73.11	94.10	2.79	0.35	0.05	184.75	3.35	1.53	0.17	1.44	0.87	9.33	2.10	28.27	1.53
GT1-3247.5		47	0.49	73.03	93.83	2.88	0.34	0.06	174.11	2.89	1.60	0.20	1.84	0.87	9.47	2.12	28.85	1.41
GT1-3249		45	0.65	73.66	94.21	2.73	0.34	0.05	192.14	3.33	1.86	0.15	1.57	0.80	8.25	1.87	30.52	1.67
GT1-3249.5		55	0.23	74.73	95.00	2.79	0.34	0.04	192.95	2.74	1.69	0.09	1.21	0.79	8.80	2.01	29.80	7.57
GT1-3270				71.85	92.38	2.74	0.33	0.07	106.60	3.67	1.19	0.17	1.18	0.80	8.14	2.02	32.15	
GT1-3280				72.80	93.05	2.77	0.33	0.06	202.27	3.30	1.25	0.17	1.24	0.74	7.84	1.91	32.49	
GT1-3308		11	0.16	73.69	93.01	3.13	0.30	0.06	120.33	5.07	2.52	0.12	1.27	0.89	10.66	2.19	25.32	
GT1-3308.8		21	0.14	72.89	92.18	3.17	0.29	0.07	130.88	4.61	2.27	0.13	1.32	0.86	10.47	2.13	26.35	
GT1-3330				73.08	93.41	3.20	0.33	0.06	150.95	4.41	2.71	0.14	1.64	0.85	10.63	1.99	25.20	
GT1-3361.5		0	0.09	76.71	94.79	3.13	0.28	0.05	115.34	4.03	3.31	0.13	1.88	0.83	11.03	2.59	25.90	
GT1-3362.5		0	0.05	76.29	94.25	3.08	0.27	0.05	116.37	4.61	2.24	0.22	2.42	0.84	10.79	2.03	26.79	
GT1-3364.5		1		77.27	95.06	3.11	0.28	0.04	119.41	4.73	3.18	0.17	2.51	0.84	10.77	1.95	26.19	
GT1-3370				69.72	92.40	3.65	0.39	0.07	76.38	4.45	3.27	0.22	2.39	1.06	13.56	2.43	19.38	
GT1-3406.5		1	0.75	72.19	90.99	2.49	0.27	0.08	115.71	5.42	0.65	0.54	1.99	0.93	8.12	1.99	33.21	5.02
GT1-3406.8		33	0.85	69.41	88.85	2.77	0.27	0.11	146.97	4.38	0.79	0.61	2.06	0.81	8.82	2.10	32.41	3.70
GT1-3407.8		1	0.53	68.29	87.36	2.74	0.25	0.12	111.97	5.19	0.76	0.41	1.84	0.88	8.84	1.95	30.93	6.58
GT1-3409.5		1	4.30	74.16	91.79	2.38	0.25	0.08	120.58	3.54	0.64	1.62	2.26	0.82	7.14	2.49	29.92	42.95
GT1-3440				70.67	90.44	2.94	0.30	0.09	135.95	4.34	1.01	0.35	1.82	0.84	9.75	1.96	27.86	
GT1-3477.5		1	0.36	67.21	86.97	3.36	0.27	0.13	95.63	4.07	0.79	0.61	2.08	0.81	10.95	1.78	28.46	1.57
GT1-3478.5		1	0.62	71.08	90.05	2.76	0.27	0.09	121.90	4.71	0.68	0.48	1.79	0.86	9.99	1.88	28.24	2.20
GT1-3479.5		1	0.49	72.84	91.28	2.51	0.26	0.08	125.63	5.10	0.64	0.44	1.72	0.78	8.57	1.85	30.55	3.28
GT1-3480.5		1	0.34	72.64	91.64	2.51	0.28	0.08	131.62	5.85	0.62	0.35	1.56	0.83	7.61	1.91	32.34	6.78
GT1-3510				68.69	88.98	2.99	0.30	0.11	163.32	4.00	1.01	0.43	2.49	0.80	9.38	2.00	29.68	

Gosau	Samples	Location	Type	Unit / DL	SiO_2 [%] 0.01	Al_2O_3 [%] 0.01	Fe_2O_3 [%] 0.04	MgO [%] 0.01	CaO [%] 0.01	Na_2O [%] 0.01	K_2O [%] 0.01	TiO_2 [%] 0.01	P_2O_5 [%] 0.01	MnO [%] 0.01	Cr_2O_3 [%] 0.002	LOI [%] -5.1	Sum [%] 0.01	Sc [ppm] 1	Ba [ppm] 1	Be [ppm] 1
Glinzendorf S.	GT1-3552	Glinzendorf T1	core		55.12	19.57	7.37	1.95	0.87	0.81	3.04	1.00	0.13	0.13	0.016	9.8	99.81	18	264	2
Glinzendorf S.	GT1-3553	Glinzendorf T1	core		54.32	20.10	7.39	2.01	0.93	0.83	3.12	1.02	0.13	0.14	0.016	9.8	99.80	19	261	2
Glinzendorf S.	GT1-3554	Glinzendorf T1	core		57.19	18.20	7.16	1.97	1.70	2.12	2.50	0.80	0.20	0.13	0.014	7.8	99.79	17	322	2
Glinzendorf S.	GT1-3554.5	Glinzendorf T1	core		55.15	19.34	7.23	2.36	1.53	1.33	3.15	0.84	0.15	0.19	0.016	8.5	99.79	18	342	2
Glinzendorf S.	GT1-3570	Glinzendorf T1	cutting		54.29	17.16	6.85	2.28	3.90	1.88	2.58	0.76	0.19	0.24	0.015	9.7	99.85	16	293	2
Glinzendorf S.	GT1-3611.5	Glinzendorf T1	core		57.65	20.29	5.51	1.90	0.56	1.33	2.93	0.93	0.12	0.13	0.018	8.4	99.80	18	269	2
Glinzendorf S.	GT1-3613	Glinzendorf T1	core		56.79	19.26	7.37	2.24	0.86	1.33	3.33	0.81	0.10	0.15	0.017	7.5	99.78	17	281	2
Glinzendorf S.	GT1-3615.2	Glinzendorf T1	core		70.68	6.00	7.13	1.58	5.18	0.49	0.77	0.42	0.07	0.36	0.007	7.2	99.87	6	166	0
Glinzendorf S.	GT1-3630	Glinzendorf T1	cutting		55.50	15.63	6.58	1.98	5.37	0.96	2.93	0.65	0.15	0.24	0.026	9.8	99.84	15	361	2
Glinzendorf S.	GT1-3651.5	Glinzendorf T1	core		64.00	16.49	6.80	1.71	0.11	0.60	3.28	0.79	0.13	0.05	0.035	5.8	99.81	17	299	3
Glinzendorf S.	GT1-3652.5	Glinzendorf T1	core		64.66	15.05	7.83	1.57	0.45	0.62	3.08	0.72	0.14	0.04	0.057	5.6	99.83	15	220	2
Glinzendorf S.	GT1-3680	Glinzendorf T1	cutting		52.91	17.41	7.73	2.18	4.57	0.79	3.18	0.74	0.14	0.11	0.028	10.1	99.86	17	226	2
Glinzendorf S.	GT1-3713.5	Glinzendorf T1	core		53.48	16.36	7.04	2.21	5.74	0.93	2.55	0.77	0.12	0.07	0.025	10.5	99.84	16	189	2
Glinzendorf S.	GT1-3714.5	Glinzendorf T1	core		56.04	17.84	7.87	2.44	2.34	0.86	2.94	0.80	0.11	0.07	0.026	8.4	99.81	18	211	2
Glinzendorf S.	GT1-3716.5	Glinzendorf T1	core		53.42	15.76	7.82	2.25	5.68	0.99	2.47	0.75	0.13	0.08	0.028	10.4	99.83	16	191	2
Glinzendorf S.	GT1-3717	Glinzendorf T1	core		39.86	11.86	3.40	3.10	18.04	0.70	2.25	0.55	0.06	0.16	0.093	19.7	99.83	14	161	0
Glinzendorf S.	GT1-3785	Glinzendorf T1	cutting		52.43	15.64	6.84	2.21	6.96	0.85	2.72	0.70	0.12	0.14	0.045	11.2	99.85	16	210	2
Glinzendorf S.	GT1-3825	Glinzendorf T1	cutting		52.22	14.79	7.38	2.07	7.66	0.75	2.57	0.67	0.12	0.12	0.054	11.4	99.87	16	184	2
Glinzendorf S.	GT1-3870	Glinzendorf T1	cutting		56.74	19.12	7.24	2.14	1.14	1.07	3.13	0.80	0.21	0.23	0.017	8.0	99.84	18	290	2
Glinzendorf S.	GT1-3900	Glinzendorf T1	core		54.50	20.32	8.02	2.17	0.78	1.14	2.75	0.88	0.20	0.24	0.018	8.8	99.82	18	243	3
Glinzendorf S.	GT1-3901	Glinzendorf T1	core		55.30	20.33	7.69	2.15	0.64	1.09	2.93	0.86	0.18	0.16	0.017	8.5	99.81	18	265	2
Glinzendorf S.	GT1-3903	Glinzendorf T1	core		55.08	20.68	7.43	2.23	0.67	1.04	3.21	0.87	0.09	0.21	0.017	8.3	99.83	19	262	3
Glinzendorf S.	GT1-3904.5	Glinzendorf T1	core		54.76	20.40	7.74	2.18	0.58	1.17	3.01	0.87	0.11	0.22	0.020	8.7	99.79	18	254	3
Glinzendorf S.	GT1-3925	Glinzendorf T1	cutting		55.03	17.63	7.35	2.18	3.21	1.18	2.75	0.75	0.16	0.23	0.017	9.3	99.85	16	295	2
Glinzendorf S.	GT1-3945.5	Glinzendorf T1	core		58.72	19.41	6.48	2.04	0.98	0.90	3.19	0.81	0.11	0.12	0.016	7.0	99.82	18	276	3
Glinzendorf S.	GT1-3946.5	Glinzendorf T1	core		56.64	20.43	6.65	1.96	1.54	0.86	2.95	0.87	0.11	0.08	0.019	7.7	99.83	18	254	2
Glinzendorf S.	GT1-3947.5 RED	Glinzendorf T1	core		54.84	14.44	7.91	1.16	7.01	0.59	1.95	0.81	0.06	0.12	0.022	11.0	99.88	15	113	3
Glinzendorf S.	GT1-3947.5 BLACK	Glinzendorf T1	core		55.60	20.44	7.84	2.10	0.94	0.95	2.81	0.84	0.15	0.14	0.018	8.0	99.82	18	246	3
Glinzendorf S.	GT1-3948.5	Glinzendorf T1	core		49.98	13.95	5.51	1.11	11.74	0.56	1.91	0.72	0.06	0.15	0.017	14.2	99.87	14	105	2
Glinzendorf S.	GT1-3949.5	Glinzendorf T1	core		52.29	17.13	6.48	1.53	6.44	0.57	2.40	0.74	0.09	0.13	0.060	11.9	99.86	17	127	4
Glinzendorf S.	GFT3-3050	Gänserndorf T3	cutting		50.22	13.29	5.00	3.57	9.37	0.99	2.82	0.61	0.12	0.10	0.013	13.7	99.80	13	349	2
Glinzendorf S.	GFT3-3079	Gänserndorf T3	core		12.84	4.66	1.44	1.44	41.35	0.14	0.84	0.17	0.24	0.10	0.017	36.6	99.86	5	88	0
Glinzendorf S.	GFT3-3079.5	Gänserndorf T3	core		25.53	9.92	3.57	1.63	29.27	0.25	1.86	0.33	0.09	0.08	0.045	27.2	99.85	11	147	2
Glinzendorf S.	GFT3-3080.5	Gänserndorf T3	core		23.28	8.51	3.21	1.60	31.62	0.21	1.52	0.30	0.05	0.08	0.028	29.4	99.84	9	123	2
Glinzendorf S.	GFT3-3081	Gänserndorf T3	core		6.55	1.99	0.93	1.00	48.23	0.08	0.29	0.06	0.04	0.07	0.005	40.6	99.85	2	93	0
Glinzendorf S.	GFT3-3083	Gänserndorf T3	core		31.88	12.01	3.39	1.68	24.25	0.26	2.20	0.43	0.06	0.06	0.029	23.6	99.85	11	168	2
Glinzendorf S.	GFT3-3083.5	Gänserndorf T3	core		45.44	17.42	3.96	1.94	11.43	0.32	3.41	0.58	0.10	0.05	0.032	15.1	99.82	17	228	1
Glinzendorf S.	GFT3-3100	Gänserndorf T3	cutting		32.25	9.57	3.86	3.10	22.58	0.61	1.95	0.41	0.09	0.13	0.011	25.3	99.83	9	244	1
Glinzendorf S.	GFT3-3125	Gänserndorf T3	cutting		38.96	12.05	5.38	3.23	14.16	0.61	2.18	0.48	0.09	0.08	0.034	22.5	99.82	12	260	2
Glinzendorf S.	GFT3-3146	Gänserndorf T3	core		29.94	7.87	4.53	6.36	22.78	0.32	1.38	0.37	0.06	0.13	0.053	26.0	99.81	9	136	1
Glinzendorf S.	GFT3-3147 RED	Gänserndorf T3	core		35.19	7.93	7.63	6.50	18.65	0.30	1.27	0.39	0.04	0.10	0.123	21.6	99.78	11	247	1
Glinzendorf S.	GFT3-3147 GREY	Gänserndorf T3	core		36.46	7.40	4.51	6.56	20.00	0.33	1.17	0.42	0.04	0.10	0.118	22.6	99.79	10	253	2
Glinzendorf S.	GFT3-3148	Gänserndorf T3	core		34.27	10.78	5.05	5.31	18.99	0.46	1.76	0.44	0.05	0.10	0.039	22.5	99.80	12	159	1
Grünbach S.	M-1	Maiersdorf (Grünbach Fm)	outcrop		24.81	12.75	7.18	0.88	1.28	0.18	2.24	0.51	0.06	0.05	0.012	49.8	99.77	16	1473	4
Grünbach S.	M-1B	Maiersdorf (Grünbach Fm)	outcrop		5.94	2.59	3.75	0.42	9.52	0.06	0.49	0.12	0.04	0.17	0.008	73.0	96.09	5	86	0

Samples	Co	Cs	Ga	Hf	Nb	Rb	Sn	Sr	Ta	Th	U	V	W	Zr	Y	La	Ce	Pr	Nd	Sm	Eu	Gd	Tb	Dy	Ho
Unit	[ppm]	[ppm]	[ppm]	[ppm]	[ppm]	[ppm]	[ppm]	[ppm]	[ppm]	[ppm]	[ppm]	[ppm]	[ppm]	[ppm]	[ppm]	[ppm]	[ppm]	[ppm]	[ppm]	[ppm]	[ppm]	[ppm]	[ppm]	[ppm]	[ppm]
DL	0.2	0.1	0.5	0.1	0.1	0.1	1	0.5	0.1	0.2	0.1	8	0.5	0.1	0.1	0.1	0.1	0.02	0.3	0.05	0.02	0.05	0.01	0.05	0.02
GT1-3552	21.4	8.3	22.9	6.3	20.1	122.6	3	186.2	1.5	15.1	3.5	179	2.2	204.1	27.7	38.9	91.7	9.58	37.9	6.24	1.23	5.00	0.83	4.64	0.97
GT1-3553	19.1	8.5	21.7	5.9	20.0	121.2	3	183.0	1.4	15.5	3.4	173	2.0	191.8	26.3	39.0	92.1	9.48	36.6	6.24	1.22	4.79	0.83	4.72	0.98
GT1-3554	24.2	7.4	19.1	5.0	12.8	91.8	3	190.2	0.9	13.8	3.0	143	2.0	173.5	25.4	24.4	58.5	6.26	24.6	5.74	1.29	5.58	0.89	5.05	0.93
GT1-3554.5	20.8	8.6	21.0	4.8	15.1	118.4	3	283.9	1.0	15.6	2.9	165	2.1	159.0	24.1	33.8	78.7	8.12	30.2	5.40	1.08	4.37	0.77	4.47	0.91
GT1-3570	18.1	7.6	19.7	4.8	13.5	101.7	3	195.9	1.0	12.6	2.7	136	2.6	164.0	25.3	28.9	64.5	7.14	28.1	5.71	1.23	5.20	0.86	4.55	0.90
GT1-3611.5	23.8	8.4	22.0	5.7	16.8	112.5	3	195.6	1.1	15.0	3.0	173	2.5	197.0	23.7	34.5	78.6	8.02	29.4	4.95	0.98	4.18	0.72	4.10	0.86
GT1-3613	20.3	9.1	21.0	5.0	14.8	127.8	3	136.7	1.1	14.6	2.9	165	2.3	163.5	23.1	33.3	74.8	7.81	28.6	5.14	1.06	4.25	0.76	4.38	0.87
GT1-3615.2	18.8	1.9	7.4	5.2	8.0	29.6	0	169.5	0.6	6.4	1.7	64	2.2	184.9	16.9	16.6	43.6	4.45	18.5	3.71	0.83	3.56	0.58	3.11	0.60
GT1-3630	18.8	8.2	18.5	4.7	13.0	123.0	3	245.4	1.1	12.9	3.0	121	4.8	153.8	27.6	29.5	63.5	7.20	27.5	5.61	1.13	5.25	0.89	4.87	0.96
GT1-3651.5	33.2	10.2	18.6	5.4	15.2	137.6	3	130.3	1.2	14.9	2.7	121	2.7	189.9	33.3	41.0	94.8	10.35	40.3	8.36	1.64	7.43	1.14	6.33	1.23
GT1-3652.5	31.1	8.2	16.8	5.6	14.4	119.0	2	105.3	1.1	13.4	2.7	124	2.5	205.5	30.3	33.8	78.5	8.11	32.0	6.18	1.22	5.68	0.98	5.30	1.08
GT1-3680	23.1	9.7	21.1	4.4	13.7	136.9	4	146.7	1.1	13.6	2.8	136	4.3	149.8	25.4	31.3	67.6	7.46	30.2	5.56	1.17	5.02	0.82	4.45	0.88
GT1-3713.5	23.3	8.7	16.9	4.4	13.7	106.9	2	136.9	1.0	14.0	2.5	135	2.1	145.8	24.4	30.4	67.9	7.34	28.6	5.81	1.15	5.06	0.86	4.79	0.95
GT1-3714.5	26.5	9.7	18.9	4.3	14.1	122.3	3	142.3	1.1	13.6	2.8	143	2.0	145.0	23.7	31.2	70.6	7.48	27.6	5.50	1.11	4.85	0.79	4.78	0.93
GT1-3716.5	21.9	8.0	17.4	4.2	13.7	98.5	3	156.3	1.0	12.5	2.5	127	2.0	148.7	23.9	28.8	65.0	6.93	26.8	5.58	1.15	5.07	0.83	4.75	0.93
GT1-3717	30.5	10.2	14.7	2.9	10.7	100.0	2	285.3	0.6	10.5	2.5	121	1.9	114.4	19.5	22.6	50.6	5.52	19.1	3.89	0.80	3.42	0.61	3.28	0.72
GT1-3785	24.9	8.5	18.1	4.2	13.5	118.0	3	145.2	1.0	13.2	2.8	123	5.0	146.4	25.6	31.4	66.7	7.48	29.9	5.63	1.13	5.01	0.83	4.59	0.92
GT1-3825	24.8	8.3	17.9	4.4	12.7	110.3	3	145.6	1.0	12.4	2.7	120	4.4	155.2	26.3	29.6	62.3	6.98	27.6	5.52	1.10	4.90	0.83	4.54	0.91
GT1-3870	20.2	9.6	22.3	4.6	15.1	129.3	3	109.0	1.0	14.7	2.9	153	3.2	165.5	25.8	31.7	71.4	7.51	28.5	5.64	1.21	5.07	0.85	4.64	0.93
GT1-3900	26.6	8.8	22.9	5.3	14.4	111.5	3	125.5	1.0	16.2	3.0	180	2.1	181.8	27.9	33.6	85.1	8.46	32.5	7.35	1.56	6.10	1.00	5.13	1.00
GT1-3901	25.6	8.8	22.3	6.4	15.4	119.0	3	132.3	1.0	16.9	2.9	178	2.8	198.2	28.8	35.0	86.0	8.24	30.5	6.20	1.27	5.36	0.90	4.78	0.98
GT1-3903	24.0	10.2	22.8	5.4	15.7	133.4	4	132.7	1.0	15.4	2.7	177	2.7	173.2	24.9	35.3	84.0	7.85	27.0	4.66	0.94	3.72	0.69	3.84	0.92
GT1-3904.5	31.0	9.3	22.9	5.0	15.1	122.4	3	132.2	1.2	16.3	2.8	176	2.7	174.6	26.0	31.9	80.5	7.65	28.7	5.05	1.05	4.19	0.76	4.16	0.89
GT1-3925	19.0	8.4	19.6	4.2	13.4	116.3	3	137.3	1.0	12.5	2.8	136	5.5	155.4	25.5	30.3	66.4	7.24	28.3	5.52	1.20	5.01	0.84	4.65	0.90
GT1-3945.5	21.9	10.1	21.7	4.9	16.0	137.5	3	117.8	1.0	15.4	3.0	166	2.7	171.3	26.4	35.7	83.3	8.33	30.4	5.09	1.04	3.99	0.76	4.14	0.96
GT1-3946.5	22.7	8.5	21.8	4.9	16.1	126.0	4	111.2	1.1	16.4	3.9	171	2.4	176.9	30.6	36.8	82.4	8.71	31.6	6.41	1.26	4.92	0.88	4.88	1.08
GT1-3947.5 RED	18.6	10.0	17.2	5.4	13.8	116.7	2	113.7	1.0	10.7	2.2	137	2.1	181.0	38.2	38.8	71.4	8.55	32.0	5.96	1.28	5.24	0.94	5.17	1.15
GT1-3947.5 BLACK	25.4	8.3	22.9	4.8	14.8	113.3	3	113.8	0.9	14.6	2.9	170	2.4	162.6	27.3	35.8	85.1	8.85	32.6	6.22	1.29	5.00	0.88	4.59	1.01
GT1-3948.5	16.0	10.6	15.7	4.4	13.0	110.4	3	129.1	1.0	12.4	2.2	117	1.6	165.7	37.6	37.7	65.6	7.99	29.7	5.47	1.17	4.94	0.91	5.00	1.04
GT1-3949.5	30.0	14.7	20.2	5.0	15.9	150.8	3	116.2	1.3	16.9	3.2	113	2.8	175.5	40.2	38.8	77.1	9.12	33.5	6.71	1.28	6.03	1.05	6.21	1.28
GFT3-3050	12.2	9.3	16.2	3.2	11.3	118.1	3	324.0	0.9	11.7	3.1	107	2.0	121.3	20.3	26.1	53.8	6.22	24.1	4.54	0.96	4.12	0.68	3.83	0.73
GFT3-3079	6.8	11.3	5.2	1.3	3.4	46.1	0	652.0	0.2	3.8	1.8	35	0.6	44.7	14.5	11.6	27.1	3.06	11.8	2.35	0.54	2.68	0.44	2.20	0.43
GFT3-3079.5	22.1	16.3	13.2	1.8	6.4	101.8	2	484.2	0.4	6.9	2.8	84	1.9	65.2	15.3	18.4	40.1	4.38	17.0	3.17	0.61	2.83	0.46	2.48	0.54
GFT3-3080.5	14.4	16.4	10.1	2.0	6.5	86.5	2	607.4	0.4	6.7	2.3	72	0.9	68.9	13.2	16.3	36.3	3.94	15.5	2.79	0.50	2.54	0.40	2.20	0.45
GFT3-3081	3.2	2.7	2.7	0.5	1.2	17.7	0	896.8	0.0	1.7	12.1	50	0.0	12.9	3.7	3.9	8.3	0.94	3.3	0.57	0.12	0.61	0.11	0.61	0.11
GFT3-3083	23.1	18.4	14.5	2.4	9.0	118.5	2	483.5	0.5	9.1	3.0	99	1.6	94.4	17.0	22.7	49.4	5.31	19.8	3.75	0.68	3.03	0.53	2.95	0.60
GFT3-3083.5	18.4	16.7	22.1	3.7	11.6	181.1	4	389.6	0.6	12.7	4.1	150	2.2	121.0	23.1	30.0	68.2	7.43	27.2	5.15	0.94	4.44	0.75	4.36	0.79
GFT3-3100	9.4	7.1	11.6	2.1	7.6	81.9	2	439.3	0.5	7.4	2.8	78	1.5	71.0	13.1	17.6	36.4	4.16	16.6	3.10	0.63	2.65	0.45	2.53	0.49
GFT3-3125	27.6	11.7	13.3	2.5	9.0	92.7	3	337.1	0.6	8.5	5.8	109	1.6	86.2	15.1	20.2	41.5	4.60	17.9	3.42	0.70	3.02	0.50	2.79	0.55
GFT3-3146	30.5	8.8	9.8	1.8	7.1	65.4	1	336.1	0.5	6.6	2.0	69	0.8	67.6	14.6	15.6	34.9	3.86	15.1	2.97	0.62	2.83	0.44	2.38	0.48
GFT3-3147 RED	38.2	6.8	10.0	2.3	7.3	59.8	1	291.2	0.3	6.0	1.9	76	1.4	80.4	14.5	16.4	34.6	4.00	14.9	2.93	0.63	2.71	0.46	2.36	0.53
GFT3-3147 GREY	34.7	5.5	7.8	3.0	8.3	50.3	1	290.8	0.4	6.3	1.8	64	1.2	95.3	14.9	15.9	34.3	3.92	14.7	2.91	0.58	2.65	0.44	2.62	0.53
GFT3-3148	35.6	11.9	13.8	1.9	8.8	92.2	3	341.8	0.3	7.4	2.0	88	1.3	74.4	14.3	17.5	38.5	4.17	15.7	3.00	0.66	2.71	0.45	2.43	0.51
M-1	16.7	14.6	16.4	2.1	8.5	96.3	1	127.1	0.4	7.6	9.1	117	2.0	88.2	22.3	19.2	43.4	4.80	20.2	4.02	0.93	3.81	0.64	3.45	0.74
M-1B	7.2	1.6	12.3	0.9	9.4	20.4	0	255.4	0.1	2.3	4.0	260	3.6	35.0	8.3	5.7	13.3	1.54	5.7	1.36	0.34	1.40	0.27	1.41	0.30

Samples	Unit / DL	Er	Tm	Yb	Lu	TOT/C	TOT/S	Mo	Cu	Pb	Zn	Ni	As	Cd	Sb	Bi	Ag	Au	Hg	Tl	Se	B	$\delta^{13}C$	$\delta^{18}O$
	Unit	[ppm]	[ppm]	[ppm]	[ppm]	[%]	[%]	[ppm]	[ppm]	[ppm]	[ppm]	[ppm]	[ppm]	[ppm]	[ppm]	[ppm]	[ppm]	[ppm]	[ppm]	[ppm]	[ppm]	[ppm]	[VPDB]	[VPDB]
	DL	0.03	0.01	0.05	0.01	0.02	0.02	0.1	0.1	0.1	1	0.1	0.5	0.1	0.1	0.1	0.1	0.5	0.01	0.1	0.5	3	0.06	0.08
GT1-3552		3.01	0.49	3.06	0.46	1.54	0.54	11.5	7.0	15.8	44	52.0	24.3	0.0	0.6	0.4	0.0	1.3	0.08	0.0	0.7	137	-8.97	-3.10
GT1-3553		2.88	0.46	3.03	0.46	1.53	0.32	3.5	5.8	11.8	44	50.5	17.0	0.0	0.4	0.4	0.0	0.0	0.07	0.0	0.7	145		
GT1-3554		2.69	0.44	2.83	0.42	1.46	0.79	1.0	13.6	38.1	50	61.6	42.7	0.0	0.7	0.5	0.1	0.0	0.16	0.0	1.0	112		
GT1-3554.5		2.75	0.45	2.77	0.42	1.25	0.65	0.8	23.5	16.7	50	63.7	24.6	0.0	0.3	0.5	0.0	1.1	0.12	0.0	0.7	136	-6.29	-5.99
GT1-3570		2.68	0.41	2.67	0.40	2.04	0.49	1.4	35.5	24.4	51	58.4	21.7	0.0	0.3	0.5	0.0	1.3	0.12	0.0	0.9	124		
GT1-3611.5		2.68	0.44	2.86	0.43	1.06	0.93	0.8	54.7	55.1	54	64.5	33.4	0.0	0.4	0.6	0.1	0.0	0.12	0.0	0.7	100		
GT1-3613		2.64	0.46	2.93	0.42	0.91	0.55	1.1	139.2	15.9	118	67.8	30.6	0.1	0.4	0.5	0.0	0.0	0.09	0.0	0.0	117		
GT1-3615.2		1.59	0.25	1.70	0.23	1.97	1.04	9.9	11.1	31.3	31	50.0	30.8	0.0	1.5	0.1	0.1	0.0	0.15	0.0	0.0	38	-9.14	-7.87
GT1-3630		2.76	0.44	2.76	0.41	1.90	0.38	1.0	31.4	17.1	61	94.8	15.8	0.0	0.3	0.3	0.0	2.3	0.08	0.0	0.0	109		
GT1-3651.5		3.52	0.54	3.32	0.49	0.04	0.00	0.6	11.0	11.0	60	183.4	9.0	0.0	0.7	0.4	0.0	0.0	0.06	0.2	0.0	102		
GT1-3652.5		3.32	0.49	3.11	0.46	0.11	0.00	0.8	8.4	18.0	51	148.0	12.7	0.0	0.8	0.4	0.0	1.7	0.05	0.2	0.0	96		
GT1-3680		2.67	0.41	2.59	0.40	1.24	0.14	0.9	44.2	19.5	73	153.4	17.0	0.0	0.4	0.4	0.0	3.1	0.09	0.1	0.0	121		
GT1-3713.5		2.86	0.44	2.85	0.41	1.32	0.00	0.4	15.4	11.6	59	131.5	9.9	0.1	0.5	0.3	0.0	2.2	0.11	0.1	0.0	85	-6.57	-5.07
GT1-3714.5		2.74	0.44	2.78	0.40	0.62	0.03	0.6	20.3	13.4	80	201.3	10.7	0.0	0.4	0.3	0.0	2.8	0.08	0.0	0.0	97	-5.31	-5.89
GT1-3716.5		2.68	0.42	2.70	0.40	1.34	0.00	0.6	20.9	14.5	67	124.7	14.7	0.0	0.6	0.3	0.0	2.1	0.08	0.0	0.0	89	-5.21	-5.16
GT1-3717		1.88	0.33	2.01	0.30	4.50	0.03	0.2	69.1	10.8	54	460.6	0.9	0.1	0.0	0.3	0.0	0.5	0.02	0.0	0.0	98	-3.35	-5.06
GT1-3785		2.74	0.42	2.58	0.40	1.83	0.03	0.8	36.7	18.5	74	226.7	14.4	0.1	0.3	0.4	0.0	3.2	0.08	0.1	0.0	109		
GT1-3825		2.60	0.42	2.59	0.41	1.87	0.00	0.7	20.0	18.4	67	220.6	14.2	0.0	0.3	0.3	0.0	1.7	0.08	0.0	0.0	105		
GT1-3870		2.80	0.43	2.71	0.41	0.98	0.17	0.7	74.8	28.5	91	72.6	16.5	0.0	0.1	0.5	0.0	2.3	0.12	0.0	0.7	122		
GT1-3900		2.88	0.45	3.15	0.47	1.18	0.67	0.5	74.0	28.1	100	71.5	21.2	0.0	0.3	0.5	0.0	0.8	0.14	0.0	0.0	109		
GT1-3901		2.91	0.46	3.08	0.47	0.95	0.59	0.4	99.6	23.0	86	72.0	23.9	0.0	0.3	0.5	0.0	1.0	0.13	0.0	0.0	108		
GT1-3903		2.78	0.45	2.91	0.43	0.80	0.25	0.3	92.4	23.6	81	69.4	12.9	0.0	0.2	0.5	0.0	0.7	0.10	0.0	0.0	114		
GT1-3904.5		2.70	0.43	2.85	0.44	1.13	0.49	0.7	81.0	25.9	86	74.3	20.5	0.0	0.3	0.5	0.0	0.6	0.10	0.0	0.0	109		
GT1-3925		2.65	0.42	2.57	0.40	1.73	0.36	1.2	59.3	33.7	95	76.2	25.1	0.0	0.2	0.4	0.0	2.1	0.12	0.1	0.0	103		
GT1-3945.5		2.91	0.42	2.85	0.42	0.79	0.13	0.5	68.3	35.4	71	62.4	16.3	0.0	0.2	0.5	0.0	0.7	0.05	0.0	0.0	106		
GT1-3946.5		3.01	0.50	3.08	0.47	0.77	0.16	2.3	129.9	17.0	87	65.7	26.2	0.0	0.4	0.9	0.1	1.2	0.18	0.0	0.6	128		
GT1-3947.5 RED		3.42	0.50	3.33	0.49	1.52	0.00	0.4	7.5	15.5	34	75.1	8.5	0.0	0.6	0.3	0.0	1.0	0.14	0.0	0.0	80	-7.48	-5.55
GT1-3947.5 BLACK		3.08	0.46	3.00	0.44	0.94	0.29	8.0	50.8	116.5	120	62.5	17.9	0.5	0.2	0.5	0.0	0.0	0.07	0.0	0.0	100		
GT1-3948.5		3.12	0.48	3.13	0.47	2.62	0.00	0.4	13.1	13.8	29	68.6	6.7	0.1	0.5	0.3	0.0	1.9	0.14	0.0	0.0	71	-7.63	-5.84
GT1-3949.5		3.59	0.55	3.53	0.51	1.40	0.00	0.5	30.1	13.7	51	315.8	7.2	0.1	0.5	0.3	0.0	1.6	0.05	0.1	0.0	86	-7.63	-6.21
GFT3-3050		2.09	0.32	1.96	0.30	2.89	0.20	1.8	29.7	89.3	87	50.8	21.6	0.2	0.7	0.3	0.0	1.2	0.13	0.2	1.1	106		
GFT3-3079		1.06	0.15	0.84	0.13	9.89	0.11	0.5	10.3	5.0	22	91.3	2.5	0.0	0.0	0.1	0.0	0.0	0.01	0.0	0.0	37	0.15	-5.37
GFT3-3079.5		1.60	0.25	1.40	0.22	6.99	0.13	1.6	20.9	8.1	36	311.2	4.2	0.1	0.1	0.2	0.0	0.5	0.03	0.0	0.0	76	-1.64	-6.08
GFT3-3080.5		1.34	0.20	1.48	0.21	7.80	0.32	2.7	17.8	11.2	38	164.4	5.5	0.2	0.2	0.2	0.0	0.0	0.02	0.0	1.5	56	-1.74	-6.54
GFT3-3081		0.32	0.05	0.23	0.05	11.76	0.29	2.7	15.2	3.4	27	48.8	5.8	0.0	0.3	0.0	0.0	0.0	0.03	0.0	0.7	14	-3.48	-7.36
GFT3-3083		1.77	0.28	1.89	0.27	6.00	0.36	2.9	16.6	11.1	63	216.2	11.0	0.2	0.2	0.2	0.0	0.0	0.02	0.0	0.0	74	-0.75	-5.60
GFT3-3083.5		2.52	0.40	2.54	0.37	3.13	0.03	0.1	31.5	10.2	39	215.0	2.4	0.2	0.0	0.4	0.0	0.0	0.02	0.0	2.4	112	-2.17	-5.50
GFT3-3100		1.37	0.21	1.38	0.21	7.29	0.27	1.1	21.8	14.9	52	47.7	16.4	0.1	0.3	0.2	0.0	0.9	0.05	0.0	1.1	74		
GFT3-3125		1.60	0.28	1.63	0.25	8.07	1.53	3.1	33.0	96.7	88	356.2	24.9	0.2	0.8	0.3	0.0	2.1	0.08	0.1	1.3	98		
GFT3-3146		1.32	0.21	1.44	0.21	6.30	0.02	0.2	25.0	19.5	42	433.3	1.9	0.1	0.2	0.2	0.0	0.8	0.01	0.0	0.0	62	-4.35	-4.67
GFT3-3147 RED		1.51	0.23	1.45	0.21	4.99	0.02	0.4	23.6	18.1	49	667.0	6.1	0.1	0.8	0.2	0.0	0.8	0.01	0.0	0.0	67	-4.73	-4.87
GFT3-3147 GREY		1.47	0.25	1.61	0.22	5.43	0.02	0.1	19.2	14.9	44	568.3	0.8	0.3	0.1	0.1	0.0	0.0	0.00	0.0	0.0	64	-4.58	-4.59
GFT3-3148		1.47	0.23	1.54	0.24	4.97	0.03	0.2	25.2	21.1	51	549.4	2.8	0.1	0.3	0.2	0.0	0.7	0.04	0.0	0.0	86	-4.84	-4.53
M-1		2.10	0.33	2.10	0.30	32.04	3.64	3.3	37.9	9.6	70	38.5	34.4	0.2	1.3	0.3	0.0	1.1	1.54	0.0	2.1	132		
M-1B		0.84	0.15	0.84	0.14	49.65	0.13	1.0	7.6	4.5	13	12.4	40.5	0.0	4.8	0.0	0.0	0.0	1.25	0.0	0.6	187		

Samples	$^{87}Sr/^{86}Sr$	$CaCO_3$	TOC	CIA	CPA	Si/Al	K/Al	Na/Al	B/Al*	Th/U	Cr/V	Y/Ni	Cr/Ni	Th/Sc	Zr/Sc	La/Sc	Ti/Zr	TOC/S
Unit		[%]	[%]															
DL	0.000005	1	0.1															
GT1-3552		9	1.38	76.67	93.63	2.49	0.24	0.06	132.31	4.31	0.60	0.53	2.08	0.84	11.34	2.16	29.37	2.56
GT1-3553		6	1.42	76.69	93.64	2.39	0.24	0.06	136.34	4.56	0.62	0.52	2.14	0.82	10.09	2.05	31.88	4.42
GT1-3554		0	1.54	65.28	83.92	2.78	0.22	0.16	116.31	4.60	0.66	0.41	1.54	0.81	10.21	1.44	27.64	1.94
GT1-3554.5		9	1.26	71.30	89.84	2.52	0.26	0.10	132.91	5.38	0.66	0.38	1.70	0.87	8.83	1.88	31.67	1.94
GT1-3570				65.65	84.73	2.79	0.24	0.15	136.57	4.67	0.75	0.43	1.74	0.79	10.25	1.81	27.78	
GT1-3611.5		1	0.82	72.89	90.27	2.51	0.23	0.09	93.15	5.00	0.70	0.37	1.89	0.83	10.94	1.92	28.30	0.88
GT1-3613		1	0.86	70.70	89.80	2.60	0.27	0.10	114.81	5.03	0.70	0.34	1.69	0.86	9.62	1.96	29.70	1.56
GT1-3615.2		18	0.64	71.04	88.16	10.41	0.20	0.11	119.70	3.76	0.74	0.34	0.95	1.07	30.82	2.77	13.62	0.62
GT1-3630				71.17	90.82	3.14	0.29	0.09	131.80	4.30	1.45	0.29	1.85	0.86	10.25	1.97	25.34	
GT1-3651.5		0	0.01	74.91	94.35	3.43	0.31	0.05	116.91	5.52	1.95	0.18	1.29	0.88	11.17	2.41	24.94	
GT1-3652.5		1	0.05	73.69	93.65	3.80	0.32	0.06	120.56	4.96	3.11	0.20	2.60	0.89	13.70	2.25	21.00	
GT1-3680				74.24	93.05	2.68	0.29	0.06	131.36	4.86	1.39	0.17	1.23	0.80	8.81	1.84	29.61	
GT1-3713.5		11	0.11	73.76	91.45	2.89	0.24	0.08	98.20	5.60	1.25	0.19	1.28	0.88	9.11	1.90	31.66	
GT1-3714.5		11	0.16	74.79	92.65	2.77	0.26	0.07	102.76	4.86	1.23	0.12	0.87	0.76	8.06	1.73	33.08	5.42
GT1-3716.5		13	0.18	72.66	90.63	2.99	0.25	0.09	106.73	5.00	1.49	0.19	1.52	0.78	9.29	1.80	30.24	
GT1-3717		29	0.33	71.45	91.15	2.97	0.30	0.08	156.17	4.20	5.19	0.04	1.36	0.75	8.17	1.61	28.82	10.98
GT1-3785				73.15	91.79	2.96	0.27	0.08	131.72	4.71	2.47	0.11	1.34	0.83	9.15	1.96	28.66	
GT1-3825				73.80	92.30	3.12	0.27	0.07	134.18	4.59	3.04	0.12	1.65	0.78	9.70	1.85	25.88	
GT1-3870				73.46	91.57	2.62	0.26	0.08	120.60	5.07	0.75	0.36	1.58	0.82	9.19	1.76	28.98	
GT1-3900		0	1.16	75.13	91.55	2.37	0.21	0.08	101.38	5.40	0.68	0.39	1.70	0.90	10.10	1.87	29.02	1.72
GT1-3901		1	0.82	75.05	91.89	2.40	0.23	0.08	100.40	5.83	0.65	0.40	1.60	0.94	11.01	1.94	26.01	1.40
GT1-3903		1	0.61	74.99	92.36	2.35	0.24	0.07	104.19	5.70	0.65	0.36	1.66	0.81	9.12	1.86	30.11	2.44
GT1-3904.5		1	1.18	74.16	91.38	2.37	0.23	0.08	100.99	5.82	0.77	0.35	1.82	0.91	9.70	1.77	29.87	2.40
GT1-3925				71.99	90.08	2.76	0.24	0.09	110.42	4.46	0.84	0.33	1.51	0.78	9.71	1.89	28.93	
GT1-3945.5		0	0.58	75.16	92.91	2.67	0.26	0.07	103.21	5.13	0.65	0.42	1.73	0.86	9.52	1.98	28.35	4.48
GT1-3946.5		1	0.66	77.23	93.52	2.45	0.23	0.06	118.41	4.21	0.75	0.47	1.95	0.91	9.83	2.04	29.48	4.15
GT1-3947.5 RED		20	0.13	78.09	93.70	3.35	0.21	0.06	104.71	4.86	1.09	0.51	1.98	0.71	12.07	2.59	26.83	
GT1-3947.5 BLACK		0	1.04	76.82	92.90	2.40	0.22	0.07	92.47	5.03	0.72	0.44	1.95	0.81	9.03	1.99	30.97	3.59
GT1-3948.5		21	0.19	78.11	93.81	3.16	0.21	0.06	96.19	5.64	0.98	0.55	1.67	0.89	11.84	2.69	26.05	
GT1-3949.5		21	0.19	79.29	94.81	2.70	0.22	0.05	94.89	5.28	3.59	0.13	1.28	0.99	10.32	2.28	25.28	
GFT3-3050				67.81	89.08	3.34	0.33	0.10	150.75	3.77	0.82	0.40	1.73	0.90	9.33	2.01	30.15	
GFT3-3079		80	0.51	77.28	95.29	2.43	0.28	0.04	150.06	2.11	3.28	0.16	1.26	0.76	8.94	2.32	22.80	4.63
GFT3-3079.5		47	0.51	77.77	96.02	2.27	0.29	0.04	144.80	2.46	3.62	0.05	0.98	0.63	5.93	1.67	30.34	3.88
GFT3-3080.5		59	0.58	78.46	96.10	2.42	0.28	0.03	124.37	2.91	2.63	0.08	1.15	0.74	7.66	1.81	26.10	1.81
GFT3-3081		88	1.10	77.52	93.80	2.91	0.23	0.06	132.96	0.14	0.68	0.08	0.69	0.85	6.45	1.95	27.88	3.78
GFT3-3083		55	0.79	78.77	96.56	2.34	0.29	0.03	116.45	3.03	1.98	0.08	0.91	0.83	8.58	2.06	27.31	2.20
GFT3-3083.5		24	0.84	78.60	97.07	2.30	0.31	0.03	121.52	3.10	1.44	0.11	1.01	0.75	7.12	1.76	28.74	28.13
GFT3-3100				69.92	90.51	2.98	0.32	0.09	146.14	2.64	0.95	0.27	1.56	0.82	7.89	1.96	34.62	
GFT3-3125				73.40	92.31	2.86	0.28	0.07	153.71	1.47	2.11	0.04	0.64	0.71	7.18	1.68	33.38	
GFT3-3146		37	0.43	75.55	93.73	3.36	0.28	0.06	148.89	3.30	5.19	0.03	0.83	0.73	7.51	1.73	32.81	21.48
GFT3-3147 RED		31	0.22	77.05	94.14	3.92	0.25	0.05	159.68	3.16	10.94	0.02	1.25	0.55	7.31	1.49	29.08	10.98
GFT3-3147 GREY		43	0.25	75.88	93.17	4.35	0.25	0.06	163.46	3.50	12.46	0.03	1.40	0.63	9.53	1.59	26.42	12.28
GFT3-3148		38	0.74	75.92	93.44	2.81	0.26	0.06	150.78	3.70	2.99	0.03	0.48	0.62	6.20	1.46	35.45	24.62
M-1		0	33.75	80.87	97.73	1.72	0.28	0.02	195.67	0.84	0.69	0.58	2.11	0.48	5.51	1.20	34.66	9.27
M-1B				78.06	96.33	2.03	0.30	0.03	1364.60	0.58	0.21	0.67	4.36	0.46	7.00	1.14	20.55	

Gosau	Samples	Location	Type	Unit	SiO_2 [%]	Al_2O_3 [%]	Fe_2O_3 [%]	MgO [%]	CaO [%]	Na_2O [%]	K_2O [%]	TiO_2 [%]	P_2O_5 [%]	MnO [%]	Cr_2O_3 [%]	LOI [%]	Sum [%]	Sc [ppm]	Ba [ppm]	Be [ppm]
				DL	0.01	0.01	0.04	0.01	0.01	0.01	0.01	0.01	0.01	0.01	0.002	-5.1	0.01	1	1	1
Grünbach S.	M-2	Maiersdorf (Grünbach Fm)	outcrop																	
Grünbach S.	M-3	Maiersdorf (Grünbach Fm)	outcrop		65.44	17.06	5.12	1.48	0.31	0.50	3.81	0.97	0.20	0.03	0.014	4.9	99.83	16	622	3
Grünbach S.	M-4	Maiersdorf (Grünbach Fm)	outcrop																	
Grünbach S.	M-5	Maiersdorf (Grünbach Fm)	outcrop		27.00	9.26	12.98	1.13	5.56	0.24	1.96	0.47	0.08	0.10	0.009	41.1	99.89	13	290	2
Grünbach S.	M-6	Maiersdorf (Grünbach Fm)	outcrop		52.87	23.42	5.92	2.12	0.94	0.38	4.56	1.07	0.08	0.13	0.020	8.3	99.83	24	628	3
Grünbach S.	M-7	Maiersdorf (Grünbach Fm)	outcrop		46.62	18.05	7.23	2.13	4.62	0.43	3.96	0.85	0.11	0.09	0.017	15.7	99.84	20	524	2
Grünbach S.	M-9A	Maiersdorf (Grünbach Fm)	outcrop																	
Grünbach S.	M-9B	Maiersdorf (Grünbach Fm)	outcrop		49.69	26.47	3.61	1.82	1.29	0.31	4.03	1.17	0.08	0.03	0.023	11.3	99.83	27	598	4
Grünbach S.	M-12	Maiersdorf (Grünbach Fm)	outcrop		42.38	16.56	7.55	1.40	1.59	0.35	3.44	0.77	0.09	0.06	0.015	25.7	99.87	18	441	3
Grünbach S.	M-16	Maiersdorf (Grünbach Fm)	outcrop		52.92	22.29	6.03	2.40	1.35	0.40	4.72	1.04	0.11	0.17	0.020	8.4	99.82	23	637	2
Grünbach S.	M-17	Maiersdorf (Grünbach Fm)	outcrop		11.72	6.01	5.68	0.48	1.95	0.12	1.29	0.23	0.06	0.06	0.005	72.3	99.94	7	183	1
Grünbach S.	M-18	Maiersdorf (Grünbach Fm)	outcrop		51.43	19.54	6.68	2.44	3.00	0.48	4.31	0.89	0.12	0.11	0.017	10.8	99.83	20	533	3
Grünbach S.	M-23	Maiersdorf (Grünbach Fm)	outcrop		52.93	14.82	5.31	2.24	8.56	0.62	3.26	0.83	0.14	0.10	0.011	11.0	99.85	14	480	0
Grünbach S.	M-24	Maiersdorf (Grünbach Fm)	outcrop		53.20	23.58	5.91	2.26	0.43	0.42	4.88	1.07	0.09	0.14	0.019	7.8	99.82	24	661	4
Grünbach S.	M-27	Maiersdorf (Grünbach Fm)	outcrop																	
Grünbach S.	M-31	Maiersdorf (Grünbach Fm)	outcrop		52.73	22.21	4.93	2.42	2.63	0.46	5.04	1.02	0.11	0.03	0.019	8.2	99.83	22	612	4
Grünbach S.	M-33	Maiersdorf (Grünbach Fm)	outcrop		66.30	14.72	4.02	1.65	0.75	0.71	2.95	0.85	0.31	0.02	0.016	7.6	99.87	15	430	2
Grünbach S.	M-36	Maiersdorf (Grünbach Fm)	outcrop																	
Grünbach S.	M-37	Maiersdorf (Grünbach Fm)	outcrop		54.91	21.26	6.33	2.34	1.32	0.45	4.76	1.00	0.12	0.11	0.018	7.2	99.83	21	668	2
Grünbach S.	M-42	Maiersdorf (Grünbach Fm)	outcrop		66.58	15.37	5.40	1.90	0.49	0.50	3.19	0.97	0.15	0.07	0.014	5.2	99.84	15	491	2
Grünbach S.	M-46	Maiersdorf (Grünbach Fm)	outcrop		45.05	19.72	7.66	2.96	6.50	0.39	4.35	0.91	0.13	0.16	0.016	12.0	99.83	21	551	4
Grünbach S.	M-48	Maiersdorf (Grünbach Fm)	outcrop		53.49	18.86	6.09	2.23	4.23	0.40	4.27	0.94	0.13	0.09	0.015	9.1	99.84	19	534	2
Grünbach S.	M-50	Maiersdorf (Grünbach Fm)	outcrop		54.17	20.93	4.96	2.14	2.89	0.52	4.64	1.01	0.10	0.05	0.016	8.4	99.83	20	624	4
Grünbach S.	M-53	Maiersdorf (Grünbach Fm)	outcrop		54.77	21.65	6.34	2.33	0.74	0.32	4.76	1.00	0.06	0.07	0.019	7.8	99.84	22	593	3
Grünbach S.	M-55	Maiersdorf (Grünbach Fm)	outcrop																	
Grünbach S.	M-57	Maiersdorf (Grünbach Fm)	outcrop		54.84	17.95	5.69	1.94	4.72	0.52	3.93	0.94	0.11	0.16	0.014	9.0	99.85	18	526	1
Grünbach S.	M-60	Maiersdorf (Grünbach Fm)	outcrop		34.06	11.20	17.19	1.11	10.04	0.27	2.24	0.54	0.08	0.09	0.010	23.1	99.90	14	292	3
Grünbach S.	M-62	Maiersdorf (Grünbach Fm)	outcrop																	
Grünbach S.	M-64	Maiersdorf (Grünbach Fm)	outcrop																	
Grünbach S.	M-65	Maiersdorf (Grünbach Fm)	outcrop		48.60	19.90	4.40	2.21	6.88	0.55	4.77	0.80	0.09	0.04	0.019	11.6	99.85	19	562	4
Grünbach S.	M-66	Maiersdorf (Grünbach Fm)	outcrop																	
Grünbach S.	M-67	Maiersdorf (Grünbach Fm)	outcrop		31.01	11.89	6.05	0.63	3.87	0.28	2.15	0.47	0.06	0.08	0.010	43.4	99.92	13	315	5
Grünbach S.	M-68	Maiersdorf (Grünbach Fm)	outcrop		50.54	24.07	4.71	1.23	1.91	0.33	4.85	1.06	0.05	0.00	0.021	11.1	99.86	25	641	2
Grünbach S.	M-69	Maiersdorf (Grünbach Fm)	outcrop		54.83	14.52	7.36	1.65	7.27	0.53	3.07	0.80	0.14	0.17	0.013	9.5	99.86	16	434	2
Grünbach S.	M-71	Maiersdorf (Grünbach Fm)	outcrop																	
Grünbach S.	M-72	Maiersdorf (Grünbach Fm)	outcrop		49.87	16.59	6.49	1.91	7.99	0.46	3.64	0.81	0.13	0.13	0.016	11.8	99.86	18	490	3
Grünbach S.	M-73	Maiersdorf (Grünbach Fm)	outcrop																	
Grünbach S.	M-74	Maiersdorf (Grünbach Fm)	outcrop		21.87	9.17	8.19	0.76	5.56	0.20	1.86	0.37	0.06	0.02	0.009	51.8	99.93	13	263	3
Grünbach S.	M-75	Maiersdorf (Grünbach Fm)	outcrop		47.03	15.14	7.24	1.72	10.27	0.51	3.44	0.76	0.13	0.12	0.015	13.5	99.86	16	450	2
Grünbach S.	M-77	Maiersdorf (Grünbach Fm)	outcrop		46.04	14.16	5.39	1.52	13.31	0.49	3.09	0.77	0.15	0.14	0.012	14.8	99.87	15	449	3
Grünbach S.	M-78	Maiersdorf (Grünbach Fm)	outcrop		50.48	17.53	4.39	1.85	7.95	0.49	3.76	0.85	0.12	0.11	0.015	12.3	99.86	17	539	2
Grünbach S.	M-79	Maiersdorf (Grünbach Fm)	outcrop		43.42	13.48	15.62	1.14	1.60	0.43	2.80	0.70	0.09	0.03	0.015	20.5	99.88	16	416	5
Grünbach S.	M-82	Maiersdorf (Grünbach Fm)	outcrop																	
Grünbach S.	M-84	Maiersdorf (Grünbach Fm)	outcrop		44.13	14.35	5.34	1.64	14.33	0.47	3.11	0.72	0.14	0.10	0.012	15.5	99.87	14	441	1
Grünbach S.	M-85	Maiersdorf (Grünbach Fm)	outcrop																	

Samples	Co	Cs	Ga	Hf	Nb	Rb	Sn	Sr	Ta	Th	U	V	W	Zr	Y	La	Ce	Pr	Nd	Sm	Eu	Gd	Tb	Dy	Ho
Unit	[ppm]	[ppm]	[ppm]	[ppm]	[ppm]	[ppm]	[ppm]	[ppm]	[ppm]	[ppm]	[ppm]	[ppm]	[ppm]	[ppm]	[ppm]	[ppm]	[ppm]	[ppm]	[ppm]	[ppm]	[ppm]	[ppm]	[ppm]	[ppm]	[ppm]
DL	0.2	0.1	0.5	0.1	0.1	0.1	1	0.5	0.1	0.2	0.1	8	0.5	0.1	0.1	0.1	0.1	0.02	0.3	0.05	0.02	0.05	0.01	0.05	0.02
M-2																									
M-3	10.5	7.3	21.4	6.5	16.9	139.5	4	89.1	1.3	12.4	3.0	137	2.9	252.6	32.1	43.0	94.7	10.31	38.1	6.92	1.40	5.89	0.94	5.29	1.07
M-4																									
M-5	17.3	4.9	14.0	2.6	8.4	73.0	2	191.1	0.5	6.3	4.4	76	2.5	104.0	21.2	19.8	45.0	5.11	22.2	4.23	0.97	4.09	0.68	3.72	0.70
M-6	22.2	14.3	29.0	4.8	17.9	188.8	5	101.2	1.4	14.2	4.6	199	2.9	164.5	30.0	37.5	79.0	8.94	35.3	6.48	1.39	5.56	0.93	5.38	1.09
M-7	19.1	11.2	23.9	4.0	15.5	154.6	4	179.4	1.1	11.9	5.9	163	2.2	145.8	30.8	30.9	66.9	7.54	31.5	6.04	1.35	5.53	0.91	5.27	1.01
M-9A																									
M-9B	28.3	19.2	32.6	5.4	21.0	181.5	6	121.5	1.6	16.7	8.7	236	3.1	183.1	28.0	39.6	83.8	9.60	38.7	7.02	1.51	5.62	0.91	5.01	1.03
M-12	16.6	9.0	21.0	3.9	13.5	133.6	3	112.9	1.0	10.1	4.4	159	2.2	133.4	23.4	28.6	58.8	6.71	28.0	5.07	1.13	4.45	0.74	4.27	0.85
M-16	24.5	12.3	27.9	4.6	18.1	182.5	5	124.6	1.2	13.6	3.6	189	2.7	154.9	28.7	36.6	75.7	8.51	33.7	6.37	1.37	5.31	0.92	5.19	1.05
M-17	7.2	3.9	9.0	0.9	4.5	52.6	1	149.2	0.2	2.9	8.2	98	1.0	38.1	13.0	10.2	23.4	2.67	10.5	2.23	0.52	2.46	0.38	2.03	0.39
M-18	20.2	12.2	24.5	4.3	16.3	159.6	4	135.9	1.2	13.8	4.2	147	2.7	149.8	27.3	33.4	72.3	7.91	30.8	6.30	1.37	5.36	0.88	4.76	0.94
M-23	14.9	7.3	19.0	5.4	14.7	122.0	3	139.3	0.9	11.1	3.2	135	2.6	189.0	28.8	32.6	71.4	7.91	31.3	5.65	1.21	5.30	0.86	4.77	0.95
M-24	27.0	12.8	31.4	5.1	19.1	199.3	5	105.0	1.2	16.3	4.2	219	3.4	177.2	30.9	43.0	91.4	10.12	41.6	7.27	1.49	6.44	0.99	5.66	1.16
M-27																									
M-31	18.7	12.5	29.6	4.6	17.8	199.3	5	124.6	1.2	13.6	3.5	199	2.9	177.8	30.1	37.3	79.9	8.95	33.8	6.17	1.24	5.28	0.86	5.12	1.00
M-33	15.2	7.5	19.0	4.9	15.2	129.6	3	86.7	1.1	10.6	3.6	125	2.6	194.9	31.4	40.4	88.6	9.84	39.1	7.09	1.50	6.38	1.03	5.62	1.05
M-36																									
M-37	17.6	11.4	27.1	5.0	16.9	190.5	6	101.7	1.1	16.0	3.2	189	2.7	178.9	31.8	39.2	86.8	9.72	36.8	6.93	1.38	6.05	0.96	5.68	1.08
M-42	21.2	7.5	19.9	7.0	17.1	126.6	4	69.4	1.2	12.5	3.6	146	2.7	271.5	33.4	37.9	80.7	8.91	35.1	6.38	1.40	6.12	1.00	5.79	1.14
M-46	23.0	10.1	25.8	3.9	16.0	168.4	4	136.5	0.8	13.1	3.9	174	2.2	138.4	28.8	35.4	78.0	8.54	35.5	6.16	1.31	5.51	0.86	4.95	0.96
M-48	22.7	10.6	24.1	4.9	16.3	168.1	5	112.5	1.1	13.3	3.4	157	2.7	178.8	32.2	37.3	81.9	9.21	35.8	6.54	1.36	5.95	0.98	5.26	1.09
M-50	23.6	13.0	27.5	5.5	18.1	202.5	5	94.5	1.1	15.3	3.9	185	2.8	185.9	32.4	42.0	88.7	10.22	40.8	7.32	1.51	6.32	1.00	5.58	1.10
M-53	27.2	13.7	28.6	5.2	18.2	196.3	5	92.1	1.3	15.7	3.2	181	2.7	170.5	28.5	39.8	87.0	9.87	38.0	6.84	1.32	5.53	0.89	5.22	1.03
M-55																									
M-57	22.4	10.3	22.9	5.9	16.4	156.9	4	85.3	1.1	13.1	3.4	144	2.6	210.3	33.4	39.0	83.3	9.61	36.8	6.87	1.44	6.27	1.01	5.99	1.15
M-60	12.5	7.0	16.1	3.1	10.2	92.7	3	129.5	0.7	9.3	4.5	106	2.3	116.3	25.4	24.8	54.2	6.36	25.6	4.92	1.14	5.03	0.79	4.36	0.89
M-62																									
M-64																									
M-65	19.4	15.5	25.4	4.2	15.9	198.8	5	94.8	1.1	14.7	3.0	133	3.6	152.8	23.9	34.9	73.8	8.52	32.8	5.77	1.11	4.89	0.75	4.49	0.89
M-66																									
M-67	27.2	7.5	15.3	2.6	7.5	89.5	3	67.6	0.5	6.8	3.4	93	2.0	103.1	29.6	21.3	48.7	5.76	23.5	5.21	1.18	5.59	0.94	5.41	1.06
M-68	3.2	21.8	32.6	4.9	18.9	216.6	5	92.2	1.3	17.4	3.7	203	3.2	166.3	24.1	41.6	86.3	9.48	34.8	6.03	1.21	4.73	0.72	4.10	0.85
M-69	18.3	7.4	18.0	4.8	14.1	115.2	3	119.9	0.9	10.4	2.7	116	2.4	182.4	31.2	32.9	71.7	8.12	31.9	6.22	1.33	5.80	0.92	5.23	1.06
M-71																									
M-72	24.3	10.2	20.2	4.4	14.3	143.3	4	122.8	1.0	12.4	2.8	149	2.1	153.2	31.0	35.4	77.8	8.65	32.8	6.60	1.35	6.26	0.98	5.49	1.07
M-73																									
M-74	7.0	6.8	17.1	2.0	7.1	77.7	2	72.4	0.4	6.9	3.7	90	2.9	71.9	23.0	17.1	36.8	4.27	16.2	3.59	0.83	3.76	0.67	3.70	0.78
M-75	19.9	10.6	19.4	4.9	14.2	137.5	3	145.4	0.8	11.3	3.1	121	2.2	165.3	28.2	34.5	73.4	8.38	33.3	6.03	1.28	5.44	0.90	4.80	0.98
M-77	17.2	8.0	18.4	5.3	14.1	121.8	3	137.3	0.8	11.9	3.2	114	2.7	163.5	28.8	32.5	68.8	7.99	31.3	5.87	1.26	5.57	0.91	4.96	1.04
M-78	18.6	10.9	21.9	4.7	15.0	154.9	4	91.0	1.0	13.3	3.6	148	2.6	157.3	27.6	35.1	74.7	8.53	32.3	6.08	1.23	5.29	0.87	4.65	1.00
M-79	17.8	8.4	18.8	4.4	12.8	112.5	3	61.1	0.9	10.7	5.4	172	2.1	165.7	28.6	30.7	64.9	7.64	30.8	5.56	1.20	5.10	0.86	4.98	1.00
M-82																									
M-84	17.6	10.1	17.7	4.1	13.2	126.3	3	140.8	0.7	10.8	2.6	119	2.4	143.6	25.6	30.0	65.3	7.24	29.3	5.37	1.07	4.79	0.78	4.38	0.88
M-85																									

Samples	Er	Tm	Yb	Lu	TOT/C	TOT/S	Mo	Cu	Pb	Zn	Ni	As	Cd	Sb	Bi	Ag	Au	Hg	Tl	Se	B	$\delta^{13}C$	$\delta^{18}O$
Unit	[ppm]	[ppm]	[ppm]	[ppm]	[%]	[%]	[ppm]	[ppm]	[ppm]	[ppm]	[ppm]	[ppm]	[ppm]	[ppm]	[ppm]	[ppm]	[ppm]	[ppm]	[ppm]	[ppm]	[ppm]	[VPDB]	[VPDB]
DL	0.03	0.01	0.05	0.01	0.02	0.02	0.1	0.1	0.1	1	0.1	0.5	0.1	0.1	0.1	0.1	0.5	0.01	0.1	0.5	3	0.06	0.08
M-2																						-2.28	-5.73
M-3	3.15	0.46	3.14	0.45	0.19	0.00	0.3	36.8	9.6	49	33.6	13.3	0.0	1.0	0.5	0.1	2.7	2.55	0.0	0.0	179		
M-4																						-2.93	-5.67
M-5	2.07	0.33	1.94	0.28	24.72	4.83	5.9	27.6	20.7	42	62.6	300.4	0.2	6.5	0.2	0.1	0.0	4.12	0.3	0.8	214	-4.70	-6.42
M-6	3.18	0.51	3.22	0.46	0.63	0.11	0.2	65.3	15.6	55	40.3	3.4	0.0	0.3	0.5	0.1	2.8	0.27	0.0	0.5	225		
M-7	2.94	0.45	3.00	0.44	6.38	3.00	2.3	41.1	12.7	180	50.0	70.2	0.3	0.9	0.4	0.1	1.5	1.41	0.1	0.9	160	-2.04	-6.40
M-9A																						-3.04	-5.84
M-9B	3.14	0.47	3.22	0.50	1.28	0.13	1.5	78.3	21.7	66	55.7	13.4	0.2	1.2	0.6	0.2	1.6	0.96	0.0	1.0	272		
M-12	2.51	0.37	2.46	0.37	10.73	0.51	2.9	37.6	15.9	55	56.4	59.3	0.1	4.4	0.4	0.0	1.1	2.38	0.1	2.0	146		
M-16	3.05	0.46	3.21	0.44	0.88	0.07	0.6	64.4	12.5	53	51.5	5.9	0.0	0.4	0.5	0.0	2.8	0.34	0.0	0.0	179	-2.88	-5.27
M-17	1.09	0.16	0.91	0.16	48.96	0.25	5.6	16.6	5.0	43	22.6	18.9	0.3	0.4	0.1	0.0	0.0	0.78	0.0	1.5	168		
M-18	2.85	0.44	2.83	0.42	2.64	0.98	1.1	51.6	10.6	50	51.6	24.2	0.1	0.6	0.5	0.1	0.9	0.71	0.0	0.0	164	-1.42	-5.15
M-23	2.87	0.44	2.66	0.44	2.10	0.38	1.1	40.6	7.5	43	38.4	17.3	0.0	0.7	0.3	0.0	1.0	0.71	0.0	0.5	146	-4.03	-5.97
M-24	3.36	0.53	3.31	0.51	0.48	0.25	1.3	67.8	14.6	65	64.0	11.5	0.2	0.3	0.5	0.1	1.4	0.64	0.0	0.0	160		
M-27																						-3.21	-6.51
M-31	2.99	0.45	3.04	0.46	0.97	0.02	0.3	55.3	16.3	49	49.0	9.6	0.0	0.7	0.5	0.0	1.1	0.66	0.0	0.0	178		
M-33	3.13	0.46	2.86	0.46	1.97	0.04	0.3	45.6	6.0	63	41.6	21.2	0.0	0.8	0.3	0.0	0.6	0.46	0.0	0.6	111		
M-36																						-7.19	-8.41
M-37	3.29	0.51	3.26	0.50	0.34	0.00	1.0	49.1	10.1	47	56.1	10.6	0.0	0.5	0.4	0.0	2.1	0.66	0.0	0.0	170		
M-42	3.43	0.52	3.41	0.51	0.07	0.00	0.2	50.1	7.9	44	53.6	5.6	0.0	0.4	0.3	0.0	2.3	0.50	0.0	0.0	123		
M-46	2.91	0.44	2.79	0.44	1.68	0.00	1.5	54.7	12.4	62	53.5	11.7	0.2	0.6	0.4	0.0	2.1	0.51	0.0	0.0	167	-4.35	-6.86
M-48	3.36	0.49	3.27	0.48	0.84	0.00	0.1	50.0	13.9	56	52.6	3.1	0.1	0.2	0.4	0.0	2.6	0.74	0.0	0.0	173	-5.67	-7.09
M-50	3.30	0.51	3.38	0.53	0.69	0.00	1.5	58.3	17.7	62	51.8	32.5	0.0	0.9	0.4	0.0	1.2	1.66	0.0	0.0	163		
M-53	3.35	0.49	3.26	0.49	0.11	0.00	0.0	53.9	15.6	54	58.7	0.7	0.0	0.1	0.4	0.0	1.8	1.23	0.0	0.0	154		
M-55																						-7.18	-7.43
M-57	3.45	0.51	3.25	0.51	0.99	0.00	0.2	51.3	11.4	47	56.1	5.6	0.0	0.2	0.4	0.0	2.3	0.60	0.0	0.0	132	-9.03	-8.34
M-60	2.60	0.38	2.44	0.38	7.53	0.13	10.6	26.0	9.9	39	60.7	128.4	0.3	2.6	0.2	0.1	0.0	2.22	0.2	0.8	89	-7.61	-8.39
M-62																						-3.69	-6.78
M-64																						-9.21	-8.46
M-65	2.56	0.40	2.54	0.40	1.53	0.00	0.6	38.6	16.2	52	51.5	10.7	0.1	0.1	0.4	0.0	2.1	0.30	0.0	0.0	150	-5.83	-7.44
M-66																						-5.32	-7.42
M-67	3.14	0.47	2.89	0.45	20.88	0.82	17.3	28.7	5.8	79	75.4	110.5	0.1	1.6	0.2	0.1	0.9	4.99	0.1	1.9	74		
M-68	2.73	0.40	2.75	0.43	1.41	0.00	1.3	28.8	25.2	6	5.1	33.9	0.0	0.5	0.5	0.2	3.5	1.85	0.1	0.0	190	-8.94	-10.01
M-69	3.10	0.46	3.02	0.46	1.44	0.00	0.8	43.1	12.2	41	70.2	21.0	0.1	0.9	0.3	0.0	1.4	0.81	0.0	0.0	128	-4.60	-6.37
M-71																						-9.32	-8.85
M-72	3.07	0.45	2.96	0.45	1.79	0.00	1.2	44.6	13.5	52	74.5	20.6	0.1	0.4	0.4	0.0	1.3	0.63	0.0	0.0	147	-5.82	-7.04
M-73																						-9.27	-9.03
M-74	2.32	0.36	2.28	0.37	25.61	0.02	5.5	33.2	10.2	45	45.1	27.5	0.2	2.2	0.2	0.0	0.0	4.95	0.2	1.1	62		
M-75	2.96	0.42	2.78	0.41	2.26	0.00	1.3	37.1	15.9	63	68.5	41.0	0.2	1.0	0.4	0.0	2.1	1.26	0.0	0.0	133	-3.58	-6.49
M-77	3.04	0.43	2.76	0.43	2.86	0.00	0.4	40.1	10.1	39	49.0	11.0	0.0	0.2	0.3	0.0	1.6	0.24	0.0	0.0	115	-5.85	-7.48
M-78	2.96	0.44	2.88	0.43	1.80	0.00	0.6	42.1	8.8	41	68.8	26.9	0.2	0.1	0.4	0.0	1.4	0.48	0.0	0.0	139	-9.27	-8.71
M-79	3.02	0.46	3.01	0.45	7.62	0.25	19.4	50.7	16.6	46	78.5	80.8	0.4	7.6	0.4	0.2	1.1	4.46	0.4	1.2	114		
M-82																						-6.38	-7.97
M-84	2.61	0.40	2.62	0.38	3.07	0.00	0.7	34.6	10.1	42	60.2	22.8	0.1	0.4	0.3	0.0	1.3	0.65	0.0	0.0	112	-6.36	-7.53
M-85																						0.28	-5.35

Samples	$^{87}Sr/^{86}Sr$	$CaCO_3$	TOC	CIA	CPA	Si/Al	K/Al	Na/Al	B/Al*	Th/U	Cr/V	Y/Ni	Cr/Ni	Th/Sc	Zr/Sc	La/Sc	Ti/Zr	TOC/S
Unit		[%]	[%]															
DL	0.000005	1	0.1															
M-2		20	1.68															
M-3		0	0.15	74.73	95.40	3.39	0.35	0.04	198.31	4.13	0.69	0.96	2.82	0.78	15.79	2.69	23.02	
M-4		16	1.80															
M-5		17	26.30	76.08	95.91	2.58	0.33	0.04	436.78	1.43	0.80	0.34	0.97	0.48	8.00	1.52	27.09	5.45
M-6		0	0.56	79.11	97.40	1.99	0.31	0.02	181.58	3.09	0.68	0.74	3.35	0.59	6.85	1.56	38.99	5.06
M-7		12	4.85	76.00	96.23	2.28	0.34	0.03	167.53	2.02	0.70	0.62	2.30	0.60	7.29	1.55	34.95	1.62
M-9A		13	0.09															
M-9B		4	1.06	83.10	98.11	1.66	0.24	0.02	194.21	1.92	0.66	0.50	2.79	0.62	6.78	1.47	38.31	8.15
M-12		9	12.05	77.26	96.64	2.26	0.33	0.03	166.63	2.30	0.64	0.41	1.80	0.56	7.41	1.59	34.60	23.63
M-16		10	0.62	77.62	97.13	2.10	0.33	0.03	151.78	3.78	0.72	0.56	2.62	0.59	6.73	1.59	40.25	8.84
M-17		0	52.80	77.04	96.82	1.72	0.34	0.03	528.32	0.35	0.34	0.58	1.49	0.41	5.44	1.46	36.19	211.20
M-18		13	2.16	75.78	96.12	2.33	0.35	0.03	158.63	3.29	0.78	0.53	2.23	0.69	7.49	1.67	35.62	2.20
M-23		20	0.35	72.69	93.56	3.16	0.35	0.06	186.19	3.47	0.55	0.75	1.94	0.79	13.50	2.33	26.33	0.91
M-24		0	0.46	77.97	97.15	1.99	0.32	0.02	128.24	3.88	0.59	0.48	2.01	0.68	7.38	1.79	36.20	1.83
M-27		11	1.72															
M-31		0	0.58	76.12	96.71	2.10	0.36	0.03	151.47	3.89	0.65	0.61	2.62	0.62	8.08	1.70	34.39	29.18
M-33		9	2.09	72.69	92.65	3.98	0.31	0.07	142.52	2.94	0.86	0.75	2.60	0.71	12.99	2.69	26.15	52.25
M-36		20	0.12															
M-37		6	0.18	76.22	96.64	2.28	0.35	0.03	151.13	5.00	0.64	0.57	2.17	0.76	8.52	1.87	33.51	
M-42		0	0.04	75.09	94.92	3.83	0.33	0.05	151.25	3.47	0.65	0.62	1.76	0.83	18.10	2.53	21.42	
M-46		13	0.33	76.70	96.85	2.02	0.35	0.03	160.06	3.36	0.62	0.54	2.02	0.62	6.59	1.69	39.42	
M-48		14	0.09	76.05	96.63	2.51	0.36	0.03	173.37	3.91	0.65	0.61	1.93	0.70	9.41	1.96	31.52	
M-50		4	0.19	75.66	96.07	2.29	0.35	0.03	147.19	3.92	0.58	0.63	2.09	0.77	9.30	2.10	32.57	
M-53		0	0.05	77.72	97.63	2.23	0.34	0.02	134.44	4.91	0.71	0.49	2.19	0.71	7.75	1.81	35.16	
M-55		18	0.11															
M-57		11	0.11	75.06	95.45	2.70	0.34	0.04	138.99	3.85	0.66	0.60	1.69	0.73	11.68	2.17	26.80	
M-60		19	6.41	77.17	96.19	2.69	0.31	0.03	150.19	2.07	0.64	0.42	1.11	0.66	8.31	1.77	27.84	49.27
M-62		18	0.12															
M-64		18	0.14															
M-65		18	0.17	74.05	95.65	2.16	0.38	0.04	142.46	4.90	0.97	0.46	2.49	0.77	8.04	1.84	31.39	
M-66		21	0.24															
M-67		0	21.45	78.54	96.27	2.30	0.28	0.03	117.63	2.00	0.73	0.39	0.90	0.52	7.93	1.64	27.33	26.16
M-68		11	1.36	79.16	97.79	1.85	0.32	0.02	149.19	4.70	0.70	4.73	27.82	0.70	6.65	1.66	38.21	
M-69		17	0.08	74.13	94.34	3.34	0.33	0.05	166.61	3.85	0.76	0.44	1.25	0.65	11.40	2.06	26.29	
M-71		14	1.89															
M-72		18	0.24	75.26	95.64	2.66	0.34	0.04	167.47	4.43	0.73	0.42	1.45	0.69	8.51	1.97	31.70	
M-73		12	0.98															
M-74		0	26.90	77.44	96.54	2.11	0.32	0.03	127.79	1.86	0.68	0.51	1.35	0.53	5.53	1.32	30.85	1345.00
M-75		22	0.17	73.70	94.75	2.74	0.36	0.05	166.03	3.65	0.84	0.41	1.48	0.71	10.33	2.16	27.56	
M-77		25	0.13	74.07	94.61	2.87	0.34	0.05	153.50	3.72	0.71	0.59	1.65	0.79	10.90	2.17	28.23	
M-78		19	0.25	75.52	95.60	2.54	0.34	0.04	149.86	3.69	0.68	0.40	1.47	0.78	9.25	2.06	32.40	
M-79		0	7.36	75.20	95.01	2.85	0.33	0.04	159.84	1.98	0.59	0.36	1.29	0.67	10.36	1.92	25.33	29.44
M-82		22	0.19															
M-84		27	0.20	74.50	94.89	2.72	0.34	0.05	147.51	4.15	0.68	0.43	1.35	0.77	10.26	2.14	30.06	
M-85																		

Gosau	Samples	Location	Type	Unit / DL	SiO_2 [%] 0.01	Al_2O_3 [%] 0.01	Fe_2O_3 [%] 0.04	MgO [%] 0.01	CaO [%] 0.01	Na_2O [%] 0.01	K_2O [%] 0.01	TiO_2 [%] 0.01	P_2O_5 [%] 0.01	MnO [%] 0.01	Cr_2O_3 [%] 0.002	LOI [%] -5.1	Sum [%] 0.01	Sc [ppm] 1	Ba [ppm] 1	Be [ppm] 1
Grünbach S.	M-87	Maiersdorf (Grünbach Fm)	outcrop																	
Grünbach S.	M-88	Maiersdorf (Grünbach Fm)	outcrop		28.35	10.62	10.05	0.80	4.48	0.21	1.73	0.46	0.09	0.10	0.014	43.0	99.92	14	263	6
Grünbach S.	M-89	Maiersdorf (Grünbach Fm)	outcrop																	
Grünbach S.	M-90	Maiersdorf (Grünbach Fm)	outcrop		60.27	18.26	3.66	1.72	2.99	0.41	3.26	0.95	0.08	0.02	0.018	8.2	99.86	18	456	2
Grünbach S.	M-92	Maiersdorf (Grünbach Fm)	outcrop		49.67	19.69	5.94	2.08	6.07	0.45	4.15	0.90	0.11	0.12	0.016	10.7	99.85	19	575	2
Studienka G.	STU83-3102-06_3	Studienka 83	core		13.79	3.33	1.06	1.52	42.13	0.16	0.99	0.17	0.05	0.03	0.000	36.7	99.90	3	79	0
Studienka G.	STU83-3430-35	Studienka 83	core		59.82	17.31	6.16	2.28	1.00	1.80	2.95	0.78	0.15	0.13	0.012	7.5	99.87	15	342	2
Studienka G.	STU83-4114-17_2	Studienka 83	core		35.77	13.45	5.13	2.17	19.02	0.91	2.11	0.52	0.20	0.09	0.009	20.5	99.87	12	187	2
Studienka G.	Z57-4020-23	Závod 57	core		15.05	3.26	1.43	7.63	35.22	0.24	0.96	0.16	0.05	0.03	0.008	35.8	99.80	4	79	1
Studienka G.	Z68-3721-22	Závod 68	core		52.26	12.39	4.52	3.86	9.60	1.37	2.83	0.62	0.09	0.08	0.011	12.2	99.83	12	349	4
Studienka G.	Z68-3872,5-83,6	Závod 68	core		43.63	11.68	4.12	4.46	15.12	1.16	2.53	0.57	0.12	0.08	0.008	16.3	99.81	11	295	2
Studienka G.	Z68-3883,6-89	Závod 68	core		43.10	11.91	4.12	5.78	13.78	1.12	2.67	0.57	0.09	0.08	0.008	16.5	99.78	12	457	2
Studienka G.	Z68-3948-63	Závod 68	core		37.94	11.22	3.67	5.51	17.31	0.91	2.54	0.51	0.07	0.08	0.009	20.0	99.79	11	311	2
Studienka G.	Z68-3948,5-63	Závod 68	core		45.65	13.13	4.53	4.43	12.55	1.20	2.97	0.61	0.10	0.08	0.008	14.6	99.81	12	309	1
Studienka G.	Z68-4018-36	Závod 68	core		42.73	11.75	4.38	4.73	14.23	1.11	2.63	0.57	0.17	0.08	0.008	17.4	99.81	11	270	1
Studienka G.	Z68-4063-81_1	Závod 68	core		34.44	10.01	3.53	3.86	21.91	0.78	2.30	0.44	0.06	0.08	0.008	22.4	99.81	9	272	1
Studienka G.	Z68-4063-81_2	Závod 68	core		26.55	9.24	3.39	9.47	20.58	0.52	2.46	0.38	0.06	0.08	0.007	27.0	99.74	8	242	0
Studienka G.	Z68-4063-81_3	Závod 68	core		33.57	10.11	4.32	3.24	22.47	0.73	2.35	0.44	0.66	0.09	0.008	21.8	99.81	10	284	2
Studienka G.	Z68-4137-42	Závod 68	core		22.61	6.92	2.26	2.04	33.17	0.41	1.70	0.29	0.06	0.09	0.009	30.3	99.84	7	162	1
Studienka G.	Z68-4183-86,2	Závod 68	core		18.06	5.09	2.08	1.91	36.48	0.31	1.28	0.22	0.05	0.05	0.008	34.3	99.84	5	110	1
Studienka G.	Z68-4590-99_1	Závod 68	core		29.15	2.18	0.99	2.53	33.77	0.33	0.49	0.15	0.03	0.02	0.011	30.2	99.83	2	57	0
Studienka G.	Z68-4590-99_2	Závod 68	core		40.17	3.00	1.20	3.08	26.13	0.35	0.65	0.21	0.05	0.02	0.019	25.0	99.84	3	62	0

Samples	Co	Cs	Ga	Hf	Nb	Rb	Sn	Sr	Ta	Th	U	V	W	Zr	Y	La	Ce	Pr	Nd	Sm	Eu	Gd	Tb	Dy	Ho
Unit	[ppm]	[ppm]	[ppm]	[ppm]	[ppm]	[ppm]	[ppm]	[ppm]	[ppm]	[ppm]	[ppm]	[ppm]	[ppm]	[ppm]	[ppm]	[ppm]	[ppm]	[ppm]	[ppm]	[ppm]	[ppm]	[ppm]	[ppm]	[ppm]	[ppm]
DL	0.2	0.1	0.5	0.1	0.1	0.1	1	0.5	0.1	0.2	0.1	8	0.5	0.1	0.1	0.1	0.1	0.02	0.3	0.05	0.02	0.05	0.01	0.05	0.02
M-87																									
M-88	16.2	23.5	15.7	2.6	8.1	86.0	2	66.1	0.6	7.2	3.4	111	2.1	100.9	27.9	22.0	45.7	5.44	22.4	4.54	1.03	4.78	0.77	4.47	0.87
M-89																									
M-90	23.4	15.0	22.3	5.2	15.8	149.4	4	73.7	1.0	12.5	3.0	146	2.8	186.5	28.6	36.5	78.2	8.76	34.6	6.32	1.30	5.57	0.90	4.93	1.02
M-92	23.6	11.3	24.4	4.0	15.1	163.7	4	100.3	1.0	14.0	3.2	159	3.2	145.9	27.3	35.6	74.9	8.68	33.5	6.25	1.33	5.51	0.87	4.74	1.00
STU83-3102-06_3	2.5	2.4	4.1	1.4	3.8	39.0	0	488.4	0.3	2.6	1.3	32	0.0	46.3	8.6	9.6	17.8	2.23	8.7	1.58	0.34	1.53	0.24	1.43	0.27
STU83-3430-35	14.2	9.8	20.8	5.8	13.9	122.7	4	121.0	0.9	14.5	3.5	115	2.8	184.6	28.8	33.4	69.4	7.93	30.7	5.83	1.17	5.41	0.84	4.65	0.96
STU83-4114-17_2	13.7	6.7	16.6	2.4	11.8	90.3	3	392.0	0.9	8.6	2.1	97	1.9	90.0	21.5	26.9	55.2	6.37	25.4	4.87	1.01	4.40	0.68	3.61	0.74
Z57-4020-23	4.6	2.8	4.3	1.1	3.4	37.9	0	475.6	0.2	2.4	2.4	57	1.5	42.1	8.1	8.5	16.4	1.90	8.2	1.41	0.29	1.33	0.20	1.10	0.23
Z68-3721-22	13.3	6.0	15.3	4.2	11.5	116.9	3	238.8	0.8	9.3	2.3	113	1.9	164.8	24.9	31.5	66.9	7.95	33.3	5.82	1.20	5.33	0.81	4.50	0.92
Z68-3872,5-83,6	9.3	6.1	14.3	4.1	10.8	107.9	3	388.9	0.8	8.8	2.4	102	1.6	142.5	24.4	25.5	54.1	6.21	25.0	4.84	1.04	4.37	0.71	4.09	0.85
Z68-3883,6-89	9.1	6.1	15.3	3.5	10.9	114.0	3	318.5	0.9	8.3	2.4	102	1.7	141.5	21.2	25.0	51.2	6.10	23.7	4.66	0.96	4.07	0.66	3.65	0.75
Z68-3948-63	10.6	6.1	14.0	3.3	9.8	106.7	3	437.8	0.8	8.7	2.1	106	1.3	113.8	18.8	24.4	48.5	5.96	22.7	4.33	0.89	3.69	0.61	3.58	0.67
Z68-3948,5-63	10.9	6.9	16.7	4.3	12.4	134.2	5	318.1	1.0	10.0	2.4	103	2.0	143.1	22.6	26.8	54.0	6.56	25.4	4.81	1.02	4.20	0.72	3.97	0.82
Z68-4018-36	8.9	5.9	15.0	4.3	10.9	113.9	3	364.3	0.8	8.3	2.4	96	1.9	154.8	27.4	27.8	56.4	7.14	29.0	5.80	1.28	5.26	0.88	4.69	0.93
Z68-4063-81_1	9.4	6.0	12.0	3.1	8.7	98.1	2	566.6	0.7	7.8	2.0	86	1.6	100.7	19.7	24.7	48.8	5.97	23.8	4.25	0.88	3.75	0.59	3.48	0.67
Z68-4063-81_2	5.8	4.0	11.8	2.4	7.8	92.8	2	394.0	0.5	8.3	2.1	73	2.2	94.2	13.7	20.2	39.3	4.75	18.4	3.37	0.67	2.91	0.46	2.44	0.50
Z68-4063-81_3	10.6	6.0	13.0	3.1	9.0	99.1	3	607.9	0.7	8.1	3.0	87	1.5	100.4	28.9	29.0	55.6	6.90	27.9	5.48	1.12	5.31	0.81	4.47	0.89
Z68-4137-42	11.1	5.0	8.8	1.6	5.7	71.3	1	752.1	0.3	5.5	1.2	73	1.0	56.4	14.4	17.4	31.0	4.13	15.5	2.88	0.63	2.48	0.41	2.47	0.46
Z68-4183-86,2	5.3	3.3	7.1	1.3	4.6	52.2	0	881.3	0.2	4.3	1.0	49	0.8	42.1	11.8	14.4	24.4	3.33	13.2	2.49	0.53	2.28	0.37	1.95	0.39
Z68-4590-99_1	2.8	1.1	2.5	1.6	3.2	19.1	0	895.7	0.2	2.6	1.3	24	0.0	64.2	8.5	9.4	18.5	2.27	8.8	1.59	0.29	1.44	0.23	1.32	0.26
Z68-4590-99_2	4.3	1.3	3.8	2.3	4.2	24.6	0	695.7	0.3	3.7	1.6	30	0.6	91.0	9.1	11.3	22.1	2.69	11.8	2.00	0.36	1.66	0.27	1.54	0.30

Samples	Er	Tm	Yb	Lu	TOT/C	TOT/S	Mo	Cu	Pb	Zn	Ni	As	Cd	Sb	Bi	Ag	Au	Hg	Tl	Se	B	$\delta^{13}C$	$\delta^{18}O$
Unit	[ppm]	[ppm]	[ppm]	[ppm]	[%]	[%]	[ppm]	[ppm]	[ppm]	[ppm]	[ppm]	[ppm]	[ppm]	[ppm]	[ppm]	[ppm]	[ppm]	[ppm]	[ppm]	[ppm]	[ppm]	[VPDB]	[VPDB]
DL	0.03	0.01	0.05	0.01	0.02	0.02	0.1	0.1	0.1	1	0.1	0.5	0.1	0.1	0.1	0.1	0.5	0.01	0.1	0.5	3	0.06	0.08
M-87																						-0.57	-5.40
M-88	2.55	0.38	2.48	0.38	21.43	0.66	5.6	54.0	13.0	90	97.0	51.4	0.3	3.4	0.2	0.2	0.7	1.83	0.1	1.6	67		
M-89																						-3.29	-6.98
M-90	3.03	0.44	2.92	0.44	0.83	0.00	0.0	49.1	11.9	39	42.2	21.5	0.0	0.3	0.4	0.0	2.2	0.46	0.0	0.0	138		
M-92	2.88	0.42	2.88	0.45	1.33	0.00	0.5	49.3	11.6	52	63.0	14.9	0.0	0.3	0.4	0.0	1.9	0.53	0.0	0.0	148	-6.34	-7.86
STU83-3102-06_3	0.82	0.12	0.73	0.11	9.37	0.00	0.1	6.8	4.3	18	12.2	4.1	0.0	0.0	0.0	0.0	0.0	0.01	0.0	0.0	29	0.22	-1.91
STU83-3430-35	2.96	0.43	2.94	0.45	1.00	0.03	0.8	33.5	17.2	91	41.0	10.3	0.0	0.0	0.5	0.0	0.0	0.04	0.0	0.0	78		
STU83-4114-17_2	2.09	0.29	1.99	0.29	4.79	0.51	0.3	19.3	9.4	54	23.0	9.8	0.0	0.0	0.2	0.0	0.6	0.04	0.0	0.0	122		
Z57-4020-23	0.70	0.11	0.62	0.09	9.56	0.26	0.4	5.8	9.4	26	19.3	5.6	0.2	0.2	0.0	0.0	0.7	0.02	0.0	0.0	41	1.41	-2.27
Z68-3721-22	2.42	0.37	2.56	0.36	2.73	0.07	0.1	17.3	10.8	51	23.8	27.2	0.0	0.2	0.3	0.0	0.0	0.07	0.0	0.0	74	0.36	-5.42
Z68-3872,5-83,6	2.49	0.35	2.21	0.33	4.04	0.04	0.1	17.1	9.7	48	22.9	6.7	0.1	0.2	0.2	0.0	0.0	0.04	0.0	0.0	78	0.41	-4.95
Z68-3883,6-89	2.08	0.32	2.05	0.30	4.18	0.06	0.2	16.6	10.3	52	22.2	8.9	0.0	0.2	0.2	0.0	0.0	0.05	0.0	0.0	76	0.60	-5.13
Z68-3948-63	2.05	0.29	1.80	0.28	4.88	0.00	0.2	21.2	12.8	48	26.0	3.9	0.1	0.1	0.3	0.0	0.0	0.04	0.0	0.0	88	0.93	-5.04
Z68-3948,5-63	2.24	0.35	2.20	0.33	3.41	0.00	0.2	20.1	11.6	56	27.7	3.9	0.1	0.2	0.3	0.0	0.0	0.03	0.0	0.0	81	0.77	-5.05
Z68-4018-36	2.71	0.38	2.48	0.38	3.95	0.00	0.2	15.0	7.1	50	23.0	3.7	0.1	0.1	0.2	0.0	0.5	0.04	0.0	0.0	78	0.98	-5.04
Z68-4063-81_1	1.88	0.28	1.87	0.27	5.37	0.00	0.3	14.0	8.0	42	24.0	7.2	0.2	0.2	0.2	0.0	0.7	0.05	0.0	0.0	83	1.43	-3.48
Z68-4063-81_2	1.48	0.22	1.47	0.21	6.79	0.00	0.4	10.7	8.4	55	13.5	6.4	0.2	0.2	0.3	0.0	0.8	0.03	0.0	0.0	97	0.72	-5.49
Z68-4063-81_3	2.39	0.35	2.27	0.32	5.14	0.00	0.9	26.1	15.5	42	25.4	15.5	0.1	0.5	0.3	0.0	0.0	0.04	0.0	0.0	87	1.72	-3.01
Z68-4137-42	1.31	0.20	1.28	0.18	7.51	0.00	0.0	14.3	6.9	31	28.7	8.3	0.2	0.0	0.2	0.0	0.6	0.07	0.0	0.0	64	1.75	-2.05
Z68-4183-86,2	1.11	0.17	1.04	0.15	8.41	0.00	0.0	9.1	5.8	23	18.0	4.7	0.1	0.0	0.1	0.0	0.6	0.03	0.0	0.0	54	1.50	-1.46
Z68-4590-99_1	0.76	0.11	0.70	0.10	8.03	0.17	0.2	3.0	3.1	14	15.5	6.8	0.1	0.1	0.0	0.0	0.0	0.02	0.0	0.0	33	0.20	-2.35
Z68-4590-99_2	0.93	0.15	0.94	0.13	6.45	0.22	0.2	4.0	4.3	13	27.7	7.0	0.0	0.2	0.0	0.0	0.0	0.02	0.0	0.0	43	0.20	-2.75

Samples	$^{87}Sr/^{86}Sr$	$CaCO_3$	TOC	CIA	CPA	Si/Al	K/Al	Na/Al	B/Al*	Th/U	Cr/V	Y/Ni	Cr/Ni	Th/Sc	Zr/Sc	La/Sc	Ti/Zr	TOC/S
Unit		[%]	[%]															
DL	0.000005	1	0.1															
M-87		47	0.70															
M-88		5	21.45	80.55	96.85	2.36	0.26	0.03	119.24	2.12	0.85	0.29	0.98	0.51	7.21	1.57	27.33	32.50
M-89		26	0.48															
M-90		4	0.41	78.92	96.44	2.92	0.28	0.03	142.84	4.17	0.83	0.68	2.88	0.69	10.36	2.03	30.54	
M-92		16	0.19	76.73	96.38	2.23	0.33	0.03	142.06	4.38	0.68	0.43	1.72	0.74	7.68	1.87	36.98	
STU83-3102-06_3		78	0.11	67.57	92.67	3.66	0.47	0.07	164.59	2.00	0.00	0.70	0.00	0.87	15.43	3.20	22.01	
STU83-3430-35		0	0.89	65.50	85.39	3.05	0.27	0.15	85.16	4.14	0.71	0.70	1.98	0.97	12.31	2.23	25.33	29.80
STU83-4114-17_2				71.82	89.98	2.35	0.25	0.09	171.44	4.10	0.63	0.93	2.64	0.72	7.50	2.24	34.64	
Z57-4020-23		61	0.27	64.06	89.20	4.08	0.46	0.10	237.70	1.00	0.95	0.42	2.80	0.60	10.53	2.13	22.78	1.04
Z68-3721-22		25	0.23	62.07	84.61	3.73	0.36	0.16	112.88	4.04	0.66	1.05	3.12	0.78	13.73	2.63	22.55	3.25
Z68-3872,5-83,6		30	0.20	64.05	85.96	3.30	0.34	0.14	126.22	3.67	0.53	1.07	2.36	0.80	12.95	2.32	23.98	4.95
Z68-3883,6-89		27	0.24	64.43	86.60	3.20	0.35	0.13	120.60	3.46	0.53	0.95	2.43	0.69	11.79	2.08	24.15	4.08
Z68-3948-63		31	0.16	66.14	88.23	2.99	0.36	0.11	148.24	4.14	0.57	0.72	2.34	0.79	10.35	2.22	26.87	
Z68-3948,5-63		25	0.21	64.70	86.93	3.07	0.35	0.13	116.60	4.17	0.52	0.82	1.95	0.83	11.93	2.23	25.56	
Z68-4018-36		25	0.15	64.39	86.55	3.21	0.35	0.13	125.46	3.46	0.56	1.19	2.35	0.75	14.07	2.53	22.07	
Z68-4063-81_1		42	0.10	66.44	88.64	3.04	0.36	0.11	156.71	3.90	0.63	0.82	2.25	0.87	11.19	2.74	26.19	
Z68-4063-81_2		42	0.08	67.87	91.53	2.54	0.42	0.08	198.41	3.95	0.65	1.01	3.50	1.04	11.78	2.53	24.18	
Z68-4063-81_3		41	0.10	67.15	89.38	2.93	0.36	0.10	162.64	2.70	0.62	1.14	2.13	0.81	10.04	2.90	26.27	
Z68-4137-42		63	0.11	68.45	91.12	2.89	0.39	0.08	174.80	4.58	0.83	0.50	2.12	0.79	8.06	2.49	30.83	
Z68-4183-86,2		70	0.11	67.91	90.89	3.13	0.39	0.09	200.51	4.30	1.10	0.66	3.00	0.86	8.42	2.88	31.33	
Z68-4590-99_1		67	0.17	57.43	80.06	11.81	0.35	0.21	286.10	2.00	3.10	0.55	4.80	1.30	32.10	4.70	14.01	1.02
Z68-4590-99_2		58	0.27	61.79	83.90	11.83	0.34	0.16	270.90	2.31	4.28	0.33	4.63	1.23	30.33	3.77	13.83	1.23

Gosau	Sample	Formation	Age	zrn [%]	tur [%]	rut [%]	grt [%]	chr [%]	cld [%]	sta [%]	mon [%]	tit [%]	epi [%]	hbl [%]	gln [%]	dis [%]	sil [%]	bkt/ana [%]	ZTR [%]	META [%]	grains
Gießhübl	Ad82-1	Con-San Sst	Con-San	47.0	1.0	12.0	1.0	39.0	0.0	0.0	0.0	0.0	0.0	0.0	0.0	0.0	0.0	0.0	60.0	1.0	144
Gießhübl	SchoeT11-1	Con-San Sst	Con-San	70.0	2.0	9.0	0.0	19.0	0.0	0.0	0.0	0.0	0.0	0.0	0.0	0.0	0.0	0.0	81.0	0.0	56
Gießhübl	SchoeT11-2	Con-San Sst	Con-San	30.0	1.0	4.0	3.0	62.0	0.0	0.0	0.0	0.0	0.0	0.0	0.0	0.0	0.0	0.0	35.0	3.0	100
Gießhübl	Strasshof T1-1	Con-San Sst	Con-San	28.0	1.0	4.0	1.0	66.0	0.0	0.0	0.0	0.0	0.0	0.0	0.0	0.0	0.0	0.0	33.0	1.0	108
Gießhübl	SchoeT90-1	Con-San Sst	Con-San	11.0	0.0	5.0	1.0	83.0	0.0	0.0	0.0	0.0	0.0	0.0	0.0	0.0	0.0	0.0	16.0	1.0	112
Gießhübl	SchoeT90-2	Con-San Sst	Con-San	7.0	0.0	4.0	4.0	85.0	0.0	0.0	0.0	0.0	0.0	0.0	0.0	0.0	0.0	0.0	11.0	4.0	217
Gießhübl	Strassh T9-45	Con-San Sst	Con-San	46.0	0.5	12.5	7.5	33.5	0.0	0.0	0.0	0.0	0.0	0.0	0.0	0.0	0.0	0.0	59.0	7.5	200
Gießhübl	Strassh T9-46	Con-San Sst	Con-San	1.6	14.1	10.9	1.6	67.1	3.1	0.0	0.0	0.0	0.0	0.0	0.0	0.0	0.0	1.6	26.6	4.7	64
Gießhübl	Strassh T9-47	Con-San Sst	Con-San	7.2	0.0	2.1	0.0	90.7	0.0	0.0	0.0	0.0	0.0	0.0	0.0	0.0	0.0	0.0	9.3	0.0	978
Gießhübl	Strassh T9-48	Con-San Sst	Con-San	9.2	18.5	4.6	1.5	66.2	0.0	0.0	0.0	0.0	0.0	0.0	0.0	0.0	0.0	0.0	32.3	1.5	65
Gießhübl	Strassh T9-49	Con-San Sst	Con-San	31.1	3.3	1.6	0.0	64.0	0.0	0.0	0.0	0.0	0.0	0.0	0.0	0.0	0.0	0.0	36.0	0.0	61
Gießhübl	Strassh T9-50	Con-San Sst	Con-San	18.6	0.0	19.1	60.8	1.5	0.0	0.0	0.0	0.0	0.0	0.0	0.0	0.0	0.0	0.0	37.7	60.8	204
Gießhübl	Strassh T9a-1	Con-San Sst	Con-San	49.7	4.0	14.6	0.5	30.7	0.0	0.0	0.5	0.0	0.0	0.0	0.0	0.0	0.0	0.0	68.3	0.5	200
Gießhübl	Strassh T9a-2	Con-San Sst	Con-San	53.9	1.6	15.2	0.5	28.8	0.0	0.0	0.0	0.0	0.0	0.0	0.0	0.0	0.0	0.0	70.7	0.5	184
Gießhübl	Strassh T9a-3	Con-San Sst	Con-San	7.0	1.0	4.0	0.0	88.0	0.0	0.0	0.0	0.0	0.0	0.0	0.0	0.0	0.0	0.0	12.0	0.0	200
Gießhübl	Strassh T9a-4	Con-San Sst	Con-San	12.0	2.5	5.5	0.0	79.5	0.0	0.0	0.0	0.0	0.0	0.0	0.0	0.0	0.0	0.5	20.0	0.0	200
Gießhübl	Strassh T9a-5	Con-San Sst	Con-San	31.7	4.5	15.8	32.7	5.0	8.9	0.0	0.5	0.0	0.0	0.0	0.0	0.0	0.0	1.0	51.9	41.6	202
Gießhübl	Strassh T9a-6	Con-San Sst	Con-San	21.0	15.0	26.0	28.0	4.0	6.0	0.0	0.0	0.0	0.0	0.0	0.0	0.0	0.0	0.0	62.0	34.0	100
Gießhübl	Strassh T9b-1	Con-San Sst	Con-San	22.2	5.6	12.5	54.2	5.6	0.0	0.0	0.0	0.0	0.0	0.0	0.0	0.0	0.0	0.0	40.3	54.2	73
Gießhübl	Strassh T9b-2	Con-San Sst	Con-San	63.3	8.4	12.4	3.0	11.9	0.0	0.0	0.5	0.0	0.5	0.0	0.0	0.0	0.0	0.0	84.1	3.5	202
Gießhübl	Strassh T9b-3	Con-San Sst	Con-San	62.0	4.0	16.0	2.0	15.5	0.0	0.0	0.0	0.0	0.0	0.0	0.0	0.0	0.0	0.5	82.0	2.0	200
Gießhübl	Strassh T9b-4	Con-San Sst	Con-San	48.3	5.7	15.4	2.2	27.3	0.0	0.0	1.1	0.0	0.0	0.0	0.0	0.0	0.0	0.0	69.4	2.2	178
Gießhübl	Strassh T9b-5	Con-San Sst	Con-San	60.7	6.3	12.7	1.3	17.7	0.0	1.3	0.0	0.0	0.0	0.0	0.0	0.0	0.0	0.0	79.7	2.6	79
Gießhübl	Strassh T9b-6	Con-San Sst	Con-San	8.9	0.0	3.3	1.4	86.4	0.0	0.0	0.0	0.0	0.0	0.0	0.0	0.0	0.0	0.0	12.2	1.4	214
Gießhübl	Strassh T9b-7	Con-San Sst	Con-San	5.2	1.7	6.9	0.0	86.2	0.0	0.0	0.0	0.0	0.0	0.0	0.0	0.0	0.0	0.0	13.8	0.0	58
Gießhübl	Strassh T9b-8	Con-San Sst	Con-San	10.3	4.7	0.9	1.9	82.2	0.0	0.0	0.0	0.0	0.0	0.0	0.0	0.0	0.0	0.0	15.9	1.9	107
Gießhübl	Strassh T9b-9	Con-San Sst	Con-San	11.1	3.0	3.0	3.0	79.9	0.0	0.0	0.0	0.0	0.0	0.0	0.0	0.0	0.0	0.0	17.1	3.0	99
Gießhübl	Ad02-1	Nierental Fm	Camp-L-Maastr	12.4	9.3	14.4	45.4	11.3	5.2	0.0	0.0	0.0	0.0	0.0	0.0	0.0	0.0	2.1	36.1	50.5	66
Gießhübl	Ad02-2	Nierental Fm	Camp-L-Maastr	21.3	9.6	10.6	31.9	17.0	8.5	0.0	0.0	0.0	0.0	0.0	0.0	0.0	0.0	1.1	41.5	40.4	202
Gießhübl	Ad02-3	Nierental Fm	Camp-L-Maastr	4.5	7.8	7.8	67.0	4.5	5.6	0.3	0.0	0.0	0.3	0.0	0.0	0.0	0.0	2.2	20.1	73.2	205
Gießhübl	Ad02-4	Nierental Fm	Camp-L-Maastr	4.5	6.7	11.2	60.7	6.7	4.5	1.1	0.0	0.0	2.2	0.0	0.0	0.0	0.0	2.2	22.5	68.5	205
Gießhübl	Ad02-5	Nierental Fm	Camp-L-Maastr	4.6	9.2	10.3	66.4	4.6	3.4	0.0	0.3	0.0	0.0	0.0	0.0	0.0	0.0	1.1	24.1	69.9	203
Gießhübl	Ad02-6	Nierental Fm	Camp-L-Maastr	7.4	3.2	10.6	52.1	18.1	2.1	0.0	0.0	0.0	3.2	0.0	0.0	0.0	0.0	3.2	21.3	57.4	115
Gießhübl	Ad02-7	Nierental Fm	Camp-L-Maastr	33.3	10.8	7.5	4.3	39.8	3.2	0.0	0.0	0.0	1.1	0.0	0.0	0.0	0.0	0.0	51.6	8.6	68
Gießhübl	Ad02-8	Nierental Fm	Camp-L-Maastr	24.4	12.2	7.8	15.6	36.7	2.2	0.0	0.0	0.0	0.0	0.0	0.0	0.0	0.0	1.1	44.4	17.8	140
Gießhübl	Ad02-9	Nierental Fm	Camp-L-Maastr	21.1	18.0	8.5	5.3	42.3	0.3	0.0	0.3	0.0	0.0	0.0	0.0	0.0	0.0	4.2	47.6	5.6	203
Gießhübl	Ad02-10	Nierental Fm	Camp-L-Maastr	25.8	5.2	9.3	18.6	35.1	2.1	0.0	0.0	0.0	1.0	0.0	0.0	0.0	0.0	3.1	40.2	21.6	206
Gießhübl	Ad02-11	Nierental Fm	Camp-L-Maastr	21.4	14.3	10.2	33.7	11.2	7.1	0.0	1.0	0.0	0.0	0.0	0.0	0.0	0.0	1.0	45.9	40.8	70
Gießhübl	Ad02-13	Nierental Fm	Camp-L-Maastr	23.2	11.6	12.6	12.6	32.6	5.3	0.0	0.0	0.0	0.0	0.0	0.0	0.0	0.0	2.1	47.4	17.9	65
Gießhübl	Ad02-14	Nierental Fm	Camp-L-Maastr	24.1	17.8	11.5	14.6	28.2	3.1	0.0	0.0	0.0	0.3	0.0	0.0	0.0	0.0	0.3	53.3	18.1	200
Gießhübl	Ad02-16	Nierental Fm	Camp-L-Maastr	21.3	8.5	16.0	30.9	16.0	1.1	2.1	0.0	0.0	3.2	0.0	0.0	0.0	0.0	1.1	45.7	37.2	119
Gießhübl	Strassh T9-1	L-Gießhübl Fm	L-Paleoc	4.4	2.5	9.9	82.8	0.0	0.5	0.0	0.0	0.0	0.0	0.0	0.0	0.0	0.0	0.0	16.7	83.3	203
Gießhübl	Strassh T9-2	L-Gießhübl Fm	L-Paleoc	8.0	1.5	5.0	85.6	0.0	0.0	0.0	0.0	0.0	0.0	0.0	0.0	0.0	0.0	0.0	14.4	85.6	201
Gießhübl	Strassh T9-3	L-Gießhübl Fm	L-Paleoc	4.4	0.0	2.5	93.1	0.0	0.0	0.0	0.0	0.0	0.0	0.0	0.0	0.0	0.0	0.0	6.9	93.1	203
Gießhübl	Strassh T9-4	L-Gießhübl Fm	L-Paleoc	1.0	1.0	1.5	96.6	0.0	0.0	0.0	0.0	0.0	0.0	0.0	0.0	0.0	0.0	0.0	3.4	96.6	203
Gießhübl	Strassh T9-5	L-Gießhübl Fm	L-Paleoc	0.0	0.5	0.5	99.0	0.0	0.0	0.0	0.0	0.0	0.0	0.0	0.0	0.0	0.0	0.0	1.0	99.0	202
Gießhübl	Strassh T9-6	L-Gießhübl Fm	L-Paleoc	2.0	0.5	5.5	92.0	0.0	0.0	0.0	0.0	0.0	0.0	0.0	0.0	0.0	0.0	0.0	8.0	92.0	200

Gosau	Sample	Formation	Age	zrn [%]	tur [%]	rut [%]	grt [%]	chr [%]	cld [%]	sta [%]	mon [%]	tit [%]	epi [%]	hbl [%]	gln [%]	dis [%]	sil [%]	bkt/ana [%]	ZTR [%]	META [%]	grains
Gießhübl	Strassh T9-7	L-Gießhübl Fm	L-Paleoc	9.3	1.4	7.9	80.4	0.0	0.0	0.0	0.9	0.0	0.0	0.0	0.0	0.0	0.0	0.0	18.7	80.4	214
Gießhübl	Strassh T9-8	L-Gießhübl Fm	L-Paleoc	9.6	0.4	10.0	79.9	0.0	0.0	0.0	0.0	0.0	0.0	0.0	0.0	0.0	0.0	0.0	20.1	79.9	229
Gießhübl	Strassh T9-9	L-Gießhübl Fm	L-Paleoc	4.0	0.0	5.0	90.0	0.0	1.0	0.0	0.0	0.0	0.0	0.0	0.0	0.0	0.0	0.0	9.0	91.0	200
Gießhübl	Strassh T9-10	L-Gießhübl Fm	L-Paleoc	6.3	0.5	10.2	82.5	0.0	0.5	0.0	0.0	0.0	0.0	0.0	0.0	0.0	0.0	0.0	17.0	83.0	206
Gießhübl	Strassh T9-11	L-Gießhübl Fm	L-Paleoc	9.3	0.0	10.7	79.9	0.0	0.0	0.0	0.0	0.0	0.0	0.0	0.0	0.0	0.0	0.0	20.1	79.9	214
Gießhübl	Strassh T9-12	L-Gießhübl Fm	L-Paleoc	9.0	1.0	9.0	80.5	0.0	0.5	0.0	0.0	0.0	0.0	0.0	0.0	0.0	0.0	0.0	19.0	81.0	200
Gießhübl	Strassh T9-13	L-Gießhübl Fm	L-Paleoc	6.4	0.0	4.5	88.6	0.5	0.0	0.0	0.0	0.0	0.0	0.0	0.0	0.0	0.0	0.0	10.9	88.6	202
Gießhübl	Strassh T9-14	L-Gießhübl Fm	L-Paleoc	3.8	1.4	10.9	82.9	0.5	0.5	0.0	0.0	0.0	0.0	0.0	0.0	0.0	0.0	0.0	16.1	83.4	211
Gießhübl	Strassh T9-15	L-Gießhübl Fm	L-Paleoc	8.0	2.0	11.0	78.5	0.0	0.5	0.0	0.0	0.0	0.0	0.0	0.0	0.0	0.0	0.0	21.0	79.0	200
Gießhübl	Strassh T9-16	L-Gießhübl Fm	L-Paleoc	9.5	0.5	10.0	80.0	0.0	0.0	0.0	0.0	0.0	0.0	0.0	0.0	0.0	0.0	0.0	20.0	80.0	200
Gießhübl	Strassh T9-17	L-Gießhübl Fm	L-Paleoc	0.5	2.0	8.0	88.5	0.0	1.0	0.0	0.0	0.0	0.0	0.0	0.0	0.0	0.0	0.0	10.5	89.5	200
Gießhübl	Strassh T9-18	L-Gießhübl Fm	L-Paleoc	7.8	2.0	17.6	72.5	0.0	0.0	0.0	0.0	0.0	0.0	0.0	0.0	0.0	0.0	0.0	27.5	72.5	204
Gießhübl	Strassh T9-19	L-Gießhübl Fm	L-Paleoc	8.5	0.5	12.9	77.6	0.0	0.5	0.0	0.0	0.0	0.0	0.0	0.0	0.0	0.0	0.0	21.9	78.1	201
Gießhübl	Strassh T9-20	L-Gießhübl Fm	L-Paleoc	20.1	3.3	16.3	59.3	0.5	0.5	0.0	0.0	0.0	0.0	0.0	0.0	0.0	0.0	0.0	39.7	59.8	209
Gießhübl	Strassh T9-21	L-Gießhübl Fm	L-Paleoc	4.5	2.0	2.0	90.0	0.5	0.5	0.0	0.0	0.5	0.0	0.0	0.0	0.0	0.0	0.0	8.5	91.0	200
Gießhübl	Strassh T9-22	L-Gießhübl Fm	L-Paleoc	7.8	1.0	14.2	73.5	2.0	1.5	0.0	0.0	0.0	0.0	0.0	0.0	0.0	0.0	0.0	23.0	75.0	204
Gießhübl	Strassh T9-23	L-Gießhübl Fm	L-Paleoc	7.8	2.2	4.4	85.6	0.0	0.0	0.0	0.0	0.0	0.0	0.0	0.0	0.0	0.0	0.0	14.4	85.6	90
Gießhübl	Strassh T9-24	L-Gießhübl Fm	L-Paleoc	2.5	1.5	6.9	88.7	0.0	0.5	0.0	0.0	0.0	0.0	0.0	0.0	0.0	0.0	0.0	10.8	89.2	203
Gießhübl	Strassh T9-25	L-Gießhübl Fm	L-Paleoc	13.6	3.3	12.2	66.7	3.3	0.9	0.0	0.0	0.0	0.0	0.0	0.0	0.0	0.0	0.0	29.1	67.6	213
Gießhübl	Strassh T9-26	L-Gießhübl Fm	L-Paleoc	7.3	1.0	8.7	81.1	1.0	1.0	0.0	0.0	0.0	0.0	0.0	0.0	0.0	0.0	0.0	17.0	82.0	206
Gießhübl	Strassh T9-27	L-Gießhübl Fm	L-Paleoc	8.3	1.0	4.4	85.9	0.5	0.0	0.0	0.0	0.0	0.0	0.0	0.0	0.0	0.0	0.0	13.7	85.9	205
Gießhübl	Strassh T9-28	L-Gießhübl Fm	L-Paleoc	11.1	4.0	8.5	75.4	0.0	1.0	0.0	0.0	0.0	0.0	0.0	0.0	0.0	0.0	0.0	23.6	76.4	199
Gießhübl	Ad02-17	L-Gießhübl Fm	L-Paleoc	3.0	4.0	1.0	91.1	0.0	1.0	0.0	0.0	0.0	0.0	0.0	0.0	0.0	0.0	0.0	7.9	92.1	200
Gießhübl	Ad02-18	L-Gießhübl Fm	L-Paleoc	7.2	11.3	5.2	73.2	0.0	2.1	0.0	0.0	0.0	0.0	0.0	0.0	0.0	0.0	1.0	23.7	75.3	204
Gießhübl	Ad02-19	L-Gießhübl Fm	L-Paleoc	2.1	10.3	4.1	80.2	1.0	0.0	0.0	0.0	0.0	0.3	0.0	0.0	0.0	0.0	2.1	16.4	80.5	201
Gießhübl	Ad02-20	L-Gießhübl Fm	L-Paleoc	5.3	12.6	3.2	76.8	0.0	1.1	0.0	0.0	0.0	0.0	0.0	0.0	0.0	0.0	1.1	21.1	77.9	153
Gießhübl	Ad02-21	L-Gießhübl Fm	L-Paleoc	3.1	5.2	6.2	80.4	2.1	3.1	0.0	0.0	0.0	0.0	0.0	0.0	0.0	0.0	0.0	14.4	83.5	65
Gießhübl	Ad02-22	L-Gießhübl Fm	L-Paleoc	3.1	1.0	5.1	85.5	2.0	0.0	0.3	0.0	0.0	0.0	0.0	0.0	0.0	0.0	3.1	9.2	85.8	230
Gießhübl	Ad02-23	L-Gießhübl Fm	L-Paleoc	1.0	4.1	5.1	89.8	0.0	0.0	0.0	0.0	0.0	0.0	0.0	0.0	0.0	0.0	0.0	10.2	89.8	205
Gießhübl	Ad02-24	L-Gießhübl Fm	L-Paleoc	1.0	1.0	3.1	93.6	0.0	0.0	0.0	0.3	0.0	0.0	0.0	0.0	0.0	0.0	1.0	5.1	93.6	218
Gießhübl	Ad02-25	L-Gießhübl Fm	L-Paleoc	2.1	3.2	6.4	84.8	1.1	1.1	0.0	0.0	0.0	0.3	0.0	0.0	0.0	0.0	1.1	11.7	86.2	203
Gießhübl	Ad02-26	L-Gießhübl Fm	L-Paleoc	1.0	2.1	9.3	86.2	0.0	0.0	0.0	0.0	0.0	0.3	0.0	0.0	0.0	0.0	1.0	12.5	86.5	211
Gießhübl	Ad02-27	L-Gießhübl Fm	L-Paleoc	1.0	0.3	2.1	95.2	0.0	0.3	0.0	0.0	0.0	0.0	0.0	0.0	0.0	0.0	1.0	3.5	95.5	207
Gießhübl	Ad02-28	L-Gießhübl Fm	L-Paleoc	2.0	2.0	4.1	90.5	0.0	0.3	0.0	0.0	0.0	0.0	0.0	0.0	0.0	0.0	1.0	8.1	90.8	206
Gießhübl	Ad02-29	L-Gießhübl Fm	L-Paleoc	2.0	0.3	4.0	92.4	0.0	0.3	0.0	0.0	0.0	0.0	0.0	0.0	0.0	0.0	1.0	6.3	92.7	207
Gießhübl	Ad02-30	L-Gießhübl Fm	L-Paleoc	0.0	3.0	4.0	92.4	0.3	0.3	0.0	0.0	0.0	0.0	0.0	0.0	0.0	0.0	0.0	7.0	92.7	214
Gießhübl	Ad02-31	L-Gießhübl Fm	L-Paleoc	0.0	2.0	4.1	93.9	0.0	0.0	0.0	0.0	0.0	0.0	0.0	0.0	0.0	0.0	0.0	6.1	93.9	213
Gießhübl	Ad02-32	L-Gießhübl Fm	L-Paleoc	2.1	1.0	6.3	90.6	0.0	0.0	0.0	0.0	0.0	0.0	0.0	0.0	0.0	0.0	0.0	9.4	90.6	204
Gießhübl	Ad02-33	L-Gießhübl Fm	L-Paleoc	1.0	4.1	3.1	90.8	0.0	0.0	0.0	0.0	0.0	1.0	0.0	0.0	0.0	0.0	0.0	8.2	91.8	204
Gießhübl	Ad02-34	L-Gießhübl Fm	L-Paleoc	4.1	5.1	4.1	85.7	0.0	1.0	0.0	0.0	0.0	0.0	0.0	0.0	0.0	0.0	0.0	13.3	86.7	226
Gießhübl	Ad02-35	L-Gießhübl Fm	L-Paleoc	2.0	4.0	3.0	90.9	0.0	0.0	0.0	0.0	0.0	0.0	0.0	0.0	0.0	0.0	0.0	9.1	90.9	225
Gießhübl	Ad02-36	L-Gießhübl Fm	L-Paleoc	2.1	2.1	4.2	90.2	0.0	0.0	0.3	0.0	0.0	0.0	0.0	0.0	0.0	0.0	1.0	8.4	90.6	203
Gießhübl	Ad02-37	L-Gießhübl Fm	L-Paleoc	0.3	0.3	3.1	95.9	0.0	0.0	0.0	0.0	0.0	0.0	0.0	0.0	0.0	0.0	0.3	3.8	95.9	208
Gießhübl	Ad02-38	L-Gießhübl Fm	L-Paleoc	0.3	2.0	3.1	93.6	0.0	0.0	0.0	0.0	0.0	0.0	0.0	0.0	0.0	0.0	1.0	5.4	93.6	206
Gießhübl	Ad02-39	L-Gießhübl Fm	L-Paleoc	2.0	1.0	5.1	90.9	0.0	0.3	0.3	0.0	0.0	0.3	0.0	0.0	0.0	0.0	0.0	8.2	91.8	204

Gosau	Sample	Formation	Age	zrn [%]	tur [%]	rut [%]	grt [%]	chr [%]	cld [%]	sta [%]	mon [%]	tit [%]	epi [%]	hbl [%]	gln [%]	dis [%]	sil [%]	bkt/ana [%]	ZTR [%]	META [%]	grains
Gießhübl	Ad02-40	L-Gießhübl Fm	L-Paleoc	3.1	3.1	6.1	86.5	0.0	1.0	0.0	0.0	0.0	0.0	0.0	0.0	0.0	0.0	0.3	12.2	87.5	226
Gießhübl	Ad02-41	L-Gießhübl Fm	L-Paleoc	6.2	1.0	4.1	87.4	0.0	1.0	0.0	0.0	0.0	0.3	0.0	0.0	0.0	0.0	0.0	11.3	88.7	209
Gießhübl	Ad02-42	L-Gießhübl Fm	L-Paleoc	1.0	0.0	8.2	88.8	0.0	0.0	0.0	0.0	0.0	0.0	0.0	0.0	0.0	0.0	2.0	9.2	88.8	200
Gießhübl	Ad02-43	L-Gießhübl Fm	L-Paleoc	0.3	0.3	5.0	93.4	0.0	1.0	0.0	0.0	0.0	0.0	0.0	0.0	0.0	0.0	0.0	5.6	94.4	210
Gießhübl	Ad02-44	L-Gießhübl Fm	L-Paleoc	2.0	2.0	5.0	90.4	0.0	0.0	0.0	0.3	0.0	0.0	0.0	0.0	0.0	0.0	0.3	9.0	90.4	204
Gießhübl	Ad02-45	L-Gießhübl Fm	L-Paleoc	2.0	2.0	2.0	93.6	0.0	0.0	0.0	0.0	0.0	0.0	0.0	0.0	0.0	0.0	0.3	6.1	93.6	203
Gießhübl	Ad02-46	L-Gießhübl Fm	L-Paleoc	2.1	4.2	3.2	89.5	0.0	1.1	0.0	0.0	0.0	0.0	0.0	0.0	0.0	0.0	0.0	9.5	90.5	204
Gießhübl	Ad02-47	L-Gießhübl Fm	L-Paleoc	0.3	2.1	4.2	91.4	0.0	1.0	0.0	0.0	0.0	0.0	0.0	0.0	0.0	0.0	1.0	6.5	92.4	205
Gießhübl	Ad02-48	L-Gießhübl Fm	L-Paleoc	1.1	4.2	6.3	86.3	0.0	1.1	0.0	0.0	0.0	0.0	0.0	0.0	0.0	0.0	1.1	11.6	87.4	202
Gießhübl	Ad02-49	L-Gießhübl Fm	L-Paleoc	5.1	4.1	4.1	85.8	0.0	0.3	0.0	0.3	0.0	0.0	0.0	0.0	0.0	0.0	0.3	13.3	86.1	204
Gießhübl	Ad02-50	L-Gießhübl Fm	L-Paleoc	2.0	1.0	5.1	91.2	0.0	0.3	0.0	0.0	0.0	0.0	0.0	0.0	0.0	0.0	0.3	8.2	91.5	201
Gießhübl	Ad02-51	L-Gießhübl Fm	L-Paleoc	1.0	3.1	5.2	90.3	0.0	0.3	0.0	0.0	0.0	0.0	0.0	0.0	0.0	0.0	0.0	9.3	90.7	230
Gießhübl	Ad02-52	L-Gießhübl Fm	L-Paleoc	1.0	2.0	4.1	91.3	0.0	1.0	0.0	0.3	0.0	0.0	0.0	0.0	0.0	0.0	0.3	7.1	92.3	207
Gießhübl	Ad02-53	L-Gießhübl Fm	L-Paleoc	0.0	5.2	1.0	91.4	0.0	2.1	0.0	0.0	0.0	0.0	0.0	0.0	0.0	0.0	0.3	6.2	93.5	206
Gießhübl	Ad02-54	L-Gießhübl Fm	L-Paleoc	3.0	4.0	8.1	83.6	1.0	0.3	0.0	0.0	0.0	0.0	0.0	0.0	0.0	0.0	0.0	15.1	83.9	216
Gießhübl	Ad02-55	L-Gießhübl Fm	L-Paleoc	2.1	7.5	2.1	86.8	0.0	1.1	0.0	0.0	0.0	0.3	0.0	0.0	0.0	0.0	0.0	11.8	88.2	204
Gießhübl	Ad02-56	L-Gießhübl Fm	L-Paleoc	2.1	2.1	8.4	85.3	0.0	1.1	0.0	0.0	0.0	0.0	0.0	0.0	0.0	0.0	1.1	12.6	86.3	221
Gießhübl	Ad02-57	L-Gießhübl Fm	L-Paleoc	2.1	4.2	5.3	82.1	0.0	4.2	0.0	0.0	0.0	1.1	0.0	0.0	0.0	0.0	1.1	11.6	87.4	200
Gießhübl	Ad02-58	L-Gießhübl Fm	L-Paleoc	1.0	10.5	7.3	79.7	0.0	1.0	0.0	0.0	0.0	0.0	0.0	0.0	0.0	0.0	0.3	18.9	80.8	207
Gießhübl	Ad02-59	L-Gießhübl Fm	L-Paleoc	2.1	10.6	8.5	76.4	0.0	2.1	0.0	0.0	0.0	0.3	0.0	0.0	0.0	0.0	0.0	21.2	78.8	217
Gießhübl	Ad02-60	L-Gießhübl Fm	L-Paleoc	2.1	6.2	2.1	87.0	0.0	0.3	1.0	0.0	0.0	0.3	0.0	0.0	0.0	0.0	1.0	10.4	88.6	202
Gießhübl	Ad02-61	L-Gießhübl Fm	L-Paleoc	2.1	8.5	2.1	81.9	0.0	4.3	0.0	0.0	0.0	0.0	0.0	0.0	0.0	0.0	1.1	12.8	86.2	206
Gießhübl	Ad02-62	L-Gießhübl Fm	L-Paleoc	4.4	1.1	3.3	84.4	0.0	5.6	0.0	0.0	0.0	0.0	0.0	0.0	0.0	0.0	1.1	8.9	90.0	204
Gießhübl	Ad02-63	L-Gießhübl Fm	L-Paleoc	3.1	0.3	5.2	89.3	0.0	1.0	0.0	0.0	0.0	0.0	0.0	0.0	0.0	0.0	1.0	8.6	90.3	209
Gießhübl	Ad02-64	L-Gießhübl Fm	L-Paleoc	4.2	5.2	6.3	79.2	0.0	2.1	1.0	0.0	0.0	1.0	0.0	0.0	0.0	0.0	1.0	15.6	83.3	209
Gießhübl	Ad02-65	L-Gießhübl Fm	L-Paleoc	3.2	4.2	7.4	79.5	0.0	1.1	0.0	0.0	0.0	0.3	0.0	0.0	0.0	0.0	4.2	14.8	80.9	207
Gießhübl	Ad02-66	L-Gießhübl Fm	L-Paleoc	1.1	2.1	6.3	86.7	0.0	1.1	0.3	0.0	0.0	0.3	0.0	0.0	0.0	0.0	2.1	9.5	88.4	214
Gießhübl	Ad02-67	L-Gießhübl Fm	L-Paleoc	3.2	4.2	5.3	86.7	0.0	0.3	0.0	0.0	0.0	0.0	0.0	0.0	0.0	0.0	0.3	12.7	87.0	206
Gießhübl	Ad02-68	L-Gießhübl Fm	L-Paleoc	3.1	3.1	9.4	83.9	0.0	0.0	0.0	0.0	0.0	0.0	0.0	0.0	0.0	0.0	0.3	15.7	83.9	207
Gießhübl	Ad02-69	L-Gießhübl Fm	L-Paleoc	4.1	2.1	8.2	78.4	2.1	3.1	0.0	1.0	0.0	0.0	0.0	0.0	0.0	0.0	1.0	14.4	81.4	106
Gießhübl	Ad02-70	L-Gießhübl Fm	L-Paleoc	5.2	1.0	6.3	85.0	0.3	1.0	0.0	0.0	0.0	0.0	0.0	0.0	0.0	0.0	1.0	12.6	86.0	204
Gießhübl	Ad02-71	L-Gießhübl Fm	L-Paleoc	6.2	4.1	6.2	80.7	0.3	2.1	0.0	0.0	0.0	0.0	0.0	0.0	0.0	0.0	0.3	16.6	82.8	205
Gießhübl	Ad02-72	L-Gießhübl Fm	L-Paleoc	5.3	4.2	3.2	79.3	0.3	5.3	0.3	0.0	0.0	0.0	0.0	0.0	0.0	0.0	2.1	12.7	84.9	214
Gießhübl	Ad02-73	L-Gießhübl Fm	L-Paleoc	4.3	6.5	5.4	79.3	0.0	1.1	0.0	0.0	0.0	1.1	0.0	0.0	0.0	0.0	2.2	16.3	81.5	205
Gießhübl	Ad02-74	L-Gießhübl Fm	L-Paleoc	3.2	5.4	5.4	79.3	0.0	4.3	0.0	0.3	0.0	0.0	0.0	0.0	0.0	0.0	2.1	13.9	83.6	204
Gießhübl	Ad02-75	L-Gießhübl Fm	L-Paleoc	3.3	10.9	2.2	78.6	0.0	2.2	1.1	0.0	0.3	0.3	0.0	0.0	0.0	0.0	1.1	16.4	82.5	201
Gießhübl	Ad02-76	L-Gießhübl Fm	L-Paleoc	2.1	6.3	10.4	80.2	0.0	1.0	0.0	0.0	0.0	0.0	0.0	0.0	0.0	0.0	0.0	18.8	81.3	210
Gießhübl	Ad02-77	L-Gießhübl Fm	L-Paleoc	2.2	8.6	5.4	80.7	0.3	0.3	0.0	0.0	0.0	0.3	0.0	0.0	0.0	0.0	2.2	16.1	81.4	201
Gießhübl	RaasT1-1	L-Gießhübl Fm	L-Paleoc	22.0	0.0	19.0	58.0	0.0	1.0	0.0	0.0	0.0	0.0	0.0	0.0	0.0	0.0	0.0	41.0	59.0	336
Gießhübl	RaasT1-2	L-Gießhübl Fm	L-Paleoc	28.0	1.0	25.0	46.0	0.0	0.0	0.0	0.0	0.0	0.0	0.0	0.0	0.0	0.0	0.0	54.0	46.0	307
Gießhübl	RaasT1-3	L-Gießhübl Fm	L-Paleoc	2.0	1.0	7.0	89.0	0.0	1.0	0.0	0.0	0.0	0.0	0.0	0.0	0.0	0.0	0.0	10.0	90.0	364
Gießhübl	RaasT1-4	L-Gießhübl Fm	L-Paleoc	3.0	3.0	6.0	87.0	0.0	1.0	0.0	0.0	0.0	0.0	0.0	0.0	0.0	0.0	0.0	12.0	88.0	304
Gießhübl	RaasT1-5	L-Gießhübl Fm	L-Paleoc	1.0	1.0	7.1	90.8	0.0	0.0	0.0	0.0	0.0	0.0	0.0	0.0	0.0	0.0	0.0	9.2	90.8	337
Gießhübl	RaasT1-6	L-Gießhübl Fm	L-Paleoc	45.2	9.7	11.8	28.0	2.2	2.2	0.0	0.0	0.0	0.0	0.0	0.0	0.0	0.0	1.1	66.7	30.1	218

Gosau	Sample	Formation	Age	zrn [%]	tur [%]	rut [%]	grt [%]	chr [%]	cld [%]	sta [%]	mon [%]	tit [%]	epi [%]	hbl [%]	gln [%]	dis [%]	sil [%]	bkt/ana [%]	ZTR [%]	META [%]	grains
Gießhübl	RaasT1-7	L-Gießhübl Fm	L-Paleoc	51.1	14.4	8.9	21.1	1.1	1.1	0.0	0.0	0.0	0.0	0.0	0.0	0.0	0.0	2.2	74.4	22.2	205
Gießhübl	RaasT1-10	L-Gießhübl Fm	L-Paleoc	55.4	14.5	10.8	12.0	2.4	2.4	0.0	0.0	0.0	2.4	0.0	0.0	0.0	0.0	0.0	80.7	16.9	109
Gießhübl	RaasT1-11	L-Gießhübl Fm	L-Paleoc	16.7	0.0	41.7	40.6	0.0	1.0	0.0	0.0	0.0	0.0	0.0	0.0	0.0	0.0	0.0	58.3	41.7	395
Gießhübl	RaasT1-12	L-Gießhübl Fm	L-Paleoc	5.1	14.3	14.3	66.3	0.0	0.0	0.0	0.0	0.0	0.0	0.0	0.0	0.0	0.0	0.0	33.7	66.3	269
Gießhübl	RaasT1-13	L-Gießhübl Fm	L-Paleoc	18.0	1.0	21.0	60.0	0.0	0.0	0.0	0.0	0.0	0.0	0.0	0.0	0.0	0.0	0.0	40.0	60.0	191
Gießhübl	RaasT1-14	L-Gießhübl Fm	L-Paleoc	3.0	1.0	11.1	82.8	0.0	2.0	0.0	0.0	0.0	0.0	0.0	0.0	0.0	0.0	0.0	15.2	84.8	143
Gießhübl	RaasT1-15	L-Gießhübl Fm	L-Paleoc	26.0	0.0	22.0	51.0	1.0	0.0	0.0	0.0	0.0	0.0	0.0	0.0	0.0	0.0	0.0	48.0	51.0	212
Gießhübl	RaasT1-16	L-Gießhübl Fm	L-Paleoc	23.2	4.0	18.2	52.5	1.0	1.0	0.0	0.0	0.0	0.0	0.0	0.0	0.0	0.0	0.0	45.5	53.5	281
Gießhübl	SchoeT32-1	L-Gießhübl Fm	L-Paleoc	31.0	0.0	69.0	0.0	0.0	0.0	0.0	0.0	0.0	0.0	0.0	0.0	0.0	0.0	0.0	100.0	0.0	13
Gießhübl	SchoeT32-2	L-Gießhübl Fm	L-Paleoc	40.8	0.0	29.6	29.6	0.0	0.0	0.0	0.0	0.0	0.0	0.0	0.0	0.0	0.0	0.0	70.4	29.6	24
Gießhübl	SchoeT32-3	L-Gießhübl Fm	L-Paleoc	50.0	0.0	25.0	25.0	0.0	0.0	0.0	0.0	0.0	0.0	0.0	0.0	0.0	0.0	0.0	75.0	25.0	4
Gießhübl	SchoeT32-4	L-Gießhübl Fm	L-Paleoc	5.0	0.0	15.0	80.0	0.0	0.0	0.0	0.0	0.0	0.0	0.0	0.0	0.0	0.0	0.0	20.0	80.0	120
Gießhübl	SchoeT32-5	L-Gießhübl Fm	L-Paleoc	26.3	1.0	52.5	19.2	1.0	0.0	0.0	0.0	0.0	0.0	0.0	0.0	0.0	0.0	0.0	79.8	19.2	117
Gießhübl	Strassh T9-36	M-Gießhübl Fm	M-Paleoc	1.2	3.1	9.9	85.7	0.0	0.0	0.0	0.0	0.0	0.0	0.0	0.0	0.0	0.0	0.0	14.3	85.7	161
Gießhübl	Strassh T9-37	M-Gießhübl Fm	M-Paleoc	2.8	3.2	7.9	82.9	0.9	2.3	0.0	0.0	0.0	0.0	0.0	0.0	0.0	0.0	0.0	13.9	85.2	216
Gießhübl	Strassh T9-38	M-Gießhübl Fm	M-Paleoc	3.0	2.0	5.0	89.0	0.5	0.5	0.0	0.0	0.0	0.0	0.0	0.0	0.0	0.0	0.0	10.0	89.5	200
Gießhübl	Strassh T9-39	M-Gießhübl Fm	M-Paleoc	3.5	0.0	7.0	87.5	0.0	2.0	0.0	0.0	0.0	0.0	0.0	0.0	0.0	0.0	0.0	10.5	89.5	200
Gießhübl	Strassh T9-40	M-Gießhübl Fm	M-Paleoc	1.1	4.3	5.4	88.0	1.1	0.0	0.0	0.0	0.0	0.0	0.0	0.0	0.0	0.0	0.0	10.9	88.0	92
Gießhübl	Strassh T9-41	M-Gießhübl Fm	M-Paleoc	3.4	2.0	5.9	87.3	0.0	1.5	0.0	0.0	0.0	0.0	0.0	0.0	0.0	0.0	0.0	11.3	88.7	204
Gießhübl	Strassh T9-42	M-Gießhübl Fm	M-Paleoc	1.1	4.0	6.3	88.6	0.0	0.0	0.0	0.0	0.0	0.0	0.0	0.0	0.0	0.0	0.0	11.4	88.6	176
Gießhübl	Strassh T9-43	M-Gießhübl Fm	M-Paleoc	6.8	1.0	7.7	83.6	0.5	0.0	0.0	0.5	0.0	0.0	0.0	0.0	0.0	0.0	0.0	15.5	83.6	207
Gießhübl	Strassh T9-44	M-Gießhübl Fm	M-Paleoc	11.9	2.8	11.0	73.4	0.0	0.9	0.0	0.0	0.0	0.0	0.0	0.0	0.0	0.0	0.0	25.7	74.3	218
Gießhübl	SchoeT32-6	M-Gießhübl Fm	M-Paleoc	57.6	0.0	21.2	7.1	14.1	0.0	0.0	0.0	0.0	0.0	0.0	0.0	0.0	0.0	0.0	78.8	7.1	14
Gießhübl	SchoeT32-7	M-Gießhübl Fm	M-Paleoc	55.6	22.2	18.9	0.0	3.3	0.0	0.0	0.0	0.0	0.0	0.0	0.0	0.0	0.0	0.0	96.7	0.0	30
Gießhübl	SchoeT32-8	M-Gießhübl Fm	M-Paleoc	60.0	12.0	16.0	12.0	0.0	0.0	0.0	0.0	0.0	0.0	0.0	0.0	0.0	0.0	0.0	88.0	12.0	26
Gießhübl	SchoeT32-9	M-Gießhübl Fm	M-Paleoc	92.0	0.0	7.0	1.0	0.0	0.0	0.0	0.0	0.0	0.0	0.0	0.0	0.0	0.0	0.0	99.0	1.0	100
Gießhübl	SchoeT32-10	M-Gießhübl Fm	M-Paleoc	53.0	9.3	30.1	5.2	0.3	2.1	0.0	0.0	0.0	0.0	0.0	0.0	0.0	0.0	0.0	92.4	7.3	177
Gießhübl	SchoeT32-11	M-Gießhübl Fm	M-Paleoc	55.7	3.1	27.8	12.4	0.0	1.0	0.0	0.0	0.0	0.0	0.0	0.0	0.0	0.0	0.0	86.6	13.4	151
Gießhübl	SchoeT32-12	M-Gießhübl Fm	M-Paleoc	34.0	3.0	15.0	48.0	0.0	0.0	0.0	0.0	0.0	0.0	0.0	0.0	0.0	0.0	0.0	52.0	48.0	246
Gießhübl	SchoeT32-13	M-Gießhübl Fm	M-Paleoc	11.0	0.0	37.0	52.0	0.0	0.0	0.0	0.0	0.0	0.0	0.0	0.0	0.0	0.0	0.0	48.0	52.0	130
Gießhübl	SchoeT32-14	M-Gießhübl Fm	M-Paleoc	31.0	1.0	7.0	61.0	0.0	0.0	0.0	0.0	0.0	0.0	0.0	0.0	0.0	0.0	0.0	39.0	61.0	127
Gießhübl	SchoeT32-15	M-Gießhübl Fm	M-Paleoc	43.0	0.0	23.0	34.0	0.0	0.0	0.0	0.0	0.0	0.0	0.0	0.0	0.0	0.0	0.0	66.0	34.0	115
Gießhübl	SchoeT32-16	M-Gießhübl Fm	M-Paleoc	20.0	0.0	46.0	34.0	0.0	0.0	0.0	0.0	0.0	0.0	0.0	0.0	0.0	0.0	0.0	66.0	34.0	234
Gießhübl	SchoeT32-17	M-Gießhübl Fm	M-Paleoc	16.7	4.2	12.5	62.5	0.0	4.2	0.0	0.0	0.0	0.0	0.0	0.0	0.0	0.0	0.0	33.3	66.7	25
Gießhübl	SchoeT32-18	M-Gießhübl Fm	M-Paleoc	42.0	25.0	25.0	0.0	0.0	8.0	0.0	0.0	0.0	0.0	0.0	0.0	0.0	0.0	0.0	92.0	8.0	12
Gießhübl	SchoeT32-19	M-Gießhübl Fm	M-Paleoc	71.0	7.0	13.0	6.0	0.0	3.0	0.0	0.0	0.0	0.0	0.0	0.0	0.0	0.0	0.0	91.0	9.0	103
Gießhübl	RaasT1-17	M-Gießhübl Fm	M-Paleoc	15.0	8.0	8.0	54.0	15.0	0.0	0.0	0.0	0.0	0.0	0.0	0.0	0.0	0.0	0.0	31.0	54.0	13
Gießhübl	Ad02-78	M-Gießhübl Fm	M-Paleoc	4.4	7.7	1.1	85.7	0.0	0.0	0.0	0.0	0.0	0.0	0.0	0.0	0.0	0.0	1.1	13.2	85.7	202
Gießhübl	Ad02-79	M-Gießhübl Fm	M-Paleoc	4.3	7.5	5.4	79.3	0.0	1.1	0.3	0.0	0.0	0.0	0.0	0.0	0.0	0.0	2.1	17.1	80.7	203
Gießhübl	Ad02-80	M-Gießhübl Fm	M-Paleoc	8.4	6.3	1.0	83.7	0.0	0.3	0.0	0.0	0.0	0.0	0.0	0.0	0.0	0.0	0.3	15.7	84.0	207
Gießhübl	Ad02-81	M-Gießhübl Fm	M-Paleoc	8.2	6.2	4.1	81.2	0.0	0.0	0.0	0.0	0.0	0.0	0.0	0.0	0.0	0.0	0.3	18.5	81.2	208
Gießhübl	Ad02-82	M-Gießhübl Fm	M-Paleoc	8.6	11.8	3.2	75.3	0.0	0.0	0.0	0.0	0.0	0.0	0.0	0.0	0.0	0.0	1.1	23.7	75.3	203
Gießhübl	Ad02-83	M-Gießhübl Fm	M-Paleoc	1.1	4.3	5.4	89.0	0.0	0.0	0.0	0.0	0.0	0.0	0.0	0.0	0.0	0.0	0.3	10.7	89.0	208
Gießhübl	Ad02-84	M-Gießhübl Fm	M-Paleoc	2.0	5.0	3.0	89.0	0.0	0.0	0.0	0.0	0.0	0.0	0.0	0.0	0.0	0.0	1.0	10.0	89.0	200
Gießhübl	Ad02-85	M-Gießhübl Fm	M-Paleoc	4.2	1.0	1.0	91.7	0.0	1.0	0.0	0.0	0.0	0.0	0.0	0.0	0.0	0.0	1.0	6.3	92.7	211
Gießhübl	Ad02-86	M-Gießhübl Fm	M-Paleoc	2.1	5.3	4.2	87.7	0.3	0.0	0.0	0.0	0.0	0.0	0.0	0.0	0.0	0.0	0.3	11.6	87.7	208
Gießhübl	Ad02-87	M-Gießhübl Fm	M-Paleoc	3.1	9.3	2.1	84.1	0.0	0.0	0.0	0.0	0.3	0.0	0.0	0.0	0.0	0.0	1.0	14.5	84.4	202

Gosau	Sample	Formation	Age	zrn [%]	tur [%]	rut [%]	grt [%]	chr [%]	cld [%]	sta [%]	mon [%]	tit [%]	epi [%]	hbl [%]	gln [%]	dis [%]	sil [%]	bkt/ana [%]	ZTR [%]	META [%]	grains
Gießhübl	Ad02-88	M-Gießhübl Fm	M-Paleoc	3.0	10.1	4.0	82.6	0.0	0.0	0.0	0.0	0.0	0.0	0.0	0.0	0.0	0.0	0.3	17.1	82.6	209
Gießhübl	Ad02-89	M-Gießhübl Fm	M-Paleoc	3.2	6.3	3.2	85.6	0.0	1.1	0.3	0.0	0.0	0.0	0.0	0.0	0.0	0.0	0.3	12.7	87.0	208
Gießhübl	Ad02-90	M-Gießhübl Fm	M-Paleoc	4.2	7.4	6.3	81.1	0.0	0.3	0.3	0.0	0.0	0.0	0.0	0.0	0.0	0.0	0.3	17.9	81.8	204
Gießhübl	Ad02-91	M-Gießhübl Fm	M-Paleoc	5.1	3.1	5.1	85.3	0.0	1.0	0.0	0.0	0.0	0.0	0.0	0.0	0.0	0.0	0.3	13.4	86.3	202
Gießhübl	Ad02-92	M-Gießhübl Fm	M-Paleoc	5.2	12.4	4.1	76.6	0.0	0.3	0.0	0.0	0.0	0.3	0.0	0.0	0.0	0.0	1.0	21.7	77.2	202
Gießhübl	Ad02-93	M-Gießhübl Fm	M-Paleoc	2.0	4.0	2.0	90.1	0.0	1.0	0.0	0.0	0.0	0.0	0.0	0.0	0.0	0.0	1.0	7.9	91.1	200
Gießhübl	Ad02-94	M-Gießhübl Fm	M-Paleoc	3.0	5.1	3.0	86.9	0.0	1.0	0.0	0.0	0.0	0.0	0.0	0.0	0.0	0.0	1.0	11.1	87.9	208
Gießhübl	Strassh T9-29	M-Gießhübl Fm	U-Paleoc	4.9	2.0	6.8	86.3	0.0	0.0	0.0	0.0	0.0	0.0	0.0	0.0	0.0	0.0	0.0	13.7	86.3	205
Gießhübl	Strassh T9-30	M-Gießhübl Fm	U-Paleoc	1.9	0.5	7.2	90.4	0.0	0.0	0.0	0.0	0.0	0.0	0.0	0.0	0.0	0.0	0.0	9.6	90.4	209
Gießhübl	Strassh T9-31	M-Gießhübl Fm	U-Paleoc	0.5	0.0	1.0	97.0	0.0	1.5	0.0	0.0	0.0	0.0	0.0	0.0	0.0	0.0	0.0	1.5	98.5	200
Gießhübl	Strassh T9-32	M-Gießhübl Fm	U-Paleoc	3.5	0.5	9.0	86.6	0.0	0.5	0.0	0.0	0.0	0.0	0.0	0.0	0.0	0.0	0.0	12.9	87.1	201
Gießhübl	Strassh T9-33	M-Gießhübl Fm	U-Paleoc	3.4	1.0	6.9	88.7	0.0	0.0	0.0	0.0	0.0	0.0	0.0	0.0	0.0	0.0	0.0	11.3	88.7	203
Gießhübl	Strassh T9-34	M-Gießhübl Fm	U-Paleoc	4.0	4.0	7.9	84.2	0.0	0.0	0.0	0.0	0.0	0.0	0.0	0.0	0.0	0.0	0.0	15.8	84.2	202
Gießhübl	Strassh T9-35	M-Gießhübl Fm	U-Paleoc	3.5	2.5	11.5	81.0	0.0	0.5	0.0	0.0	0.0	0.0	0.0	0.0	0.0	0.0	1.0	17.5	81.5	200
Gießhübl	Ad02-95	U-Gießhübl Fm	U-Paleoc	3.1	4.1	4.1	88.1	0.3	0.3	0.0	0.0	0.0	0.0	0.0	0.0	0.0	0.0	0.0	11.3	88.4	204
Gießhübl	Ad02-96	U-Gießhübl Fm	U-Paleoc	5.3	1.1	4.2	87.7	0.3	0.0	0.0	0.0	0.0	0.3	0.0	0.0	0.0	0.0	1.1	10.6	88.1	210
Gießhübl	Ad02-97	U-Gießhübl Fm	U-Paleoc	4.2	4.2	2.1	87.5	0.0	0.0	1.0	0.0	0.0	0.0	0.0	0.0	0.0	0.0	1.0	10.4	88.5	219
Gießhübl	Ad02-98	U-Gießhübl Fm	U-Paleoc	4.2	1.0	5.2	87.9	0.0	0.3	0.0	0.0	0.3	0.0	0.0	0.0	0.0	0.0	1.0	10.5	88.5	212
Gießhübl	Ad02-99	U-Gießhübl Fm	U-Paleoc	3.2	8.6	2.2	83.9	0.0	0.0	1.1	0.0	0.0	0.0	0.0	0.0	0.0	0.0	1.1	14.0	84.9	209
Gießhübl	Ad02-100	U-Gießhübl Fm	U-Paleoc	5.4	7.6	7.6	78.1	0.3	0.0	0.3	0.0	0.0	0.3	0.0	0.0	0.0	0.0	0.3	20.6	78.7	207
Gießhübl	Ad02-101	U-Gießhübl Fm	U-Paleoc	7.1	5.9	3.6	78.3	0.0	0.4	0.0	0.0	0.0	0.0	0.0	0.0	0.0	0.0	4.7	16.6	78.6	203
Gießhübl	Ad02-102	U-Gießhübl Fm	U-Paleoc	4.3	5.4	4.3	83.2	0.0	0.3	0.0	0.3	0.0	0.0	0.0	0.0	0.0	0.0	2.2	14.0	83.5	213
Gießhübl	Ad02-103	U-Gießhübl Fm	U-Paleoc	3.2	4.2	5.3	84.8	0.0	0.0	0.3	0.0	0.0	0.0	0.0	0.0	0.0	0.0	2.1	12.7	85.2	205
Gießhübl	Ad02-104	U-Gießhübl Fm	U-Paleoc	6.9	15.0	4.6	70.4	0.0	0.3	0.3	0.0	0.0	0.0	0.0	0.0	0.0	0.0	2.3	26.6	71.1	210
Gießhübl	Ad02-105	U-Gießhübl Fm	U-Paleoc	7.5	7.5	2.2	80.7	0.0	0.3	0.0	0.0	0.0	0.3	0.3	0.0	0.0	0.0	1.1	17.2	81.7	204
Gießhübl	Ad02-106	U-Gießhübl Fm	U-Paleoc	5.7	7.9	4.5	70.2	0.0	0.3	0.0	0.0	0.0	3.4	6.8	0.0	0.0	0.0	1.1	18.1	80.7	201
Gießhübl	Ad02-107	U-Gießhübl Fm	U-Paleoc	2.2	11.2	4.5	77.6	0.0	0.0	0.3	0.0	0.0	0.3	0.3	0.0	0.0	0.0	3.4	18.0	78.6	202
Gießhübl	Ad02-108	U-Gießhübl Fm	U-Paleoc	8.5	7.5	5.3	72.6	0.0	0.0	0.3	0.3	0.0	0.0	0.0	0.0	0.0	0.0	5.3	21.4	73.0	201
Gießhübl	Ad02-109	U-Gießhübl Fm	U-Paleoc	7.6	6.5	3.3	79.1	0.0	0.0	0.0	0.3	0.0	0.0	0.0	0.0	0.0	0.0	3.3	17.3	79.1	210
Gießhübl	Ad02-110	U-Gießhübl Fm	U-Paleoc	6.9	4.6	2.3	82.5	0.0	0.3	0.0	0.0	0.0	0.0	0.0	0.0	0.0	0.0	3.4	13.7	82.8	208
Gießhübl	Ad02-111	U-Gießhübl Fm	U-Paleoc	7.4	6.3	2.1	83.2	0.0	0.0	0.0	0.0	0.0	0.0	0.0	0.0	0.0	0.0	1.1	15.8	83.2	204
Gießhübl	Ad02-112	U-Gießhübl Fm	U-Paleoc	4.1	3.1	1.0	88.4	0.3	0.0	0.0	0.0	0.0	0.0	0.0	0.0	0.0	0.0	3.1	8.2	88.4	206
Gießhübl	Ad02-113	U-Gießhübl Fm	U-Paleoc	8.3	9.3	3.1	76.8	0.3	0.0	0.0	0.0	0.0	0.0	0.0	0.0	0.0	0.0	2.1	20.8	76.8	221
Gießhübl	Ad02-114	U-Gießhübl Fm	U-Paleoc	1.0	5.2	1.0	91.3	0.0	0.3	0.0	0.0	0.0	0.0	0.0	0.0	0.0	0.0	1.0	7.3	91.6	204
Gießhübl	Ad02-115	U-Gießhübl Fm	U-Paleoc	6.5	6.5	4.3	81.3	0.0	0.3	0.0	0.0	0.0	0.0	0.0	0.0	0.0	0.0	1.1	17.3	81.6	207
Gießhübl	Ad02-116	U-Gießhübl Fm	U-Paleoc	5.3	6.3	4.2	82.1	0.0	0.0	0.0	0.0	0.0	0.0	0.0	0.0	0.0	0.0	2.1	15.8	82.1	202
Gießhübl	Ad02-117	U-Gießhübl Fm	U-Paleoc	10.2	8.0	1.1	77.3	0.0	1.1	0.0	0.0	0.0	0.0	0.0	0.0	0.0	0.0	2.3	19.3	78.4	206
Gießhübl	Ad02-118	U-Gießhübl Fm	U-Paleoc	2.2	7.6	2.2	87.0	0.0	1.1	0.0	0.0	0.0	0.0	0.0	0.0	0.0	0.0	0.0	12.0	88.0	194
Gießhübl	Ad02-119	U-Gießhübl Fm	U-Paleoc	4.3	15.1	3.2	75.6	0.0	0.3	0.0	0.0	0.0	0.3	0.0	0.0	0.0	0.0	1.1	22.7	76.2	214
Gießhübl	Ad02-120	U-Gießhübl Fm	U-Paleoc	4.4	14.4	2.2	76.4	0.0	1.1	0.0	0.0	0.0	0.3	0.0	0.0	0.0	0.0	1.1	21.0	77.9	202
Gießhübl	Ad02-121	U-Gießhübl Fm	U-Paleoc	6.4	7.4	5.3	79.8	0.0	1.1	0.0	0.0	0.0	0.0	0.0	0.0	0.0	0.0	0.0	19.1	80.9	200
Gießhübl	Ad02-122	U-Gießhübl Fm	U-Paleoc	8.6	7.5	5.4	77.5	0.3	0.0	0.3	0.0	0.0	0.3	0.0	0.0	0.0	0.0	0.0	21.5	78.1	209
Gießhübl	Ad02-123	U-Gießhübl Fm	U-Paleoc	8.4	10.5	4.2	72.7	0.0	0.0	0.3	0.3	0.0	0.0	0.3	0.0	0.0	0.0	3.2	23.2	73.3	209
Gießhübl	Ad02-124	U-Gießhübl Fm	U-Paleoc	2.1	8.4	3.2	83.0	0.0	0.3	0.0	0.3	0.0	0.3	0.3	0.0	0.0	0.0	2.1	13.7	83.9	205
Gießhübl	Ad02-125	U-Gießhübl Fm	U-Paleoc	1.0	6.3	2.1	88.1	0.0	0.3	0.0	0.0	0.0	0.0	1.0	0.0	0.0	0.0	1.0	9.4	89.5	211
Gießhübl	Ad02-126	U-Gießhübl Fm	U-Paleoc	5.5	8.8	1.1	80.6	0.0	1.1	0.0	0.3	0.0	0.3	0.0	0.0	0.0	0.0	2.2	15.5	82.0	206
Gießhübl	Ad02-127	U-Gießhübl Fm	U-Paleoc	4.2	4.2	0.3	91.0	0.0	0.0	0.3	0.0	0.0	0.0	0.0	0.0	0.0	0.0	0.0	8.7	91.3	208

Gosau	Sample	Formation	Age	zrn [%]	tur [%]	rut [%]	grt [%]	chr [%]	cld [%]	sta [%]	mon [%]	tit [%]	epi [%]	hbl [%]	gln [%]	dis [%]	sil [%]	bkt/ana [%]	ZTR [%]	META [%]	grains
Gießhübl	Ad02-128	U-Gießhübl Fm	U-Paleoc	3.3	5.4	4.3	83.4	0.0	1.1	0.0	0.0	0.0	0.3	0.0	0.0	0.0	0.0	2.2	13.0	84.8	201
Gießhübl	Ad02-129	U-Gießhübl Fm	U-Paleoc	4.4	6.7	6.7	80.0	0.0	0.0	0.0	0.0	0.0	0.0	0.0	0.0	0.0	0.0	2.2	17.8	80.0	204
Gießhübl	Ad02-130	U-Gießhübl Fm	U-Paleoc	2.2	6.5	5.4	83.7	0.0	1.1	0.0	0.0	0.0	0.0	0.0	0.0	0.0	0.0	1.1	14.1	84.8	206
Gießhübl	Ad02-131	U-Gießhübl Fm	U-Paleoc	3.1	7.3	4.2	83.9	0.0	0.3	0.0	0.0	0.0	0.0	0.0	0.0	0.0	0.0	1.0	14.7	84.3	210
Gießhübl	Ad02-132	U-Gießhübl Fm	U-Paleoc	9.4	7.3	2.1	78.5	0.3	0.3	0.0	0.0	0.0	0.0	0.0	0.0	0.0	0.0	2.1	18.8	78.8	210
Grünbach	GRÜN 09/6	Kreuzgraben Fm	U-San	5.4	18.0	7.2	5.4	58.6	0.0	0.0	0.0	1.8	0.0	0.0	0.0	0.0	0.0	3.6	30.6	7.2	111
Grünbach	GRÜN 09/6B	Kreuzgraben Fm	U-San	7.6	27.6	6.2	37.8	18.5	0.0	0.0	0.0	0.0	0.0	0.0	0.0	0.0	0.0	2.2	41.5	37.8	275
Grünbach	GRÜN 09/26	Kreuzgraben Fm	U-San	26.8	22.5	37.8	0.5	1.0	0.0	0.0	1.9	3.3	0.0	0.0	0.0	0.0	0.0	6.2	87.1	3.8	209
Grünbach	GRÜN 09/2	Maiersdorf Fm	U-San	8.0	9.1	1.8	50.4	4.3	3.3	2.5	0.7	1.4	1.4	7.2	0.0	0.4	0.0	9.1	18.8	66.3	276
Grünbach	GRÜN 09/3	Maiersdorf Fm	U-San	12.2	7.1	4.1	56.6	7.1	2.6	2.0	1.0	1.0	0.0	0.5	0.0	0.0	0.0	5.6	23.5	62.8	196
Grünbach	GRÜN 09/09	Maiersdorf Fm	U-San	5.9	45.1	5.6	14.3	19.9	5.6	0.3	0.0	0.7	0.0	0.0	0.0	0.0	0.0	2.1	56.6	21.0	286
Grünbach	GRÜN 09/12	Maiersdorf Fm	U-San	8.4	34.1	7.0	16.8	25.7	3.3	0.0	0.9	0.0	0.0	0.0	0.0	0.0	0.0	3.7	49.5	20.1	214
Grünbach	GRÜN 09/16	Maiersdorf Fm	U-San	3.1	14.6	5.2	49.0	13.5	4.2	1.0	0.0	0.0	0.0	2.1	0.0	0.0	0.0	7.3	22.9	56.3	96
Grünbach	GRÜN 09/17	Maiersdorf Fm	U-San	11.5	15.2	15.2	26.3	24.0	0.9	0.0	0.0	0.0	0.0	0.0	0.0	0.0	0.0	6.9	41.9	27.2	217
Grünbach	GRÜN 09/27	Maiersdorf Fm	U-San	15.3	13.9	9.1	24.9	34.4	0.0	0.0	0.0	0.5	0.0	0.0	0.0	0.0	0.0	1.9	38.3	25.4	209
Grünbach	GRÜN 09/5	Grünbach Fm	L-Camp	27.5	16.0	31.5	7.5	0.0	0.5	0.0	1.0	1.0	0.0	0.0	0.0	0.0	0.0	15.0	75.0	9.0	200
Grünbach	GRÜN 09/18	Grünbach Fm	L-Camp	11.5	28.3	23.9	15.9	4.4	3.5	0.9	1.8	0.0	0.9	0.0	0.0	0.0	0.0	8.8	63.7	21.2	113
Grünbach	GRÜN 09/22	Grünbach Fm	L-Camp	3.3	16.1	9.0	14.7	46.0	1.9	0.0	0.0	2.4	0.0	0.5	1.9	0.0	0.0	3.8	28.4	21.3	211
Grünbach	GRÜN 09/22	Grünbach Fm	L-Camp	1.5	28.0	7.5	14.0	40.5	2.5	0.0	1.0	2.5	0.5	0.0	1.0	0.0	0.0	1.0	37.0	20.5	200
Grünbach	GRÜN 09/23	Grünbach Fm	L-Camp	7.1	23.0	8.7	13.8	37.2	0.0	0.0	0.5	6.6	0.0	0.0	2.6	0.0	0.0	0.5	38.8	23.0	196
Grünbach	GRÜN 09/24	Grünbach Fm	L-Camp	21.8	15.2	22.3	4.3	1.9	30.8	0.0	0.0	0.9	0.0	0.0	0.0	0.0	0.0	2.8	59.2	36.0	211
Grünbach	GRÜN 09/25	Grünbach Fm	L-Camp	1.1	42.0	4.5	8.5	33.0	6.8	0.0	0.0	1.7	0.0	0.0	0.6	0.0	0.0	1.1	47.7	17.6	176
Grünbach	GRÜN 09/28	Grünbach Fm	L-Camp	18.5	18.0	17.0	3.0	14.5	23.5	0.0	0.0	1.5	0.0	0.0	0.5	0.0	0.0	3.5	53.5	28.5	200
Grünbach	GRÜN 09/35	Grünbach Fm	L-Camp	52.9	9.9	20.6	1.3	0.4	4.9	0.0	2.2	0.9	0.4	0.0	0.0	0.0	0.0	6.3	83.4	7.6	223
Grünbach	GRÜN 09/36	Grünbach Fm	L-Camp	31.5	18.5	30.4	2.2	5.4	8.7	0.0	0.0	1.1	0.0	0.0	0.0	0.0	0.0	2.2	80.4	12.0	92
Grünbach	GRÜN 09/40	Grünbach Fm	L-Camp	14.6	12.7	15.1	5.9	18.0	28.3	0.0	0.0	0.5	0.0	0.0	0.0	0.0	0.0	4.4	42.4	34.6	205
Grünbach	GRÜN 09/42	Grünbach Fm	L-Camp	22.6	35.3	12.8	6.0	6.0	3.0	0.0	2.3	0.8	0.0	0.0	0.0	0.0	0.0	11.3	70.7	9.8	133
Grünbach	GRÜN 09/43	Grünbach Fm	L-Camp	35.4	29.2	13.5	6.3	0.0	2.1	0.0	1.0	0.0	1.0	0.0	0.0	0.0	0.0	11.5	78.1	9.4	96
Grünbach	GRÜN 09/44B	Grünbach Fm	L-Camp	23.6	16.7	20.8	1.9	0.9	22.7	0.0	0.9	0.5	0.0	0.5	0.0	0.0	0.0	11.6	61.1	25.5	216
Grünbach	GRÜN 09/45	Grünbach Fm	L-Camp	17.8	7.3	1.8	5.9	0.0	63.5	0.0	0.9	0.0	0.0	0.0	0.0	0.0	0.0	2.7	26.9	69.4	219
Grünbach	GRÜN 09/47B	Grünbach Fm	L-Camp	22.2	27.5	13.0	5.3	3.4	16.9	0.0	1.4	0.5	0.0	0.0	0.0	0.0	0.0	9.7	62.8	22.7	207
Grünbach	GRÜ 09/47C	Grünbach Fm	L-Camp	15.7	25.5	12.5	5.6	10.2	26.4	0.0	0.0	0.0	0.0	0.0	0.0	0.0	0.0	4.2	53.7	31.9	216
Grünbach	GRÜN 09/47D	Grünbach Fm	L-Camp	32.7	20.3	21.7	3.2	2.3	0.9	0.0	3.2	0.5	0.0	0.0	0.0	0.0	0.0	15.2	74.7	4.6	217
Grünbach	GRÜN 09/48	Grünbach Fm	L-Camp	4.5	3.7	4.5	85.7	0.4	0.0	0.0	0.4	0.0	0.0	0.0	0.0	0.0	0.0	0.8	12.7	85.7	244
Grünbach	GRÜN 09/49	Grünbach Fm	L-Camp	2.7	3.6	4.5	84.7	0.5	0.0	0.0	0.9	0.5	0.0	0.0	0.0	0.0	0.0	2.7	10.8	85.1	222
Grünbach	GRÜN 09/50	Grünbach Fm	L-Camp	23.8	14.3	19.0	2.9	1.9	32.9	0.0	0.5	0.5	0.0	0.0	0.0	0.0	0.0	4.3	57.1	36.2	210
Grünbach	M 10	Grünbach Fm	L-Camp	19.7	9.4	15.5	5.2	5.2	31.5	0.0	1.4	0.9	0.0	0.0	0.0	0.0	0.5	10.8	44.6	37.6	213
Grünbach	M 15	Grünbach Fm	L-Camp	51.9	4.8	11.5	1.0	0.5	14.4	0.0	7.7	1.4	0.0	0.0	0.0	0.0	0.0	6.7	68.3	16.8	208
Grünbach	M 19	Grünbach Fm	L-Camp	11.4	28.4	2.5	1.0	0.5	45.8	0.0	1.0	2.0	0.0	0.5	0.0	0.0	0.0	7.0	42.3	49.3	201
Grünbach	M 30	Grünbach Fm	L-Camp	30.2	26.7	16.3	0.0	0.0	14.0	0.0	1.2	0.0	0.0	0.0	0.0	0.0	0.0	11.6	73.3	14.0	86
Grünbach	M 32	Grünbach Fm	L-Camp	20.4	13.3	20.9	1.9	12.8	20.4	0.0	0.5	1.9	0.0	0.0	0.0	0.0	0.0	8.1	54.5	24.2	211
Grünbach	M 34	Grünbach Fm	L-Camp	41.7	4.1	8.7	3.2	12.8	15.1	0.0	4.1	1.4	0.0	0.0	0.0	0.0	0.0	8.7	54.6	19.7	218
Grünbach	M 35	Grünbach Fm	L-Camp	11.8	14.7	13.2	0.0	4.4	33.8	0.0	0.0	0.0	0.0	2.9	0.0	0.0	0.0	19.1	39.7	36.8	68
Grünbach	M 37	Grünbach Fm	L-Camp	18.5	16.6	14.7	2.4	9.0	19.4	0.0	1.9	1.4	0.0	0.0	0.0	0.0	0.0	16.1	49.8	23.2	211
Grünbach	M 40	Grünbach Fm	L-Camp	4.6	18.5	27.7	0.0	0.0	32.3	0.0	0.0	1.5	0.0	0.0	0.0	0.0	0.0	15.4	50.8	33.8	65
Grünbach	M 43	Grünbach Fm	L-Camp	18.6	19.5	29.8	0.0	0.5	21.4	0.0	0.5	1.9	0.0	0.0	0.0	0.0	0.0	7.9	67.9	23.3	215
Grünbach	M 44	Grünbach Fm	L-Camp	29.3	6.0	41.9	0.0	2.3	16.3	0.0	0.9	0.5	0.0	0.0	0.0	0.0	0.0	2.8	77.2	16.7	215

Gosau	Sample	Formation	Age	zrn [%]	tur [%]	rut [%]	grt [%]	chr [%]	cld [%]	sta [%]	mon [%]	tit [%]	epi [%]	hbl [%]	gln [%]	dis [%]	sil [%]	bkt/ana [%]	ZTR [%]	META [%]	grains
Grünbach	M 45	Grünbach Fm	L-Camp	20.8	13.9	45.5	2.0	1.5	7.4	0.0	1.5	1.5	0.0	0.0	0.0	0.0	0.0	5.9	80.2	10.9	202
Grünbach	M 49	Grünbach Fm	L-Camp	22.9	13.7	31.7	2.4	0.5	19.5	0.0	2.0	1.5	0.0	0.0	0.0	0.0	0.0	5.9	68.3	23.4	205
Grünbach	M 51	Grünbach Fm	L-Camp	7.9	10.7	40.0	1.4	0.9	29.3	0.0	0.5	1.4	0.0	0.0	0.0	0.0	0.0	7.9	58.6	32.1	215
Grünbach	M 52	Grünbach Fm	L-Camp	6.8	13.6	46.1	1.0	1.9	22.3	0.0	1.0	0.5	0.0	0.0	0.0	0.0	0.0	6.8	66.5	23.8	206
Grünbach	M 56	Grünbach Fm	L-Camp	7.2	5.3	26.9	0.0	0.5	48.1	0.0	1.0	2.9	0.0	0.0	0.0	0.0	0.0	8.2	39.4	51.0	208
Grünbach	M 58	Grünbach Fm	L-Camp	13.5	24.5	18.8	1.0	1.0	31.7	0.0	0.5	1.4	0.0	0.0	0.0	0.0	0.0	7.7	56.7	34.1	208
Grünbach	M 59	Grünbach Fm	L-Camp	24.8	11.2	28.0	0.0	3.7	25.2	0.0	2.3	0.5	0.0	0.0	0.0	0.0	0.0	4.2	64.0	25.7	214
Grünbach	M 61	Grünbach Fm	L-Camp	14.8	24.1	30.1	0.5	1.9	24.1	0.0	2.3	0.5	0.0	0.0	0.0	0.0	0.0	1.9	69.0	25.0	216
Grünbach	M 63	Grünbach Fm	L-Camp	1.4	14.4	4.7	0.9	60.5	17.2	0.0	0.0	0.0	0.0	0.0	0.0	0.0	0.0	0.9	20.5	18.1	215
Grünbach	M 70	Grünbach Fm	L-Camp	12.5	23.6	41.7	1.4	2.3	12.5	0.0	0.5	2.3	0.0	0.0	0.0	0.0	0.0	3.2	77.8	16.2	216
Grünbach	M 76	Grünbach Fm	L-Camp	4.3	15.9	37.2	1.0	0.5	37.2	0.0	0.5	1.0	0.0	0.0	0.0	0.0	0.0	2.4	57.5	39.1	207
Grünbach	M 80	Grünbach Fm	L-Camp	8.5	26.5	37.9	0.0	0.9	19.4	0.0	0.9	1.9	0.0	0.0	0.0	0.0	0.0	3.8	73.0	21.3	211
Grünbach	M 81	Grünbach Fm	L-Camp	23.1	13.0	28.7	1.9	7.4	18.5	0.0	0.5	3.2	0.0	0.0	0.0	0.0	0.0	3.2	64.8	23.6	216
Grünbach	M 83	Grünbach Fm	L-Camp	3.3	33.8	15.0	0.0	20.2	23.5	0.0	0.5	1.9	0.0	0.0	0.0	0.0	0.0	1.9	52.1	25.4	213
Grünbach	M 91	Grünbach Fm	L-Camp	11.5	20.7	30.0	1.4	8.8	23.0	0.0	0.9	0.5	0.0	0.0	0.0	0.0	0.0	3.2	62.2	24.9	217
Grünbach	GRÜN 09/10	Piesting Fm	U-Camp	27.3	18.2	25.5	0.9	0.4	17.3	0.0	1.3	0.0	0.4	0.0	0.0	0.0	0.0	8.7	71.0	18.6	231
Grünbach	GRÜ 09/11	Piesting Fm	U-Camp	31.4	17.5	11.2	4.9	14.3	13.0	0.0	0.4	1.3	0.0	0.0	0.0	0.9	0.0	4.9	60.1	19.3	223
Grünbach	GRÜN 09/29A	Piesting Fm	U-Camp	32.4	13.0	9.3	9.3	1.9	13.9	0.0	0.9	0.9	3.7	0.0	0.0	0.0	0.0	14.8	54.6	27.8	108
Grünbach	GRÜN 09/29B	Piesting Fm	U-Camp	22.7	28.9	19.9	0.9	1.4	8.5	0.0	1.4	1.4	0.5	0.0	0.0	0.0	0.0	14.2	71.6	11.4	211
Grünbach	GRÜN 09/37	Piesting Fm	U-Camp	6.9	28.3	13.0	0.8	0.0	44.1	0.0	0.0	0.0	0.0	0.0	0.0	0.0	0.0	6.9	48.2	44.9	247
Grünbach	GRÜN 09/32	Piesting Fm	Maastr	1.9	13.6	3.4	36.4	0.0	29.6	0.0	1.5	2.4	0.0	0.5	0.0	0.5	0.0	10.2	18.9	68.9	206
Grünbach	GRÜN 09/13	Zweiersdor Fm	Paleoc	0.8	2.3	6.6	85.7	0.0	0.0	0.0	0.4	0.4	0.0	0.0	0.0	0.0	0.0	3.9	9.7	86.0	258
Grünbach	GRÜN 09/14	Zweiersdor Fm	Paleoc	0.0	1.3	7.5	87.5	0.0	0.8	0.0	0.0	0.8	0.0	0.0	0.0	0.0	0.4	1.7	8.8	89.2	240
Glinzendorf	T1-3910	Limnic-marine	L-San	6.0	4.5	11.0	68.0	5.5	1.5	1.0	0.0	0.0	0.0	0.0	0.0	0.0	0.0	2.5	21.5	70.5	200
Glinzendorf	T1-3930	Limnic-marine	L-San	7.8	5.4	12.3	62.3	7.8	2.0	1.5	0.5	0.0	0.0	0.0	0.0	0.0	0.0	0.5	25.5	65.7	204
Glinzendorf	T1-3950	Limnic-marine	L-San	6.0	3.5	7.5	77.5	2.5	1.5	0.0	0.0	0.0	0.0	0.0	0.0	0.0	0.0	1.5	17.0	79.0	200
Glinzendorf	T1-3970	Limnic-marine	L-San	3.0	2.5	8.0	77.6	4.5	2.0	0.0	1.5	0.0	0.0	0.0	0.0	0.0	0.0	1.0	13.4	79.6	201
Glinzendorf	T1-3990	Limnic-marine	L-San	5.0	2.0	4.5	57.5	28.5	2.5	0.0	0.0	0.0	0.0	0.0	0.0	0.0	0.0	0.0	11.5	60.0	200
Glinzendorf	T1-4020	Limnic-marine	L-San	9.1	1.8	3.7	53.7	26.8	3.0	0.0	0.0	0.0	0.0	0.0	0.0	0.0	0.0	1.8	14.6	56.7	164
Glinzendorf	T1-4040	Limnic-marine	L-San	6.0	1.0	3.5	23.0	63.5	1.5	0.5	1.0	0.0	0.0	0.0	0.0	0.0	0.0	0.0	10.5	25.0	200
Glinzendorf	T1-4060	Limnic-marine	L-San	11.7	1.7	6.7	13.3	63.3	1.7	0.0	0.0	0.0	0.0	0.0	0.0	0.0	0.0	1.7	20.0	15.0	60
Glinzendorf	T1-4080	Limnic-marine	L-San	8.7	5.4	4.3	14.1	67.4	0.0	0.0	0.0	0.0	0.0	0.0	0.0	0.0	0.0	0.0	18.5	14.1	92
Glinzendorf	T1-4100	Limnic-marine	L-San	19.7	9.1	9.1	13.6	36.4	1.5	0.0	7.6	0.0	0.0	0.0	0.0	0.0	0.0	3.0	37.9	15.2	66
Glinzendorf	T1-4120	Limnic-marine	L-San	16.9	3.2	9.7	37.1	30.6	0.8	0.0	1.6	0.0	0.0	0.0	0.0	0.0	0.0	0.0	29.8	37.9	124
Glinzendorf	T1-4140	Limnic-marine	L-San	36.0	7.9	9.5	34.4	8.5	0.0	0.0	2.1	0.5	0.0	0.0	0.0	0.0	0.0	1.1	53.4	34.9	189
Glinzendorf	T1-4160	Limnic-marine	L-San	33.0	7.5	12.0	28.0	13.5	0.0	0.0	3.5	1.5	0.0	0.0	0.0	0.0	0.0	1.0	52.5	29.5	200
Glinzendorf	T1-4185	Limnic-marine	L-San	19.4	6.5	9.0	12.4	51.7	0.0	0.0	0.0	0.5	0.0	0.0	0.0	0.0	0.0	0.5	34.8	12.9	201
Glinzendorf	T1-4200	Limnic-marine	L-San	10.8	2.7	4.3	4.9	76.8	0.0	0.0	0.5	0.0	0.0	0.0	0.0	0.0	0.0	0.0	17.8	4.9	185
Glinzendorf	GT1-3940	Limnic-marine	L-San	29.3	2.4	12.2	20.7	32.9	0.0	0.0	2.4	0.0	0.0	0.0	0.0	0.0	0.0	0.0	43.9	20.7	82
Glinzendorf	T1-3710	Limnic-marine	U-San	10.8	1.0	4.4	80.4	2.0	0.0	0.0	0.5	0.5	0.0	0.0	0.0	0.0	0.0	0.5	16.2	80.9	204
Glinzendorf	T1-3730	Limnic-marine	U-San	8.8	1.4	9.3	75.0	1.4	2.3	0.9	0.5	0.0	0.0	0.0	0.5	0.0	0.0	0.0	19.4	78.7	216
Glinzendorf	T1-3755	Limnic-marine	U-San	6.9	2.8	8.3	74.2	2.8	1.8	0.9	0.5	0.5	0.0	0.0	0.0	0.0	0.0	1.4	18.0	77.4	217
Glinzendorf	T1-3770	Limnic-marine	U-San	7.6	5.2	8.6	72.9	2.9	0.0	1.0	1.4	0.0	0.0	0.0	0.0	0.0	0.0	0.5	21.4	73.8	210
Glinzendorf	T1-3790	Limnic-marine	U-San	10.3	1.5	10.3	72.9	2.0	3.0	0.0	0.0	0.0	0.0	0.0	0.0	0.0	0.0	0.0	22.2	75.9	203
Glinzendorf	T1-3820	Limnic-marine	U-San	7.3	1.0	10.7	75.6	1.0	2.9	1.0	0.5	0.0	0.0	0.0	0.0	0.0	0.0	0.0	19.0	79.5	205
Glinzendorf	T1-3840	Limnic-marine	U-San	6.9	4.3	11.2	71.6	1.7	0.9	0.9	0.9	0.0	0.0	0.0	0.0	0.0	0.0	1.7	22.4	73.3	116
Glinzendorf	T1-3860	Limnic-marine	U-San	6.9	3.0	10.3	66.0	9.4	0.5	1.5	1.0	0.0	0.0	0.0	0.0	0.0	0.0	1.5	20.2	68.0	203

Gosau	Sample	Formation	Age	zrn [%]	tur [%]	rut [%]	grt [%]	chr [%]	cld [%]	sta [%]	mon [%]	tit [%]	epi [%]	hbl [%]	gln [%]	dis [%]	sil [%]	bkt/ana [%]	ZTR [%]	META [%]	grains
Glinzendorf	T1-3880	Limnic-marine	U-San	15.3	4.5	6.4	56.4	14.9	1.0	0.5	1.0	0.0	0.0	0.0	0.0	0.0	0.0	0.0	26.2	57.9	202
Glinzendorf	GT1-3700	Limnic-marine	U-San	8.0	0.5	2.0	2.0	87.5	0.0	0.0	0.0	0.0	0.0	0.0	0.0	0.0	0.0	0.0	10.5	2.0	200
Glinzendorf	GT1-3740	Limnic-marine	U-San	5.0	0.5	1.5	3.5	89.5	0.0	0.0	0.0	0.0	0.0	0.0	0.0	0.0	0.0	0.0	7.0	3.5	200
Glinzendorf	GT1-3780	Limnic-marine	U-San	5.1	1.7	1.7	10.9	80.6	0.0	0.0	0.0	0.0	0.0	0.0	0.0	0.0	0.0	0.0	8.6	10.9	175
Glinzendorf	GT1-3820	Limnic-marine	U-San	4.0	2.0	1.0	1.5	91.6	0.0	0.0	0.0	0.0	0.0	0.0	0.0	0.0	0.0	0.0	6.9	1.5	202
Glinzendorf	GT1-3860	Limnic-marine	U-San	7.3	0.0	1.2	4.9	84.1	0.0	2.4	0.0	0.0	0.0	0.0	0.0	0.0	0.0	0.0	8.5	7.3	82
Glinzendorf	T1-3500	Limnic-marine	L-Camp	23.3	7.1	21.9	35.7	9.0	0.5	0.0	1.9	0.5	0.0	0.0	0.0	0.0	0.0	0.0	52.4	36.7	210
Glinzendorf	T1-3520	Limnic-marine	L-Camp	12.1	4.6	12.1	64.2	3.5	1.7	0.6	1.2	0.0	0.0	0.0	0.0	0.0	0.0	0.0	28.9	66.5	173
Glinzendorf	T1-3540	Limnic-marine	L-Camp	10.0	4.0	14.5	62.0	7.0	1.5	0.0	1.0	0.0	0.0	0.0	0.0	0.0	0.0	0.0	28.5	63.5	200
Glinzendorf	T1-3570	Limnic-marine	L-Camp	11.2	1.0	17.3	60.2	7.1	0.0	0.0	3.1	0.0	0.0	0.0	0.0	0.0	0.0	0.0	29.6	60.2	98
Glinzendorf	T1-3590	Limnic-marine	L-Camp	10.5	1.5	8.0	70.0	6.0	2.5	1.5	0.0	0.0	0.0	0.0	0.0	0.0	0.0	0.0	20.0	74.0	200
Glinzendorf	T1-3610	Limnic-marine	L-Camp	8.5	10.6	13.6	57.8	4.5	2.0	1.0	1.0	0.0	0.0	0.0	0.0	0.0	0.0	1.0	32.7	60.8	200
Glinzendorf	T1-3640	Limnic-marine	L-Camp	13.2	2.0	12.3	65.7	3.9	1.0	0.5	0.5	0.5	0.0	0.0	0.0	0.0	0.0	0.5	27.5	67.6	204
Glinzendorf	T1-3660	Limnic-marine	L-Camp	12.5	3.5	7.5	69.0	2.5	3.0	0.5	0.5	0.5	0.0	0.0	0.0	0.0	0.0	0.5	23.5	73.0	200
Glinzendorf	T1-3680	Limnic-marine	L-Camp	8.5	3.5	10.1	66.3	3.0	2.5	2.0	0.5	0.5	0.0	0.0	0.0	0.0	0.0	3.0	22.1	71.4	200
Glinzendorf	GT1-3550	Limnic-marine	L-Camp	14.0	1.0	6.0	79.0	0.0	0.0	0.0	0.0	0.0	0.0	0.0	0.0	0.0	0.0	0.0	21.0	79.0	140
Glinzendorf	GT1-3620	Limnic-marine	L-Camp	29.6	7.0	15.5	23.9	18.3	1.4	0.0	2.8	1.4	0.0	0.0	0.0	0.0	0.0	0.0	52.1	26.8	72
Glinzendorf	GT1-3660	Limnic-marine	L-Camp	12.2	2.0	2.4	0.5	82.9	0.0	0.0	0.0	0.0	0.0	0.0	0.0	0.0	0.0	0.0	16.6	0.5	205
Glinzendorf	T1-3310	Limnic-marine	M-Camp	12.0	2.3	12.0	65.4	4.5	1.5	0.0	1.5	0.0	0.0	0.0	0.0	0.0	0.0	0.8	26.3	66.9	133
Glinzendorf	T1-3327.4	Limnic-marine	M-Camp	29.2	8.1	7.0	14.1	41.3	0.0	0.0	0.0	0.0	0.3	0.0	0.0	0.0	0.0	0.0	44.3	14.4	197
Glinzendorf	T1-3328.5	Limnic-marine	M-Camp	23.2	0.3	4.0	16.1	54.4	0.0	0.0	0.0	1.0	0.0	0.0	0.0	0.0	0.0	1.0	27.5	17.1	201
Glinzendorf	T1-3330	Limnic-marine	M-Camp	30.0	5.0	23.5	22.0	15.0	1.5	0.5	2.0	0.5	0.0	0.0	0.0	0.0	0.0	0.0	58.5	24.5	200
Glinzendorf	T1-3331.1	Limnic-marine	M-Camp	31.3	1.0	4.0	27.3	34.3	0.0	0.0	0.0	1.0	0.0	0.0	0.0	0.0	0.0	1.0	36.4	28.3	157
Glinzendorf	T1-3332.1	Limnic-marine	M-Camp	23.2	6.3	8.4	25.3	32.6	0.0	0.0	0.0	1.1	0.0	0.0	0.0	0.0	0.0	3.2	37.9	26.3	144
Glinzendorf	T1-3350	Limnic-marine	M-Camp	23.3	3.3	18.9	41.1	8.9	1.1	1.1	1.1	1.1	0.0	0.0	0.0	0.0	0.0	0.0	45.6	44.4	90
Glinzendorf	T1-3370	Limnic-marine	M-Camp	20.5	5.3	29.5	24.7	16.8	0.0	0.5	1.6	0.0	0.0	0.0	0.0	0.0	0.5	0.5	55.3	25.3	190
Glinzendorf	T1-3390	Limnic-marine	M-Camp	9.1	2.0	11.2	68.5	7.1	1.5	0.0	0.0	0.0	0.0	0.0	0.0	0.0	0.5	0.0	22.3	70.1	197
Glinzendorf	T1-3405	Limnic-marine	M-Camp	15.3	10.2	22.4	37.8	7.7	3.6	1.0	0.5	0.5	0.0	0.0	0.0	0.0	0.0	1.0	48.0	42.9	196
Glinzendorf	T1-3430	Limnic-marine	M-Camp	18.1	3.1	13.5	56.0	4.7	1.6	1.0	1.6	0.5	0.0	0.0	0.0	0.0	0.0	0.0	34.7	59.1	193
Glinzendorf	T1-3450	Limnic-marine	M-Camp	15.2	2.0	17.3	48.2	12.2	3.0	0.5	0.5	1.0	0.0	0.0	0.0	0.0	0.0	0.0	34.5	52.8	197
Glinzendorf	T1-3465	Limnic-marine	M-Camp	17.4	2.2	23.2	39.1	14.5	0.7	1.4	0.7	0.7	0.0	0.0	0.0	0.0	0.0	0.0	42.8	42.0	138
Glinzendorf	GT1-3340	Limnic-marine	M-Camp	8.9	0.6	3.8	17.1	67.7	0.6	0.6	0.0	0.0	0.0	0.0	0.0	0.0	0.0	0.6	13.3	18.4	158
Glinzendorf	GT1-3360	Limnic-marine	M-Camp	5.0	0.0	2.0	0.0	93.0	0.0	0.0	0.0	0.0	0.0	0.0	0.0	0.0	0.0	0.0	7.0	0.0	58
Glinzendorf	GT1-3380	Limnic-marine	M-Camp	5.8	0.5	0.5	1.5	91.7	0.0	0.0	0.0	0.0	0.0	0.0	0.0	0.0	0.0	0.0	6.8	1.5	206
Glinzendorf	GT1-3420	Limnic-marine	M-Camp	6.7	1.9	4.8	19.2	62.5	0.0	1.0	0.0	0.0	0.0	0.0	0.0	0.0	0.0	3.8	13.5	20.2	104
Glinzendorf	GT1-3481	Limnic-marine	M-Camp	98.0	0.0	0.0	0.0	2.0	0.0	0.0	0.0	0.0	0.0	0.0	0.0	0.0	0.0	0.0	98.0	0.0	87
Glinzendorf	T1-3100	Limnic-marine	U-Camp	9.0	4.0	8.5	73.4	1.0	2.0	1.0	0.5	0.0	0.0	0.5	0.0	0.0	0.0	0.0	21.6	76.9	199
Glinzendorf	T1-3120	Limnic-marine	U-Camp	6.6	3.5	7.6	76.3	1.0	0.5	3.0	0.5	0.5	0.0	0.0	0.5	0.0	0.0	0.0	17.7	80.8	198
Glinzendorf	T1-3140	Limnic-marine	U-Camp	4.8	1.4	9.2	81.6	1.0	0.0	0.0	1.0	0.5	0.0	0.0	0.0	0.0	0.0	0.5	15.5	82.1	207
Glinzendorf	T1-3160	Limnic-marine	U-Camp	9.6	1.5	5.1	79.8	1.0	0.0	1.5	0.5	0.0	0.0	0.0	0.0	0.0	0.0	1.0	16.2	81.3	198
Glinzendorf	T1-3180	Limnic-marine	U-Camp	7.9	1.5	6.9	81.2	0.5	0.0	1.0	1.0	0.0	0.0	0.0	0.0	0.0	0.0	0.0	16.3	82.2	202
Glinzendorf	T1-3200	Limnic-marine	U-Camp	10.7	0.6	6.8	78.5	0.0	0.6	0.0	1.7	0.0	0.0	0.0	0.0	0.0	0.6	0.6	18.1	79.1	177
Glinzendorf	T1-3220	Limnic-marine	U-Camp	11.8	2.6	14.9	62.1	6.2	2.1	0.5	0.0	0.0	0.0	0.0	0.0	0.0	0.0	0.0	29.2	64.6	195
Glinzendorf	T1-3240	Limnic-marine	U-Camp	13.7	2.0	9.8	68.6	2.9	1.0	1.0	0.0	0.0	0.0	0.0	0.0	0.0	0.0	1.0	25.5	70.6	102
Glinzendorf	T1-3265	Limnic-marine	U-Camp	18.7	4.5	15.2	52.0	5.6	1.5	0.5	1.5	0.0	0.0	0.0	0.0	0.0	0.0	0.5	38.4	54.0	198
Glinzendorf	T1-3290	Limnic-marine	U-Camp	14.5	3.5	12.5	62.0	6.0	0.0	0.0	1.5	0.0	0.0	0.0	0.0	0.0	0.0	0.0	30.5	62.0	200

Gosau	Sample	Formation	Age	zrn [%]	tur [%]	rut [%]	grt [%]	chr [%]	cld [%]	sta [%]	mon [%]	tit [%]	epi [%]	hbl [%]	gln [%]	dis [%]	sil [%]	bkt/ana [%]	ZTR [%]	META [%]	grains
Glinzendorf	GT1-3220	Limnic-marine	U-Camp	20.3	0.0	10.2	66.1	0.0	0.0	1.7	0.0	0.0	0.0	0.0	0.0	0.0	0.0	1.7	30.5	67.8	60
Studienka	K09/4A	Ostrež Fm	L-Con	61.3	0.0	23.8	3.8	5.0	0.0	0.0	1.3	1.3	0.0	0.0	0.0	0.0	0.0	3.8	85.0	5.0	80
Studienka	K9/5A	Ostrež Fm	M-U-Con	6.2	13.3	3.3	0.0	66.7	5.7	0.0	0.0	1.4	0.0	0.0	0.5	0.0	0.0	2.9	22.9	7.6	210
Studienka	K09/5B	Ostrež Fm	M-U-Con	5.9	17.1	4.4	1.0	62.4	5.4	0.0	1.0	0.5	0.0	0.5	0.0	0.0	0.0	2.0	27.3	7.3	205
Studienka	K09/8A	Stvernik Fm	U-Con-L-San	7.3	43.2	3.2	0.9	33.6	5.9	0.0	1.4	0.9	0.9	0.0	0.0	0.0	0.0	2.7	53.6	8.6	220
Studienka	K09/8B	Stvernik Fm	U-Con-L-San	16.4	15.0	8.5	0.0	50.7	0.5	0.0	1.4	0.5	0.5	0.0	0.0	0.0	0.0	6.6	39.9	1.4	213
Studienka	09/6A	Košariská Fm	L-Camp	22.3	13.7	10.2	2.5	35.0	6.6	0.0	2.0	3.0	0.0	0.0	0.0	0.0	0.0	4.6	46.2	12.2	197
Studienka	K09/6C	Košariská Fm	L-Camp	19.2	33.3	13.1	2.3	16.4	8.9	0.0	0.9	0.5	0.0	0.0	0.0	0.0	0.0	5.2	65.7	11.7	213
Studienka	K09/7A	Podbradlo Fm	M-U-Camp	30.7	14.9	9.8	2.3	24.7	6.0	0.0	1.9	0.5	0.0	0.0	0.0	0.0	0.0	9.3	55.3	8.8	215
Studienka	K09/7B	Podbradlo Fm	M-U-Camp	15.3	42.4	10.2	3.4	16.9	6.8	0.0	0.0	0.0	0.0	0.0	0.0	0.0	0.0	5.1	67.8	10.2	59
Studienka	K09/2A	Priepastné Fm	Paleoc	14.9	34.3	3.7	20.9	3.0	17.9	0.0	1.5	0.0	0.0	0.0	1.5	0.7	0.0	1.5	53.0	40.3	134
Studienka	K09/2B	Priepastné Fm	Paleoc	8.4	67.8	2.6	4.4	7.9	4.8	0.0	0.9	0.0	0.0	0.0	0.0	0.0	0.0	3.1	78.9	9.3	227
Studienka	K09/3A	Jablonka Fm	M-Eoc	13.5	14.9	13.0	41.3	0.5	2.9	0.5	1.9	4.8	0.0	0.0	0.0	0.0	0.0	6.7	41.3	49.5	208
Studienka	K09/3B	Jablonka Fm	M-Eoc	7.1	20.5	11.0	47.1	0.0	3.8	0.5	1.4	4.3	0.0	0.0	0.0	0.0	0.0	4.3	38.6	55.7	210

Gosau	Sample	Formation	Age	Location	SiO_2 [wt.%]	FeO [wt.%]	Al_2O_3 [wt.%]	MgO [wt.%]	MnO [wt.%]	CaO [wt.%]	TiO_2 [wt.%]	Cr_2O_3 [wt.%]	Na_2O [wt.%]	NiO [wt.%]	Total [wt.%]	Alm [wt.%]	Sps [wt.%]	Prp [wt.%]	Grs [wt.%]	And [wt.%]	Uva [wt.%]
Gießhübl	L16_grt1	not defined	Con-San	Lilienfeld	40.71	15.25	23.38	12.74	0.30	8.45	0.05	0.00	0.02	0.00	100.91	31.1	0.6	46.3	21.9	0.1	0.0
Gießhübl	L221_grt1	not defined	Con-San	Lilienfeld	38.20	27.89	22.05	6.79	3.31	2.11	0.04	0.00	0.00	0.00	100.39	60.6	7.3	26.3	5.8	0.1	0.0
Gießhübl	TA8_grt1	Nierental Fm	Campanian	Tasshof	38.13	23.89	21.56	4.10	2.43	9.82	0.14	0.00	0.00	0.00	100.07	51.7	5.3	15.8	26.8	0.4	0.0
Gießhübl	A3_grt1	L-Gießhübl Fm	Maastr	Aderklaa 92	37.56	28.19	21.39	2.27	3.33	7.68	0.09	0.00	0.03	0.00	100.54	62.0	7.4	8.9	21.4	0.3	0.0
Gießhübl	A3_grt2	L-Gießhübl Fm	Maastr	Aderklaa 92	37.43	31.56	21.46	2.21	0.14	7.38	0.11	0.00	0.03	0.00	100.30	70.0	0.3	8.7	20.7	0.3	0.0
Gießhübl	A3_grt3	L-Gießhübl Fm	Maastr	Aderklaa 92	36.88	26.70	20.90	0.83	8.12	6.01	0.09	0.00	0.09	0.00	99.63	60.5	18.7	3.4	17.2	0.3	0.0
Gießhübl	A3_grt4	L-Gießhübl Fm	Maastr	Aderklaa 92	37.25	29.30	21.44	2.28	2.17	7.31	0.04	0.00	0.07	0.00	99.86	65.2	4.9	9.1	20.7	0.1	0.0
Gießhübl	A3_grt5	L-Gießhübl Fm	Maastr	Aderklaa 92	37.20	26.99	21.13	1.25	6.07	8.07	0.11	0.00	0.02	0.00	100.85	59.1	13.4	4.9	22.3	0.3	0.0
Gießhübl	A3_grt6	L-Gießhübl Fm	Maastr	Aderklaa 92	37.32	27.35	21.38	2.20	4.62	7.09	0.10	0.00	0.01	0.00	100.06	60.7	10.4	8.7	19.9	0.3	0.0
Gießhübl	A3_grt7	L-Gießhübl Fm	Maastr	Aderklaa 92	37.30	29.12	21.32	2.18	2.94	7.01	0.17	0.00	0.02	0.00	100.06	64.8	6.6	8.6	19.5	0.5	0.0
Gießhübl	A3_grt8	L-Gießhübl Fm	Maastr	Aderklaa 92	38.55	28.00	21.99	7.94	0.95	2.91	0.04	0.00	0.01	0.00	100.39	59.8	2.0	30.2	7.8	0.1	0.0
Gießhübl	A3_grt9	L-Gießhübl Fm	Maastr	Aderklaa 92	37.43	27.98	21.38	1.84	3.30	8.33	0.12	0.00	0.03	0.00	100.41	61.8	7.4	7.2	23.2	0.4	0.0
Gießhübl	A3_grt10	L-Gießhübl Fm	Maastr	Aderklaa 92	37.37	30.87	21.53	1.79	1.36	7.71	0.10	0.00	0.02	0.00	100.76	68.1	3.0	7.1	21.5	0.3	0.0
Gießhübl	A3_grt11	L-Gießhübl Fm	Maastr	Aderklaa 92	37.44	28.77	21.52	2.14	2.59	7.57	0.12	0.00	0.04	0.00	100.19	64.1	5.8	8.5	21.2	0.4	0.0
Gießhübl	A3_grt12	L-Gießhübl Fm	Maastr	Aderklaa 92	37.61	29.12	21.46	2.43	2.58	7.10	0.02	0.00	0.02	0.00	100.33	64.5	5.8	9.6	20.1	0.1	0.0
Gießhübl	A3_grt13	L-Gießhübl Fm	Maastr	Aderklaa 92	37.08	31.79	21.06	1.24	1.36	7.03	0.17	0.00	0.02	0.00	99.75	71.6	3.1	5.0	19.8	0.5	0.0
Gießhübl	A3_grt14	L-Gießhübl Fm	Maastr	Aderklaa 92	37.15	27.76	21.19	0.85	2.49	10.50	0.14	0.00	0.15	0.00	100.22	61.4	5.6	3.3	29.3	0.4	0.0
Gießhübl	A3_grt15	L-Gießhübl Fm	Maastr	Aderklaa 92	37.49	29.21	21.61	2.23	3.11	7.12	0.07	0.00	0.01	0.00	100.86	64.3	6.9	8.8	19.9	0.2	0.0
Gießhübl	A3_grt16	L-Gießhübl Fm	Maastr	Aderklaa 92	37.44	29.53	21.10	1.31	1.43	9.04	0.11	0.00	0.04	0.00	99.98	65.8	3.2	5.2	25.5	0.3	0.0
Gießhübl	A3_grt17	L-Gießhübl Fm	Maastr	Aderklaa 92	37.81	32.13	21.57	4.42	0.48	3.95	0.06	0.00	0.00	0.00	100.41	70.5	1.1	17.3	10.9	0.2	0.0
Gießhübl	A3_grt18	L-Gießhübl Fm	Maastr	Aderklaa 92	37.42	32.75	21.65	3.43	2.28	2.86	0.00	0.00	0.04	0.00	100.42	73.1	5.1	13.6	8.2	0.0	0.0
Gießhübl	A3_grt19	L-Gießhübl Fm	Maastr	Aderklaa 92	37.26	28.20	21.24	1.34	3.94	7.95	0.10	0.00	0.03	0.00	100.05	63.0	8.9	5.3	22.5	0.3	0.0
Gießhübl	A3_grt20	L-Gießhübl Fm	Maastr	Aderklaa 92	36.93	36.16	21.34	2.82	1.01	1.65	0.09	0.00	0.06	0.00	100.05	81.6	2.3	11.3	4.5	0.3	0.0
Gießhübl	A3_grt21	L-Gießhübl Fm	Maastr	Aderklaa 92	37.46	28.93	21.38	1.33	2.74	8.68	0.14	0.00	0.02	0.00	100.69	64.0	6.1	5.2	24.2	0.4	0.0
Gießhübl	A3_grt22	L-Gießhübl Fm	Maastr	Aderklaa 92	37.38	33.08	21.42	4.06	2.64	1.69	0.01	0.00	0.05	0.00	100.34	73.3	5.9	16.0	4.8	0.0	0.0
Gießhübl	A3_grt23	L-Gießhübl Fm	Maastr	Aderklaa 92	37.58	27.31	21.63	2.16	2.37	9.51	0.10	0.00	0.07	0.00	100.73	59.7	5.2	8.4	26.3	0.3	0.0
Gießhübl	A3_grt24	L-Gießhübl Fm	Maastr	Aderklaa 92	37.44	31.42	21.37	1.85	0.79	7.50	0.11	0.00	0.05	0.00	100.52	69.6	1.8	7.3	21.0	0.3	0.0
Gießhübl	A3_grt25	L-Gießhübl Fm	Maastr	Aderklaa 92	37.79	32.45	21.68	4.84	1.51	2.35	0.00	0.00	0.07	0.00	100.68	71.2	3.4	18.9	6.6	0.0	0.0
Gießhübl	A3_grt26	L-Gießhübl Fm	Maastr	Aderklaa 92	37.55	29.11	21.62	2.24	1.23	8.59	0.09	0.00	0.04	0.00	100.48	64.2	2.8	8.8	24.0	0.3	0.0
Gießhübl	A3_grt27	L-Gießhübl Fm	Maastr	Aderklaa 92	37.27	29.86	21.14	1.26	2.36	8.02	0.17	0.00	0.02	0.00	100.10	66.7	5.3	5.0	22.5	0.5	0.0
Gießhübl	A3_grt28	L-Gießhübl Fm	Maastr	Aderklaa 92	37.61	29.15	21.57	2.27	1.90	7.86	0.08	0.00	0.08	0.00	100.52	64.5	4.3	9.0	22.1	0.2	0.0
Gießhübl	A3_grt29	L-Gießhübl Fm	Maastr	Aderklaa 92	36.95	34.18	20.94	1.51	1.46	5.22	0.14	0.00	0.05	0.00	100.43	75.9	3.3	6.0	14.4	0.4	0.0
Gießhübl	A3_grt30	L-Gießhübl Fm	Maastr	Aderklaa 92	37.99	30.29	21.62	5.50	1.11	3.28	0.16	0.00	0.03	0.00	99.97	66.7	2.5	21.6	8.8	0.5	0.0
Gießhübl	A3_grt31	L-Gießhübl Fm	Maastr	Aderklaa 92	37.44	30.10	21.39	2.17	1.10	7.91	0.06	0.00	0.05	0.00	100.21	66.6	2.5	8.6	22.2	0.2	0.0
Gießhübl	A4_grt1	L-Gießhübl Fm	Paleocene	Aderklaa 92	37.11	28.18	21.13	0.69	4.21	8.51	0.14	0.00	0.05	0.00	100.01	63.2	9.6	2.7	24.0	0.4	0.0
Gießhübl	A4_grt2	L-Gießhübl Fm	Paleocene	Aderklaa 92	37.71	30.13	21.50	2.22	0.63	8.06	0.13	0.00	0.03	0.00	100.41	66.9	1.4	8.8	22.5	0.4	0.0
Gießhübl	A4_grt3	L-Gießhübl Fm	Paleocene	Aderklaa 92	37.58	27.55	21.37	3.80	0.93	8.44	0.13	0.00	0.03	0.00	99.82	59.8	2.1	14.7	23.1	0.4	0.0
Gießhübl	A4_grt4	L-Gießhübl Fm	Paleocene	Aderklaa 92	37.15	32.39	21.41	3.96	2.16	2.48	0.04	0.00	0.00	0.00	99.59	72.3	4.9	15.8	7.0	0.1	0.0
Gießhübl	A4_grt5	L-Gießhübl Fm	Paleocene	Aderklaa 92	37.25	28.91	21.15	1.59	2.65	8.53	0.13	0.00	0.08	0.00	100.30	63.7	5.9	6.3	23.7	0.4	0.0
Gießhübl	A4_grt6	L-Gießhübl Fm	Paleocene	Aderklaa 92	37.19	29.62	21.44	2.00	2.16	7.16	0.17	0.00	0.06	0.00	99.80	66.5	4.9	8.0	20.1	0.5	0.0
Gießhübl	A4_grt7	L-Gießhübl Fm	Paleocene	Aderklaa 92	36.98	32.10	21.17	1.87	1.26	6.32	0.10	0.00	0.06	0.00	99.86	71.7	2.8	7.4	17.8	0.3	0.0
Gießhübl	A4_grt8	L-Gießhübl Fm	Paleocene	Aderklaa 92	37.21	29.74	21.38	1.75	2.74	7.14	0.13	0.00	0.01	0.00	100.11	66.4	6.2	7.0	20.0	0.4	0.0
Gießhübl	A4_grt9	L-Gießhübl Fm	Paleocene	Aderklaa 92	36.93	28.77	21.20	1.05	4.47	7.21	0.14	0.00	0.08	0.00	99.85	64.8	10.2	4.2	20.4	0.4	0.0
Gießhübl	A4_grt10	L-Gießhübl Fm	Paleocene	Aderklaa 92	37.47	30.21	21.41	2.78	0.65	7.35	0.08	0.00	0.06	0.00	100.00	66.8	1.4	11.0	20.6	0.2	0.0
Gießhübl	A4_grt11	L-Gießhübl Fm	Paleocene	Aderklaa 92	36.68	34.34	21.39	3.77	1.95	1.00	0.03	0.00	0.11	0.00	99.25	77.5	4.5	15.2	2.8	0.1	0.0
Gießhübl	A4_grt12	L-Gießhübl Fm	Paleocene	Aderklaa 92	36.52	34.96	21.00	1.66	2.58	2.89	0.04	0.00	0.02	0.00	99.68	79.0	5.9	6.7	8.3	0.1	0.0
Gießhübl	A4_grt13	L-Gießhübl Fm	Paleocene	Aderklaa 92	36.73	33.89	21.29	2.46	3.32	2.08	0.04	0.00	0.00	0.00	99.81	76.5	7.6	9.9	5.9	0.1	0.0

Gosau	Sample	Formation	Age	Location	SiO_2 [wt.%]	FeO [wt.%]	Al_2O_3 [wt.%]	MgO [wt.%]	MnO [wt.%]	CaO [wt.%]	TiO_2 [wt.%]	Cr_2O_3 [wt.%]	Na_2O [wt.%]	NiO [wt.%]	Total [wt.%]	Alm [wt.%]	Sps [wt.%]	Prp [wt.%]	Grs [wt.%]	And [wt.%]	Uva [wt.%]
Gießhübl	A4_grt14	L-Gießhübl Fm	Paleocene	Aderklaa 92	37.06	28.26	21.15	1.36	3.09	8.26	0.29	0.00	0.04	0.00	99.51	63.7	7.0	5.5	23.0	0.9	0.0
Gießhübl	A4_grt15	L-Gießhübl Fm	Paleocene	Aderklaa 92	37.26	31.18	21.46	2.21	0.94	6.98	0.06	0.00	0.01	0.00	100.10	69.3	2.1	8.8	19.7	0.2	0.0
Gießhübl	A4_grt16	L-Gießhübl Fm	Paleocene	Aderklaa 92	37.26	31.01	21.52	2.72	0.43	7.04	0.05	0.00	0.03	0.00	100.05	68.5	1.0	10.7	19.8	0.1	0.0
Gießhübl	A4_grt17	L-Gießhübl Fm	Paleocene	Aderklaa 92	37.18	27.16	21.40	1.25	3.78	9.43	0.15	0.00	0.00	0.00	100.33	60.0	8.5	4.9	26.2	0.5	0.0
Gießhübl	A4_grt18	L-Gießhübl Fm	Paleocene	Aderklaa 92	37.46	29.47	21.32	2.59	1.71	7.41	0.15	0.00	0.00	0.00	100.10	65.1	3.8	10.2	20.5	0.5	0.0
Gießhübl	A4_grt19	L-Gießhübl Fm	Paleocene	Aderklaa 92	37.07	26.06	21.17	0.67	4.83	10.10	0.10	0.00	0.06	0.00	100.06	57.8	10.9	2.6	28.4	0.3	0.0
Gießhübl	A4_grt20	L-Gießhübl Fm	Paleocene	Aderklaa 92	37.19	29.48	21.23	2.55	2.00	7.12	0.15	0.00	0.03	0.00	99.75	65.3	4.5	10.1	19.7	0.5	0.0
Gießhübl	A4_grt21	L-Gießhübl Fm	Paleocene	Aderklaa 92	37.19	28.93	21.31	2.41	2.85	6.99	0.06	0.00	0.00	0.00	99.75	64.2	6.4	9.5	19.7	0.2	0.0
Gießhübl	A4_grt22	L-Gießhübl Fm	Paleocene	Aderklaa 92	37.46	29.00	21.24	1.75	1.82	8.68	0.10	0.00	0.02	0.00	100.05	64.3	4.1	6.9	24.4	0.3	0.0
Gießhübl	A4_grt23	L-Gießhübl Fm	Paleocene	Aderklaa 92	37.04	34.47	21.21	2.76	0.14	4.26	0.09	0.00	0.04	0.00	100.01	76.6	0.3	10.9	11.9	0.3	0.0
Gießhübl	A4_grt24	L-Gießhübl Fm	Paleocene	Aderklaa 92	37.41	30.98	21.53	2.95	0.36	7.10	0.07	0.00	0.07	0.00	100.46	67.8	0.8	11.5	19.7	0.2	0.0
Gießhübl	A4_grt25	L-Gießhübl Fm	Paleocene	Aderklaa 92	37.20	29.19	21.33	2.27	1.95	7.78	0.11	0.00	0.03	0.00	99.84	64.6	4.4	8.9	21.7	0.3	0.0
Gießhübl	A4_grt26	L-Gießhübl Fm	Paleocene	Aderklaa 92	37.28	27.29	21.26	2.24	4.09	7.74	0.09	0.00	0.07	0.00	100.04	60.2	9.1	8.8	21.6	0.3	0.0
Gießhübl	A4_grt27	L-Gießhübl Fm	Paleocene	Aderklaa 92	36.95	28.29	21.15	1.51	4.21	7.70	0.14	0.00	0.12	0.00	100.07	62.7	9.5	6.0	21.4	0.4	0.0
Gießhübl	A4_grt28	L-Gießhübl Fm	Paleocene	Aderklaa 92	37.20	31.53	21.49	2.00	0.31	7.41	0.07	0.00	0.03	0.00	100.02	70.2	0.7	7.9	21.0	0.2	0.0
Gießhübl	A2_gr1	M-Gießhübl Fm	Paleocene	Aderklaa 92	37.42	29.21	21.29	1.67	2.83	8.26	0.10	0.01	0.03	0.00	100.82	64.0	6.3	6.5	22.9	0.3	0.0
Gießhübl	A2_gr2	M-Gießhübl Fm	Paleocene	Aderklaa 92	37.79	30.87	21.51	2.85	0.36	6.91	0.06	0.06	0.04	0.00	100.45	68.3	0.8	11.2	19.3	0.2	0.1
Gießhübl	A2_gr3	M-Gießhübl Fm	Paleocene	Aderklaa 92	37.38	30.29	21.37	2.13	2.16	6.87	0.09	0.01	0.03	0.00	100.32	67.2	4.9	8.4	19.2	0.3	0.0
Gießhübl	A2_gr4	M-Gießhübl Fm	Paleocene	Aderklaa 92	37.72	29.00	21.63	3.73	0.83	7.20	0.04	0.00	0.04	0.03	100.21	63.4	1.8	14.5	20.1	0.1	0.0
Gießhübl	A2_gr5	M-Gießhübl Fm	Paleocene	Aderklaa 92	37.34	29.42	21.28	2.08	3.22	6.85	0.10	0.00	0.01	0.00	100.29	65.1	7.2	8.2	19.1	0.3	0.0
Gießhübl	A2_gr6	M-Gießhübl Fm	Paleocene	Aderklaa 92	37.90	26.59	21.71	3.24	1.25	9.77	0.08	0.02	0.00	0.00	100.54	57.6	2.7	12.5	26.9	0.2	0.0
Gießhübl	A2_gr7	M-Gießhübl Fm	Paleocene	Aderklaa 92	37.02	33.81	21.20	1.51	0.09	6.49	0.11	0.00	0.02	0.02	100.27	75.3	0.2	6.0	18.2	0.3	0.0
Gießhübl	A2_gr8	M-Gießhübl Fm	Paleocene	Aderklaa 92	37.39	29.16	21.27	2.36	2.59	7.32	0.07	0.02	0.05	0.00	100.24	64.3	5.8	9.3	20.4	0.2	0.0
Gießhübl	A2_gr9	M-Gießhübl Fm	Paleocene	Aderklaa 92	37.53	30.57	21.44	2.72	0.88	7.12	0.10	0.00	0.02	0.00	100.37	67.3	2.0	10.7	19.8	0.3	0.0
Gießhübl	A2_gr10	M-Gießhübl Fm	Paleocene	Aderklaa 92	37.63	26.14	21.44	1.90	3.29	10.01	0.10	0.02	0.00	0.00	100.52	57.2	7.3	7.4	27.8	0.3	0.0
Gießhübl	A2_gr11	M-Gießhübl Fm	Paleocene	Aderklaa 92	37.52	31.12	21.14	2.76	2.43	5.60	0.09	0.04	0.05	0.00	100.75	68.1	5.4	10.8	15.4	0.3	0.1
Gießhübl	A2_gr12	M-Gießhübl Fm	Paleocene	Aderklaa 92	37.52	28.88	21.36	2.33	3.00	7.29	0.08	0.02	0.02	0.00	100.50	63.6	6.7	9.2	20.3	0.2	0.0
Gießhübl	A2_gr13	M-Gießhübl Fm	Paleocene	Aderklaa 92	37.41	30.32	21.73	4.49	2.53	3.74	0.03	0.04	0.04	0.00	100.32	66.4	5.6	17.5	10.3	0.1	0.1
Gießhübl	A2_gr14	M-Gießhübl Fm	Paleocene	Aderklaa 92	37.25	30.33	21.11	1.83	3.60	5.96	0.12	0.04	0.00	0.00	100.22	67.6	8.1	7.3	16.6	0.4	0.1
Gießhübl	A2_gr15	M-Gießhübl Fm	Paleocene	Aderklaa 92	37.50	30.07	21.49	2.73	1.26	7.14	0.11	0.04	0.03	0.00	100.37	66.3	2.8	10.7	19.8	0.3	0.1
Gießhübl	A2_gr16	M-Gießhübl Fm	Paleocene	Aderklaa 92	37.62	29.82	21.54	2.53	1.84	7.03	0.12	0.02	0.02	0.01	100.55	66.0	4.1	10.0	19.5	0.3	0.0
Gießhübl	A2_gr17	M-Gießhübl Fm	Paleocene	Aderklaa 92	37.26	30.49	21.27	2.60	3.02	5.36	0.06	0.01	0.01	0.00	100.09	67.7	6.8	10.3	15.0	0.2	0.0
Gießhübl	A2_gr18	M-Gießhübl Fm	Paleocene	Aderklaa 92	37.43	31.08	21.47	2.22	0.79	7.47	0.10	0.02	0.01	0.04	100.64	68.4	1.8	8.7	20.7	0.3	0.0
Gießhübl	A2_gr19	M-Gießhübl Fm	Paleocene	Aderklaa 92	37.20	28.07	21.10	1.40	4.56	7.72	0.17	0.03	0.02	0.00	100.26	62.3	10.2	5.5	21.4	0.5	0.1
Gießhübl	A2_gr20	M-Gießhübl Fm	Paleocene	Aderklaa 92	37.34	29.27	21.40	2.09	1.89	8.14	0.11	0.04	0.05	0.00	100.31	64.6	4.2	8.2	22.6	0.3	0.1
Gießhübl	A2_gr21	M-Gießhübl Fm	Paleocene	Aderklaa 92	37.12	21.28	21.08	1.22	13.76	6.04	0.13	0.01	0.01	0.00	100.63	47.2	30.9	4.8	16.7	0.4	0.0
Gießhübl	A1_gr2	U-Gießhübl Fm	Paleocene	Aderklaa 84	37.63	28.97	21.17	1.41	1.78	9.11	0.09	0.00	0.03	0.00	100.19	64.4	4.0	5.6	25.7	0.3	0.0
Gießhübl	A1_gr3	U-Gießhübl Fm	Paleocene	Aderklaa 84	38.10	24.95	21.67	3.04	1.90	10.79	0.20	0.05	0.02	0.01	100.71	54.1	4.2	11.7	29.3	0.6	0.1
Gießhübl	A1_gr4	U-Gießhübl Fm	Paleocene	Aderklaa 84	37.86	30.91	21.42	2.73	0.54	6.99	0.05	0.04	0.02	0.02	100.55	68.3	1.2	10.7	19.5	0.2	0.1
Gießhübl	A1_gr5	U-Gießhübl Fm	Paleocene	Aderklaa 84	37.89	28.71	21.35	2.91	1.99	7.19	0.06	0.02	0.01	0.01	100.13	63.6	4.5	11.5	20.2	0.2	0.0
Gießhübl	A1_gr6	U-Gießhübl Fm	Paleocene	Aderklaa 84	37.28	33.15	20.88	1.25	0.19	7.18	0.11	0.03	0.03	0.02	100.12	74.0	0.4	5.0	20.2	0.3	0.1
Gießhübl	A1_gr7	U-Gießhübl Fm	Paleocene	Aderklaa 84	37.81	30.30	21.48	3.58	1.46	5.59	0.08	0.00	0.01	0.00	100.31	66.8	3.3	14.1	15.6	0.2	0.0
Gießhübl	A1_gr8	U-Gießhübl Fm	Paleocene	Aderklaa 84	37.84	29.61	21.41	2.97	1.20	7.26	0.06	0.00	0.06	0.01	100.41	65.2	2.7	11.6	20.3	0.2	0.0
Gießhübl	A1_gr10	U-Gießhübl Fm	Paleocene	Aderklaa 84	37.80	28.86	21.28	2.47	2.57	7.34	0.12	0.04	0.01	0.02	100.50	63.8	5.7	9.7	20.4	0.3	0.1
Gießhübl	A1_gr11	U-Gießhübl Fm	Paleocene	Aderklaa 84	37.75	30.51	21.28	2.29	1.22	7.33	0.10	0.01	0.01	0.02	100.52	67.5	2.7	9.0	20.4	0.3	0.0
Gießhübl	A1_gr12	U-Gießhübl Fm	Paleocene	Aderklaa 84	37.60	30.37	21.35	2.60	1.24	7.14	0.03	0.00	0.01	0.02	100.36	66.9	2.8	10.2	20.0	0.1	0.0
Gießhübl	A1_gr13	U-Gießhübl Fm	Paleocene	Aderklaa 84	37.79	30.77	21.36	2.75	0.75	6.94	0.09	0.03	0.03	0.02	100.54	67.9	1.7	10.8	19.3	0.3	0.1

Gosau	Sample	Formation	Age	Location	SiO_2 [wt.%]	FeO [wt.%]	Al_2O_3 [wt.%]	MgO [wt.%]	MnO [wt.%]	CaO [wt.%]	TiO_2 [wt.%]	Cr_2O_3 [wt.%]	Na_2O [wt.%]	NiO [wt.%]	Total [wt.%]	Alm [wt.%]	Sps [wt.%]	Prp [wt.%]	Grs [wt.%]	And [wt.%]	Uva [wt.%]
Gießhübl	A1_gr15	U-Gießhübl Fm	Paleoc	Aderklaa 84	37.42	30.63	21.21	2.47	2.34	6.20	0.08	0.03	0.01	0.01	100.40	67.5	5.2	9.7	17.2	0.2	0.1
Gießhübl	A1_gr16	U-Gießhübl Fm	Paleoc	Aderklaa 84	38.60	30.43	21.85	7.61	0.77	1.46	0.02	0.04	0.01	0.02	100.82	65.2	1.7	29.1	3.9	0.0	0.1
Glinzend.	T106_grt1	not defined	Camp	Markgrn. T1	37.09	32.92	21.00	1.12	0.93	7.36	0.04	0.00	0.01	0.00	100.48	72.7	2.1	4.4	20.7	0.1	0.0
Glinzend.	T107_grt1	not defined	Camp	Markgrn. T1	37.21	26.89	21.07	0.60	4.02	10.26	0.18	0.00	0.04	0.00	100.25	59.6	9.0	2.3	28.6	0.5	0.0
Glinzend.	T107_grt2	not defined	Camp	Markgrn. T1	37.09	28.24	21.01	2.28	4.32	7.31	0.01	0.00	0.02	0.00	100.26	61.4	9.5	8.8	20.3	0.0	0.0
Glinzend.	T107_grt3	not defined	Camp	Markgrn. T1	36.94	35.72	21.26	1.85	0.15	4.14	0.07	0.00	0.04	0.00	100.17	80.3	0.3	7.4	11.7	0.2	0.0
Glinzend.	T107_grt4	not defined	Camp	Markgrn. T1	37.25	28.66	21.39	1.28	1.41	9.97	0.16	0.00	0.03	0.00	100.13	63.5	3.2	5.0	27.8	0.5	0.0
Glinzend.	T107_grt5	not defined	Camp	Markgrn. T1	36.72	33.31	20.79	1.08	0.73	6.95	0.02	0.00	0.00	0.00	99.59	74.2	1.7	4.3	19.8	0.0	0.0
Glinzend.	T102_gr1	not defined	Camp	Markgrn. T1	38.14	28.50	22.08	7.03	2.45	1.72	0.02	0.11	0.00	0.00	100.05	62.3	5.4	27.4	4.6	0.0	0.2
Glinzend.	T102_gr2	not defined	Camp	Markgrn. T1	38.66	24.32	21.77	6.64	0.71	7.75	0.11	0.00	0.00	0.04	100.00	52.0	1.5	25.3	20.9	0.3	0.0
Glinzend.	T102_gr5	not defined	Camp	Markgrn. T1	38.66	21.95	21.96	6.40	0.81	10.19	0.08	0.06	0.02	0.00	100.13	46.5	1.7	24.1	27.3	0.2	0.1
Glinzend.	T102_gr6	not defined	Camp	Markgrn. T1	38.63	22.68	21.85	5.71	0.92	10.20	0.18	0.00	0.00	0.00	100.18	48.4	2.0	21.7	27.4	0.5	0.0
Glinzend.	T102_gr7	not defined	Camp	Markgrn. T1	38.20	23.71	21.20	3.09	1.93	11.85	0.24	0.01	0.05	0.00	100.28	51.1	4.2	11.9	32.0	0.7	0.0
Glinzend.	T102_gr8	not defined	Camp	Markgrn. T1	38.77	23.20	21.94	6.79	0.74	8.78	0.11	0.02	0.01	0.02	100.39	49.0	1.6	25.6	23.4	0.3	0.0
Glinzend.	T102_gr9	not defined	Camp	Markgrn. T1	37.81	25.81	21.44	3.71	2.99	8.18	0.11	0.00	0.04	0.00	100.08	56.2	6.6	14.4	22.5	0.3	0.0
Glinzend.	T102_gr10	not defined	Camp	Markgrn. T1	37.62	26.36	21.53	4.16	7.27	3.64	0.02	0.04	0.00	0.00	100.64	57.6	16.1	16.2	10.1	0.1	0.1
Glinzend.	T102_gr11	not defined	Camp	Markgrn. T1	36.60	26.74	20.91	1.11	12.67	2.15	0.08	0.03	0.01	0.00	100.28	60.4	29.0	4.5	5.9	0.2	0.1
Glinzend.	T102_gr12	not defined	Camp	Markgrn. T1	37.22	27.63	21.06	2.30	8.84	2.77	0.12	0.04	0.03	0.01	100.02	62.4	20.2	9.3	7.6	0.4	0.1
Glinzend.	T102_gr13	not defined	Camp	Markgrn. T1	38.91	23.51	22.08	7.07	0.62	8.02	0.12	0.05	0.00	0.02	100.39	50.0	1.3	26.8	21.4	0.3	0.1
Glinzend.	T104_grt1	not defined	Camp	Markgrn. T1	36.71	32.32	20.94	1.14	2.36	6.72	0.04	0.00	0.06	0.00	100.29	71.3	5.3	4.5	18.9	0.1	0.0
Grünbach	G6B_gr1	Kreuzgr. Fm	Con-San	Grünbach	37.65	31.99	21.15	4.78	2.80	1.26	0.03	0.33	0.00	0.00	99.99	71.1	6.3	19.0	2.8	0.1	0.7
Grünbach	G6B_gr2	Kreuzgr. Fm	Con-San	Grünbach	38.09	24.25	21.68	3.82	1.38	10.82	0.17	0.00	0.04	0.04	100.29	52.3	3.0	14.7	29.4	0.5	0.0
Grünbach	G6B_gr3	Kreuzgr. Fm	Con-San	Grünbach	39.17	21.72	22.21	7.70	0.54	8.98	0.05	0.02	0.00	0.07	100.45	45.7	1.2	28.9	24.0	0.1	0.0
Grünbach	G6B_gr4	Kreuzgr. Fm	Con-San	Grünbach	37.24	34.34	21.24	3.49	2.64	1.23	0.08	0.11	0.06	0.04	100.45	76.6	6.0	13.9	3.1	0.2	0.2
Grünbach	G6B_gr5	Kreuzgr. Fm	Con-San	Grünbach	37.34	33.30	21.36	4.44	1.77	1.46	0.03	0.24	0.03	0.00	99.97	74.2	4.0	17.6	3.6	0.1	0.5
Grünbach	G6B_gr6	Kreuzgr. Fm	Con-San	Grünbach	38.47	25.12	21.56	3.85	2.58	9.24	0.09	0.02	0.05	0.00	100.97	54.1	5.6	14.8	25.2	0.3	0.0
Grünbach	G6B_gr7	Kreuzgr. Fm	Con-San	Grünbach	37.45	32.43	21.26	4.52	2.27	1.95	0.02	0.12	0.00	0.00	100.02	71.6	5.1	17.8	5.2	0.1	0.2
Grünbach	G6B_gr8	Kreuzgr. Fm	Con-San	Grünbach	37.91	30.58	21.39	5.47	2.82	1.81	0.03	0.26	0.00	0.00	100.28	67.2	6.3	21.4	4.5	0.1	0.5
Grünbach	G6B_gr9	Kreuzgr. Fm	Con-San	Grünbach	38.72	23.16	21.57	5.32	0.70	10.81	0.13	0.18	0.03	0.00	100.61	49.1	1.5	20.1	28.6	0.4	0.4
Grünbach	G6B_gr10	Kreuzgr. Fm	Con-San	Grünbach	38.22	24.86	21.52	4.04	2.94	8.77	0.08	0.07	0.05	0.00	100.54	53.7	6.4	15.6	23.9	0.2	0.1
Grünbach	G6B_gr11	Kreuzgr. Fm	Con-San	Grünbach	38.14	24.74	21.35	4.03	2.86	8.66	0.10	0.08	0.02	0.00	99.98	53.9	6.3	15.6	23.7	0.3	0.2
Grünbach	G6B_gr12	Kreuzgr. Fm	Con-San	Grünbach	38.88	22.19	21.57	6.80	0.54	9.63	0.09	0.15	0.00	0.00	99.85	47.0	1.1	25.7	25.6	0.3	0.3
Grünbach	G6B_gr13	Kreuzgr. Fm	Con-San	Grünbach	38.59	22.95	21.62	6.01	0.77	10.04	0.12	0.05	0.00	0.05	100.20	48.5	1.7	22.7	26.8	0.3	0.1
Grünbach	G6B_gr14	Kreuzgr. Fm	Con-San	Grünbach	37.62	24.19	21.05	2.98	7.81	6.53	0.04	0.13	0.00	0.00	100.35	52.8	17.3	11.6	17.9	0.1	0.3
Grünbach	G6B_gr15	Kreuzgr. Fm	Con-San	Grünbach	38.73	22.44	21.90	5.96	0.55	10.57	0.11	0.01	0.02	0.00	100.30	47.6	1.2	22.5	28.4	0.3	0.0
Grünbach	G9_gr1	Maiersdorf Fm	Con-San	Grünbach	38.29	22.36	21.34	4.00	2.85	10.77	0.18	0.03	0.05	0.00	99.88	48.4	6.2	15.5	29.3	0.5	0.1
Grünbach	G9_gr2	Maiersdorf Fm	Con-San	Grünbach	38.60	22.58	21.79	5.52	0.66	11.08	0.06	0.03	0.06	0.00	100.37	47.8	1.4	20.8	29.8	0.2	0.1
Grünbach	G9_gr3	Maiersdorf Fm	Con-San	Grünbach	39.15	22.84	21.77	8.09	0.39	7.76	0.07	0.04	0.04	0.00	100.16	48.0	0.8	30.3	20.6	0.2	0.1
Grünbach	G9_gr4	Maiersdorf Fm	Con-San	Grünbach	38.61	23.22	21.64	5.76	0.65	10.08	0.09	0.02	0.04	0.00	100.10	49.3	1.4	21.8	27.2	0.2	0.0
Grünbach	G9_gr5	Maiersdorf Fm	Con-San	Grünbach	38.75	22.98	21.75	6.04	0.58	10.14	0.09	0.03	0.03	0.00	100.39	48.6	1.2	22.8	27.1	0.3	0.1
Grünbach	G9_gr6	Maiersdorf Fm	Con-San	Grünbach	38.17	26.36	21.65	5.03	4.68	4.61	0.00	0.04	0.00	0.02	100.56	57.4	10.3	19.5	12.8	0.0	0.1
Grünbach	G9_gr7	Maiersdorf Fm	Con-San	Grünbach	39.28	22.10	22.08	7.77	0.47	8.74	0.04	0.07	0.00	0.03	100.56	46.4	1.0	29.1	23.3	0.1	0.1
Grünbach	G9_gr8	Maiersdorf Fm	Con-San	Grünbach	38.28	23.80	21.72	3.57	1.13	11.71	0.13	0.00	0.01	0.00	100.35	51.4	2.5	13.8	32.0	0.4	0.0
Grünbach	G9_gr9	Maiersdorf Fm	Con-San	Grünbach	38.62	23.33	21.31	4.72	0.72	11.00	0.14	0.00	0.00	0.00	99.84	50.1	1.6	18.1	29.9	0.4	0.0
Grünbach	G9_gr10	Maiersdorf Fm	Con-San	Grünbach	38.18	24.23	21.42	3.38	1.50	10.88	0.16	0.04	0.03	0.01	99.83	53.0	3.3	13.2	29.9	0.5	0.1
Grünbach	G9_gr11	Maiersdorf Fm	Con-San	Grünbach	38.80	22.03	21.72	6.07	1.07	10.43	0.10	0.06	0.02	0.01	100.31	46.6	2.3	22.9	27.9	0.3	0.1
Grünbach	G9_gr12	Maiersdorf Fm	Con-San	Grünbach	38.53	22.66	21.74	5.10	0.73	11.46	0.14	0.00	0.02	0.02	100.41	48.0	1.6	19.3	30.7	0.4	0.0

Gosau	Sample	Formation	Age	Location	SiO_2 [wt.%]	FeO [wt.%]	Al_2O_3 [wt.%]	MgO [wt.%]	MnO [wt.%]	CaO [wt.%]	TiO_2 [wt.%]	Cr_2O_3 [wt.%]	Na_2O [wt.%]	NiO [wt.%]	Total [wt.%]	Alm [wt.%]	Sps [wt.%]	Prp [wt.%]	Grs [wt.%]	And [wt.%]	Uva [wt.%]
Grünbach	G9_gr13	Maiersdorf Fm	Con-San	Grünbach	38.79	22.82	21.62	7.05	0.55	8.89	0.12	0.07	0.03	0.01	99.95	48.2	1.2	26.6	23.6	0.3	0.1
Grünbach	G9_gr14	Maiersdorf Fm	Con-San	Grünbach	37.04	31.67	21.00	2.60	5.01	2.13	0.01	0.07	0.00	0.02	99.55	71.8	11.5	10.5	6.0	0.0	0.1
Grünbach	G9_gr15	Maiersdorf Fm	Con-San	Grünbach	38.44	23.14	21.64	5.34	0.82	10.59	0.11	0.03	0.00	0.01	100.12	49.2	1.8	20.2	28.5	0.3	0.1
Grünbach	G22_gr1	Grünbach Fm	Campanian	Grünbach	38.56	23.57	21.60	5.00	0.91	10.20	0.19	0.11	0.04	0.03	100.20	50.7	2.0	19.2	27.3	0.6	0.2
Grünbach	G22_gr2	Grünbach Fm	Campanian	Grünbach	37.99	1.45	21.10	0.02	0.14	37.30	1.50	0.06	0.00	0.00	99.57	2.9	0.3	0.1	92.5	4.1	0.1
Grünbach	G22_gr4	Grünbach Fm	Campanian	Grünbach	38.46	23.56	21.47	5.24	1.70	9.64	0.05	0.00	0.00	0.02	100.13	50.2	3.7	19.9	26.2	0.1	0.0
Grünbach	G22_gr5	Grünbach Fm	Campanian	Grünbach	38.90	22.14	22.03	6.13	0.88	10.09	0.12	0.06	0.04	0.03	100.42	47.2	1.9	23.3	27.1	0.3	0.1
Grünbach	G22_gr6	Grünbach Fm	Campanian	Grünbach	38.44	23.39	21.86	5.06	1.01	10.32	0.12	0.08	0.03	0.00	100.30	50.1	2.2	19.3	27.8	0.3	0.2
Grünbach	G22_gr7	Grünbach Fm	Campanian	Grünbach	38.22	22.93	21.53	3.95	2.47	11.19	0.11	0.04	0.02	0.02	100.48	49.0	5.4	15.0	30.2	0.3	0.1
Grünbach	G22_gr8	Grünbach Fm	Campanian	Grünbach	39.13	20.80	22.22	7.54	0.09	10.28	0.08	0.06	0.00	0.00	100.21	43.8	0.2	28.3	27.4	0.2	0.1
Grünbach	G22_gr9	Grünbach Fm	Campanian	Grünbach	37.67	30.77	21.55	5.21	2.90	2.14	0.10	0.05	0.00	0.01	100.38	67.3	6.4	20.3	5.6	0.3	0.1
Grünbach	G22_gr10	Grünbach Fm	Campanian	Grünbach	37.73	30.90	21.53	5.31	2.78	1.71	0.04	0.01	0.00	0.00	100.01	68.1	6.2	20.9	4.7	0.1	0.0
Grünbach	G22_gr11	Grünbach Fm	Campanian	Grünbach	38.94	22.93	21.82	5.77	0.35	10.53	0.08	0.01	0.01	0.00	100.44	48.7	0.8	21.9	28.4	0.2	0.0
Grünbach	G22_gr12	Grünbach Fm	Campanian	Grünbach	38.67	23.86	21.76	6.41	1.04	8.02	0.12	0.06	0.01	0.00	99.95	51.2	2.3	24.5	21.6	0.4	0.1
Grünbach	G22_gr13	Grünbach Fm	Campanian	Grünbach	36.74	27.07	20.88	1.57	12.70	1.21	0.10	0.02	0.02	0.03	100.32	61.2	29.0	6.3	3.2	0.3	0.0
Grünbach	G22_gr14	Grünbach Fm	Campanian	Grünbach	37.16	33.96	21.28	3.54	2.31	1.53	0.05	0.12	0.02	0.01	99.98	76.2	5.2	14.2	4.0	0.1	0.3
Grünbach	G22_gr15	Grünbach Fm	Campanian	Grünbach	38.48	23.06	21.66	5.31	0.57	11.19	0.07	0.06	0.01	0.00	100.40	48.6	1.2	20.0	29.9	0.2	0.1
Grünbach	G22_gr16	Grünbach Fm	Campanian	Grünbach	38.65	22.68	21.72	6.05	0.62	10.18	0.11	0.07	0.01	0.01	100.10	48.1	1.3	22.9	27.2	0.3	0.1
Grünbach	M81_gr1	Grünbach Fm	Campanian	Maiersdorf	38.24	23.15	21.68	4.37	1.96	10.76	0.19	0.04	0.03	0.04	100.46	49.6	4.3	16.7	28.9	0.5	0.1
Grünbach	M81_gr2	Grünbach Fm	Campanian	Maiersdorf	37.49	32.98	21.28	4.74	2.27	1.47	0.04	0.02	0.00	0.00	100.29	72.3	5.0	18.5	4.0	0.1	0.0
Grünbach	M81_gr3	Grünbach Fm	Campanian	Maiersdorf	36.99	32.07	21.08	2.88	5.12	1.29	0.01	0.00	0.00	0.02	99.45	72.8	11.8	11.6	3.7	0.0	0.0
Grünbach	G10_grt1	Piesting Fm	Campanian	Grünbach	36.59	21.34	21.17	0.65	14.97	5.24	0.11	0.00	0.04	0.00	100.09	48.1	34.2	2.6	14.8	0.3	0.0
Grünbach	G14_gr1	Zweiersdorf Fm	Paleocene	Grünbach	37.14	24.93	20.99	1.93	12.42	3.15	0.08	0.01	0.02	0.00	100.66	55.4	28.0	7.7	8.7	0.2	0.0
Grünbach	G14_gr2	Zweiersdorf Fm	Paleocene	Grünbach	37.76	33.34	21.68	5.15	1.25	1.31	0.03	0.01	0.00	0.02	100.53	73.4	2.8	20.2	3.6	0.1	0.0
Grünbach	G14_gr3	Zweiersdorf Fm	Paleocene	Grünbach	38.02	27.02	21.86	2.85	0.46	10.34	0.08	0.01	0.03	0.00	100.67	59.0	1.0	11.1	28.7	0.2	0.0
Grünbach	G14_gr4	Zweiersdorf Fm	Paleocene	Grünbach	37.03	26.23	20.94	1.03	8.69	6.39	0.21	0.02	0.01	0.01	100.56	58.2	19.5	4.1	17.5	0.6	0.0
Grünbach	G14_gr5	Zweiersdorf Fm	Paleocene	Grünbach	37.96	28.57	21.10	2.01	3.64	7.05	0.12	0.03	0.06	0.02	100.56	63.7	8.2	8.0	19.7	0.3	0.1
Grünbach	G14_gr6	Zweiersdorf Fm	Paleocene	Grünbach	37.77	32.27	21.31	2.65	0.10	6.27	0.06	0.01	0.03	0.00	100.47	71.5	0.2	10.5	17.6	0.2	0.0
Grünbach	G14_gr7	Zweiersdorf Fm	Paleocene	Grünbach	37.26	29.07	20.97	1.19	4.38	7.17	0.13	0.02	0.02	0.00	100.21	64.9	9.9	4.7	20.1	0.4	0.0
Grünbach	G14_gr8	Zweiersdorf Fm	Paleocene	Grünbach	37.73	26.88	21.49	2.36	2.31	9.30	0.17	0.01	0.02	0.00	100.27	59.3	5.2	9.3	25.8	0.5	0.0
Grünbach	G14_gr9	Zweiersdorf Fm	Paleocene	Grünbach	37.60	33.78	21.18	3.82	1.81	1.84	0.23	0.02	0.01	0.01	100.28	75.4	4.1	15.2	4.5	0.7	0.0
Grünbach	G14_gr10	Zweiersdorf Fm	Paleocene	Grünbach	37.11	35.49	21.18	2.36	1.89	2.46	0.06	0.03	0.01	0.01	100.60	79.3	4.3	9.4	6.8	0.2	0.1
Grünbach	G14_gr11	Zweiersdorf Fm	Paleocene	Grünbach	38.97	24.94	21.98	7.93	1.24	5.19	0.10	0.01	0.00	0.00	100.36	53.1	2.7	30.1	13.9	0.3	0.0
Grünbach	G14_gr12	Zweiersdorf Fm	Paleocene	Grünbach	38.37	29.60	22.03	7.45	1.32	1.50	0.04	0.02	0.03	0.01	100.35	64.2	2.9	28.8	4.0	0.1	0.0
Grünbach	G14_gr13	Zweiersdorf Fm	Paleocene	Grünbach	37.69	29.91	21.27	2.32	1.96	7.07	0.13	0.04	0.03	0.00	100.40	66.4	4.4	9.2	19.6	0.4	0.1
Grünbach	G14_gr14	Zweiersdorf Fm	Paleocene	Grünbach	37.35	34.57	21.03	1.36	0.09	5.60	0.08	0.00	0.05	0.00	100.14	78.1	0.2	5.5	15.9	0.3	0.0
Grünbach	G14_gr15	Zweiersdorf Fm	Paleocene	Grünbach	37.48	28.85	21.15	1.98	3.31	7.41	0.08	0.00	0.05	0.01	100.30	63.8	7.4	7.8	20.7	0.2	0.0
Grünbach	G14_gr16	Zweiersdorf Fm	Paleocene	Grünbach	37.42	29.74	21.53	2.45	1.44	7.45	0.07	0.00	0.02	0.01	100.14	65.9	3.2	9.7	20.9	0.2	0.0
Grünbach	G14_gr17	Zweiersdorf Fm	Paleocene	Grünbach	37.81	31.21	21.38	3.47	0.42	5.93	0.07	0.04	0.03	0.01	100.35	68.7	0.9	13.6	16.4	0.2	0.1
Grünbach	G14_gr18	Zweiersdorf Fm	Paleocene	Grünbach	37.73	30.87	21.40	2.89	0.53	6.73	0.11	0.02	0.03	0.01	100.32	68.3	1.2	11.4	18.7	0.3	0.0
Grünbach	G14_gr19	Zweiersdorf Fm	Paleocene	Grünbach	37.15	27.45	21.39	1.29	5.88	7.38	0.16	0.01	0.01	0.00	100.72	60.8	13.2	5.1	20.4	0.5	0.0
Grünbach	G14_gr20	Zweiersdorf Fm	Paleocene	Grünbach	37.33	32.87	21.50	3.76	0.49	4.07	0.08	0.02	0.05	0.01	100.17	72.6	1.1	14.8	11.2	0.2	0.0
Grünbach	G14_gr21	Zweiersdorf Fm	Paleocene	Grünbach	37.37	30.74	21.54	2.27	1.39	7.20	0.09	0.01	0.03	0.01	100.65	67.7	3.1	8.9	20.0	0.3	0.0
Grünbach	G14_gr23	Zweiersdorf Fm	Paleocene	Grünbach	37.55	31.16	21.61	2.60	0.91	6.89	0.07	0.02	0.02	0.01	100.83	68.4	2.0	10.2	19.1	0.2	0.0
Grünbach	G14_gr24	Zweiersdorf Fm	Paleocene	Grünbach	37.69	30.75	21.75	3.06	0.35	7.19	0.06	0.02	0.02	0.00	100.89	67.2	0.8	11.9	19.9	0.2	0.0
Grünbach	G14_gr25	Zweiersdorf Fm	Paleocene	Grünbach	37.82	30.58	21.61	3.11	0.13	7.16	0.07	0.02	0.03	0.01	100.52	67.3	0.3	12.2	20.0	0.2	0.0
Grünbach	G14_gr26	Zweiersdorf Fm	Paleocene	Grünbach	37.85	27.93	21.69	2.65	2.87	7.85	0.18	0.01	0.02	0.00	101.06	61.2	6.4	10.4	21.5	0.5	0.0

Gosau	Sample	Formation	Age	Location	SiO_2 [wt.%]	FeO [wt.%]	Al_2O_3 [wt.%]	MgO [wt.%]	MnO [wt.%]	CaO [wt.%]	TiO_2 [wt.%]	Cr_2O_3 [wt.%]	Na_2O [wt.%]	NiO [wt.%]	Total [wt.%]	Alm [wt.%]	Sps [wt.%]	Prp [wt.%]	Grs [wt.%]	And [wt.%]	Uva [wt.%]
Grünbach	G14_gr27	Zweiersdorf Fm	Paleocene	Grünbach	37.36	32.52	21.46	2.88	1.67	4.75	0.04	0.02	0.02	0.01	100.73	71.6	3.7	11.3	13.3	0.1	0.0
Grünbach	G14_gr28	Zweiersdorf Fm	Paleocene	Grünbach	37.40	30.88	21.65	2.40	0.82	7.34	0.09	0.03	0.03	0.00	100.62	68.1	1.8	9.4	20.4	0.3	0.1
Grünbach	G14_gr29	Zweiersdorf Fm	Paleocene	Grünbach	37.53	27.99	21.48	2.14	2.47	8.53	0.09	0.02	0.02	0.00	100.27	61.9	5.5	8.4	23.8	0.3	0.0
Grünbach	G14_gr30	Zweiersdorf Fm	Paleocene	Grünbach	37.32	26.71	21.17	1.24	3.74	10.28	0.11	0.01	0.02	0.00	100.60	58.2	8.2	4.8	28.4	0.3	0.0
Grünbach	G14_gr31	Zweiersdorf Fm	Paleocene	Grünbach	38.46	28.36	21.71	6.73	1.21	4.25	0.04	0.02	0.00	0.00	100.77	60.3	2.6	25.5	11.4	0.1	0.0
Grünbach	G14_gr32	Zweiersdorf Fm	Paleocene	Grünbach	38.08	29.19	21.61	3.68	0.76	7.35	0.06	0.00	0.01	0.03	100.76	63.6	1.7	14.3	20.3	0.2	0.0
Grünbach	G14_gr33	Zweiersdorf Fm	Paleocene	Grünbach	37.53	30.17	21.71	2.74	1.19	7.15	0.02	0.00	0.02	0.01	100.54	66.4	2.7	10.7	20.1	0.1	0.0
Grünbach	G14_gr34	Zweiersdorf Fm	Paleocene	Grünbach	37.83	27.22	21.76	2.72	2.27	8.83	0.04	0.02	0.02	0.01	100.71	59.6	5.0	10.6	24.6	0.1	0.0
Grünbach	G14_gr35	Zweiersdorf Fm	Paleocene	Grünbach	37.57	29.26	21.43	1.67	2.28	8.30	0.13	0.03	0.03	0.02	100.73	64.8	5.1	6.6	23.1	0.4	0.1
Grünbach	G14_gr36	Zweiersdorf Fm	Paleocene	Grünbach	37.47	31.60	21.31	1.87	0.98	7.19	0.14	0.04	0.02	0.03	100.64	70.0	2.2	7.4	19.9	0.4	0.1
Grünbach	G14_gr37	Zweiersdorf Fm	Paleocene	Grünbach	37.66	30.76	21.70	2.76	0.43	7.31	0.04	0.01	0.02	0.00	100.67	67.6	1.0	10.8	20.5	0.1	0.0
Grünbach	G14_gr38	Zweiersdorf Fm	Paleocene	Grünbach	37.31	25.44	21.24	1.16	3.71	10.67	0.31	0.02	0.04	0.00	99.90	56.6	8.4	4.6	29.5	0.9	0.0
Grünbach	G14_gr39	Zweiersdorf Fm	Paleocene	Grünbach	37.71	24.86	21.40	1.69	6.27	8.81	0.12	0.00	0.02	0.01	100.87	54.6	13.9	6.6	24.5	0.3	0.0
Grünbach	G14_gr40	Zweiersdorf Fm	Paleocene	Grünbach	37.70	31.81	21.59	3.54	1.12	4.96	0.05	0.02	0.03	0.00	100.82	69.7	2.5	13.8	13.8	0.1	0.0
Studienka	B6C_grt1	Košariská Fm	Campanian	Brezová	37.05	19.74	20.59	0.53	13.76	7.95	0.16	0.00	0.00	0.00	99.77	44.1	31.1	2.1	22.3	0.5	0.0
Studienka	B6C_grt2	Košariská Fm	Campanian	Brezová	36.78	27.40	20.88	0.82	10.93	3.33	0.17	0.00	0.03	0.00	100.34	62.0	25.0	3.3	9.1	0.5	0.0
Studienka	B6C_grt3	Košariská Fm	Campanian	Brezová	36.60	18.08	20.65	0.56	19.35	4.47	0.23	0.00	0.00	0.00	99.94	40.7	44.1	2.2	12.2	0.7	0.0
Studienka	B2B_grt1	Priepastné Fm	Paleocene	Brezová	36.20	25.83	20.92	0.99	9.68	4.86	0.16	0.00	0.05	0.00	98.69	59.2	22.5	4.0	13.8	0.5	0.0
Studienka	B2B_grt2	Priepastné Fm	Paleocene	Brezová	37.04	27.84	21.01	0.59	5.47	8.23	0.13	0.00	0.03	0.00	100.35	61.9	12.3	2.3	23.0	0.4	0.0
Studienka	B2B_grt3	Priepastné Fm	Paleocene	Brezová	37.52	30.72	21.53	3.01	0.65	6.65	0.08	0.00	0.08	0.00	100.23	67.9	1.5	11.9	18.6	0.3	0.0
Studienka	B2B_grt4	Priepastné Fm	Paleocene	Brezová	36.94	28.88	21.17	0.88	5.19	6.81	0.10	0.00	0.05	0.00	100.00	65.0	11.8	3.5	19.3	0.3	0.0
Studienka	B2B_grt5	Priepastné Fm	Paleocene	Brezová	36.69	32.32	21.16	1.14	4.78	3.90	0.04	0.00	0.01	0.00	100.04	73.1	10.9	4.6	11.2	0.1	0.0
Studienka	B2B_grt6	Priepastné Fm	Paleocene	Brezová	37.03	32.54	21.29	1.30	0.98	6.83	0.08	0.00	0.05	0.00	100.10	73.0	2.2	5.2	19.4	0.2	0.0
Studienka	B2B_grt7	Priepastné Fm	Paleocene	Brezová	36.77	28.60	20.99	1.27	7.69	4.37	0.13	0.00	0.00	0.00	99.82	64.6	17.6	5.1	12.3	0.4	0.0
Studienka	B2B_grt8	Priepastné Fm	Paleocene	Brezová	36.43	28.16	20.89	0.97	9.32	3.29	0.10	0.00	0.07	0.00	99.21	64.7	21.7	4.0	9.4	0.3	0.0
Studienka	B2B_grt9	Priepastné Fm	Paleocene	Brezová	36.52	32.93	20.91	1.24	5.89	2.30	0.08	0.00	0.00	0.00	99.88	74.8	13.5	5.0	6.4	0.3	0.0
Studienka	B2B_grt10	Priepastné Fm	Paleocene	Brezová	36.56	30.40	20.72	1.18	7.23	3.43	0.15	0.00	0.05	0.00	99.73	68.7	16.6	4.8	9.5	0.4	0.0
Studienka	B2B_grt11	Priepastné Fm	Paleocene	Brezová	37.51	28.48	21.53	3.86	5.85	3.27	0.05	0.00	0.09	0.00	100.64	62.6	13.0	15.1	9.1	0.2	0.0
Studienka	B2B_grt12	Priepastné Fm	Paleocene	Brezová	36.80	32.47	21.09	1.36	3.86	4.37	0.11	0.00	0.01	0.00	100.07	73.1	8.8	5.5	12.3	0.3	0.0
Studienka	B2B_grt13	Priepastné Fm	Paleocene	Brezová	36.70	33.65	21.07	1.42	3.25	3.70	0.10	0.00	0.03	0.00	99.91	76.1	7.4	5.7	10.4	0.3	0.0
Studienka	B2B_grt14	Priepastné Fm	Paleocene	Brezová	36.88	31.41	21.22	0.93	3.98	5.79	0.09	0.00	0.04	0.00	100.34	70.6	9.1	3.7	16.4	0.3	0.0
Studienka	B2B_grt15	Priepastné Fm	Paleocene	Brezová	37.86	30.25	21.82	6.51	1.77	1.65	0.05	0.00	0.03	0.00	99.94	66.1	3.9	25.4	4.5	0.2	0.0
Studienka	B1_grt1	not defined	Paleocene	Brezová	36.58	29.06	21.14	2.09	9.47	1.39	0.09	0.00	0.07	0.00	99.89	65.8	21.7	8.4	3.7	0.3	0.0
Studienka	B1_grt2	not defined	Paleocene	Brezová	36.78	29.40	21.18	2.50	8.12	1.67	0.06	0.00	0.02	0.00	99.72	66.5	18.6	10.1	4.6	0.2	0.0
Studienka	B1_grt3	not defined	Paleocene	Brezová	36.00	34.13	20.71	0.27	7.63	0.85	0.09	0.00	0.01	0.00	99.67	78.6	17.8	1.1	2.2	0.3	0.0
Studienka	B1_grt4	not defined	Paleocene	Brezová	37.40	30.91	21.50	1.96	0.59	7.90	0.09	0.00	0.03	0.00	100.37	68.5	1.3	7.7	22.2	0.3	0.0
Studienka	B1_grt5	not defined	Paleocene	Brezová	37.68	29.28	21.66	4.04	3.40	3.66	0.22	0.00	0.02	0.00	99.94	65.6	7.7	16.1	9.9	0.7	0.0
Studienka	B1_grt6	not defined	Paleocene	Brezová	37.00	32.25	21.59	3.17	3.70	2.33	0.07	0.00	0.01	0.00	100.13	72.2	8.4	12.7	6.5	0.2	0.0
Studienka	B1_grt7	not defined	Paleocene	Brezová	36.81	34.32	21.34	2.69	0.95	3.59	0.05	0.00	0.05	0.00	99.78	76.8	2.1	10.7	10.1	0.1	0.0
Studienka	B1_grt8	not defined	Paleocene	Brezová	37.95	30.85	22.04	5.85	1.68	1.99	0.06	0.00	0.04	0.00	100.46	67.8	3.7	22.9	5.4	0.2	0.0
Studienka	B1_grt9	not defined	Paleocene	Brezová	36.71	37.46	21.07	2.39	1.60	0.43	0.05	0.00	0.05	0.00	99.77	85.3	3.7	9.7	1.1	0.2	0.0
Studienka	B1_grt10	not defined	Paleocene	Brezová	37.43	32.12	21.45	4.62	1.87	2.03	0.07	0.00	0.06	0.00	99.65	71.6	4.2	18.4	5.6	0.2	0.0
Studienka	B1_grt11	not defined	Paleocene	Brezová	36.73	33.78	21.02	1.25	2.51	4.57	0.06	0.00	0.08	0.00	99.99	76.1	5.7	5.0	13.0	0.2	0.0
Studienka	B1_grt12	not defined	Paleocene	Brezová	37.45	31.87	21.72	5.24	1.96	1.83	0.02	0.00	0.00	0.00	100.09	70.0	4.4	20.5	5.1	0.1	0.0
Studienka	B1_grt13	not defined	Paleocene	Brezová	37.15	31.34	21.19	1.21	0.93	7.92	0.20	0.00	0.03	0.00	99.95	70.3	2.1	4.8	22.1	0.6	0.0
Studienka	B1_grt14	not defined	Paleocene	Brezová	37.13	30.15	21.37	2.64	3.89	4.26	0.04	0.00	0.06	0.00	99.55	68.1	8.9	10.6	12.2	0.1	0.0
Studienka	B1_grt15	not defined	Paleocene	Brezová	36.95	32.43	21.59	3.21	4.42	1.18	0.08	0.00	0.00	0.00	99.86	73.5	10.1	13.0	3.2	0.2	0.0

Gosau	Sample	Formation	Age	Location	SiO_2 [wt.%]	FeO [wt.%]	Al_2O_3 [wt.%]	MgO [wt.%]	MnO [wt.%]	CaO [wt.%]	TiO_2 [wt.%]	Cr_2O_3 [wt.%]	Na_2O [wt.%]	NiO [wt.%]	Total [wt.%]	Alm [wt.%]	Sps [wt.%]	Prp [wt.%]	Grs [wt.%]	And [wt.%]	Uva [wt.%]
Studienka	B1_grt16	not defined	Paleocene	Brezová	37.46	31.30	21.40	3.44	3.04	3.51	0.03	0.00	0.03	0.00	100.20	69.6	6.8	13.6	9.9	0.1	0.0
Studienka	B1_grt17	not defined	Paleocene	Brezová	36.86	33.58	21.36	1.87	1.99	4.48	0.03	0.00	0.01	0.00	100.17	75.2	4.5	7.5	12.7	0.1	0.0
Studienka	Z1_gr2	not defined	Paleocene	Závod 68	37.35	29.31	21.42	3.36	2.79	5.81	0.04	0.01	0.00	0.04	100.13	64.3	6.2	13.1	16.2	0.1	0.0
Studienka	Z1_gr3	not defined	Paleocene	Závod 68	37.47	31.46	21.32	1.74	0.40	7.82	0.10	0.03	0.00	0.00	100.34	69.9	0.9	6.9	21.9	0.3	0.1
Studienka	Z1_gr4	not defined	Paleocene	Závod 68	37.20	30.36	21.31	1.07	1.18	9.00	0.06	0.02	0.00	0.02	100.22	67.5	2.7	4.2	25.4	0.2	0.0
Studienka	Z1_gr6	not defined	Paleocene	Závod 68	37.05	29.03	21.16	0.86	5.52	6.94	0.14	0.03	0.02	0.02	100.76	64.4	12.4	3.4	19.3	0.4	0.1
Studienka	Z1_gr7	not defined	Paleocene	Závod 68	37.82	31.14	21.66	5.58	1.36	2.17	0.03	0.05	0.00	0.04	99.86	68.8	3.1	22.0	5.9	0.1	0.1
Studienka	Z1_gr8	not defined	Paleocene	Závod 68	37.49	30.75	21.23	1.53	1.01	8.28	0.12	0.02	0.01	0.00	100.44	68.2	2.3	6.0	23.1	0.4	0.1
Studienka	Z1_gr9	not defined	Paleocene	Závod 68	37.06	34.22	21.19	1.26	0.33	6.12	0.09	0.01	0.00	0.03	100.29	76.7	0.7	5.0	17.3	0.3	0.0
Studienka	Z1_gr10	not defined	Paleocene	Závod 68	37.15	23.36	21.08	0.67	8.29	9.37	0.15	0.00	0.02	0.00	100.09	52.0	18.7	2.7	26.3	0.4	0.0
Studienka	Z1_gr11	not defined	Paleocene	Závod 68	37.22	26.15	21.16	1.77	4.94	8.25	0.03	0.01	0.00	0.00	99.52	58.3	11.1	7.0	23.5	0.1	0.0
Studienka	Z1_gr13	not defined	Paleocene	Závod 68	36.72	29.41	21.02	1.21	6.85	4.80	0.08	0.02	0.03	0.00	100.13	65.9	15.5	4.8	13.5	0.2	0.0
Studienka	Z1_gr14	not defined	Paleocene	Závod 68	37.39	28.23	21.45	2.13	2.95	7.82	0.03	0.02	0.00	0.03	100.04	62.7	6.6	8.4	22.1	0.1	0.0
Studienka	Z1_gr15	not defined	Paleocene	Závod 68	37.11	31.56	21.13	2.63	4.40	3.04	0.03	0.03	0.02	0.00	99.95	70.8	10.0	10.5	8.6	0.1	0.1
Studienka	Z1_gr17	not defined	Paleocene	Závod 68	37.96	29.32	21.55	5.32	1.23	4.35	0.03	0.01	0.01	0.02	99.78	64.3	2.7	20.8	12.1	0.1	0.0
Studienka	Z1_gr18	not defined	Paleocene	Závod 68	37.76	31.44	21.69	5.60	1.42	2.24	0.02	0.06	0.00	0.01	100.25	68.8	3.1	21.8	6.1	0.1	0.1
Studienka	Z1_gr19	not defined	Paleocene	Závod 68	37.34	30.43	21.12	1.52	0.96	8.29	0.14	0.00	0.04	0.03	99.87	68.0	2.2	6.1	23.3	0.4	0.0
Studienka	Z1_gr20	not defined	Paleocene	Závod 68	37.28	32.02	21.11	2.04	1.48	5.56	0.06	0.00	0.06	0.00	99.60	72.3	3.4	8.2	15.9	0.2	0.0
Studienka	Z1_gr21	not defined	Paleocene	Závod 68	37.24	32.66	21.21	3.44	3.04	2.22	0.04	0.00	0.01	0.00	99.86	73.0	6.9	13.7	6.3	0.1	0.0
Studienka	Z1_gr22	not defined	Paleocene	Závod 68	36.99	31.91	21.12	1.85	1.36	5.87	0.09	0.01	0.00	0.00	99.21	72.3	3.1	7.5	16.8	0.3	0.0
Studienka	Z1_gr23	not defined	Paleocene	Závod 68	36.82	26.81	21.10	0.90	7.37	6.99	0.06	0.01	0.02	0.03	100.10	59.8	16.6	3.6	19.8	0.2	0.0
Studienka	Z1_gr24	not defined	Paleocene	Závod 68	37.24	26.59	21.08	0.78	4.75	9.40	0.16	0.04	0.00	0.00	100.03	59.3	10.7	3.1	26.3	0.5	0.1
Studienka	B3B_grt1	Jablonka Fm	Eocene	Brezová	36.93	27.02	20.94	0.84	7.41	6.29	0.09	0.00	0.00	0.00	99.52	61.3	17.0	3.4	18.0	0.3	0.0
Studienka	B3B_grt2	Jablonka Fm	Eocene	Brezová	36.97	25.68	20.83	1.06	8.99	6.17	0.14	0.00	0.00	0.00	99.83	57.6	20.4	4.2	17.3	0.4	0.0
Studienka	B3B_grt3	Jablonka Fm	Eocene	Brezová	36.87	30.12	21.08	0.78	2.63	7.78	0.10	0.00	0.03	0.00	99.39	68.2	6.0	3.2	22.3	0.3	0.0
Studienka	B3B_grt4	Jablonka Fm	Eocene	Brezová	37.89	11.04	21.40	0.48	8.56	20.67	0.07	0.00	0.01	0.00	100.12	23.5	18.4	1.8	56.1	0.2	0.0
Studienka	B3B_grt5	Jablonka Fm	Eocene	Brezová	37.37	30.54	21.62	3.93	2.67	3.69	0.00	0.00	0.00	0.00	99.82	67.9	6.0	15.6	10.5	0.0	0.0
Studienka	B3B_grt6	Jablonka Fm	Eocene	Brezová	37.95	31.33	21.91	6.14	1.11	1.26	0.00	0.00	0.03	0.00	99.72	69.6	2.5	24.3	3.6	0.0	0.0

Gosau	Sample	Formation	Age	Location	SiO_2 [%]	FeO [%]	Al_2O_3 [%]	MgO [%]	MnO [%]	CaO [%]	TiO_2 [%]	Cr_2O_3 [%]	NiO [%]	ZnO [%]	Total [%]	Mg# [%]	Cr# [%]	Fe^{2+} [%]
Gießhübl	MTW4_sp1	not defined	Con-San	Mitterwäldchen	0.00	17.61	15.99	10.14	0.21	0.00	0.08	54.49	0.03	0.20	98.73	0.51	0.81	3.83
Gießhübl	MTW4_sp2	not defined	Con-San	Mitterwäldchen	0.02	15.92	12.40	12.21	0.22	0.00	0.13	58.49	0.06	0.10	99.53	0.58	0.86	3.45
Gießhübl	MTW4_sp3	not defined	Con-San	Mitterwäldchen	0.00	17.98	19.10	12.05	0.18	0.00	0.04	50.58	0.08	0.07	100.09	0.54	0.77	3.79
Gießhübl	MTW4_sp4	not defined	Con-San	Mitterwäldchen	0.00	15.43	26.01	12.45	0.14	0.00	0.08	43.85	0.13	0.14	98.22	0.59	0.68	3.18
Gießhübl	MTW4_sp5	not defined	Con-San	Mitterwäldchen	0.12	17.64	23.62	10.18	0.24	0.00	0.10	45.27	0.10	0.09	97.35	0.51	0.71	3.74
Gießhübl	MTW4_sp6	not defined	Con-San	Mitterwäldchen	0.00	14.35	26.96	9.25	0.12	0.00	0.06	45.35	0.14	0.09	96.31	0.54	0.68	3.01
Gießhübl	MTW4_sp7	not defined	Con-San	Mitterwäldchen	0.00	17.39	28.55	12.65	0.17	0.02	0.16	40.65	0.09	0.19	99.86	0.57	0.65	3.51
Gießhübl	MTW4_sp8	not defined	Con-San	Mitterwäldchen	0.02	16.39	24.38	13.41	0.18	0.01	0.06	44.70	0.12	0.11	99.38	0.59	0.70	3.37
Gießhübl	MTW4_sp9	not defined	Con-San	Mitterwäldchen	0.00	20.16	20.83	12.07	0.24	0.00	0.07	45.36	0.13	0.12	98.98	0.52	0.74	4.28
Gießhübl	MTW4_sp1	not defined	Con-San	Mitterwäldchen	0.00	15.63	30.41	11.47	0.16	0.01	0.06	40.08	0.10	0.20	98.11	0.57	0.63	3.17
Gießhübl	MTW4_sp1	not defined	Con-San	Mitterwäldchen	0.01	12.91	28.70	12.93	0.12	0.00	0.02	43.11	0.07	0.15	98.01	0.64	0.66	2.61
Gießhübl	MTW4_sp1	not defined	Con-San	Mitterwäldchen	0.00	16.84	26.68	13.04	0.16	0.00	0.07	42.36	0.08	0.19	99.42	0.58	0.67	3.43
Gießhübl	L16_sp3	not defined	Con-San	Lilienfeld	0.03	12.35	42.07	17.76	0.12	0.02	0.07	26.58	0.27	0.12	99.38	0.72	0.45	2.31
Gießhübl	L16_sp4	not defined	Con-San	Lilienfeld	0.02	12.59	54.30	18.55	0.08	0.02	0.04	13.30	0.34	0.20	99.43	0.72	0.24	2.24
Gießhübl	L16_sp5	not defined	Con-San	Lilienfeld	0.01	16.94	23.36	12.68	0.17	0.01	0.07	44.90	0.11	0.11	98.36	0.57	0.71	3.54
Gießhübl	L16_sp6	not defined	Con-San	Lilienfeld	0.02	15.69	32.01	14.52	0.15	0.00	0.09	36.74	0.11	0.14	99.47	0.62	0.59	3.10
Gießhübl	L16_sp7	not defined	Con-San	Lilienfeld	0.01	16.79	29.69	13.98	0.15	0.01	0.05	38.04	0.12	0.17	99.01	0.60	0.62	3.38
Gießhübl	L16_sp8	not defined	Con-San	Lilienfeld	0.00	16.48	27.33	13.67	0.13	0.02	0.11	41.42	0.12	0.14	99.40	0.60	0.66	3.34
Gießhübl	L16_sp9	not defined	Con-San	Lilienfeld	0.00	17.01	28.31	13.84	0.17	0.00	0.05	39.73	0.12	0.20	99.44	0.59	0.64	3.44
Gießhübl	L16_sp10	not defined	Con-San	Lilienfeld	0.00	18.72	22.50	11.96	0.17	0.00	0.04	45.81	0.13	0.17	99.51	0.53	0.72	3.91
Gießhübl	L16_sp11	not defined	Con-San	Lilienfeld	0.04	15.95	26.34	13.88	0.15	0.01	0.09	42.52	0.08	0.03	99.08	0.61	0.67	3.25
Gießhübl	L16_sp12	not defined	Con-San	Lilienfeld	0.04	17.43	20.41	13.23	0.17	0.00	0.05	47.36	0.17	0.10	98.95	0.58	0.75	3.67
Gießhübl	L16_sp13	not defined	Con-San	Lilienfeld	0.01	12.59	32.90	16.04	0.16	0.00	0.09	37.08	0.20	0.08	99.15	0.69	0.59	2.46
Gießhübl	L16_sp14	not defined	Con-San	Lilienfeld	0.02	14.96	23.62	13.20	0.18	0.00	0.10	45.97	0.12	0.08	98.25	0.61	0.71	3.11
Gießhübl	L16_sp15	not defined	Con-San	Lilienfeld	0.02	18.95	14.33	10.19	0.29	0.00	0.08	54.17	0.06	0.22	98.30	0.49	0.83	4.18
Gießhübl	L16_sp16	not defined	Con-San	Lilienfeld	0.01	15.22	27.99	14.21	0.15	0.00	0.05	41.58	0.10	0.15	99.46	0.63	0.66	3.06
Gießhübl	L16_sp17	not defined	Con-San	Lilienfeld	0.03	19.40	23.32	11.51	0.18	0.00	0.05	44.08	0.10	0.22	98.88	0.51	0.71	4.07
Gießhübl	L16_sp18	not defined	Con-San	Lilienfeld	0.01	16.67	25.01	13.28	0.16	0.00	0.03	43.79	0.07	0.12	99.15	0.59	0.69	3.43
Gießhübl	L16_sp19	not defined	Con-San	Lilienfeld	0.00	15.13	35.01	15.70	0.17	0.01	0.09	32.72	0.15	0.12	99.09	0.65	0.54	2.95
Gießhübl	L16_sp20	not defined	Con-San	Lilienfeld	0.00	15.65	21.84	12.74	0.11	0.00	0.03	48.47	0.13	0.16	99.14	0.59	0.74	3.26
Gießhübl	L16_sp21	not defined	Con-San	Lilienfeld	0.02	15.68	26.83	14.20	0.19	0.01	0.06	42.34	0.09	0.12	99.52	0.62	0.67	3.17
Gießhübl	L16_sp22	not defined	Con-San	Lilienfeld	0.01	14.64	29.47	14.80	0.11	0.00	0.06	39.70	0.12	0.07	98.98	0.64	0.63	2.93
Gießhübl	L16_sp23	not defined	Con-San	Lilienfeld	0.02	13.88	28.92	15.47	0.13	0.00	0.14	40.68	0.16	0.09	99.49	0.67	0.64	2.76
Gießhübl	L16_sp24	not defined	Con-San	Lilienfeld	0.05	15.19	24.59	14.66	0.10	0.00	0.28	43.75	0.20	0.12	98.94	0.63	0.69	3.11
Gießhübl	L16_sp25	not defined	Con-San	Lilienfeld	0.03	15.30	28.80	14.02	0.16	0.01	0.02	41.01	0.10	0.12	99.57	0.62	0.65	3.06
Gießhübl	L221_sp1	not defined	Con-San	Lilienfeld	0.02	14.75	26.85	12.83	0.13	0.00	0.04	43.41	0.11	0.11	98.23	0.61	0.67	3.02
Gießhübl	L221_sp2	not defined	Con-San	Lilienfeld	0.00	16.63	26.40	13.53	0.14	0.01	0.04	42.42	0.08	0.11	99.35	0.59	0.67	3.39
Gießhübl	L221_sp3	not defined	Con-San	Lilienfeld	0.01	15.33	26.61	14.13	0.15	0.00	0.02	42.48	0.12	0.14	99.00	0.62	0.67	3.12
Gießhübl	L221_sp4	not defined	Con-San	Lilienfeld	0.00	15.10	26.01	13.88	0.13	0.01	0.02	43.45	0.10	0.18	98.89	0.62	0.68	3.08
Gießhübl	L221_sp5	not defined	Con-San	Lilienfeld	0.00	18.44	21.94	11.90	0.21	0.00	0.02	47.07	0.03	0.21	99.80	0.54	0.73	3.85
Gießhübl	L221_sp6	not defined	Con-San	Lilienfeld	0.01	14.17	26.83	14.05	0.19	0.01	0.13	43.56	0.07	0.11	99.14	0.64	0.68	2.86
Gießhübl	L221_sp7	not defined	Con-San	Lilienfeld	0.00	14.19	25.69	14.20	0.13	0.01	0.03	45.19	0.09	0.23	99.75	0.64	0.69	2.87
Gießhübl	L221_sp8	not defined	Con-San	Lilienfeld	0.03	15.22	25.08	14.02	0.12	0.00	0.05	44.29	0.15	0.08	99.02	0.62	0.69	3.11
Gießhübl	L221_sp9	not defined	Con-San	Lilienfeld	0.00	18.47	18.42	11.63	0.16	0.01	0.04	50.38	0.08	0.15	99.32	0.53	0.78	3.94
Gießhübl	L221_sp1	not defined	Con-San	Lilienfeld	0.01	19.00	24.85	11.54	0.20	0.00	0.09	42.79	0.14	0.12	98.75	0.52	0.69	3.96
Gießhübl	L221_sp1	not defined	Con-San	Lilienfeld	0.46	15.43	20.09	11.75	0.19	0.20	0.05	50.03	0.08	0.10	98.37	0.58	0.76	3.26
Gießhübl	L221_sp1	not defined	Con-San	Lilienfeld	0.05	14.64	21.13	12.70	0.14	0.01	0.11	49.88	0.05	0.15	98.86	0.61	0.75	3.06

Gosau	Sample	Formation	Age	Location	SiO_2 [%]	FeO [%]	Al_2O_3 [%]	MgO [%]	MnO [%]	CaO [%]	TiO_2 [%]	Cr_2O_3 [%]	NiO [%]	ZnO [%]	Total [%]	Mg# [%]	Cr# [%]	Fe^{2+} [%]
Gießhübl	L221_sp1	not defined	Con-San	Lilienfeld	0.00	16.85	21.69	11.09	0.17	0.01	0.16	47.96	0.06	0.16	98.13	0.54	0.74	3.57
Gießhübl	L221_sp1	not defined	Con-San	Lilienfeld	0.00	14.21	33.81	15.21	0.15	0.00	0.09	35.29	0.11	0.13	99.00	0.66	0.57	2.78
Gießhübl	L221_sp1	not defined	Con-San	Lilienfeld	0.00	23.07	16.81	7.50	0.28	0.02	0.16	49.93	0.03	0.20	98.00	0.37	0.79	5.14
Gießhübl	L221_sp1	not defined	Con-San	Lilienfeld	0.00	22.09	11.70	8.46	0.29	0.00	0.21	55.99	0.08	0.28	99.09	0.41	0.86	4.97
Gießhübl	L221_sp1	not defined	Con-San	Lilienfeld	0.01	19.57	16.48	10.42	0.22	0.00	0.04	52.47	0.08	0.20	99.47	0.49	0.80	4.23
Gießhübl	L221_sp1	not defined	Con-San	Lilienfeld	0.00	13.57	20.56	13.98	0.15	0.00	0.01	51.11	0.07	0.08	99.54	0.65	0.76	2.81
Gießhübl	L221_sp1	not defined	Con-San	Lilienfeld	0.01	16.14	21.62	12.29	0.15	0.01	0.43	48.06	0.08	0.16	98.95	0.58	0.74	3.37
Gießhübl	L221_sp2	not defined	Con-San	Lilienfeld	0.00	15.54	24.74	11.55	0.15	0.00	0.06	45.59	0.10	0.18	97.91	0.57	0.70	3.24
Gießhübl	TA8_sp1	Nierental Fm	Campanian	Tasshof	0.02	16.06	25.67	13.14	0.18	0.00	0.02	44.58	0.08	0.14	99.89	0.59	0.69	3.26
Gießhübl	TA8_sp2	Nierental Fm	Campanian	Tasshof	0.00	20.27	20.00	12.00	0.17	0.01	0.23	46.49	0.06	0.13	99.36	0.51	0.75	4.31
Gießhübl	TA8_sp3	Nierental Fm	Campanian	Tasshof	0.00	17.37	21.83	12.76	0.19	0.02	0.07	47.08	0.06	0.07	99.45	0.57	0.73	3.62
Gießhübl	TA8_sp4	Nierental Fm	Campanian	Tasshof	0.02	19.50	18.70	10.96	0.22	0.03	0.03	50.23	0.08	0.19	99.96	0.50	0.77	4.15
Gießhübl	TA8_sp5	Nierental Fm	Campanian	Tasshof	0.01	18.01	21.94	12.41	0.18	0.01	0.05	46.75	0.08	0.13	99.57	0.55	0.73	3.76
Gießhübl	TA8_sp6	Nierental Fm	Campanian	Tasshof	0.00	14.78	26.68	14.02	0.18	0.02	0.06	43.73	0.07	0.18	99.72	0.63	0.68	2.98
Gießhübl	TA8_sp7	Nierental Fm	Campanian	Tasshof	0.00	18.75	24.61	13.23	0.18	0.00	0.07	42.10	0.11	0.10	99.14	0.56	0.69	3.88
Gießhübl	TA8_sp8	Nierental Fm	Campanian	Tasshof	0.00	15.66	34.38	14.41	0.16	0.01	0.06	34.72	0.10	0.31	99.79	0.62	0.56	3.06
Gießhübl	TA8_sp9	Nierental Fm	Campanian	Tasshof	0.00	20.62	15.76	9.56	0.26	0.03	0.06	53.16	0.07	0.17	99.68	0.45	0.81	4.49
Gießhübl	TA8_sp10	Nierental Fm	Campanian	Tasshof	0.00	21.15	13.25	8.87	0.26	0.00	0.11	55.34	0.02	0.24	99.26	0.43	0.84	4.69
Gießhübl	TA8_sp11	Nierental Fm	Campanian	Tasshof	0.01	18.77	17.17	11.03	0.19	0.02	0.06	52.05	0.05	0.17	99.51	0.51	0.80	4.03
Gießhübl	TA8_sp12	Nierental Fm	Campanian	Tasshof	0.02	19.41	11.78	9.67	0.24	0.00	0.07	58.32	0.07	0.13	99.71	0.47	0.86	4.29
Gießhübl	TA8_sp13	Nierental Fm	Campanian	Tasshof	0.03	14.57	31.93	15.28	0.12	0.00	0.06	37.57	0.09	0.18	99.84	0.65	0.60	2.86
Gießhübl	TA8_sp14	Nierental Fm	Campanian	Tasshof	0.00	21.20	25.09	11.23	0.21	0.00	0.04	40.99	0.11	0.23	99.11	0.49	0.68	4.44
Gießhübl	TA8_sp15	Nierental Fm	Campanian	Tasshof	0.02	20.51	12.33	9.26	0.27	0.00	0.06	56.74	0.05	0.24	99.47	0.45	0.86	4.55
Gießhübl	TA9_sp1	Nierental Fm	Campanian	Tasshof	0.00	15.16	33.80	14.91	0.13	0.00	0.06	34.77	0.15	0.17	99.15	0.64	0.57	2.98
Gießhübl	TA9_sp2	Nierental Fm	Campanian	Tasshof	0.00	16.67	37.24	14.33	0.15	0.01	0.05	30.55	0.18	0.30	99.47	0.61	0.51	3.23
Gießhübl	TA9_sp3	Nierental Fm	Campanian	Tasshof	0.00	18.12	24.91	12.48	0.17	0.00	0.03	43.60	0.11	0.17	99.58	0.55	0.69	3.73
Gießhübl	TA9_sp4	Nierental Fm	Campanian	Tasshof	0.00	16.15	24.52	12.83	0.18	0.00	0.06	45.46	0.08	0.22	99.50	0.59	0.70	3.32
Gießhübl	TA9_sp5	Nierental Fm	Campanian	Tasshof	0.00	15.54	32.82	14.91	0.14	0.00	0.04	35.59	0.15	0.22	99.41	0.63	0.58	3.06
Gießhübl	TA9_sp6	Nierental Fm	Campanian	Tasshof	0.00	15.81	27.67	14.25	0.12	0.01	0.20	41.67	0.15	0.07	99.94	0.62	0.66	3.17
Gießhübl	TA9_sp7	Nierental Fm	Campanian	Tasshof	0.00	17.68	14.85	11.02	0.20	0.00	0.07	55.36	0.08	0.13	99.39	0.53	0.83	3.83
Gießhübl	TA9_sp8	Nierental Fm	Campanian	Tasshof	0.00	19.10	21.92	11.14	0.14	0.03	0.03	46.51	0.07	0.21	99.15	0.51	0.73	4.03
Gießhübl	TA9_sp9	Nierental Fm	Campanian	Tasshof	0.00	17.82	20.21	12.31	0.18	0.00	0.06	48.72	0.09	0.14	99.53	0.55	0.76	3.75
Gießhübl	TA9_sp10	Nierental Fm	Campanian	Tasshof	0.00	16.21	32.76	14.42	0.14	0.00	0.05	35.32	0.15	0.25	99.30	0.61	0.58	3.21
Gießhübl	TA9_sp11	Nierental Fm	Campanian	Tasshof	0.00	17.33	23.01	12.33	0.20	0.02	0.18	46.41	0.04	0.20	99.72	0.56	0.72	3.59
Gießhübl	TA9_sp12	Nierental Fm	Campanian	Tasshof	0.00	19.03	19.46	11.01	0.20	0.02	0.11	49.69	0.04	0.19	99.73	0.51	0.77	4.04
Gießhübl	A3_sp1	L-Gießhübl Fm	Maastr	Aderklaa 92	0.04	20.16	14.81	10.12	0.22	0.00	0.06	52.85	0.08	0.19	98.53	0.47	0.82	4.44
Gießhübl	A3_sp2	L-Gießhübl Fm	Maastr	Aderklaa 92	0.01	17.64	25.29	12.92	0.17	0.02	0.10	42.01	0.19	0.17	98.51	0.57	0.68	3.65
Gießhübl	A3_sp3	L-Gießhübl Fm	Maastr	Aderklaa 92	0.01	19.31	17.17	11.01	0.24	0.00	0.13	50.59	0.04	0.13	98.63	0.50	0.79	4.19
Gießhübl	A3_sp4	L-Gießhübl Fm	Maastr	Aderklaa 92	0.01	14.75	24.92	11.91	0.12	0.02	0.07	45.11	0.10	0.18	97.19	0.59	0.70	3.08
Glinzendorf	T1-02_sp	not defined	Campanian	Markgrn. T1	0.00	19.24	23.69	11.42	0.19	0.01	0.23	44.39	0.06		99.22	0.51	0.71	4.02
Glinzendorf	T1-02_sp	not defined	Campanian	Markgrn. T1	0.00	14.01	44.60	17.11	0.14	0.01	0.04	22.68	0.25		98.82	0.69	0.39	2.62
Glinzendorf	T1-02_sp	not defined	Campanian	Markgrn. T1	0.00	14.33	39.74	16.32	0.10	0.01	0.08	27.89	0.18		98.65	0.67	0.47	2.74
Glinzendorf	T1-02_sp	not defined	Campanian	Markgrn. T1	0.00	18.28	46.71	13.12	0.16	0.02	0.10	19.97	0.23		98.58	0.56	0.35	3.46
Glinzendorf	T1-02_sp	not defined	Campanian	Markgrn. T1	0.02	11.07	52.50	19.02	0.11	0.00	0.11	16.43	0.32		99.58	0.75	0.29	1.97
Glinzendorf	T1-02_sp	not defined	Campanian	Markgrn. T1	0.00	12.64	50.11	18.38	0.09	0.01	0.00	17.74	0.27		99.24	0.72	0.31	2.29
Glinzendorf	T1-02_sp	not defined	Campanian	Markgrn. T1	0.02	15.77	16.43	9.80	0.20	0.00	0.11	55.20	0.08		97.61	0.53	0.81	3.44
Glinzendorf	T1-02_sp	not defined	Campanian	Markgrn. T1	0.03	13.87	38.79	16.81	0.11	0.01	0.07	29.40	0.18		99.27	0.68	0.49	2.64

Gosau	Sample	Formation	Age	Location	SiO_2 [%]	FeO [%]	Al_2O_3 [%]	MgO [%]	MnO [%]	CaO [%]	TiO_2 [%]	Cr_2O_3 [%]	NiO [%]	ZnO [%]	Total [%]	Mg# [%]	Cr# [%]	Fe^{2+} [%]
Glinzendorf	T1-02_sp	not defined	Campanian	Markgrn. T1	0.03	13.86	39.23	16.86	0.09	0.00	0.07	29.07	0.20		99.40	0.68	0.49	2.63
Glinzendorf	T1-02_sp	not defined	Campanian	Markgrn. T1	0.01	19.36	40.18	14.58	0.15	0.00	0.10	24.36	0.24		98.99	0.57	0.44	3.75
Glinzendorf	T1-02_sp	not defined	Campanian	Markgrn. T1	0.02	16.72	30.91	14.23	0.13	0.00	0.34	36.96	0.11		99.41	0.60	0.60	3.33
Glinzendorf	T1-02_sp	not defined	Campanian	Markgrn. T1	0.02	17.62	26.99	12.18	0.18	0.01	0.18	42.10	0.09		99.38	0.55	0.67	3.60
Glinzendorf	T1-02_sp	not defined	Campanian	Markgrn. T1	0.00	21.09	9.99	9.26	0.26	0.00	0.23	57.70	0.08		98.62	0.44	0.88	4.78
Glinzendorf	T1-02_sp	not defined	Campanian	Markgrn. T1	0.00	25.27	10.65	7.26	0.30	0.01	0.34	54.21	0.07		98.10	0.34	0.87	5.84
Glinzendorf	T1-02_sp	not defined	Campanian	Markgrn. T1	0.02	21.46	16.78	6.77	0.25	0.01	0.16	51.13	0.06		96.63	0.36	0.80	4.83
Glinzendorf	T1-01_sp	not defined	Campanian	Markgrn. T1	0.01	16.36	45.57	16.21	0.11	0.01	0.06	20.44	0.24		99.00	0.64	0.36	3.06
Glinzendorf	T1-01_sp	not defined	Campanian	Markgrn. T1	0.03	15.00	27.64	14.48	0.16	0.00	0.03	42.24	0.10		99.69	0.63	0.66	3.01
Glinzendorf	T1-01_sp	not defined	Campanian	Markgrn. T1	0.00	19.59	18.50	10.86	0.24	0.01	0.17	49.51	0.07		98.96	0.50	0.77	4.21
Grünbach	G6B_sp1	Kreuzgraben Fm	Con-San	Grünbach	0.02	19.14	15.61	10.49	0.27	0.00	0.13	53.02	0.10		98.78	0.49	0.81	4.43
Grünbach	G6B_sp2	Kreuzgraben Fm	Con-San	Grünbach	0.01	20.83	21.81	11.12	0.22	0.00	0.12	44.66	0.09		98.86	0.43	0.72	5.02
Grünbach	G6B_sp3	Kreuzgraben Fm	Con-San	Grünbach	0.01	23.00	17.96	9.87	0.23	0.00	0.28	47.41	0.10		98.87	0.66	0.77	2.74
Grünbach	G6B_sp4	Kreuzgraben Fm	Con-San	Grünbach	0.00	14.36	39.14	15.91	0.11	0.00	0.03	29.41	0.13		99.09	0.54	0.49	3.92
Grünbach	G6B_sp5	Kreuzgraben Fm	Con-San	Grünbach	0.03	18.73	22.56	12.24	0.22	0.00	0.05	45.38	0.11		99.31	0.48	0.72	4.18
Grünbach	G6B_sp6	Kreuzgraben Fm	Con-San	Grünbach	0.01	19.25	17.26	9.84	0.22	0.00	0.17	51.87	0.08		98.69	0.61	0.79	3.23
Grünbach	G6B_sp7	Kreuzgraben Fm	Con-San	Grünbach	0.00	15.78	23.91	13.74	0.16	0.00	0.03	45.92	0.11		99.66	0.43	0.71	4.57
Grünbach	G6B_sp8	Kreuzgraben Fm	Con-San	Grünbach	0.00	20.47	13.40	8.48	0.30	0.00	0.21	55.56	0.03		98.44	0.38	0.84	5.08
Grünbach	G6B_sp9	Kreuzgraben Fm	Con-San	Grünbach	0.03	22.44	10.53	7.78	0.29	0.00	0.19	57.85	0.02		99.12	0.62	0.88	3.17
Grünbach	G6B_sp10	Kreuzgraben Fm	Con-San	Grünbach	0.01	15.86	30.29	14.50	0.16	0.02	0.02	38.02	0.11		98.98	0.53	0.62	4.04
Grünbach	G6B_sp11	Kreuzgraben Fm	Con-San	Grünbach	0.00	19.33	23.23	12.31	0.18	0.01	0.17	43.75	0.09		99.07	0.56	0.71	3.53
Grünbach	G6B_sp12	Kreuzgraben Fm	Con-San	Grünbach	0.01	17.85	33.38	12.87	0.13	0.00	0.24	35.01	0.13		99.62	0.52	0.57	4.15
Grünbach	G6B_sp13	Kreuzgraben Fm	Con-San	Grünbach	0.05	19.94	24.54	12.15	0.17	0.00	0.18	42.05	0.09		99.16	0.53	0.69	4.16
Grünbach	G6B_sp14	Kreuzgraben Fm	Con-San	Grünbach	0.01	20.50	29.80	13.00	0.19	0.00	0.12	35.52	0.14		99.27	0.47	0.60	4.45
Grünbach	G6B_sp15	Kreuzgraben Fm	Con-San	Grünbach	0.02	20.74	19.03	10.26	0.22	0.00	0.21	48.76	0.14		99.38	0.72	0.77	2.32
Grünbach	G6B_sp16	Kreuzgraben Fm	Con-San	Grünbach	0.03	12.68	48.92	17.98	0.11	0.00	0.04	18.73	0.27		98.75	0.58	0.33	3.55
Grünbach	G9_sp1	Maiersdorf Fm	Con-San	Grünbach	0.03	17.43	27.16	13.23	0.13	0.00	0.06	41.26	0.11		99.40	0.54	0.66	4.02
Grünbach	G9_sp2	Maiersdorf Fm	Con-San	Grünbach	0.01	19.94	31.42	13.06	0.19	0.00	0.12	34.18	0.15		99.06	0.34	0.58	5.85
Grünbach	G9_sp3	Maiersdorf Fm	Con-San	Grünbach	0.00	25.20	11.82	7.16	0.27	0.01	0.26	52.26	0.09		97.07	0.53	0.85	4.08
Grünbach	G9_sp4	Maiersdorf Fm	Con-San	Grünbach	0.00	20.34	32.70	13.01	0.16	0.00	0.19	32.68	0.18		99.27	0.51	0.56	4.12
Grünbach	G9_sp5	Maiersdorf Fm	Con-San	Grünbach	0.00	19.70	25.58	11.66	0.20	0.01	0.10	40.89	0.11		98.25	0.67	0.67	2.83
Grünbach	G9_sp6	Maiersdorf Fm	Con-San	Grünbach	0.00	15.25	47.50	16.97	0.11	0.01	0.05	18.45	0.24		98.58	0.61	0.33	3.19
Grünbach	G9_sp7	Maiersdorf Fm	Con-San	Grünbach	0.00	16.22	33.66	14.10	0.13	0.00	0.16	35.12	0.13		99.52	0.54	0.57	3.71
Grünbach	G9_sp8	Maiersdorf Fm	Con-San	Grünbach	0.03	17.41	19.41	11.34	0.20	0.00	0.15	50.16	0.09		98.79	0.29	0.77	5.21
Grünbach	G9_sp10	Maiersdorf Fm	Con-San	Grünbach	0.00	15.76	35.65	15.58	0.14	0.00	0.15	32.78	0.14		100.21	0.64	0.54	3.04
Grünbach	G9_sp11	Maiersdorf Fm	Con-San	Grünbach	0.00	22.03	27.80	10.94	0.23	0.00	0.08	37.18	0.12		98.38	0.47	0.63	4.59
Grünbach	G9_sp12	Maiersdorf Fm	Con-San	Grünbach	0.00	24.34	21.48	9.83	0.22	0.01	0.24	42.28	0.10		98.48	0.42	0.72	5.26
Grünbach	G9_sp13	Maiersdorf Fm	Con-San	Grünbach	0.00	14.40	29.45	14.98	0.16	0.00	0.08	40.36	0.14		99.56	0.65	0.64	2.86
Grünbach	G9_sp14	Maiersdorf Fm	Con-San	Grünbach	0.03	18.47	37.89	14.87	0.15	0.00	0.11	27.40	0.23		99.16	0.59	0.48	3.59
Grünbach	G9_sp15	Maiersdorf Fm	Con-San	Grünbach	0.00	20.66	19.49	10.52	0.24	0.00	0.03	48.18	0.07		99.19	0.48	0.76	4.43
Grünbach	G9_sp16	Maiersdorf Fm	Con-San	Grünbach	0.00	13.48	51.60	18.36	0.12	0.00	0.07	15.55	0.27		99.45	0.71	0.28	2.43
Grünbach	M81_sp1	Grünbach Fm	Campanian	Grünbach	0.01	13.90	39.27	16.50	0.13	0.00	0.15	28.96	0.19		99.10	0.68	0.49	2.65
Grünbach	M81_sp2	Grünbach Fm	Campanian	Grünbach	0.00	17.54	21.13	12.06	0.20	0.00	0.12	47.62	0.07		98.73	0.55	0.74	3.70
Grünbach	M81_sp3	Grünbach Fm	Campanian	Grünbach	0.00	14.81	43.51	17.03	0.11	0.00	0.20	23.59	0.24		99.50	0.67	0.41	2.77
Grünbach	M81_sp4	Grünbach Fm	Campanian	Grünbach	0.02	14.36	36.97	15.15	0.10	0.01	0.16	31.92	0.14		98.83	0.65	0.52	2.78
Grünbach	M81_sp5	Grünbach Fm	Campanian	Grünbach	0.01	14.59	41.79	16.13	0.09	0.00	0.14	26.25	0.17		99.16	0.66	0.45	2.76
Grünbach	M81_sp6	Grünbach Fm	Campanian	Grünbach	0.02	23.82	11.39	8.14	0.28	0.01	0.36	53.76	0.07		97.85	0.38	0.86	5.46

Gosau	Sample	Formation	Age	Location	SiO_2 [%]	FeO [%]	Al_2O_3 [%]	MgO [%]	MnO [%]	CaO [%]	TiO_2 [%]	Cr_2O_3 [%]	NiO [%]	ZnO [%]	Total [%]	Mg# [%]	Cr# [%]	Fe^{2+} [%]
Grünbach	M63_sp1	Grünbach Fm	Campanian	Grünbach	0.00	14.35	48.36	17.47	0.13	0.00	0.21	18.68	0.29		99.49	0.69	0.33	2.62
Grünbach	M63_sp2	Grünbach Fm	Campanian	Grünbach	0.01	14.87	32.74	15.66	0.14	0.00	0.06	35.55	0.20		99.23	0.65	0.58	2.92
Grünbach	M63_sp3	Grünbach Fm	Campanian	Grünbach	0.02	20.14	21.15	10.94	0.24	0.00	0.02	46.75	0.04		99.30	0.49	0.74	4.27
Grünbach	M63_sp4	Grünbach Fm	Campanian	Grünbach	0.01	17.28	23.76	12.53	0.17	0.01	0.03	45.45	0.10		99.34	0.56	0.71	3.58
Grünbach	M63_sp5	Grünbach Fm	Campanian	Grünbach	0.03	16.22	21.96	13.30	0.19	0.02	0.14	47.63	0.11		99.61	0.59	0.74	3.36
Grünbach	M63_sp6	Grünbach Fm	Campanian	Grünbach	0.00	19.80	22.26	11.33	0.24	0.02	0.11	45.25	0.06		99.06	0.51	0.72	4.18
Grünbach	M63_sp7	Grünbach Fm	Campanian	Grünbach	0.01	20.96	11.17	8.69	0.30	0.01	0.09	57.23	0.07		98.52	0.43	0.87	4.73
Grünbach	M63_sp8	Grünbach Fm	Campanian	Grünbach	0.00	17.16	30.00	13.73	0.15	0.00	0.09	38.68	0.09		99.90	0.59	0.62	3.43
Grünbach	M63_sp9	Grünbach Fm	Campanian	Grünbach	0.00	16.28	20.40	13.32	0.15	0.00	0.06	49.02	0.03		99.25	0.59	0.75	3.41
Grünbach	M63_sp10	Grünbach Fm	Campanian	Grünbach	0.00	19.64	29.55	13.09	0.14	0.00	0.25	36.41	0.15		99.23	0.54	0.61	3.98
Grünbach	M63_sp11	Grünbach Fm	Campanian	Grünbach	0.03	15.94	15.38	12.74	0.17	0.00	0.08	55.38	0.06		99.77	0.59	0.82	3.40
Grünbach	M63_sp12	Grünbach Fm	Campanian	Grünbach	0.03	14.73	17.16	13.05	0.24	0.00	0.11	53.89	0.08		99.29	0.61	0.80	3.12
Grünbach	M63_sp13	Grünbach Fm	Campanian	Grünbach	0.04	15.03	34.51	15.76	0.16	0.02	0.07	34.31	0.13		100.02	0.65	0.56	2.91
Grünbach	M63_sp14	Grünbach Fm	Campanian	Grünbach	0.01	19.82	12.95	10.72	0.21	0.01	0.07	54.94	0.08		98.81	0.49	0.84	4.38
Grünbach	M63_sp15	Grünbach Fm	Campanian	Grünbach	0.00	15.49	30.15	14.86	0.15	0.02	0.10	38.60	0.14		99.50	0.63	0.62	3.08
Grünbach	M63_sp16	Grünbach Fm	Campanian	Grünbach	0.00	14.92	34.44	15.72	0.13	0.00	0.05	34.16	0.20		99.61	0.65	0.56	2.90
Grünbach	M63_sp17	Grünbach Fm	Campanian	Grünbach	0.02	14.27	25.99	14.99	0.16	0.00	0.06	43.76	0.11		99.36	0.65	0.68	2.88
Grünbach	M63_sp18	Grünbach Fm	Campanian	Grünbach	0.01	15.57	39.08	15.82	0.11	0.00	0.06	28.67	0.12		99.44	0.64	0.48	2.98
Grünbach	M63_sp19	Grünbach Fm	Campanian	Grünbach	0.00	14.74	35.85	15.77	0.09	0.00	0.07	32.96	0.17		99.65	0.66	0.54	2.85
Grünbach	M63_sp20	Grünbach Fm	Campanian	Grünbach	0.00	16.36	26.38	13.86	0.17	0.00	0.07	42.43	0.12		99.39	0.60	0.67	3.33
Grünbach	G22_sp1	Grünbach Fm	Campanian	Grünbach	0.01	15.65	34.58	13.74	0.14	0.00	0.07	34.02	0.10		98.30	0.61	0.56	3.09
Grünbach	G22_sp2	Grünbach Fm	Campanian	Grünbach	0.02	10.98	53.39	19.23	0.08	0.01	0.00	15.79	0.38		99.88	0.76	0.27	1.94
Grünbach	G22_sp3	Grünbach Fm	Campanian	Grünbach	0.03	13.17	46.88	17.77	0.10	0.00	0.13	20.99	0.26		99.32	0.71	0.36	2.42
Grünbach	G22_sp4	Grünbach Fm	Campanian	Grünbach	0.00	23.93	29.13	11.95	0.15	0.02	0.40	32.10	0.17		97.84	0.47	0.59	4.99
Grünbach	G22_sp5	Grünbach Fm	Campanian	Grünbach	0.06	18.27	27.84	14.39	0.14	0.03	0.35	37.84	0.14		99.05	0.58	0.63	3.71
Grünbach	G22_sp6	Grünbach Fm	Campanian	Grünbach	0.02	12.70	56.30	19.06	0.12	0.00	0.04	10.73	0.34		99.32	0.73	0.20	2.24
Grünbach	G22_sp7	Grünbach Fm	Campanian	Grünbach	0.01	11.92	51.42	18.41	0.10	0.02	0.08	16.69	0.32		98.97	0.73	0.29	2.15
Grünbach	G22_sp8	Grünbach Fm	Campanian	Grünbach	0.03	11.01	55.02	19.68	0.13	0.00	0.07	13.09	0.32		99.33	0.76	0.23	1.94
Grünbach	G22_sp9	Grünbach Fm	Campanian	Grünbach	0.04	15.11	28.47	13.24	0.13	0.03	0.02	41.65	0.10		98.79	0.61	0.65	3.05
Grünbach	G22_sp11	Grünbach Fm	Campanian	Grünbach	0.04	22.28	28.46	11.52	0.25	0.00	0.22	35.80	0.15		98.72	0.75	0.62	2.06
Grünbach	G22_sp12	Grünbach Fm	Campanian	Grünbach	0.01	11.65	54.13	19.38	0.11	0.01	0.03	13.85	0.36		99.52	0.52	0.25	3.64
Grünbach	G22_sp13	Grünbach Fm	Campanian	Grünbach	0.00	17.66	29.27	10.69	0.15	0.00	0.13	39.74	0.08		97.72	0.70	0.63	2.49
Grünbach	G22_sp14	Grünbach Fm	Campanian	Grünbach	0.01	13.70	49.81	18.01	0.10	0.02	0.08	17.13	0.32		99.17	0.63	0.31	3.08
Grünbach	G22_sp15	Grünbach Fm	Campanian	Grünbach	0.00	15.93	37.21	15.31	0.16	0.01	0.12	30.46	0.18		99.37	0.58	0.51	3.42
Grünbach	G22_sp16	Grünbach Fm	Campanian	Grünbach	0.00	16.65	24.95	12.78	0.20	0.00	0.11	44.45	0.06		99.21	0.43	0.70	4.70
Grünbach	G22_sp17	Grünbach Fm	Campanian	Grünbach	0.00	21.08	16.59	9.07	0.19	0.02	0.13	49.92	0.09		97.09	0.55	0.79	3.73
Grünbach	G22_sp18	Grünbach Fm	Campanian	Grünbach	0.00	17.76	22.69	12.30	0.19	0.01	0.10	45.40	0.04		98.49	0.55	0.72	3.69
Grünbach	G22_sp19	Grünbach Fm	Campanian	Grünbach	0.02	17.09	14.55	11.84	0.16	0.02	0.07	55.65	0.08		99.47	0.49	0.83	4.18
Studienka	B5B_sp1	not defined	Con-San	Brezová	0.01	17.94	21.07	9.58	0.30	0.00	0.14	47.61	0.06	0.29	97.00	0.49	0.74	0.01
Studienka	B5B_sp2	not defined	Con-San	Brezová	0.04	15.42	26.76	13.98	0.11	0.01	0.03	41.25	0.10	0.13	97.82	0.62	0.66	0.02
Studienka	B5B_sp3	not defined	Con-San	Brezová	0.00	16.49	31.53	14.07	0.13	0.00	0.06	35.22	0.15	0.18	97.82	0.60	0.59	0.03
Studienka	B5B_sp4	not defined	Con-San	Brezová	0.02	15.68	25.80	13.16	0.19	0.00	0.05	42.66	0.10	0.26	97.92	0.60	0.68	0.02
Studienka	B5B_sp5	not defined	Con-San	Brezová	0.01	18.20	28.96	12.95	0.20	0.00	0.05	37.62	0.06	0.16	98.21	0.56	0.62	0.01
Studienka	B5B_sp6	not defined	Con-San	Brezová	0.02	14.90	31.07	14.94	0.14	0.00	0.03	37.07	0.13	0.16	98.44	0.64	0.60	0.03
Studienka	B5B_sp7	not defined	Con-San	Brezová	0.04	15.39	26.85	13.98	0.14	0.00	0.03	41.22	0.09	0.14	97.88	0.62	0.66	0.02
Studienka	B8A_sp1	Štvernik Fm	Con-San	Brezová	0.04	16.31	23.80	13.33	0.14	0.01	0.03	45.41	0.08		99.12	0.59	0.71	3.36
Studienka	B8A_sp2	Štvernik Fm	Con-San	Brezová	0.08	16.74	25.09	13.36	0.17	0.03	0.12	43.20	0.12		98.90	0.59	0.69	3.44

Gosau	Sample	Formation	Age	Location	SiO_2 [%]	FeO [%]	Al_2O_3 [%]	MgO [%]	MnO [%]	CaO [%]	TiO_2 [%]	Cr_2O_3 [%]	NiO [%]	ZnO [%]	Total [%]	Mg# [%]	Cr# [%]	Fe^{2+} [%]
Studienka	B8A_sp3	Štvernik Fm	Con-San	Brezová	0.01	18.06	21.80	12.41	0.20	0.02	0.05	46.92	0.09		99.57	0.55	0.73	3.77
Studienka	B8A_sp4	Štvernik Fm	Con-San	Brezová	0.02	17.04	15.38	11.27	0.33	0.01	0.05	54.61	0.07		98.76	0.54	0.82	3.70
Studienka	B8A_sp5	Štvernik Fm	Con-San	Brezová	0.01	15.99	23.65	13.55	0.14	0.01	0.07	45.48	0.10		98.99	0.60	0.71	3.30
Studienka	B8A_sp6	Štvernik Fm	Con-San	Brezová	0.00	19.61	23.05	11.01	0.17	0.02	0.12	45.09	0.06		99.13	0.50	0.71	4.12
Studienka	B8A_sp7	Štvernik Fm	Con-San	Brezová	0.02	16.63	23.15	12.29	0.17	0.00	0.23	46.22	0.11		98.82	0.57	0.72	3.46
Studienka	B8A_sp8	Štvernik Fm	Con-San	Brezová	0.00	15.74	27.11	14.13	0.19	0.00	0.11	42.63	0.11		100.02	0.62	0.67	3.16
Studienka	B8A_sp9	Štvernik Fm	Con-San	Brezová	0.03	19.22	16.51	10.91	0.25	0.00	0.10	51.94	0.05		99.01	0.50	0.80	4.16
Studienka	B8A_sp10	Štvernik Fm	Con-San	Brezová	0.00	18.83	23.28	11.97	0.23	0.00	0.04	45.00	0.05		99.41	0.53	0.71	3.93
Studienka	B8A_sp11	Štvernik Fm	Con-San	Brezová	0.00	18.06	27.00	12.43	0.20	0.00	0.07	41.25	0.11		99.11	0.55	0.66	3.70
Studienka	B8A_sp12	Štvernik Fm	Con-San	Brezová	0.01	17.74	23.12	12.77	0.20	0.00	0.07	45.16	0.09		99.16	0.56	0.71	3.69
Studienka	B8A_sp13	Štvernik Fm	Con-San	Brezová	0.03	18.08	29.52	13.14	0.18	0.00	0.04	37.71	0.14		98.85	0.56	0.62	3.67
Studienka	B8A_sp14	Štvernik Fm	Con-San	Brezová	0.01	15.66	27.73	14.33	0.15	0.01	0.07	41.23	0.08		99.26	0.62	0.66	3.16
Studienka	B8A_sp15	Štvernik Fm	Con-San	Brezová	0.02	13.85	28.90	14.78	0.15	0.01	0.07	41.46	0.12		99.36	0.66	0.65	2.76
Studienka	B8A_sp16	Štvernik Fm	Con-San	Brezová	0.03	17.56	16.87	12.55	0.21	0.00	0.09	52.11	0.13		99.54	0.56	0.80	3.74
Studienka	B8A_sp17	Štvernik Fm	Con-San	Brezová	0.06	15.61	27.77	14.36	0.19	0.00	0.09	41.30	0.14		99.52	0.62	0.66	3.14
Studienka	B8A_sp18	Štvernik Fm	Con-San	Brezová	0.02	19.68	19.42	11.30	0.25	0.00	0.32	47.85	0.10		98.93	0.51	0.76	4.21
Studienka	B8A_sp19	Štvernik Fm	Con-San	Brezová	0.00	16.36	26.85	13.39	0.20	0.01	0.02	42.55	0.05		99.41	0.59	0.67	3.32
Studienka	B8A_sp20	Štvernik Fm	Con-San	Brezová	0.02	16.56	23.97	13.54	0.15	0.00	0.09	44.55	0.07		98.95	0.59	0.70	3.42
Studienka	B8A_sp21	Štvernik Fm	Con-San	Brezová	0.02	16.61	34.33	14.49	0.18	0.00	0.09	33.77	0.21		99.70	0.61	0.56	3.25
Studienka	B8A_sp22	Štvernik Fm	Con-San	Brezová	0.00	17.58	16.10	11.63	0.19	0.00	0.11	53.88	0.06		99.56	0.54	0.81	3.77
Studienka	B8A_sp23	Štvernik Fm	Con-San	Brezová	0.01	16.53	20.55	12.84	0.16	0.00	0.13	48.94	0.05		99.22	0.58	0.75	3.46
Studienka	B8A_sp24	Štvernik Fm	Con-San	Brezová	0.00	15.94	20.93	13.40	0.15	0.01	0.13	48.63	0.07		99.26	0.60	0.75	3.32
Studienka	B8A_sp25	Štvernik Fm	Con-San	Brezová	0.01	14.40	29.11	15.08	0.13	0.00	0.07	40.50	0.12		99.42	0.65	0.64	2.87
Studienka	B6C_sp1	Košariská Fm	Campanian	Brezová	0.03	14.52	27.67	14.73	0.08	0.01	0.10	40.99	0.13	0.16	98.42	0.64	0.65	2.94
Studienka	B6C_sp2	Košariská Fm	Campanian	Brezová	0.02	15.90	39.77	15.90	0.10	0.01	0.15	26.41	0.23	0.22	98.70	0.64	0.46	3.06
Studienka	B6C_sp3	Košariská Fm	Campanian	Brezová	0.00	16.83	35.54	14.65	0.15	0.00	0.04	31.94	0.08	0.30	99.54	0.61	0.53	3.29
Studienka	B6C_sp4	Košariská Fm	Campanian	Brezová	0.02	15.75	37.42	15.70	0.13	0.01	0.12	29.43	0.17	0.17	98.92	0.64	0.50	3.05
Studienka	B6C_sp5	Košariská Fm	Campanian	Brezová	0.04	14.22	35.97	15.39	0.13	0.03	0.16	32.15	0.16	0.25	98.50	0.66	0.53	2.77
Studienka	B6C_sp6	Košariská Fm	Campanian	Brezová	0.00	13.89	36.43	16.03	0.10	0.01	0.09	31.77	0.14	0.21	98.68	0.67	0.53	2.69
Studienka	B6C_sp7	Košariská Fm	Campanian	Brezová	0.05	13.06	40.35	16.86	0.11	0.00	0.18	27.79	0.15	0.20	98.75	0.70	0.47	2.48
Studienka	B6C_sp8	Košariská Fm	Campanian	Brezová	0.00	15.50	30.39	14.69	0.14	0.00	0.13	38.01	0.14	0.21	99.21	0.63	0.62	3.09
Studienka	B6C_sp9	Košariská Fm	Campanian	Brezová	0.02	17.34	34.24	13.93	0.15	0.00	0.06	33.19	0.11	0.22	99.25	0.59	0.55	3.42
Studienka	B6C_sp10	Košariská Fm	Campanian	Brezová	0.05	16.23	24.06	13.64	0.13	0.01	0.10	44.28	0.12	0.09	98.72	0.60	0.70	3.36
Studienka	B6C_sp11	Košariská Fm	Campanian	Brezová	0.02	16.84	32.44	14.29	0.13	0.01	0.08	34.51	0.16	0.19	98.67	0.60	0.58	3.36
Studienka	B6C_sp12	Košariská Fm	Campanian	Brezová	0.00	19.82	26.70	12.65	0.15	0.00	0.18	38.87	0.09	0.26	98.71	0.53	0.65	4.10
Studienka	B6C_sp13	Košariská Fm	Campanian	Brezová	0.02	15.23	41.18	15.75	0.13	0.01	0.13	26.09	0.17	0.26	98.98	0.65	0.45	2.90
Studienka	B6C_sp14	Košariská Fm	Campanian	Brezová	0.03	17.88	20.28	12.11	0.17	0.01	0.12	47.78	0.08	0.12	98.56	0.55	0.75	3.80
Studienka	B6C_sp15	Košariská Fm	Campanian	Brezová	0.05	20.72	25.27	11.82	0.18	0.00	0.15	39.92	0.10	0.23	98.43	0.50	0.67	4.34
Studienka	B6C_sp16	Košariská Fm	Campanian	Brezová	0.05	15.52	31.15	14.81	0.17	0.01	0.07	36.98	0.14	0.21	99.11	0.63	0.60	3.09
Studienka	B6C_sp17	Košariská Fm	Campanian	Brezová	0.01	13.65	32.66	15.93	0.14	0.00	0.10	36.10	0.10	0.10	98.79	0.68	0.59	2.68
Studienka	B6C_sp18	Košariská Fm	Campanian	Brezová	0.02	17.21	42.98	15.37	0.14	0.00	0.39	22.76	0.27	0.27	99.40	0.61	0.40	3.26
Studienka	B6C_sp19	Košariská Fm	Campanian	Brezová	0.02	15.79	28.60	13.71	0.17	0.00	0.12	40.30	0.10	0.20	99.00	0.61	0.64	3.19
Studienka	B6C_sp20	Košariská Fm	Campanian	Brezová	0.02	14.20	34.80	15.87	0.16	0.02	0.06	34.09	0.15	0.17	99.52	0.67	0.56	2.75
Studienka	B6C_sp21	Košariská Fm	Campanian	Brezová	0.01	14.91	28.72	14.36	0.13	0.00	0.13	40.18	0.09	0.19	98.71	0.63	0.64	3.00
Studienka	B6C_sp22	Košariská Fm	Campanian	Brezová	0.01	15.41	38.92	16.04	0.12	0.02	0.12	28.08	0.21	0.18	99.11	0.65	0.48	2.96
Studienka	B6C_sp23	Košariská Fm	Campanian	Brezová	0.02	15.36	38.67	15.95	0.11	0.00	0.18	27.83	0.18	0.14	98.42	0.65	0.48	2.97
Studienka	B6C_sp24	Košariská Fm	Campanian	Brezová	0.02	14.40	30.53	15.12	0.12	0.01	0.13	38.66	0.13	0.16	99.28	0.65	0.62	2.86

Gosau	Sample	Formation	Age	Location	SiO_2 [%]	FeO [%]	Al_2O_3 [%]	MgO [%]	MnO [%]	CaO [%]	TiO_2 [%]	Cr_2O_3 [%]	NiO [%]	ZnO [%]	Total [%]	Mg# [%]	Cr# [%]	Fe^{2+} [%]
Studienka	B6C_sp25	Košariská Fm	Campanian	Brezová	0.06	18.01	36.71	14.50	0.20	0.03	0.08	29.33	0.16	0.21	99.29	0.59	0.51	3.52
Studienka	B6C_sp26	Košariská Fm	Campanian	Brezová	0.02	12.86	46.02	17.58	0.11	0.01	0.07	22.27	0.23	0.20	99.38	0.71	0.38	2.37
Studienka	B7A_sp1	Podbradlo Fm	Campanian	Brezová	0.00	14.57	34.67	15.62	0.14	0.02	0.04	34.37	0.13		99.56	0.66	0.56	2.83
Studienka	B7A_sp2	Podbradlo Fm	Campanian	Brezová	0.03	17.51	30.74	13.62	0.18	0.01	0.15	36.82	0.13		99.18	0.58	0.61	3.51
Studienka	B7A_sp3	Podbradlo Fm	Campanian	Brezová	0.00	12.00	44.89	17.23	0.12	0.01	0.16	24.25	0.20		98.86	0.72	0.41	2.23
Studienka	B7A_sp4	Podbradlo Fm	Campanian	Brezová	0.00	21.05	25.67	10.73	0.22	0.00	0.17	40.59	0.07		98.50	0.48	0.67	4.42
Studienka	B7A_sp5	Podbradlo Fm	Campanian	Brezová	0.03	22.97	12.80	6.83	0.32	0.01	0.19	53.59	0.07		96.80	0.35	0.84	5.29
Studienka	B7A_sp6	Podbradlo Fm	Campanian	Brezová	0.06	15.65	17.53	10.37	0.14	0.01	0.16	53.98	0.07		97.96	0.54	0.80	3.38
Studienka	B7A_sp7	Podbradlo Fm	Campanian	Brezová	0.01	13.83	40.31	16.74	0.14	0.02	0.15	28.17	0.16		99.52	0.68	0.47	2.61
Studienka	B7A_sp8	Podbradlo Fm	Campanian	Brezová	0.04	16.13	20.78	12.95	0.12	0.02	0.11	48.62	0.06		98.84	0.59	0.75	3.38
Studienka	B7A_sp9	Podbradlo Fm	Campanian	Brezová	0.04	14.32	27.31	13.52	0.14	0.00	0.23	42.99	0.13		98.69	0.63	0.67	2.90
Studienka	B7A_sp10	Podbradlo Fm	Campanian	Brezová	0.03	17.16	22.19	12.94	0.20	0.00	0.02	46.47	0.10		99.11	0.57	0.73	3.58
Studienka	B7A_sp11	Podbradlo Fm	Campanian	Brezová	0.00	17.71	36.59	14.33	0.18	0.00	0.15	30.04	0.12		99.12	0.59	0.51	3.46
Studienka	B7A_sp12	Podbradlo Fm	Campanian	Brezová	0.04	15.76	19.20	13.51	0.18	0.00	0.18	51.01	0.13		100.00	0.61	0.77	3.29
Studienka	B7A_sp13	Podbradlo Fm	Campanian	Brezová	0.01	15.42	23.35	13.83	0.15	0.00	0.07	46.05	0.09		98.97	0.62	0.72	3.18
Studienka	B7A_sp14	Podbradlo Fm	Campanian	Brezová	0.00	15.98	27.18	13.70	0.14	0.01	0.05	42.12	0.09		99.25	0.60	0.66	3.24
Studienka	B7A_sp15	Podbradlo Fm	Campanian	Brezová	0.01	18.62	18.76	10.70	0.22	0.00	0.19	50.21	0.06		98.75	0.51	0.77	3.99
Studienka	B2B_sp1	Priepastné Fm	Paleocene	Brezová	0.04	15.14	32.06	14.80	0.17	0.01	0.10	35.74	0.12	0.13	98.32	0.64	0.59	0.02
Studienka	B2B_sp2	Priepastné Fm	Paleocene	Brezová	0.02	14.25	32.80	15.25	0.13	0.00	0.16	36.13	0.18	0.15	99.07	0.66	0.58	0.04
Studienka	B2B_sp3	Priepastné Fm	Paleocene	Brezová	0.01	14.04	34.48	15.57	0.10	0.00	0.16	34.21	0.17	0.11	98.86	0.66	0.56	0.03
Studienka	B2B_sp4	Priepastné Fm	Paleocene	Brezová	0.01	21.36	20.52	10.22	0.21	0.01	0.13	45.38	0.07	0.21	98.12	0.46	0.74	0.02
Studienka	B2B_sp5	Priepastné Fm	Paleocene	Brezová	0.03	17.64	21.42	11.87	0.19	0.02	0.11	46.96	0.07	0.25	98.57	0.55	0.74	0.02
Studienka	B2B_sp6	Priepastné Fm	Paleocene	Brezová	0.03	16.25	40.62	16.39	0.12	0.02	0.14	25.15	0.24	0.13	99.10	0.64	0.44	0.05
Studienka	B2B_sp7	Priepastné Fm	Paleocene	Brezová	0.02	18.74	23.44	12.10	0.14	0.01	0.06	43.83	0.10	0.15	98.57	0.54	0.71	0.02
Studienka	B2B_sp8	Priepastné Fm	Paleocene	Brezová	0.02	18.33	23.60	12.16	0.17	0.00	0.10	43.53	0.04	0.27	98.23	0.54	0.70	0.01
Studienka	B2B_sp9	Priepastné Fm	Paleocene	Brezová	0.01	14.67	27.50	14.48	0.15	0.00	0.10	41.51	0.09	0.19	98.70	0.64	0.66	0.02
Studienka	B2B_sp10	Priepastné Fm	Paleocene	Brezová	0.00	13.93	33.81	15.13	0.10	0.02	0.17	35.18	0.16	0.09	98.59	0.66	0.57	0.03
Studienka	B2B_sp11	Priepastné Fm	Paleocene	Brezová	0.02	17.04	24.08	12.81	0.17	0.01	0.05	43.95	0.10	0.19	98.42	0.57	0.70	0.02
Studienka	B2B_sp12	Priepastné Fm	Paleocene	Brezová	0.01	16.45	30.30	14.73	0.13	0.02	0.07	36.47	0.11	0.14	98.43	0.62	0.61	0.02
Studienka	B2B_sp13	Priepastné Fm	Paleocene	Brezová	0.01	13.79	31.47	15.37	0.14	0.00	0.10	37.65	0.14	0.19	98.85	0.67	0.60	0.03
Studienka	B2B_sp14	Priepastné Fm	Paleocene	Brezová	0.03	13.58	35.50	16.21	0.14	0.00	0.19	33.08	0.16	0.13	99.03	0.68	0.54	0.03
Studienka	B2B_sp15	Priepastné Fm	Paleocene	Brezová	0.03	20.63	24.96	11.10	0.23	0.01	0.08	40.49	0.08	0.31	97.90	0.49	0.67	0.02
Studienka	B2B_sp16	Priepastné Fm	Paleocene	Brezová	0.01	15.48	28.21	14.05	0.20	0.02	0.03	40.64	0.10	0.14	98.88	0.62	0.65	0.02

Gosau	Sample	Grain	Formation	Age	Location	SiO_2 [%]	FeO [%]	Al_2O_3 [%]	MgO [%]	MnO [%]	CaO [%]	TiO_2 [%]	B_2O_3 [%]	F [%]	Na_2O [%]	K_2O [%]	Total [%]
Gießhübl	MTW4_Tu1	core	not defined	Con-San	Mitterwäldchen	35.90	8.00	33.03	5.86	0.04	0.42	0.69	9.66	0.11	2.17	0.03	95.90
Gießhübl	MTW4_Tu1	rim	not defined	Con-San	Mitterwäldchen	35.80	7.22	33.81	5.84	0.04	0.53	0.65	9.66	0.00	1.89	0.02	95.46
Gießhübl	MTW4_Tu2	core	not defined	Con-San	Mitterwäldchen	35.70	7.37	34.28	5.73	0.02	0.65	0.80	9.66	0.27	1.81	0.01	96.30
Gießhübl	MTW4_Tu2	rim	not defined	Con-San	Mitterwäldchen	35.28	6.98	34.47	5.64	0.02	0.90	1.17	9.66	0.18	1.64	0.03	95.96
Gießhübl	MTW4_Tu3	core	not defined	Con-San	Mitterwäldchen	36.11	9.61	30.89	6.39	0.00	0.04	0.10	9.66	0.00	2.67	0.00	95.46
Gießhübl	MTW4_Tu3	rim	not defined	Con-San	Mitterwäldchen	35.65	12.00	28.50	6.25	0.00	0.19	0.69	9.66	0.00	2.77	0.00	95.71
Gießhübl	MTW4_Tu4	core	not defined	Con-San	Mitterwäldchen	36.55	4.30	30.66	9.57	0.02	1.08	0.78	9.66	0.15	2.17	0.00	94.94
Gießhübl	MTW4_Tu4	rim	not defined	Con-San	Mitterwäldchen	36.46	4.66	30.19	9.51	0.01	1.12	1.11	9.66	0.24	2.24	0.02	95.20
Gießhübl	MTW4_Tu5	core	not defined	Con-San	Mitterwäldchen	35.22	7.99	33.06	5.73	0.05	0.86	0.86	9.66	0.00	1.79	0.03	95.25
Gießhübl	MTW4_Tu5	rim	not defined	Con-San	Mitterwäldchen	35.67	8.01	32.77	5.72	0.08	0.87	0.80	9.66	0.18	1.81	0.03	95.61
Gießhübl	MTW4_Tu6	core	not defined	Con-San	Mitterwäldchen	35.71	6.40	34.32	5.94	0.02	0.40	0.97	9.66	0.00	2.02	0.03	95.48
Gießhübl	MTW4_Tu6	rim	not defined	Con-San	Mitterwäldchen	36.37	7.33	31.05	7.81	0.02	0.08	0.51	9.66	0.15	2.72	0.01	95.71
Gießhübl	MTW4_Tu9	core	not defined	Con-San	Mitterwäldchen	35.53	9.71	30.83	5.83	0.01	0.25	0.84	9.66	0.18	2.47	0.03	95.34
Gießhübl	MTW4_Tu9	rim	not defined	Con-San	Mitterwäldchen	36.03	7.49	32.07	6.54	0.01	0.16	0.72	9.66	0.02	2.42	0.03	95.14
Gießhübl	MTW4_Tu10	core	not defined	Con-San	Mitterwäldchen	35.49	6.52	34.17	6.18	0.05	0.69	0.80	9.66	0.00	2.06	0.05	95.66
Gießhübl	MTW4_Tu10	rim	not defined	Con-San	Mitterwäldchen	35.89	9.45	31.51	5.22	0.01	0.07	1.07	9.66	0.00	2.33	0.06	95.26
Gießhübl	L16_Tu1	core	not defined	Con-San	Lilienfeld	34.31	13.77	34.05	1.50	0.06	0.11	0.46	9.66	0.63	2.00	0.05	96.60
Gießhübl	L16_Tu1	rim	not defined	Con-San	Lilienfeld	35.90	10.48	31.50	5.38	0.03	0.06	0.57	9.66	0.24	2.49	0.01	96.33
Gießhübl	L16_Tu2	core	not defined	Con-San	Lilienfeld	36.51	6.03	33.06	7.50	0.04	0.91	0.31	9.66	0.06	1.86	0.03	95.98
Gießhübl	L16_Tu2	rim	not defined	Con-San	Lilienfeld	36.10	6.06	32.16	7.98	0.04	1.44	0.95	9.66	0.00	1.73	0.00	96.11
Gießhübl	L16_Tu3	core	not defined	Con-San	Lilienfeld	36.12	4.16	33.54	8.64	0.01	1.08	0.74	9.66	0.00	1.96	0.03	95.94
Gießhübl	L16_Tu3	rim	not defined	Con-San	Lilienfeld	36.19	4.08	33.61	8.47	0.00	1.18	0.70	9.66	0.21	1.94	0.04	96.08
Gießhübl	L16_Tu4	core	not defined	Con-San	Lilienfeld	35.75	5.82	34.74	6.42	0.02	0.57	0.62	9.66	0.17	2.00	0.02	95.78
Gießhübl	L16_Tu4	rim	not defined	Con-San	Lilienfeld	36.11	5.58	34.26	6.90	0.01	0.61	0.68	9.66	0.08	1.99	0.04	95.93
Gießhübl	L16_Tu5	core	not defined	Con-San	Lilienfeld	36.26	5.16	32.99	7.93	0.01	0.65	0.80	9.66	0.09	2.27	0.02	95.84
Gießhübl	L16_Tu5	rim	not defined	Con-San	Lilienfeld	36.24	5.17	33.07	7.85	0.00	0.68	0.81	9.66	0.00	2.24	0.02	95.72
Gießhübl	L16_Tu6	core	not defined	Con-San	Lilienfeld	36.13	5.54	33.90	6.88	0.00	0.49	0.74	9.66	0.00	2.03	0.00	95.37
Gießhübl	L16_Tu6	rim	not defined	Con-San	Lilienfeld	36.46	5.86	33.68	7.02	0.01	0.52	0.75	9.66	0.00	2.01	0.02	95.98
Gießhübl	L16_Tu7	core	not defined	Con-San	Lilienfeld	36.22	6.32	33.89	6.21	0.03	0.73	0.83	9.66	0.00	1.74	0.02	95.64
Gießhübl	L16_Tu7	rim	not defined	Con-San	Lilienfeld	36.29	6.72	33.22	6.32	0.05	0.81	1.01	9.66	0.00	1.78	0.01	95.87
Gießhübl	L16_Tu8	core	not defined	Con-San	Lilienfeld	35.50	9.52	32.51	5.68	0.04	1.02	0.07	9.66	0.20	1.77	0.01	95.97
Gießhübl	L16_Tu8	rim	not defined	Con-San	Lilienfeld	35.09	10.56	31.35	5.43	0.05	1.63	0.17	9.66	0.33	1.50	0.01	95.78
Gießhübl	L16_Tu9	core	not defined	Con-San	Lilienfeld	36.36	5.17	32.02	8.70	0.02	0.51	0.75	9.66	0.09	2.51	0.03	95.81
Gießhübl	L16_Tu9	rim	not defined	Con-San	Lilienfeld	36.34	5.09	31.69	8.57	0.01	0.55	0.77	9.66	0.00	2.48	0.04	95.19
Gießhübl	L16_Tu10	core	not defined	Con-San	Lilienfeld	36.30	3.94	33.14	8.73	0.00	0.75	0.62	9.66	0.10	2.29	0.04	95.56
Gießhübl	L16_Tu10	rim	not defined	Con-San	Lilienfeld	36.16	3.93	33.15	8.74	0.00	0.71	0.52	9.66	0.00	2.19	0.02	95.09
Gießhübl	L16_Tu11	core	not defined	Con-San	Lilienfeld	33.94	11.21	33.62	3.26	0.12	0.70	1.19	9.66	0.28	1.80	0.05	95.81
Gießhübl	L16_Tu11	rim	not defined	Con-San	Lilienfeld	36.17	8.47	32.69	5.70	0.04	0.09	0.48	9.66	0.20	2.11	0.00	95.61
Gießhübl	L16_Tu13	core	not defined	Con-San	Lilienfeld	35.27	5.49	34.68	6.87	0.01	1.05	0.76	9.66	0.08	1.72	0.02	95.62
Gießhübl	L16_Tu13	rim	not defined	Con-San	Lilienfeld	35.59	5.40	34.43	7.03	0.01	1.03	0.70	9.66	0.00	1.84	0.03	95.72
Gießhübl	L16_Tu14	core	not defined	Con-San	Lilienfeld	35.81	5.66	34.85	6.54	0.01	0.63	0.70	9.66	0.36	2.11	0.06	96.39
Gießhübl	L16_Tu14	rim	not defined	Con-San	Lilienfeld	35.80	5.96	34.92	6.13	0.04	0.48	0.66	9.66	0.02	1.86	0.04	95.56
Gießhübl	L16_Tu15	core	not defined	Con-San	Lilienfeld	36.03	8.39	31.45	6.47	0.03	0.58	0.78	9.66	0.06	2.11	0.01	95.57
Gießhübl	L16_Tu15	rim	not defined	Con-San	Lilienfeld	36.61	6.37	31.77	7.75	0.02	0.11	0.03	9.66	0.00	2.01	0.05	94.38
Gießhübl	L16_Tu16	core	not defined	Con-San	Lilienfeld	35.63	6.27	34.56	6.01	0.03	0.43	0.89	9.66	0.55	1.84	0.06	95.92
Gießhübl	L16_Tu16	rim	not defined	Con-San	Lilienfeld	35.47	6.86	33.72	5.99	0.02	0.39	1.37	9.66	0.03	2.16	0.04	95.70
Gießhübl	L16_Tu17	core	not defined	Con-San	Lilienfeld	34.69	11.19	32.83	3.78	0.07	0.37	0.82	9.66	0.35	2.12	0.03	95.91

Gosau	Sample	Grain	Formation	Age	Location	SiO_2 [%]	FeO [%]	Al_2O_3 [%]	MgO [%]	MnO [%]	CaO [%]	TiO_2 [%]	B_2O_3 [%]	F [%]	Na_2O [%]	K_2O [%]	Total [%]
Gießhübl	L16_Tu17	rim	not defined	Con-San	Lilienfeld	34.66	12.28	32.10	3.37	0.15	0.31	0.74	9.66	0.14	2.27	0.05	95.71
Gießhübl	L221_Tu1	core	not defined	Con-San	Lilienfeld	35.00	10.31	31.93	5.28	0.07	0.66	0.79	9.66	0.11	2.04	0.07	95.93
Gießhübl	L221_Tu1	rim	not defined	Con-San	Lilienfeld	35.94	9.95	31.50	5.01	0.04	0.07	1.01	9.66	0.00	2.30	0.04	95.52
Gießhübl	L221_Tu2	core	not defined	Con-San	Lilienfeld	35.77	6.86	32.04	7.22	0.00	0.81	0.84	9.66	0.10	2.15	0.02	95.46
Gießhübl	L221_Tu2	rim	not defined	Con-San	Lilienfeld	35.88	6.62	31.76	7.54	0.02	0.78	0.91	9.66	0.00	2.23	0.03	95.43
Gießhübl	L221_Tu3	core	not defined	Con-San	Lilienfeld	35.13	11.08	34.50	2.99	0.06	0.41	0.44	9.66	0.00	1.73	0.04	96.04
Gießhübl	L221_Tu3	rim	not defined	Con-San	Lilienfeld	36.56	8.23	33.69	5.09	0.01	0.04	0.47	9.66	0.02	1.61	0.03	95.42
Gießhübl	L221_Tu4	core	not defined	Con-San	Lilienfeld	35.48	8.16	33.61	5.22	0.05	0.61	0.93	9.66	0.00	1.89	0.04	95.66
Gießhübl	L221_Tu4	rim	not defined	Con-San	Lilienfeld	35.22	8.00	33.97	5.15	0.03	0.52	1.06	9.66	0.00	1.99	0.06	95.67
Gießhübl	L221_Tu5	core	not defined	Con-San	Lilienfeld	35.95	7.97	32.14	6.24	0.07	0.30	1.13	9.66	0.00	2.12	0.04	95.63
Gießhübl	L221_Tu5	rim	not defined	Con-San	Lilienfeld	35.69	7.89	31.41	6.59	0.05	0.35	1.42	9.66	0.00	2.18	0.06	95.30
Gießhübl	L221_Tu6	core	not defined	Con-San	Lilienfeld	35.84	4.54	34.63	7.19	0.04	0.51	0.84	9.66	0.11	2.05	0.03	95.44
Gießhübl	L221_Tu6	rim	not defined	Con-San	Lilienfeld	35.88	9.98	31.01	5.43	0.00	0.07	1.23	9.66	0.14	2.53	0.01	95.94
Gießhübl	L221_Tu7	core	not defined	Con-San	Lilienfeld	35.61	10.03	30.21	6.01	0.02	0.25	0.92	9.66	0.00	2.65	0.02	95.38
Gießhübl	L221_Tu7	rim	not defined	Con-San	Lilienfeld	36.01	6.91	31.38	7.69	0.00	0.83	0.83	9.66	0.21	2.23	0.02	95.78
Gießhübl	L221_Tu8	core	not defined	Con-San	Lilienfeld	36.36	3.81	32.91	8.62	0.00	0.72	0.61	9.66	0.00	2.08	0.01	94.77
Gießhübl	L221_Tu8	rim	not defined	Con-San	Lilienfeld	35.91	10.34	30.22	6.02	0.00	0.10	0.30	9.66	0.00	2.45	0.02	95.01
Gießhübl	L221_Tu9	core	not defined	Con-San	Lilienfeld	35.93	6.76	33.67	6.54	0.03	0.75	0.79	9.66	0.00	1.84	0.01	95.98
Gießhübl	L221_Tu9	rim	not defined	Con-San	Lilienfeld	35.46	6.54	33.62	6.68	0.00	0.79	0.79	9.66	0.00	1.97	0.02	95.52
Gießhübl	L221_Tu11	core	not defined	Con-San	Lilienfeld	35.17	11.42	33.98	2.60	0.10	0.21	0.60	9.66	0.26	1.84	0.04	95.89
Gießhübl	L221_Tu11	rim	not defined	Con-San	Lilienfeld	34.83	11.86	33.59	2.51	0.12	0.20	0.74	9.66	0.26	1.90	0.07	95.74
Gießhübl	L221_Tu12	core	not defined	Con-San	Lilienfeld	36.97	3.94	34.28	7.92	0.00	0.04	0.09	9.66	0.00	2.95	0.00	95.84
Gießhübl	L221_Tu12	rim	not defined	Con-San	Lilienfeld	36.60	5.20	32.42	8.34	0.00	0.04	0.10	9.66	0.00	2.73	0.01	95.10
Gießhübl	L221_Tu13	core	not defined	Con-San	Lilienfeld	35.76	6.43	34.98	5.66	0.04	0.45	0.79	9.66	0.00	1.59	0.03	95.38
Gießhübl	L221_Tu13	rim	not defined	Con-San	Lilienfeld	35.76	6.44	34.58	5.97	0.04	0.47	1.00	9.66	0.06	1.73	0.03	95.74
Gießhübl	L221_Tu14	core	not defined	Con-San	Lilienfeld	35.99	10.33	31.48	5.20	0.03	0.05	0.54	9.66	0.00	2.42	0.02	95.72
Gießhübl	L221_Tu14	rim	not defined	Con-San	Lilienfeld	35.01	10.00	27.79	8.13	0.13	2.44	0.55	9.66	0.00	1.33	0.08	95.12
Gießhübl	L221_Tu16	core	not defined	Con-San	Lilienfeld	35.32	10.83	28.95	6.64	0.02	0.00	0.32	9.66	0.00	2.98	0.04	94.75
Gießhübl	L221_Tu16	rim	not defined	Con-San	Lilienfeld	35.39	12.34	27.62	6.47	0.03	0.04	0.39	9.66	0.00	2.96	0.04	94.93
Gießhübl	TA8_Tu1	core	Nierental Fm	Campanian	Tasshof	36.06	10.07	29.77	6.61	0.00	0.03	0.50	9.66	0.00	2.80	0.01	95.51
Gießhübl	TA8_Tu1	rim	Nierental Fm	Campanian	Tasshof	36.27	9.02	30.80	6.93	0.01	0.03	0.22	9.66	0.00	2.87	0.03	95.83
Gießhübl	TA8_Tu2	core	Nierental Fm	Campanian	Tasshof	36.34	9.63	30.31	6.96	0.00	0.03	0.13	9.66	0.33	2.68	0.01	96.07
Gießhübl	TA8_Tu2	rim	Nierental Fm	Campanian	Tasshof	34.69	15.65	32.82	0.17	0.14	0.13	0.22	9.66	0.68	2.09	0.04	96.28
Gießhübl	A3_tu1	core	L-Gießhübl Fm	Maastr	Aderklaa 92	35.50	9.58	33.57	4.62	0.03	0.30	0.92	9.66	0.23	1.74	0.01	96.17
Gießhübl	A3_tu1	rim	L-Gießhübl Fm	Maastr	Aderklaa 92	35.35	10.39	33.64	3.74	0.04	0.30	0.90	9.66	0.22	1.78	0.04	96.06
Gießhübl	A3_tu4	core	L-Gießhübl Fm	Maastr	Aderklaa 92	35.71	8.31	34.94	4.44	0.06	0.25	0.69	9.66	0.27	1.75	0.04	96.12
Gießhübl	A3_tu4	rim	L-Gießhübl Fm	Maastr	Aderklaa 92	35.48	9.99	31.69	4.53	0.05	0.26	2.39	9.66	0.00	2.02	0.03	96.11
Gießhübl	A3_tu5	core	L-Gießhübl Fm	Maastr	Aderklaa 92	34.22	13.32	33.71	1.87	0.05	0.34	0.57	9.66	0.72	1.95	0.05	96.47
Gießhübl	A3_tu5	rim	L-Gießhübl Fm	Maastr	Aderklaa 92	36.38	8.24	31.79	6.63	0.02	0.17	0.72	9.66	0.74	2.27	0.03	96.64
Gießhübl	A3_tu7	core	L-Gießhübl Fm	Maastr	Aderklaa 92	35.94	7.05	31.91	7.56	0.00	0.45	0.69	9.66	0.67	2.37	0.02	96.32
Gießhübl	A3_tu7	rim	L-Gießhübl Fm	Maastr	Aderklaa 92	35.62	11.07	30.06	5.87	0.01	0.05	0.80	9.66	0.48	2.67	0.03	96.33
Gießhübl	A3_tu11	core	L-Gießhübl Fm	Maastr	Aderklaa 92	35.41	8.39	32.08	6.74	0.02	0.71	0.40	9.66	0.41	2.17	0.03	96.02
Gießhübl	A3_tu11	rim	L-Gießhübl Fm	Maastr	Aderklaa 92	35.80	10.78	29.81	6.11	0.06	0.24	0.68	9.66	0.57	2.60	0.01	96.31
Gießhübl	A3_tu12	core	L-Gießhübl Fm	Maastr	Aderklaa 92	35.96	7.30	33.02	6.57	0.03	0.54	0.44	9.66	0.00	1.93	0.01	95.48
Gießhübl	A3_tu12	rim	L-Gießhübl Fm	Maastr	Aderklaa 92	36.83	4.38	34.76	7.64	0.00	0.33	0.49	9.66	0.35	1.82	0.02	96.30
Gießhübl	A3_tu14	core	L-Gießhübl Fm	Maastr	Aderklaa 92	36.43	4.50	35.50	7.17	0.00	0.22	0.40	9.66	0.33	1.98	0.03	96.22
Gießhübl	A3_tu14	rim	L-Gießhübl Fm	Maastr	Aderklaa 92	36.27	5.02	33.22	7.55	0.00	0.33	1.62	9.66	0.37	2.11	0.02	96.16

Gosau	Sample	Grain	Formation	Age	Location	SiO_2 [%]	FeO [%]	Al_2O_3 [%]	MgO [%]	MnO [%]	CaO [%]	TiO_2 [%]	B_2O_3 [%]	F [%]	Na_2O [%]	K_2O [%]	Total [%]
Gießhübl	A4_tu1	core	L-Gießhübl Fm	Paleocene	Aderklaa 92	35.66	10.28	31.01	5.72	0.01	0.13	0.26	9.66	0.51	2.64	0.00	95.88
Gießhübl	A4_tu1	rim	L-Gießhübl Fm	Paleocene	Aderklaa 92	35.24	11.86	28.53	5.90	0.02	0.16	0.55	9.66	0.31	2.67	0.02	94.91
Gießhübl	A4_tu2	core	L-Gießhübl Fm	Paleocene	Aderklaa 92	36.15	6.86	32.35	7.15	0.00	0.28	0.48	9.66	0.00	2.40	0.03	95.36
Gießhübl	A4_tu2	rim	L-Gießhübl Fm	Paleocene	Aderklaa 92	35.93	9.47	32.19	5.42	0.02	0.05	0.59	9.66	0.00	2.40	0.02	95.74
Gießhübl	A4_tu7	core	L-Gießhübl Fm	Paleocene	Aderklaa 92	35.87	8.45	32.13	6.33	0.02	0.23	0.42	9.66	0.00	2.48	0.01	95.59
Gießhübl	A4_tu7	rim	L-Gießhübl Fm	Paleocene	Aderklaa 92	35.73	9.04	30.94	6.00	0.01	0.21	1.25	9.66	0.22	2.38	0.02	95.44
Gießhübl	A4_tu9	core	L-Gießhübl Fm	Paleocene	Aderklaa 92	33.87	9.13	35.35	4.20	0.05	0.62	0.61	9.66	0.00	1.91	0.05	95.44
Gießhübl	A4_tu9	rim	L-Gießhübl Fm	Paleocene	Aderklaa 92	35.92	6.07	32.67	7.48	0.01	0.83	0.90	9.66	0.07	2.07	0.07	95.76
Glinzendorf	T102_Tur1	core	not defined	Campanian	Markgrn. T1	36.34	4.59	32.14	8.73	0.03	1.38	0.69	9.66	0.70	1.92	0.02	96.20
Glinzendorf	T102_Tur1	rim	not defined	Campanian	Markgrn. T1	36.25	4.56	32.17	8.86	0.00	1.13	0.85	9.66	0.66	2.05	0.01	96.21
Glinzendorf	T102_Tur3	core	not defined	Campanian	Markgrn. T1	35.77	9.49	32.12	5.14	0.01	0.78	0.99	9.66	0.50	1.70	0.04	96.20
Glinzendorf	T102_Tur3	rim	not defined	Campanian	Markgrn. T1	36.86	6.06	31.85	7.92	0.00	0.04	0.02	9.66	0.00	1.70	0.02	94.14
Glinzendorf	T102_Tur5	core	not defined	Campanian	Markgrn. T1	34.82	11.60	33.52	2.94	0.14	0.29	0.61	9.66	0.04	1.95	0.04	95.60
Glinzendorf	T102_Tur5	rim	not defined	Campanian	Markgrn. T1	35.91	5.20	33.35	7.63	0.00	0.70	0.81	9.66	0.00	2.08	0.02	95.34
Glinzendorf	T102_Tur6	core	not defined	Campanian	Markgrn. T1	35.89	9.07	31.32	6.06	0.04	0.29	0.81	9.66	0.45	2.46	0.03	96.08
Glinzendorf	T102_Tur6	rim	not defined	Campanian	Markgrn. T1	36.29	5.79	33.70	6.89	0.00	0.19	0.74	9.66	0.21	2.28	0.03	95.78
Glinzendorf	T102_Tur8	core	not defined	Campanian	Markgrn. T1	36.52	7.95	33.31	5.85	0.00	0.11	0.43	9.66	0.10	2.34	0.03	96.29
Glinzendorf	T102_Tur8	rim	not defined	Campanian	Markgrn. T1	35.78	6.04	34.29	6.53	0.01	0.62	0.63	9.66	0.38	2.08	0.03	96.06
Glinzendorf	T102_Tur9	core	not defined	Campanian	Markgrn. T1	35.63	10.02	31.47	5.47	0.03	0.12	0.47	9.66	0.10	2.47	0.00	95.43
Glinzendorf	T102_Tur9	rim	not defined	Campanian	Markgrn. T1	35.75	9.33	32.44	5.36	0.04	0.04	0.39	9.66	0.28	2.20	0.00	95.49
Glinzendorf	T102_Tur12	core	not defined	Campanian	Markgrn. T1	35.33	8.12	27.90	8.97	0.03	2.26	1.56	9.66	0.00	1.51	0.04	95.39
Glinzendorf	T102_Tur12	rim	not defined	Campanian	Markgrn. T1	35.78	8.44	29.04	7.94	0.02	1.30	1.27	9.66	0.14	2.02	0.02	95.63
Glinzendorf	T102_Tur13	core	not defined	Campanian	Markgrn. T1	35.43	6.20	34.93	6.24	0.04	0.67	0.68	9.66	0.20	1.83	0.04	95.91
Glinzendorf	T102_Tur13	rim	not defined	Campanian	Markgrn. T1	36.15	9.84	31.33	5.79	0.01	0.01	0.04	9.66	0.41	2.23	0.00	95.48
Glinzendorf	T102_Tur14	core	not defined	Campanian	Markgrn. T1	35.34	9.85	33.02	4.03	0.17	0.28	0.95	9.66	0.00	2.04	0.03	95.37
Glinzendorf	T102_Tur14	rim	not defined	Campanian	Markgrn. T1	36.15	7.28	33.59	6.08	0.04	0.57	0.48	9.66	0.11	1.94	0.01	95.92
Glinzendorf	T102_Tur15	core	not defined	Campanian	Markgrn. T1	35.23	8.68	31.58	5.93	0.01	1.27	1.23	9.66	0.26	1.76	0.03	95.64
Glinzendorf	T102_Tur15	rim	not defined	Campanian	Markgrn. T1	35.37	8.46	32.30	5.73	0.03	1.00	1.13	9.66	0.14	1.72	0.03	95.57
Glinzendorf	T102_Tur16	core	not defined	Campanian	Markgrn. T1	35.87	7.09	31.43	7.49	0.01	0.91	0.93	9.66	0.65	2.20	0.02	96.25
Glinzendorf	T102_Tur16	rim	not defined	Campanian	Markgrn. T1	35.93	7.12	31.32	7.58	0.01	0.93	0.89	9.66	0.27	2.12	0.01	95.83
Glinzendorf	T102_Tur17	core	not defined	Campanian	Markgrn. T1	36.52	7.25	27.66	10.71	0.00	0.00	0.18	9.66	0.00	2.92	0.08	94.96
Glinzendorf	T102_Tur17	rim	not defined	Campanian	Markgrn. T1	36.03	10.15	26.55	9.18	0.00	0.00	0.61	9.66	0.01	2.92	0.07	95.18
Glinzendorf	T102_Tur18	core	not defined	Campanian	Markgrn. T1	36.35	6.08	32.39	7.76	0.01	0.42	0.65	9.66	0.00	2.22	0.00	95.53
Glinzendorf	T102_Tur18	rim	not defined	Campanian	Markgrn. T1	35.39	7.21	34.73	5.33	0.01	0.48	0.85	9.66	0.22	1.77	0.01	95.68
Glinzendorf	T101_Tur1	core	not defined	Campanian	Markgrn. T1	36.49	9.81	30.87	5.83	0.01	0.14	1.40	9.66	0.56	2.47	0.03	97.27
Glinzendorf	T101_Tur1	rim	not defined	Campanian	Markgrn. T1	35.80	9.33	31.03	5.63	0.00	0.10	1.16	9.66	0.56	2.40	0.01	95.68
Grünbach	M63_Tur1	core	Grünbach Fm	Campanian	Grünbach	36.29	9.15	28.46	8.54	0.01	0.04	0.21	9.66	0.00	2.88	0.03	95.26
Grünbach	M63_Tur1	rim	Grünbach Fm	Campanian	Grünbach	36.68	8.41	29.23	8.73	0.00	0.06	0.20	9.66	0.18	2.82	0.04	96.00
Grünbach	M63_Tur3	core	Grünbach Fm	Campanian	Grünbach	34.58	12.66	33.88	2.11	0.12	0.17	0.65	9.66	0.36	1.83	0.04	96.06
Grünbach	M63_Tur3	rim	Grünbach Fm	Campanian	Grünbach	36.54	7.55	32.44	6.91	0.00	0.00	0.12	9.66	0.24	2.18	0.01	95.65
Grünbach	M63_Tur5	core	Grünbach Fm	Campanian	Grünbach	35.25	3.82	31.47	8.64	0.00	2.12	0.84	9.66	0.51	1.51	0.04	93.87
Grünbach	M63_Tur5	rim	Grünbach Fm	Campanian	Grünbach	36.40	8.86	32.09	5.83	0.02	0.31	0.48	9.66	0.00	2.17	0.12	95.93
Grünbach	M63_Tur7	core	Grünbach Fm	Campanian	Grünbach	35.30	6.97	35.03	5.68	0.05	0.81	0.98	9.66	0.00	1.80	0.05	96.33
Grünbach	M63_Tur7	rim	Grünbach Fm	Campanian	Grünbach	36.19	9.72	33.99	4.00	0.01	0.05	0.44	9.66	0.38	1.52	0.01	95.97
Grünbach	G22_Tur1	core	Grünbach Fm	Campanian	Grünbach	35.77	5.47	33.23	7.60	0.02	1.24	0.92	9.66	0.45	1.76	0.02	96.14
Grünbach	G22_Tur1	rim	Grünbach Fm	Campanian	Grünbach	36.58	6.73	34.18	6.14	0.01	0.03	0.10	9.66	0.23	1.91	0.00	95.57
Grünbach	G22_Tur3	core	Grünbach Fm	Campanian	Grünbach	36.58	6.49	31.86	8.13	0.01	0.03	0.07	9.66	0.00	2.47	0.01	95.31

Gosau	Sample	Grain	Formation	Age	Location	SiO_2 [%]	FeO [%]	Al_2O_3 [%]	MgO [%]	MnO [%]	CaO [%]	TiO_2 [%]	B_2O_3 [%]	F [%]	Na_2O [%]	K_2O [%]	Total [%]
Grünbach	G22_Tur3	rim	Grünbach Fm	Campanian	Grünbach	36.58	5.10	33.50	7.73	0.00	0.04	0.14	9.66	0.19	3.01	0.03	95.98
Grünbach	G22_Tur4	core	Grünbach Fm	Campanian	Grünbach	35.09	8.84	34.94	4.12	0.05	0.37	0.86	9.66	0.11	1.86	0.04	95.93
Grünbach	G22_Tur4	rim	Grünbach Fm	Campanian	Grünbach	35.87	10.34	29.55	6.30	0.01	0.08	0.85	9.66	0.37	2.78	0.01	95.81
Grünbach	G22_Tur6	core	Grünbach Fm	Campanian	Grünbach	36.70	5.46	35.48	6.22	0.01	0.24	0.17	9.66	0.17	1.41	0.02	95.53
Grünbach	G22_Tur6	rim	Grünbach Fm	Campanian	Grünbach	39.44	4.71	31.40	7.96	0.01	0.02	0.63	9.66	0.00	1.89	0.01	95.74
Grünbach	G22_Tur7	core	Grünbach Fm	Campanian	Grünbach	35.62	9.38	35.51	3.28	0.04	0.10	0.32	9.66	0.43	1.51	0.04	95.87
Grünbach	G22_Tur7	rim	Grünbach Fm	Campanian	Grünbach	36.86	3.87	34.56	7.95	0.01	0.01	0.01	9.66	0.02	1.37	0.01	94.32
Grünbach	G22_Tur10	core	Grünbach Fm	Campanian	Grünbach	36.73	5.91	31.25	8.80	0.00	0.04	0.20	9.66	0.71	2.96	0.02	96.27
Grünbach	G22_Tur10	rim	Grünbach Fm	Campanian	Grünbach	36.77	6.14	30.88	9.20	0.00	0.02	0.20	9.66	0.41	2.98	0.00	96.25
Grünbach	G22_Tur11	core	Grünbach Fm	Campanian	Grünbach	36.14	9.13	28.04	8.77	0.00	0.02	0.21	9.66	0.18	2.95	0.07	95.17
Grünbach	G22_Tur11	rim	Grünbach Fm	Campanian	Grünbach	36.07	9.05	27.98	8.69	0.00	0.01	0.23	9.66	0.20	2.99	0.03	94.91
Grünbach	G22_Tur12	core	Grünbach Fm	Campanian	Grünbach	36.36	5.44	32.62	7.76	0.00	0.47	0.71	9.66	0.51	2.37	0.03	95.93
Grünbach	G22_Tur12	rim	Grünbach Fm	Campanian	Grünbach	36.84	8.11	34.12	5.26	0.00	0.02	0.03	9.66	0.24	1.00	0.01	95.28
Grünbach	G22_Tur14	core	Grünbach Fm	Campanian	Grünbach	35.52	7.51	33.97	5.60	0.05	0.49	0.81	9.66	0.08	2.04	0.04	95.76
Grünbach	G22_Tur14	rim	Grünbach Fm	Campanian	Grünbach	35.52	7.22	34.25	5.52	0.04	0.45	0.83	9.66	0.48	1.94	0.03	95.94
Grünbach	G22_Tur15	core	Grünbach Fm	Campanian	Grünbach	37.06	5.80	32.26	8.11	0.00	0.00	0.05	9.66	0.06	2.33	0.02	95.36
Grünbach	G22_Tur15	rim	Grünbach Fm	Campanian	Grünbach	36.23	8.36	30.47	7.49	0.00	0.01	0.23	9.66	0.36	2.97	0.00	95.78
Grünbach	G22_Tur16	core	Grünbach Fm	Campanian	Grünbach	36.36	6.81	31.71	7.56	0.00	0.07	0.39	9.66	0.28	2.72	0.00	95.56
Grünbach	G22_Tur16	rim	Grünbach Fm	Campanian	Grünbach	35.80	8.60	30.96	6.48	0.03	0.15	1.03	9.66	0.38	2.68	0.01	95.78
Grünbach	G10_tu1	core	Piesting Fm	Campanian	Grünbach	36.20	5.76	31.40	8.40	0.01	0.22	1.06	9.66	0.54	2.71	0.03	95.99
Grünbach	G10_tu1	rim	Piesting Fm	Campanian	Grünbach	36.21	8.60	31.58	6.56	0.01	0.00	0.08	9.66	0.62	2.18	0.05	95.56
Grünbach	G10_tu2	core	Piesting Fm	Campanian	Grünbach	32.10	14.49	34.10	0.39	0.55	0.55	0.49	9.66	0.84	2.09	0.01	95.27
Grünbach	G10_tu2	rim	Piesting Fm	Campanian	Grünbach	35.60	9.54	30.24	6.01	0.02	0.32	1.60	9.66	0.76	2.65	0.01	96.40
Grünbach	G10_tu4	core	Piesting Fm	Campanian	Grünbach	35.36	10.57	30.84	5.52	0.00	0.48	0.78	9.66	0.22	2.42	0.03	95.89
Grünbach	G10_tu4	rim	Piesting Fm	Campanian	Grünbach	35.46	8.40	33.23	5.76	0.01	0.06	0.02	9.66	0.24	1.30	0.03	94.17
Grünbach	G10_tu7	core	Piesting Fm	Campanian	Grünbach	34.76	13.74	34.18	1.01	0.21	0.07	0.16	9.66	0.54	1.68	0.03	96.03
Grünbach	G10_tu7	rim	Piesting Fm	Campanian	Grünbach	35.97	8.88	32.78	5.48	0.00	0.06	0.42	9.66	1.06	2.15	0.01	96.48
Grünbach	G10_tu9	core	Piesting Fm	Campanian	Grünbach	35.63	6.32	32.40	8.09	0.04	1.20	0.24	9.66	0.37	1.90	0.03	95.88
Grünbach	G10_tu9	rim	Piesting Fm	Campanian	Grünbach	36.05	7.39	32.46	6.91	0.03	0.12	0.34	9.66	0.34	2.38	0.00	95.67
Grünbach	G37_tu1	core	Piesting Fm	Maastr	Grünbach	34.37	13.62	34.97	0.77	0.23	0.11	0.38	9.66	0.55	1.66	0.03	96.36
Grünbach	G37_tu1	rim	Piesting Fm	Maastr	Grünbach	35.74	9.39	32.37	5.21	0.02	0.03	0.74	9.66	0.09	2.10	0.00	95.34
Grünbach	G37_tu2	core	Piesting Fm	Maastr	Grünbach	36.23	6.17	32.25	7.54	0.01	0.35	1.00	9.66	0.27	2.25	0.03	95.76
Grünbach	G37_tu2	rim	Piesting Fm	Maastr	Grünbach	35.58	10.14	31.33	5.24	0.02	0.16	1.01	9.66	0.40	2.29	0.04	95.87
Grünbach	G37_tu6	core	Piesting Fm	Maastr	Grünbach	35.93	6.85	32.26	7.23	0.02	0.56	0.75	9.66	0.22	2.18	0.06	95.70
Grünbach	G37_tu6	rim	Piesting Fm	Maastr	Grünbach	38.65	7.29	30.21	7.02	0.02	0.11	0.14	9.66	0.16	3.24	0.02	96.52
Grünbach	G37_tu8	core	Piesting Fm	Maastr	Grünbach	36.31	6.49	32.49	7.37	0.01	0.35	0.91	9.66	0.18	2.46	0.01	96.23
Grünbach	G37_tu8	rim	Piesting Fm	Maastr	Grünbach	35.49	11.88	30.83	4.84	0.00	0.02	0.45	9.66	0.59	2.38	0.01	96.13
Grünbach	G37_tu10	core	Piesting Fm	Maastr	Grünbach	35.26	9.43	34.37	4.27	0.07	0.31	0.47	9.66	0.07	2.01	0.06	95.96
Grünbach	G37_tu10	rim	Piesting Fm	Maastr	Grünbach	36.54	7.01	32.92	6.97	0.03	0.04	0.32	9.66	0.00	2.48	0.02	95.99
Grünbach	G37_tu15	core	Piesting Fm	Maastr	Grünbach	36.28	5.77	32.40	7.95	0.00	0.69	0.76	9.66	0.71	2.20	0.00	96.43
Grünbach	G37_tu15	rim	Piesting Fm	Maastr	Grünbach	35.92	9.93	29.08	7.46	0.01	0.03	0.73	9.66	0.30	2.70	0.02	95.84
Grünbach	G37_tu16	core	Piesting Fm	Maastr	Grünbach	36.25	5.26	34.77	6.69	0.01	0.31	0.56	9.66	0.07	1.77	0.02	95.37
Grünbach	G37_tu16	rim	Piesting Fm	Maastr	Grünbach	35.53	10.15	30.19	5.46	0.08	0.16	1.50	9.66	0.04	2.57	0.03	95.36
Grünbach	G37_tu17	core	Piesting Fm	Maastr	Grünbach	36.28	5.96	37.12	4.89	0.08	0.09	0.10	9.66	0.54	1.73	0.01	96.43
Grünbach	G37_tu17	rim	Piesting Fm	Maastr	Grünbach	36.01	10.71	28.90	7.12	0.01	0.02	0.41	9.66	0.00	2.84	0.03	95.72

curriculum vitae

Gerald Hofer
Master of Science

30.10.1983

Burggasse 114/2/9, 1070 Vienna

gerald.hofer@univie.ac.at



Academic Career:

June 2002:
School leaving examination graduated with honors (BG/BRG Leoben)

October 2002 - September 2003:
Civilian service in a shelter for homeless men (Salztorzentrum, Salvation Army, Vienna)

October 2003:
Start of the academic studies of earth sciences (University of Vienna)

September 2007:
Bachelor of Science graduated with honors
(Thesis: "Geomorphologic and sedimentologic investigations of the north-eastern part of the Lake Neusiedl")

December 2009:
Master of Science graduated with honors
(Thesis: "Geochemical investigation on lacustrine-marine sediments of the borehole Markgrafneusiedl T1 (Upper Cretaceous, Gosau Group)"

January 2009
Start with PhD-thesis

Professional Career:

August 2008 - December 2008:
Scientific employee at the Department of Geodynamics and Sedimentology in the OMV-"Gosau Project"
(Pilot study: "Geochemistry and isotope geochemistry of limnic-marine cycles, Upper Cretaceous; Borehole Markgrafneusiedl T1")

January 2009 - March 2011:
Scientific employee at the Department of Geodynamics and Sedimentology in the OMV-"Gosau Project"

April 2011 - March 2013:
Two years grant from ÖAW (Austrian Academy of Science, DOC-program)

Various tutor activities at the University of Vienna (Stratigraphy, microscopy, field mapping, historical geology)

Additional Courses:

Chemostratigraphy: applications, limitations and implications for global environmental change (H. Jenkyns; Trieste, Italy)

Sedimentary Provenance Analysis: short course (H. Von Eynatten; Göttingen, Germany)

Special Skills:

Good basic skills in various programs widly used in geoscience
Languages: German, English; basics in French and Spanish